U.S. DEPARTMENT OF COMMERCE
National Technical Information Service

PB-260 570

Ozone and Other Photochemical Oxidants Volume 1 (Chapters 1-7)

National Research Council, Washington, D C

Prepared for

Health Effects Research Lab, Research Triangle Park, N C

Aug 76

328135

PB 260 570

EPA-600/1-76-027a
August 1976

Environmental Health Effects Research Series

UNITED STATES ENVIRONMENTAL PROTECTION AGENCY

REPRODUCED BY
NATIONAL TECHNICAL
INFORMATION SERVICE
U. S. DEPARTMENT OF COMMERCE
SPRINGFIELD, VA. 22161

RESEARCH REPORTING SERIES

Research reports of the Office of Research and Development, U.S. Environmental Protection Agency, have been grouped into five series. These five broad categories were established to facilitate further development and application of environmental technology. Elimination of traditional grouping was consciously planned to foster technology transfer and a maximum interface in related fields. The five series are:

1. Environmental Health Effects Research
2. Environmental Protection Technology
3. Ecological Research
4. Environmental Monitoring
5. Socioeconomic Environmental Studies

This report has been assigned to the ENVIRONMENTAL HEALTH EFFECTS RESEARCH series. This series describes projects and studies relating to the tolerances of man for unhealthful substances or conditions. This work is generally assessed from a medical viewpoint, including physiological or psychological studies. In addition to toxicology and other medical specialities, study areas include biomedical instrumentation and health research techniques utilizing animals—but always with intended application to human health measures.

This document is available to the public through the National Technical Information Service, Springfield, Virginia 22161.

TECHNICAL REPORT DATA
(Please read Instructions on the reverse before completing)

1. RE EPA-600/1-76-027a	2.	3. RECIPIENT'S ACCESSION NO. PB-260 570
4. TITLE AND SUBTITLE Ozone and Other Photochemical Oxidants.		5. REPORT DATE August 1976 6. PERFORMING ORGANIZATION CODE
7. AUTHOR(S) Subcommittee on Ozone and Other Photochemical Oxidants		8. PERFORMING ORGANIZATION REPORT NO.
9. PERFORMING ORGANIZATION NAME AND ADDRESS Committee on Medical and Biologic Effects of Environmental Pollutants National Academy of Sciences Washington, D.C.		10. PROGRAM ELEMENT NO. 1AA601 11. CONTRACT/GRANT NO. 68-02-1226
12. SPONSORING AGENCY NAME AND ADDRESS Health Effects Research Laboratory Office of Research and Development U.S. Environmental Protection Agency Research Triangle Park, N.C. 27711		13. TYPE OF REPORT AND PERIOD COVERED 14. SPONSORING AGENCY CODE EPA-ORD

15. SUPPLEMENTARY NOTES
In two volumes - Vol. 1, Chapters 1 through 7. Vol. 2, Chapters 8 through 15

16. ABSTRACT

This report deals primarily with the origins and effects of ozone and other photochemical oxidants. It is limited, more or less, to the problem of urban pollution and to such closely related topics as natural background in the earth's boundary layer. No consideration is given to the stratospheric ozone layer and the effects produced by Supersonic Transport emissions or halocarbons.

The first third of the report is concerned with the origins and measurement of ozone and other photochemical oxidants and the relationship of atmospheric concentrations to emissions. The middle third deals with toxicologic studies and effects on humans, and the last with effects on plants, ecosystems, and materials.

17. KEY WORDS AND DOCUMENT ANALYSIS

a. DESCRIPTORS	b. IDENTIFIERS/OPEN ENDED TERMS	c. COSATI Field/Group
ozone photochemical reactions oxidizers measurement air pollution toxicity		06 F, T 07, C

PRICES SUBJECT TO CHANGE

18. DISTRIBUTION STATEMENT RELEASE TO PUBLIC	19. SECURITY CLASS *(This Report)* UNCLASSIFIED	21. NO. OF PAGES 552
	20. SECURITY CLASS *(This page)* UNCLASSIFIED	22. PRICE 13.50-3.00

EPA Form 2220-1 (9-73)

EPA-600/1-76-027a
August 1976

OZONE AND OTHER PHOTOCHEMICAL OXIDANTS

Volume 1

By

Subcommittee on Ozone and Other Photochemical Oxidants
Committee on Medical and Biologic Effects of
Environmental Pollution
National Research Council
National Academy of Sciences

Contract No. 68-02-1226

Project Officer

Orin Stopinski
Criteria and Special Studies Office
Health Effects Research Laboratory
Research Triangle Park, N.C. 27711

U.S. ENVIRONMENTAL PROTECTION AGENCY
OFFICE OF RESEARCH AND DEVELOPMENT
HEALTH EFFECTS RESEARCH LABORATORY
RESEARCH TRIANGLE PARK, N.C. 27711

DISCLAIMER

This report has been reviewed by the Health Effects Research Laboratory, U.S. Environmental Protection Agency, and approved for publication. Approval does not signify that the contents necessarily reflect the views and policies of the U.S. Environmental Protection Agency, nor does mention of trade names or commercial products constitute endorsement or recommendation for use.

NOTICE

The project reported on here was approved by the Governing Board of the National Research Council, whose members are drawn from the Councils of the National Academy of Sciences, the National Academy of Engineering, and the Institute of Medicine. The members of the committee responsible for the report were chosen for their special competences and with regard for appropriate representation of experience and disciplines. The findings and conclusions presented are entirely those of that committee.

This report has been critically reviewed according to procedures approved by a Report Review Committee consisting of members of the National Academy of Sciences, the National Academy of Engineering, and the Institute of Medicine. Only after completion of the review process has it been released for publication.

The work on which this publication is based was performed pursuant to Contract No. 68-02-1226 with the Environmental Protection Agency.

FOREWORD

The many benefits of our modern, developing, industrial society are accompanied by certain hazards. Careful assessment of the relative risk of existing and new man-made environmental hazards is necessary for the establishment of sound regulatory policy. These regulations serve to enhance the quality of our environment in order to promote the public health and welfare and the productive capacity of our Nation's population.

The Health Effects Research Laboratory, Research Triangle Park conducts a coordinated environmental health research program in toxicology, epidemiology, and clinical studies using human volunteer subjects. These studies address problems in air pollution, non-ionizing radiation, environmental carcinogenesis and the toxicology of pesticides as well as other chemical pollutants. The Laboratory develops and revises air quality criteria documents on pollutants for which national ambient air quality standards exist or are proposed, provides the data for registration of new pesticides or proposed suspension of those already in use, conducts research on hazardous and toxic materials, and is preparing the health basis for non-ionizing radiation standards. Direct support to the regulatory function of the Agency is provided in the form of expert testimony and preparation of affidavits as well as expert advice to the Administrator to assure the adequacy of health care and surveillance of persons having suffered imminent and substantial endangerment of their health.

To aid the Health Effects Research Laboratory to fulfill the functions listed above, the National Academy of Sciences (NAS) under EPA Contract No. 68-02-1226 prepares evaluative reports of current knowledge of selected atmospheric pollutants. These documents serve as background material for the preparation or revision of criteria documents, scientific and technical assessment reports, partial bases for EPA decisions and recommendations for research needs. "Ozone and Other Photochemical Oxidants" is one of these reports.

JHKnelson

John H. Knelson, M.D.
Director
Health Effects Research Laboratory

SUBCOMMITTEE ON OZONE AND OTHER PHOTOCHEMICAL OXIDANTS

SHELDON K. FRIEDLANDER, California Institute of Technology, Pasadena, Chairman

BERNARD ALTSHULER, Institute of Environmental Medicine, New York University Medical Center, New York

KYLE D. BAYES, Department of Chemistry, University of California, Los Angeles

ALAN Q. ESCHENROEDER, Environmental Research and Technology, Inc., Santa Barbara, California

JACK D. HACKNEY, University of Southern California, Downey

WALTER W. HECK, Agricultural Research Service, U.S. Department of Agriculture, North Carolina State University, Raleigh

JAMES R. MC CARROLL, Medical Services Division, City of Los Angeles, California

JAMES R. MC NESBY, Office of Air and Water Measurement, National Bureau of Standards, Washington, D.C.

PAUL R. MILLER, Pacific Southwest Forest and Range Experiment Station, U.S. Forest Service, Berkeley, California

PETER K. MUELLER, Environmental Research and Technology, Inc.. Westlake Village, California

SHELDON D. MURPHY, Department of Physiology, Harvard School of Public Health, Boston, Massachusetts

Consultants

KARL A. BELL, Environmental Health Department, Rancho Los Amigos Hospital, Downey, California, and Departments of Environmental and Chemical Engineering, School of Engineering, University of Southern California, Los Angeles

BERNARD D. GOLDSTEIN, Institute of Environmental Medicine, New York University Medical Center, New York

DANIEL GROSJEAN, Statewide Air Pollution Research Center, University of California, Riverside

MARGARET HITCHCOCK, Yale University School of Medicine, New Haven, Connecticut

JOHN B. MUDD, Department of Biochemistry, University of California, Riverside

MARSHALL WHITE, University of California, Berkeley

JAMES A. FRAZIER, Division of Medical Sciences, National Research Council, Washington, D.C., Staff Officer

COMMITTEE ON MEDICAL AND BIOLOGIC EFFECTS OF ENVIRONMENTAL POLLUTANTS

HERSCHEL E. GRIFFIN, Graduate School of Public Health, University of Pittsburgh, Pennsylvania, Chairman

RONALD F. COBURN, Department of Physiology, University of Pennsylvania School of Medicine, Philadelphia

T. TIMOTHY CROCKER, Department of Community and Environmental Medicine, University of California College of Medicine, Irvine

CLEMENT A. FINCH, Department of Hematology, University of Washington, Seattle

SHELDON K. FRIEDLANDER, W. M. Keck Laboratories, California Institute of Technology, Pasadena

ROBERT I. HENKIN, Department of Pediatrics, Georgetown University Hospital, Washington, D.C.

IAN T. T. HIGGINS, School of Public Health, University of Michigan, Ann Arbor

JOE W. HIGHTOWER, Department of Chemical Engineering, Rice University, Houston, Texas

HENRY KAMIN, Department of Biochemistry, Duke University Medical Center, Durham, North Carolina

ORVILLE A. LEVANDER, Nutrition Institute, Agricultural Research Center, Beltsville, Maryland

DWIGHT F. METZLER, Kansas State Department of Health and Environment, Topeka

I. HERBERT SCHEINBERG, Department of Medicine, Albert Einstein College of Medicine, Bronx, New York

RALPH G. SMITH, Department of Environmental and Industrial Health, School of Public Health, University of Michigan, Ann Arbor

ROGER P. SMITH, Department of Pharmacology and Toxicology, Dartmouth Medical School, Hanover, New Hampshire

T. D. BOAZ, JR., Division of Medical Sciences, National Research Council, Washington, D.C., Executive Director

ACKNOWLEDGMENTS

This document was written by the Subcommittee on Ozone and Other Photochemical Oxidants under the chairmanship of Dr. Sheldon K. Friedlander. The members of the Subcommittee and its consultants were chosen for their competence to prepare sections of the report. The entire document was critically reviewed by the Subcommittee, and it represents the combined effort and cooperation of all its members and consultants.

The authors of the individual sections were as follows: Dr. Kyle D. Bayes, the material on chemical origin; Dr. Daniel Grosjean, on aerosols; Dr. Alan Q. Eschenroeder, on atmospheric concentrations of photochemical oxidants and models for predicting air quality; Dr. Peter K. Mueller, on measurement and methods; Drs. Karl A. Bell and Bernard Altshuler, on respiratory transport and absorption; Dr. Sheldon D. Murphy in collaboration with Drs. Bernard D. Goldstein and Margaret Hitchcock, on toxicology; Dr. Jack D. Hackney, on controlled studies on humans; Dr. James R. McCarroll, on epidemiologic studies; Dr. Walter W. Heck in collaboration with Drs. John B. Mudd and Paul R. Miller, on plants and microorganisms; Dr. Miller in collaboration with Dr. Marshall White, on ecosystems; and Dr. James R. McNesby, on effects of photochemical oxidants on materials. Dr. Friedlander prepared the executive summary.

The document was reviewed by the Report Review Committee of the National Academy of Sciences; by the parent Committee on Medical and Biologic Effects of Environmental Pollutants (MBEEP); by the Associate Editor, Dr. Ronald F. Coburn, and several anonymous reviewers; by the Advisory Center on Toxicology of the Assembly of Life Sciences (ALS); by the Committee on Atmospheric Sciences of the Commission on Natural Resources' Environmental Studies Board; and by the Committee on National Statistics of the Assembly of Mathematical and Physical Sciences.

The Subcommittee is indebted to Mr. James A. Frazier, staff officer in the ALS Division of Medical Sciences, for his special efforts and assistance. The report was edited by Mr. Norman Grossblatt, Editor for the Assembly of Life Sciences. This is the largest of the MBEEP reports yet produced, and we wish to acknowledge the editorial assistance of Mrs. Renee Ford on one of the chapters.

COMMITTEE ON MEDICAL AND BIOLOGIC EFFECTS OF ENVIRONMENTAL POLLUTANTS
Division of Medical Sciences, National Research Council
Assembly of Life Sciences

SUBCOMMITTEE ON OZONE AND OTHER PHOTOCHEMICAL OXIDANTS

OUTLINE OF THE REPORT

1. EXECUTIVE SUMMARY
2. CHEMICAL ORIGIN
3. AEROSOLS
4. ATMOSPHERIC CONCENTRATIONS OF PHOTOCHEMICAL OXIDANTS
5. MODELS FOR PREDICTING AIR QUALITY
6. MEASUREMENT METHODS
7. RESPIRATORY TRANSPORT AND ABSORPTION
8. TOXICOLOGY
9. CONTROLLED STUDIES ON HUMANS
10. EPIDEMIOLOGIC STUDIES
11. PLANTS AND MICROORGANISMS
12. ECOSYSTEMS
13. EFFECTS OF PHOTOCHEMICAL OXIDANTS ON MATERIALS
14. GENERAL SUMMARY AND CONCLUSIONS
15. RECOMMENDATIONS FOR FUTURE RESEARCH

Chapter 1

EXECUTIVE SUMMARY

In the early 1950's, it was reported by Haagen-Smit[1] that many of the characteristics of photochemical smog could be explained by the presence of ozone and other photochemical oxidants. These substances, he believed, were formed in the atmosphere as a result of chemical reactions involving nitrogen oxides and hydrocarbons present in automobile exhaust. Significant quantities of nitrogen oxides were also emitted by power plants.

Considerable time elapsed before there was general acceptance of Haagen-Smit's important discovery, in part because of its subtle nature. For the first time, a major air pollution problem was demonstrated to be caused by a pollutant generated in the atmosphere. Its effect often did not become apparent until many miles downwind from the source. (The same suspicion has been attached to sulfate-containing aerosols for many years, but the proof that the sulfate is damaging is not as well established.) In addition, a new pollution source, automobile exhaust, had been shown to be of prime importance.

After the pioneering studies of Haagen-Smit, an extensive scientific literature developed on the properties, measurement, and effects of photochemical smog. The attempt to control engine emission has had a profound effect on the automobile and petroleum industries. Estimated costs and associated benefits of automobile emission control each run into the billions per year.[2]

By the Clean Air Act Amendment of 1970, Congress set automobile emission standards and instructed the Environmental Protection Agency (EPA) to set ambient air quality standards. Included in the Act was a requirement to review the standards periodically. It is hoped that this report will be of value to both Congress and the EPA in discharging their responsibilities for the review of these standards.

However, the Subcommittee on Ozone and Other Photochemical Oxidants did not discuss—and does not necessarily endorse—the adoption of fixed federal standards as the prime approach to pollution control. The Subcommittee also did not attempt to determine the concentration at which the standard should be set, except to recognize the difficulty of arriving at such a number. There was, however, general skepticism concerning the applicability of the concept of the threshold concentration - the concentration below which there are no biologic effects.

This report deals primarily with the origins and effects of ozone and other photochemical oxidants. It is limited, more or less, to the problem of urban pollution and to such closely related topics as natural background in the earth's boundary layer. No consideration is given to the stratospheric ozone layer and the effects produced by SST* emissions or halocarbons.

The reference method recommended by the federal government for the determination of oxidant measures ozone, which serves as an indicator of photochemical smog. Other agents formed in the photochemical system include a variety of free radicals in the gas phase and sulfates, nitrates, and oxygenated organic compounds in the particulate phase. A measurement of ozone, alone, provides only limited information on the concentrations of the other agents, because of the complex chemical and mixing processes involved. How these other agents form and what their effects are remain poorly understood. Recommendations on studies involving such agents will be found throughout the report.

---

*Supersonic Transport

We still lack an adequate dose-response relationship for humans exposed to ozone, particularly at concentrations less than about 0.2 ppm. The data base for the development of such a relationship for both short- and long-term exposures is inadequate. Although some data from controlled studies are available for concentrations above 0.3 ppm, methods for extrapolating to lower concentrations are needed. Moreover, it is not clear how to weight the results of pulmonary function tests on humans, animal studies, and epidemiologic studies in a general dose-response relationship.

Despite uncertainties concerning the causative agents and their effects, we must proceed with the regulation of emissions that lead to the formation of photochemical smog. At the same time, research should continue on identifying the individual harmful agents in photochemical smog and their effects. Otherwise, there is danger of focusing on an indicator (ozone) while the formation and behavior of associated pollutants, which create a major part of the problem, are not adequately understood.

Roughly speaking, the first third of this report is concerned with the origins and measurement of ozone and other photochemical oxidants and the relationship of atmospheric concentrations to emissions. The middle third deals with toxicologic studies and effects on humans, and the last with effects on plants, ecosystems, and materials.

Each chapter is accompanied by a summary and/or a set of recommendations prepared by the individual author. Some of the most important points have been identified in the Executive Summary, particularly those which cut across several fields. In some cases, the recommendations have been abstracted directly from the other chapters. For detailed recommendations, however, the reader should turn to the separate chapters.

ORIGINS AND MEASUREMENT

The extensive scientific literature covering the chemistry of smog reactions is reviewed in Chapter 2. Even in the case of a single hydrocarbon with typical concentrations of the oxides of nitrogen, carbon monoxide, water vapor, and other trace components, several hundred chemical reactions take place. The urban atmosphere contains not just one but hundreds of different hydrocarbons, each with its own reactivity and oxidation products. Most of the reaction mechanisms and rate constants needed to construct realistic models of polluted atmospheres have been determined in laboratory studies under carefully controlled conditions. Serious gaps remain in the present models, and further fundamental research on kinetics and mechanisms is necessary. For example, rate constants are needed for almost all the reactions of hydroperoxy and alkylperoxy radicals. The homogeneous and heterogeneous reactions of the oxides of nitrogen with water also need study.

Smog-chamber studies are needed for validating both detailed chemical models and lumped models. Measurements of more products and the reactive intermediates, including such free radicals as hydroxyl and hydroperoxy, will provide more stringent tests for models. There are useful interactions among modeling studies, smog-chamber experiments, atmospheric measurements, and fundamental chemical kinetics; it is not possible to ignore one without hindering progress in the others.

The possibility that free radicals, particularly hydroperoxy, have significant effects on biologic surfaces should be investigated.

The available information on aerosol formation in photochemical smog is reviewed in Chapter 3. The story told there is still not complete, but there is evidence that reactions involving ozone contribute significantly to the formation of both the organic and sulfate-containing components of the aerosol. Laboratory studies show that both cyclic olefins and C_{6+} diolefins are efficient aerosol precursors that lead to the formation of difunctional oxygenated organic compounds (such as dicarboxylic acids) of low vapor pressure. These compounds have also been found in the smog aerosol. Cyclic olefins have been identified in both gasoline and auto exhaust and might be an important source of secondary aerosol organics; there are no known sources of diolefins. The role of aromatics as aerosol precursors is not understood.

Aerosol organics in the atmosphere could be reduced by control of emission of nitrogen oxides and total hydrocarbons. However, the identification and control of a few specific aerosol precursors in gasoline and other sources might prove a more efficient approach.

Our knowledge of the chemical and physical processes that govern aerosol formation in the atmosphere is limited, and further research in the field is badly needed. Attention should be focused on laboratory studies of aerosol formation from aromatic hydrocarbons. The concentrations of aerosol precursors in the atmosphere should be determined; more data on organic compounds in ambient aerosols are needed to estimate the relative importance of olefinic and aromatic hydrocarbons as aerosol precursors.

The health effects of difunctional oxygenated organic compounds should be investigated in both animal and human studies.

A critical question concerning atmospheric concentrations of ozone and other photochemical oxidants is: "What fraction of the observed values in each locale can be controlled by reduction of emissions?" Some contend that natural background concentrations exceed the federal ambient air quality standard (0.08). Another point of view is that background ozone concentrations rarely exceed about 0.05 - 0.06 ppm at the surface and that higher concentrations are caused by man-made sources.

The data reviewed in Chapter 4 support the second point of view. Measurements in remote areas of the Northern Hemisphere, when compared with those in the lower 48 states of the United States, support the contention that man-made sources are involved in cases where the standard is exceeded. Further measurements are needed to establish this contention with more certainty. Some of the difficulties involved in such studies become apparent when it is noted that the effect of pollution--particularly nitric oxide emissions--is to reduce ozone concentrations locally.

Theoretical interpretation of the experimental observations will help in determining the relative roles played by stratospheric injection, plant emissions, background methane, and transport to surfaces in the natural portion of the tropospheric ozone cycle.

The most complete data on ozone and other oxidant concentrations have been obtained for the Los Angeles air basin, because of the severity of the problem there. Further measurements are needed in the central and eastern areas of the United States, to broaden the foundations of a national control strategy. Such studies should be designed with specific goals in mind, and not carried out as routine monitoring exercises.

Rational air pollution control strategies require the establishment of reliable relationships between air quality and emissions.(Chapter 5). Diffusion models for inert (nonreacting) agents have long been used in air pollution control and in the study of air pollution effects. Major advances have been made in incorporating the complex chemical reaction schemes of photochemical smog in diffusion models for air basins. In addition to these deterministic models, statistical relationships that are based on aerometric data and that relate oxidant concentrations to emission measurements have been determined.

Improvements in deterministic (photochemical/diffusion) methods are based largely on accounting for more physicochemical effects in the structure of the model. Specific research subjects for improved models include photochemical aerosol formation and the effects of turbulence on chemical reaction rates. The challenge to the researcher is to incorporate the study of these subjects without needlessly complicating already complex models. How accurate a mathematical simulation is required? What, roughly, will be the effect of omitting some particular chemical or physical component? What is the sensitivity of model outputs to inaccuracies in the inputs?

One of the most important contributions of research in this field will be the development of criteria to define the limits of applicability of existing models, rather than a single supermodel that will incorporate all effects.

Specific goals are essential in model development and in data collection for model-testing. Examples of goals are the determination of oxidant isopleths and the relating of visibility degradation to emission sources. Monitoring programs should be designed with specific goals of data analysis or modeling. It should not be expected that from the data alone useful information will emerge directly or that someone else will spontaneously dig out the important results. Two important steps that can be undertaken by those who produce models to encourage application and aid the user are the compilation of a catalog of air quality models that describes their capabilities in terms of a common set of performance standards and the improvement of model output to permit easy access by the user.

Methods of measuring the components of photochemical smog are reviewed in Chapter 6. There have been significant advances in the calibration of instruments for monitoring ozone in ambient air. A method based on the absorption of ultraviolet radiation at 254 nm has been adopted by California for the calibration of air monitoring instruments. The method is based on the use of a commerically available instrument that measures ultraviolet absorption as a transfer standard in the calibration process.

It is important to separate, conceptually and in practice, the calibration process from the monitoring process. Photochemical oxidants consisting primarily of ozone were continuously monitored first in southern California by measuring the color change of potassium iodide solutions brought into contact with ambient air. This measurement continues to yield valid photochemical oxidant data in California. However, it has yielded questionable data at ambient air monitoring sites elsewhere in the United States. For this reason, at the end of 1971, the EPA adopted a continuous monitoring process that involves the measurement of the chemiluminescence produced when ozone in air is brought into contact with ethylene. When it is calibrated with the ultraviolet-absorption method, this reference procedure for monitoring ozone in ambient air is widely accepted. The evaluation of nationally applicable primary calibration procedures for ozone measurement should continue.

Instruments based on differential ultraviolet absorption still need to be evaluated, and possibly modified, before their acceptance for monitoring ozone in polluted atmospheres on a nationwide scale. The California Air Resources Board and other air pollution control agencies are evaluating ultraviolet absorption side-by-side with chemiluminescence and potassium iodide instruments.

There is no commercially available instrument for the continuous monitoring of any of the chemical species present in the particulate component of photochemical smog. Methods should be developed for the direct and continuous measurement of such species. Species of interest include sulfates, nitrates, some oxygenated organic compounds, and lead.

HEALTH EFFECTS

A great deal is known about the deposition of aerosol particles in the lung and their later clearance. Less is known about the uptake of gases such as ozone and other oxidants that can react with biopolymers in the mucous and tissue layers. Such information is important in understanding the site and mechanism of pollutant gas action in humans and the effects of copollutants like nitrogen dioxide and ozone, and in the extrapolation of dose-response data from animals to humans. What has been done in this field is reviewed in Chapter 7, which also discusses the information necessary for improved understanding of the transport process.

The solubility of the gas is important. For example, experimental data from studies carried out with dogs show that nearly 100% of highly soluble sulfur dioxide inhaled through the nose is removed before reaching the first bifurcation in the lung, whereas 27-70% (depending on initial concentration) of ozone, which is less soluble in water, is removed in the same region. In addition to solubility, chemical reactions in the surface layers are of great importance.

A concerted effort is needed to increase our understanding of the transfer and uptake of reactive gases in the lung. A program in this field should involve in vitro model studies, animal experiments, and clinical studies. More information is required on the chemical, physical, and morphologic properties of the mucous layer and the kinetics of the reactions of ozone in the mucous and tissue layers. Experimental data on uptake and dosage for ozone and other oxidants are difficult to obtain for the tracheobronchial and pulmonary regions. Such data for animals and humans will be needed to test the present simple transport models, before further refinements are made.

Toxicologic research (Chapter 8) on the effects of ozone in laboratory animals has demonstrated that exposure to airborne ozone at less than 1 ppm for a few hours produces numerous changes in cell and organ structure and function. The lowest concentrations that produce these changes differ somewhat among different species of laboratory animals and with the effect under observation. However, several functional and morphologic indexes of response to ozone are altered with exposures to concentrations of about 0.2 - 0.5 ppm over periods ranging from a few minutes to several weeks.

Recent studies involving repeated or prolonged exposures of laboratory animals to ozone have suggested that changes indicative of chronic lung disease (such as decreased elasticity of the lungs) also require concentrations of 0.2 - 0.5 ppm.

Exposures to ozone for a few hours result in a marked increase in the susceptibility of animals to controlled doses of infectious organisms introduced into the lung. This is the most sensitive test of any yet reported; significantly increased susceptibility of mice to one microorganism occurred after exposure to ozone at a concentration as low as 0.08 ppm. Other reports with different microorganisms or different species have suggested that somewhat higher concentrations are required. These findings suggest the need for carefully planned epidemiologic studies on the incidence of lung infection in human populations exposed to oxidant air pollution. How do such studies relate to reported cases of human adaptation to long-term oxidant exposure?

Extrapulmonary effects have also been observed in laboratory animals at concentrations of about 0.2 ppm. These include reduced voluntary activity, chromosomal aberrations in circulating lymphocytes of hamsters, increased neonatal mortality, and greater incidence of jaw abnormalities in offspring of mice exposed to ozone. The mechanisms of these effects are largely unknown. Reports of chromosomal aberrations in hamsters and of mutagenic activity of ozone in microorganisms and tissue cultures raise the question of a possible genetic or carcinogenic hazard. This should be tested experimentally and epidemiologically.

There is evidence that nutrition affects animal response to ozone. Increased susceptibility has been reported in animals deficient in vitamin E--or the converse (protection conferred by administration of vitamin E).

Convincing new information on the health effects of oxidant exposure has emerged from controlled studies on humans, from which tentative dose-response curves have been constructed. These data are reviewed in Chapter 9, with the types of experimental facilities now available for such measurements. The new data show reduced pulmonary function in healthy smokers and nonsmokers after exposure to ozone at 0.37 ppm and higher for 2 h. (The federal standard is 0.08 ppm for a 1-h exposure.) Other gases and aerosols found in an urban atmosphere were not present in these experiments.

With various tests of ventilatory function, it has been shown that healthy male college students experienced no effect of sulfur dioxide at 0.37 ppm, a 10% decline in function with ozone at 0.37 ppm, and a 20-40% decline in function with a combination of sulfur dioxide at 0.37 ppm and ozone at 0.37 ppm. Other experiments have suggested an adaptation of southern Californians to chronic exposure to ambient ozone.

Further studies are needed to give better dose-response information, and to provide a frequency distribution of the population response to oxidants alone and in combination with other pollutants at various concentrations. Such studies should include the effects of mixed pollutants over ranges corresponding to the ambient atmosphere. The mixtures should be carefully characterized to be sure of the effects of trace pollutants on sulfate aerosol formation. The design of such studies should permit extrapolation from animals to humans and from small groups of humans to populations. Further research on the possibility of human adaptation to chronic exposure to oxidants is desirable.

Safety, ethical, and legal considerations require that the utmost care be exercised in human experimentation. The risk inherent in this work can be minimized by the proper design of facilities for human exposure to reactive gases, such as ozone and sulfur dioxide, and reactive gas mixtures. Standards for the exposures of humans to such controlled atmospheres should be discussed by national groups and agencies, such as the American Medical Association, and the National Institutes of Health.

Studies of the reactions of population groups to photochemical smog are reviewed in Chapter 10. Such studies played a major role in the establishment of the current federal standards. Included were eye irritation studies, effects on asthmatics, and the responses of groups of high school athletes. Uncertainties in the design of these experiments and interpretation of the data make further epidemiologic studies essential.

Two major studies are being conducted by the EPA in Los Angeles on the effects of photochemical oxidants on health. The first is a survey of schoolchildren in seven communities representing different degrees of oxidant exposure. In addition to rather detailed environmental monitoring data, specific health characteristics will be followed, including chronic respiratory disease in adults, lower respiratory disease in children, acute respiratory disease in both children and adults, pulmonary function in children, aggravation of asthma, irritation of mucous membranes, and tissue residues of trace metals. Complete data from this study will not be available for another 5 years.

The second study is only beginning and will attempt to correlate the effects of photochemical oxidants and cigarette-smoking in promoting chronic respiratory signs and symptoms in cohorts of adolescents and their families. Pulmonary function tests will be included.

These studies are being carried out by EPA as part of the CHESS program. The results of these studies should be released as soon as possible for evaluation by the general scientific community. This will permit the design and initiation of additional studies with modifications where necessary to supplement what has been done. The continuation of epidemiologic studies, including those of the CHESS program, is vital to our understanding of the effects of air pollution on health.

Other epidemiologic studies should be designed to seek analogues in human populations of effects observed in toxicologic and clinical studies, including the results of pulmonary function tests, evidence of chronic lung disease in animals, and evidence of increased susceptibility to microbial infection.

EFFECTS ON PLANTS, ECOSYSTEMS, AND MATERIALS

The major phytotoxic components of the photochemical oxidant system, discussed in Chapter 11, are ozone and peroxyacetylnitrate (PAN), but there is indirect evidence that other phytotoxicants are present. Considerable effort has gone into controlled exposures to ozone and into field studies. Leaf stomata are the principal sites for ozone and PAN entry into plant tissue. Closed stomata will protect plants from these oxidants. Both ozone and PAN may interfere with various oxidative reactions within plant cells. Membrane sulfhydryl groups and unsaturated lipid components may be primary targets of oxidants. Young leaf tissue is more sensitive to PAN; newly expanding and maturing tissue is most sensitive to ozone. Light is required before plant tissue will respond to PAN; that is not the case with ozone.

Oxidants reduce yields of many plants, especially sensitive cultivars. Chronic exposures to concentrations between 0.05 and 0.15 ppm will reduce soybean, corn, and radish yields. The threshold appears to be between 0.05 and 0.1 ppm for some sensitive cultivars--well within values monitored in the eastern United States. Growth or flowering effects on carnation, geranium, radish, and pinto bean have been found at chronic exposures to ozone at 0.05 - 0.15 ppm. Estimated costs to consumers of agricultural losses from oxidant damage are several hundred million dollars a year.

There have been three main approaches to protecting plants from air pollution. Several researchers are including pollutant stress in standard breeding programs and thus are breeding for tolerance. Interim measures involve the use of chemical sprays. Such sprays are not now economically feasible, but they are being tested, and some are protective. Cultural and land-use practices may also be used to control pollution effects, especially on a short-term basis.

A few definitive experiments are needed to complete our knowledge of acute dose-response relationships for ozone. Research is necessary in the case of PAN and other oxidants. More important is the need for studies of crop and native species over growing seasons with chronic oxidant exposures. At the same time, additional work with field chambers, filtered or nonfiltered, is needed.

There is a critical need to understand the interaction of multiple pollutants on the plant systems. These are believed to be important, but little is known about these interactions with respect to most plants.

Although the plant membrane is considered the primary site of action for the oxidants, there is no definitive work on this. The mechanism of response and the biochemical systems affected are not understood. An understanding of these responses would be supportive of breeding and spray protective programs.

Effects on ecosystems are considered in Chapter 12. The permanent vegetation constituting natural ecosystems receives much greater chronic exposure than the short-lived vegetation that makes up the agroecosystem subject to intermittent short-term fumigations. Each situation has measurable economic and aesthetic effects, but on different time scales. The single agricultural ecologic system (the agroecosystem) has little resilience to pollutant stress; losses are sometimes immediate and occasionally catastrophic. The natural ecosystem is initially more resistant to pollutant stress because of species diversity, but the longer chronic exposures disrupt the system. Simulation models of ecosystem components are under development. The study of such models and their interaction offers the possibility of determining the long-term effects of pollutants on natural ecosystems and agroecosystems.

There is convincing evidence of large-scale damage to natural ecosystems in regions downwind from Los Angeles. The injury to the mixed-conifer stands of the San Bernadino National Forest began in the early 1940's and is well advanced. A similar problem is developing in the forests of the southern Sierra Nevada. Both direct and indirect effects have been observed on most components of the forest ecosystem, including producers, consumers and decomposers. These effects are the results of reactions in the Los Angeles urban plume, which generate oxidants as the pollutants are transported downwind. Other cities of the western United States—namely, Salt Lake City and Denver, where basin-mountain terrain is contiguous—may show similar injury to forest ecosystems as their oxidant air pollution problems grow.

The socioeconomic consequences of the continued degradation of natural ecosystems and agroecosystems should be investigated in more detail. The indirect effects on man's health and the direct effects on his welfare resulting from ecosystem deterioration by oxidant injury should be taken into account in developing air pollution control strategies. Land-use planning and airshed classification schemes may be useful in averting further deterioration.

Dose-response relations in key primary-producer species in service-important ecosystems should be examined under field conditions.

Material damage by oxidants is reviewed in Chapter 13. In test chambers with external "ozone" generators that operate at or near atmospheric pressure, ozone is the only likely oxidizing species. In ambient air, however, the presence of other oxidants and sunlight may contribute to material damage. Laboratory studies of the mechanisms and effects of oxidants other than ozone—including PAN, atomic oxygen, and some free radicals—on specific materials are needed. The concentration of these agents in the atmosphere should be determined.

The most economically important materials with respect to ozone damage are paint, elastomers (rubbers), and textile fiber-dye systems. Damage to polyethylene by ozone is considered to be negligible. The ozone damage in 1970 to materials has been estimated as follows: paint, $540 million; elastomers, $569 million; and textile fibers and dyes, $84 million—for a total of over $1 billion. Thus, the total combined material and crop damage falls between $1.5 and 2 billion per year. Estimates of damage to natural ecosystems are not available.

REFERENCES

1. Haagen-Smit, A. J. Chemistry and physiology of Los Angeles smog. Ind. Eng. Chem. 44:1342-1346, 1952.
2. National Academy of Sciences. National Academy of Engineering. Air Quality and Automobile Emission Control. A Report by the Coordinating Committee on Air Quality Studies. Vol.4. The Costs and Benefits of Automobile Emission Control. U.S. Senate Committee Print Serial No. 93-24. Washington, D.C.: U.S. Government Printing Office, 1974. 470 pp.

CHAPTER 2

CHEMICAL ORIGIN

The photochemistry of the polluted atmosphere is exceedingly complex. Even if one considers only a single hydrocarbon pollutant, with typical concentrations of nitrogen oxides, carbon monoxide, water vapor, and other trace components of air, several hundred chemical reactions are involved in a realistic assessment of the chemical evolution of such a system. The actual urban atmosphere contains not just one, but hundreds of different hydrocarbons, each with its own reactivity and oxidation products.

The atmosphere is complicated in other ways. The emission of primary pollutants occurs throughout the day and night (varying with time and location), adding to some of the previous day's well-aged pollutants. As the sun rises, the light intensity increases in a nonlinear fashion. The movement of air is important -- vertical mixing and lateral transport from one community to another. It is not practical to construct a model that includes the detailed chemistry and all these variables with present computers.

Several approaches have been used to reduce the problem to manageable proportions. The chemistry of photochemical oxidant formation can best be understood by considering laboratory experiments with one hydrocarbon (at most, two) and typical amounts of the nitrogen oxides, carbon monoxide, and water vapor. A model is developed on the basis of all the chemical reactions that are thought to be relevant, with their measured or estimated rate constants. Calculations and observations are then compared to assess the accuracy and completeness of the chemical model. Alternatively, one can reduce the chemistry to just a few generalized or lumped reactions, and then include the temporal and spatial changes that occur as a polluted air mass moves through an urban environment. Both approaches provide valuable insights.

This chapter offers a brief introduction to present understanding of the chemistry of photochemical oxidant formation (thorough reviews are available elsewhere [1-5, 5a]), some comments on the state of knowledge of the chemistry of the polluted atmosphere, a review of some recent developments in instrumentation that promise to increase understanding of atmospheric chemistry.

BASIC CHEMISTRY OF OXIDANT FORMATION

Brief Review

This section covers some of the more important chemical reactions that occur in the polluted atmosphere and attempts to show how these reactions result in photochemical oxidant formation. For a more thorough understanding of the chemistry involved, the reader should consult several of the recent reviews[1-4,5a] and computer modeling studies by Demerjian, Kerr, and Calvert[5] and by Calvert and McQuigg.[6] Unless otherwise noted, the mechanisms and rate constants of these modeling studies are used in this discussion.

Three properties of photochemical smog were evident first in Los Angeles: eye irritation; haze (aerosol) formation; and the degradation of rubber products. All three are associated with oxidants, although aerosols can also be formed by other pollutants, particularly sulfur dioxide.

The photochemical oxidants that are observed in the atmosphere are ozone, O_3; nitrogen dioxide, NO_2; and peroxyacetylnitrate (PAN). Several other substances, such as hydrogen peroxide, H_2O_2, may be classified as photochemical oxidants, but their common presence in smog is not well established. The oxidants are secondary pollutants; i.e., they are formed as a result of chemical reactions in the atmosphere. Primary pollutants are those emitted directly by pollution sources.

The classes of major primary pollutants that are important in urban areas are listed in Table 2-1. The pollutants most responsible for oxidant formation in the air are the nitrogen oxides, hydrocarbons, aldehydes, and carbon monoxide. The internal-combustion engine is a major source of emission of these primary pollutants, although many stationary sources, such as electric power generating plants, also contribute heavily to emission of nitrogen oxides.[7]

TABLE 2-1

Some Primary Pollutants Involved in Photochemical Oxidant Formation

Hydrocarbons:

- Alkanes: n-butane, isopentane, isooctane
- Cycloalkanes: cyclohexane, methylcyclopentane
- Olefins (sometimes called "alkenes"): ethylene, propylene, butene
- Cycloolefins: cyclohexene
- Alkynes: acetylene
- Aromatics: toluene, xylene

Chlorinated hydrocarbons

Aldehydes, RCHO[a]: Formaldehyde, acetaldehyde

Ketones, RCOR[a]: Acetone, methylethylketone

Nitric oxide, NO[b]

Carbon monoxide, CO

Sulfur dioxide, SO_2

---

[a] R = a hydrocarbon group, such as methyl, CH_3, or benzyl, C_6H_5.

[b] "NO_x" is often used to indicate "oxides of nitrogen." In practice, this usually means the sum, NO + NO_2, although it should include such other forms as NO_3, N_2O_5, and HNO_3. Nitrous oxide, N_2O, is relatively inert in the lower atmosphere and is not included in the term "NO_x."

The amount of oxidant formed in the atmosphere has a complex dependence on time of day, meteorologic conditions, and amounts of the various primary pollutants. A typical time dependence for a smoggy day in Los Angeles is shown in Figure 2-1. Early in the morning the concentration of ozone is very low. As the day progresses, the ozone increases. The complementary behavior of nitric oxide and nitrogen dioxide is of major importance here. The rapid increase in nitric oxide is the result of the morning rush-hour traffic. The nitric oxide concentration then falls, even though automobile emission is still strong, and nitrogen dioxide begins to increase. As the nitrogen dioxide concentration increases, so does that of ozone.

It should be noted that the concentrations shown in Figure 2-1 represent averaged hourly values. Recent continuous monitoring of nitrogen dioxide at one site shows a more complex time dependence, seen in Figure 2-2. These rapid fluctuations in concentration within a few minutes are probably the result of the movement of air masses and varying emission from local sources.[8] Figure 2-2 underlines the importance of air transport and variable emission, as well as of chemical changes, in the modeling of concentration at a single monitoring station.

The time dependence of the oxidant concentration shown in Figure 2-1 can be mimicked in laboratory studies. The results of a typical smog-chamber experiment are shown in Figure 2-3. A sample of air initially containing propylene at 2.2 ppm and nitric oxide at 1.0 ppm is irradiated starting at time zero. Although the hydrocarbon begins to disappear almost immediately, ozone does not develop until almost all the nitric oxide has been converted to nitrogen dioxide. This relationship between nitric oxide, nitrogen dioxide, and ozone is of central importance in attempts to under-

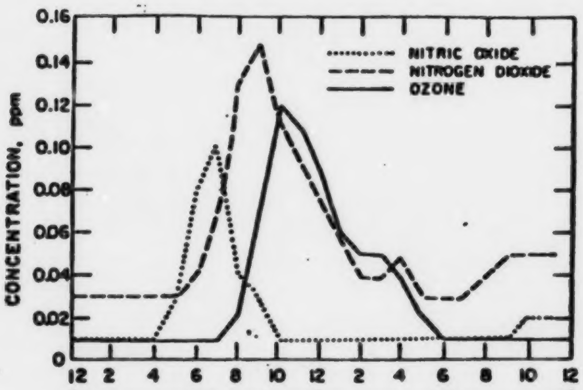

FIGURE 2-1. Diurnal variation of nitric oxide, nitrogen dioxide, and ozone concentrations in Los Angeles. July 19, 1965.
(Reprinted from Air Quality Criteria for Photochemical Oxidants.[19])

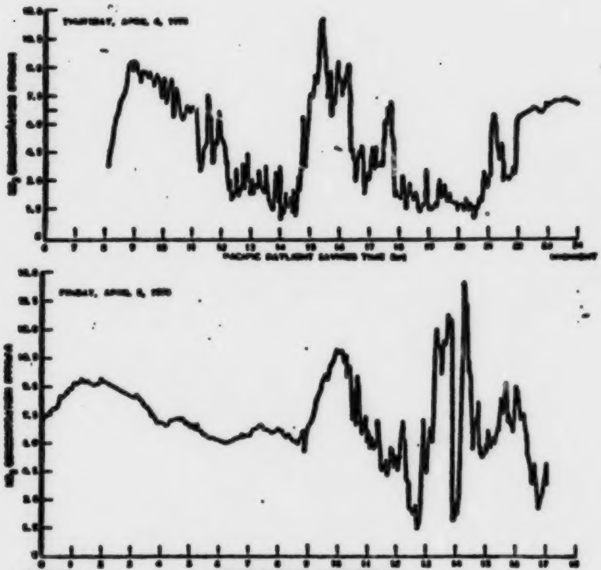

FIGURE 2-2. Atmospheric nitrogen dioxide concentrations, El Segundo, California, April 4-5, 1974. (Reprinted with permission from Tucker *et al.*[8])

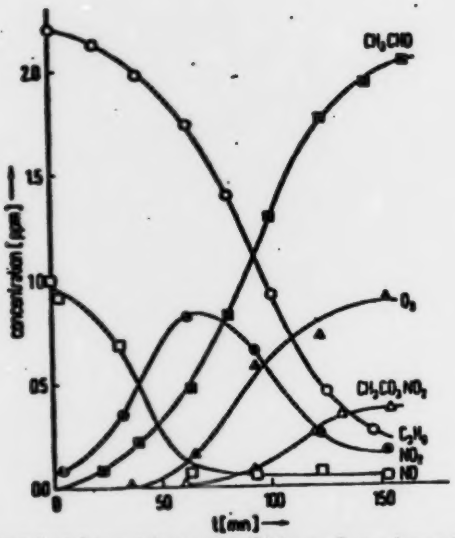

FIGURE 2-3. Typical concentration-time profiles for irradiation of a propylene-NO$_x$ mixture in a smog chamber. (Reprinted with permission from Niki *et al.*[20])

stand the chemistry of these systems. Note also in Figure 2-3 the development of PAN, $CH_3CO_3NO_2$.

Laboratory experiments of this type have the great advantage that the initial conditions can be well defined (although often they are not[5]), in contrast with the average sample of urban air, which is a mixture of new and old pollutants. Also, in laboratory experiments, the same sample of air is observed over a long period, which is not possible with most air pollution monitoring networks. For these reasons, most attempts to understand the chemistry of oxidant formation have concentrated on smog-chamber experiments, rather than the real atmosphere.

The major oxidant in smog is ozone, and early research efforts concentrated on the mechanism of its formation. Attention was focused on the nitrogen oxides, specifically nitrogen dioxide, because it was known that the nitrogen dioxide molecule could absorb blue and near-ultraviolet sunlight and break apart (undergo photolysis):

$$NO_2 + \text{light}(\lambda \leq 430\text{ nm}) \rightarrow O + NO. \qquad (1)$$

In the lower atmosphere, the oxygen atoms react quickly with molecular oxygen to form ozone:

$$O + O_2 + M \rightarrow O_3 + M. \qquad (2)$$

Equation 2 is actually a three-body process, in that another molecule (M), usually nitrogen or oxygen, is necessary to carry off the energy released in the newly formed bond. These two reactions then form a mechanism for ozone formation in the atmosphere. They would not be complete without the additional reaction,

$$NO + O_3 \rightarrow NO_2 + O_2 \qquad (3)$$

which is known to be fast. Because Eq. 3 consumes the molecule of ozone that was formed in Eq. 2 and regenerates the molecule of nitrogen dioxide that was photolyzed in Eq. 1, the three reactions form a cycle, which is shown schematically in Figure 2-4. The net result of this cycle is that the absorbed sunlight is degraded into thermal energy. Several other minor reactions occur in this system, but they will not be discussed here (see page 17 of reference 5).

Equations 1-3 show the most common chemical reactions that occur in the polluted atmosphere. That is because nitrogen dioxide is the strongest absorber of sunlight. At a latitude of 40°, the typical turnover lifetime for nitrogen dioxide is about 1.4 min. This means that, on the average, half the nitrogen dioxide molecules are photodisssociated in Eq. 1 and reformed in Eq. 3 every 1.4 min. No other molecule in smog is so active.

An important consequence of this rapid turnover is the establishment of a steady-state concentration of ozone. One can express this dynamic equilibrium as follows:

$$[O_3] = \frac{k_1 \; [NO_2]}{k_3 \; [NO]}, \qquad (4)$$

where k_1 is the rate at which sunlight dissociates nitrogen dioxide, k_3 is the rate constant for Eq. 3, and the brackets indicate concentrations. With a typical value for k_1 (8×10^{-3}/s) and the known rate constant for Eq. 3, Eq. 4 becomes:

$$[O_3] = (0.021 \text{ ppm}) \; \frac{[NO_2]}{[NO]}. \qquad (5)$$

Modeling studies show that Eq. 4 should be obeyed quite closely.[5] Tests of this equation on atmospheric data show good agreement, at least for ozone concentrations of 0.1 ppm or less.[64,65] At higher ozone concentrations, deviations have been observed, although it was suggested that

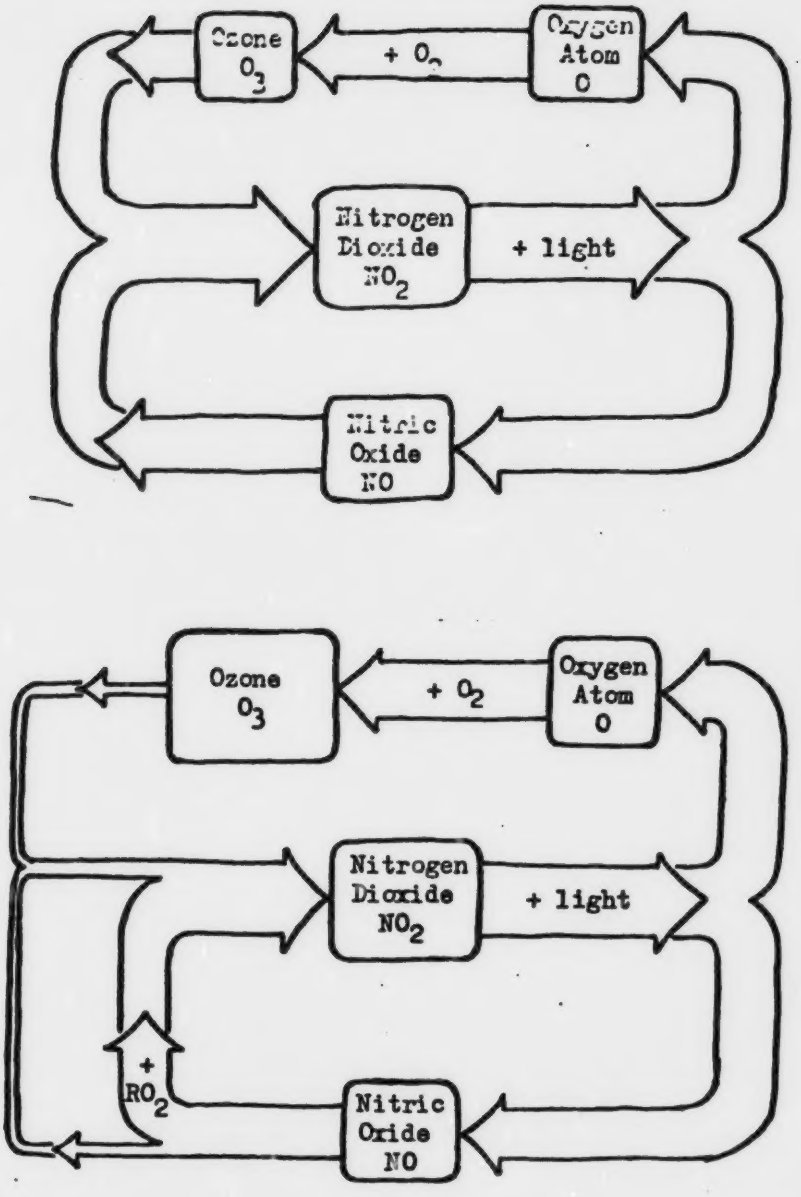
Ozone O_3
+ O_2
Oxygen Atom O
Nitrogen Dioxide NO_2
+ light
Nitric Oxide NO
Ozone O_3
+ O_2
Oxygen Atom O
Nitrogen Dioxide NO_2
+ light
+ RO_2
Nitric Oxide NO

FIGURE 2-4. The NO-NO_2-O_3 cycle in air contaminated with NO_x only (above) and with NO_x and hydrocarbons (below). Above, the dissociation of nitrogen dioxide by sunlight forms equal numbers of nitric oxide molecules and oxygen atoms. The latter are rapidly converted to ozone molecules. The ozone then reacts with the nitric oxide, again on a 1:1 basis, to reform nitrogen dioxide. Only a small steady-state concentration of ozone results from this cycle. Below, when hydrocarbons, aldehydes, or other reactive contaminants are present, they can form peroxy radicals that oxidize the nitric oxide, pumping it directly to nitrogen dioxide. This leaves very little of the nitric oxide to react with the ozone, so the ozone builds up to large concentrations.

the method of averaging was responsible, rather than a real failure of Eq. 4.[65]

Equation 4 does appear to explain, at least qualitatively, the time dependence of the ozone concentration. For example, as long as the ratio $[NO_2]$: $[NO]$ is less than 1:1 in Figure 2-3, the ozone concentration is very low. However, when most of the nitric oxide has been converted to nitrogen dioxide, the ozone concentration increases rapidly. Similar behavior is observed in the Los Angeles atmosphere (Figure 2-1).

Although of central importance in smog chemistry, Eqs. 1-3 cannot by themselves explain the buildup of ozone. If only these three reactions were important, the photodissociation of nitrogen dioxide would rapidly establish a small ozone concentration within a few minutes, after which no further changes would occur. During this ozone buildup, the nitrogen dioxide concentration would only decrease. Contrast this behavior with the observations in Figures 2-1 and 2-3. The actual ozone buildup occurs over a period of hours and is accompanied by an increase in the nitrogen dioxide concentration. Thus, the photolysis of nitrogen dioxide alone cannot explain the ozone buildup, even though it is the mechanism of ozone formation. The dominant factor in these systems is the ratio of nitrogen dioxide to nitric oxide. The challenge, then, is to explain the conversion of nitric oxide to nitrogen dioxide. Once that is done, the ozone concentration will follow the $[NO_2]$: $[NO]$ ratio.

Another difficulty was apparent in the early chemical studies on polluted air.[8/] It was known from laboratory studies that both ozone and the ground-state oxygen atoms that are formed in Eq. 1 would attack reactive hydrocarbons. However, the experimentally observed rate of loss of the hydrocarbons was often greater than could be explained by the attack of ozone and oxygen atoms. Figure 2-5 shows this effect for the case of propylene. Note that the discrepancy is especially large in the earlier parts of the reaction.

Some new mechanism was required to explain the rapid oxidation of nitric oxide to nitrogen dioxide; and one or more reactive intermediates, in addition to ozone and oxygen atoms, were needed to explain the observed hydrocarbon loss rates. Several people suspected that these two problems were connected to some free-radical chain mechanism. Many reactive intermediates were suggested, including the hydroxyl radical, OH; the hydroperoxy radical, HO_2; the methoxy radical, CH_3O; nitrogen trioxide, NO_3; and "singlet oxygen" (meaning O_2 in one of its low-lying metastable states, $a^1\Delta$ or $b^1\Sigma$).

About 1970, two research groups suggested that hydroxyl radicals (OH) were the solution to the above problems.[9,10] They suggested the following reaction cycle:

$$OH + CO \rightarrow H + CO_2, \quad (6)$$

$$H + O_2 + M \rightarrow HO_2 + M; \quad (7)$$

$$HO_2 + NO \rightarrow OH + NO_2. \quad (8)$$

Equation 6 is sufficiently fast to be important in the atmosphere. For a carbon monoxide concentration of 5 ppm, the average lifetime of a hydroxyl radical is about 0.01 s, owing to Eq. 6 (other reactions may decrease the lifetime even further). Equation 7 is a three-body recombination and is known to be fast at atmospheric pressures. The rate constant for Eq. 8 is not well established, although several experimental studies support its occurence.[11-13,13b] On the basis of the most recently reported value for the rate constant of Eq. 8, which is an indirect determination,[13a] the average lifetime of a hydroperoxy radical is about 2 s for a nitric oxide concentration of 0.05 ppm. Equation 8 is the pivotal reaction for this cycle, and it deserves more direct experimental study.

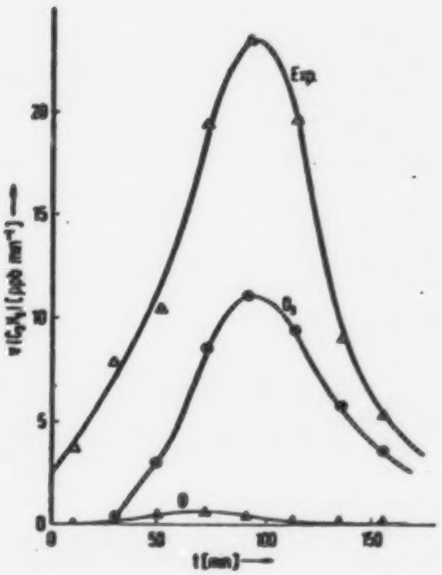

FIGURE 2-5. Comparison of the experimentally observed rate of propylene loss with that calculated for its reactions with ozone and oxygen atoms. (Reprinted with permission from Niki _et_ _al_.[20]).

Equations 6-8 form a catalytic cycle, in that the hydroxyl radical that is used in Eq. 6 is regenerated in Eq. 8. The net results of this cycle are the oxidations of nitric oxide to nitrogen dioxide and carbon monoxide to carbon dioxide by the oxygen present in the air.

Other oxidation chains can be constructed. For example, when methyl radicals are generated by other reactions, as in the ozonolysis of olefins, then the following reactions can occur:

$$CH_3 + O_2 + M \rightarrow CH_3O_2 + M, \tag{9}$$

$$CH_3O_2 + NO \rightarrow CH_3O + NO_2, \tag{10}$$

$$CH_3O + O_2 \rightarrow CH_2O + HO_2. \tag{11}$$

The methyl radical rapidly (in 10^{-7} s) combines with oxygen to form the methylperoxy radical, CH_3O_2. A recent study has confirmed that nitric oxide is oxidized by methylperoxy, although the rate constant is still unknown.[14] The methoxy radical, CH_3O, should then react predominantly with oxygen to form formaldehyde, CH_2O, and hydroperoxy radical. The net result of this sequence is the oxidation of one molecule of nitric oxide to nitrogen dioxide and the conversion of an alkyl radical into a hydroperoxy radical, which can then react as in Eq. 8. Similar sequences can be written for larger alkyl radicals.

There were two important innovations in the development of these oxidative cycles: the use of carbon monoxide, which had previously been considered a relatively inert molecule in the atmosphere, to regenerate the hydroperoxy radical via Eqs. 6 and 7; and the use of peroxy radicals, HO_2 and RO_2, to oxidize nitric oxide to nitrogen dioxide.

These oxidative cycles have a drastic effect on the concentration of ozone, as is summarized in Figure 2-4. The peroxy radicals oxidize the nitric oxide back to nitrogen dioxide, increasing the ratio $[NO_2]:[NO]$ and, as a result of Eq. 5, the concentration of ozone. Expressed in words, the photolysis of nitrogen dioxide continues to generate ozone, but the balancing reaction of ozone with nitric oxide becomes less probable, because most of the nitric oxide is reacting with peroxy radicals. As a result, more ozone is being formed than is being destroyed, and so its concentration increases. It is this interaction of the $NO-NO_2-O_3$ cycle with the free radicals generated from hydrocarbons and other reactive pollutants that is the basis of photochemical oxidant formation.

The participation of hydroxyl and hydroperoxy radicals in the oxidation of nitric oxide raises the possibility that these radicals might also attack hydrocarbons. In the case of hydroxyl, these reactions are known to be fairly rapid. On the basis of the rate constants that have been measured and estimates of those which have not, the rates of attack of hydroxyl and hydroperoxy radicals appear to be large enough to explain the excess consumption of propylene shown in Figure 2-5.

A detailed chemical model has been constructed with these free-radical chain reactions and all the other reactions that are thought to be important in the atmosphere. It is possible to evaluate quantitatively the various reactions that destroy the olefin and to determine which intermediates are most important. Figure 2-6 shows the results of such a summation for a mixture of trans-2-butene, NO_x, and aldehydes.[6] The vertical distances between lines on Figure 2-6 are proportional to the various rates of attack. The graph shows that destruction of olefin by hydroxyl radical is a major process, although attack by ozone, hydroperoxy radical and oxygen atoms is also significant. Olefin attack by other intermediates, such as nitrogen trioxide and methoxy radical, are less significant, but not insignificant.

Taking propylene as a typical example, the reactions with hydroxyl radical would be:

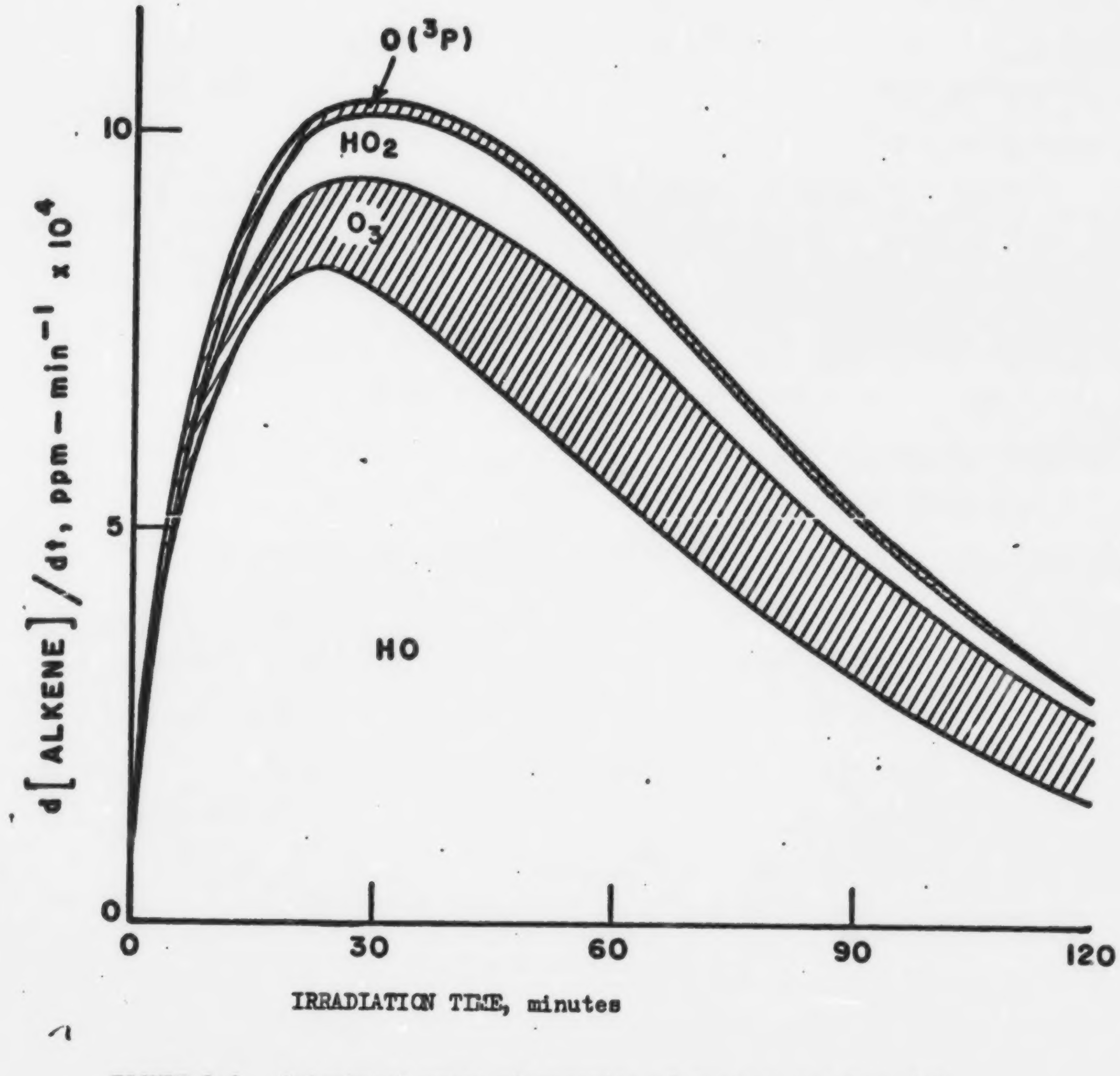

FIGURE 2-6. Calculated rates of reaction of various species with trans-2-butene as a function of irradiation time. The initial conditions are as specified in Table 2-2, except that the aldehydes are not initially present. (Reprinted with permission from Calvert and McQuigg.[6]).

$$\cdot OH + C_3H_6 \rightarrow .CH_2CHCH_2 + H_2O, \qquad (12)$$

$$\cdot OH + C_3H_6 \rightarrow CH_3\dot{C}HCH_2OH, \qquad (13)$$

where the dots on the free radicals indicate the dominant positions of the unpaired electrons. Evidence of both abstraction reactions, such as Eq. 12, and addition reactions, such as Eq. 13, has been obtained recently.[15] The relative importance of addition and abstraction will depend on the structure of the olefin; these numbers are not well established.

Each of the radicals formed in Eqs. 12 and 13 will react with molecular oxygen to form a peroxy radical,

$$R\cdot + O_2 \rightarrow RO_2^{\bullet}, \qquad (14)$$

which can then oxidize nitric oxide:

$$RO_2\cdot + NO \rightarrow RO\cdot + NO_2. \qquad (15)$$

The RO· formed in Eq. 15 is still a free radical, so it will react further.

Most free radicals contain odd numbers of electrons, and most stable molecules contain even numbers of electrons (nitric oxide and nitrogen dioxide are two important exceptions, being stable molecules with odd numbers of electrons). Therefore, in the reaction, free radical + stable molecule →, another free radical is usually generated. This free-radical chain process is stopped only when one of the following types of processes occurs.

Radical-radical reactions, e.g.,

$$H\dot{O}_2 + H\dot{O}_2 \rightarrow H_2O_2 + O_2, \qquad (16)$$

$$CH_3\dot{O}_2 + H\dot{O}_2 \rightarrow CH_3O_2H + O_2. \qquad (17)$$

Radical-NO_x reactions, e.g.,

$$H\dot{O}_2 + NO_2 \rightarrow HONO + O_2 \text{ (or } HOONO_2 \text{ ?)}, \qquad (18)$$

$$CH_3CO\dot{O}_2 + NO_2 \rightarrow CH_3COO_2NO_2 \text{ (PAN)}. \qquad (19)$$

Radical-surface reaction, e.g.,

$$\dot{H}O_2 + \text{surface} \rightarrow \text{absorbed radical}. \qquad (20)$$

The rate constants for these chain-terminating steps are not well established. However, present estimates are probably not greatly in error because radical-radical reactions tend to be fast.

What is the initial source of the free radicals that are so important for oxidant development? Calvert and McQuigg[6] attempted to answer this question by evaluating the many proposed reactions with their detailed chemical model. Although the actual importance of any particular source will depend on the concentration of pollutants assumed and the time of irradiation, they found for a typical mixture (nitric oxide, nitrogen dioxide, trans-2-butene, formaldehyde, acetaldehyde, carbon monoxide, water, and methane) that the following reactions were the most important radical sources:

$$\text{HONO} + \text{sunlight} \rightarrow \text{OH} + \text{NO}, \qquad (21)$$

$$CH_2O + \text{sunlight} \rightarrow \text{CHO} + \text{H}, \qquad (22)$$

$$CH_3CHO + \text{sunlight} \rightarrow CH_3 + \text{CHO}, \qquad (23)$$

$$O_3 + C_4H_8 \rightarrow \text{various radicals}. \qquad (24)$$

Of special interest here is the radical generation during the early part of the irradiation, before the oxidant concentration has developed; photodissociation of nitrous acid, HONO, and aldehydes is very important. The concentration of nitrous acid in the atmosphere due to the reaction,

$$\text{NO} + NO_2 + H_2O \rightarrow 2\text{HONO}, \qquad (25)$$

is controversial,[16] but the presence of aldehydes in the urban atmosphere is not. It is established that aldehydes will absorb sunlight and dissociate into free radicals. The mechanism of the reaction of ozone with olefins in the gas phase appears to be very complicated, but recent experimental evidence shows that some free radicals are formed.[17]

Although the above reactions generate a few free radicals, most of the oxidation of nitric oxide to nitrogen dioxide is carried out by the alkylperoxy, RO_2, and hydroperoxy radicals that are formed in later reactions involving reactive hydrocarbons, aldehydes, or even carbon monoxide. One such example is shown in Figure 2-7. There is still considerable uncertainty as to the mechanism of these secondary reactions. The modeling studies should be consulted for details.[5,6]

The importance of the secondary reactions can be expressed as a radical chain length, which is the total rate of all reactions involving a particular radical divided by the primary rate of formation of that radical. For a particular set of conditions chosen in the modeling studies, chain lengths of about 4 for the hydroperoxy radical and about 8 for the alkylperoxy and hydroxyl radicals were calculated early in the irradiation period.[6] After further irradiation, the chains became shorter.

The oxidizable pollutants -- such as hydrocarbons, aldehydes, and carbon monoxide -- serve the function of regenerating free radicals that will react with the oxygen in the air to form alkylperoxy and hydroperoxy. Thus, these oxidizable pollutants can be thought of as pumping the nitric oxide to nitrogen dioxide. In the process, they become degraded to other compounds, some of which are still reactive (e.g., formaldehyde, CH_2O, in Figure 2-7). The amount of pumping that can be done, and thus the amount of photochemical oxidant formed, depends on both the reactivity of the oxidizable pollutant and its concentration in a nonlinear way. As the oxidant concentration builds up, the probability of ozone's reacting with hydrocarbons and various free radicals increases, and the rate of ozone accumulation decreases.

Early attention focused on the most reactive of the hydrocarbons, the olefins, because it was expected and was observed by atmospheric sampling that they were preferentially consumed during smog formation.[18] Laboratory studies confirm that olefin-NO_x mixtures are very prolific sources of ozone. However, these olefins are not essential to oxidant formation. Both the

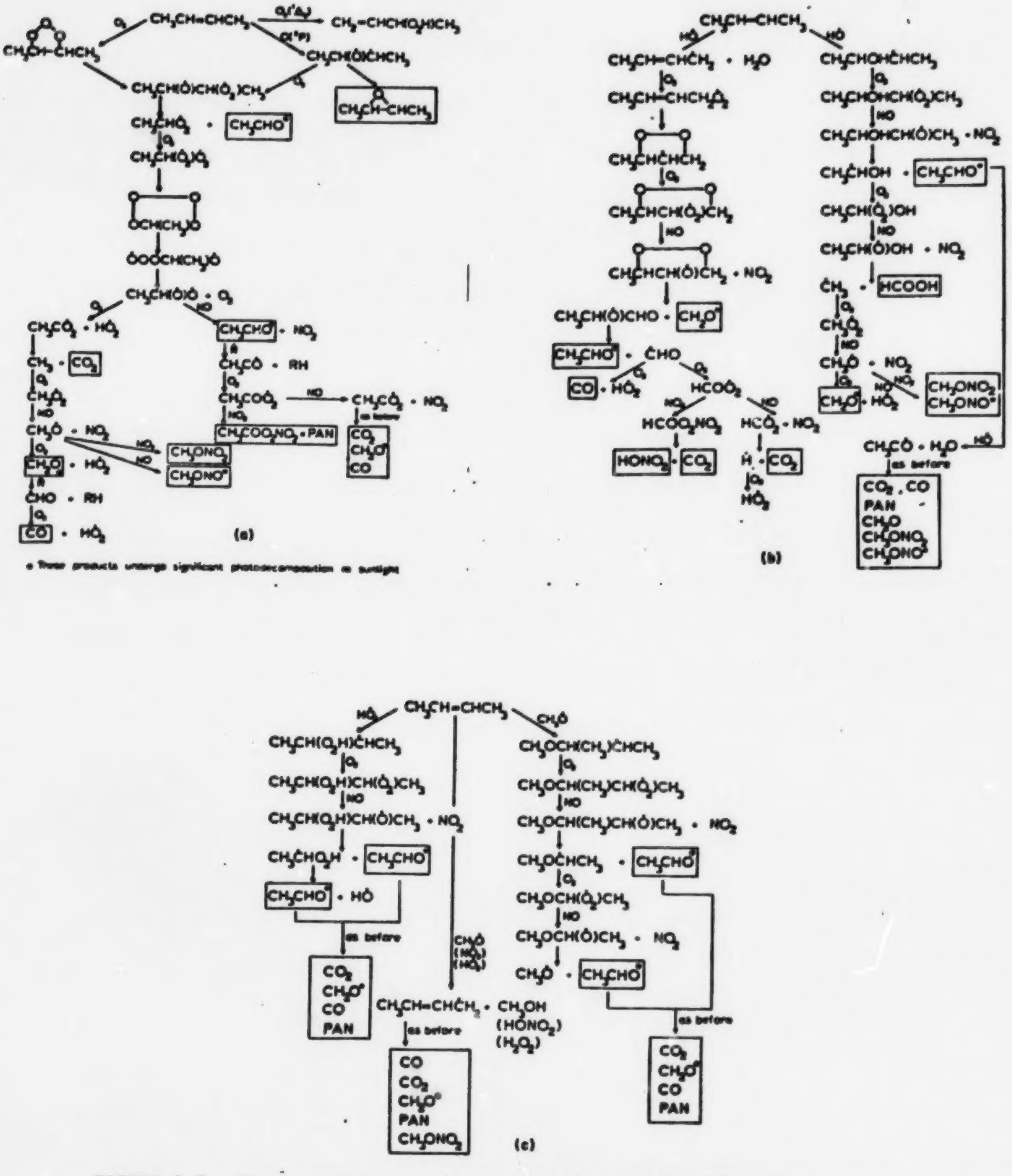
(a)
* These products undergo significant photodecomposition in sunlight
(b)
(c)

FIGURE 2-7. Major reaction paths for the degradation of *trans*-2-butene in an irradiated NO_x-polluted atmosphere. (Reprinted with permission from Demerjian *et al.*[5])

modeling studies and smog-chamber simulations show significant oxidant formation with NO_x + aldehydes, NO_x + alkanes (except methane), or even NO_x + carbon monoxide in moist air. The development of significant oxidant from NO_x + aldehydes is particularly ominous, because aldehyde emission is not now controlled. As the modelers state:[6]

> "It appears from these data that the O_3 standard (i.e. 0.08 ppm for one hour) could not be met if the aldehydes remained high, $[CH_2O]$ = 0.10, $[CH_3CHO]$ = 0.06 ppm, even if nearly all of the olefinic hydrocarbon were removed .... We should learn from these data that the true relationship between non-methane hydrocarbons and maximum 1-hour oxidant at low hydrocarbon levels could be a critical function of a variable which is not routinely measured now, namely the concentration of the impurity aldehyde."

A similar statement could probably be made concerning ketones. These compounds are commonly used as solvents, and they are known to form free radicals when photolyzed. Many chlorinated hydrocarbons, which are also widely used as solvents, can be attacked by hydroxyl radicals and thus contribute to peroxy radical formation.

No one pollutant can be blamed as the major cause of ozone formation. Replacing the more reactive hydrocarbons with less reactive ones would delay the formation of ozone, but would not prevent it. Reducing the NO_x concentration seems to reduce the maximal oxidant concentrations observed, but the effect is nonlinear. Heavy injections of nitric oxide into the air can temporarily reduce the local ozone concentration, as often happens in urban centers, but additional oxidant formation can be expected later downwind. Although these effects can be understood qualitatively, it is not yet possible to make accurate predictions of oxidant formation, even in laboratory experiments.

In summary, the concentration of ozone in the polluted atmosphere is controlled by the intensity of sunlight and the ratio of nitrogen dioxide to nitric oxide. Hydrocarbons and other pollutants -- such as aldehydes, ketones, chlorinated hydrocarbons, and carbon monoxide -- react to form peroxy radicals. These, in turn, react with nitric oxide, causing the ratio $[NO_2]:[NO]$ to increase. As a consequence of Eq. 5, the ozone concentration also increases.

This brief description of oxidant formation in polluted air is based on our current understanding of the chemistry involved. It is evident from an examination of the detailed mechanism that many of the important reactions have not been well studied. For example, the sequences of degradation reactions for the hydrocarbons are only poorly understood. As a result of these uncertainties, it is not possible to make accurate predictions of photochemical oxidant concentrations. However, with another 5 years of progress similar to the last 5, it should be possible to construct chemical models that will permit ozone predictions accurate to within 30% for laboratory studies. Although many of the chemical details in the current models are certain to be altered as more experimental data become available, it seems probable that at least the backbone of our present understanding is correct.

Recent Chemical Modeling Studies -- Results and Uncertainties

The state of our current understanding of the chemistry of oxidant formation can be judged by examining recent modeling studies, in which all the reactions that are considered important are combined and the resulting differential equations are integrated numerically. Experimental rate constants from the literature are accepted (unless they are judged unreasonable), and others are estimated. In the system NO_x-propylene-air, 242 different reactions are included; another 100 reactions are neglected as probably unimportant. Roughly half the rate constants used in the model are not firm experimental values.

The success of these computer simulations must be rated as quite good. Figure 2-8 compares concentration-time measurements from a smog-chamber study of NO_x-propylene-air with computer-calculated results based on the same initial conditions. The time dependences and absolute concentrations agree fairly well, but not perfectly. Note that the calculated maximal concentrations of ozone and PAN are less than the measured values by about a factor of 2. The rapid conversion of nitric oxide to nitrogen dioxide and the time dependence of ozone and PAN are reproduced quite well. These results are impressive, considering that the mechanism and rate constants in the model were not considered variables to be adjusted until a best fit is obtained. Once the reactions and rate constants were selected, they were used for a variety of simulations, with fair to excellent agreement.[5]

However, the number of concentrations being fitted is fairly small, compared with the number of parameters going into the model. The computer calculations can be used to predict the concentrations of other trace compounds that should be present in smog chambers. If these compounds are later found at approximately the predicted concentrations, the model will be strengthened. If not, changes will have to be made in the model. A more stringent test of the model will occur when it becomes possible to measure the actual concentrations of the free radicals in the atmosphere.

Many of the values of the rate constants that go into the model are not critical, but some are. As the modelers state:

> "Even these systems are very complex and difficult to treat quantitatively since many reactions which appear to be important in theory have not been studied in detail, and theoretical estimates of rate constants must be made in desperation...."[6]

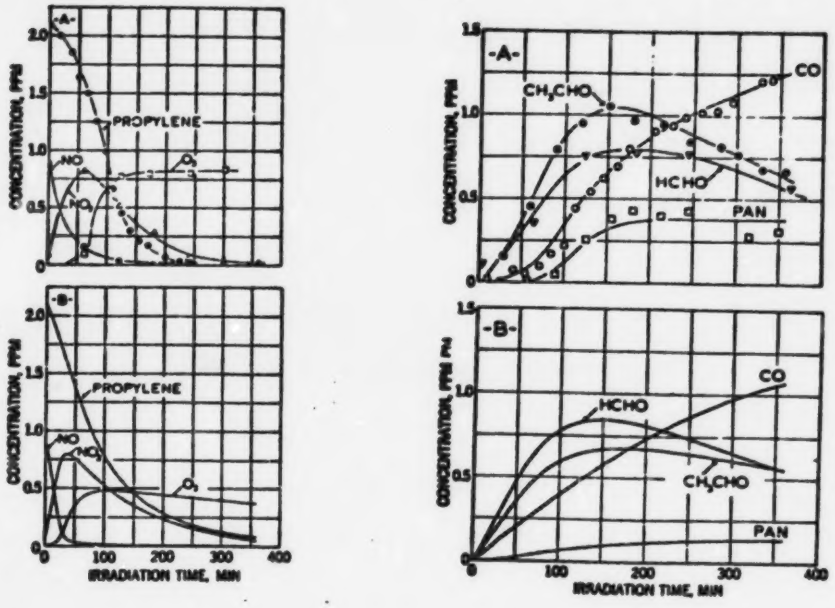

FIGURE 2-8. Photooxidation of propylene in irradiated C_3H_6-NO-NO_2 mixtures in moist air. A, experimental rate data from smog-chamber experiment of A. P. Altshuller *et al.* (Environ. Sci. Technol. *1*, 899 (1967)). Initial concentrations: C_3H_6, 2.09 ppm; NO, 0.90 ppm; NO_2, 0.09 ppm. Relative humidity at 31.5 C, 50%. B, computer simulation of product concentration-time curves for same initial conditions. (Reprinted with permission from Demerjian *et al.*[5]).

Some of the most serious current uncertainties are as follows:

- Direct determinations of rate constants are needed for almost all the reactions of hydroperoxy radical and RO_2.
- "The rate constants for both homogeneous and heterogeneous reactions related to the oxides of nitrogen and water vapor should be characterized carefully.... Furthermore, the actual levels of nitrous acid, nitric acid, H_2O, NO, and NO_2 should be determined simultaneously in real auto-exhaust-polluted atmospheres...."[5]
- "The primary quantum yield of radical formation in nitrous acid, CH_2O, and CH_3CHO photolyses should be better established as a function of the appropriate wavelength range of sunlight."[5]
- "The chemical details of the reaction sequence following OH radical addition and abstraction from olefins should be explored fully...."[5]
- The chemical details of the reactions of representative alkyl radicals, alkoxy radicals, and biradicals with oxygen should be established. Both the rate constants and the immediate products are needed to construct realistic mechanisms for the model.
- The gas-phase stability of a variety of possible products -- such as the olefin ozonide, peroxyformyl nitrate, and peroxynitric acid -- are not known.

These assignments represent formidable tasks for the experimentalists, but recent developments in instrumentation and techniques suggest that substantial progress should be made soon.

The present smog models are probably most vulnerable to the possibility that some important mechanism or intermediate has been omitted altogether. The modelers themselves recognize the uncertainties involved:

> "One must not take too seriously the results from complex simulations at this stage of our knowledge. In particular the development of sound reaction schemes and realistic smog models require much more quantitative kinetic information as to the detailed reaction paths which appear to be important in photochemical smog. ...There is no question that as such information becomes available, present models will require substantial changes."[6]

A realistic and detailed chemical model has great value. The stepwise addition of various primary pollutants can be made to evaluate the importance of each. The effects of various emission control strategies on the chemistry of oxidant formation can be studied easily and quickly. It is possible to calculate the importance and concentration of various reactive intermediates. One can estimate the concentrations of various compounds that have not yet been observed in smog. And it is possible to pinpoint some of the important gaps, in order to stimulate future experimental studies.

The detailed chemical model has been used to make the following observations and predictions; some of these statements are common to other models and are in accord with experimental observations:

- Complete elimination of olefinic hydrocarbons without controlling aldehyde emission will not ensure low oxidant readings in the atmosphere.[21]
- If no hydrocarbons or aldehydes were present in the atmosphere, but carbon monoxide and NO_x were present, significant ozone concentrations would develop. With reactive hydrocarbons present, the addition of carbon monoxide does not have a strong effect on oxidant concentration, unless it is added in very large amounts (2,000 ppm).[22]

- Reactions of the hydroxyl radical dominate the removal of hydrocarbons. However, several other reactants make significant contributions, including hydroperoxy radical, ozone, and oxygen atoms. (This conclusion depends on the hydrocarbon being considered: it is claimed that some terpenes in air are attacked mainly by ozone.[23])
- The hydroperoxy radical has the highest concentration of all the free radicals in smog. The concentrations of both hydroperoxy and hydroxyl radicals are rather insensitive to primary pollutant concentration.
- The concentration of ozone generated photochemically goes through a maximum as the NO_x concentration is increased.[24]
- The total oxidant dosage varies in a nonlinear manner with dilution of the primary pollutant.[25,26]
- The participation of singlet oxygen in the development of photochemical oxidant is minor, but its human health consequences should be considered.[27]

A good understanding of the detailed chemistry of oxidant formation makes it possible to construct more compact chemical models. These generalized or lumped mechanism models reduce the number of individual chemical reactions by combining similar or sequential reactions and ignoring minor ones.[28-30] Averaged reactivities and averaged product yields may be used. The simplified mechanisms can also reproduce smog-chamber data very well, although the construction of the simplified model is semiempirical, so good agreement is not unexpected. These generalized mechanisms are very valuable for modeling the real atmosphere, because the reduction in chemical complexity allows the inclusion of other important variables, such as transport and pollutant inputs. (The use of these models is covered in Chapter 5.)

Which Reactive Intermediates Are Important?

The concentrations of the various reactive intermediates can be calculated with a detailed chemical model. This information is not available elsewhere, because it is not yet possible to measure these reactive intermediates in the atmosphere. Table 2-2 shows the calculated concentrations of several intermediates and ozone for a simulated polluted atmosphere. Table 2-3 gives the calculated rates of attack of the same intermediates on the olefin *trans*-2-butene for the same irradiation times. By comparing these two tables, one can judge the importance of various intermediates. For example, the concentration of singlet oxygen is high, but its rate of attack on the olefin is insignificant, compared with that of hydroxyl radical. The steady-state concentration of hydroxyl radical is very low, owing mainly to its high reactivity. Early in the irradiation, hydroxyl radicals account for 90% of the *trans*-2-butene removal and even after 60 min, when the oxone concentration has developed, they still account for 50% of the removal. The hydroperoxy radicals show both a relatively high concentration -- by far the highest of the free radicals -- and a significant rate of attack on the olefin.

Average Lifetimes of Reactive Intermediates

It is well established that both ozone and PAN can cause damage to biologic systems (see Chapters 8 and 11). The possibility that the reactive intermediates in smog could directly cause biologic damage has been suggested,[1] but experiments are seldom designed to test this possibility.

The lifetimes of the various reactive intermediates shown in Table 2-4 were calculated with the assumption of a sudden termination of sunlight, as would occur when air is inhaled. The long lifetime of the hydroperoxy radical means that almost all of it will survive long enough to be transported into the lungs.

TABLE 2-2

Calculated Concentrations of Reactive Species in a Simulated Smog Mixture at Several Irradiation Times[a]

Species	Concentration, ppb 2 min	 30 min	 60 min
Ozone, O_3	8.5	84	139
Hydroperoxy radical, HO_2	0.21	0.32	0.37
Singlet oxygen, O_2 $(a^1\Delta)$	3.9×10^{-3}	5.1×10^{-3}	5.2×10^{-3}
Nitrogen trioxide, NO_3	0.03×10^{-3}	2.2×10^{-3}	7.4×10^{-3}
Hydroxyl radical, OH	1.7×10^{-4}	0.88×10^{-4}	0.72×10^{-4}
Oxygen atoms, O	3.8×10^{-6}	8.9×10^{-6}	9.5×10^{-6}

[a] Data from Demerjian *et al.*[5] Initial conditions: [NO], 0.075 ppm; [NO_2], 0.025 ppm; [*trans*-2-butene], 0.10 ppm; [CO], 10 ppm; [CH_2O], 0.10 ppm; [CH_3CHO], 0.06 ppm; [CH_4], 1.5 ppm; relative humidity, 50%.

TABLE 2-3

Calculated Rates of Attack on trans-2-Butene by Various Reactive Species in Simulated Smog Mixture at Several Irradiation Times.[a]

	Attack Rate, ppb/min		
Species	2 min.	30 min.	60 min.
Ozone	0.026	0.16	0.16
Hydroperoxy radical	0.16	0.15	0.09
Singlet oxygen	2.9×10^{-6}	2.1×10^{-6}	1.3×10^{-6}
Nitrogen trioxide	0.05×10^{-4}	2.2×10^{-4}	2.6×10^{-4}
Hydroxyl radical	1.72	0.55	0.27
Oxygen atoms	0.013	0.018	0.011

[a] Data from Demerjian *et al*.[5] Conditions same as in Table 2-2.

TABLE 2-4

Calculated Average Lifetimes of Several Reactive Intermediates in a Simulated Smog Mixture.[a]

Species	Lifetime,s
Ozone	250
Hydroperoxy radical	7
Singlet oxygen	0.05
Nitrogen trioxide	0.1
Hydroxyl radical	0.0030
Oxygen atoms	10^{-5}

[a] Data from Pitts and Finlayson (p.8).[4] Conditions same as in Table 2-2. Irradiation time, 60 min.

In contrast, the hydroxyl radicals will decay within a few milliseconds. As a computer simulation has shown, even though the half-life of singlet oxygen appears short, compared with the breathing cycle of several seconds, a significant fraction of it should survive into the lungs.[31]

Whether such species as hydroperoxy radicals and singlet oxygen will survive collisions with the surfaces of the upper breathing tract and reach the lower lungs, as ozone does, must await further experiments. Clearly, if all the ozone molecules and all the hydroperoxy radicals are eventually absorbed in the lungs, the ozone damage will dominate, unless hydroperoxy radicals are several hundred times more damaging, which seems unlikely.

Free radicals could have a significant effect on biologic surfaces that are in direct contact with irradiated smog, such as leaves and human skin. The effective dose delivered to a surface depends on the bulk concentration of the species, the sticking coefficient (the probability that a molecule that hits a surface will be absorbed), and the damage once it is absorbed. Very little is known about sticking coefficients, especially of free radicals. It is known that singlet oxygen will survive approximately 10,000 collisions with aqueous phosphoric acid[32] and that ozone is not immediately absorbed in the upper bronchial tubes. There is an indication that hydroperoxy radicals might be absorbed readily on surfaces.[33] If the sticking coefficient of hydroperoxy radicals were unity for biologic surfaces (which might be reasonable, inasmuch as it has the ability to make hydrogen bonds) and the sticking coefficient for ozone were 10^{-4}, the actual influxes of hydroperoxy radicals and ozone to a surface might be comparable, even though the ozone concentration is approximately 300 times greater. This calculation is pure speculation, but it does show that the influx of free radicals to a sunlit surface should not be neglected.

It is known that free radicals are formed when ozone reacts with carbon-carbon double bonds. Recently, it has been suggested that PAN probably forms free radicals when it reacts with aldehydes.[34] Because hydroperoxy radicals are free radicals, they may have biologic effects similar to those of ozone and PAN. Certainly, for experiments in which the observed biologic damage cannot be attributed to the measured concentrations of ozone and PAN, free radicals or unstable compounds should be considered.

Summary

The major primary pollutants of importance to oxidant formation are nitric oxide, hydrocarbons, aldehydes, and carbon monoxide. A few free radicals are formed by photolysis of aldehydes and nitrous acid by sunlight or by the reaction of traces of ozone with reactive hydrocarbons. These free radicals initiate chain reactions involving hydroperoxy and alkylperoxy radicals. During these chain reactions, the nitric oxide is converted to nitrogen dioxide, and the hydrocarbons and aldehydes are degrated. The photolysis of nitrogen dioxide by sunlight forms a free oxygen atom, which combines with an oxygen molecule to form ozone. Because of the $NO-NO_2-O_3$ cycle (Eqs. 1-3), the ozone concentration is determined primarily by the ratio $[NO_2] : [NO]$ and so does not become large until most of the nitric oxide has been converted to nitrogen dioxide. The total amount of oxidant formed depends, in a nonlinear fashion, on the amount of hydrocarbons available to continue pumping the nitric oxide to nitrogen dioxide. Aldehydes and even carbon monoxide can also serve this pumping function. When some of the peroxy radicals recombine or react with the nitrogen oxides, many secondary products, such as hydrogen peroxide and PAN, are formed.

Recent chemical modeling studies have been reasonably successful in reproducing the concentration -- time histories of smog-chamber experiments. An examination of these models shows a need for much more detailed chemical knowledge. Modeling studies also point out the necessity of carefully defining the initial conditions of smog-chamber experiments. Some observations that have been made with these models are:

- Even if hydrocarbons are completely removed from the air, aldehydes and NO_x can generate high concentrations of photochemical oxidants.
- If both hydrocarbons and aldehydes are eliminated, carbon monoxide and NO_x alone can generate significant concentrations of ozone.
- The concentration of ozone generated photochemically goes through a maximum as the NO_x concentration is increased.
- The steady-state concentration of free radicals in smog is approximately 0.3 ppb and is rather insensitive to primary pollutant concentration.

The concentrations, average lifetimes, and rates of attack of the reactive intermediates can be calculated with chemical models.

The effects of free radicals on biologic surfaces cannot be ignored.

NEW EXPERIMENTAL METHODS OF STUDYING AIR CHEMISTRY

Lasers

The development of reliable lasers with a variety of wavelengths, both fixed and variable, has generated many ideas of applications to air pollution monitoring and to chemical kinetics. Most of these techniques are still in the developmental stage. Whether they will have the reliability and low cost needed for widespread use is not known. Proposed methods include the following:

- Long-path infrared absorption, using a tunable diode laser, which is claimed to have a sensitivity of 5 ppb for carbon monoxide over a 610-m pathlength.[35]
- Differential laser absorption, with measurement of two or more wavelengths simultaneously and claimed sensitivity in the parts-per-billion range.[36]
- Laser backscattering, either Raman or fluorescence, which does not require a remote detector, can thus be used for detecting atmospheric pollutants at a distance, and has sensitivity less than that with direct absorption techniques.
- Laser-induced electronic fluorescence; two devices reported recently look very promising for continuous atmospheric monitoring; sensitivities of 0.6 ppb for nitrogen dioxide and 50 ppb for formaldehyde are claimed;[8,37] careful attention to possible interference from other species is necessary; detection of the hydroxyl radical in air ($\sim 10^8$ molecules/cm^3) has been claimed for this technique,[38] but it has been pointed out that this concentration seems much too high,[6] especially because the air had been removed from the sunlight 6 s before analysis; spurious effects, such as photolysis of the ozone in the air by the laser beam and two-photon absorption by water vapor, might have been responsible for the hydroxyl radical that was observed.
- Photoacoustic or optoacoustic spectroscopy, which detects the absorption of a pulsed laser in a cell by the pressure pulses generated when the light energy is degraded to heat,[39] which is claimed to have sensitivities of 0.4 ppb for nitric oxide and 5 ppb for ethylene, and which can measure the absorption spectra of solids and dusts.[40]

- **Laser magnetic resonance**, which has already been used to detect the free hydroxyl, methynyl (CH), hydroperoxy, formyl (HCO), and amino radicals in low-pressure gases[41] and could be used to determine rate constants for the reactions of the smaller free radicals.

Several recent reviews on lasers and laser spectroscopy should be consulted for details of these promising new techniques.[42-44]

Photoionization Mass Spectrometry

The use of high-intensity resonance lamps in the vacuum ultraviolet as photoionization sources for mass spectrometers allows many free radicals to be observed directly in reacting gases.[45] With the proper choice of lamp, photoionization causes no fragmentation of other molecules to interfere with the free-radical peaks -- a major problem in conventional electron bombardment sources. Steady-state concentrations of free radicals have been observed when oxygen atoms react with hydrocarbons and in ozone-olefin reactions.[17,46-48] With this technique, it was possible to resolve an argument of long standing concerning the immediate products formed by the attack of oxygen atoms on ethylene (mainly methyl and formyl radicals, with about 5% formaldehyde and hydrogen).

The photoionization mass spectrometer can detect singlet oxygen in a large excess of ground-state oxygen, and nitric oxide an excess of nitrogen dioxide.[50,51] Attempts to detect hydroperoxy radicals have not been successful, probably because of a low photoionization cross section, but the methylperoxy radical has been observed with this technique.[52]

Future research using the photoionization mass spectrometer should result in significant progress in resolving some of the uncertainties in current chemical smog models, namely, detection of the immediate products formed when hydroxyl radical reacts with olefins, determination of rate constants and mechanisms for oxygen reacting with free radicals, identification of the immediate products formed in ozone-olefin reactions, and determination of the rate constants and products of the reactions of alkylperoxy radicals with olefins and other hydrocarbons.

Computer-Controlled High-Resolution Mass Spectrometry

The powerful technique of coupling a computer to a high-resolution mass spectrometer has been used to analyze air pollutants.[53] Both particulate matter and gases can be scanned for up to 300 pollutants. Only stable compounds will be detected by this method, because the samples are concentrated before analysis.

The advantage of this technique is the rapidity of monitoring for many compounds simultaneously, including some of the liquid and solid inorganic materials -- such as sulfuric acid, ammonium sulfate, and ammonium nitrate — which may be the final products of the primary pollutants nitric oxide and sulfur dioxide. Also, monitoring the many partially oxidized hydrocarbons, such as aldehydes and acids, will give useful insight into the reaction mechanisms involved in the atmosphere. One disadvantage of this system is that only compounds that the computer is programed for will be reported; unexpected compounds may be overlooked. A careful study of sampling efficiency will be needed before quantitative concentrations in the atmosphere can be reported.

Summary

The development of lasers has opened up several new techniques for monitoring pollutants in the atmosphere. Sensitivities down to the parts-per-billion range are claimed, and continuous monitoring is possible.

The photoionization mass spectrometer has been developed as a sensitive detector for free radicals in the gas phase. A high-resolution mass spectrometer coupled to a computer is capable of detecting up to 300 compounds in air, both in particulate form and in the gas phase.

PRODUCTS OF PHOTOCHEMICAL SMOG -- OBSERVATIONS AND SPECULATION

A large number of compounds can be formed in the polluted atmosphere. As a result of the small concentrations involved and the great variety of possible products, very few compounds have actually been observed. The gaseous compounds for which quantitative measurements have been reported are listed in Table 2-5 with typical concentrations. Compounds observed in particulate matter will be discussed in the next chapter.

Which of the compounds in Table 2-5 are considered oxidants depends on the reactant being considered. Certainly ozone, PAN, and hydrogen peroxide are strong oxidants when biologic materials are considered. This list is certain to grow as more sensitive analytic techniques are used and as modeling studies suggest other important species that should be present.

Table 2-6 is a list of some compounds that may be present in photochemical smog, but have not yet been reported. The presence of some of these compounds seems very probable, in that they have been observed in smog-chamber studies (such as PBzN and ketene), whereas others are very speculative. For example, organic peroxy radicals, RO_2, are almost certainly important intermediates in the conversion of nitric oxide to nitrogen dioxide. When these radicals undergo a chain termination reaction with hydroperoxy radical, the corresponding organic hydroperoxide, ROOH, or peracid, $RCOO_2H$ (if an acylperoxy radical is involved), will be formed. Although the rate of this hydroperoxide formation is estimated[6] to be less than that of the similar formation of hydrogen peroxide by approximately a factor of 100,

TABLE 2-5

Compounds Observed in Photochemical Smog

Compound	Typical (or Maximal) Concentration Reported, ppm	Reference
Ozone, O_3	0.1 (0.7)	Chapter 4
PAN, $CH_3COO_2NO_2$	0.004 (0.01)	Chapter 4
Hydrogen peroxide, H_2O_2	(0.18)	58
Formaldehyde, CH_2O	0.04	Chapter 4
Higher aldehydes, RCHO	0.04	Chapter 4
Acrolein, CH_2CHCHO	0.007	Chapter 4
Formic acid, HCOOH	(0.05)	59

TABLE 2-6

Compounds That May Be Formed in Photochemical Smog

Compound	Possible Reaction of Formation	Reference
Peroxybenzoylnitrate, $C_6H_5COO_2NO_2$		57
Nitric acid, $HONO_2$		60, 59
Organic hydroperoxides, ROOH	$RO_2 + HO_2$	5 (p. 75)
Organic peracids, $RCOO_2H$	$RCOO_2 + HO_2$	5 (p. 75)
Organic peroxynitrates, RO_2NO_2	$RO_2 + NO_2 + M$	54
Ozonides, 0_3-olefin	0_3 + olefin + M	17
Ketene, CH_2CO	0_3 + olefin	61
Nitrous acid, HONO	$NO_2 + HO_2$	62
Pernitric acid, HO_2NO_2	$NO_2 + HO2 + M$	
Pernitrous acid, HO_2NO	$NO + HO_2 + M$	12
Sulfoxyperoxynitrate, $HOSO_2O_2NO_2$	$HOSO_2O_2 + NO_2 + M$	6

the potential concentration must be combined with toxicity and other information before a substance can be dismissed as unimportant.

Similarly, chain termination by $RO_2 + NO_2$ could form organic peroxynitrates. These would probably be less toxic than PAN, but they could be present in comparable amounts. The formation of organic peroxynitrites and peroxynitrates has been considered,[54] but they have not been observed in smog.

If ozone-olefin adducts are stable in the gas phase, as a recent study hinted,[17] then they are almost certainly present in the urban atmosphere. Their concentrations will depend on their stability in the sunlit atmosphere. If present, they are expected to be very reactive.

Pernitric (or peroxynitric) acid is an example of a compound that could be present in significant quantities. This proposal is very speculative, because there is no evidence of this compound in the gas phase, although there is evidence of some such species in solutions.[55] The reaction of hydroperoxy radical with nitrogen dioxide is usually written as,

$$H\dot{O}_2 + NO_2 \rightarrow HONO + O_2, \qquad (18)$$

which is certainly reasonable. However, at a pressure of 1 atm, the three-body recombination step,

$$H\dot{O}_2 + NO_2 + M \rightarrow HOONO_2 + M, \qquad (26)$$

also seems probable. The laboratory experiments that support Eq. 18 cannot rule out the formation of some pernitric acid. The chemical modeling studies show that, if Eq. 26 is assumed to be half as probable as Eq. 18, the formation of pernitric acid would be comparable with that of PAN.[6]

Similarly, recent experiments[12] have been interpreted to mean that about 10% of the reaction of hydroperoxy radical with nitric oxide gives pernitrous acid, HOONO, instead of nitrogen dioxide and hydroxyl radical. Because this reaction is of major importance, even 10% of a second channel would be important, although it has been argued that such compounds would not be sufficiently stable to accumulate in the atmosphere.[54] Whether such peroxynitrogen compounds are stable in the gas phase and whether they can be found in the atmosphere must await further experiments.

The last entry in Table 2-6, sulfoxyperoxynitrate, is an inorganic analogue of PAN. It was suggested in a computer study that investigated the addition of sulfur dioxide to the NO_x-hydrocarbon system.[6] Although this is only speculative, such unpleasant compounds may become more important if the sulfur content of fuels is allowed to increase in areas where an oxidizing photochemical smog is common. It is known that sulfur dioxide, when present in photochemical smog, is rapidly oxidized to sulfuric acid, and a recent mass-spectrometric study also indicated the presence of organic sulfur dioxide compounds.[63]

Table 2-6 is only a sampling of the compounds that might be found in photochemical smog in the future. The possible combinations among the many free radicals and the oxides of sulfur and nitrogen are almost limitless. Many undiscovered exotic compounds are present in photochemical smog, but their concentration and importance remain to be established.

RECOMMENDATIONS FOR FUTURE RESEARCH

- Rate constants are needed for almost all the reactions of HO_2 and RO_2.
- The homogeneous and heterogeneous reactions of the oxides of nitrogen with water vapor need study.
- The yields of free radicals from the photolysis of nitrous acid and of aldehydes should be established.

- Equation 4, $[O_3] = k_1[NO_2]/k_3[NO]$, should be tested in the real atmosphere, as well as in laboratory experiments. Simultaneous measurements of the concentrations of ozone, nitric oxide, and nitrogen dioxide and of the intensity of sunlight for a variety of conditions will provide a much-needed check on this dynamic equilibrium.
- A quantitative measure of the concentration of free radicals in smog (probably OH or HO_2) under well-defined conditions will provide an important test of present chemical models.
- Strong support for fundamental gas-phase kinetics is needed. Most of the reaction mechanisms and rate constants that are needed to construct realistic and detailed models of the polluted atmosphere are determined in laboratory studies under very special conditions, not in smog simulations at a pressure of 1 atm. Because there are still very serious gaps in the present models, further research should be supported.
- Smog-chamber studies are needed for validating both the detailed chemical models and the lumped models. Many of the past chamber studies have not used sufficiently well-defined initial conditions. Measurements of more products and of the reactive intermediates will provide more stringent tests for models.
- Modeling studies are very useful in pointing out the important kinetic data that are lacking, in clarifying some of the past smog-chamber studies, and generally in making the very complex chemistry more comprehensible. Accurate models can make unique predictions about the polluted atmosphere. There are very useful interactions between the modeling studies, the smog-chamber

experiments, and fundamental chemical kinetics; it is not possible to ignore one without hurting progress in the others.

- It seems probable that many new and unstable compounds are present in the polluted atmosphere or in smog chambers. A careful search for some of these compounds may provide some surprises.
- Promising new instrumental techniques should be supported, both for monitoring pollutants and for following reactive intermediates in kinetic studies. A reliable and accurate method of standardizing concentrations in the parts-per-billion range is needed.
- The possibility that free radicals, particularly HO_2, have significant effects on biologic surfaces exposed to the irradiated atmosphere should be investigated. Sticking coefficients are needed. In experiments in which the observed biologic effects cannot be attributed to the measured ozone and PAN concentrations, the possibility of damage by the steady-state concentrations of free radicals in the atmosphere should be considered.

REFERENCES

1. Leighton, P. A. Photochemistry of Air Pollution. New York: Academic Press, 1961. 300 pp.

2. Altshuller, A. P., and J. H. Bufalini. Photochemical aspects of air pollution. A review. Photochem. Photobiol. 4:97-146, 1965.

3. Altshuller, A. P., and J. J. Bufalini. Photochemical aspects of air pollution: A review. Environ. Sci. Technol. 5:39-64, 1971.

4. Pitts, J. N., Jr., and B. J. Finlayson. Mechanisms of photochemical air pollution. Angew. Chem. (Engl.) 14:1-15, 1975.

5. Demerjian, K. L., J. A. Kerr, and J. G. Calvert. The mechanism of photochemical smog formation. Adv. Environ. Sci. Technol. 4:1-262, 1974.

5a. Levy, H., II. Photochemistry of the troposphere. Adv. Photochem. 9:369-524, 1974.

6. Calvert, J. G., and R. D. McQuigg.

Int. J. Chem. Kinet. (in press) (UNVERIFIED)

7a. Stern, A. C., Ed. Air Pollution. Vol. 1. Air Pollution and Its Effects. (2nd ed.) New York: Academic Press, 1968. 694 pp.

7b. Stern, A. C., Ed. Air Pollution. Vol. 2. Analysis, Monitoring, and Surveying. (2nd ed.) New York: Academic Press, 1968. 684 pp.

7c. Stern, A. C., Ed. Air Pollution. Vol. 3. Sources of Air Pollution and Their Control. (2nd ed.) New York: Academic Press, 1968. 866 pp.

7d. Stern, A. C., Ed. Air Pollution. Vol. 4. (ed.) New York: Academic Press, (in press) (UNVERIFIED)

8. Tucker, A. W., M. Birnbaum, and C. L. Fincher. Atmospheric NO_2 determination by 442-nm laser induced fluorescence. Appl. Optics 14:1418-1422, 1975.

9. Heicklen, J., K. Westberg, and N. Cohen. Conversion of NO to NO_2 in Polluted Atmospheres. Center for Air Environment Studies Publication No. 115-69. University Park: The Pennsylvania State University, 1969. 5 pp.

10. Stedman, D. H., E. D. Norris, E. E. Daby, H. Niki, and B. Weinstock. The role of OH radicals in photochemical smog reactions. Paper Presented at 160th National Meeting of the American Chemical Society, Chicago, September, 1970.

11. Payne, W. A., L. J. Stief, and D. D. Davis. A kinetics study of the reaction of HO_2 with SO_2 and NO. J. Amer. Chem. Soc. 95:7614-7619, 1973.

12. Cox, R. A., and R. G. Derwent. Kinetics of the reaction of HO_2 with nitric oxide and nitrogen dioxide. J. Photochem. 4:139-153, 1975.

13. Simonaitis, R., and J. Heicklen. Reaction of HO_2 with NO and NO_2. J. Phys. Chem. 78:653-657, 1974.

13a. Hack, W. K. Hoyermann, and H. G. Wagner. Über einiae Radikalreaktionen im H-O-N-System. Z. Naturforschung. 29A:1236-1237, 1974.

13b. Hack, W., K. Hoyermann, and H. Gg. Wagner. The reaction $NO + HO_2 \longrightarrow NO_2 + OH$ with $OH + H_2O_2 \longrightarrow HO_2 + H_2O$ as an HO_2-source. Int. J. Chem. Kinetics, Symp. No. 1 (Chemical Kinetic Data for the Lower and Upper Atmosphere):329-339, 1975.

14. Pate, C. T., B. J. Finlayson, and J. N. Pitts, Jr. A long path infrared spectroscopic study of the reaction of methylperoxy free radicals with nitric oxide. J. Amer. Chem. Soc. 96:6554-6558, 1973.

15. Slagle, I. R., J. R. Gilbert, R. E. Graham, and D. Gutman. Direct identification of reactive channels in the reactions of hydroxyl radicals with allene, propylene and 2-butene. Int. J. Chem. Kinetics, Symp. No. 1 (Chemical Kinetic Data for the Lower and Upper Atmosphere):317-328, 1975.

16. Demerjian, K. L., J. A. Kerr, and J. G. Calvert. The mechanism of photochemical smog formation. Adv. Environ. Sci. Technol. 4:166, 1974.

17. Atkinson, R., B. J. Finlayson, and J. N. Pitts, Jr. Photoionization mass spectrometer studies of gas phase ozone-olefin reactions. J. Amer. Chem. Soc. 95:7592-7599, 1973.

18. Stephens, E. R., and F. R. Burleson. Distribution of light hydrocarbons in ambient air. J. Air Pollut. Control Assoc. 19:929-936, 1969.

19. U. S. Department of Health, Education, and Welfare. Public Health Service. Air Quality Criteria for Photochemical Oxidants. National Air Pollution Control Administration Publ. No. AP-63. Washington, D. C.: U. S. Government Printing Office, 1970.

20. Niki, H., E. E. Daby, and B. Weinstock. Mechanisms of smog reactions. Adv. Chem. Ser. 113:16-57, 1972.

21. Bufalini, J. J., and K. L. Brubaker. The photooxidation of formaldehyde at low partial pressures, pp. 225-238. In C. S. Tuesday, Ed. Chemical Reactions in Urban Atmospheres. Proceedings of the Symposium held at General Motors Research Laboratories, Warren, Michigan, 1969. New York: American Elsevier, 1971.

22. Glasson, W. A. Effect of carbon monoxide on atmospheric photooxidation of nitric oxide--hydrocarbon mixtures. Environ. Sci. Technol. 9:343-347, 1975.

23. Grimsrud, E. P., H. H. Westberg, and R. A. Rasmussen. Atmospheric reactivity of monoterpene hydrocarbons, NO_x photooxidation and ozonolysis. Int. J. Chem. Kinetics Symp. No. 1, 1975 (Chemical Kinetic Data for the Lower and Upper Atmosphere):183-195, 1975.

24. Tuesday, C. S. The atmospheric photooxidation of *trans*-butene-2 and nitric oxide, pp. 15-49. In Chemical Reactions in the Lower and Upper Atmosphere. Proceedings of an International Symposium Arranged by Stanford Research Institute, San Francisco, California, April 18-20, 1961. New York: Interscience Publishers, 1961.

25. Schuck, E. A., A. P. Altshuller, D. S. Barth, and G. B. Morgan. Relationship of hydrocarbons to oxidants in ambient atmospheres. J. Air Pollut. Control Assoc. 20:297-302, 1970.

26. Glasson, W. A., and C. S. Tuesday. Hydrocarbon reactivity and the kinetics of the atmospheric photooxidation of nitric oxide. J. Air Pollut. Control Assoc. 20:239-244, 1970.

27. Pitts, J. N., Jr., and B. J. Finlayson. Mechanisms of photochemical air pollution. Angew. Chem. (Engl.) 14:8, 1975.

28. Eschenroeder, A. Q., and J. R. Martinez. Concept and applications of photochemical smog models. Adv. Chem. Ser. 113:101-168, 1972.

29. Hecht, T. A., and J. H. Seinfeld. Development and validation of a generalized mechanism for photochemical smog. Environ. Sci. Technol. 5:47-57, 1972.

30. Hecht, T. A., J. H. Seinfeld, and M. C. Dodge. Further development of generalized kinetic mechanism for photochemical smog. Environ. Sci. Technol. 8: 327-339, 1974.

31. Firestone, R. F., and J. G. Calvert.

(in press)

32. Wayne, R. P. Singlet molecular oxygen. Adv. Photochem. 7:311-371, 1969.

33. Lloyd, A. C. Evaluated and estimated kinetic data for phase reactions of the hydroperoxyl radical. Int. J. Chem. Kinetics 6:169-228, 1974.

34. Wendschuh, P. H., C. T. Pate, and J. N. Pitts, Jr. The reaction of peroxyacetyl nitrate with aldehydes. Tetrahedron Lett. 31:2931-2934, 1973.

35. Ku, R. T., E. D. Hinkley, and J. O. Sample. Long-path monitoring of atmospheric carbon monoxide with a tunable diode laser system. Appl. Optics 14:854-861, 1975.

36a. O'Shea, D. C., and L. G. Dodge. NO_2 concentration measurements in an urban atmosphere using differential absorption techniques. Appl. Optics 13:1481-1486, 1974.

36b. Menzies, R. T., and M. T. Chahine. Remote atmospheric sensing with an airborne laser absorption spectrometer. Appl. Optics 13:2840-2849, 1974.

36c. Patty, R. R., G. M. Russwurm, W. A. McClenny, and D. R. Morgan. CO_2 laser absorption coefficients for determining ambient levels of O_3, NH_3, and C_2H_4. Appl. Optics 13:2850-2854, 1974.

37. Becker, K. H., U. Schurath, and T. Tatarczyk. Fluorescence determination of low formaldehyde concentrations in air by dye laser excitation. Appl. Optics 14:310-313, 1975.

38. Wang, C. C., and L. I. Davis, Jr. Measurement of hydroxyl concentrations in air using a tunable uv laser beam. Phys. Rev. Lett. 32:349-352, 1974.

39. Kreuzer, L. B., N. D. Kenyon, and C. K. N. Patel. Air pollution: Sensitive detection of ten pollutant gases by carbon monoxide and carbon dioxide lasers. Science 177:347-349, 1972.

40. Maugh, T. H., II. Photoacoustic spectroscopy: New uses for an old technique. Science 188:38-39, 1975.

41. Davies, P. B., D. K. Russell, B. A. Thrush, and F. D. Wayne. Detection of amino radical NH_2 by laser magnetic resonance spectroscopy. J. Chem. Phys. 62:3739-3742, 1975.

42. Colles, M. J., and C. R. Pidgeon. Tunable lasers. Rep. Prog. Phys. 38: 329-460, 1975.

43. Melngailis, I.

IEEE J. Quant. Electr. QE-10:7- , 1972.

44. Hinkley, E. D., K. W. Nill, and F. A. Blum.

pp. . In H. Walther, Ed. Laser Spectroscopy of Atoms and Molecules. (in press)

45. Jones, I. T. N., and K. D. Bayes. Detection of steady-state free-radical concentrations by photoionization. J. Amer. Chem. Soc. 94:6869-6871, 1972.

46. Jones, I. T. N., and K. D. Bayes. Free radical formation in the atomic oxygen plus acetylene reaction, pp. 277-284. In Proceedings of 14th Symposium (International) on Combustion, 1972. Pittsburg: The Combustion Institute, 1973.

47a. Washida, N., and K. D. Bayes. The reaction of methyl radicals with atomic oxygen. Chem. Phys. Lett. 23:373-375, 1973.

47b. Slagle, I. R., F. J. Pruss, Jr., and D. Gutman. Kinetics into the steady state. I. Study of the reaction of oxygen atoms with methyl radicals. Int. J. Chem. Kinetics. 6:111-123, 1974.

48. Washida, N., R. I. Martinez, and K. D. Bayes. The oxidation of formyl radicals. Z. Naturforsch. 29A:251-255, 1974.

49a. Kanofsky, J. R., and D. Gutman. Direct observation of the products produced by the O-atom reactions with ethylene and propylene studied in high-intensity molecular beams. Chem. Phys. Lett. 15:236-239, 1972.

49b. Kanofsky, J. R., D. Lucas, and D. Gutman. Direct identification of free-radical products of oxygen atom reactions with olefins, using high-intensity molecular beams, pp. 285-294. In Proceedings of 14th Symposium (International) on Combustion, 1972. Pittsburgh: The Combustion Institute, 1973.

49c. Pruss, F. J., Jr., I. R. Slagle, and D. Gutman. Determination of branching ratios for the reaction of oxygen atoms with ethylene. J. Phys. Chem. 76:663-665, 1974.

50. Jones, I. T. N., and K. D. Bayes. Formation of O_2 ($\underline{a}\,{}^1\Delta_g$) by electronic energy transfer in mixtures of NO_2 and O_2. J. Chem. Phys. 59:3119-3124, 1973.

51. Jones, I. T. N., and K. D. Bayes. Photolysis of nitrogen dioxide. J. Chem. Phys. 59:4836-4833, 1973.

52. Washida, N., and K. D. Bayes.

(in press)

53. Schuetzle, D., A. L. Crittenden, and R. J. Charlson. Application of computer controlled high resolution mass spectrometry to the analysis of air pollutants. J. Air Pollut. Control Assoc. 23:704-709, 1973.

54. Demerjian, K. L., J. A. Kerr, and J. G. Calvert, The mechanism of photochemical smog formation. Adv. Environ. Sci. Technol. 4:77, 1974.

55. Moeller, T. Inorganic Chemistry. New York: John Wiley & Sons, 1952. p. 613.

Delete 56--omitted.

57. Heuss, J. M., and W. A. Glasson. Hydrocarbon reactivity and eye irritation. Environ. Sci. Technol. 2:1109-1116, 1968.

58. Bufalini, J. J., B. W. Gay, Jr., and K. L. Brubaker. Hydrogen peroxide formation from formaldehyde photooxidation and its presence in urban atmospheres. Environ. Sci. Technol. 6:816-821, 1972.

59. Hanst, P. L., W. E. Wilson, R. K. Patterson, B. W. Gay, and L. W. Chaney. Paper Presented at 167th National Meeting of the American Chemical Society, Los Angeles, April 1974. (UNVERIFIED)

60. Miller, D. F., and C. W. Spicer. A Continuous Analyzer for Detecting Nitric Acid. Paper 74-17, Presented at 67th Annual Meeting of the Air Pollution Control Association, Denver, Colorado, June 1974.

61. McAfee, J. M., A. M. Winer, and J. N. Pitts. In CODATA (Committee on Data for Science and Technology) Symposium on Chemical Kinetics Data for the Lower and Upper Atmosphere, Warrenton, Virginia, Sept. 1974. (in press) (UNVERIFIED)

62. McAfee, J. M., J. N. Pitts, and A. M. Winer. In Pacific Conference on Chemistry and Spectroscopy, San Francisco, October 1974. (in press) (UNVERIFIED)

63. Schulten, H.-R., and U. Schurath. Analysis of aerosols from the ozonolysis of 1-butene by high-resolution field desorption mass spectrometry. J. Phys. Chem. 79:51-57, 1975.

64. Stedman, D. H., and J. O. Jackson. The photostationary state in photochemical smog. Int. J. Chem. Kinetics Symp. No. 1, 1975 (Chemical Kinetic Data for the Lower and Upper Atmosphere):493-501, 1975.

65. Eschenroeder, A. Q., and J. R. Martinez. Analysis of Los Angeles Atmospheric Reaction Data from 1968 to 1969. General Research Corp. CR-1-170, 1970. (UNVERIFIED)

CHAPTER 3

AEROSOLS

Organic compounds were recognized long ago as key ingredients of the polluted atmosphere and constitute a significant fraction of the urban aerosol associated with photochemical smog.[1] Although there is no air quality standard for organic aerosols, ambient concentrations of particulate organic substances are related to the concentrations of total suspended particles, for which there are federal and state standards,* and to prevailing visibility. Primary organic compounds are emitted directly into the atmosphere, and their concentrations can be reduced through emission control.[3] Secondary organic compounds result from gas-phase photochemical reactions involving hydrocarbons, nitrogen oxides, and ozone and thus imply the same type of control strategies as for ozone and photochemical oxidants.[4,5] However, control of secondary organic compounds would require a more elaborate approach, with the identification of specific hydrocarbon precursors as a necessary step (Figure 3-1). Because of their accumulation in the submicrometer range, secondary organic aerosols may be responsible for adverse health effects and contribute significantly to visibility degradation. Despite its importance, the gas-to-particle conversion of organic pollutants has received much less attention than other aspects of air pollution. This section deals with the identification of secondary organic aerosols in the atmosphere and the physical and chemical aspects of their formation. The relative importance of their gas-phase hydrocarbon precursors, including naturally emitted terpenes,

---

*The national ambient air quality standards for particulate matter are:[2] 24-h averages, not to be exceeded more than once a year: primary, 260 μg/m^3; secondary, 150 μg/m^3. Annual geometric means: primary, 75 μg/m^3; secondary, 60 μg/m^3.

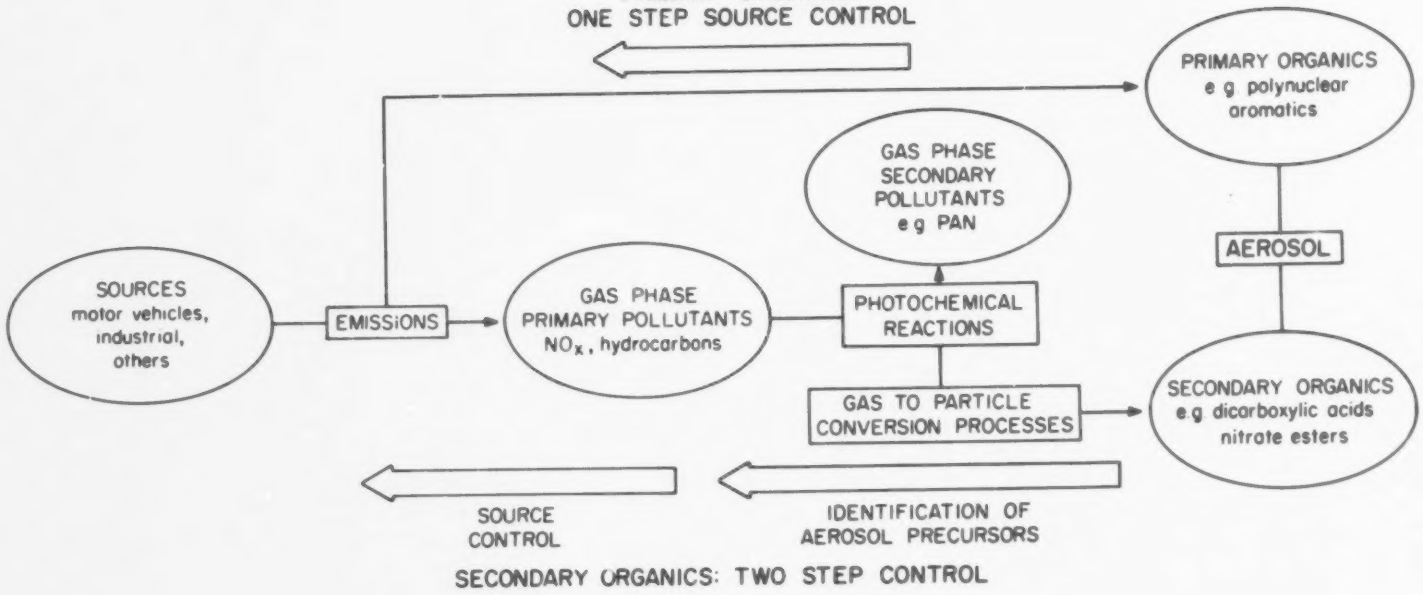
PRIMARY ORGANICS:
ONE STEP SOURCE CONTROL
SOURCES
motor vehicles,
industrial,
others
EMISSIONS
GAS PHASE
PRIMARY POLLUTANTS
NO_x, hydrocarbons
GAS PHASE
SECONDARY
POLLUTANTS
e g PAN
PHOTOCHEMICAL
REACTIONS
GAS TO PARTICLE
CONVERSION PROCESSES
PRIMARY ORGANICS
e g polynuclear
aromatics
AEROSOL
SECONDARY ORGANICS
e.g dicarboxylic acids
nitrate esters
SOURCE
CONTROL
IDENTIFICATION OF
AEROSOL PRECURSORS
SECONDARY ORGANICS: TWO STEP CONTROL

Figure 3-1. Control strategies for primary and secondary organic aerosols.

will be discussed, and the contribution of hydrocarbon photochemical reactions to the formation of inorganic sulfate and nitrate aerosols will be briefly reviewed.

Atmospheric Observations

Analytic Techniques. Identifying the chemical composition of urban aerosols, in which hundreds of components may be present, is a formidable task for the analyst. Although rather simple techniques can be used to quantify the aerosol composition by elemental analysis (e.g., organic carbon) and groups of compounds (e.g., nitrates, sulfates, and organics or aliphatics, aromatics, and oxygenates in the organic fraction), only more sophisticated techniques can provide individual identification of compounds present at very low concentrations. The necessary selectivity and sensitivity are then gained at the expense of a general picture of the aerosol composition.

Aerosol samples can be analyzed without further preparation for organic carbon[6] and for carbon, hydrogen, oxygen, and nitrogen (CHON);[7] with infrared spectroscopy;[8,9] with photoelectron spectroscopy;[10] and with mass spectrometry.[11] However, organic analysis is generally conducted after solvent extraction of samples collected on glass-fiber filters.[12] The organic extract can be further fractionated by thin-layer, paper, liquid, or column chromatography, by ion-exchange chromatography,[13] or by separation into different types of solvents.[14] The extracts or fractions are then analyzed for organic carbon[6] or for CHON[15-19] by infrared,[15,16,18-21] ultraviolet fluorescence,[22-29] gas chromatography,[23,30-34] high-pressure liquid chromatography,[35] and mass spectrometry.[36-40] For example, more than 70 polynuclear aromatics have been identified with mass spectrometry.[41] Some of these techniques have been used in conjunction with size distribution measurements.[9,10,18,19,29] Vacuum sublimation[34] and, more recently, ultrasonic extraction[42] have been proposed as alternative techniques for the time-consuming process that uses the Soxhlet extractor. However, most of the later analyses depend on the extraction efficiency of the organic solvent. Although nonpolar solvents were most widely used in the past (cyclohexane, benzene for the National Air Surveillance Network[43]), it has been found recently[6] that solvent extraction efficiencies depend on solvent polarity characteristics (Figure 3-2) and that binary mixtures of a polar solvent and a nonpolar one can extract up to 48% more organics than benzene alone from samples collected in areas of heavy photochemical pollution (Table 3-1)

Primary Organic Aerosols. Primary organics are emitted to the atmosphere by industrial sources (oil refineries, chemical plants, producers and users of solvents and plasticizers), vehicles (as a result of incomplete fuel combustion, oxygenated degradation products of lubricating oil, polymers from tires), and agricultural activities (use of pesticides). An exhaustive literature survey is beyond the scope of this section, but can be found in Air Quality Criteria for Particulate Matter;[44] many useful references are also available.[6-43]

Among the identified primary organics are linear and branched alkanes and alkenes, substituted benzenes and styrenes, quinones, acridines, quinolines, phenols, cresols, phthalates, fatty acids, carbonyl compounds, and some pesticide compounds. Diurnal concentration profiles of primary pollutants emitted in auto exhaust parallel vehicle activity and show two

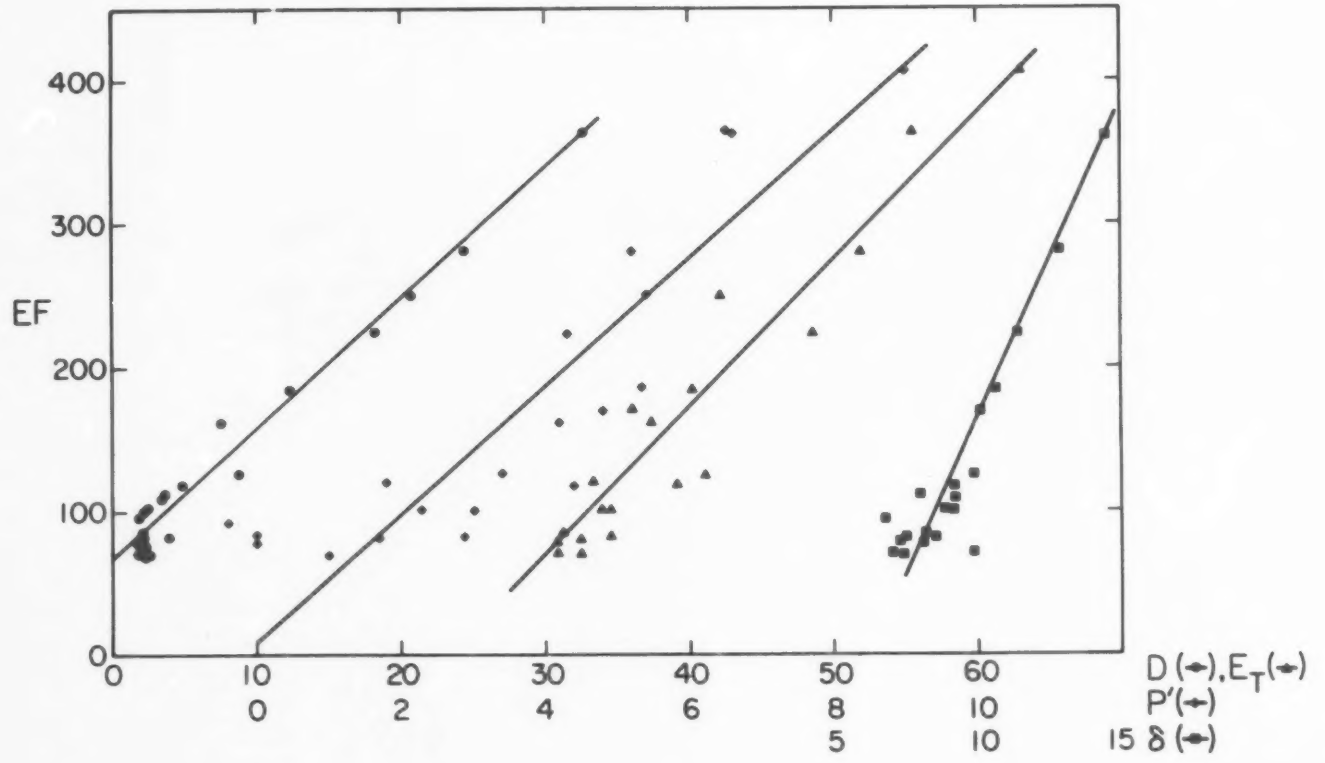

Figure 3-2. Solvent extraction efficiencies (EF) as function of dielectric constants (D), solubility parameters (δ), and polarity parameters (P′ and E_T). Solvents studied: silicon tetrachloride, carbon disulfide, n-pentane, Freon 113, cyclopentane, n-hexane, carbon tetrachloride, diethylether, cyclohexane, isooctane, benzene (reference, EF=100), toluene, trichloroethylene, diethylamine, chloroform, triethylamine, methylene chloride, tetrahydrofuran, 1,4-dioxane, pyridine, 2-propanol, acetone, ethanol, methanol, dimethyl sulfoxide, and water. (Reprinted with permission from Grosjean, ref. 6.)

Table 3-1

Extraction Efficiencies (EF) and Organic Carbon Extraction Efficiencies (OCEF) of Various Solvents and Binary Mixtures for Atmospheric Aerosol Samples[a]

Solvent	EF	OCEF	Binary Mixture[b,c]		EF	OCEF
Silicon tetrachloride	69	-	Freon 113	2-Propanol	157	119
Carbon disulfide	70	69		Acetone	191	131
n-Pentane	71	-		Ethanol	198	134
Freon 113	76	76		Methanol	220	147
Cyclopentane	77	-	Cyclohexane	2-Propanol	210	125
n-Hexane	78	78		Acetone	230	136
Carbon tetrachloride	81	80		Ethanol	242	130
Diethylether	82	80		Methanol	252	144
Cyclohexane	84	84	Isooctane	2-Propanol	220	131
Isooctane	95	94		Acetone	241	132
BENZENE (reference)	100	100		Ethanol	255	130
Toluene	102	-		Methanol	281	144
Trichloroethylene	109	108	Benzene	2-Propanol	225	135
Diethylamine	112	-		Acetone	240	140
Chloroform	118	114		Ethanol	268	135
Triethylamine	120	116		Methanol	301	145
Methylene chloride	126	120	Chloroform	2-Propanol	218	131
Tetrahydrofuran	100-260	54-115		Acetone	248	137
1,4-Dioxane	112-262	47-110		Ethanol	260	139
Pyridine	115-295	52-116		Methanol	312	149
2-Propanol	70-327	61-167	Methylene chloride	2-Propanol	219	140
Acetone	71-388	60-170		Acetone	249	144
Ethanol	95-421	64-190		Ethanol	260	142
Methanol	85-560	69-200		Methanol	320	151
Dimethyl sulfoxide	90-520	-				
Water	183-594	74-230				

---

[a] Data from Grosjean.[6]

[b] 50%:50% by volume.

[c] Polar-solvent EF and OCEF measured for the same sampling period:
2-propanol: 230 and 107 acetone: 260 and 120
ethanol: 291 and 122 methanol: 374 and 144

$$EF_i = 100 \times \frac{\text{total extracted, solvent i}}{\text{total extracted, benzene, same sample}}$$

$$OCEF_i = 100 \times \frac{\text{extracted organic carbon, solvent i}}{\text{extracted organic carbon, benzene, same sample}}$$

characteristic peaks associated with morning and evening traffic periods.[45] Because of their potential carcinogenic activity, polynuclear aromatic hydrocarbons have been extensively studied (see Foster et al.[35]). Recent studies have reported their identification in automobile exhaust,[40] their ambient distribution with respect to particle size,[29] the close relation between their ambient concentrations and automobile traffic in the Los Angeles area,[28,46] and their possible loss during sampling as a function of their volatility.[47] The recent observation of chemiluminescence associated with particles in auto exhaust[48] is of interest, in view of the fact that the carcinogenic action of electronically excited molecules is much greater than that of the corresponding ground state.[49]

Secondary Organic Aerosols. Organic aerosols formed by gas-phase photochemical reactions of hydrocarbons, ozone, and nitrogen oxides have been identified recently in both urban and rural atmospheres. Aliphatic organic nitrates,[19,50,51] such dicarboxylic acids as adipic and glutaric acids,[50] carboxylic acids derived from aromatic hydrocarbons (benzoic and phenylacetic acids) and from terpenes emitted by vegetation, such as pinonic acid from α-pinene,[52] have been identified. The most important contribution in this field has been that of Schuetzle et al., who used computer-controlled high-resolution mass spectrometry and thermal analysis,[11,53,54] the only available technique that combines the resolving power necessary to identify individual pollutants at very low concentrations with the ability to detect the wide range of compounds (metals, inorganics, organics) present in polluted atmospheres. Organic aerosols of secondary origin identified by the University of Washington group--Schuetzle et al.[11,53,54] and Knights et al.[45] --are listed in Tables 3-2 and 3-3. It can be seen that most of them are difunctional compounds, most probably formed in the atmosphere by photochemical oxidation of cyclic alkenes and alkadienes. The sensitivity of the technique permits obtaining diurnal variations of primary and secondary organics from 2-h size-resolved samples. Diurnal concentration profiles of secondary organic aerosols follow ozone variations closely. Such typical profiles are illustrated for some selected compounds in Figure 3-3.

Relative Abundance of Primary and Secondary Organic Aerosols. If primary organic aerosols are preponderant in urban areas where photochemical reactions are not significant, secondary organic aerosols are predominant in photochemically polluted areas, such as the south California basin. As part of the recently completed California Air Characterization Study (ACHEX),[55,56,57] a close relation between visibility reduction and photochemical smog was observed at eight sampling locations where the extinction coefficient, b_{scat}, due to light scattering from airborne particles was measured when ozone concentration was at its maximum (Figure 3-4). Good correlations were obtained between the organic aerosol fractions,[51,58] their carbonyl infrared absorption band intensities,[51] and ozone concentrations.

With the concept of chemical-element balance developed by Friedlander,[59] secondary organic aerosols have been estimated to account for 82% and 76% of the aerosol carbon balance in 24-h and 2-h samples (Pasadena, September 29, 1973[60]). During a severe photochemical episode, secondary organics reached up to 95% of the total organics (Pasadena, July 25, 1973; maximal ozone

Table 7-1

Secondary Organic Aerosols[a]

Compounds Identified			Possible Gas-Phase Hydrocarbon Precursors
Aliphatic multifunctional compounds:			
1. $X-(CH_2)_n-Y$ (n=3,4,5):			1. Cyclic olefins 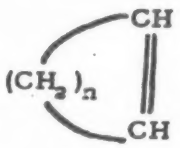 and/or diolefins $>C=CH-(CH_2)_n-CH=C<$
	X	Y	
	COOH	CH_2OH	
	COOH	COH	
	COOH	COOH	
	COOH	CH_2ONO	
	or [b]COH	CH_2ONO_2	
	COH	CH_2OH	
	COH	COH	
	COOH	COONO	
	or [b]COH	$COONO_2$	
	COH	COONO	
	COOH	$COONO_2$	
	COOH	CH_2ONO_2	
2. Others: $CH_2OH-CH=C(COOH)-CHO$ $CH_2OH-CH_2-CH=C(COOH)-CHO$ $CHO-CH=CH-CH(CH_3)CHO$ $CH_2OH-CH=CH-CH=C(CH_3)CHO$ $C_5H_8O_3$ isomers[b] Nitrocresols $C_6H_6O_2$ isomers [b]			2. Not known; possibly from aromatic ring cleavage
Aromatic monofunctional compounds:			
3. $C_6H_5-(CH_2)_n-COOH$ (n = 0,1,2,3)			3. Alkenylbenzenes $C_6H_5-(CH_2)_n-CH=CHR$; also toluene for C_6H_5COOH
4. $C_6H_5-CH_2OH$ C_6H_5CHO Hydroxynitrobenzyl alcohol			4. Toluene, styrene, other monoalkylbenzenes?
Terpene-derived oxygenates:			
5. Pinonic acid Pinic acid Norpinonic acid			5. α-Pinene
6. Isomers of pinonic acid:[b] $C_9H_{14}O_2$ isomers $C_{10}H_{14}O_3$ isomers $C_{10}H_{16}O_2$ isomers			6. Other terpenes?

---

[a] Data from Knights *et al.*;[45] compounds identified at West Covina, California, July 24, 1974.

[b] Isomers not resolved by mass spectrometry.

Table 3-3

Relative Importance of Aliphatic and Aromatic Precursors[a]

Gas-Phase Hydrocarbon Precursors	Secondary Organic Aerosols				
	X-$(CH_2)_n$-Y		Concentration,[b] µg/m^3		
	X	Y	n=3	n=4	n=5
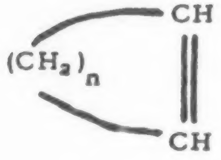	COOH	CH_2OH	2.18	3.40	0.65
	COOH	COH	1.39	2.59	0.82
	COOH	COOH	1.35	0.78	0.15
	or {COOH COH	CH_2ONO CH_2ONO_2	1.01	0.40	0.27
	COH	CH_2OH	0.31	0.40	0.13
	COH	COH	0.30	0.24	-
or/and	or {COOH COH	COONO $COONO_2$	0.14	0.24	-
	COH	COONO	1.01	0.14	-
	COOH	$COONO_2$	-	-	-
	COOH	CH_2ONO_2	0.12	0.15	-
>C=CH-$(CH_2)_n$-CH=C<	Total		7.81	8.34	2.02
	COOH-CH_2-COOH		0.15		
	COOH-$(CH_2)_2$-COOH		0.57		
	Total difunctional compounds:		18.89		
C_6H_5-CH=CHR	C_6H_5-$(CH_2)_n$-COOH		n=0:0.38 n=1:0.41 n=2:0.52 n=3:0.03		
	Total from aromatics:		1.34		

---

[a] Of aerosols in Pasadena, California, September 22, 1972; sampling period, 7:30 a.m. to 12:35 p.m. Adapted from Schuetzle *et al.*[54]

[b] The same response factor (that of adipic acid) was used for all difunctional compounds.

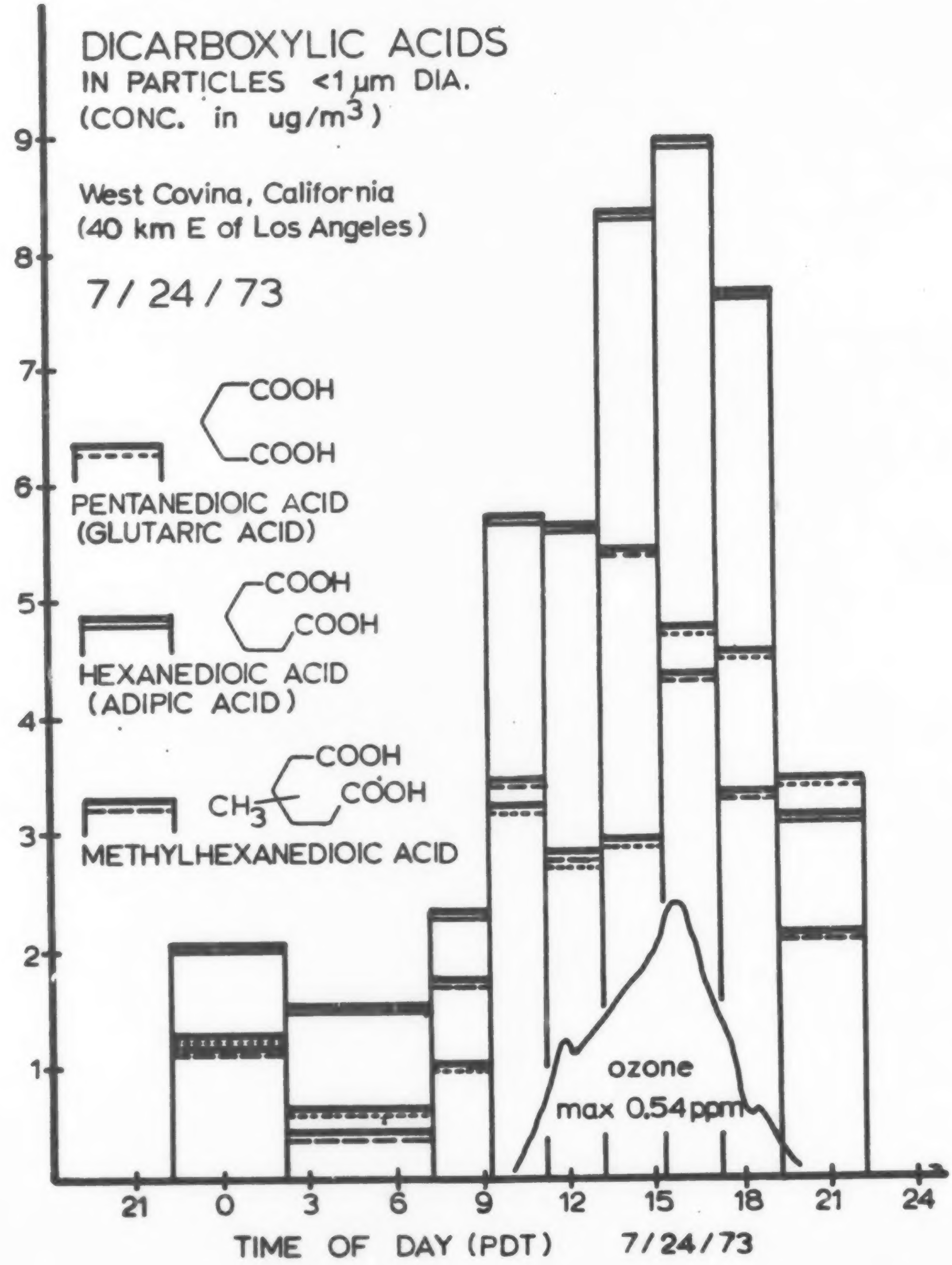

Figure 3-3. Dicarboxylic acid diurnal profiles. (Reprinted with permission from Knights et al.[45])

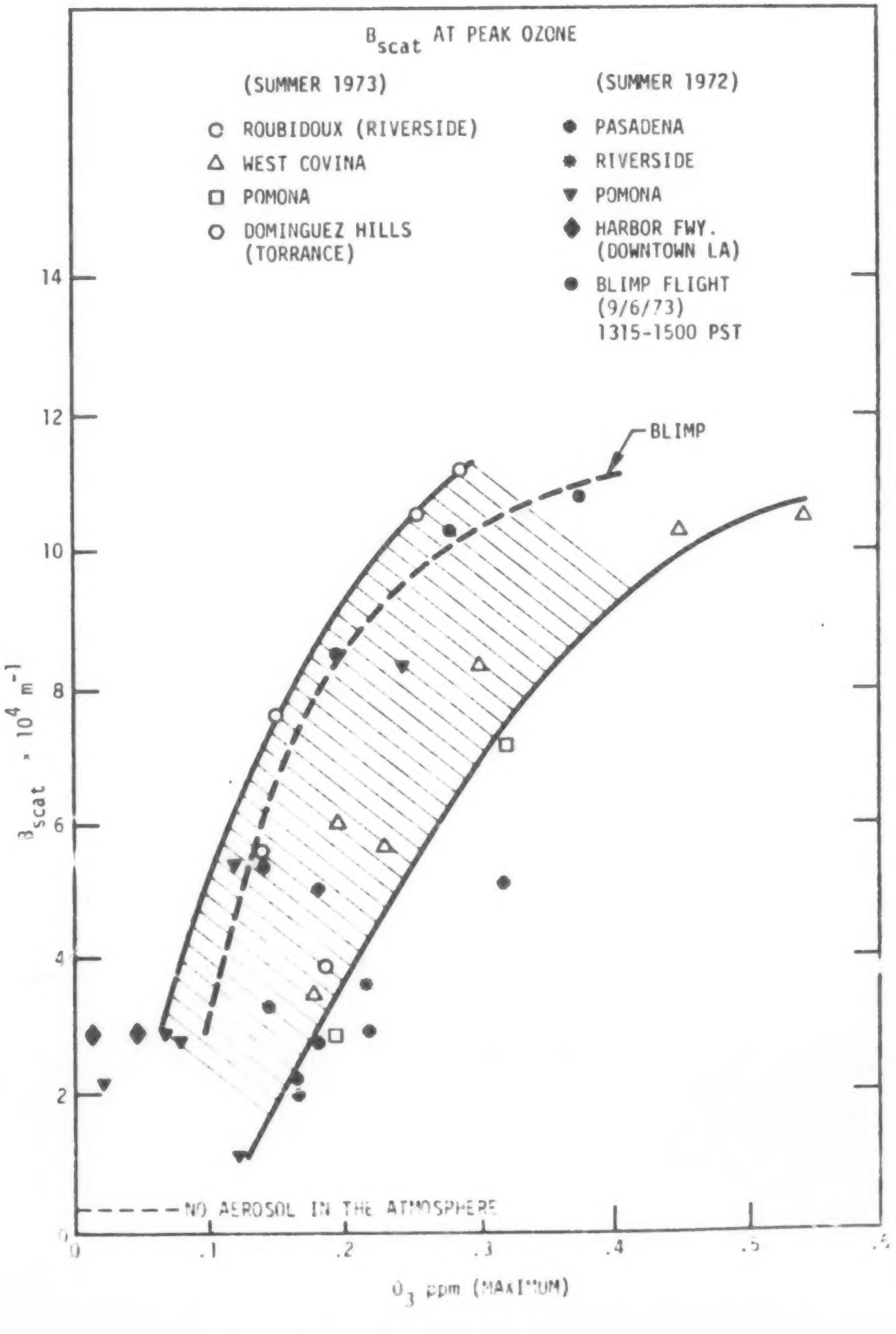

Figure 3-4. Correlation between b_{scat} and maximal ozone concentration. Based on 2-h averaged data taken in the Los Angeles area. (Reprinted with permission from Hidy et al.[56])

concentration, 0.67 ppm[51]). In such extreme situations, all secondary material resulting from gas-to-particle conversion (secondary organics plus nitrates plus sulfates) accounts for up to 95.5% of the total aerosol mass (Figure 3-5). Size distribution measurements on short-period samples, first developed by Lundgren,[61] show that difunctional compounds listed in Tables 3-2 and 3-3 accumulate in the submicrometer range[45,54] and that a significant fraction of the organic carbon is found below 0.5 µm.[55,56] These results clearly illustrate the potential health hazards associated with human exposure to high concentration ($\geq 300\ \mu g/m^3$) of respirable secondary particles during acute photochemical episodes.

Gas-Particle Distribution Factors. The extent of gas-to-aerosol conversion of secondary pollutants can be estimated by measuring gas-particle distribution factors for carbon, nitrogen, and sulfur species.[51] For example $f_C = P/(P+G)$, where P = particulate organic carbon ($\mu g/m^3$ as carbon) and G = gas-phase reactive hydrocarbons (total hydrocarbons - [methane + acetylene]) converted from ppm as methane to $\mu g/m^3$ as carbon. It can be seen from measured values of f_N, f_S, and f_C (Table 3-4) that the extent of conversion of organic gases is much lower than that of sulfur and nitrogen oxides. Similar f_N, f_S, and f_C values were calculated from ACHEX data.[56,57] The maximal f_C, measured over a 1-h period when the highest ozone concentration in several years was recorded in Pasadena, was only about 6%, and average values are in the range of 1-2%. This, combined with estimates of air-mass travel times based on air trajectory analysis,[62] provides an upper limit of about 2%/h for the ambient gas-to-aerosol conversion rate of organic gases in photochemically polluted atmospheres.[51] Although organics always account for an important

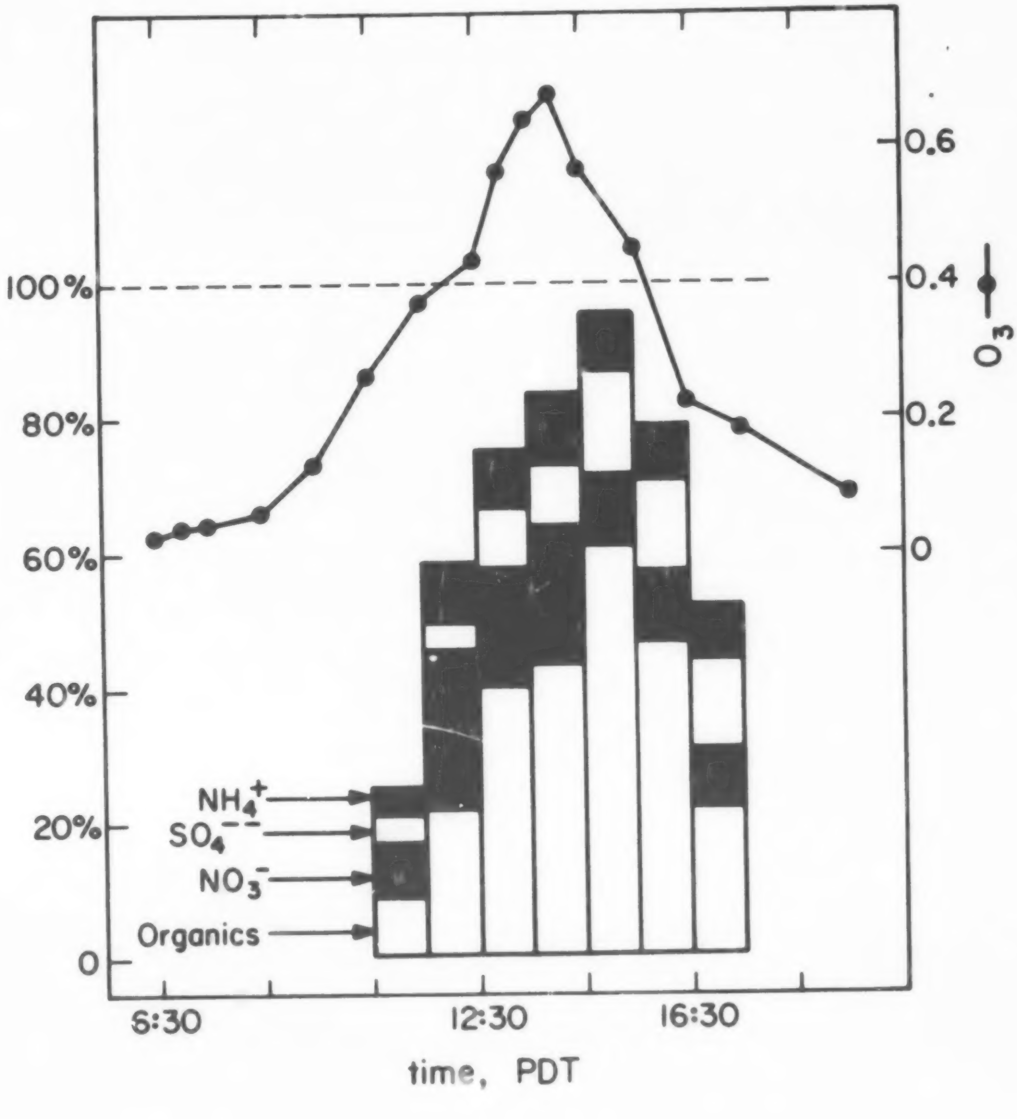

Figure 3-5. Hourly variations of secondary aerosol: organics, nitrates, sulfates, and ammonium as percent of total aerosol. Pasadena, July 25, 1973. (Reprinted with permission from Grosjean and Friedlander.[21])

Table 3-4

Gas-Particle Distribution Factors for Organics (f_C), Nitrates (f_N), and Sulfates (f_S)[a]

Sampling Date	Concentration, $\mu g/m^3$ Organics	NO_3^-	$SO_4^=$	Gas-Particle Distribution Factor f_C	f_N[b]	f_S[c]
7/12/73	22.7	3.9	49.8	0.014	0.013	—
	37.2	5.3	31.8	0.0235	0.018	0.324
	26.3	4.5	44.5	0.0175	0.017	0.333
	45.5	4.0	24.4	0.0300	0.018	0.230
	28.4	2.5	—	0.0120	0.012	—
	11.6	2.9	—	0.0090	0.015	—
7/25/73	50.5	7	—	0.020	0.019	—
	79.1	8.5	—	0.0365	0.023	—
	54.0	12	8.6	0.029	0.041	0.16
	20.0	19.7	10.7	0.009	0.074	0.13
	47.0	50	9.2	0.021	0.165	0.18
	118.5	53	24.4	0.0385	0.152	0.36
	132.5	64	27.7	0.0515	0.168	0.37
	141.0	25.4	34.1	0.0615	0.077	0.39
	85.6	19.5	24.4	0.0495	0.061	0.25
	28.7	11.2	18.5	0.020	0.037	0.26
	37.3	5.0	—	0.0235	0.019	—
10/17/73	16.6	6.3	10.3	0.0042	0.012	0.393
	15.1	3.8	9.0	0.0079	0.011	0.171
	43	14.3	12.2	0.0205	0.032	0.466
	15.1	1.8	5.4	0.0088	0.007	0.297
	8.1	4.0	—	0.0066	0.017	—

---

[a] Data from Grosjean and Friedlander.[51] Sampling in Pasadena. Sampling time: 7/12, 8:00-12:00, 12:00-14:00, 14:00-16:00, 16:00-18:00, 18:00-20:00, and 20:00-24:00; 7/25, 1 h 7:30-17:30, last sample 17:30-19:30; 10/17, 8:00-10:00, 10:00-12:00, 12:00-13:00, 13:00-15:00, and 15:00-17:00.

[b] $f_N = [NO_3^-]_P/[NO_3^-]_P + [NO_x]_G$; units, $\mu g/m^3$ as NO_2.

[c] $f_S = [SO_4^=]_P/[SO_4^=]_P + [SO_2]_G$; units, $\mu g/m^3$ as SO_2.

$[X]_P$ = particulate-phase concentration; $[X]_G$ = gas-phase concentration fraction of urban aerosols, only a small fraction of the organic gas is converted to particulate material. This, and the fact that most of the secondary organics identified in ambient aerosols are difunctional compounds that can be formed from a few possible precursors (such as cyclic olefins and diolefins), leads us to review next data obtained in smog-chamber studies of organic aerosol formation from olefinic and other hydrocarbons.

Smog-Chamber Studies

Since the pioneering work of Haagen-Smit and co-workers more than three decades ago,[63] the chemistry of polluted air has been simulated in laboratory studies and a good understanding of the reactions occurring in the complex atmospheric mix has been gained by investigating the behavior of simple pollutant mixtures under controlled conditions. However, aerosol formation in smog-chamber experiments has not been studied as much as gas-phase photochemistry. In most studies, aerosol formation was observed only by monitoring the light-scattering increase during the experiment, and aerosol chemical composition was not sought. Moreover, a quantitative comparison of data obtained by all investigators is practically impossible, in view of the differences in smog-chamber design and material, mode of irradiation, initial reactant concentrations, available instrumentation, etc. Systems investigated included ozone-hydrocarbon reactions in the dark, in irradiated mixtures of hydrocarbon with nitric oxide or nitrogen dioxide or both, in "clean" air, in ambient air, and with or without addition of sulfur dioxide, water, and ammonia. Over compounds that have been investigated are listed in Table 3-5.[52,64-100]

Table 3-5

Compounds Investigated in Smog-Chamber Studies, with References

I. OLEFINS

Alkenes:

Ethylene	65,66,68,69,73,75,79,88,89,91.
Propylene	69,70,73,79,86,90,91,95,96.
1-Butene	68,70,75,80,84,87,88,89,95,99.
cis- and *trans*-2-Butene	65,66,68,70,72,85,97.
Isobutene	65,66,68,69,70.
2-Methyl-1-butene	70
2-Methyl-2-butene	65,66,67,70,88,89,90.
3-Methyl-1-butene	68,70.
1-Pentene	65,66,68,70,74,88,89.
cis- and *trans*-2-Pentene	68,70,85,90.
1-Hexene	64,68,70,72,74,77,80,82,85,87,95,98
cis- and *trans*-2-Hexene	68,70,82.
2-Methyl-1-pentene	85
4-Methyl-1-pentene	70,90.
cis-3-Methyl-2-pentene	68
2,3-Dimethyl-2-butene	65,66,69,70,100.
1-Heptene	52,72,79,84,88,89,94.
cis- and *trans*-3-heptene	68,72,79,88,89.
5-Methyl-1-hexene	94
1-Octene	76,79,81,94,95.
trans-4-Octene	94
2,4,4-Trimethyl-1-pentene(isooctene)	68,79.

Table 3-5 (Cont.)

Compounds Investigated in Smog-Chamber Studies, with References

1-Decene	95
1-Dodecene	95,98.
Cyclic Olefins:	
Cyclopentene	68,79,100.
Cyclohexene	52,64,65,66,68,72,79,81,82,88,89,92,94,95,98,100.
Diolefins:	
1,3-Butadiene	65,66,68,75,79.
Isoprene	79
1,3-Hexadiene	98
1,5-Hexadiene	68,82,94,98.
1,6-Heptadiene	94
2-Methyl-1,5-hexadiene	94
1,7-Octadiene	94,100.
2,6-Octadiene	94
Dicyclopentadiene	68
Other Olefins:	
Indene	94
Turpentine	81
Styrene	79
α-Pinene	52,78,79,82,92,94,98.

Table 3-5 (Cont.)

Compounds Investigated in Smog-Chamber Studies, with References

II.	PARAFFINS	
	Methane	65,66,79.
	Cyclopropane	68
	n-Butane	68,88,89.
	n-Pentane	65,66.
	2,2-Dimethylpropane	65,66.
	Cyclopentane	65,66.
	2-Methylbutane	65,66,68,89.
	2-Methylpentane	68
	3-Methylpentane	75
	n-Hexane	75
	Cyclohexane	68,75,82,88,89.
	2,4,4-Trimethylpentane (isooctane)	75,79,84,88,89.
	2,6-Dimethylheptane	94
III.	ACETYLENIC	
	1-Butyne	65,66.
IV.	AROMATICS	
	Benzene	65,66,71,79,81,88,89,93.
	Toluene	52,65,66,71,75,80,81,82,83,84,88,89,92,93,98,100,147.
	o-, m-, and p-Xylene	65,66,71,75,81,88,89,93,94,98,147.
	Ethylbenzene	65,66,71,79,94.

Table 3-5 (Cont.)

Compounds Investigated in Smog-Chamber Studies, with References

	1,3,5-Trimethylbenzene (mesitylene)	71,72,75,79,80,88,89,94.
	Isopropylbenzene	71,81.
	1,2,4-Trimethylbenzene	71
	1,2,3-Dimethylbenzene	71
	3-Ethyltoluene	71
	1,2-Diethylbenzene	88,89.
	tert-Butylbenzene	88,89.
	n-Butylbenzene	88,89.
	1,4-Diethylbenzene	71
	1,2,3,5-Tetramethylbenzene	71
V.	ALDEHYDES	
	Formaldehyde	75
	Propionaldehyde	75
	Hexanal	88,89.
	Heptanal	147
	Benzaldehyde	81
	Glutaraldehyde	94
VI.	KETONES	
	Mesityl oxide	83
	Isophorone	83
	Methylisobutylketone	83
	Cyclohexanone	82

Aerosol Formation from Different Types of Hydrocarbons. Extensive discussion of data represented in Table 3-5 is beyond the scope of this review, and only the most important aspects of aerosol formation are reported here and in the next few sections. Many of the conclusions presented thereafter were reached in the early studies reported by the Stanford Research Institute, Air Pollution Foundation, and Franklin Institute groups.[64-69,101-103] Results obtained in the presence of sulfur dioxide are discussed toward the end of this chapter.

In the absence of sulfur dioxide, aerosol formation depends strongly on the type of hydrocarbon precursor studied. The following qualitative trends are observed:

- Most paraffins do not generate aerosol, even when irradiated at high concentrations. However, some aerosol can be formed from the more "reactive" branched paraffins having more than six carbon atoms (such as isooctane) after long irradiation periods.
- Acetylenics do not form aerosol.
- All unsaturated compounds can form organic aerosol when reacting with ozone at high concentrations, as observed by Cvetanovic.[70] However, studies conducted at much lower alkene concentration (1-10 ppm) show a marked effect of alkene chain length on aerosol formation. Alkenes with fewer than six carbon atoms do not form aerosol; those with six or more carbon atoms form aerosol when they yield (after rupture of the double bond) a fragment with at least five carbon atoms. For example, 1-heptene forms much more aerosol than 3-heptene, and 2,4,4-trimethyl-1-pentene (isooctene) forms more aerosol than its isomer trans-4-octene.

Amounts of aerosol formed from 1-alkenes increase regularly with the number of carbon atoms (Figure 3-6).

- Cyclic olefins and diolefins form much more aerosol than 1-alkenes that have the same number of carbon atoms (for example, cyclohexene >> 1-hexene, and 1,7-octadiene >> 1-octene). The same effect of chain length and double-bond position is observed for diolefins (1,7-octadiene > 1,6-heptadiene > 1,5-hexadiene, and 1,7-octadiene >> 2,6-octadiene). Heavier unsaturated cyclic compounds, such as indene and terpenes, form even more aerosol.

- Conflicting results have been reported for aromatic compounds. Aerosol formation has been reported from benzene, toluene, and other alkylbenzenes by several investigators,[88,92,93] whereas no aerosol formation was observed in other studies.[66,94,100] This merits further investigation, in view of the large fraction of aromatic hydrocarbons present in polluted atmospheres.

- Carbonyl compounds (ketones, C_{1-7} aldehydes, dialdehydes) do not generate aerosol.

- Data on aerosol formation from irradiated automobile exhaust[88,101-105] confirm the marked sensitivity to hydrocarbon type observed in individual hydrocarbon studies. Aerosol formation increases with the olefinic[103] and aromatic[105] fuel content. However, changes in mode of engine operation (acceleration, idle) and inorganic variables (sulfur dioxide, relative humidity) have a more pronounced effect on aerosol formation than change in fuel composition.[88]

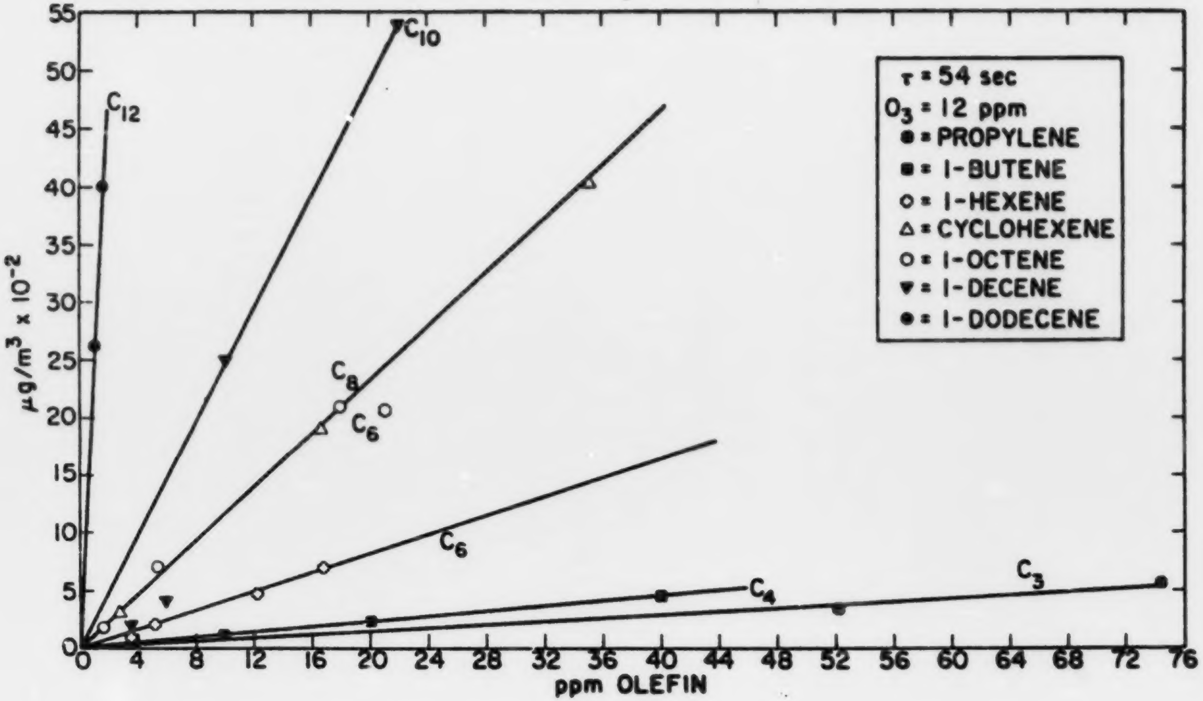

Figure 3-6. Mass concentration of aerosol formation from olefin-ozone reaction as a function of olefin concentration. τ , residence time in the flow reactor. (Reprinted with permission from Burton et al.[95])

Photochemical Reactivity and Aerosol Formation Ability. We have listed in Table 3-6 the relative rates of conversion of nitric oxide to nitrogen dioxide measured by Glasson and Tuesday[106] and the amounts of aerosol formed, relative to cyclohexene, from data of Renzetti and Doyle,[66] Prager *et al.*,[68] Groblicki and Nebel,[79] Wilson *et al.*,[88,89] O'Brien *et al.*,[94] and Grosjean[100] for different types of hydrocarbon precursors. Table 3-7 summarizes the experimental conditions for data presented in Table 3-6. As mentioned before, data reported by these investigators are in good qualitative agreement for all precursor classes except aromatics. It is clear from the data in Table 3-6 that there is no straightforward relation between the amount of aerosol formed and the gas-phase photochemical reactivity of the various precursors. The overall hydrocarbon photochemical reactivity is a complex function of the rate constants of reaction with various species (ozone, oxygen atom, hydroxyl and hydroperoxy radicals, other free radicals) during the photooxidation process. Therefore, relative rates of hydrocarbon decay, of ozone (or oxidant) formation, or of conversion of nitric oxide to nitrogen dioxide can be used as empirical photochemical reactivity (PR) indexes. As we will see in a more quantitative manner later, the ability of a given hydrocarbon to form aerosol depends on the *nature* of the products formed (chemical dependence) and on their *volatility* (physical dependence), and an aerosol formation ability (AFA) index can be derived from physical and chemical aerosol data. Therefore, the amount of aerosol formed appears to be the product of two terms:

$$[\text{aerosol}] = (\text{photochemical reactivity}) \times (\text{aerosol formation ability}).$$

Table 3-6

Aerosol Formation and Gas-Phase Reactivity

Precursor	Aerosol Formation Ability[a]											Gas-Phase Reactivity[a,h]
	Without Sulfur Dioxide						With Sulfur Dioxide					
	b	*c*	*d*	*e*	*f*	*g*	*b*	*c*	*d*	*e*	*g*	
I. **OLEFINS**												
Alkenes:												
Ethylene	0	2.8	-	-	-	-	12.6	63	44	1	-	48.5
Propylene	-	-	12.4	-	-	-	-	-	69	-	-	100
1-Butene	-	1.4	-	-	-	-	-	81	-	1	-	83
cis-2-Butene	-	1.4	-	-	-	-	-	86				202
trans-2-Butene	0						144		-	-	-	320
Isobutene	0	0	-	-	-	-	40	-	-	-	-	100
2-Methyl-2-butene	3.6	-	-	-	-	-	96	-	-	2.6	-	543
3-Methyl-1-butene	-	2.8	-	-	-	-	-	-	-	-	-	77
1-Pentene	0.9	2.8	-	-	-	-	96	87	-	2.7	-	60
cis- and *trans*-2-Pentene	-	0	-	-	-	-	-	86	-	-	-	187
1-Hexene	-	1.4	-	-	-	-	-	96	-	-	-	48.5
cis- and *trans*-2-Hexene	-	7	-	-	-	-	-	86	-	-	-	171 (trans)
cis-3-Methyl-2-pentene	-	5.6	-	-	-	-	-	-	-	-	-	-
2,3-Dimethyl-2-butene	2.7	-	-	-	-	0	100	-	-	-	-	10^3
1-Heptene	-	-	10.5	≈0	1	-	-	-	-	6.5	-	43
cis- and *trans*-3-Heptene	-	12.6	0	-	-	-	-	96	-	11.7	-	134 (trans)
5-Methyl-1-hexene	-	-	-	-	1	-	-	-	-	-	-	-

Table 3-6 (Cont.)

Aerosol Formation and Gas-Phase Reactivity

	Aerosol Formation Ability[a]											
	Without Sulfur Dioxide						With Sulfur Dioxide					
Precursor	*b*	*c*	*d*	*e*	*f*	*g*	*b*	*c*	*d*	*e*	*g*	Gas-Phase Reactivity[a,h]
1-Octene	-	-	-	-	1	-	-	-	88	-	-	42.8
trans-4-Octene	-	-	-	-	1	-	-	-	-	-	-	94.5
Isooctene	-	94	28	-	-	-	-	94	81	-	-	-
Cyclic Olefins:												
Cyclopentene	-	75	58	-	-	-	-	-	-	-	-	657
Cyclohexene	100	100	100	-	100	100	107	100	91	100	-	100
α-Pinene	-	-	140	-	200	-	-	-	137	-	-	-
Diolefins:												
1,3-Butadiene	3.6	33	-	-	-	-	150	91	85	-	-	123
Isoprene	-	-	-	-	-	-	-	-	75	-	-	106
1,5-Hexadiene	-	104	-	-	45	-	-	111	-	-	-	-
1,6-Heptadiene	-	-	-	-	178	-	-	-	-	-	-	-
2-Methyl-1,5-hexadiene	-	-	-	-	122	-	-	-	-	-	-	-
1,7-Octadiene	-	-	-	-	200	-	-	-	-	-	-	-
2,6-Octadiene	-	-	-	-	1	-	-	-	-	-	-	-
Dicyclopentadiene	-	124	-	-	-	-	-	111	-	-	-	-

Table 3-6 (Cont.)

Aerosol Formation and Gas-Phase Reactivity

	Aerosol Formation Ability[a]											
	Without Sulfur Dioxide						With Sulfur Dioxide					Gas-Phase Reactivity[a,h]
Precursor	*b*	*c*	*d*	*e*	*f*	*g*	*b*	*c*	*d*	*e*	*g*	
II. **PARAFFINS**												
Methane	0	-	-	-	-	-	0	-	25	-	-	2.86
•Cyclopropane	-	4.3	-	-	-	-	-	-	-	-	-	-
n-Butane	-	-	-	-	-	-	-	2.8	-	.55	-	21.2
n-Pentane	0	-	-	-	-	-	0	-	-	-	-	26.5
2,2-Dimethylpropane	0	-	-	-	-	-	0	-	-	-	-	10.0
Cyclopentane	0	-	-	-	-	-	0	-	-	-	-	26.2
2-Methylbutane	0	-	-	-	-	-	0	-	-	.65	-	28.0
2-Methylpentane	-	-	-	-	-	-	-	0	-	-	-	26.8
Cyclohexane	-	0	-	-	-	-	-	-	-	1.4	-	27.6
Isooctane	-	-	6.2	-	-	-	-	-	12.4	.25	-	21.1
2,6-Dimethylheptane	-	-	-	-	1	-	-	-	-	-	-	-
III. **AROMATICS**												
Benzene	0	-	10.5	-	-	-	4.5	-	-	10.8	-	9.4
Toluene	0	-	-	8.5	-	0	9	-	-	8.6	-	37.2
o-Xylene	-	-	-	-	9	-	-	-	-	-	-	74.5
m-Xylene	-	-	-	-	-	-	-	-	-	29.4	-	106
p-Xylene	0	-	-	-	-	-	0	-	-	-	-	60
Ethylbenzene	0	-	-	-	1	-	12.6	-	69	-	-	34.3
Mesitylene	-	-	-	9	1	-	-	-	50	9.0	-	146

Table 3-6 (Cont.)

Aerosol Formation and Gas-Phase Reactivity

Precursor	Aerosol Formation Ability[a]											Gas-Phase Reactivity[a,h]
	Without Sulfur Dioxide						With Sulfur Dioxide					
	b	*c*	*d*	*e*	*f*	*g*	*b*	*c*	*d*	*e*	*g*	
1,2-Diethylbenzene	-	-	-	-	-	-	-	-	-	23.4	-	48.5
tert-Butylbenzene	-	-	-	-	-	-	-	-	-	24.4	-	16.8
n-Butylbenzene	-	-	-	-	-	-	-	-	-	22.2	-	-
IV. ALDEHYDES												
Hexanal	-	-	-	-	-	-	-	-	-	0	-	-
Heptanal	-	-	-	-	0	-	-	-	-	-	-	-
Glutaraldehyde	-	-	-	-	0	-	-	-	-	-	-	-
V. ACETYLENIC												
1-Butyne	0	-	-	-	-	-	0.9	-	-	-	-	-

---

[a] Relative to cyclohexene = 100.
[b] Data from Renzetti and Doyle, ref. 66
[c] Data from Prager *et al*., ref. 68
[d] Data from Groblicki and Nebel, ref. 79
[e] Data from Wilson *et al*., ref. 88,89
[f] Data from O'Brien *et al*., ref. 94
[g] Data from Grosjean *et al*., ref. 100
[h] Data from Glasson and Tuesday, ref. 106; nitric oxide photooxidation rates.

Table 3-7

Experimental Conditions in Smog-Chamber Studies

Smog Chamber	Renzetti and Doyle[66]	Prager et al.[68]	Groblicki and Nebel[79]	Wilson et al.[88,89]	O'Brien et al.[94]	Grosjean et al.[100]
Material	Pyrex	Glass	Stainless steel	Glass	Glass	Teflon
Volume	50 liters	640 liters	300 ft^3	200 liters	1,100 ft^3	80 m^3
Irradiation	Mercury lamps	Mercury lamps	Fluorescent tubes	Black fluorescent lamps	Black fluorescent lamps	Solar
Diluent gas	Clean air	Air	Clean Air + CO at 50 ppm	Clean air	Clean air	Ambient air
Hydrocarbon impurities	?	?	<0.6 ppm as hexane	Produce ozone at $\leq$3 ppb	Nonmethane hydrocarbon at 1 ppb	Ambient (high)
Reactor type	Stirred flow	Stirred flow and batch	Batch	Flow	Batch	Batch
Stirring	Yes	Yes	Yes	No	No	No
Temperature	Ambient	Ambient	95 F	82 F	22 C	Ambient
Initial Concentrations						
Hydrocarbon, ppm	3	10	4	3	2	1
Nitric oxide, ppm	1	0	2	0.37	1	0.33
Nitrogen dioxide, ppm	0	5	0	0.37	0	0.16
Sulfur dioxide (when added), ppm	0.1-0.6	2	1	0.1	Not studied	0.04
Water	50% relative humidity	100 ppm	3 torr	50% relative humidity	70% relative humidity	Ambient, 35% relative humidity
Aerosol Measurement	*a*	*b*	*b*	*b*	*c*	*c*

---

[a] 90° light scattering relative to air

[b] Sinclair Phoenix forward scattering smoke photometer (logarithmic, 1 unit reading increase = mass x 10 increase)

[c] b_{scat}, integrating nephelometer (linear, reading proportional to mass)

Bearing in mind that product volatility decreases regularly when the size of the hydrocarbon precursor increases, this provides a rational approach for a qualitative estimate of aerosol formed from any type of precursor. Aerosol formation can be "PR-controlled" (paraffins, acetylenics; PR = 0) or "AFA-controlled" (low-molecular-weight alkenes, carbonyl compounds; high PR, but AFA = 0). In the same way, aerosol formation from 1-alkenes having similar PR is controlled by their AFA factor, which increases with chain length; whereas relative amounts of aerosol formed from hydrocarbons leading to products of similar volatility (for example, *n*-heptane, toluene, and 1-heptene, with similar AFA factors) are controlled by their relative gas-phase reactivities. Therefore, hydrocarbons providing the bulk of secondary organic aerosols in the atmosphere are not necessarily those prevailing in oxidant formation. An important consequence is that control of atmospheric organic aerosol concentrations can be achieved by two types of control strategies: *specific* control of precursors with high AFA may prove to be as efficient as *total* hydrocarbon and nitrogen oxides emission control.

Application of Smog-Chamber Data to the Atmosphere. Many difficulties arise in the application of laboratory data to the more complex atmospheric processes. This is illustrated by the following examples:

- Depending on meteorologic conditions, aerosol formation in the atmosphere is better approximated, but never fully simulated, by smog-chamber studies under either static (batch-reactor) or dynamic (flow-reactor) conditions.

- Small differences in light sources have definite effects on photochemical processes. Some irradiation systems match the solar spectrum poorly, thus affecting the relative importance of the various photodissociation processes occurring in the atmosphere.[107] Ambient variations in the nitrogen dioxide photolysis pseudo-first-order rate constant, K_d, are difficult to reproduce with artificial irradiation systems. "Transparent" smog-chamber materials, such as fluoroolefinic polymers, fail to transmit the entire solar radiation: Mylar absorbs strongly in the < 3300 Å region,[108] and Teflon shows a pronounced decrease in transmission, owing to aging.[100,109] Different smog profiles were obtained when identical experiments were conducted in aluminum, stainless steel, Pyrex, and Teflon smog chambers.[107] Furthermore, a so-called inert material, such as Teflon, reacts with ozone.[71,110]

- Mechanical stirring dramatically inhibits aerosol formation,[80] and data obtained in smog chambers equipped with stirring accessories are questionable.

- Significant aerosol losses on the walls are observed in smog chambers with high surface:volume (S:V) ratios. Typical smog chambers have S:V ratios of around 3:1 to 5:1 m^{-1}. Although wall losses are minimized in bigger smog chambers, with S:V ratios of 0.1:1 to 1:1 m^{-1} range, this is still much higher than typical ambient S:V values. For example, a typical ambient concentration of 150 $\mu g/m^3$ corresponds to an S:V ratio of about 9×10^{-4}:1 m^{-1} (assuming a density of 1 and a diameter of 1 μm). Formation of water layers on the smog-chamber walls would promote heterogeneous reactions and thus affect the chemical composition of the aerosol formed. Nitric oxide and, to a lesser extent, nitrogen dioxide are poorly soluble in water, whereas sulfur dioxide and nitrogen pentoxide are readily soluble and their liquid-phase oxidation to form sulfate and nitric acid, respectively, is quite significant.

- Errors may be due to the instrumentation itself. Improper calibration of condensation nuclei counters may lead to poor nuclei concentration data.[111] In many experiments, the aerosol mass concentration was deduced from the light-scattering measurements by using Charlson's relation,[112] which was established from data on ambient, well-aged aerosols. Use of this relation is questionable for automobile exhaust data,[105,169] and it does not apply to fresh aerosols generated in smog chambers.[94,100] Interference due to ozone and to nitrogen-containing compounds has been reported when nitrogen oxide concentrations have been measured by the colorimetric[113] and chemiluminescence[114] techniques. Significant differences have been observed in the measurement of ozone by different techniques, and a standard procedure has been recently recommended.[115]

- Use of clean air, although important for obtaining quantitative gas-phase data, would favor homogeneous nucleation to the detriment of the heterogeneous process, which is preponderant in the polluted atmosphere, thus providing aerosol kinetic and growth data of questionable significance. Moreover, the background composition of individual hydrocarbons in clean air is generally not specified, and only an upper limit of "total hydrocarbon" concentration is provided. Therefore, a significant fraction of the nuclei formed may well originate from a few C_{6+} alkenes or cyclic olefins present as traces in the hydrocarbon background.

- Because of the abundance of smog-chamber data on homogeneous gas-phase photochemical reactions, the possible importance of heterogeneous reactions in the formation of organic aerosols has been somewhat overlooked. However, reactions in the liquid phase and reactions catalyzed by airborne particles containing metals, oxides, and salts--similar to the reactions occurring in the well-known heterogeneous oxidation of sulfur dioxide--may be of some importance. As demonstrated by Judeikis and Siegel,[116] heterogeneous reactions can compete with and, under favorable conditions, outweigh the homogeneous gas-phase reactions that are usually considered to be important. Free radicals (hydroxyl, hydroperoxy, and so on) may be efficiently trapped by aerosol particles and react further in the particle-water layer[117] or at the particle surface.[118] These reactions have been incorporated in a recent mathematical simulation study.[117]

We have seen that aerosol data obtained in environmental chambers may be seriously affected by many empirical characteristics, such as smog-chamber design and materials, stirring, mode of irradiation, and wall losses. Moreover, only homogeneous systems have been studied, and the importance of heterogeneous organic reactions is not assessed. Therefore, caution must be exercised when extrapolating smog-chamber data to atmospheric processes.

Chemical Composition of Model Aerosols

As mentioned earlier, there is little information on the chemical composition of "model" organic aerosols generated from a single hydrocarbon in a smog chamber. Prager *et al.*[68] and Endow *et al.*[69] reported the presence of absorption bands due to carbonyl, carboxylic acid, and nitrate ester groups in the infrared spectra of aerosols produced from various olefins. In their study of the gas-phase olefin-ozone reaction at high concentrations, Vrbaski and Cvetanovic[119] reported the formation of aerosols that initially had a peroxidic character and whose later decomposition produced carbonyl compounds identified by gas chromatography. Kopzcynski[71] reported absorption bands due to carbonyl, hydroxyl, nitrate ester, and nitro groups in the infrared spectra of aerosol generated from mesitylene at 25 ppm. Barlage and Alley[74] studied, by mass spectrometry, aerosols formed from 1-pentene and 1-hexene at 10 ppm. They found peaks corresponding to masses in the range 120-160 a.m.u., indicating the presence of polymeric material. Groblicki and Nebel[79] and Ripperton *et al*.[82] reported similar infrared spectra for α-pinene aerosol generated by either dark reaction with ozone or irradiation with nitrogen oxides. Infrared spectra of α-pinene, 1-hexene, and dodecene aerosols were recently reported by Lipeles.[98] Chu and Orr[93] studied aerosols formed from benzene, toluene, and *o*-xylene and found similarities between *o*-xylene aerosol and diethylphthalate (infrared spectra) and between benzene aerosol and such aromatic ketones as fluorenone (mass spectra). O'Brien *et al*.[94] reported carbonyl, hydroxyl, carboxyl, and nitrate ester absorption bands in the infrared spectra of 1-octene and 1,7-octadiene aerosols and found that infrared spectra of indene aerosol resembles that of homophthalic acid, an expected product of indene photooxidation. Paper chromatography indicated the presence of several carboxylic acids in the 1-octene aerosol and the presence of acidic difunctional compounds (α, ω diacids, α, ω acid nitrate, and other ω-substituted acids) in the 1,7-octadiene aerosol. Some ammonium nitrate was found, indicating that nitric acid was formed photochemically. The molecular weight of 1,7-octadiene aerosol was determined, and its value[256] indicates that the difunctional compounds are present as dimers, or possibly higher polymers, in the aerosol.

This survey shows that highly oxygenated compounds (carbonyls, acids, nitrate esters) constitute the bulk of model organic aerosols, and that smog-chamber data on chemical composition are in qualitative agreement with atmospheric observations. However, positive identification of individual organic compounds present in model aerosols cannot be achieved from infrared, carbon-hydrogen-nitrogen, and paper-chromatography analysis or from limited mass-spectrometry data. Only since 1973 have firm product identifications been reported. Lipeles _et_ _al_.[87] and Schulten and Schurath[99] studied the composition of aerosol from the reaction of ozone with 1-butene. Aerosol composition from irradiation of nitrogen oxides with cyclohexene, toluene, and α-pinene was reported by Schwartz,[92] and with cyclopentene, cyclohexene, and 1,7-octadiene, by Grosjean.[100] Mass spectrometry was used in these four studies.

Ozone-1-Butene Aerosol. The Rockwell study[87] was conducted in a flow reactor with a dry nitrogen stream and typical residence times of 20-60 s. Freshly collected aerosol showed a marked peroxidic character, but would no longer oxidize iodide after several days. Polarographic analysis confirmed the presence of peroxides. Aerosol composition was obtained by a combination of gas chromatography and electron-impact mass spectrometry. Schulten and Schurath[99] also used a flow-reactor system coupled with a high-resolution-field desorption mass spectrometer.

Hydrogen peroxide was positively identified. Other peroxides may have been present, but would decompose at the low (≈ 10^{-5} torr) pressure in the ion source of the mass spectrometer. The complete data are listed in Table 3-8. Aldehydes, ketenes, and C_{1-4} monocarboxylic acids were identified. Schulten and Schurath observed many unidentified complex ions in the higher mass region and postulated the presence of aggregates of aldehydes and acids held together by strong hydrogen bonds. This assumption is consistent with the release of carbonyl compounds observed by Cvetanovic when aerosols generated from alkenes decompose during gas-chromatography analysis.

NO_x-Toluene Aerosol. This system was studied by Schwartz.[92] Toluene at 10 ppm, nitric oxide at 1 ppm, and nitrogen dioxide at 1.2 ppm were irradiated with ultraviolet lamps in a 17-m^3 batch reactor for 270 min. Collected aerosols were successively extracted with methylene chloride and then methanol. The methylene chloride extract was fractionated into water-soluble and water-insoluble material, and the latter fraction was further divided into acidic, neutral, and basic fractions. The acidic and neutral fractions were analyzed by gas chromatography and chemical-ionization mass spectrometry; the compounds identified are shown in Figure 3-7. The two analyzed fractions represented only about 5.5% of the total aerosol mass. It is noteworthy that "classical" nitration of an aromatic ring appears to be an important process during aerosol formation and that both the alkyl group and the aromatic ring undergo attack by oxidizing species, thus leading to polyfunctional compounds of very low volatility.

Table 3-8

Composition of Aerosol from the Reaction of Ozone and 1-Butene

Identified by Lipeles et al.[87]	Identified by Schulten and Schurath[99]
Carbon dioxide	Formaldehyde
Ethane	Hydrogen peroxide
Water	Ketene
Formaldehyde	Acetaldehyde
Methanol	Formic acid
Acetaldehyde	Methylketene
Formic acid	Propionaldehyde
Propionaldehyde	Acetic acid or methylformate
Acetic acid	Ethylketene
Propionic acid	Alcohol (tentative)
Other unidentified trace	Butyraldehyde or ether, C_4H_8O
Compounds	Propionic acid
	Formic acid-formaldehyde cluster, $C_2H_4O_3$
	Butanoic acid
	Butanoic acid - water
	$C_2H_4O_4$: dimer of formic acid or dimer zwitterion
	$C_4H_8O_3$: ozonide
	+ Unidentified peaks from m/e=105 to m/e=199 ($C_xH_yO_z$ with x=3 - 8, y=5 - 13, z=2 - 6), presumably from condensates or aggregates of aldehydes and acids held together by strong hydrogen bonds

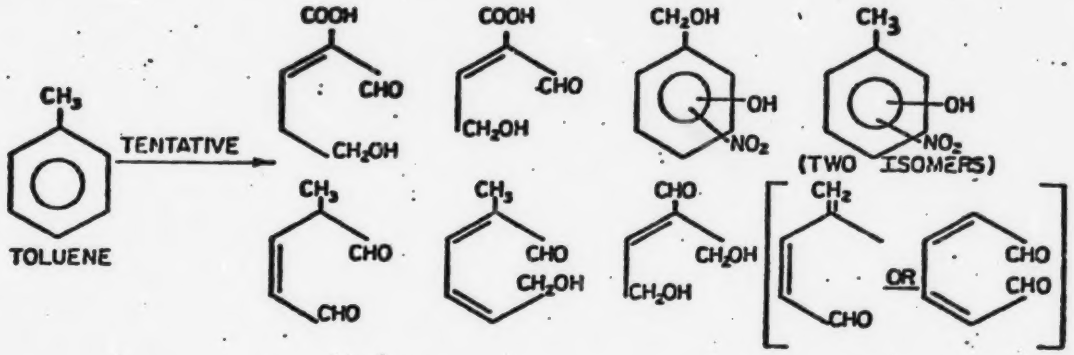

CH3
TOLUENE
TENTATIVE
COOH
CHO
CH2OH
COOH
CHO
CH2OH
CH2OH
OH
NO2
CH3
OH
NO2
(TWO ISOMERS)
CH3
CHO
CHO
CH3
CHO
CH2OH
CHO
CH2OH
CH2OH
CH2
CHO
OR
CHO
CHO

Figure 3-7. Composition of aerosol from the reaction of NO_x and toluence (according to Schwartz, ref. 92).

Aerosols from Cyclic Olefins and Diolefins. Data on cyclohexene and α-pinene aerosols were reported by Schwartz[92] after a preliminary report from the Battelle Institute group.[52] The experimental conditions and analytic techniques were identical with those just described for the toluene aerosol study. Here again, only the methylene chloride-soluble, water-insoluble fractions were studied. They accounted for about 7% and 65% of the total aerosol mass generated from cyclohexene and α-pinene, respectively. Grosjean[100] reported chemical composition of cyclopentene, cyclohexene, and 1,7-octadiene aerosols. Experiments were conducted in an 80-m^3 Teflon smog chamber filled with ambient air, with irradiation by sunlight. Typical initial concentrations were 1 ppm for hydrocarbon, 0.33 ppm for nitric oxide, and 0.16 ppm for nitrogen dioxide. Aerosols were extracted after collection and analyzed without further fractionation by combined gas chromatography and electron-impact mass spectrometry, and by combined gas chromatography and chemical-ionization mass spectrometry. Data obtained by Schwartz and Grosjean are listed in Figure 3-8 and Table 3-9. Most of the products are difunctional compounds bearing in many cases a carboxylic acid group. The ethylenic bond is retained in some compounds, indicating free-radical attack on the aliphatic chain. Good agreement is observed in the case of cyclohexene (the only compound common to the two studies), except for adipic acid, which was not reported by Schwartz, but was the major aerosol compound in Grosjean's study. However, adipic acid would not be expected to be present in the methylene chloride-soluble, water-insoluble fraction analyzed in the former study. Data for the 1,7-octadiene aerosol are also in good agreement with those obtained by O'Brien[94] by infrared and paper chromatography.

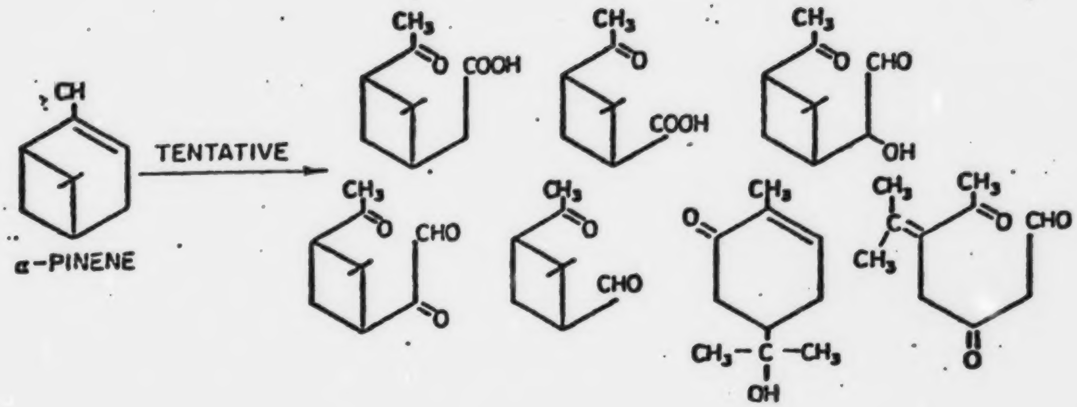

α-PINENE
TENTATIVE

Figure 3-8. Composition of aerosol from reaction of NO_x and α-pinene (according to Schwartz, ref. 92).

Table 3-9

Composition of Aerosol from the Reaction of NO_x and Various Olefins

From Cyclohexene Aerosol

Identified by Schwartz (ref. 92)	Identified by Grosjean (ref.100)
$COOH-(CH_2)_4-CHO$	$COOH-(CH_2)_4-COOH$ major
$COOH-(CH_2)_3-CHO$	$COOH-(CH_2)_4-CH_2ONO_2$
$COOH-(CH_2)_3-CH_2ONO_2$	$COOH-(CH_2)_4-CHO$
$COOH-(CH_2)_3-CH_2OH$	$COOH-(CH_2)_4-CH_2OH$
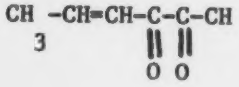 $CH_3-CH=CH-\underset{\underset{O}{\|}}{C}-\underset{\underset{O}{\|}}{C}-CH$	$COOH-(CH_2)_3-COOH$
	$COOH-(CH_2)_3-CH_2ONO_2$
$CH_2=CH-CH=CH-CH_2-CH_2OH$	$COOH-(CH_2)_3-CHO$
cyclopentene-2-aldehyde or	$COOH-(CH_2)_3-CH_2OH$
$CHO-CH=CH-CH_2-CH=CH_2$	$CHO-(CH_2)_3-CHO$

From Cyclopentene Aerosol (Identified by Grossjean, ref. 100)

$CHO-(CH_2)_3-CHO$	$COOH-(CH_2)_2-CH_2OH$
$CHO-(CH_2)_3-COOH$	$COOH-(CH_2)_2-CHO^a$
$COOH-(CH_2)_3-COOH$	$CHO-(CH_2)_2-CHO^a$
$COOH-(CH_2)_3-CH_2ONO_2$	$CHO-(CH_2)_2-CH_2ONO_2^a$

Table 3-9 (Cont.)

Composition of Aerosol from the Reaction of NO_x and Various Olefins

From 1,7-Octadiene Aerosol (Identified by Grosjean, ref. 100)

$COOH-(CH_2)_4-COOH$

$COOH-(CH_2)_4-CH_2ONO_2$

$COOH-(CH_2)_4-CHO$

$CH_2=CH-(CH_2)_4-CH_2ONO_2$ [a]

$CH_2=CH-(CH_2)_4-CHO$

$CH_2=CH-(CH_2)_4-COOH$[a]

---

[a] Tentative.

It is very significant that most of these polyfunctional compounds have also been identified in ambient aerosols (Tables 3-2 and 3-3) and that the gas-to-particle distribution factor, f_C, measured in smog-chamber studies for aerosol precursors, such as cyclic olefins and diolefins,[100] exceeds by one order of magnitude those measured in ambient atmospheres.[51]

Chemical Mechanisms of Organic Aerosol Formation

The Ozone-Olefin Reaction. Much evidence has been accumulated that the ozone-olefin reaction has a predominant role in aerosol formation from alkenes, cyclic olefins, diolefins, and other unsaturated compounds. Free radicals are formed in the reaction and can react further, along with nitric oxide and nitrogen dioxide, either with the various intermediates or with the olefin itself (see the recent review by Pitts and Finlayson[120]).

A mechanism has been proposed recently by O'Neal and Blumstein[121] for the gas-phase ozone-olefin reaction. This mechanism postulates that molozonide-biradical equilibrium is reached fast and postulates a competition between α-, β-, and γ-hydrogen abstraction reactions and the classical mechanism proposed by Criegee[122] for the liquid-phase reaction. The main features of the Criegee mechanism (Figure 3-9) are the formation, from the initial molozonide, of the major carbonyl products and a second biradical intermediate, the "zwitterion." The decomposition pathways of the zwitterion comprise unimolecular rearrangements and bimolecular reactions, the latter including ozonide formation from zwitterion-aldehyde reaction. Other aspects of the Criegee mechanism have been discussed and reviewed elsewhere.[123-127]

The Criegee mechanism, widely accepted for the liquid-phase reaction, does not adequately explain the available gas-phase data. O'Neal and

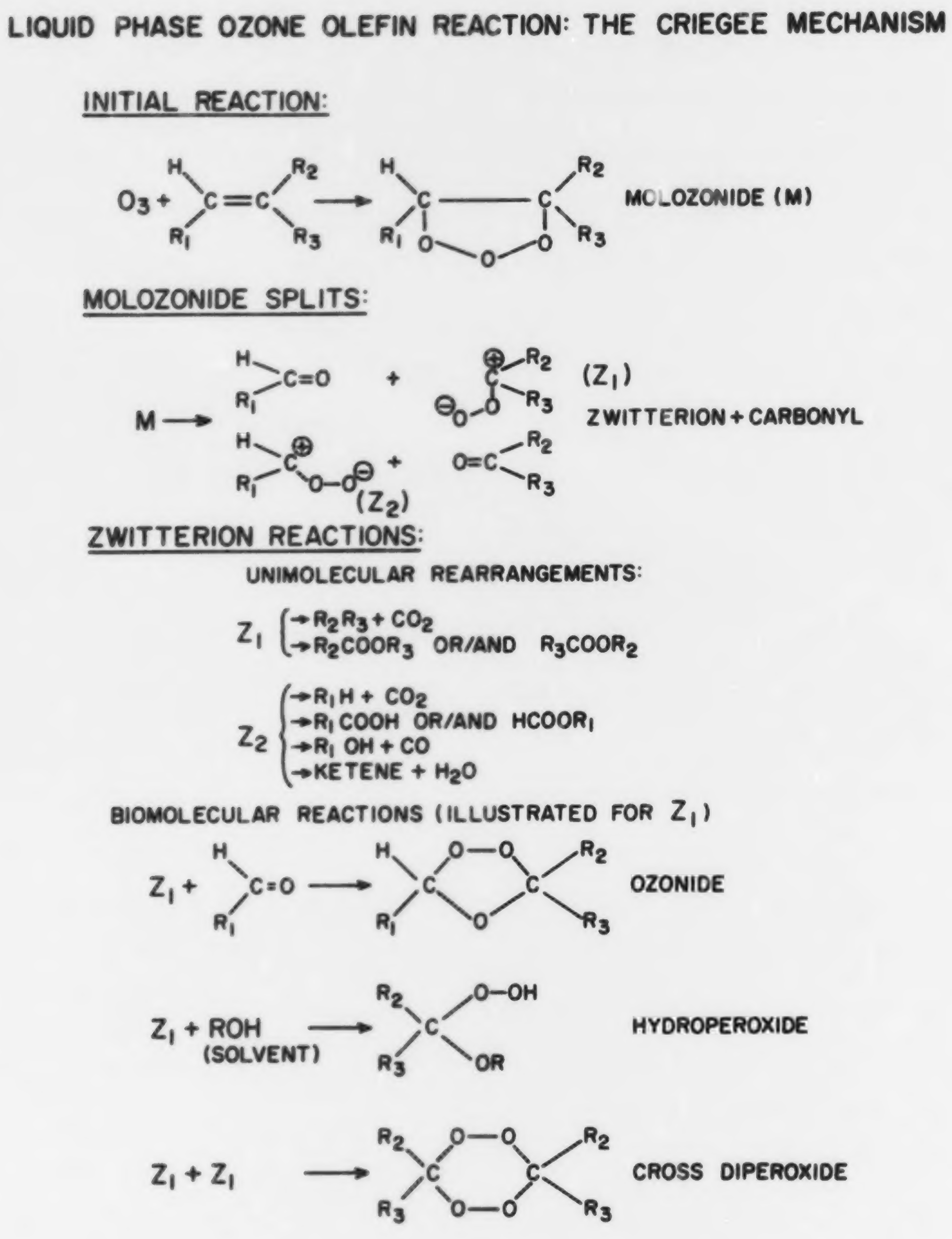
LIQUID PHASE OZONE OLEFIN REACTION: THE CRIEGEE MECHANISM
INITIAL REACTION:
O_3 +
MOLOZONIDE (M)
MOLOZONIDE SPLITS:
M →
(Z_1)
ZWITTERION + CARBONYL
(Z_2)
ZWITTERION REACTIONS:
UNIMOLECULAR REARRANGEMENTS:
Z_1 → $R_2R_3 + CO_2$
→ R_2COOR_3 OR/AND R_3COOR_2
Z_2 → $R_1H + CO_2$
→ R_1COOH OR/AND $HCOOR_1$
→ $R_1OH + CO$
→ KETENE + H_2O
BIOMOLECULAR REACTIONS (ILLUSTRATED FOR Z_1)
Z_1 +
OZONIDE
Z_1 + ROH
(SOLVENT)
HYDROPEROXIDE
$Z_1 + Z_1$
CROSS DIPEROXIDE

Figure 3-9. Liquid-phase ozone-olefin reaction: the Criegee mechanism.

Blumstein[121] suggested a biradical structure for the first gas-phase intermediate and proposed three types of unimolecular hydrogen abstraction reactions (Figure 3-10).

The α-hydrogen abstraction leads to an α-ketoperoxide, which has been tentatively identified by Pitts in the case of cis-2-butene.[128,129] Further reactions of the ketoperoxide include the formation of the "normal products," i.e., the carbonyl products that can also be explained by the Criegee mechanism. The β-hydrogen abstraction accounts for the observed α-cleavage products. The γ-hydrogen abstraction (possible for C_{4+} alkenes) should lead to a rather stable five-membered ring, dioxetane, whose existence has so far not been demonstrated experimentally. On the basis of calculations of the relative importance of the Criegee and abstraction pathways for both spontaneous and thermal reactions of the intermediate species, O'Neal and Blumstein conclude that the Criegee and abstraction mechanisms are of equal importance for butenes, that the former is predominant for ethylene and propylene, and that the latter is predominant for C_{5+} alkenes.

All aerosol products identified in the smog chamber can be reasonably explained in terms of the O'Neal and Blumstein and Criegee mechanisms, as is illustrated in Figure 3-11 for cyclohexene. The major difference between alkenes and cyclic olefins lies in the fact that, after opening of the cyclic olefin double bond, the original number of carbon atoms is conserved and the chain carries both the carbonyl group and the biradical intermediate, whose further reactions lead to the observed difunctional compounds.

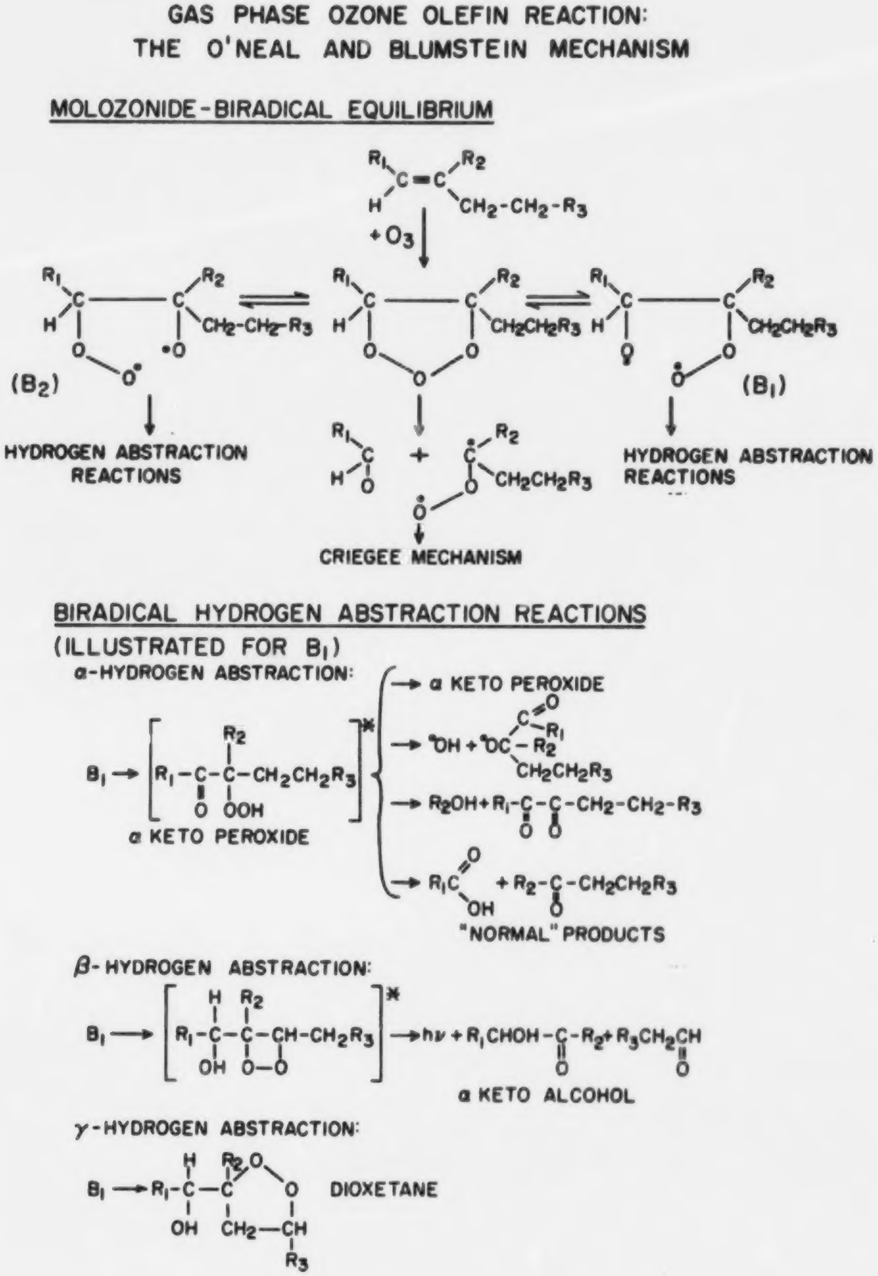
GAS PHASE OZONE OLEFIN REACTION:
THE O'NEAL AND BLUMSTEIN MECHANISM
MOLOZONIDE-BIRADICAL EQUILIBRIUM
+O3
(B2)
(B1)
HYDROGEN ABSTRACTION REACTIONS
HYDROGEN ABSTRACTION REACTIONS
CRIEGEE MECHANISM
BIRADICAL HYDROGEN ABSTRACTION REACTIONS
(ILLUSTRATED FOR B1)
α-HYDROGEN ABSTRACTION:
α KETO PEROXIDE
α KETO PEROXIDE
"NORMAL" PRODUCTS
β-HYDROGEN ABSTRACTION:
hν
α KETO ALCOHOL
γ-HYDROGEN ABSTRACTION:
DIOXETANE

Figure 3-10. Gas-phase ozone-olefin reaction: the O'Neal and Blumstein mechanism.

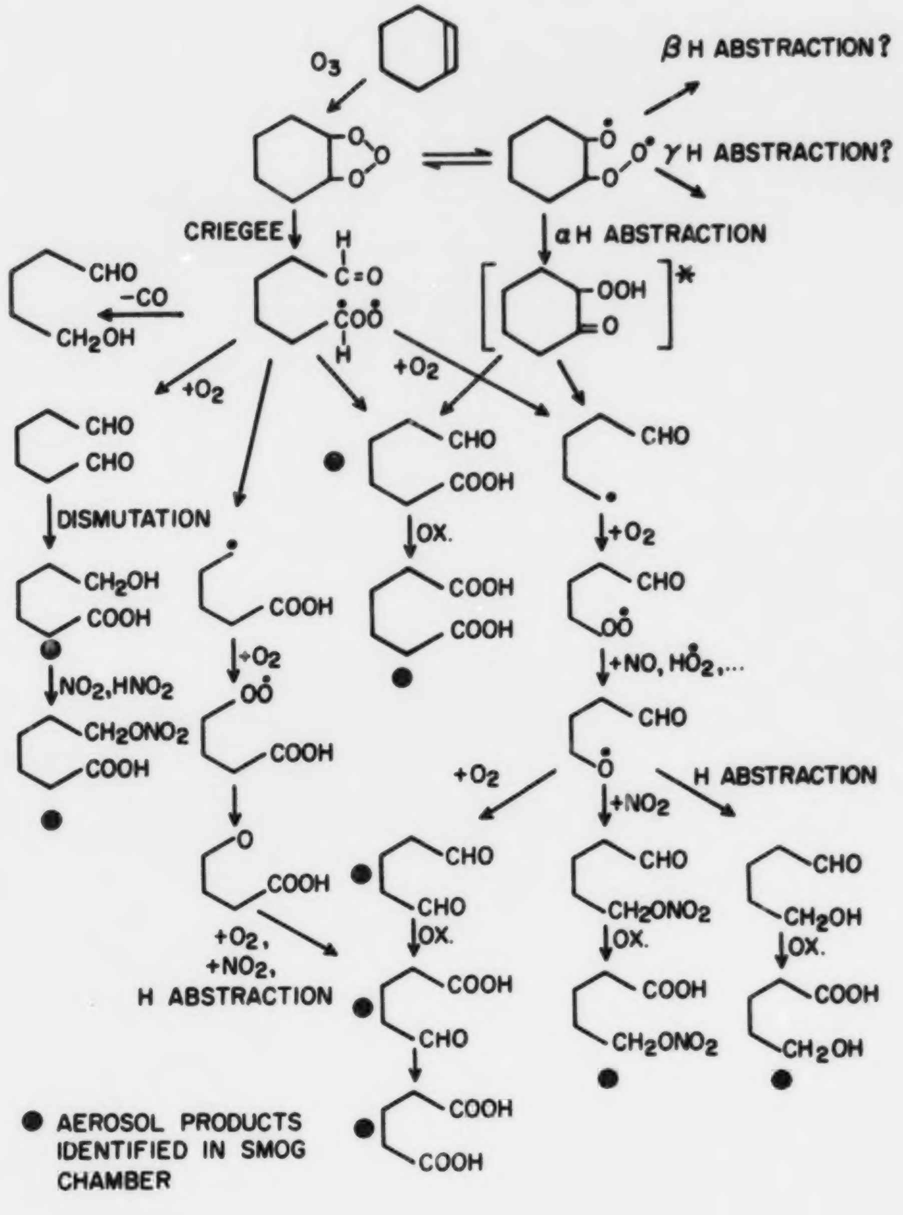

POSSIBLE FORMATION PATHWAYS FOR CYCLOHEXENE AEROSOL PRODUCTS

O3
β H ABSTRACTION?
γ H ABSTRACTION?
CRIEGEE
α H ABSTRACTION
CHO
−CO
CH2OH
C=O
COO
OOH
O
+O2
CHO
CHO
DISMUTATION
CH2OH
COOH
NO2,HNO2
CH2ONO2
COOH
COOH
CHO
COOH
OX.
COOH
COOH
CHO
+O2
CHO
OO
+NO, HO2,...
CHO
O
+O2
+NO2
H ABSTRACTION
+O2
OO
COOH
O
COOH
+O2,
+NO2,
H ABSTRACTION
CHO
CHO
OX.
COOH
CHO
COOH
COOH
CHO
CH2ONO2
OX.
COOH
CH2ONO2
CHO
CH2OH
OX.
COOH
CH2OH
● AEROSOL PRODUCTS IDENTIFIED IN SMOG CHAMBER

Figure 3-11. Possible formation pathways for cyclohexene aerosol products (after Grosjean and Friedlander.[156])

The Hydroxyl Radical-Aromatic Hydrocarbon Reaction. Very little is known about the mechanisms governing ambient reactions of aromatic hydrocarbons. The Battelle study[92] demonstrates that aromatic-ring opening, aromatic-ring nitration, and alkyl-group oxidation may occur at atmospheric concentrations. The former possibility is supported by Altschuller *et al.*,[130] who observed a decrease of infrared absorption bands due to the aromatic ring during the photooxidation of various aromatics at 5 ppm with nitric oxide at 3 ppm. Reactions of aromatic hydrocarbons with ozone, atomic oxygen, and hydroxyl radical might account for the observed polyfunctional aerosol products. The reaction of ozone with aromatics has been studied in the liquid phase by Wibaut and co-workers.[123] They reported relative rate constants of 1.9, 10, 40, 250, and 15,000 for benzene, toluene, xylenes, mesitylene, and hexamethylbenzene, respectively. Glyoxal, methylglyoxal, and biacetyl were the major products of the ozone-*o*-xylene reactions, and their formation was interpreted in terms of the Criegee mechanism. The gas-phase reaction has received little attention, and the rate constants of only three aromatics have been measured. It appears that the reaction is very slow, compared with that of olefinic compounds. Bufalini[131] estimated the rate constant k_{O_3} for mesitylene, one of the most reactive aromatics, to be only about 0.37 the rate constant for ozone reactions with the least reactive olefin, ethylene. Recent data from Stedman[132] show that toluene and xylenes react even more slowly with ozone than acetylene does.

The reaction of atomic oxygen, $O(^3P)$, has been investigated in greater detail.[93,120] Cvetanovic and co-workers[133,134] reported formation of nonvolatile polymeric material from benzene and toluene. Formation of the observed linear products can be explained by cleavage of the biradical initially formed by addition of atomic oxygen on the aromatic ring. Absolute rate constants for atomic oxygen addition to a series of aromatics were recently measured in the temperature range 299-392 K.[135]

The aromatic-hydroxyl radical reaction has been studied by Davis _et_ _al_.[136] They reported rate constants for benzene and toluene and concluded that hydroxyl additions to the aromatic ring compete favorably with the abstraction of hydrogen atom from the alkyl substituent. Doyle _et_ _al_.[137] recently published hydroxyl reaction rate constants for a series of alkylbenzenes.

Possible ozone, atomic oxygen, and hydroxyl radical reaction mechanisms, leading to linear polyfunctional products from aromatic hydrocarbons, are shown in Figure 3-12. In an attempt to assess the relative importance of the various oxidizing species in the photooxidation of olefinic and aromatic hydrocarbons, we have compared the rate constants for hydroxyl radical, atomic oxygen, and ozone reactions with the rate constants for the conversion of nitric oxide to nitrogen dioxide (Figure 3-13). Good relations are obtained between k_{O_3} and $k_{NO \rightarrow NO_2}$ for alkenes and between k_{OH} and $k_{NO \rightarrow NO_2}$ for aromatics, indicating that the structural effects prevailing in the overall conversion of nitric oxide to nitrogen dioxide are those controlling the _ozone-olefin_ and _hydroxyl radical-aromatic_ reactions. This is further substantiated by comparing the absolute reactivities of olefins and aromatics. The most reactive aromatics, _m_-xylene and mesitylene, react faster than ethylene and as fast as propylene and isobutene with the hydroxyl radical. The same reactivity

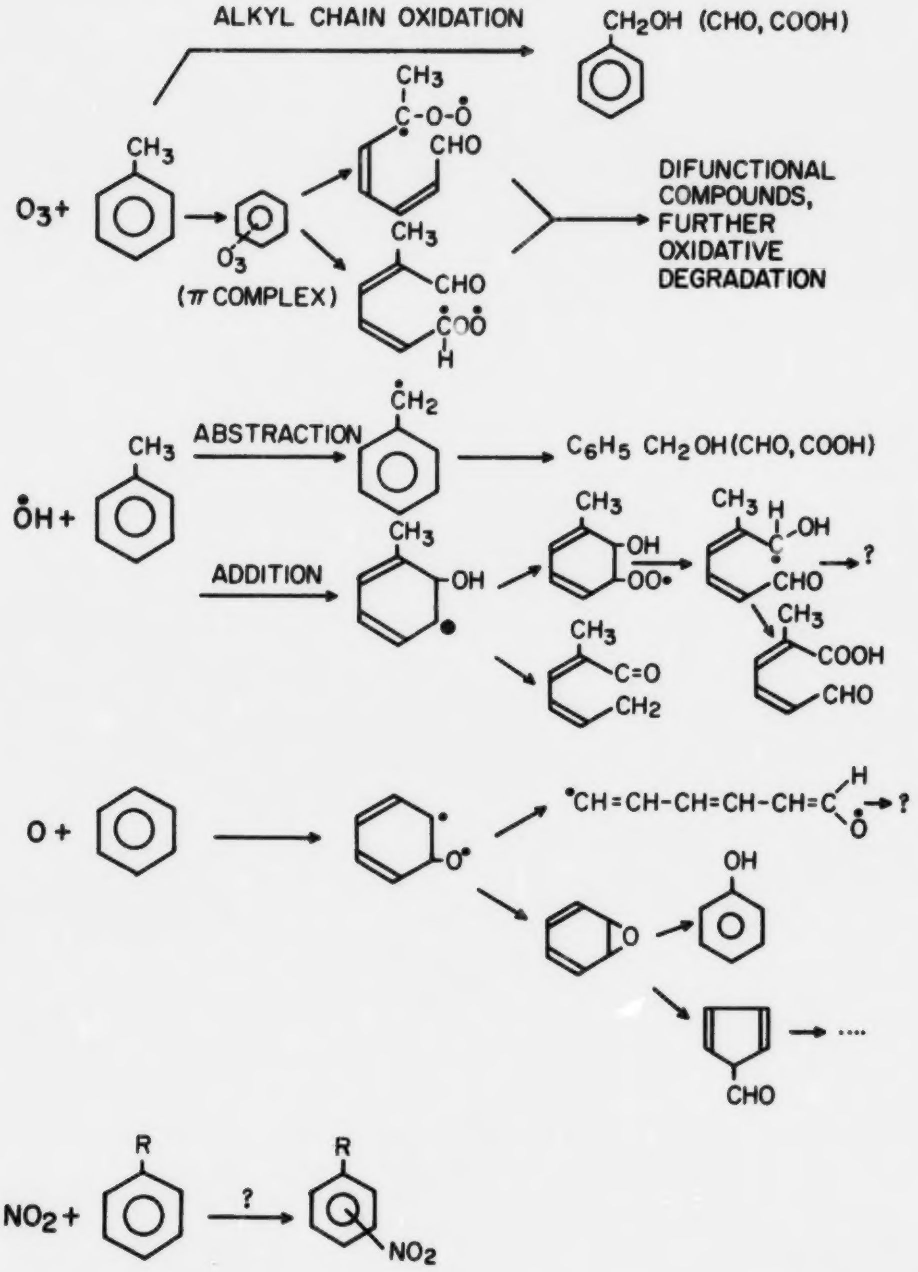
ALKYL CHAIN OXIDATION
CH2OH (CHO, COOH)
O3+
CH3
C-O-O
CHO
(π COMPLEX)
COO
H
DIFUNCTIONAL COMPOUNDS, FURTHER OXIDATIVE DEGRADATION
CH2
ABSTRACTION
C6H5 CH2OH(CHO, COOH)
OH+
ADDITION
OH
OO•
CHO
?
C=O
CH2
COOH
O+
•CH=CH-CH=CH-CH=C
H
O
?
OH
O
CHO
....
NO2+
R
?
NO2

Figure 3-12. Possible initial steps for ozone, atomic oxygen, nitrogen dioxide, and **dioxide, and** hydroxyl radical reaction with aromatic hydrocarbons.

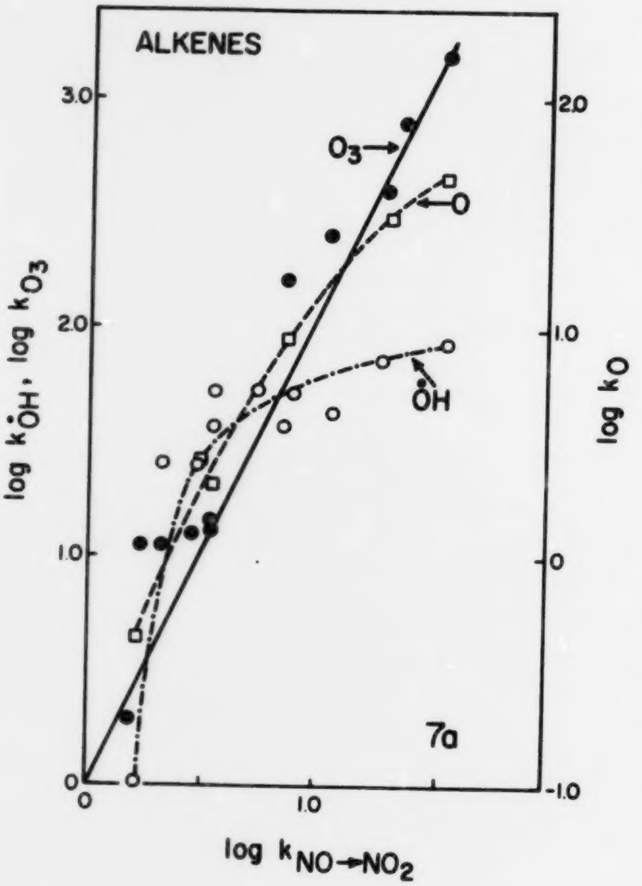

Figure 3-13a. Relations between conversion of nitric oxide to nitrogen dioxide and ozone, atomic oxygen, and hydroxyl radical reaction rate constants for (a) olefinic and (b) aromatic hydrocarbons. (Reprinted with permission from Grosjean.[157b]) ($k_{NO \rightarrow NO_2}$ from Glasson and Tuesday.[106])
Alkenes (k_{O_3} from Japar _et_ _al_.;[160] from Morris and Niki;[243] k_O from Furayama _et_ _al_.[244])

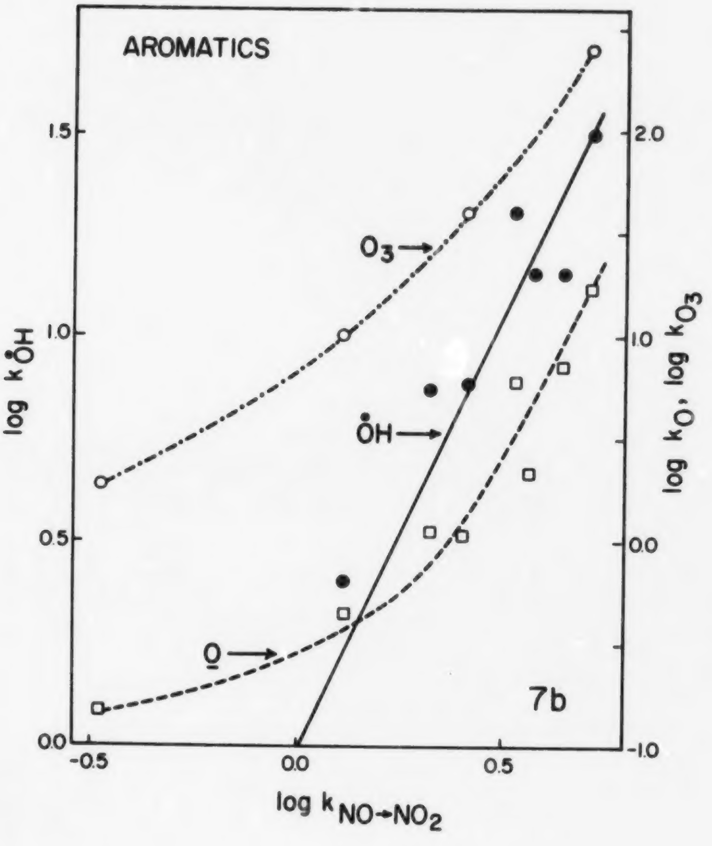

Figure 3-13b. Relations between conversion of nitric oxide to nitrogen dioxide, atomic oxygen, and hydroxyl radical reaction rate constants for (a) olefinic and (b) aromatic hydrocarbons. (Reprinted with permission from Grosjean.[157b]) Aromatics (k_O from Atkinson and Pitts;[135] Doyle *et al*.[137] k_{O_3} liquid-phase, relative to toluene, from Bailey;[123a,123b] gas-phase ozone rate constants have not been measured).

sequence is observed for the rates of conversion of nitric oxide to nitrogen dioxide, whereas ozone-aromatic reaction rate constants are too low to account for their overall photochemical reactivity. Relevant to the postulated importance of the hydroxyl radical-aromatic reaction is the observation made by Wilson _et al_.:[89] an aerosol increase from 1-heptene and an aerosol decrease from toluene when ozone is added to irradiated NO_x-hydrocarbon mixtures. In the latter case, the observed inhibiting effect results from the reaction,

$$O_3 + \dot{O}H \rightarrow H\dot{O}_2 + O_2 \quad , \qquad (1)$$

which competes with the hydroxyl radical-aromatic reaction. Many investigators also reported that aerosol formation from olefins coincides with ozone appearance, whereas aerosol buildup from aromatics starts before ozone formation and is presumably associated with the appreciable hydroxyl radical concentrations in the early stages of the photochemical process.

On the basis of all available evidence, the hydroxyl radical plays a major role in the photooxidation and aerosol formation processes for aromatic hydrocarbons. However, much research remains to be done to improve our knowledge in this field.

Physical Mechanisms of Organic Aerosol Formation

Dynamics of Gas-to-Particle Conversion.

The physical processes involved in the formation of atmospheric aerosol have been thoroughly investigated in the past few years[55-57,138-146] and will be briefly summarized here, with some emphasis on recent data obtained in smog-chamber studies.

Regardless of the chemistry, there are some physical constraints on aerosol-gas interactions. Particles must be close to or at equilibrium with respect to the surrounding vapor to exist in air for any substantial period. Thus, the partial pressure of condensed species on particles must be less than or equal to the saturation vapor pressure at atmospheric temperature for stability. As we will see later, the requirement of low vapor pressure is particularly important to the stability of organic aerosols.

Accumulation of condensed material as aerosols in the atmosphere may take place by two basic processes: by condensation of supersaturated vapor or chemical reaction that leads to spontaneous formation of new particles, and by condensation, absorption, or reaction on existing particles. In the latter case, the chemical reactions may actually take place on the surface of or within existing particles.

For condensable precursors, particle formation may occur by homogeneous or heterogeneous nucleation. It is generally accepted that heterogeneous processes are most likely in the atmosphere, because of the large number of nuclei present.

Growth of particles by accumulation on existing particles can be classed as two broad processes. If the precursor is supersaturated, growth will occur at a rate limited by vapor diffusion, which depends on the supersaturation, the temperature, the particle size, and the accommodation coefficient at the surface. The proportionality of particle size changes with the ratio of particle diameter to mean free path of the suspending gas. At one extreme, the growth depends on volume to the 2/3 power; at the other, growth is proportional to volume to the 1/3 power. When the precursor is unsaturated, growth still may take place by irreversible absorption or by chemical reactions in the particle. In this case, the rate law should be proportional to the particle volume, if the reaction is uniform throughout the particle. If the formation of material is limited by reactions in the particle, the conversion ratio should not depend on the concentration of the gaseous precursor.

There is insufficient information available to determine the rate law or physical mechanism most likely to predominate in atmospheric aerosol growth. However, there are clues to differences in the processes from the Los Angeles data. The shape of the particle volume number distribution of tropospheric aerosol is such that the 1/3 (diameter) and 2/3 (surface) moments are concentrated in the submicrometer fraction, whereas the first moment (volume) is weighted toward larger particles. Thus, the observed accumulation of organic carbon on the small particles in smog (Figure 3-14) suggest a process controlled by surface or vapor diffusion.

It is of interest that the influence of thermodynamic equilibrium must enter the growth process of particles. If the radius of the particles is too small, the partial pressure of the condensable species can increase significantly by the influence of radius of curvature (Kelvin effect). Examination of values of surface tension for a range of materials suggests that the Kelvin effect will constrain growth to particles greater than about 0.05-0.1 μm in diameter. This appears to be consistent with available observations of atmospheric growth and the distribution of secondary chemical components.

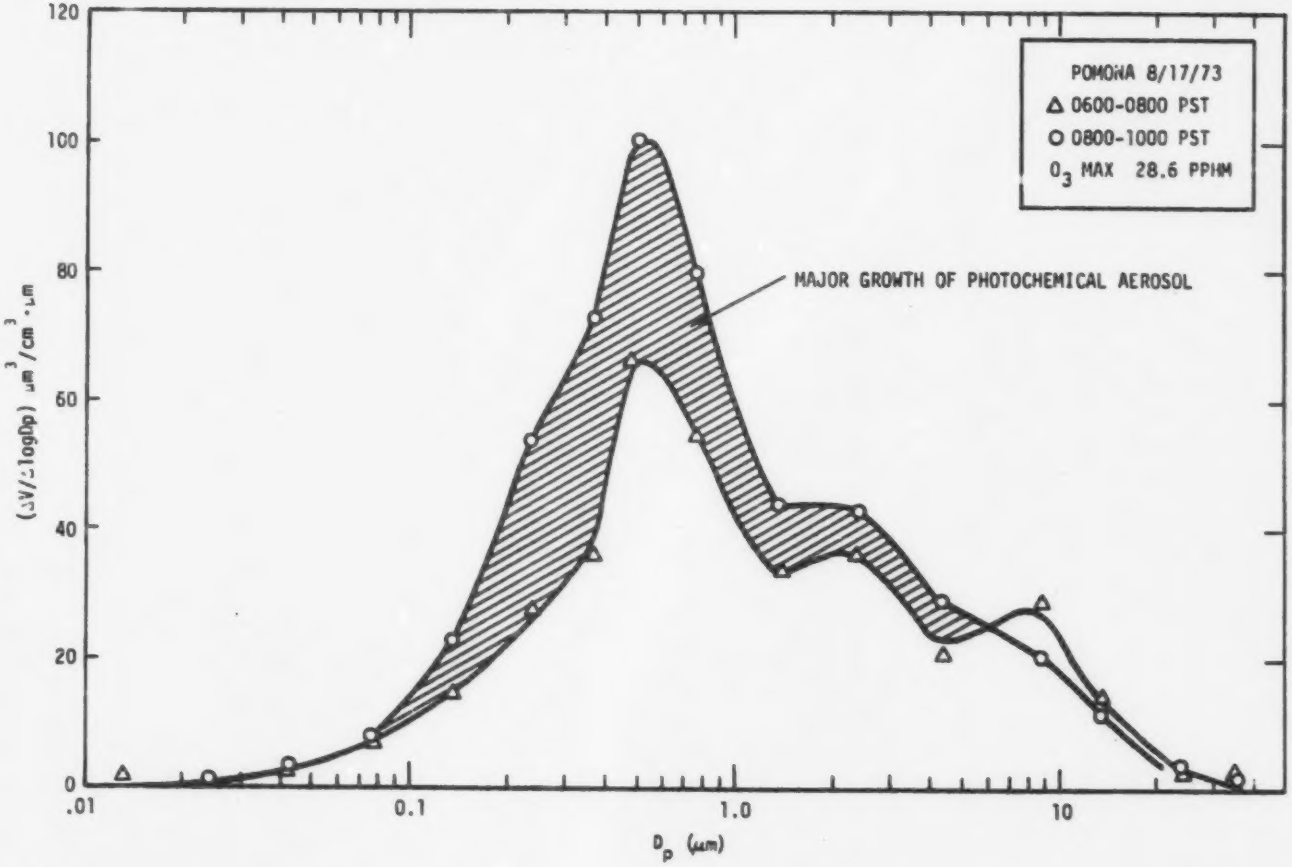

Figure 3-14. Evolution of the volume distribution of ambient smog aerosol. Compare with Figures 3-24 and 3-26. (Reprinted with permission from Hidy et al.[56])

Growth of Secondary Organic Particles. The physical mechanisms governing the formation of organic aerosols in smog-chamber experiments have recently been studied in some detail.[147,148] Two types of profiles, presented in Figure 3-15, are generally observed. Aromatic hydrocarbons and alkenes with fewer than seven carbon atoms, when present at initial concentrations of about 1 ppm, produce copious quantities of nuclei that are not able to grow in the light-scattering range. On the contrary, aerosols formed from C_{7+} alkenes, cyclic olefins, diolefins, and terpenes always grow in the light-scattering range and produce appreciable visibility reduction (Figure 3-16; compare with ambient data presented in Figure 3-14). As a result of aerosol growth, the light-scattering efficiency per aerosol mass unit increases rapidly in the early stages of the experiment (Figure 3-17; compare with the light-scattering efficiency as a function of particle size for monodisperse aerosol presented in Figure 3-18).

In the case of organic constituent formation, growth of particles is governed by physical laws of condensation, provided that the precursors are formed in the gas phase. For a diffusion-limited condensation process, the rate of volume change in particles is

$$\frac{dv}{dt} = A\,(dp - dp^*)\left(1 + \ell\,\frac{2\lambda}{dp}\right)^{-1} , \qquad (2)$$

where $A = \Sigma A_i$; $A_i = \lambda_i x_i S_i \ln S_i$; for the i th condensable species, λ_i is the particulate mole fraction and x_i is the activity coefficient; dp is the particle diameter; dp* is the initial particle size below which condensation cannot take place because of the curvature effect on equilibrium vapor pressure (Kelvin effect); S_i is the supersaturation ratio for the i^{th} species; λ is the mean free path in air; and ℓ is a parameter

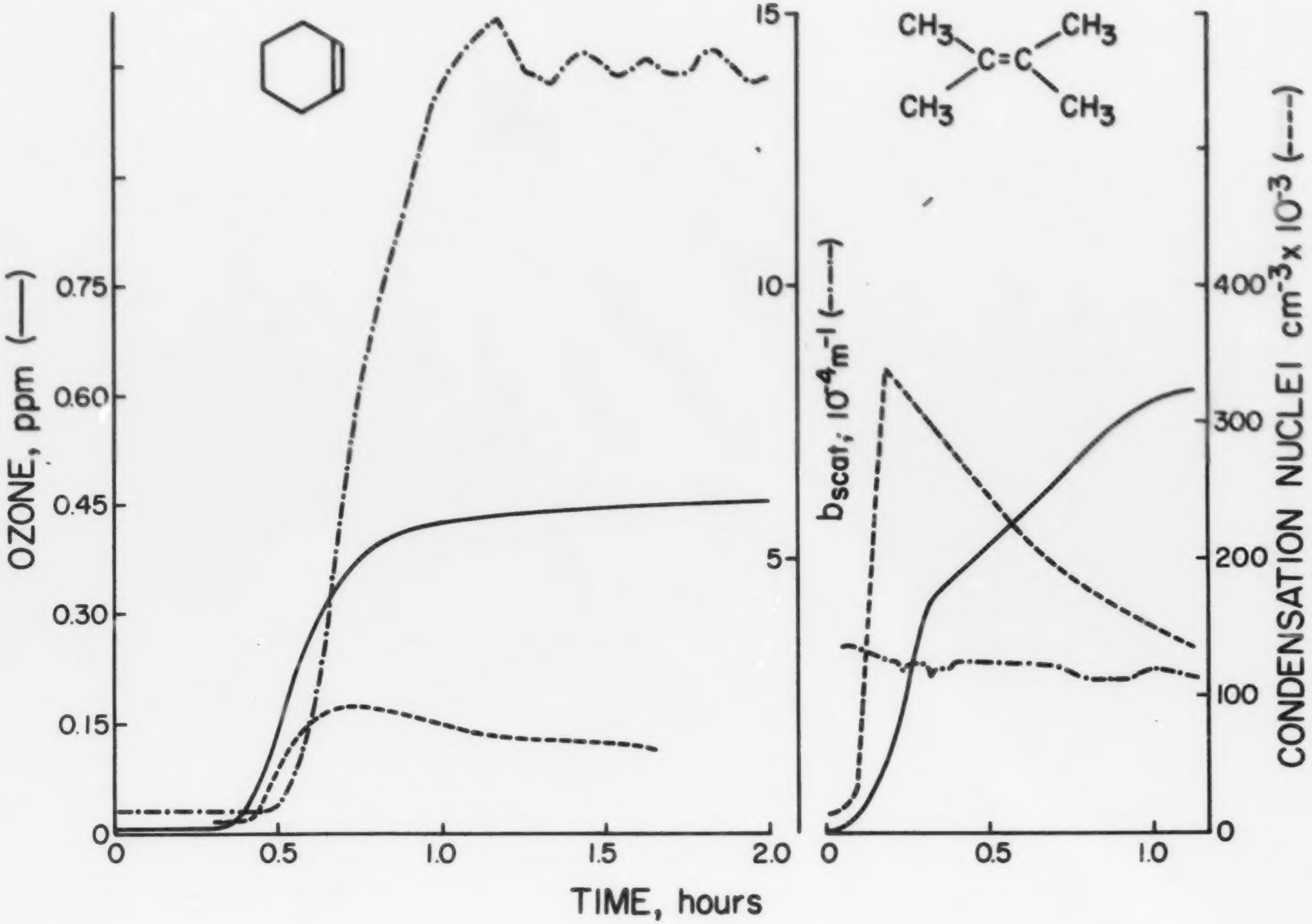

Figure 3-15. Smog-chamber profiles. Left, cyclohexene. Right, tetramethylethylene. Initial concentrations: hydrocarbon, 1 ppm; NO, 0.33 ppm; NO_2, 0.16 ppm. (Reprinted with permission from Grosjean.[100])

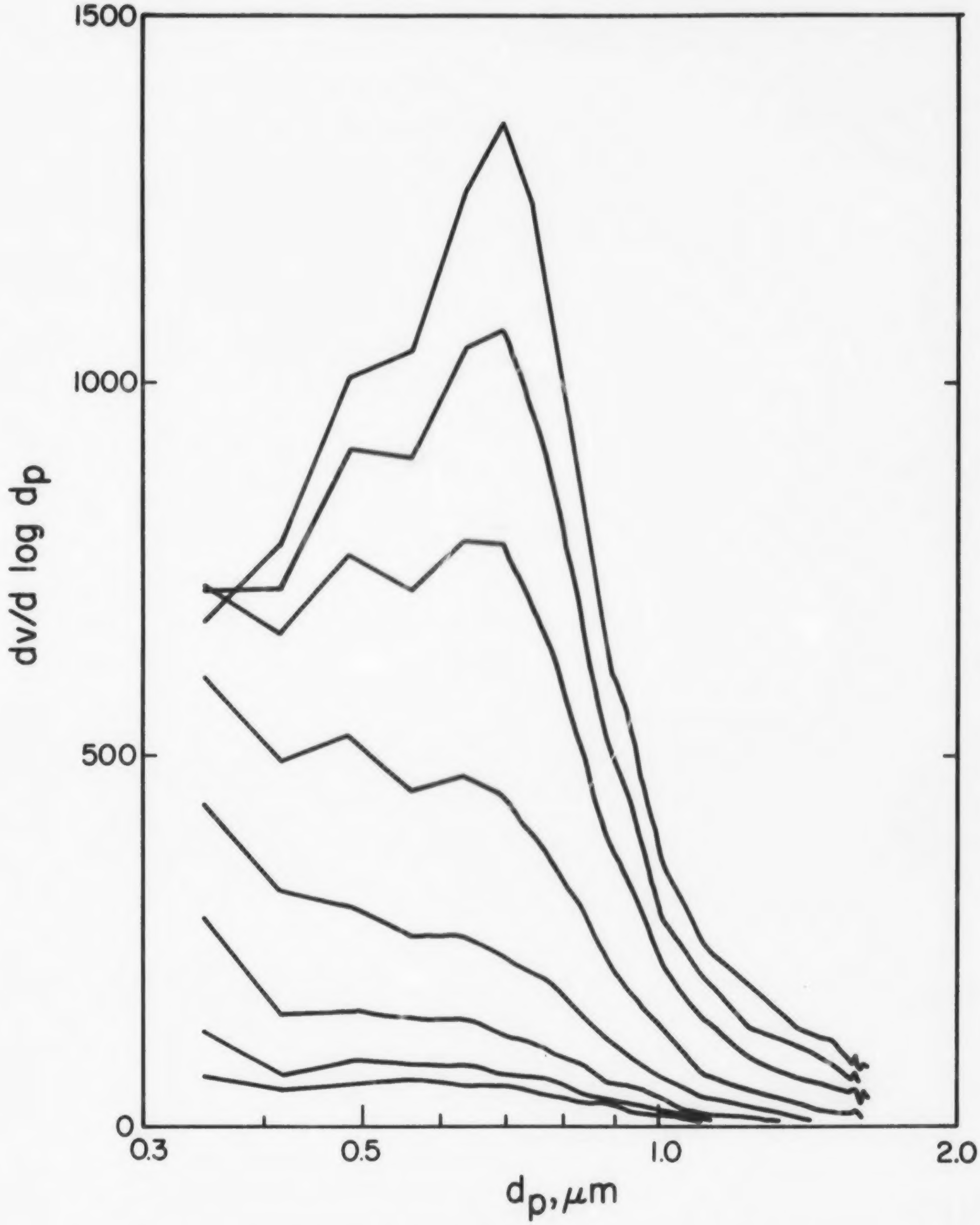

Figure 3-16. Evolution of the volume distribution of secondary organic aerosol generated in smog chamber with 1-ppm cyclohexene, 0.33-ppm NO, and 0.17-ppm NO_2. Time from bottom to top: 0, 203, 412, 631, 863, 1109, 1364, and 1626 s. Compare with Figures 3-22 and 3-26. (Reprinted with permission from Heisler *et al.*[148])

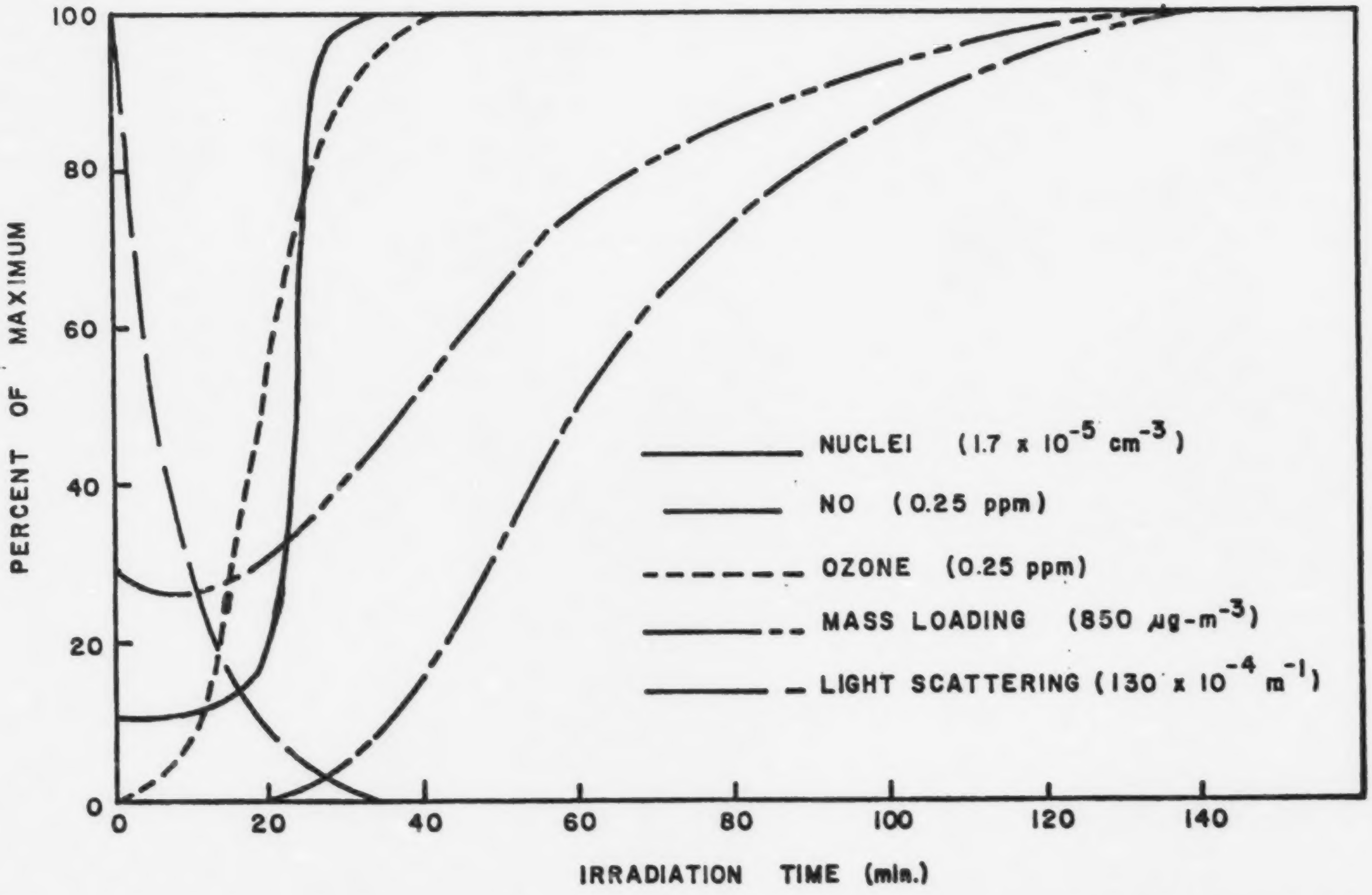

Figure 3-17. Increase in aerosol light-scattering efficiency as a result of aerosol growth. Compare with Figures 3-24 and 3-26. (Reprinted with permission from O'Brien et al.[94])

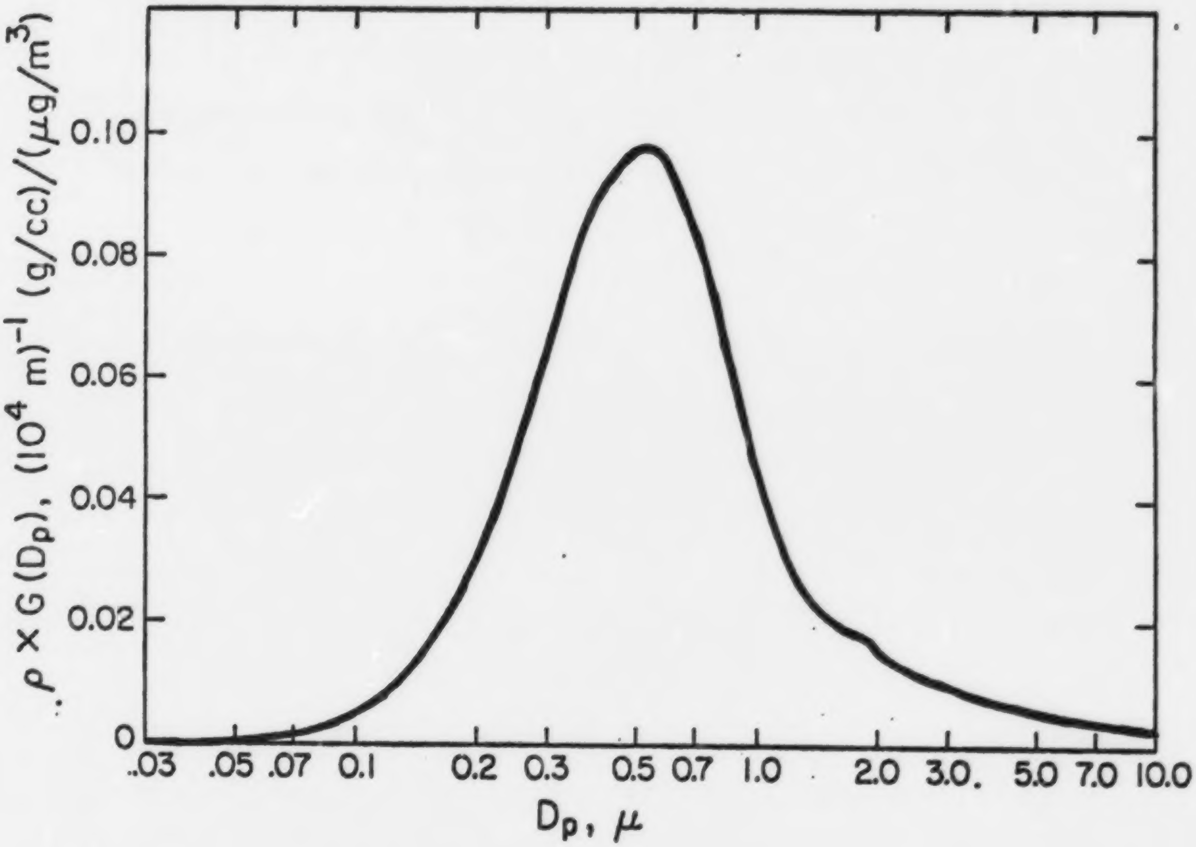

Figure 3-18. Ratio of light-scattering coefficient to mass concentration for uniform spherical particles of unit density. Refractive index, 1.5; diameter, D_p. (Reprinted with permission from Hidy *et al.*[56a])

proportional to the ratio dp/λ. This linear relation has been verified experimentally in the case of cyclic olefin and diolefin aerosols (Figure 3-19). Critical sizes of 0.13-0.24 μm and 0.26-0.28 μm have been measured for cyclohexene and 1,7-octadiene, respectively.[148] For such aerosol precursors, the gas-to-particle conversion process consists of the formation of supersaturated compounds in the gas phase followed by condensation on preexisting particles.

Condensable-Species Vapor Pressure and Aerosol Formation. As discussed earlier, the equilibrium constraint of low vapor pressure is particularly important for stability of the organic aerosols. Organic aerosol formation requires accumulation of condensable species in excess to their gas-phase saturation concentrations.[149-155] In turn, examination of vapor-pressure data for various oxygenated compounds permits estimating the minimal hydrocarbon precursor concentration required to achieve aerosol formation in ambient atmosphere. Table 3-10 gives examples of vapor pressures of various oxygenated compounds formed in hydrocarbon photooxidation reactions. It can be seen from the table and from boiling-point data that volatility decreases regularly when the number of carbon atoms increases and that, for a given chain length, carboxylic acids have the lowest vapor pressure. Moreover, the volatility of difunctional oxygenates is several orders of magnitude lower than that of the corresponding monofunctional compound.[156] Grosjean estimated the minimal ambient alkene concentration required to form the corresponding carboxylic acid in excess to its saturation concentration (Table 3-11). Because a 100% gas-to-aerosol conversion was assumed and because carboxylic acids actually represent only a fraction of the products, the precursor concentration data in Table 3-11 are, in fact, lowest

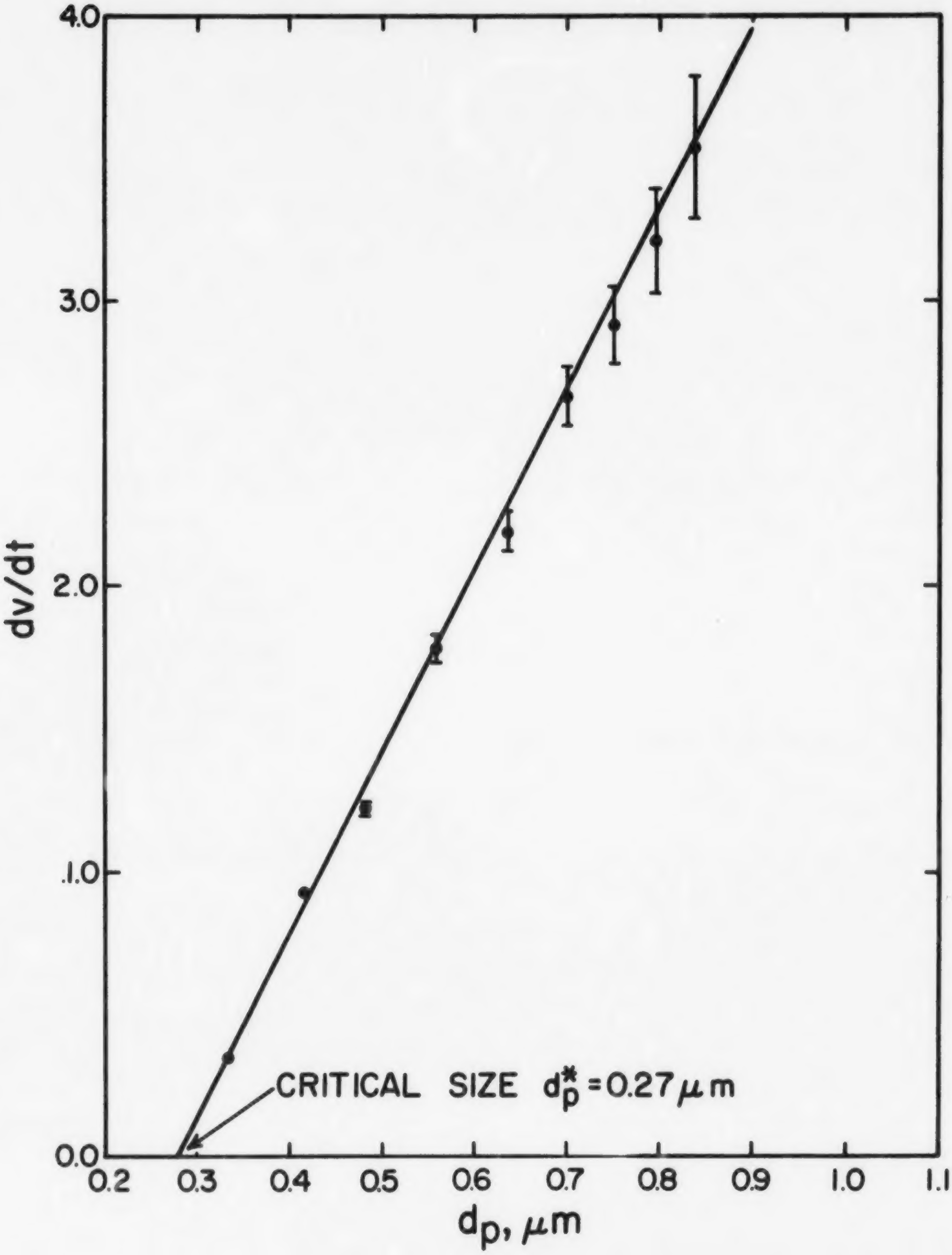

Figure 3-19. Growth of organic aerosol generated in smog chamber; same experiment as in Figure 3-24. (Reprinted with permission from Heisler.[148])

Table 3-10

Vapor Pressures of Oxygenated Compounds[a]

Carbon Number	Vapor Pressure, mm Hg at 25 C[b]				
	Alkanes[c]	Aldehydes	Alcohols[c]	Carboxylic Acids[c]	Dicarboxylic Acids
1	-	-	100(21.2 C)	40(24 C)	-
2	-	795	31.5	16	2.2×10^{-4}
3	-	200	16	4	-
4	-	-	5	1	2.97×10^{-7}
5	-	-	1.8	0.25	-
6	-	-	1(24.4 C)	0.02	6.14×10^{-8}
7	-	6	0.26	-	-
8	15.1(27 C)	-	0.11	4.4×10^{-3}	-
9	-	-	7.9×10^{-2}	-	-
10	2.28(33.6 C)	1.4×10^{-2}	4.3×10^{-2}	10^{-3}(33.6 C)	5.49×10^{-10}
11	0.48	7.2×10^{-2}	3.8×10^{-2}	-	-
12	0.117	-	10^{-2}	10^{-5}(25.3 C)	7.28×10^{-10}
13	-	-	-	8.0×10^{-5}	-
14	-	-	-	$\approx 10^{-6}$	-
15	$\approx 2 \times 10^{-3}$	-	-	-	-
16	10^{-3}(21.8 C)	-	-	$\approx 10^{-8}$	-
17	5×10^{-4}(25.7 C)	-	-	-	-
18	10^{-4}(24.8 C)	-	1.45×10^{-4}	$\approx 10^{-9}$	-

---

[a] Data from Grosjean.[156]
[b] Unless otherwise indicated in parentheses.
[c] Log Vp varies linearly with the number of carbon atoms.

Volatility sequence for C_n compounds (from boiling and melting points):
alkane > aldehyde > alcohol ≈ nitrate ester > carboxylic acid ≈ dialdehyde > diol ≈ dinitrate ≈ alcohol C_{n+6} ≈ acid aldehyde >> dicarboxylic acid.

Table 3-11

Hydrocarbon Threshold Concentration

(estimated lowest ambient olefin concentration required to form the corresponding condensable species in excess to its saturation concentration)[a]

Olefinic Precursor	Condensable Species	Condensable Species Vapor Pressure, mm Hg	Minimal Precursor Concentration[b]
Ethylene	Formic acid	40	52,400 ppm
Propylene	Acetic acid	16	20,960 ppm
1-Butene	Propionic acid	4	5,240 ppm
1-Pentene	Butanoic acid	1	1,310 ppm
1-Hexene	Pentanoic acid	0.25	327 ppm
1-Heptene	Hexanoic acid	0.02	26.2 ppm
1-Octene	Heptanoic acid	$\approx 9 \times 10^{-3}$	11.8 ppm
1-Nonene	Octanoic acid	$\approx 4 \times 10^{-3}$	5.2 ppm
1-Decene	Nonanoic acid	$\approx 6 \times 10^{-4}$	0.78 ppm
1-Tridecene	Dodecanoic acid	10^{-5}	13 ppb
Cyclopentene	Glutaric acid	2×10^{-7}	$\approx$ 0.26 ppb
Cyclohexene	Adipic acid	6×10^{-8}	0.08 ppb
Methylcyclohexene	Methyladipic acid	$\approx 2 \times 10^{-8}$	$\approx$ 0.03 ppb

---

[a] Data from Grosjean.[156]

[b] Assuming that there is 100% gas-to-particle conversion, that the formed condensable species is the one with the lowest vapor pressure (carboxylic acid), and that there is no vapor-pressure lowering by condensable species polymerization or other effect.

estimates. Vapor-pressure considerations suggest, again, cyclic olefins and diolefins as the most efficient aerosol precursors. For example, cyclohexene at only about 0.1 ppb is required to form adipic acid ($Vp \approx 6x 10^{-8}$ mm Hg) in excess to its saturation concentration, whereas 1-heptene at about 50 ppm ($5x10^{5}$ more than cyclohexene) would be necessary to form hexanoic acid ($Vp \approx 2x10^{-2}$ mm Hg) aerosol. Obviously, aerosol formation from C_{1-5} alkenes would require unrealistic ambient precursor concentrations, even if polymerization of the condensable species lowers the required precursor concentration by several orders of magnitude. Aggregation or polymerization (at least dimerization) of the condensable species formed from C_{6+} alkenes must take place to achieve aerosol formation. On the contrary, no polymerization (not even dimerization, although it may occur) is necessary to form aerosols from cyclic olefins, even when present as traces (1 ppb or below) in ambient air. Therefore, there is a threshold concentration, below which no organic aerosol is formed for each hydrocarbon precursor. The concept of precursor threshold concentration is supported by qualitative experimental observations on nuclei formation[98] (Figure 3-20) and occurrence of light scattering[94] (Figure 3-21) as a function of the precursor concentration. The low-volatility constraint for organic condensable species has major consequences for the ability of the various precursor classes to form organic aerosol in the atmosphere:

- Cyclic olefins and diolefins form aerosol even when present at very low concentrations, as confirmed by smog-chamber studies for cyclohexene[82,100] and 1,6-heptadiene.[94]

- Alkenes of C_{2-6} do not form organic aerosol in parts-per-million concentrations. Aerosol data obtained at higher concentrations, although

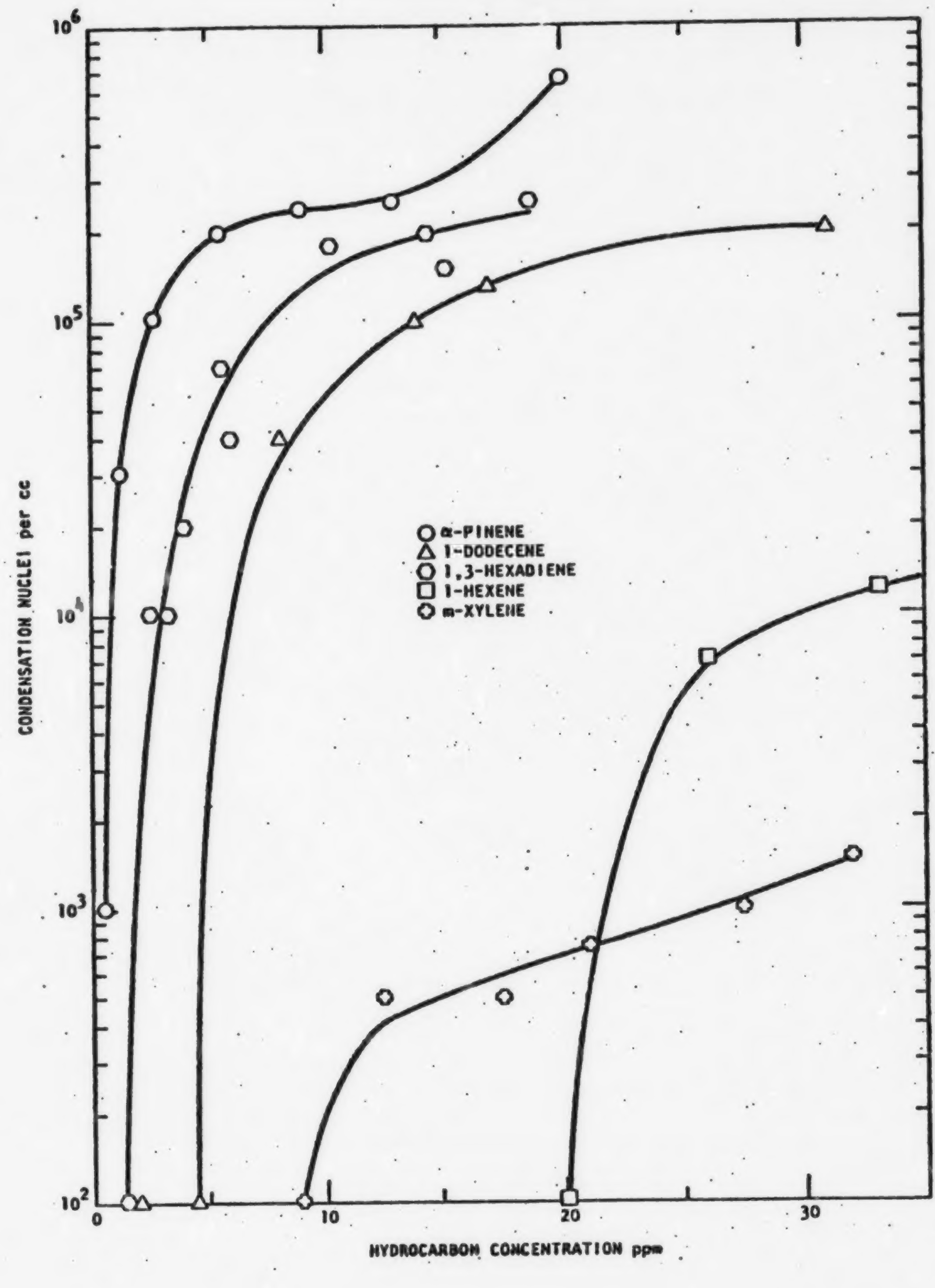

Figure 3-20. Threshold concentration for condensation nuclei formation from various hydrocarbons. (Reprinted with permission from Lipeles.[98])

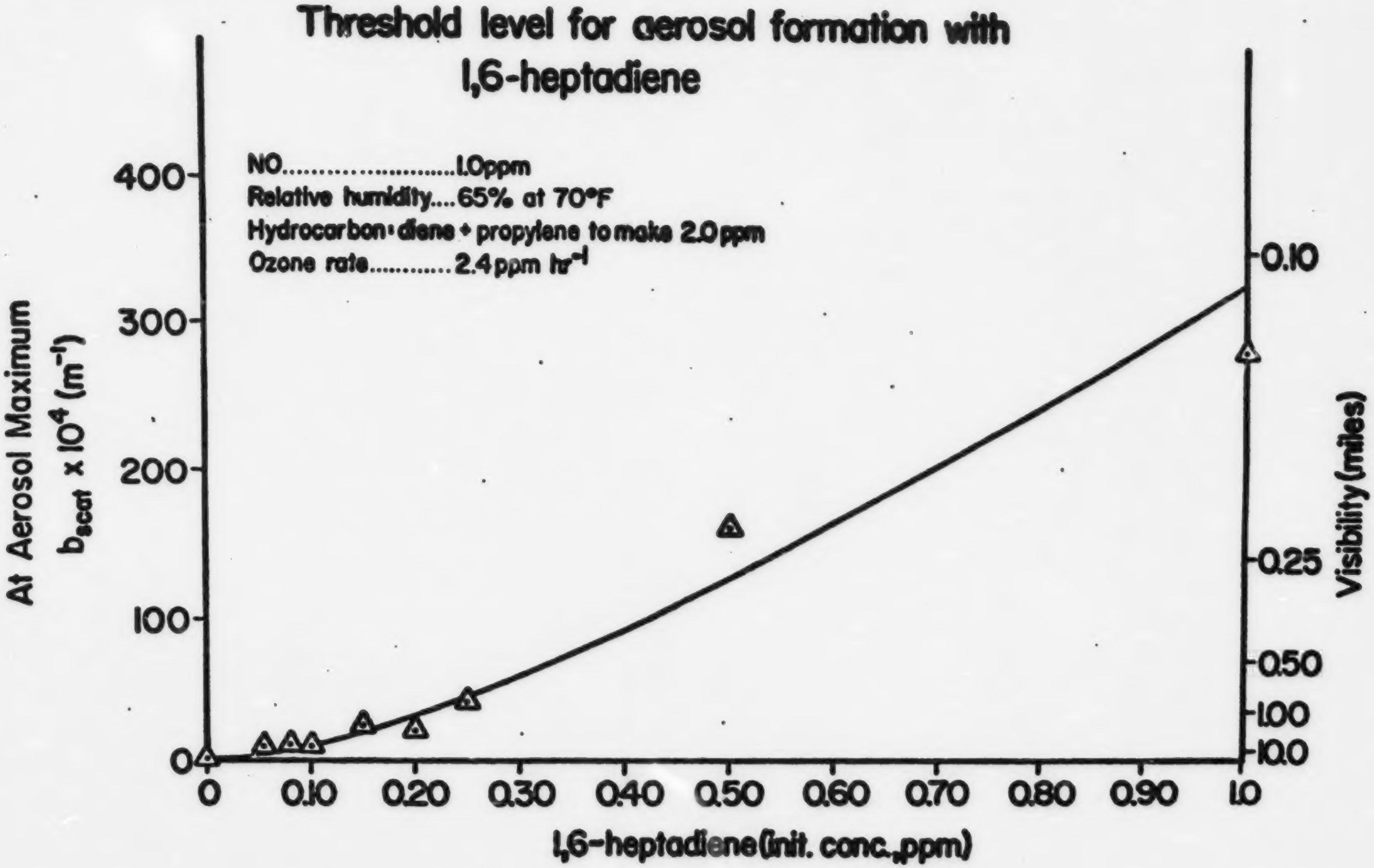

Figure 3-21. Threshold concentration for aerosol formation with 1,6-heptadiene. (Reprinted with permission from O'Brien, *et al.*[94])

useful for mechanistic studies, cannot be extrapolated to atmospheric concentrations for these low-molecular-weight alkenes.

- Threshold concentrations for C_{7+} alkenes are in the parts-per-hundred-million to parts-per-million range. Determination of their gas-phase concentration is required for assessing their contribution to atmospheric organic aerosol.

- Nothing is known about the threshold concentration for aromatic hydrocarbons. No vapor-pressure data on the polyfunctional products are available. However, a possible threshold concentration of several parts per million seems indicated by data of Kopzynski (mesitylene aerosol at 25 ppm, no aerosol at lower concentration),[71] O'Brien (mesitylene aerosol at 10 ppm, no aerosol at 2 ppm),[94] Schwartz (toluene aerosol at 10 ppm),[92] and Grosjean (no toluene aerosol at 1 ppm).[100] The situation is further complicated by the low reactivity of aromatic compounds. Monofunctional compounds formed early would stay in the gas phase, whereas polyfunctional compounds formed later by further oxidation would accumulate in the aerosol phase. Therefore, aerosol formation from aromatics would be favored by meteorologic conditions that allowed long irradiation periods. Further research is necessary for assessing in a more quantitative manner the contribution of aromatic hydrocarbons to atmospheric aerosol.

Kinetics of Organic Aerosol Formation

Assuming that some of the physical and chemical mechanisms just reviewed are predominant in the formation of organic aerosol, various schemes can be derived that permit a more quantitative description of the time evolution of atmospheric organic aerosol. For example, a kinetic scheme has been proposed recently[157a] for aerosol formation from olefinic precursors that may be applied in principle to other hydrocarbon classes. Starting with this system,

$$>C=C< \; + \left\{ \begin{array}{l} X_1 \xrightarrow{k_1} \\ \vdots \\ X_n \xrightarrow{k_n} \end{array} \right. , \qquad (3)$$

the olefin concentration is given by:

$$-\frac{d[ol]}{dt} = \sum_i k_i [X_i][ol] , \qquad (4)$$

where k_i is the rate constant of olefin reaction with the $_i$th species X_i (O_3, $\underline{O}$, $\dot{O}H$, $H\dot{O}_2$, NO_3,...). However, not all the rate constants k_i have been measured, and the olefin consumption can be estimated from empirical data, such as the nitric oxide to nitrogen dioxide conversion rate constants measured by Glasson and Tuesday.[106] Note also that Eq. 4 can be written:

$$-\frac{d[ol]}{dt} = \sum_i a_i (t)\, b_i\, k_{O_3} [O_3][ol] , \qquad (5)$$

where $k_i = b_i\, kO_3$, and that $[X_i] = a_i[O_3]$, where a_i is only a function of time and can be calculated from computer simulation data.

The Ozone-Olefin System. With Eq. 5, the general problem can be reduced to the ozone-olefin system:

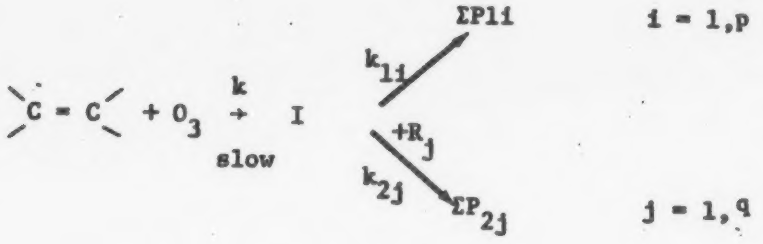

(6)

where ΣP_{1i} and ΣP_{2j} are the products (including other intermediates) that result from unimolecular and bimolecular reactions of the intermediate I, whose formation is the rate-determining step.

Assuming a steady-state concentration for I,

$$I = k[O_3][\text{olefin}] \;/\; \left[\sum_i k_{1i} + \sum_j k_{2j}\,[R_j]\right] , \tag{7}$$

where $R_j = O,\ O_3,\ O_2,\ \dot{O}H,\ H\dot{O}_2,\ NO_2,\ SO_2,$ etc.

The condensable species are generally only a fraction of the products:

$$\Sigma CS_{1i} = \alpha_1 \Sigma P_{1i} \quad \text{and} \quad \Sigma CS_{2j} = \alpha_2\, \Sigma P_{2j} .$$

Assuming that the rate of gas-to-particle conversion of any condensable species is greater than its rate of formation in the gas phase (which is the case for heterogeneous nucleation predominant in the atmosphere, but may not be valid for homogeneous nucleation in "clean-air" smog-chamber studies):

$$\begin{aligned} \frac{d[\text{aerosol}]}{dt} &= \frac{\Sigma\ dCS_{1i}}{dt} + \frac{\Sigma\ dCS_{2i}}{dt} \\ &= [I]\left(\alpha_1 \Sigma k_{1i} + \alpha_2 \Sigma k_{2j}[R_j]\right) . \end{aligned} \tag{8}$$

with Eq. 7,

$$\frac{d[\text{aerosol}]}{dt} = k[O_3][\text{olefin}]\ \frac{\alpha_1 \Sigma k_{1i} + \alpha_2 \Sigma k_{2j}[R_j]}{\Sigma k_{1i} + \Sigma k_{2j}[R_j]} . \tag{9}$$

The term $\alpha = \dfrac{d[\text{aerosol}]}{dt} \; \dfrac{1}{k[O_3][\text{olefin}]}$ is not constant, but is a function of $[R_j]$. However, α can be constant in the following cases:

- $$\alpha \equiv \alpha_1 \begin{cases} \text{if } k_{2j}[R_j] \ll k_{1i} & \text{(fast unimolecular decomposition)} \\ \text{or if } \alpha_2 = 0 & \text{(no condensable species are formed in the bimolecular pathways)} \end{cases}$$

- $$\alpha \equiv \alpha_2 \begin{cases} \text{if } k_{2j}[R_j] \gg k_{1i} \\ \text{if } \alpha_1 = 0 \end{cases}$$

- $[R_j] \approx$ constant, if the species R_j leading to condensable species by reaction with the intermediate are either in great excess (pseudo-first-order) or at steady-state concentrations (free radicals).

Note that the proposed scheme is general and that Eq. 9 can be applied to any simpler system. For example, using sulfur dioxide $\equiv R_1$, $\alpha_1 = 0$, $\alpha_{2j} = 0$ for $j \neq 1$, and $\alpha_{21} = 1$ (all sulfur trioxide formed leads to sulfuric acid aerosol), we find the Cox and Penkett[85] relation:

$$\frac{d[\text{aerosol}]}{dt} = \frac{d[H_2SO_4]}{dt} = k[\text{olefin}][O_3] \; \frac{k_{21}[SO_2]}{\Sigma k_{2j} + k_{21}[SO_2]}, \qquad (10)$$

which has been experimentally verified for the system:

$$\text{olefin} + O_3 \xrightarrow{k} I \left\{ \begin{array}{l} \xrightarrow{k_{1i}} \Sigma P_{1i}, \text{ no } CS_{1i} \\[1em] \xrightarrow[+R_j]{k_{2j}} \Sigma P_{2j}, \text{ no } CS_{2j} \\[1em] \xrightarrow[+SO_2]{k_{21}} SO_3 \rightarrow H_2SO_4 \text{ aerosol} \end{array} \right. \qquad (11)$$

A relation similar to Eq. 9 has been found to account satisfactorily for organic aerosols formed from cyclopentene, cyclohexene, and 1,7-octadiene in smog chambers.[157a] The aerosol organic carbon concentration as a function of time was measured with an organic-carbon analyzer (Figure 3-22). The relation obtained was:

$$\frac{d\ (\text{organic aerosol carbon})}{dt} = \alpha_C\ \alpha\ k[O_3][\text{olefin}]\ , \tag{12}$$

where α_C is the percent of organic carbon averaged over all condensable species.

The Ozone-Multihydrocarbon System. The same kinetic scheme can be used for the most general situation involving multicompetitive olefin-ozone reactions:

$$O_3 + \left\{ \begin{array}{l} ol_1 \xrightarrow{k_1} I_1 \left\{ \begin{array}{ll} \xrightarrow{k^1_{1i}} \Sigma P^1_{1i} & \qquad i = 1,p \\ \xrightarrow[+R_j]{k^1_{2j}} \Sigma P^1_{2j} & \qquad j = 1,q \end{array} \right. \\ \\ ol_2 \xrightarrow{k_2} I_2 \left\{ \begin{array}{l} \xrightarrow{k^2_{1i}} \Sigma P^2_{1i} \\ \xrightarrow[+R_j]{k^2_{2j}} \Sigma P^2_{2j} \end{array} \right. \\ \\ ol_n \xrightarrow{k_n} I_n \left\{ \begin{array}{l} \xrightarrow{k^n_{1i}} \Sigma P^n_{1i} \\ \xrightarrow[+R_j]{k^n_{2j}} \Sigma P^n_{2j} \end{array} \right. \end{array} \right. \tag{13}$$

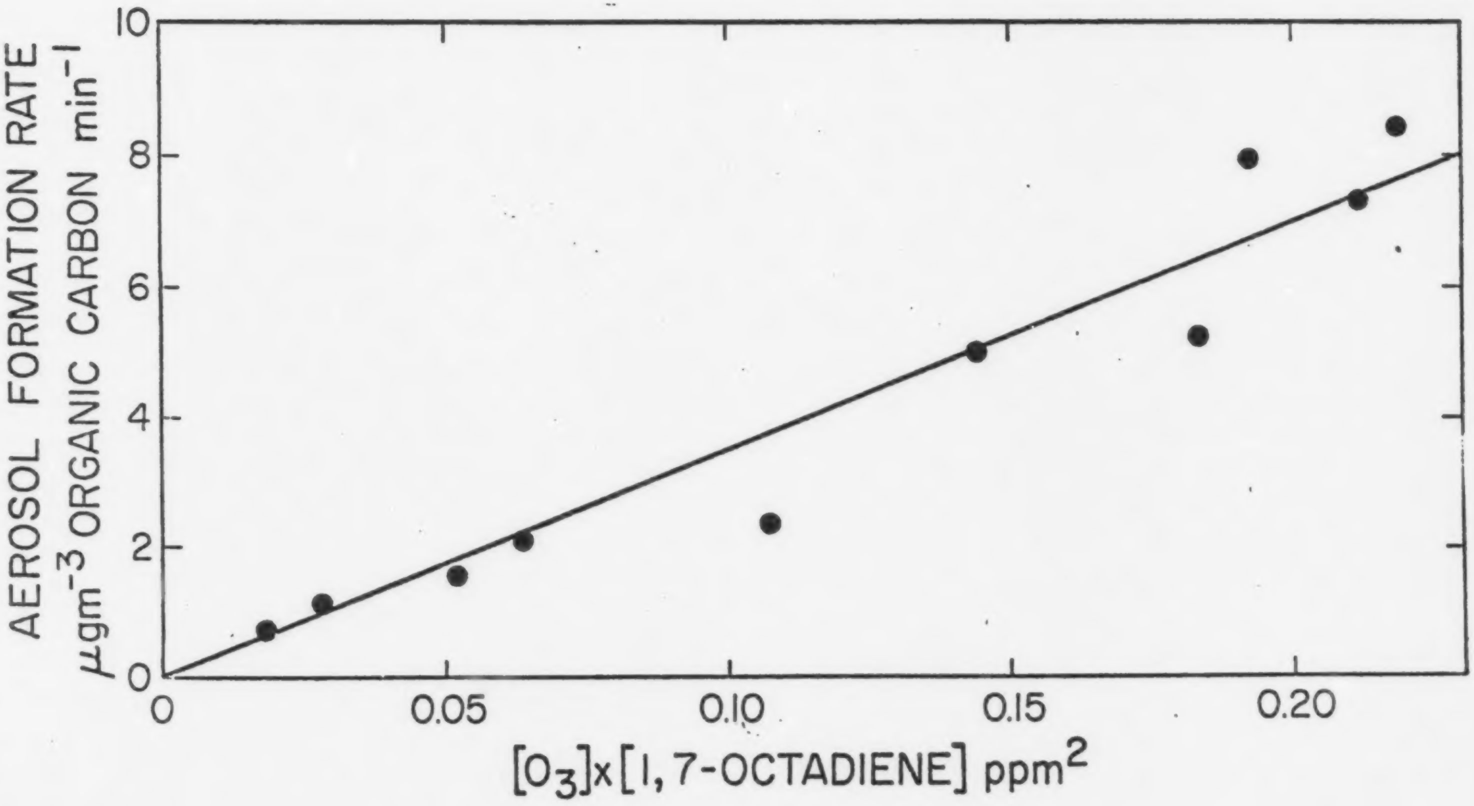

Figure 3-22. Aerosol formation rate as a function of reactant concentrations. Initial concentrations: NO, 0.17 ppm; NO_2, 0.33 ppm; 1,7-octadiene, 1.18 ppm. (Reprinted with permission from Grosjean and Friedlander.[157])

In this case, the ozone concentration is such that it satisfies simultaneously the m relations:

$$[I]_m = k_m [ol_m][O_3] / \left(\Sigma k^m_{1i} + \Sigma k^m_{2j} [R_j]\right) \qquad m = 1,n \quad (14)$$

With the only assumption being, as before, that the intermediate formation step is slower than any further reactions, including transfer of condensable species into the aerosol phase, we obtain the relation:

$$\frac{d[\text{aerosol}]}{dt} = \sum_{m=1,n} \frac{d[\text{aerosol}]_m}{dt} = [O_3] \sum_{m=1,n} \alpha_m k_m [ol]_m \ , \quad (15)$$

where, as before:

$$\alpha_n = \alpha^n_1 \Sigma k^n_{1i} + \alpha^n_2 \Sigma k^n_{2j}[R_j] / \left(\Sigma k^n_{1i} + \Sigma k^n_{2j} [R_j]\right).$$

Note that Eq. 15 expresses in a more quantitative manner the previously discussed dependence of aerosol formation on the product of a gas-phase reactivity term, k_m, and an aerosol formation ability term, α_m.

Applications to the Atmosphere. The general relation of Eq. 15 can be used for estimating amounts of organic aerosol formed from a multihydrocarbon mixture, provided that four parameters--$[O_3]$, α_m, k_m, and $[ol]_m$--are known. Ozone concentration can be readily measured. Aerosol formation ability factors, α_m, can be measured in smog-chamber experiments or estimated ($\alpha_m = 0$ for paraffins, acetylenics, and C_{1-5} alkenes). Note also that the measured ambient gas-to-particle distribution factor f_C[51] is an upper limit for $\Sigma\alpha_m$. Rate constants have been measured for some olefins.[70,85,127,131,159-162] Unknown rate constants for the ozone-olefin reaction can be estimated from published linear relations between k_{O_3} and alkene ionization potentials[163,164] and between k_{O_3} and the rate constants for other electrophilic additions.[157a,164] The last parameter, olefin concentration, can be measured or estimated from data on the composition of gasolines and automobile exhaust (see the following section). When combined with an estimation of air-mass trajectories and residence time derived from meteorologic data, use of this type of kinetic relation would permit predicting the amount of secondary organic aerosol present at a given location of an urban basin by measuring the local ozone concentration. However, it is not assumed so far that such a relation as Eq. 15 is valid for all types of unsaturated and aromatic precursors (see Grosjean and Friedlander[157a] for discussion of other complex systems), and its application to the atmosphere is limited by the scarcity of data on ambient precursor concentrations.

Gas-Phase Hydrocarbon Precursors

More than 100 compounds are released in the atmosphere of urban areas by automobiles, and there is a close relation between the atmospheric hydrocarbon composition and the composition of gasolines and automobile exhausts. The full range of compositions of gasolines has been reported by Sanders and Maynard[165,166] They identified 180 of the 240 compounds separated by capillary-column gas chromatography. Detailed fuel compositions were reported by other investigators,[167-169] and exhaust hydrocarbon compositions were reported by Neligan,[168,171] McEwen,[170] and, more recently, Papa,[172] Jacobs,[173] and Dishart.[174] Exhaust compositions were found to be very sensitive to vehicle regime[170] and fuel composition.[174] Methane, ethane, ethylene, and acetylene due to fuel cracking always represent at least 30% of the exhaust. Ambient hydrocarbons with no more than six carbon atoms are now measured on a routine basis,[171,175-180] but data on C_{7+} hydrocarbons have been limited to the paraffins and aromatics.[177-180] Figure 3-23 illustrates the wide variety of hydrocarbons found in gasoline, auto exhaust, and urban air.

Alkenes. Surprisingly, in view of the wealth of publications dealing with the hydrocarbon composition of polluted atmospheres, there is virtually no information on the existence and ambient concentrations of C_{7+} alkenes. Because of their reactivity and the stringent restriction on the olefinic content in gasolines sold in California, C_{7+} alkenes have not been found in California ambient air. Only a few of them have been identified elsewhere.[181-184] On the basis of the difference between nonmethane hydrocarbon concentrations and the sum of all $C_{\leq 6}$ hydrocarbons measured individually, the C_{7+} fraction (paraffins + olefins + aromatics) accounts for about half the nonmethane hydrocarbon concentration.[56] In the absence of any data for C_{7+} alkenes, their possible concentrations were estimated by scaling up gasoline and auto-exhaust data to match the morning ambient concentration of 1-hexene. This crude estimate indicates that C_{7+} alkenes may be present at about 100 ppb in the atmosphere during the morning traffic period.[185] These alkenes are listed in Table 3-12.

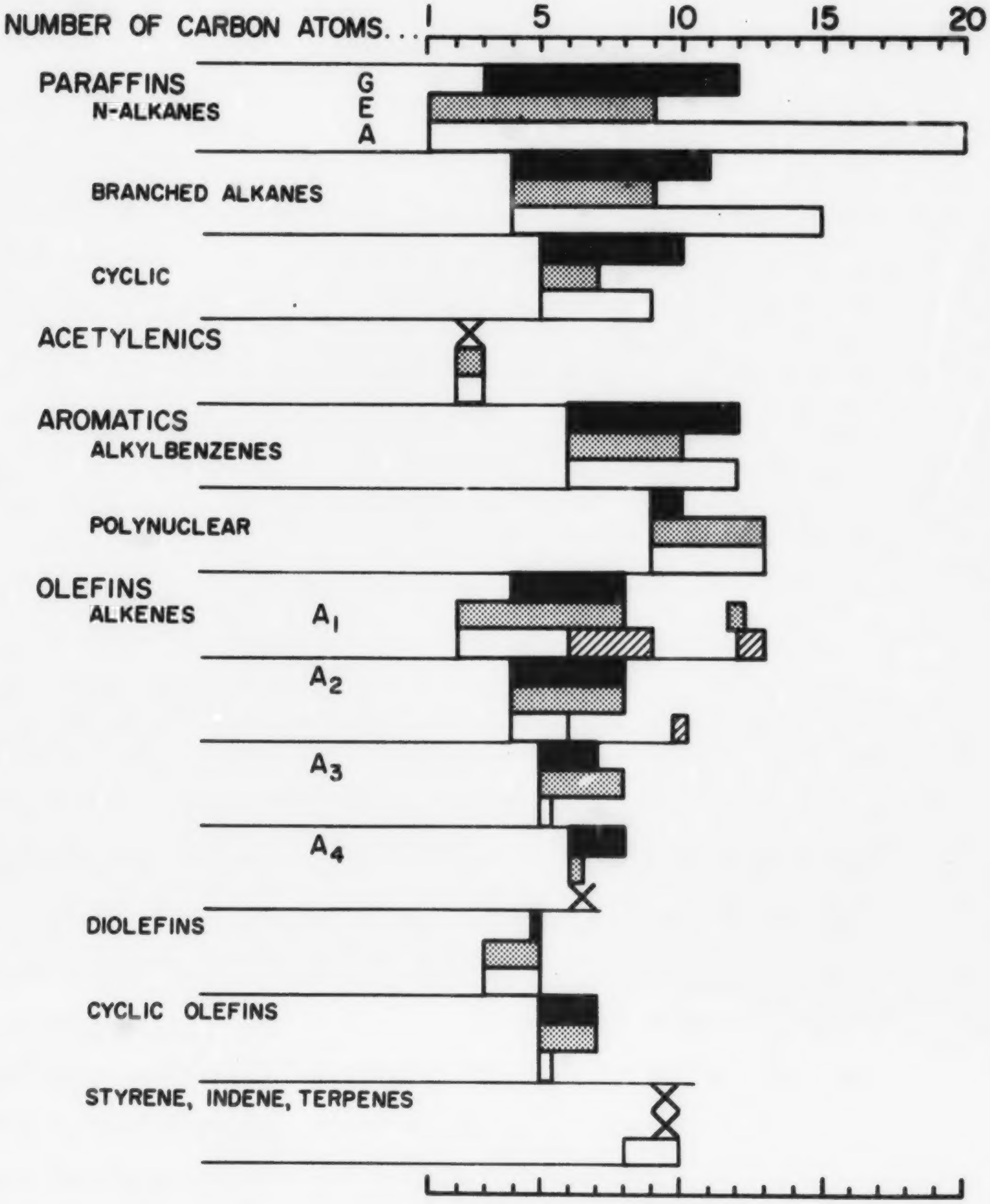

Figure 3-23. Hydrocarbons in gasolines (G), automobile exhaust (E), and ambient urban air (A). A_1, A_2, A_3, A_4 = mono-, di-, tri-, and tetra-substituted alkenes. X = not found. Hatching = not found in California.

Table 3-12

Potential Aerosol Organic Precursors Identified in Gasolines and Automobile Exhaust

Alkenes:[a]	Gasolines	Auto Exhaust	Ambient Air	Expected Photochemical Products
2,3,3-Trimethyl-1-butene	+	+	-	Monofunctional compounds: aldehydes ketones nitrates carboxylic acids (also unsaturated oxygenates if allylic oxidation occurs)
3-Methyl-2-ethyl-1-butene	+	-	-	
2,3-Dimethyl-1-pentene	+	-	-	
2,4-Dimethyl-1-pentene	+	-	-	
3,3-Dimethyl-1-pentene	+	-	-	
3,4-Dimethyl-1-pentene	-	+	-	
4,4-Dimethyl-1-pentene	+	-	-	
2-Ethyl-1-pentene	+	-	-	
3-Ethyl-1-pentene	+	-	-	
2-Methyl-1-hexene	+	-	-	
3-Methyl-1-hexene	+	-	-	
4-Methyl-1-hexene	+	-	-	
5-Methyl-1-hexene	+	+	-	
1-Heptene	+	+	+[b]	
2,4,4-Trimethyl-1-pentene	-	+	-	
2-Ethyl-1-hexene	+	-	-	
cis-2-Octene	-	+	-	
trans-2-Octene	+	+	-	
1-Octene	+	+	+[b]	
Isodecene	-	-	+[b]	
1-Dodecene	-	+	+[b]	
Diolefins:				
Propadiene	-	+	+	Dicarboxylic acids and other difunctional compounds
1,3-Butadiene	-	+	+	
2-Methyl-1,3-butadiene	+	+	+	
1,3-Pentadiene	-	+	-	
α,ω-C_5 + diolefins	-	-	-	

Table 3-12 (Cont.)

Potential Aerosol Organic Precursors Identified in Gasolines and Automobile Exhaust

	Gasolines	Auto Exhaust	Ambient Air	Expected Photochemical Products
Cyclic olefins:				
Cyclopentene	+	+	+	Dicarboxylic acids and other difunctional compounds
1-Methylcyclopentene	+	-	-	
3-Methylcyclopentene	+	-	-	
Cyclohexene	+	+	-	
3-Methylcyclohexene	-	+	-	
4-Methylcyclohexene	-	+	-	

---

[a] Alkenes leading to a C_{6+} fragment: 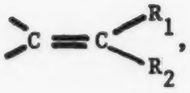, with $R_1 + R_2 \geq 5$ carbon atoms.

$>C=C<$ R_1 R_2

[b] Not identified in California.

Cyclic Olefins. Five cyclic olefins have been identified in gasolines and auto exhaust, cyclopentene being the only one detected in the atmosphere.[171,176] The five cyclic olefins account for only about 0.5% by weight of gasolines and 0.6% by volume of exhausts. Their ambient concentrations were estimated[185] by scaling up gasoline and auto-exhaust data to match the measured ambient morning cyclopentene concentration and from the measured ambient concentrations of C_{5-7} aerosol difunctional compounds. The two estimates agree and indicate that cyclic olefins may be present in the morning atmosphere at 10-50 ppb. On the contrary, C_{6+} diolefins are not present in gasolines and exhaust gases and have not been found in the atmosphere (Table 3-13).

Terpenes. The possibility of widespread haze formation by sunlight irradiation of terpenoid compounds from vegetation was first suggested by Went.[186] Went,[187] Went and Rasmussen,[188] and Rasmussen[189] estimated the annual worldwide contribution of forest hydrocarbon emissions and concluded that more reactive hydrocarbons are released by tree foliage than by man's activities. The major compounds emitted are monoterpenes (C_{10})--like α-pinene, β-pinene, limonene, and myrcene[189,190]--and the hemiterpene (C_5) isoprene.[191] The fate of these gaseous olefins in the atmosphere is still undetermined. Went[192] noticed that irradiated mixtures of nitrogen dioxide and α-pinene produced ozone and fine particles and postulated that terpene-nitrogen oxide reactions, similar to the olefin-NO_x reaction of polluted urban areas, may take place in forested rural areas. Rasmussen and Holdren[193] indicated that, on an individual basis, monoterpene hydrocarbon concentrations are in the low parts-per-billion range in rural air.

Table 3-13

Estimated Cyclic Olefin Contribution to Ambient Organic Aerosol[a]

Precursor	Gasoline, WT %[b]	Exhaust, ppb in 2-ppm NMHC[b]	Ambient Air, ppb Measured[b]	Ambient Air, ppb Estimated (morning Los Angeles)[c]
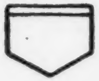	0.13-0.18	1.0	2-9 Los Angeles 4.4 Riverside	5
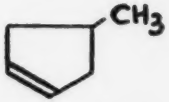	0.04-0.08	+	-	2
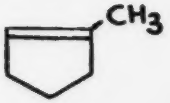	0.14-0.18	+	-	5
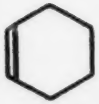	0.14-0.55	5.0	-	12
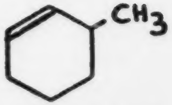	+	6.0	-	6
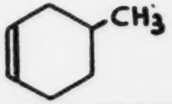	+		-	6
TOTAL	0.45-1.0	12		36

---

[a] Data from Grosjean and Friedlander.[185]

[b] +, identified, but concentration not measured; -, not found.

[c] From gasoline and automobile exhaust data; assuming an average molecular weight of 82 (that of cyclohexene), 100% gas-phase reaction, and 30% gas-to-aerosol conversion (from ref. 100), 36-ppb cyclic olefins would form aerosol difunctional compounds at about 36 μg/m^3.

The gas-phase reactivity of various terpenes has been measured. Stephens and Scott[194] were the first to include two terpenes (pinene and α-phellandrene) with their study of the relative reactivity of various hydrocarbons. Both monoterpenes showed the high reactivity predicted by their olefinic structure. Conversion of nitric oxide to nitrogen dioxide in the presence of isoprene is at a rate intermediate between those for ethylene and *trans*-2-butene,[106] and Niki reported rate constants for the α-pinene and terpinolene-ozone reactions.[195] Grimsrud et al.[196] measured the rate constants for the reaction of various terpenes with ozone and with nitric oxide, the latter at the low concentrations (10-ppb hydrocarbon and 7-ppb nitric oxide) observed in rural areas. Their data are listed in Table 3-14. Structural effects have a major influence on terpene reactivity, and olefinic terpenes react with ozone at rates comparable with those of the most reactive alkenes, such as tetramethylethylene. Grimsrud *et al*. also established that the atmospheric reactivity of very reactive terpenes is due to their reaction with ozone, whereas atmospheric reactivity of less reactive terpenes is controlled by other mechanisms that involve free radicals. Therefore, photochemical reactions of terpenes and nitric oxide may contribute, in part, to the high ozone concentrations (≥20 ppb, and sometimes exceeding 80 ppb) observed in rural daytime air.[197,198]

Table 3-14

Photooxidation and Ozonolysis Rates of Monoterpene Hydrocarbons[a]

Hydrocarbon		Photooxidation Rate (k), $sec^{-1} \times 10^4$ [b]	Ozonolysis Rate k, $ppm^{-1} sec^{-1}$ [c]	Ozonolysis Rate k x 30 ppb, $sec^{-1} \times 10^4$	Ratio, R_{O_3} : R_{NO_x} [d]
p-Menthane	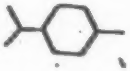	0.11	--	--	--
p-Cymene	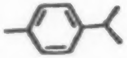	0.25	--	--	--
Isobutene	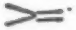	0.84	3.6×10^{-4}	0.11	0.13
β-Pinene	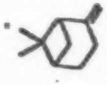	1.1	9×10^{-4}	0.27	0.25
Isoprene	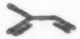	1.3	--	--	--
α-Pinene	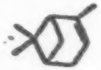	1.3	3.6×10^{-3}	1.1	0.85
3-Carene	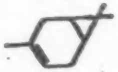	1.4	3×10^{-3}	0.9	0.64
β-Phellandrene	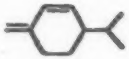	1.9	4.4×10^{-3}	1.3	0.69
γ-Terpinene	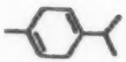	--	7×10^{-3}	2.1	--
Carvomenthene	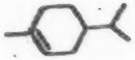	2.1	1.3×10^{-2}	3.9	2.0

Table 3-14 (Cont.)

Photooxidation and Ozonolysis Rates of Monoterpene Hydrocarbons[a]

Hydrocarbon			Ozonolysis Rate		
		Photooxidation Rate (k), $sec^{-1} \times 10^4$ [b]	k, $ppm^{-1} sec^{-1}$ [c]	k x 30 ppb, $sec^{-1} \times 10^4$	Ratio, R_{O_3} : R_{NO_x} [d]
Limonene	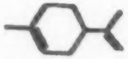	2.4	1.6×10^{-2}	4.8	2.0
Dihydromyrcene	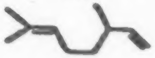	3.0	1.7×10^{-2}	5.1	1.7
Myrcene	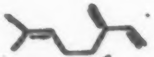	3.8	3.1×10^{-2}	9.3	2.4
Ocimene	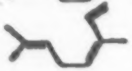	5.3	5×10^{-2}	15	2.8
Terpinolene	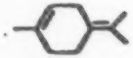	11	2.5×10^{-1}	75	6.8
α-Phellandrene	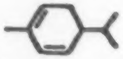	12	2.9×10^{-1}	87	7.2
α-Terpinene	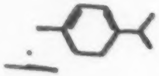	55-110	2.2	630	6.3-12.0

---

[a] Data from Grimsrud et al.[196]
[b] Irradiation vessels contained 7-ppb NO_x and 10-ppb hydrocarbon.
[c] Ozone and hydrocarbon initial concentrations, 0.1 - 5 ppm.
[d] Ratio for a typical rural ozone concentration of 30 ppb.

Aerosol formation from terpenes has not been extensively investigated. Only one olefinic terpene, α-pinene, has been studied.[78,79,82,92,98] Ripperton and Lillian[78] reported condensation nuclei formation from irradiated mixtures of 0.1-ppm nitrogen dioxide and 0.5-ppm α-pinene. Fewer condensation nuclei were obtained when increasing the water vapor concentration. Infrared spectra of α-pinene aerosol[79,82,98] indicate the presence of organic compounds, such as carbonyls, carboxylic acid, and nitrate ester. As mentioned earlier, the composition of α-pinene aerosol was studied in great detail by Schwartz (Figure 3-8). Similar polyfunctional compounds of low volatility are expected to be formed from other olefinic terpenes (β-pinene, limonene) and probably constitute a major fraction of the natural blue haze aerosols formed over forested areas. It is noteworthy that α-pinene and its aerosol products are also present at significant concentrations in urban air.[45] Diurnal profiles of the products are indicative of their secondary origin (Figure 3-24). It has not been determined whether tree foliage, solvent use (turpentine?), or transport from nearby rural regions is responsible for the presence of terpenes in urban areas.

Relative Importance of Various Hydrocarbon Classes in the Formation of Secondary Organic Aerosols. The contribution of the various classes of hydrocarbons to the formation of particulate organic compounds is a complex function of their relative ambient concentrations, gas-phase reactivity, and ability to form products whose physical properties, especially vapor pressures, are of prime importance in the physical mechanisms controlling the gas-to-aerosol conversion process. In view of the results discussed previously, cyclic olefins appear to be the most important class of organic aerosol precursors. This is due to their high gas-phase reactivity

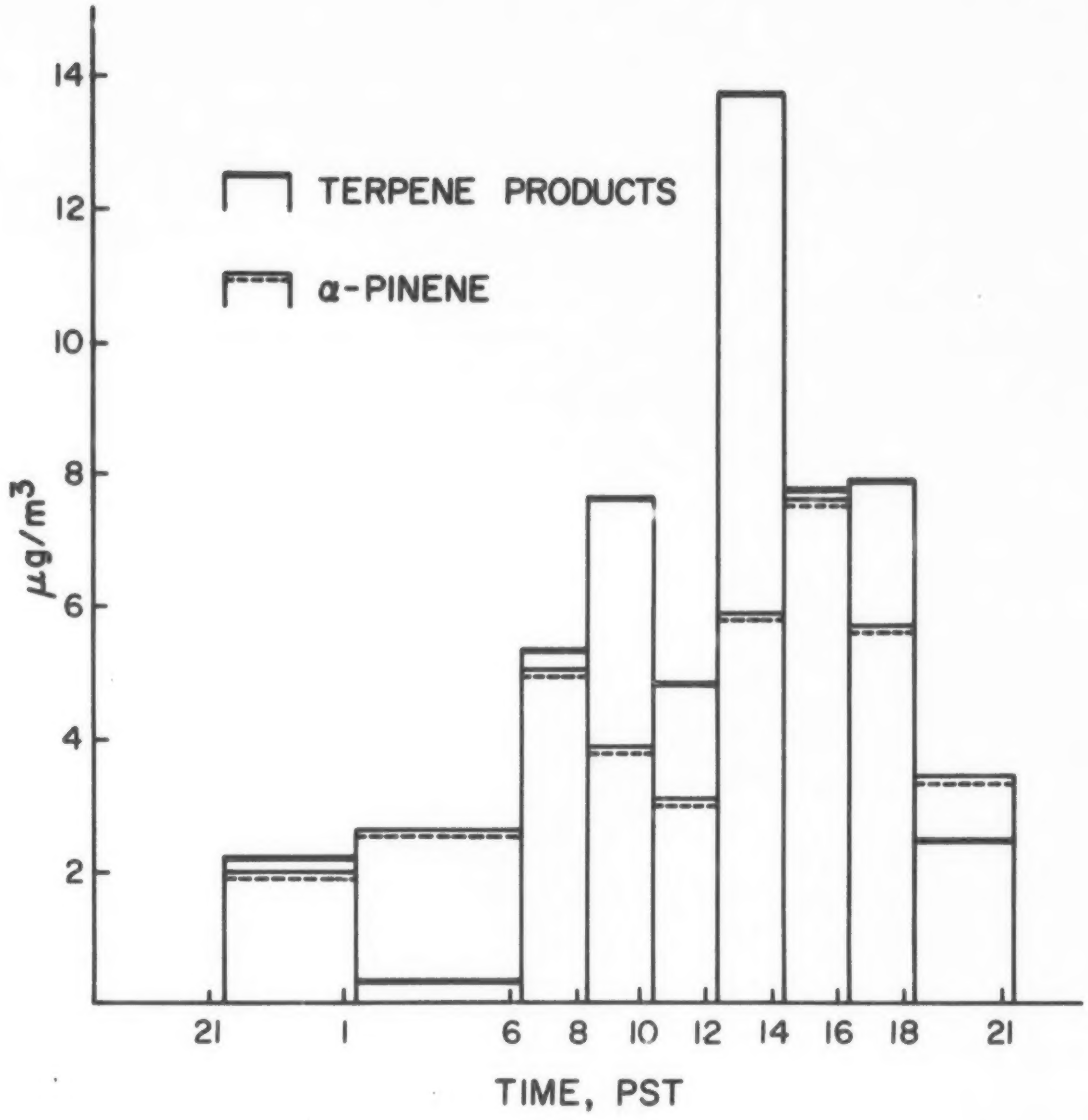

Figure 3-24. Diurnal profiles for α-pinene and total terpene products, West Covina, California, July 24, 1973. See ozone profile on Figure 3-11. (Adapted from Knights _et_ _al_.[45])

and their ability to form difunctional compounds of very low volatility. Such difunctional compounds constitute the major fraction of ambient secondary organic aerosols, and most of them have been identified in smog-chamber experiments.

The observed ambient organic aerosol formation rates are also consistent with those estimated by extrapolation of smog-chamber kinetic data. Other heavy unsaturates, such as styrene and indene, are present in the atmosphere and may contribute, in part, to the formation of benzoic acid and homophthalic acid, respectively. Diesel exhaust and industrial emission are possible sources of such heavy unsaturates. Diolefins of C_{6+} are not present in gasolines and exhaust gases and have not been found in the atmosphere, and their possible role as precursors of the C_{5-7} difunctional acidic compounds is seriously challenged. Lower diolefins are emitted in automobile exhaust. Examination of vapor-pressure data indicates that the bulk of their expected photooxidation products remains in the gas phase, including most of the less volatile C_{3-4} dicarboxylic acids.

Although the ambient concentrations of alkenes are about 10 times higher than those of cyclic olefins, their contribution to the formation of organic aerosols is much lower in both smog-chamber experiments and the ambient atmosphere. Here again, examination of vapor-pressure data reveals that vapor pressures of monofunctional oxygenates expected from alkenes exceed by several orders of magnitude those of the difunctional compounds that have the same numbers of carbon atoms. Thus, the saturation concentration for monofunctional compounds and their later gas-to-aerosol conversion can be reached only in "favorable" conditions, i.e., at high precursor (alkene) concentrations. However, ambient concentrations of C_{6+} alkenes have not been measured, and their role as aerosol precursors cannot be ruled out. The importance of aromatic hydrocarbons remains to be determined. A "compensation effect" is expected between their low reactivity and the possible aromatic ring cleavage that leads to multifunctional compounds of low volatility. On the basis of all available ambient-air and laboratory data, cyclic olefins can be reasonably postulated as the most important class of secondary organic aerosol precursors. However, aromatics and, to a lesser extent, alkenes may be important after a sufficiently long period, when the more efficient aerosol-forming precursors have disappeared. Unfortunately, there are no laboratory data based on periods long enough to simulate the slow transport of air masses ($\geq$ 12 h) encountered in some urban areas (such as the eastern part of the Los Angeles basin) where aromatics may outweigh cyclic olefins as major organic aerosol precursors.

Formation of Secondary Inorganic Aerosols in Photochemical Systems

Recent studies suggest that potentially harmful health effects may be associated with moderately high concentrations of sulfates[199] and nitrates[200] and that both sulfate and nitrate aerosols contribute more than organic particles to visibility degradation in urban areas.[51,56,201] Nitrates and sulfates in atmospheric aerosols can be formed by a wide variety of homogeneous and heterogeneous reactions. Heterogeneous reactions have been thoroughly studied and were considered, until recently, as the major pathways for sulfur dioxide and NO_x removal and particle formation. However, studies of various homogeneous reactions initiated in the last few years suggest that some of these reactions can compete effectively with heterogeneous processes. The purpose of this section is to examine the possible relation between ozone and the two major secondary inorganic aerosol species, sulfates and nitrates. Accordingly, only gas-phase photochemical reactions relevant to sulfate and nitrate formation will be reviewed, and their relative importance in the overall aerosol formation process will be assessed where possible. Information on the corresponding heterogeneous reactions can be found in several reviews.[56,57,202-206]

Nitrate Aerosols. The two important aerosol nitrate precursors are nitrous acid and nitric acid, formed mainly in the reactions:

$$NO + NO_2 + H_2O \rightarrow 2HONO \quad , \qquad (16)$$

$$N_2O_5 + H_2O \rightarrow 2HONO_2 \quad , \qquad (17)$$

$$NO_2 + OH + M \rightarrow HONO_2 + M \quad . \qquad (18)$$

With currently accepted rate constants for these reactions, Calvert[202] estimated that Reaction 18 is of principal importance for nitric acid formation in smog. Nitric acid has recently been identified in both smog chambers[206] and Los Angeles air.[208] However, both nitrous acid and nitric acid have high vapor pressures,[209] and it does not appear possible that particulate nitrogen species will exist in the atmosphere in pure form as acids. Infrared, x-ray, and chemical analyses indicate that ammonium nitrate is the major constituent of the ambient particulate nitrate fraction.[56,61,210,211] Ammonium nitrate is also found in aerosol formed from NO_x-hydrocarbon mixtures irradiated in the presence of ammonia in smog chambers.[94,100] Thus, the production of aerosol nitrate requires neutralization by ambient ammonia. It is not certain whether the reaction takes place in the gas phase or in the liquid phase after fast nitric acid diffusion into the aerosol droplets. Urban ammonia concentrations have been estimated at up to 0.2 ppm (140 $\mu g/m^3$), with averages of one-tenth that value.[212] High aerosol nitrate concentrations are observed in the eastern part of the Los Angeles basin,[56,211] where ammonia emission from feed lots is thought to be important. Also, diurnal aerosol nitrate profiles do not correlate with nitrogen oxide concentrations. Therefore, aerosol nitrate formation may be limited by ambient ammonia, rather than by any of the nitrogen oxide species.

The relative importance of the heterogeneous and photochemical nitrate formation pathways can be assessed from recently measured aerosol nitrate profiles.[51,56] On humid days, a midmorning nitrate peak is usually observed, which tracks rather poorly the morning rush hour NO_x peak and indicates that heterogeneous processes are predominant. On oxidant episode days, however, particulate nitrate concentrations correlate with ozone concentrations. Diurnal profiles of several nitrogen species are presented in Figure 3-25.[51,213] In this case, photochemical production of aerosol nitrate at a rate of about 10 $\mu g/m^3$ per hour was observed.

Sulfate Aerosols. As mentioned before, heterogeneous sulfur dioxide oxidation reactions have been extensively studied.[57,202-206] Two reactions of this type are thought to be particularly important: the aqueous oxidation of sulfur dioxide in water droplets and the catalytic oxidation of

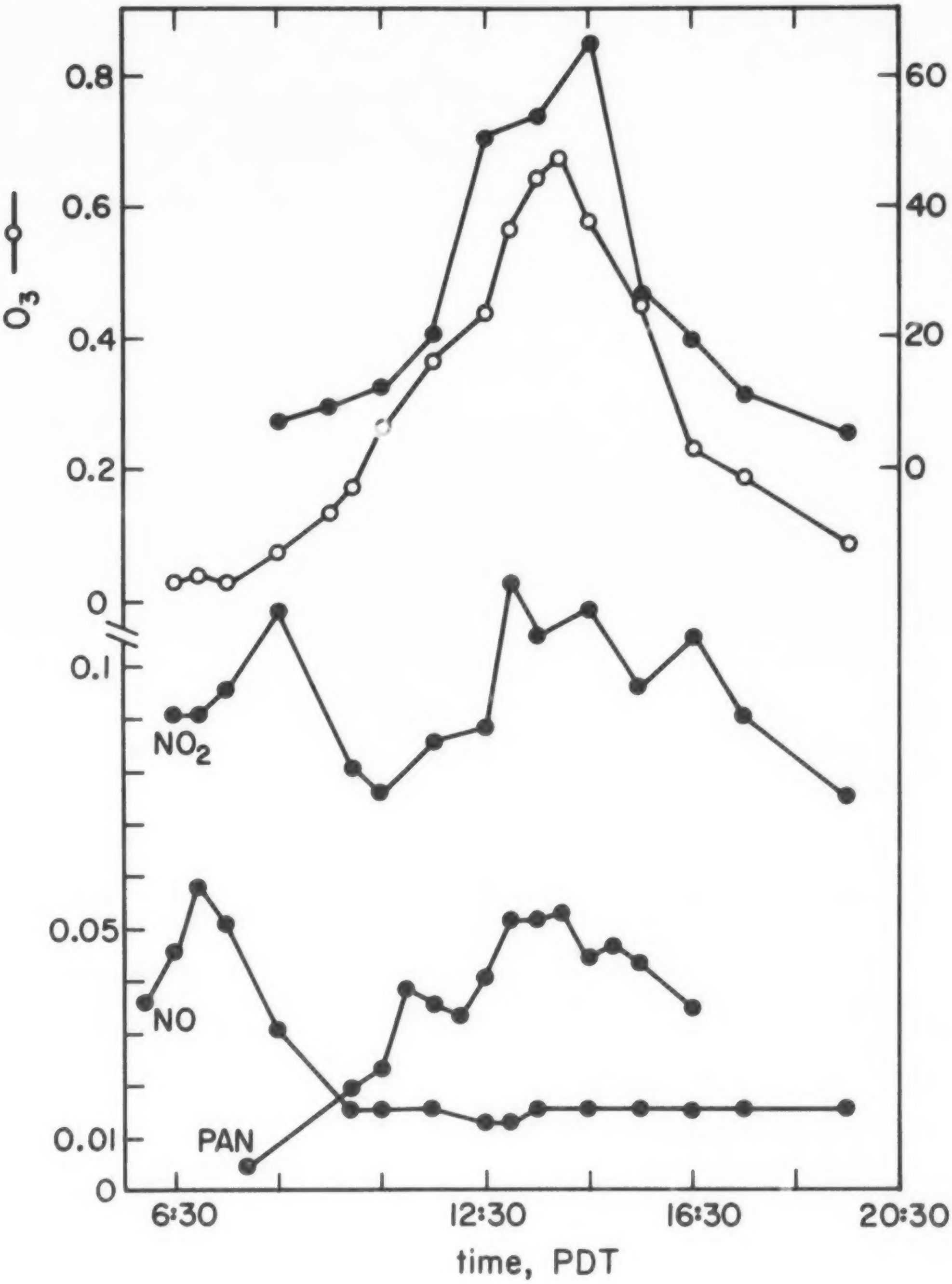

Figure 3-25. Diurnal profiles of nitrogen compounds, Pasadena, California, July 25, 1974. NO, NO_2, O_3, and PAN in ppm; and inorganic aerosol nitrates in µg/m^3. (Data from ref. 51 and 213.)

sulfur dioxide adsorbed on carbon particles. Because ozone is involved in the former reaction and carbon particles are generated by incomplete combustion of hydrocarbons, these two reactions will be examined hereafter. Novakov et al.[214,215] have observed that significant amounts of sulfate ion can be found on carbon particles generated by combustion of hydrocarbons in air enriched with sulfur dioxide in the parts-per-million range. It is difficult to assess the significance of carbon or organic particles for the sulfur dioxide oxidation in the atmosphere. There is little doubt that absorption of sulfur dioxide on carbon particles freshly generated by combustion can provide a surface-catalyzed oxidation medium. Indeed, such experiments as those of Yamamoto et al.[216] have shown that sulfur dioxide oxidation can be as high as 30%/h on activated-charcoal particles less than 5 mm in diameter. Their work also indicates that this rate is strongly reduced by sulfuric acid collection in the micropores of the charcoal. The work of Yamamoto et al. further emphasizes that such a heterogeneous oxidation mechanism depends on a variety of factors, including grain size of the carbon, temperature, and concentrations of sulfur dioxide, water vapor, and oxygen, as well as the micropore structure of the particle surface. It would seem that oily, gummy, wet particles collected from the atmosphere would be poorly suited for nonaqueous reactions to form sulfate, in that their micropore structure would be minimal. Yet such a mechanism cannot be ruled out.

The class of reactions that have been used most often to explain high sulfur dioxide rates in the presence of aerosols that contain water is the system involving sulfur dioxide absorption in water followed by oxidation by dissolved oxygen and/or ozone to form sulfate. Catalysis of the oxidation by heavy metal salts, such as Mn^{++} ion, can realize rates of oxidation in excess of 1%/h in clean water solutions (e.g., Johnstone and Coughanowr[217]). The absorption of sulfur dioxide can be promoted by the buffering effect of simultaneous absorption of ammonia. Scott and Hobbs[218] have shown that the aqueous sulfur dioxide oxidation process can be enhanced significantly by ammonium ion. Indeed, the estimates and experiments of Miller and dePena[219] suggest that rates of sulfur dioxide oxidation can be achieved in fog approaching 10%/h.

It is well known that ozone is quite soluble in water. Therefore, one expects that ozone absorption with sulfur dioxide would contribute to significant oxidation of sulfur dioxide. Experiments of Penkett[220] have shown that oxidation of sulfur dioxide in air at 7 ppb when absorbed in water droplets with ozone, which is present in surrounding air at 0.05 ppm, can be as large as 13%/h. Thus, foggy or cloudy air mixed with photochemical smog, such as occurs sometimes along the Pacific coast, could well be an important medium for sulfate ion formation. Furthermore, such an aqueous mechanism could be significant at middle altitudes over continents even at background ozone concentrations.

The reported rates of sulfur dioxide oxidation in clean water droplets must be considered maximal. It is questionable whether they can ever be achieved in the atmosphere, inasmuch as such aqueous reactions have been shown to be suppressed significantly by organic contaminants. The work of Fuller and Christ[221] and later of Schroeter[222] has indicated that the aqueous absorption of sulfur dioxide and its later oxidation are reduced by as much as an order of magnitude by dissolved organic acids or alcohols that are known to be present in atmospheric aerosol. Much experimental evidence has been accumulated on homogeneous sulfur dioxide oxidation reactions. All investigators report aerosol sulfate formation when sulfur dioxide is added to mixtures of NO_x and hydrocarbons in smog-chamber experiments (see, for example, Table 3-5). The observed enhancement of sulfur dioxide oxidation depends strongly on the hydrocarbon structure (Table 3-6). Alkenes with fewer than seven carbon atoms, which constitute the bulk of ambient unsaturates and do not form organic aerosol, always produce sulfate aerosol when sulfur dioxide is added. On the contrary, there is no significant sulfate formation and neither the nature nor the yields of organic aerosol formed by cyclic olefins are affected by adding sulfur dioxide. An "intermediate" class is represented by C_{7+} alkenes (for example, 1-heptene[84]), which produce some organic aerosol in the absence of sulfur dioxide and both organic and sulfate aerosol when sulfur dioxide is present. Addition of sulfur dioxide does not seem to affect aerosol formation from aromatic hydrocarbons significantly.[89,105] Such a striking hydrocarbon effect is not well understood and may reflect the differences in the nature or the stability of the intermediates involved for each hydrocarbon class.

Various homogeneous reactions have been postulated to account for sulfur dioxide oxidation in irradiated NO_x-hydrocarbon-sulfur dioxide systems. Gas-phase inorganic reactions of sulfur dioxide with oxygen plus light, ozone, oxygen atoms, nitrogen dioxide, nitrogen trioxide, and nitrogen pentoxide have been considered severely rate-limited on the basis of available rate data (e.g., Calvert[202,206]). Listed in Figure 3-26 are other reactions that appear to be important in the atmosphere. These

I. PRECURSOR = SULFUR TRIOXIDE

1. Reactions with intermediates of the ozone-olefin reaction:

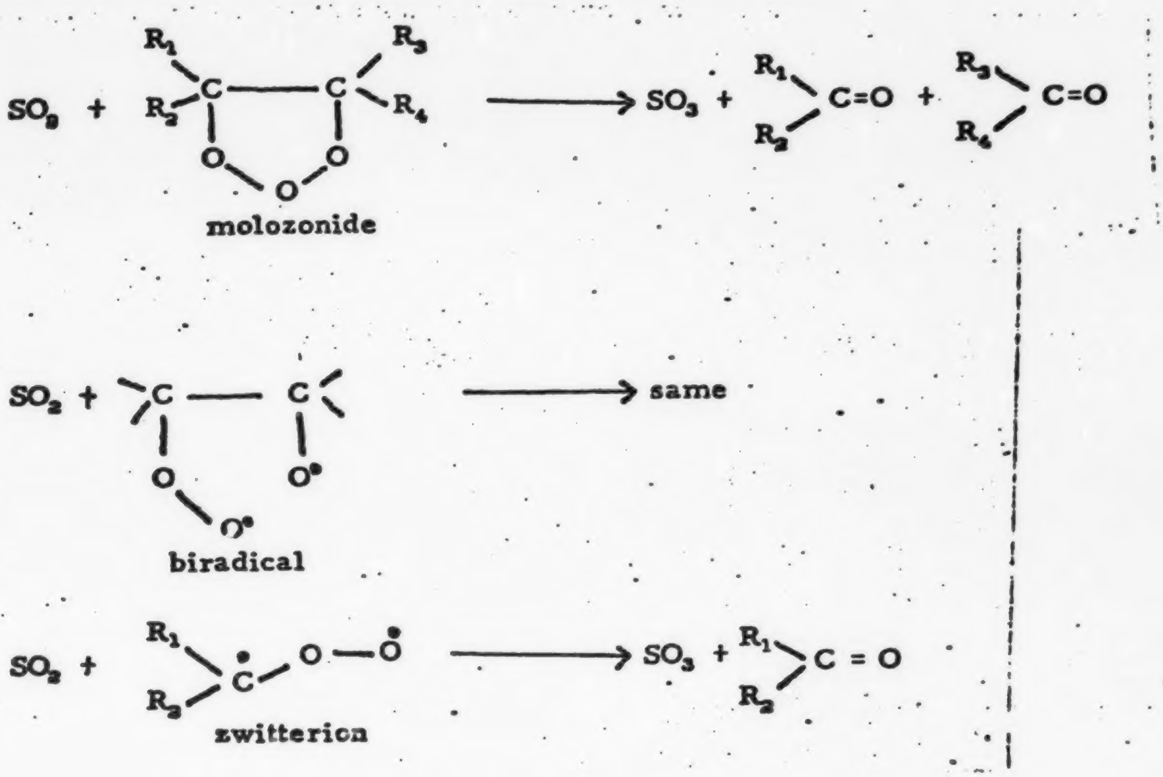
SO2 + molozonide → SO3 + R1R2C=O + R3R4C=O
molozonide
SO2 + biradical → same
biradical
SO2 + zwitterion → SO3 + R1R2C = O
zwitterion

II. 2. Reactions with organic free radicals:

$SO_2 + HO_2 \rightarrow OH + SO_3$

$SO_2 + RO_2 \rightarrow OR + SO_3$

II. PRECURSOR = ORGANOSULFUR SPECIES

$SO_2 + OH \rightarrow HOSO_2$

$SO_2 + OR \rightarrow ROSO_2$

$SO_2 + HO_2 \rightarrow HO_2SO_2$

$SO_2 + RO_2 \rightarrow RO_2SO_2$

Figure 3-26. Atmospheric SO_2 oxidation to aerosol sulfate homogeneous gas-phase organic reactions.

reactions are divided into two subcategories whose end products are sulfur trioxide and organic sulfur species. The first three reactions in Figure 3-26 correspond to the interpretation of Cox and Penkett's[85] observations that sulfur dioxide is oxidized at appreciable rates in the dark in ozone-olefin-air mixtures. The higher rate of 3%/h was found for _cis_-2-pentene, whereas the lower rate of 0.4%/h was found for propylene. Cox and Penkett suggested that either the ozonide or the zwitterion intermediates were involved in sulfur dioxide oxidation. However, Calvert's estimated lifetimes of these olefin-ozone intermediates do not favor their importance as oxidizing agents. Other radical species--such as hydroxyl, alkoxy, hydroperoxy, and alkyperoxy--may well account for sulfur dioxide oxidation.

The importance of the hydroxyl-sulfur dioxide reaction was postulated by Castelman.[223] With measured rate constants for hydroperoxy-sulfur dioxide (Davis _et al._[224]) and other reactions (James _et al._,[225] Gordon[226]), Calvert estimated sulfur dioxide oxidation rates by hydroperoxy, methylperoxy, hydroxyl, and methory radicals to be 0.85, 0.16, 0.23-1.4, and 0.48%/h, respectively.

It is generally accepted that aerosol sulfate formation requires formation of sulfur trioxide and later fast sulfur trioxide reaction with water. However, consideration should be given to other possible sulfur dioxide and sulfur trioxide reactions. For example, Urone and Schroeder[227] and Bricard _et al._[228] reported nitrosylbisulfate, $NOHSO_4$, formation during photolysis of sulfur dioxide-NO_x mixtures, whereas Daubendiek[229] reported the formation of an unidentified white solid in the sulfur trioxide-nitrogen dioxide reaction. The significance of this compound in urban aerosol formation should be evaluated. Moreover, it appears from reactions listed in Figure 3-26 that various organic sulfur species must also be considered as potential sulfate aerosol precursors. The radical addition products, such as $OHSO_2$, should react rapidly with other species to form sulfuric acid, peroxysulfuric acid, alkylsulfates, and mixed anhydrides, such as $HOSO_2ONO_2$.[202] Any of these ultimately should lead to sulfate in the presence of water.

Although no conclusive evidence has been reported so far, the possible importance of organic sulfur species as sulfate aerosol precursors is supported by several observations. Sulfuric acids, sulfonic acids, and other organic sulfur compounds are formed in sulfur dioxide-hydrocarbon reactions at high concentrations.[230-232] Organosulfur radical species, such as RSO_2 and RO_2SO_2 have been postulated as intermediates for these reactions.[233-235] Suzuki[236] observed polymer formation from

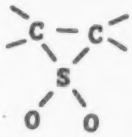

units in the sulfur dioxide-*cis*-butene reaction. More recently, Schulten and Schurath[99] reported several organosulfur compounds in aerosol formed from the sulfur dioxide-ozone-1-butene system. They tentatively identified these compounds as zwitterion-sulfur dioxide addition products and/or mixed anhydrides of sulfuric acid and sulfurous acid with several organic acids. These results are most interesting, inasmuch as the system was studied at concentrations approaching those of interest in polluted atmosphere.

Summing all the known homogeneous reactions for sulfur dioxide oxidation, it is possible to rationalize a theoretical rate of sulfate formation in the range 1.7-5.5%/h for moderate photochemical smog conditions. Sulfur dioxide oxidation rates in nonphotochemically polluted areas, such as central Europe[236] and St. Louis,[57] are in the range of 0.5-1.0%/h. Much higher sulfur dioxide oxidation rates, up to 13%/h, have been measured in the Los Angeles basin for days of low humidity and high oxidant[237] (see also gas-particle distribution factor f_S in Table 3-4). A strong influence of photochemistry is demonstrated for submicrometer sulfate aerosol by the systematic increase in $f_S < 0.5$ μm with ozone concentration at various locations in the southern California air basin (Figure 3-27). It appears, therefore, that conversion of sulfur dioxide to sulfate is significantly enhanced by homogeneous reactions in photochemically polluted atmosphere. It is possible, however, that the sulfate problem in the next few years will be dominated by other factors, such as the use of high-sulfur fuels and the use of oxidizing catalysts that cause conversion of fuel-bound sulfur to sulfuric acid aerosol.[238-242] More quantitative data on aerosol formation in sulfur dioxide-NO_x-hydrocarbon systems at atmospheric concentrations are necessary to estimate whether significant reduction in sulfate concentrations can be achieved through the control of oxidants.

Summary

Review of the literature provides ample evidence that aerosol formation is an important part of the atmospheric chemistry linked with photochemical oxidant production. The important chemical constituents of concern include sulfate, nitrate, and secondary organic material.

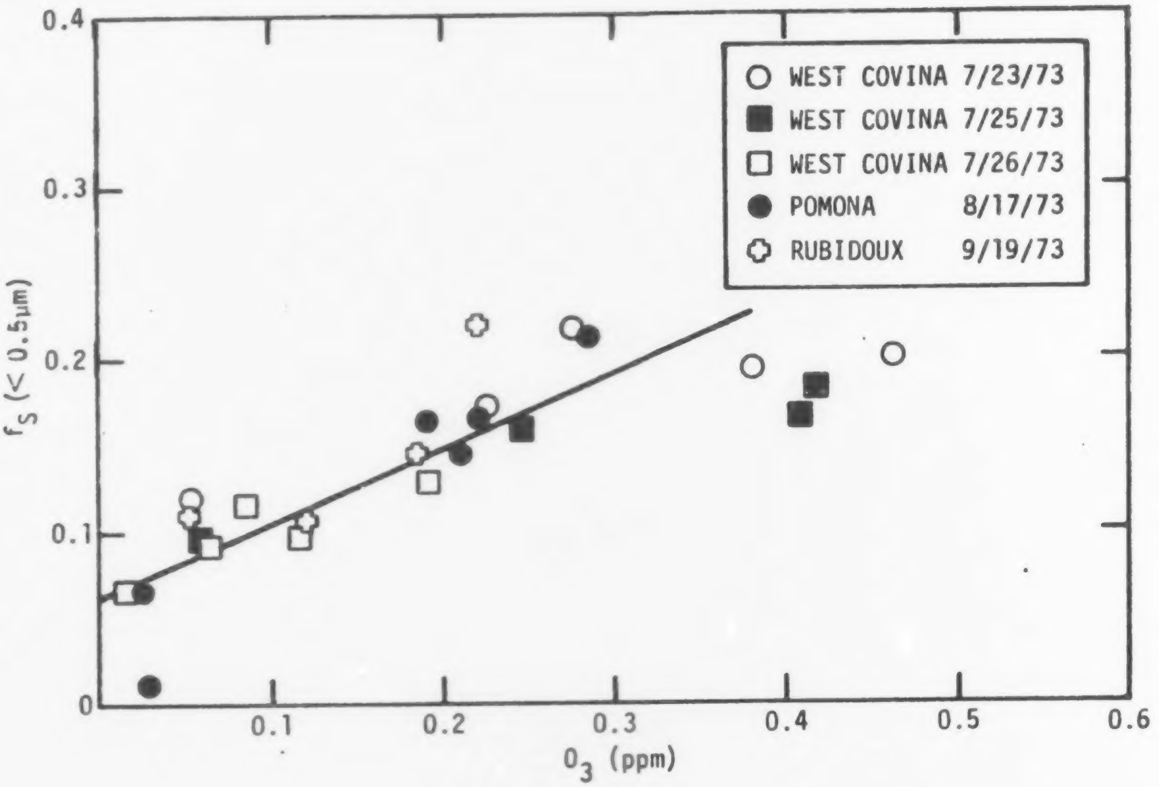

Figure 3-27. Scatter diagram of the conversion ratio f_S based on particles smaller than 0.5 μm vs. 2-h averaged ozone concentration. (Data from Hidy et al.[56,57])

Secondary organic aerosols, formed by gas-phase reaction between nitrogen oxide, ozone, and hydrocarbons constitute an important fraction of urban photochemical smog. Data obtained at high ozone concentrations (0.67 ppm) can be taken as an upper limit of the contribution of secondary organic aerosols to the organic aerosol fraction and total suspended particulate material (95% and 65%, respectively). Most of the identified ambient secondary organic aerosols are difunctional compounds that bear carboxylic, nitrate, aldehyde, and alcohol groups. The same compounds have been identified in smog chambers from C_{5+} cyclic olefins and diolefins, with gas-to-aerosol conversion factors exceeding by more than an order of magnitude those measured for the ambient average conversion of all reactive hydrocarbons. The formation of such species in the gas phase in excess of their saturation concentration followed by condensation on preexisting particles and further growth in the light-scattering range is the predominant physical mechanism that controls the gas-to-aerosol conversion process.

Because of their very low vapor pressures, difunctional compounds are readily converted to the aerosol phase, whereas more volatile monofunctional compounds require much higher precursor and ozone concentrations to reach their saturation concentration. This explains why most of the compounds formed from alkenes remain in the gas phase, whereas C_{5+} cyclic olefins and diolefins are efficient aerosol precursors. However, there is no known source of the latter class, so cyclic olefins, identified in both gasolines and auto exhaust, can be regarded as the most important source of secondary organic aerosols. The role of aromatics as aerosol precursors is essentially unknown. Because of their accumulation in the submicrometer range, all secondary organics are potentially dangerous. However, there is almost no information on health effects associated with the presence of such compounds in the atmosphere.

Because the conclusions presented in this chapter rely heavily on a few recent studies, it is extremely difficult to relate the urban concentrations of secondary aerosols to the concentration of their gas-phase precursors. Simple relations of the type d(secondary aerosol)/dt = α (precursor) (ozone) have been derived from smog-chamber data for organic aerosol formation in mixtures of cyclic olefins and NO_x and sulfate aerosol formation in mixtures of NO_x, sulfur dioxide, and C_{5-} alkenes. Such kinetic data are consistent with the organic (a few micrograms per cubic meter per hour) and sulfate (up to 13%/h) aerosol formation rates observed in photochemically polluted urban areas. More complex kinetic relations reflect certainly all the possible variations between these extreme and rather simple systems. Although control of ozone, through control of NO_x and total hydrocarbon emission, would obviously have a roughly proportional effect on the formation of organic aerosols, present data suggest the identification and control of a few specific hydrocarbon precursors as an alternative approach. The contribution of photochemical reactions involving hydrocarbons to inorganic nitrate and sulfate aerosol formation remains to be determined. More data on the identification of hydrocarbon precursors and on the kinetics of formation, physical parameters, and health effects of their products would ultimately permit quantifying the complex relations between secondary aerosols and ozone concentrations in urban atmospheres.

RECOMMENDATIONS FOR FUTURE RESEARCH

Our present knowledge of the chemical and physical processes that govern aerosol formation in the atmosphere is rather limited, and further studies are needed in most of the relevant areas of research. This may leave the reader--and the decision-maker--with a feeling of endlessness. However, substantial improvements could be made in a reasonable period by focusing research efforts in the subjects most directly involved:

- Laboratory (smog-chamber) studies of aerosol formation from aromatic hydrocarbons: gas-phase reaction mechanism, physical processes controlling gas-to-aerosol conversion, kinetic data on aerosol formation and aerosol growth, identification of the aerosol products, and effect of hydrocarbon concentration on aerosol formation (threshold).
- Careful search, in the atmosphere, for aerosol precursors, such as cyclic olefins and C_{6+} alkenes.
- Study of the possible health effects of exposure to difunctional oxygenated organics (such as dicarboxylic acids) that are present in urban aerosols.
- Identification of organic components of ambient aerosols, to permit estimation of the relative importance of olefinic and aromatic hydrocarbons as aerosol precursors.
- Estimation of the relative contributions of photochemical and nonphotochemical pathways to the formation of inorganic nitrate and sulfate aerosols.

Identification of organic components of ambient aerosols and estimation of the contributions of various pathways are of immediate interest for control strategies and could be achieved by using the existing monitoring networks so as to provide more information on aerosol chemical composition. In view of the adverse effects (e.g., on health and visibility) associated with submicrometer aerosols, an air quality standard for submicrometer particles might be more adequate than the present standard for total suspended particles.

REFERENCES

1. Leighton, P. A. Photochemistry of Air Pollution. New York: Academic Press, 1961. 300 pp.

2. U. S. Environmental Protection Agency. Part 410--National primary and secondary ambient air quality standards. Fed. Reg. 36:8186-8201, 1971.

3. TRW Systems Group. An Implementation Plan for Suspended Particulate Matter in the Los Angeles Region. Final Report to EPA, Contract #68-02-1384. Redondo Beach, Calif.: TRW Systems Group, March 1975. (UNVERIFIED)

4. National Academy of Sciences. National Academy of Engineering. Coordinating Committee on Air Quality Studies. Air Quality and Automobile Emission Control. Vol. 3. The Relationship of Emissions to Ambient Air Quality. U. S. Senate Committee Print Serial No. 93-24. Washington, D. C.: U. S. Government Printing Office, 1974. 137 pp.

5. see Chapter 5 (this report)

6. Grosjean, D. Solvent extraction and organic carbon determination in atmospheric particulate matter: The organic extraction-organic carbon analyzer (OE-OCA) technique. Anal. Chem. 47:797-805, 1975.

7. Patterson, R. K. Automated pregl-dumas technique for determining total carbon, hydrogen, and nitrogen in atmospheric aerosols. Anal. Chem. 45:605-609, 1973.

8. Stephens, E. R., and M. A. Price. Smog aerosol: Infrared spectra. Science 168:1584-1586, 1970.

9. Cunningham, P. T., S. A. Johnson, and R. T. Yang. Variations in chemistry of airborne particulate material with particle size and time. Environ. Sci. Technol. 8:131-135, 1974.

10. Novakov, T., P. K. Mueller, A. E. Alcocer, and J. W. Otvos. Chemical composition of Pasadena aerosol by particle size and time of day. III. Chemical states of nitrogen and sulfur by photoelectron spectroscopy. J. Colloid Interface Sci. 39:225-234, 1972.

11. Schuetzle, D., A. L. Crittenden, and R. J. Charlson. Application of computer controlled high resolution mass spectrometry to the analysis of air pollutants. J. Air Pollut. Control Assoc. 23:704-709, 1973.

12. Jutze, G. A., and K. E. Foster (TR-2 Air Pollution Measurements Committee) Recommended standard method for atmospheric sampling of fine particulate matter by filter media--high-volume sampler. J. Air Pollut. Control Assoc. 17:17-25, 1967.

13. Jewell, D. M., J. H. Weber, J. W. Bunger, H. Plancher, and D. R. Latham. Division of Petroleum Chemistry Paper 13 Presented at Meeting of the American Chemical Society, Washington, D. C., Sept. 12-17, 1971. (UNVERIFIED)

14. Tabor, E. C., T. E. Hauser, J. P. Lodge, and R. H. Burttschell. Characteristics of the organic particulate matter in the atmosphere of certain American cities. A.M.A. Arch. Ind. Health 17:58-63, 1958.

15. Renzetti, N. A., and G. J. Doyle. The chemical nature of the particulate in irradiated automobile exhaust. J. Air Pollut. Control Assoc. 8:293-296, 1959.

16. Cukor, P., L. L. Ciaccio, E. W. Lanning, and R. L. Rubino. Some chemical and physical characteristics of organic fractions in airborne particulate matter. Environ. Sci. Technol. 6:632-637, 1972.

17. Sawicki, E., T. W. Stanley, T. R. Hauser, H. Johnson, and W. Elbert. Correlation of piperonal test values for aromatic compounds with the atmospheric concentration of benzo(a)pyrene. Int. J. Air Water Pollut. 7: 57-70, 1963.

18. Ciaccio, L. L., R. L. Rubino, and J. Flores. Composition of organic constituents in breathable airborne particulate matter near a highway. Environ. Sci. Technol. 8:935-942, 1974.

19. Miller, D. F., W. E. Schwartz, P. W. Jones, D. W. Joseph, C. W. Spicer, C. J. Riggle, and A. Levy. Haze Formation: Its Nature and Origin, 1973. EPA-650/3-74-002. Columbus, Ohio: Battelle Columbus Laboratories, 1973. /178 pp._7

20. Frassa, K. P., R. K. Siegfriedt, and C. A. Houston. Modern analytical techniques to establish realistic crankcase drains. Society of Automotive Engineers Paper 951D, New York, January 1965.

21. Mader, P. P., R. D. MacPhee, R. T. Lofberg, and G. P. Larson. Composition of organic portion of atmospheric aerosols in the Los Angeles area. Ind. Eng. Chem. 44:1352-1355, 1952.

22. Hoffman, D., and E. L. Wynder. Analytical and biological studies on gasoline engine exhaust. Nat. Cancer Instit. Monograph 9:91-116, 1962.

23. Sawicki, E., S. P. McPherson, T. W. Stanley, J. Meeker, and W. C. Elbert. Quantitative composition of the urban atmosphere in terms of polynuclear aza heterocyclic compounds and aliphatic and polynuclear aromatic hydrocarbons. Int. J. Air Water Pollut. 9:515-524, 1965.

24. Dubois, L., A. Zdrojewski, P. Jennawar, and J. L. Monkman. The identification of the organic fraction of air sample. Atmos. Environ. 4:199-207, 1970.

25. Stanley, T. M., J. E. Meeker, and M. J. Morgan. Effects of various solvents and conditions on the recovery of benzo(a)pyrene, benz(c)acridine, and 7H-benz(de)anthracene-7-one. Environ. Sci. Technol. 1:927-931, 1967.

26. Shabad, L. M., and G. A. Smirnov. Aircraft engines as a source of carcinogenic pollution of the environment /¯benzo(a)pyrene studies_7. Atmos. Environ. 6:153-164, 1972.

27. Sawicki, E., T. W. Stanley, S. McPherson, and M. Morgan. Use of gas-liquid and thin-layer chromatography in characterising air pollutants by fluorometry. Talanta 13:619-629, 1966.

28. Gordon, R. J., and R. J. Bryan. Patterns in airborne polynuclear hydrocarbon concentrations at four Los Angeles sites. Environ. Sci. Technol. 7:1050-1053, 1973.

29. Pierce, R. C., and M. Katz. Dependency of polynuclear aromatic hydrocarbon content on size distribution of atmospheric aerosols. Environ. Sci. Technol. 9:347-353, 1975.

30. Brocco, D., V. di Palo, and M. Possanzini. Improved chromatographic evaluation of alkanes in atmospheric dust samples. J. Chromatogr. 86:234-238, 1973.

31. Hauser, T. R., and J. N. Pattison. Analysis of aliphatic fraction of air particulate matter. Environ. Sci. Technol. 6:549-555, 1972.

32. Liberti, A., G. P. Cartoni, and V. Cantuti. Gas chromatographic determination of polynuclear hydrocarbons in dust. J. Chromatogr. 15:141-148, 1964.

33. McPherson, S. P., E. Sawicki, and F. T. Fox. Characterization and estimation of n-alkanes in airborne particulates. J. Gas Chromatogr. 4:156-159, 1966.

34. Arito, H., R. Soda, and H. Matsushita. Gas chromatographic determination of polynuclear hydrocarbons in particulate air pollutants. Ind. Health 5:243-259, 1967.

35. Melton, C. W., R. I. Mitchell, D. A. Trayser, and J. F. Foster. Chemical and Physical Characterization of Automotive Exhaust Particulate Matter in the Atmosphere (Year Ending June 30, 1972). Final Report. EPA 650/3-73-001. Columbus, Ohio: Battelle Columbus Laboratories, 1973. 91 pp.

36. Shepherd, M., S. M. Rock, R. Howard, and J. Stormes. Isolation, identification, and estimation of gaseous pollutants of air. Anal. Chem. 23:1431-1440, 1951.

37. Safe, S., and O. Hutzinger. Mass Spectrometry of Pesticides and Pollutants. Cleveland, Ohio: CRC Press, 1973. 220 pp.

38. Majer, J. R., R. Perry, and J. M. Reade. The use of thin-layer chromatography and mass spectrometry for the rapid estimation of trace quantities of air pollutants. J. Chromatogr. 48:328-333, 1970.

39. Perry, R., R. Long, and J. R. Majer. The use of mass spectrometry in the analysis of air pollutants, pp. 557-562. In H. M. Englund and W. T. Beery, Eds. Proceedings of the Second International Clean Air Congress. Held at Washington, D. C., December 6-11, 1970. New York: Academic Press, 1971.

40. Boyer, K. W., and H. A. Laitinen. Automobile exhaust particulates. Properties of environmental significance. Environ. Sci. Technol. 9:457-469, 1975.

41. Lao, R. C., R. S. Thomas, H. Oja, and L. Dubois. Application of a gas chromatograph-mass spectrometer-data processor combination to the analysis of the polycyclic aromatic hydrocarbon content of airborne pollutants. Anal. Chem. 45:908-915, 1973.

42. Golden, C., and E. Sawicki. Ultrasonic extraction of total particulate aromatic hydrocarbons from airborne particles at room temperature. Int. J. Environ. Anal. Chem. (in press)

43. U. S. Environmental Protection Agency. Office of Air and Water Programs. Air Quality Data for Organics 1969 and 1970 from the National Air Surveillance Networks. Report APTD-1465. Research Triangle Park, N. C.: U. S. Environmental Protection Agency, 1973. /‾34 pp._7

44. U. S. Department of Health, Education, and Welfare. Public Health Service. National Air Pollution Control Administration. Air Quality Criteria for Particulate Matter. NAPCA Publ. No. AP-49. Washington, D. C.: U. S. Government Printing Office, 1969. 211 pp.

45. Knights, R. L., D. R. Cronn, and A. L. Crittenden. Diurnal Patterns of Several Components of Urban Particulate Air Pollution. Paper No. 3 Presented at 1975 Pittsburg Conference on Analytical Chemistry and Applied Spectroscopy, Cleveland, Ohio, March 3, 1975.

46. Gordon, R. J. Patterns in airborne particulate pollutants at several Los Angeles locations. Division of Environmental Chemistry Paper No. 40, Presented at 167th National Meeting of the American Chemical Society, Los Angeles, California, April 3, 1974.

47. Pupp, C., R. C. Lao, J. J. Murray, and R. F. Pottie. Equilibrium vapour concentrations of some polycyclic aromatic hydrocarbons, As_4O_6 and SeO_2 and the collection efficiencies of these air pollutants. Atmos. Environ. 8:915-925, 1974.

48. Stauff, J., and H. Fuhr. Chemiluminescence of the exhaust gases of an internal combustion engine. Angew. Chem. Int. Ed. Engl. 14:105-106, 1975.

49. Santamaria, L., G. G. Giordano, M. Alfisi, and F. Cascione. Effects of light on 3,4-benzpyrene carcinogenesis. Nature 210:824-825, 1966.

50. O'Brien, R. J., J. H. Crabtree, J. R. Holmes, M. C. Hoggan, and A. H. Bockian. Formation of photochemical aerosol from hydrocarbons. Atmospheric analysis. Environ. Sci. Technol. 9:577-582, 1975.

51. Grosjean, D., and S. K. Friedlander. Gas-particle distribution factors for organic and other pollutants in the Los Angeles atmosphere. J. Air Pollut. Control Assoc. 25:1038-1044, 1975.

52. Wilson, W. E., Jr., W. E. Schwartz, and G. W. Kinzer. Haze Formation. Its. Nature and Origin. Battelle Report #CPA 70-172. Columbus, Ohio: Battelle Columbus Laboratories, Jan. 28, 1972. 77 pp.

53. Schuetzle, D. Computer Controlled High Resolution Mass Spectrometric Analysis of Air Pollutants. Ph.D. Thesis. Seattle: University of Washington, 1972. 242 pp.

54. Schuetzle, D., D. Cronn, A. L. Crittenden, and R. L. Charlson. Molecular composition of secondary aerosol and its possible origin. Environ. Sci. Technol. 9:838-845, 1975.

55. Hidy, G. M., et al. Characterization of Aerosols in California (ACHEX). Interim Report, Phase I. Thousand Oaks, Calif.: Rockwell International, 1973.

56a. Hidy, G. M., et. al. Characterization of Aerosols in California. (ACHEX) Final Report. Vol. I-IV. SC524.25FR. Thousand Oaks, Calif.: Rockwell International, 1974.

56b. Hidy, G. M., B. R. Appel, R. J. Charlson, W. E. Clark, S. K. Friedlander, D. H. Hutchinson, T. B. Smith, J. Suder, J. J. Sesolowski, and K. T. Whitby. Summary of the California aerosol characterization experiment. J. Air Pollut. Control Assoc. 25:1106-1114, 1975.

57. Hidy, G. M., and C. S. Burton. Atmospheric aerosol formation by chemical reactions. Int. J. Chem. Kinetics, Symp. No. 1 (Chemical Kinetic Data for the Lower and Upper Atmosphere):509-541, 1975.

58. Appel, B. R., P. Colodny, J. J. Wesolowski, P. K. Mueller, R. Knights, J. Huntzicker, and D. Grosjean. The analysis of carbonaceous materials in California atmospheric aerosols. Paper Presented at 1974 Pacific Conference on Chemistry and Spectroscopy, San Francisco, California, October 16, 1974.

59. Friedlander, S. K. Chemical element balances and identification of air pollution sources. Environ. Sci. Technol. 7:235-240, 1972.

60. Gartrell, G., Jr., and S. K. Friedlander. Relating particulate pollution to sources: The 1972 California aerosol characterization study. Atmos. Environ. 9:279-299, 1975.

61. Lundgren, D. A. Atmospheric aerosol composition and concentration as a function of particle size and of time. J. Air Pollut. Control Assoc. 20:603-608, 1970.

62. White, W. H., R. B. Husar, and S. K. Friedlander. A Study of Los Angeles Smog Aerosol Dynamics by Air Trajectory Analyses. Paper 73-11, Presented at 66th Annual Meeting of the Air Pollution Control Association, Chicago, Illinois, June 24-28, 1973.

63a. Haagen-Smit, A. J. Chemistry and physiology of Los Angeles smog. Ind. Eng. Chem. 44:1342-1346, 1952.

63b. Haagen-Smit, A. J., C. E. Bradley and M. M. Fox. Ozone formation in photochemical oxidation of organic substances. Ind. Eng. Chem. 45:2086-2089, 1953.

63c. Haagen-Smit, A. J., and M. M. Fox. Ozone formation in photochemical oxidation of organic substances. Ind. Eng. Chem. 48:1484-1487, 1956.

64. Cadle, R. D. p. 27. In L. H. Rogers, Ed. Proceedings of the Conference on Chemical Reactions in Urban Atmospheres. Technical Report 15. San Marino, Calif.: Air Pollution Foundation, 1956.

65. Schuck, E. A., and G. J. Doyle. Photooxidation of Hydrocarbons in Mixtures Containing Oxides of Nitrogen and Sulfur Dioxide. Report No. 29. San Marino, Calif.: Air Pollution Foundation, 1959. 126 pp.

66. Renzetti, N. A., and G. J. Doyle. Photochemical aerosol formation in sulfur dioxide-hydrocarbon systems. Int. J. Air Pollut. 2:327-345, 1960.

67. Schuck, E. A., G. J. Doyle, and N. Endow. A Progress Report on the Photochemistry of Polluted Atmospheres. Technical Report 31. San Marino, Calif.: Air Pollution Foundation, 1960.

68. Prager, M. J., E. R. Stephens, and W. E. Scott. Aerosol formation from gaseous air pollutants. Ind. Eng. Chem. 52:521-524, 1960.

69. Endow, N., G. J. Doyle, and J. L. Jones. The nature of some model photochemical aerosols. J. Air Pollut. Contr. Assoc. 13:141-147, 1963.

70. Wei, Y. K., and R. J. Cvetanović. A study of the vapor phase reaction of ozone with olefins in the presence and absence of molecular oxygen. Can. J. Chem. 41:913-925, 1963.

71. Kopczynski, S. L. Photo-oxidation of alkylbenzene-nitrogen dioxide mixtures in air. Int. J. Air Water Pollut. 8:107-120, 1964.

72. Stevenson, H. J. R., D. E. Sanderson, and A. P. Altshuller. Formation of photochemical aerosols. Int. J. Air Water Pollut. 9:367-375, 1965.

73. Harkins, J., and S. W. Nicksic. Studies on the role of sulfur dioxide in visibility reduction. J. Air Pollut. Contr. Assoc. 15:218-221, 1965.

74. Barlage, W. B., Jr., and F. C. Alley. Sampling and mass spectrometer analysis of reaction products from the photochemical decomposition of various olefins. J. Air Pollut. Control Assoc. 15:235-238, 1965.

75. Altshuller, A. P., D. L. Klosterman, P. W. Leach, I. J. Hindawi, and J. E. Sigsby, Jr. Products and biological effects from irradiation of nitrogen oxides with hydrocarbons or aldehydes under dynamic conditions. Int. J. Air Water Pollut. 10:81-98, 1966.

76. Goetz, A., and R. Pueschel. Basic mechanisms of photochemical aerosol formation. Atmos. Environ. 1:287-306, 1967.

77. Urone, P., H. Lutsep, C. M. Noyes, and J. F. Parcher. Static studies of sulfur dioxide reactions in air. Environ. Sci. Technol. 2:611-618, 1968.

78. Ripperton, L. A., and D. Lillian. The effect of water vapor on ozone synthesis in the photo-oxidation of alpha-pinene. J. Air Pollut. Control Assoc. 21:629-635, 1971.

79. Groblicki, P., and G. J. Nebel. The photochemical formation of aerosols in urban atmospheres, pp. 241-263. In C. S. Tuesday, Ed. Chemical Reactions in Urban Atmospheres. Proceedings of the Symposium held at General Motors Research Laboratories, Warren, Michigan, 1969. New York: American Elsevier Publishing Company, Inc., 1971.

80. Wilson, W. E., Jr., E. L. Merryman, A. Levy, and H. R. Taliaferro. Aerosol formation in photochemical smog. I. Effect of stirring. J. Air Pollut. Control Assoc. 21:128-132, 1971.

81. Goetz, A., and O. J. Klejnot. Formation and degradation of aerocolloids by ultraviolet radiation. Environ. Sci. Technol. 6:143-151, 1972.

82. Ripperton, L. A., H. E. Jeffries, and O. White. Formation of aerosols by reaction of ozone with selected hydrocarbons. Adv. Chem. Ser. 113: 219-231, 1972.

83. Wilson, W. E., Jr., A. Levy, and E. H. McDonald. Role of SO_2 and photochemical aerosol in eye irritation from photochemical smog. Environ. Sci. Technol. 6:423-427, 1972.

84. Wilson, W. E., Jr., A. Levy, and D. B. Wimmer. A study of sulfur dioxide in photochemical smog. II. Effect of sulfur dioxide on oxidant formation in photochemical smog. J. Air Pollut. Control Assoc. 22:27-32, 1972.

85. Cox, R. A., and S. A. Penkett. Aerosol formation from sulphur dioxide in the presence of ozone and olefinic hydrocarbons. J. Chem. Soc. Faraday Trans. I. 68:1735-1753, 1972.

86. Kocmond, W. C., D. B. Kittelson, J. Y. Yang, and K. L. Demerjian. Determination of the Formation Mechanisms and Composition of Photochemical Aerosols. Report No. NA 5365-M-1. EPA-650/3-73-002. Buffalo, N.Y.: Calspan Corporation, 1973. 101 pp.

87. Lipeles, M., C. S. Burton, H. H. Wang, E. P. Parry, and G. M. Hidy. Mechanisms of Formation and Composition of Photochemical Aerosols. Final Report. EPA-R3-73-036. Thousand Oaks, Calif.: Rockwell International Corporation, July 1973. 104 pp.

88. Wilson, W. E., Jr., D. F. Miller, A. Levy, and R. K. Stone. The effect of fuel composition on atmospheric aerosol due to auto exhaust. J. Air Pollut. Control Assoc. 23:949-956, 1973.

89. Miller, D. F., A. Levy, and W. E. Wilson, Jr. A Study of Motor Fuel Composition Effects on Aerosol Formation. Part II. Aerosol Reactivity Study of Hydrocarbons. Battelle Columbus Laboratories Report to the Committee for Air And Water Conservation, American Petroleum Institute, February 21, 1972.

90. Cox, R. A., and S. A. Penkett. Oxidation of atmospheric SO_2 by products of the ozone-olefin reaction. Nature 230:321-322, 1971.

91. McNelis, D. N. Aerosol Formation from Gas-Phase Reactions of Ozone and Olefin in the Presence of Sulfur Dioxide. EPA 650-4-74-034. Research Triangle Park, N. C.: U. S. Environmental Protection Agency, 1974. 219 pp.

92. Schwartz, W. Chemical Characterization of Model Aerosols. EPA-650/3-74-011. Columbus, Ohio: Battelle Memorial Institute, 1974. 129 pp.

93. Chu, R. R., and C. Orr, Jr.
Paper 74-156, Presented at 67th Annual Meeting of the Air Pollution Control Association, Denver, Colorado, June 9-13, 1974.

94. O'Brien, J. R., J. R. Holmes, and A. H. Bockian. Formation of photochemical aerosol from hydrocarbons. Chemical reactivity and products. Environ. Sci. Technol. 9:568-576, 1975.

95. Burton, C. S., E. Franzblau, and G. M. Hidy.
Division of Colloid and Surface Chemistry Paper No. 128, Presented at the 167th National Meeting of the American Chemical Society, Los Angeles, California, March 31-April 5, 1974.

96. Smith, J. P., and P. Urone, Static studies of sulfur dioxide reactions effects of NO_2, C_3H_6, and H_2O. Environ. Sci. Technol. 8:742-746, 1974.

97. Penzhorn, R. D., and W. Schock. pp. 37-51.
In Chemische Reaktionen Atmosphärischer Schadstoffe. Institut für Radiochemie, Preport No. KFK 1975 UF, Karlsruhe, Germany, 1974.

98. Lipeles, M. The Formation of Aerosols in a Photochemical Fast Flow Reactor. Report to the Air Pollution Research Advisory Committee, Rockwell International, Thousand Oaks, California, 1975. (UNVERIFIED)

99. Schulten, H.-R., and U. Schurath. Analysis of aerosols from the ozonolysis of 1-butene by high-resolution field desorption mass spectrometry. J. Phys. Chem. 79:51-57, 1975.

100. Grosjean, D. The nature and formation of secondary aerosol organics. Part 1. Aerosol products from cyclic olefins and diolefins, pp. . In G. M. Hidy and P. K. Mueller, Eds. The Character and Origins of Smog Aerosol. Ann Arbor, Mich.: Ann Arbor Press. (in press) (UNVERIFIED)

101. Doyle, G. J., and N. A. Renzetti. The formation of aerosols by irradiation of dilute auto exhaust. J. Air Pollut. Control Assoc. 8:23-32, 1958.

102. Doyle, G. J., and J. L. Jones. Automobile exhaust-gas aerosols: A review of studies conducted at Stanford Research Institute. J. Air Pollut. Control Assoc. 13:365-367, 387, 1963.

103. Schuck, E. A., H. W. Ford, and E. R. Stephens. Air Pollution Effects of Irradiated Automobile Exhaust as Related to Fuel Composition. Report No. 26. San Marino, Calif.: Air Pollution Foundation, 1958. 91 pp.

104. Hamming, W. J., P. P. Mader, S. W. Nicksic, J. C. Romanovsky, and L. G. Wayne. Gasoline Composition and the Control of Smog. Los Angeles County Air Pollution District Report, September 1961. (UNVERIFIED)

105. Wilson, W. E., Jr., D. F. Miller, D. A. Trayser, and A. Levy. A Study of Motor Fuel Composition Effects on Aerosol Formation. Part III. Visibility Reduction from Automobile Exhaust. Battelle Columbus Laboratories Report to the Committee for Air and Water Conservation, American Petroleum Institute, February 21, 1972. (API Publ. 4147) (UNVERIFIED)

106. Glasson, W. A., and C. S. Tuesday. Hydrocarbon reactivities in the atmospheric photooxidation of nitric oxide. Environ. Sci. Technol. 4:916-924, 1970.

107. Jaffe, R. J., and F. R. Smith.
Paper 74-246, Presented at 67th Annual Meeting of the Air Pollution Control Association, Denver, Colorado, June 9-13, 1974. (UNVERIFIED)

108. Altshuller, A. P., and I. R. Cohen. Structural effects on the rate of nitrogen dioxide formation in the photo-oxidation of organic compound-nitric oxide mixtures in air. Int. J. Air Water Pollut. 7:787-797, 1963.

109. Fox, D. L., J. E. Sickles, M. R. Kuhlman, P. C. Reist, and W. E. Wilson. Design and operation parameters for a large ambient aerosol chamber. J. Air Pollut. Control Assoc. 25:1049-1053, 1975.

110. Daubendieck, R. L., and J. G. Calvert. The reaction of ozone with perfluorinated polyolefins. Environ. Lett. 6:253-272, 1974.

111. Liu, B. Y. H., and D. Y. H. Pui. A submicron aerosol standard and the primary, absolute calibration of the condensation nuclei counter. J. Colloid Interface Sci. 47:155-171, 1974.

112. Charlson, R. J. Atmospheric visibility related to aerosol mass concentration. A review. Environ. Sci. Technol. 3:913-918, 1969.

113. Baumgardner, R. E., T. A. Clark, J. A. Hodgeson, and R. K. Stevens. Determination of an ozone interference in the continuous Saltzman nitrogen dioxide procedure. Anal. Chem. 47:515-521, 1975.

114. Winer, A. M., J. W. Peters, J. P. Smith, and J. N. Pitts, Jr. Response of commercial chemiluminescent NO-NO_2 analyzers to other nitrogen-containing compounds. Environ. Sci. Technol. 8:1118-1121, 1974.

115. California Air Resources Board. Final Report of the ad hoc Oxidant Measurement Committee, Report No. 75-4-4, February 20, 1975. (UNVERIFIED)

116. Judeikis, H. S., and S. Siegel. Particle-catalyzed oxidation of atmospheric pollutants. Atmos. Environ. 7:619-631, 1973.

117. Graedel, R. E., L. A. Farrow, and T. A. Weber. The influence of aerosols on the chemistry of the troposphere. Int. J. Chem. Kinetics, Symp. No. 1 (Chemical Kinetic Data for the Lower and Upper Atmosphere): 581-594, 1975.

118. Mulcahy, M. F. R., and B. C. Young. Heterogeneous reactions of OH radicals. Int. J. Chem. Kinetics, Symp. No. 1 (Chemical Kinetic Data for the Lower and Upper Atmosphere):595-609, 1975.

119. Vrbaski, T., and R. J. Cvetanović. A study of the products of the reactions of ozone with olefins in the vapor phase as determined by gas-liquid chromatography. Can. J. Chem. 38:1063-1069, 1960.

120. Pitts, J. N., Jr., and B. J. Finlayson. Mechanisms of photochemical air pollution. Angew. Chem. (Engl.) 14:1-15, 1975.

121. O'Neal, H. E., and C. Blumstein. A new mechanism for gas phase ozone-olefin reactions. Int. J. Chem. Kinetics 5:397-413, 1973.

122a. Criegee, R., and G. Werner. Die Ozonisierung des 9,10-Oktalins. Justus Liebigs Ann. Chem. 564:9-15, 1949.

122b. Delete--same as 122a.

122c. Criegee, R. The course of ozonization of unsaturated compounds. Rec. Chem. Progr. 18:111-120, 1957.

123a. Bailey, P. S. The reactions of ozone with organic compounds. Chem. Rev. 58: 925-1010, 1958.

123b. Gould, R. F., Ed. Ozone Reactions with Organic Compounds. Advances in Chemistry Series 112. Washington, D. C.: American Chemical Society, 1972. 129 pp.

124. Gillies, C. W., R. P. Lattimer, and R. L. Kuczkowski. Microwave and mass spectral studies of the ozonlyses of ethylene, propylene, and cis- and trans-2-butene with added oxygen-18 formaldehyde and acetaldehyde. J. Amer. Chem. Soc. 96:1536-1542, 1974.

125. Fliszar, S., and J. Renard. Quantitative investigation of the ozonolysis reaction. XIV. A simple carbonium ion stabilization approach to the ozone cleavage of unsymmetrical olefins. Can. J. Chem. 48:3002-3018, 1970.

126. Hull, L. A., I. C. Hisatsune, and J. Heicklen. Low-temperature infrared studies of simple alkene-ozone reactions. J. Amer. Chem. Soc. 94: 4856-4864, 1972.

127. Hanst, P. L., E. R. Stephens, W. E. Scott, and R. C. Doerr. Atmospheric ozone-olefin reactions. Preprints Div. Petrol. Chem. Amer. Chem. Soc. 4(4):A7-A16, 1959.

128. Atkinson, R., B. J. Finlayson, and J. N. Pitts, Jr. Photoionization mass spectrometer studies of gas phase ozone-olefin reactions. J. Amer. Chem. Soc. 95:7592-7599, 1973.

129. Finlayson, B. J., J. N. Pitts, Jr., and R. Atkinson. Low-pressure gas-phase ozone-olefin reactions. Chemiluminescence, kinetics, and mechanisms. J. Amer. Chem. Soc. 96:5356-5357, 1974.

130. Altshuller, A. P., I. R. Cohen, S. F. Sleva, and S. L. Kopczynski. Air pollution: Photooxidation of aromatic hydrocarbons. Science 138: 442-443, 1962.

131. Bufalini, J. J., and A. P. Altshuller. Kinetics of vapor-phase hydrocarbon-ozone reactions. Can. J. Chem. 43:2243-2250, 1965.

132. Stedman, D. H., and H. Niki. Ozonolysis rates of some atmospheric gases. Environ. Lett. 4:303-310, 1973.

133. Boocock, G., and R. J. Cvetanović. Reaction of oxygen atoms with benzene. Can. J. Chem. 39:2436-2443, 1961.

134. Jones, G. R. H., and R. J. Cvetanović. Reaction of oxygen atoms with toluene. Can. J. Chem. 39:2444-2451, 1961.

135. Atkinson, R., and J. N. Pitts, Jr. Temperature dependence of the absolute rate constants for the reaction of $O(^3P)$ atoms with a series of aromatic hydrocarbons over the range 299-392°K. J. Phys. Chem. 79:295-297, 1975.

136. Davis, D. D., W. Bollinger, and S. Fischer. A kinetics study of the reaction of the OH free radical with aromatic compounds. I. Absolute rate constants for reactions with benzene and toluene at 300°K. J. Phys. Chem. 79:293-294, 1975.

137. Doyle, G. J., A. C. Lloyd, K. R. Darnall, A. M. Winer, and J. N. Pitts, Jr. Gas phase kinetic study of relative rates of reaction of selected aromatic compounds with hydroxyl radicals in an environmental chamber. Environ. Sci. Technol. 9:237-241, 1975.

138. Fuchs, N. A. The Mechanics of Aerosols. New York: The MacMillan Co., 1964.

139. Hidy, G. M., and J. R. Brock. The Dynamic of Aerocolloidal Systems. International Review on Aerosol Physics and Chemistry Vol. 1. New York: Pergamon Press, 1970. 379 pp.

140. Mirabel, P., and J. L. Katz, Binary homogeneous nucleation as a mechanism for the formation of aerosols. J. Chem. Phys. 60:1138-1144, 1974.

141. Husar, R. B., K. T. Whitby, and B. Y. H. Liu. Physical mechanisms governing the dynamics of Los Angeles smog aerosol. J. Colloid Interface Sci. 39:211-224, 1972.

142. Willeke, K., and K. T. Whitby. Atmospheric aerosols: Size distribution interpretation. J. Air Pollut. Control Assoc. 25:529-534, 1975.

143. Kiang, C. S., D. Stauffer, V. A. Mohnen, J. Bricard, and D. Vigla. Heteromolecular nucleation theory applied to gas-to-particle conversion. Atmos. Environ. 7:1279-1283, 1973.

144. Cadle, R. D. Formation and chemical reactions of atmospheric particles. J. Colloid Interface Sci. 39:25-31, 1972.

145. Katz, J. L., C. J. Scoppa, II., N. G. Kumar and P. Mirabel. Condensation of a supersatuated vapor. II. The homogeneous nucleation of the n-alkyl benzenes. J. Chem. Phys. 62:448-465, 1975.

146. Heisler, S., S. K. Friedlander, and R. B. Husar. The relationship of smog aerosol size and chemical element distributions to source characteristics. Atmos. Environ. 7:633-649, 1973.

147. O'Brien, J. R., J. R. Holmes, and A. H. Bockian. Formation of photochemical aerosol from hydrocarbons. Chemical reactivity and products. Environ. Sci. Technol. 9:568-576, 1975.

148a. Heisler, S. L. Gas-to-Particle Conversion in Photochemical Smog: Growth Laws and Mechanisms for Organics. Ph.D. Thesis. Pasadena: California Institute of Technology, 1976. 215 pp.

148b. Heisler, S. L., and S. K. Friedlander. Gas to particle conversion in photochemical smog: Growth laws and mechanisms for organics. Atmos. Environ. (in press)

149. Davis, M., and G. H. Thomas. The lattice energies, infra-red spectra, and pollisble cyclization of some dicarboxylic acids. Trans. Farady Soc. 56:185-192, 1960.

150. Jordan, T. E. Vapor Pressure of Organic Compounds. New York: Interscience, 1954. 266 pp.

151. Hughes, E. E., and S. G. Lias.
National Bureau of Standards Report 6435. Washington, D. C., 1960. (UNVERIFIED)

152. Aliphatic dibasic acids, Chapter 1, pp. . In J. K. Stille and T. W. Campbell, Eds. High Polymers. Vol. 27. Condensation Monomers. New York: John Wiley and Sons, 1972. (UNVERIFIED)

153. Weast, R. C., Ed. CRC Handbook of Chemistry and Physics. (47th ed.) Cleveland: The Chemical Rubber Company, 1966.

154. Rossini, F. D., B. J. Mair, and A. J. Streiff. Hydrocarbons From Petroleum. ACS Monograph Series. New York: Reinhold Publishing Corporation, 1953. 556 pp.

155. Bachman, G. B., and N. W. Connon. Nitration studies. XIV. Conversion of nitrite and nitrate esters into nitro alkanes. J. Org. Chem. 34:4121-4125, 1969.

156. Grosjean, D., and S. K. Friedlander.
Paper No. 75 Presented at Pacific Conference on Chemistry and Spectroscopy, Los Angeles, California, October 28-30, 1975. (UNVERIFIED)

157a. Grosjean, D., and S. K. Friedlander. The nature and formation of secondary aerosol organics. Part II. Kinetics of organic aerosol formation. (in press) (UNVERIFIED)

157b. Grosjean, D. Secondary organic aerosols and their gas phase hydrocarbon precursors. To be presented at the American Chemical Society Centennial Meeting, Division of Environmental Chemistry, New York, April 4-9, 1976. (UNVERIFIED)

158. Demerjian, K. L., J. A. Kerr, and J. G. Calvert. The mechanism of photochemical smog formation. Adv. Environ. Sci. Technol. 4:1-262, 1974.

159. Herron, J. T., and R. E. Huie. Int. J. Mass Spectrosc. Ion Phys. 16:125- , 1975. (UNVERIFIED)

160. Japar, S. M., C. H. Wu, and H. Niki. Rate constants for the reaction of ozone with olefins in the gas phase. J. Phys. Chem. 78:2318-2320, 1974.

161. Becker, K. H., U. Schurath, and H. Seitz. Ozone-olefin reactions in the gas phase. 1. Rate constants and activation energies. Int. J. Chem. Kinet. 6:725-739, 1974.

162. Vbraski, T., and R. J. Cvetanović. Relative rates of reaction of ozone with olefins in the vapor phase. Can. J. Chem. 38:1053-1062, 1960.

163. Masclet, P., D. Grosjean, G. Mouvier, and J. Dubois. Alkene ionization potentials. Part I: Quantitative determination of alkyl group structural effects. J. Electr. Spectrosc. Relat. Phenom. 2:225-237, 1973.

164. Grosjean, D., P. Masclet, and G. Mouvier. Potentiels d'ionisation des alcènes. III. Relations entre les Pl, les vitesses d'additions électrophiles et al réactivité des alcènes en pollution atmosphérique. Bull. Soc. Chim. Fr. 1974:573-576.

165. Sanders, W. N., and J. B. Maynard. Capillary gas chromatographic method for determining the C_3-C hydrocarbons in full-range motor gasolines. Anal. Chem. 40:527-535, 1968.

166. Maynard, J. B., and W. N. Sanders. Determination of the detailed hydrocarbon composition and potential atmospheric reactivity of full-range motor gasolines. J. Air Pollut. Control Assoc. 19:505-510, 1969.

167. Glasson, W. A., and C. S. Tuesday. Hydrocarbon reactivity and the kinetics of the atmospheric photooxidation of nitric oxide. J. Air Pollut. Control Assoc. 20:239-243, 1970.

168. Neligan, R. E., P. P. Mader, and L. A. Chambers. Exhaust composition in relation to fuel composition. J. Air Pollut. Control Assoc. 11:178-186, 1961.

169. Melton, C. W., R. I. Mitchell, D. A. Trayser, and J. F. Foster. Chemical and Physical Characterization of Automotive Exhaust Particulate Matter in the Atmosphere. CRC-APRAC Report No. CAPE-19-70-2. Columbus, Ohio: Battelle Columbus Laboratories, 1973. 90 pp.

170. McEwen, D. J. Automobile exhaust hydrocarbon analysis by gas chromatography. Anal. Chem. 38:1047-1053, 1966.

171. Neligan, R. E. Hydrocarbons in the Los Angeles atmosphere. A comparison between the hydrocarbons in automobile exhaust and those found in the Los Angeles atmosphere. Arch. Environ. Health 5:581-591, 1962.

172. Papa, L. J., D. L. Dinsel, and W. C. Harris. Gas chromatographic determination of C_1 to C_{12} hydrocarbons in automotive exhaust. J. Gas Chromatogr. 6:270-279, 1968.

173. Jacobs, E. S. Rapid gas chromatographic determination of C_1 to C_{10}. Hydrocarbons in automotive exhaust gas. Anal. Chem. 38:43-48, 1966.

174. Dishart, K. T. Exhaust hydrocarbon composition. Its relation to gasoline composition. Proc. Amer. Petrol. Inst. 50:514-540, 1970.

175. U. S. Department of Health, Education, and Welfare. Public Health Service. National Air Pollution Control Administration. Air Quality Criteria for Hydrocarbons. NAPCA Publ. No. AP-64. Washington, D. C.: U. S. Government Printing Office, 1970.

176. Stephens, E. R., and F. R. Burleson. Distribution of light hydrocarbons in ambient air. J. Air Pollut. Control Assoc. 19:929-936, 1969.

177. Altshuller, A. P., W. A. Lonneman, F. D. Sutterfield, and S. L. Kopczynski. Hydrocarbon composition of the atmosphere of the Los Angeles basin - 1967. Environ. Sci. Technol. 5:1009-1016, 1971.

178. Kopczynski, S. L., W. A. Lonneman, F. D. Sutterfield, and P. E. Darley. Photochemistry of atmospheric samples in Los Angeles. Environ. Sci. Technol. 6:342-347, 1972.

179. Siddiqui, A. A., and F. L. Worley, Jr. Hydrocarbons in Houston's atmosphere. Paper Presented at Conference on Ambient Air Qualtiy Measurements, Air Pollution Control Association, Lakeway, Texas, March 10-11, 1975.

180. Kopczynski, S. L., W. A. Lonneman, T. Winfield, and R. Seila. Gaseous pollutants in St. Louis and other cities. J. Air Pollut. Control Assoc. 25:251-255, 1975.

181. Bertsch, W., R. C. Chang, and A. Zlatkis. The determination of organic volatiles in air pollution studies: Characterization of profiles. J. Chromatogr. Sci. 12:175-182, 1974.

182. Raymond, A., and G. Guichon. Gas chromatographic analysis of C_8-C_{18} hydrocarbons in Paris air. Environ. Sci. Technol. 8:143-148, 1974.

183. Grob, K., and G. Grob. Gas-liquid chromatographic-mass spectrometric investigation of C_6-C_{20} organic compounds in an urban atmosphere. An application of ultra trace analysis on capillary columns. J. Chromatogr. 62: 1-13, 1972.

184. Jones, P. W.

Paper 74-265, Presented at 67th Annual Meeting of the Air Pollution Control Association, Denver, Colorado, June 9-13, 1974. (UNVERIFIED)

185. Grosjean, D., and S. K. Friedlander. The nature and formation of secondary aerosol organics. Part III. Cyclic olefins and diolefins as possible hydrocarbon precursors. (in press) (UNVERIFIED)

186. Went, F. W. Blue hazes in the atmosphere. Nature 187:641-643, 1960.

187. Went, F. W. Organic matter in the atmosphere, and its possible relation to petroleum formation. Proc. Nat. Acad. Sci. 46:212-221, 1960.

188. Rasmussen, R. A., and R. W. Went. Volatile organic material of plant origin in the atmosphere. Proc. Nat. Acad. Sci. 53:215-220, 1965.

189. Rasmussen, R. A. What do the hydrocarbons from trees contribute to air pollution? J. Air Pollut. Control Assoc. 22:537-543, 1972.

190. Gerhold, H. D., and G. H. Plank. Monoterpene variations in vapors from white pine and hybrids. Phytochemistry 9:1393-1398, 1970.

191. Rasmussen, R. A. Isoprene: Identified as a forest-type emission to the atmosphere. Environ. Sci. Technol. 4:667-671, 1970.

192. Went, F. W. The nature of aitken condensation nuclei in the atmosphere. Proc. Nat. Acad. Sci. 51:1259-1267, 1964.

193. Rasmussen, R. A., and M. W. Holdren. Analyses of C_5 to C_{10} Hydrocarbons in Rural Atmospheres. Paper No. 72-19 Presented at the 65th Annual Meeting of the Air Pollution Control Association, Miami Beach, Florida, June 18-22, 1972.

194. Stephens, E. R., and W. E. Scott. Relative reactivity of various hydrocarbons in polluted atmospheres. Proc. Amer. Petrol. Inst. 42(Section III Refining):665-670, 1962.

195. Japar, S. M., C. H. Wu, and H. Niki. Rate constants for the gas phase reaction of ozone with α-pinene and terpinolene. Environ. Lett. 7:245-249, 1974.

196. Grimsrud, E. P., H. H. Westberg, and R. A. Rasmussen. Atmospheric reactivity of monoterpene hydrocarbons, NO_x photooxidation and ozonolysis. Int. J. Chem. Kinetics Symp. No. 1, 1975 (Chemical Kinetic Data for the Lower and Upper Atmosphere):183-195, 1975.

197. Stasiuk, W. N., Jr., and P. E. Coffey. Rural and urban ozone relationships in New York State. J. Air Pollut. Control Assoc. 24:564-568, 1974.

198. Research Triangle Institute. Investigation of High Ozone Concentration in the Vincinity of Garrett County, Maryland and Preston County, West Virginia. Institute Final Report. EPA-R4-73-019. Research Triangle Park, N. C.: Research Triangle Institute, 1973. 105 pp.

199. U. S. Environmental Protection Agency. Office of Research and Development. National Environmental Research Center. Health Consequences of Sulfur Oxides: A Report from CHESS, 1970-71. Human Studies Laboratory. Program Element 1A1005. Research Triangle Park, N. C.: U. S. Environmental Protection Agency, 1974. 454 pp.

200. French, J. G., V. Hasselblad, R. Johnson, and K. E. McClain. The Association of Suspended Nitrates in Ambient Air with Aggravation of Asthma. Human Studies Laboratory, National Environmental Research Center. Research Triangle Park, N. C.: U. S. Environmental Protection Agency, 1975. (UNVERIFIED)

201. Barone, J., T. A. Cahill, R. G. Flocchini, and D. J. Shadoan. Visibility Reduction: A Characterization of Three Urban Sites in California. Air Quality Group, Crocker Nuclear Laboratory, University of California, Davis, 1975. (UNVERIFIED)

202. Calvert, J. G. Modes of formation of the salts of sulfur and nitrogen in an NO_x-SO_2-hydrocarbon polluted atmosphere. Paper Presented at Conference on Atmospheric Salts and Gases of Sulfur and Nitrogen in Association with Photochemical Oxidant, University of California, Irvine, January 7-9, 1974. (UNVERIFIED)

203. Urone, P. Photochemical and thermal reactions of sulfur dioxide, pp. 505-519. In Proceedings of the International Symposium on Air Pollution, Tokyo, Japan, 1972. (UNVERIFIED)

204. Bufalini, M. Oxidation of sulfur dioxide in polluted atmospheres - A review. Environ. Sci. Technol. 5:685-700, 1971.

205. Sulfur in the Environment. Missouri Botanical Gardens, St. Louis, Missouri, April 1975. (UNVERIFIED)

206. Calvert, J. G. Interactions of air pollutants, pp. 19-101. In National Academy of Sciences--National Research Council. Assembly of Life Sciences. Proceedings of the Conference on Health Effects of Air Pollutants. U. S. Senate Committee Print Serial No. 93-15. Washington, D. C.: U. S. Government Printing Office, 1973.

207. McAfee, J. M., J. N. Pitts, Jr., and A. M. Winer. In situ long path infrared spectroscopy of photochemical air pollutants in an environmental chamber. Paper Presented at Pacific Conference on Chemistry and Spectroscopy, San Francisco, Calif., October 16-18, 1974. (UNVERIFIED)

208. Miller, D. F., and C. W. Spicer. A Continuous Analyzer for Detecting Nitric Acid. Paper 74-17, Presented at 67th Annual Meeting of the Air Pollution Control Association, Denver, Colorado, June 1974.

209. Kiang, C. S., D. Stauffer, and V. A. Mohnen. Possibilities for atmospheric aerosol formation involving NH_3. Nature Phys. Sci. 244:53-54, 1973.

210. Gordon, R. J., and R. J. Bryan. Ammonium nitrate in airborne particles in Los Angeles. Environ. Sci. Technol. 7:645-647, 1973.

211. Stephens, E. R. Identification of odors from cattle feed lots. Calif. Agric. 25(1):10-11, 1971.

212. Jacobs, M. B. Table A-8. Concentrations of comon air pollutants in the average urban area, p. 413. In The Chemical Analysis of Air Pollutants. New York: Interscience Publishers, Inc., 1960.

213. Hanst, P. L., W. E. Wilson, Jr., R. K. Patterson, B. W. Gay, L. W. Chaney, and C. S. Burton. A spectroscopic study of Pasadena smog. Division of Environmental Chemistry Paper Presented at 167th National Meeting of the American Chemical Society, Los Angeles, California, April 1, 1974. (UNVERIFIED)

214. Novakov, T.
Paper 74-200, Presented at 67th Annual Meeting of the Air Pollution Control Association, Denver, Colorado, June 9-13, 1974. (UNVERIFIED)

215. Novakov, T., S. G. Chang, and A. B. Harker. Ozone concentrations in New Jersey and New York: Statistical association with related variables. Science 186:259-261, 1974.

216. Yamamoto, K., M. Seki, and K. Kawazoe. Effect of sulfuric acid accumulation on the rate of sulfur dioxide oxidation on activated carbon surface. Nippon Kaguku Kaiski 7:1268-2179, 1973. (in Japanese, summary in English)

217. Johnstone, H. F., and D. R. Coughanowr. Absorption of sulfur dioxide from air. Oxidation of drops containing dissolved catalysts. Ind. Eng. Chem. 50:1169-1172, 1958.

218. Scott, W. D., and P. V. Hobbs. The formation of sulfate in water droplets. J. Atmos. Sci. 24:54-57, 1967.

219. Miller, J. M., and R. G. de Pena. The rate of sulfate ion formation in water droplets in atmospheres with different partial pressures of SO_2, pp. 375-378. In H. M. Englund and W. T. Beery, Eds. Proceedings of the Second International Clean Air Congress. Held at Washington, D. C., December 6-11, 1970. New York: Academic Press, 1971.

220. Penkett, S. A. Oxidation of SO_2 and other atmospheric gases by ozone in aqueous solution. Nature Phys. Sci. 240:105-106, 1972.

221. Fuller, E. C., and R. H. Crist. The rate of oxidation of sulfite ions by oxygen. J. Amer. Chem. Soc. 63:1644-1650, 1941.

222. Schroeter, L. C. Kinetics of air oxidation of sulfurous acid salts. J. Pharm. Sci. 52:559-563, 1963.

223. Wood, W. P., A. W. Castelman, Jr., and I. N. Tang. Paper 74-153, Presented at 67th Annual Meeting of the Air Pollution Control Association, Denver, Colorado, June 9-13, 1974. (UNVERIFIED)

224. Davis, D. D., W. A. Payne, and L. J. Stief. The hydroperoxyl radical in atmospheric chemical dynamics: Reaction with carbon monoxide. Science 179: 280-282, 1973.

225. James, F. C., J. A. Kerr, and J. P. Simons. Direct measurement of the rate of reaction of the methyl radical with sulphur dioxide. J. Chem. Soc. Faraday Trans. I. 69:2124-2129, 1973.

226. Gordon, S., and E. Hamilton. Chem. Div., Argonne National Laboratories, Argonne, Illinois. Personal communication to J. G. Calvert, December 11, 1973. (see ref. 202)

227. Urone, P., and W. H. Schroeder. SO_2 in the atmosphere: A wealth of monitoring data, but few reactions rate studies. Environ. Sci. Technol. 3: 436-445, 1969.

228. Bourbigot, Y., J. Bricard, G. Madelaine, and D. Vigla. Pollution atmosphérique.--Identification des aérosols produits par photolyse en présence d'anhydride sulfureux. C. R. Acad. Sci. (Paris) C 276:547-550, 1973.

229. Daubendiek, R. L., and J. G. Calvert. A study of the N_2O_5-SO_2-O_3 reaction system. Environ. Lett. 8:103-116, 1975.

230. Dainton, F. S., and K. J. Ivin. The photochemical formation of sulphuric acids from sulphur dioxide and hydrocarbons. Trans. Faraday Soc. 46:374-381, 1950.

231. Johnston, H. S., and K. Dev Jain. Sulfur dioxide sensitized photochemical oxidation of hydrocarbons. Science 131:1523-1524, 1960.

232. Timmons, R. B. The photochemically induced reactions of sulfur dioxide with alkanes and carbon monoxide. Photochem. Photobiol. 12:219-230, 1970.

233. Badcock, C. C., H. W. Sidebottom, J. G. Calvert, G. W. Reinhardt, and E. K. Damon. Mechanism of the photolysis of sulfur dioxide-paraffin hydrocarbon mixtures. J. Amer. Chem. Soc. 93:3115-3121, 1971.

234. Sidebottom, H. W., C. C. Badcock, G. E. Jackson, J. G. Calvert, G. W. Reinhardt, and E. K. Damon. Photooxidation of sulfur dioxide. Environ. Sci. Technol. 6:72-79, 1972.

235. Penzhorn, R. D., W. G. Filby, K. Gunther, and L. Stieglitz. pp. 16-36. In Chemische Reaktionen Atmosphärischer Schadstoffe. Institut für Radiochemie Report KFK 1975 UF, Karlsruhe, Germany, May 1974. (UNVERIFIED)

236. Penzhorn, R. D., W. G. Filby, and H. Güsten. pp. 3-15. In Chemische Reaktionen Atmosphärischer Schadstoffe. Institut für Radiochemie Report KFK 1975 UF, Karlsruhe, Germany, May 1974. (UNVERIFIED)

237. Roberts, P. T., and S. K. Friedlander. Conversion of SO_2 to sulfur particulate in the Los Angeles atmosphere. Environ. Health Perspect. 10:103-108, 1975.

238. California Air Resources Board. Measurement of Sulfur Oxides in Auto Exhaust. Project M-274, October 1974. (UNVERIFIED)

239. Begeman, C. R., M. L. Jackson, and G. J. Nebel. Sulfate emissions from catalyst-equipped automobiles. Society of Automotive Engineers Paper No. 741060, General Motors Corp., October 1974. (UNVERIFIED)

240. Pierson, W. R., R. H. Hammerle, and H. W. Kummer. Sulfuric acid aerosol emissions from catalyst-equipped engines. Society of Automotive Engineers Paper No. 740287, Ford Motor Co., March 1974. (UNVERIFIED)

241. California Air Resources Board. Sources and Effect of Sulfates in the Atmosphere. Informational Report March 6, 1975. (UNVERIFIED)

242. U. S. Environmental Protection Agency. Issue Paper: Estimated Public Health Impact as a Result of Equipping Light-Duty Motor Vehicles with Oxidation Catalysts. January 30, 1975. (UNVERIFIED)

243. Morris, E. D., Jr., and H. Niki. Reactivity of hydroxyl radicals with olefins. J. Phys. Chem. 75:3640-3641, 1970. (letter)

244. Furayama, S., R. Atkinson, A. J. Colussi, and R. J. Cvetanović. Determination of the phase shift method of the absolute rate constants of reactions of $O(^3P)$ atoms with olefins at 25°C. Int. J. Chem. Kinetics 6: 741-751, 1974.

Chapter 4

ATMOSPHERIC CONCENTRATIONS OF PHOTOCHEMICAL OXIDANTS

The main purpose of this chapter is to survey atmospheric concentrations of photochemical oxidants, with emphasis on surface concentrations and the distribution patterns associated with them. The reason for that emphasis is that the photochemical oxidants that affect public health and welfare are largely concentrated in this region. The whole subject of stratospheric ozone (and its filtering of ultraviolet light and interactions with supersonic-transport exhaust products), nuclear weapon reaction products, and halogenated hydrocarbon decomposition products will not be treated here.

As in Air Quality Criteria for Photochemical Oxidants,[1] our concern will be with the broad subject of oxidant pollution in the atmosphere and the net oxidizing ability of the contaminants in an air sample. The standard corrections or adjustments to remove interferences from the data have already been implied in the primary references in most cases. Therefore, we need not refer to the early distinction between "oxidant" or "total oxidants" and "corrected or adjusted oxidant."

It should be noted that there are still unresolved discrepancies in oxidant data owing to differences in primary standards. Iodometric calibration techniques for ozone monitors were compared by an ad hoc committee appointed by the California Air Resources Board (CARB).[2] The committee set out to find an accurate method for measuring ozone, to relate the recommended method to earlier data, and to recommend procedures for calibrating ozone monitors in the field. It examined calibration techniques used by the

U. S. Environmental Protection Agency (EPA), the CARB, and the Los Angeles County Air Pollution Control District and concluded that the Los Angeles County method reads low by about 4% and that the CARB and EPA methods read high by about 25 - 30%. An ultraviolet procedure was used as an absolute standard, and a commercially available ultraviolet ozone monitor was calibrated to serve as a secondary standard. The committee stated that multiplication of previous CARB ozone measurements by 0.78 and of previous Los Angeles County Air Pollution Control District ozone measurements by 1.04 would yield results accurate to within 10%. (A seemingly disproportionate amount of attention must still be given to measurements available from California, because that data base continues to be the largest available.)

Ozone measurement as an indicator of the concentration of oxidants in general is widely accepted. This is not to presuppose that ozone is the cause of all oxidant-related health effects or damage, but that it serves as a surrogate compound for a complex mixture of substances that are characterized by their oxidizing ability and by the effects attributable to this property. Consequently, oxidized organic compounds like aldehydes and organic nitrates are also in the category of our subject matter. Implicit in the belief that ozone is an indicator compound is the assumption that the concentrations, or at least the adverse effects of concentrations, of nonozone oxidants bear some relationship to the ozone concentration. This assumption is a measure of the inability to analyze for the other compounds and of the sparse medical knowledge of their effects on human beings. The use of ozone as a surrogate should be carefully reevaluated.

Measurements of natural background photochemical oxidants are extremely difficult to find in the literature. Measurements that once were thought to represent the truly rural background are now suspected of having been contaminated by pollutants of man-made origin. This constitutes a critical question in the interpretation of atmospheric concentration, because some of the ozone that is present is controllable and some is not. Some of the literature cited in this chapter contains assertions that it will be impossible in some urban areas to achieve the national ambient air quality standard by local-source reductions, because "natural background" concentrations already exceed the standard. If these are not in fact natural background concentrations, they may be reducible by limiting emission of chiefly man-made precursor pollutants in upwind areas. Because the measurements are incomplete, no specific section in this chapter will be devoted to natural background concentrations of ozone; however, measurements that are available will be cited and interpreted.

It is currently advocated that atmospheric concentrations of air pollutants be expressed in micrograms per cubic meter. For ozone, the factor for converting from parts per million to micrograms per cubic meter is 1,962 for 25 C and 760 mm Hg. That is, 1 ppm = 1,962 $\mu g/m^3$. In this chapter, conversions are not always made, because of uncertainties as to the temperature and pressure at which readings were taken. These uncertainties become especially severe under conditions of high altitude. In this context, parts per million is on a molar basis.

This review begins with a summary of the sources of monitoring data operated primarily by public agencies. The spatial and temporal patterns of oxidant concentration are then discussed—urban versus rural and indoor versus outdoor relationships, diurnal and seasonal patterns, and long-term trends. The chapter includes brief discussions of photochemical oxidants other than ozone and of data quality and concludes with a set of recommendations for guidelines in future monitoring of atmospheric concentrations of ozone and other photochemical oxidants.

SOURCES OF MONITORING DATA

One of the earliest organized efforts to acquire data on photochemical oxidants was that of the Los Angeles County Air Pollution Control District, which began in the middle 1950's and has produced the largest data base now available for these studies. In 1961, the California Department of Public Health set up a 16-station Statewide Cooperative Air Monitoring Network (SCAN).

The national network of air pollution measurements is keyed to the 247 air quality control regions (AQCR's), which were classified according to the relative severity of their pollution problems.[3] The classification is a ranking of measured ambient air concentrations or the estimated air quality in the area of maximal severity. The priorities for air quality problem severity are as follows:

Priority I: Ambient concentrations significantly above primary standards.

- Priority Ia: Ambient concentrations significantly above primary standards and due to emissions from point sources.

Priority II: Ambient concentrations significantly above secondary standards.

Priority III: Ambient concentrations below secondary standards.

For photochemical oxidants, there were 55 AQCR's in the Priority I classification and 192 AQCR's in the Priority III classification in October 1973.[4] This indicates how many stations showed a severe oxidant air pollution problem.

A 1973 report issued by the EPA summarizes the history of the federal air quality program by presenting a comprehensive analysis and interpretation of data collected from federal, state, and local air quality surveillance activities.[5] Because of data-reduction lags, the report carries information up to 1971, when 183 continuous oxidant monitoring stations were in operation. It proposed 458 monitoring stations for 1974, compared with the 208 legally required. Statistics presented indicate that nine AQCR's were exceeding the primary oxidant standard in 1969; the number grew to 12 in 1970 and to 15 in 1971. Under the federal regulations, the states submit to the EPA on a quarterly basis all the air quality data obtained from their monitoring systems. The regional EPA offices edit the data for inconsistencies and errors and then forward it for inclusion in the National Aerometric Data Bank (NADB).

Of the six federal monitoring programs in operation when the report was written, two (the National Air Surveillance Networks, NASN, and CAMP) were analyzed for trends. The NASN monitors total suspended particulate matter and sulfur dioxide at over 200 stations. Nitrogen dioxide is monitored at some sites. Oxidant data obtained on a national basis are available from the CAMP, which has been operating in six major urban areas for over 10 years.

Data from the EPA's air monitoring networks described above and from networks operated by state and local governments are submitted for storage in EPA's Storage and Retrieval of Aerometric Data (SAROAD) format. Significant quantities of the information from the states were not expected to be transmitted until the summer of 1973, so the report had only limited information in this category. Extensive tabulations of air quality data and of the monitoring installations are provided.

Other data in this chapter are from special monitoring programs and from scattered reports from networks operated by public agencies. The special programs generally are experimental and are designed to elucidate specific features of the oxidant problem. The scattered data from public monitoring networks have been obtained from a variety of international sources.

A DAMAGE INDEX FOR OXIDANT IMPACT

The health effects of photochemical oxidant pollution should be measured by some kind of aggregate index that involves a weighting of pollutant concentrations according to spatial and temporal distribution. The following sections therefore examine typical values of oxidant concentration as they depend on location and time. The national ambient air quality standard concerns itself simply with the worst place at the worst time. However, in the future, damage associated with each specific effect should be incorporated in the form of a summation or in an integral, such as

$$D_{ij} = \int\int \rho_j(x,t)\Phi_{ij}(c_i)d\sigma dt, \qquad (1)$$

where D_{ij} = index of damage due to the action of the _i_th species on the _j_th type of receptor,

ρ_j = population density of *j*th receptor,

Φ_{ij} = impact function for *i*th species on *j*th receptor,

c_i = concentration of *i*th species,

x = location,

t = time, and

σ = area.

This objective index goes beyond the simpler requirements now imposed by ambient air standards; however, it can be related to ambient air standards by normalizing the impact function. For example, suppose that the impact of pollutant i on receptor j increases as the *n*th power of c_i, so that the expression

$$\Phi_{ij} = (c_i/c_{is})^n \tag{2}$$

permits a comparative evaluation of all species if c_{is} is the ambient air standard. Contributions can be aggregated to state the total damage on receptor j by summing all the D_{ij} over all i. These interactions of time and space patterns with long-term health effects are discussed further in Chapter 10. The application of this index[6] to the analysis of entire systems requires the spatial and temporal distribution of pollutants through the c_i, which implicitly depends on these variables. The sections that follow consider some of the distributions that might enter this type of damage formula.

SPATIAL PATTERNS OF OXIDANT CONCENTRATION

The early siting of monitoring stations in central business districts overlooked the fact that nitric oxide emitted by primary polluters reacts very rapidly with ozone to cause localized decreases in ozone concentration. Consequently, the ozone concentration is often higher in surburban and even rural areas than in urban areas. Before examining detailed patterns within a given urban area, it is important to look at the degrees of pollution typically found in cities throughout the United States and elsewhere.

The original criteria document for photochemical oxidants[1] included tabulations of maximal oxidant concentrations and cumulative frequency distributions of hourly average oxidant concentrations. Tables 4-1 and 4-2 show the results. The ranking of stations by yearly average concentration differs from the ranking that might come about from using peak concentrations only. This is born out by the cumulative frequency distribution: at the high-frequency end, there is very little differentiation among the cities in Table 4-2; but for the rare event, the cities are widely separated in concentration values. This must reflect the differences in mechanisms for forming the ozone that is largely responsible for the oxidant readings. This distinction may be drawn between the nonurban ozone formation processes leading to low concentrations and the urban photooxidation processes leading to the high concentrations of low frequency.

An international expert panel[7] has issued an air quality criteria document for photochemical oxidants and related hydrocarbons that builds on the U.S. Department of Health, Education, and Welfare air quality criteria document for photochemical oxidants. It discusses oxidant concentration patterns in the context of the same tabular material presented earlier.

Table 4-1

Summary of Maximal Oxidant Concentrations in
Selected Cities, 1964-1967 (from U.S. Department of H.E.W.[1])

Station	Total days of available data	Number and percent of total days with maximum hourly average equal to or greater than concentration specified						Maximum hourly average, ppm	Peak concentration, ppm
		0.15 ppm		0.10 ppm		0.05 ppm			
		Days	Percent of days	Days	Percent of Days	Days	Percent of days		
Passadena	728	299	41.1	401	55.1	546	75.0	0.46	0.67
Los Angeles	730	220	30.1	354	48.5	540	74.0	0.58	0.65
San Diego	623	35	5.6	130	20.9	440	70.6	0.38	0.46
Denver[a]	285	14	4.9	51	17.9	226	79.3	0.25	0.31
St. Louis	582	14	2.4	59	10.1	362	62.2	0.35	0.85
Philadelphia	556	13	2.3	60	10.9	233	41.9	0.21	0.25
Sacramento	711	16	2.3	104	14.6	443	62.3	0.26	0.45
Cincinnati	613	10	1.6	55	9.0	319	52.0	0.26	0.32
Santa Barbara	723	11	1.5	76	10.5	510	70.5	0.25	0.28
Washington, D.C.	577	7	1.2	65	11.3	313	54.2	0.21	0.24
San Francisco	647	6	0.9	29	4.5	185	28.6	0.18	0.22
Chicago	530	0	0	24	4.5	269	50.8	0.13	0.19

---

[a] 11 months of data beginning February, 1965.

Table 4-2

Cumulative Frequency Distribution of Hourly Average Oxidant Concentrations in Selected Cities, 1964-1965 (from U.S. Department of H.E.W[1])

City	Percent of hours with concentrations equal to or greater than stated concentrations, ppm								1964-1965 yearly average, ppm
	90	70	50	30	10	5	2	1	
Pasadena	0.01	0.01	0.02	0.04	0.12	0.18	0.23	0.26	0.042
Los Angeles	0.01	0.01	0.02	0.04	0.10	0.14	0.18	0.22	0.036
San Diego	0.01	0.02	0.03	0.04	0.08	0.10	0.12	0.14	0.036
Denver[a]	0.01	0.02	0.03	0.04	0.06	0.08	0.10	0.12	0.036
St. Louis	0.01	0.02	0.03	0.04	0.06	0.07	0.09	0.11	0.031
Philadelphia	0.01	0.02	0.02	0.03	0.06	0.08	0.11	0.14	0.026
Sacramento	0.01	0.01	0.02	0.04	0.06	0.08	0.10	0.12	0.030
Cincinnati	0.01	0.02	0.02	0.04	0.06	0.07	0.08	0.10	0.030
Santa Barbara	0.02	0.02	0.03	0.04	0.06	0.08	0.09	0.10	0.036
Washington, D.C.	0.01	0.01	0.02	0.03	0.06	0.07	0.09	0.10	0.029
San Francisco	0.01	0.01	0.02	0.03	0.04	0.05	0.06	0.07	0.019
Chicago	0.01	0.01	0.02	0.03	0.05	0.06	0.08	0.08	0.028

---

[a] 11 months of data beginning February 1965.

New information is added for the city of Delft:* The monthly means of daily maximums of hourly ozone concentrations are shown in Table 4-3, and the monthly average ozone concentrations are shown in Table 4-4. As in other cities, the worst month seems to be August, with a mean daily maximum (of hourly concentrations) of 0.071 ppm (140 $\mu g/m^3$). Table 4-5 compares the number of days in May through July of 1971 when the ozone concentration at one or more sites reached or exceeded the hourly average of 200 $\mu g/m^3$ or of 100 $\mu g/m^3$ in ref. 7. A comparison is made between Delft and five other monitoring sites in the Netherlands. Amsterdam had a peak value of 0.18 ppm in March 1971.

Measurements from a downtown site in Frankfurt-am-Main and another on a nearby 800-m mountain, Kleiner Feldberg, both in the Federal Republic of Germany, are plotted in Figure 4-1. As opposed to the pattern in New York State,[9,10] the ozone concentration at the urban sampling site was far greater than that observed at the mountain site. The peak in Frankfurt lasts from 10 a.m. to 6 p.m. Readings from two stations in Berlin are compared in Figure 4-2. One station, Steglitz, is in an area with high traffic; the other, Dahlem, is in the suburbs. It was concluded that the lower oxidant concentrations at the urban station were due to the high concentrations of hydrocarbon there. In reality, they were probably caused by the high concentration of nitric oxide that reacted with the ozone. For both cases, the concentrations of ozone were extremely low, with a maximum of 0.0132 ppm at Dahlem.

---

* The Delft data were provided to the NATO/CCMS Panel on Air Quality Criteria by L. J. Brasser of the Research Institute for Public Health Engineering, Delft, the Netherlands, in April 1973.

Table 4-3

Monthly Means of Daily Maximums of Hourly Ozone Concentrations in Delft, 1970[a]

Month	Ozone concentration	
	$\mu g/m^3$	ppm
January	4	0.002
February	23	0.012
March	90	0.046
April	104	0.053
May	116	0.059
June	121	0.062
July	88	0.045
August	140	0.071
September	113	0.058
October	58	0.030
November	46	0.023
December	29	0.015

---

[a] Reprinted with permission from ref. 7.

Table 4-4

Monthly Averages of Ozone Concentrations in Delft, 1970[a]

Month	Ozone concentration	
	$\mu g/m^3$	ppm
January	2	0.001
February	13	0.007
March	50	0.026
April	58	0.030
May	48	0.024
June	45	0.023
July	46	0.023
August	61	0.031
September	50	0.026
October	32	0.016
November	25	0.013
December	10	0.005

---

[a] Reprinted with permission from ref. 7.

Table 4-5

Days when Ozone Concentration in Delft Reached or Exceeded 200 $\mu g/m^3$, 1969–1971[a]

1969, day-mo	Maximal hourly average Ozone Concentration, $\mu g/m^3$	1970, day-mo	Maximal hourly average Ozone Concentration, $\mu g/m^3$	1971, day-mo	Maximal hourly average Ozone Concentration, $\mu g/m^3$
9–4	310	10–3	190	15–4	248
5–5	395 (440)[b]	2–5	190	4–5	200
15–6	306	14–5	287	6–5	191
16–6	285	20–6	218	11–5	214
1–7	205	21–6	313	31–5	275
16–7	370	30–7	198	1–7	25[illegible]
23–7	196	1–8	190	5–7	192
4–8	191	13–8	230	8–7	208
9–9	192	29–8	217	9–7	226
13–9	204	30–8	227	11–7	239
		31–8	190	23–7	193
		18–9	237	30–7	249
		19–9	247	19–8	249
		20–9	237	21–8	245
		29–9	211	22–8	244
				29–9	186
				2–10	228
				3–10	364 (>410)[b]

---

[a] Derived from ref. 7.

[b] Maximal concentration measured.

In 1969, 340 hourly averages were >100 $\mu g/m^3$ and 22 hourly averages were >200 $\mu g/m^3$.
In 1970, 550 hourly averages were >100 $\mu g/m^3$ and 30 hourly averages were >200 $\mu g/m^3$.
In 1971, 845 hourly averages were >100 $\mu g/m^3$ and 48 hourly averages were >200 $\mu g/m^3$.
In 1972, 236 hourly averages were >100 $\mu g/m^3$ and 9 hourly averages were >200 $\mu g/m^3$.

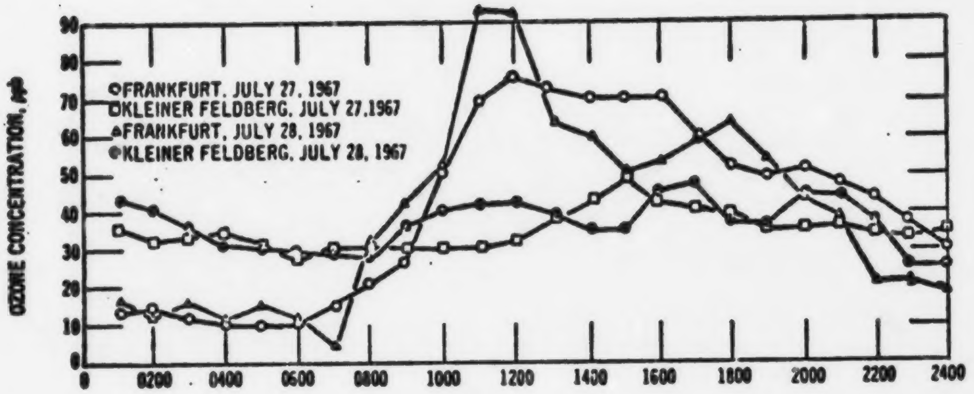

Figure 4-1. Diurnal variation in ozone concentration in Frankfurt-am-Main and at Kleiner Feldberg mountain station on July 27 and 28, 1967. (Reprinted with permission from Weber.[8])

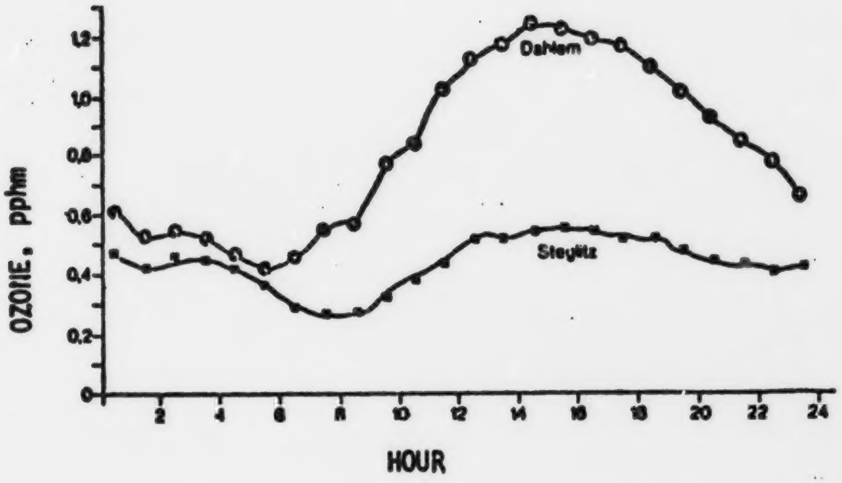

Figure 4-2. Diurnal variation in ozone concentration at two sites in Berlin, 1966-1967. (Reprinted with permission from Lahmann _et al._[11])

The NATO report also supplied ozone information for Amsterdam, University City in Rome, and Ankara, Turkey. These data are shown in Figures 4-3, 4-4, and 4-5.

An air pollution episode in Windsor, Ontario, was recorded on August 17-19, 1971.[15] Figure 4-6 shows total-oxidant peaks ranging from 0.12 to 0.20 ppm and comparable peaks for the oxides of nitrogen. An interesting feature of these measurements is the relationship between oxidants and hydrocarbon. This interpretation must not be taken too seriously, because of the large quantity of relatively unreactive material in the total-hydrocarbon reading. Figure 4-7 refers to a pollution episode at Tunney's Pasture in Ottawa in 1973 in which oxidant concentrations approached 0.14 ppm. This episode took place on a July weekend, and the nitrogen dioxide and NO_x concentrations appear to be very small. Nonmethane hydrocarbons, however, were relatively high, at about 0.6 ppm.

Bilger has documented ozone and other oxidant measurements in Australia[16] and compared them with those in other cities. Table 4-6 shows the fraction of hours during which threshold concentrations were exceeded in Sydney in 1971, 1972, and 1973. Low concentrations were recorded before 1970, probably because of the proximity to nitric oxide emission sources in the central portion of the city. It is also noteworthy that, despite the calm conditions and strong inversion in the winter months (in the southern hemisphere), high-oxidant days were relatively infrequent. Figure 4-8 outlines this seasonal variation in oxidant concentration. In Melbourne, Australia, however, a high-ozone episode was observed during December 1973. The diurnal concentration variations shown in Figure 4-9 illustrate the episode between December 10 and December 13, with a peak of 0.28 ppm on December 11, the second day of the episode. Relatively low levels were observed in other cities.

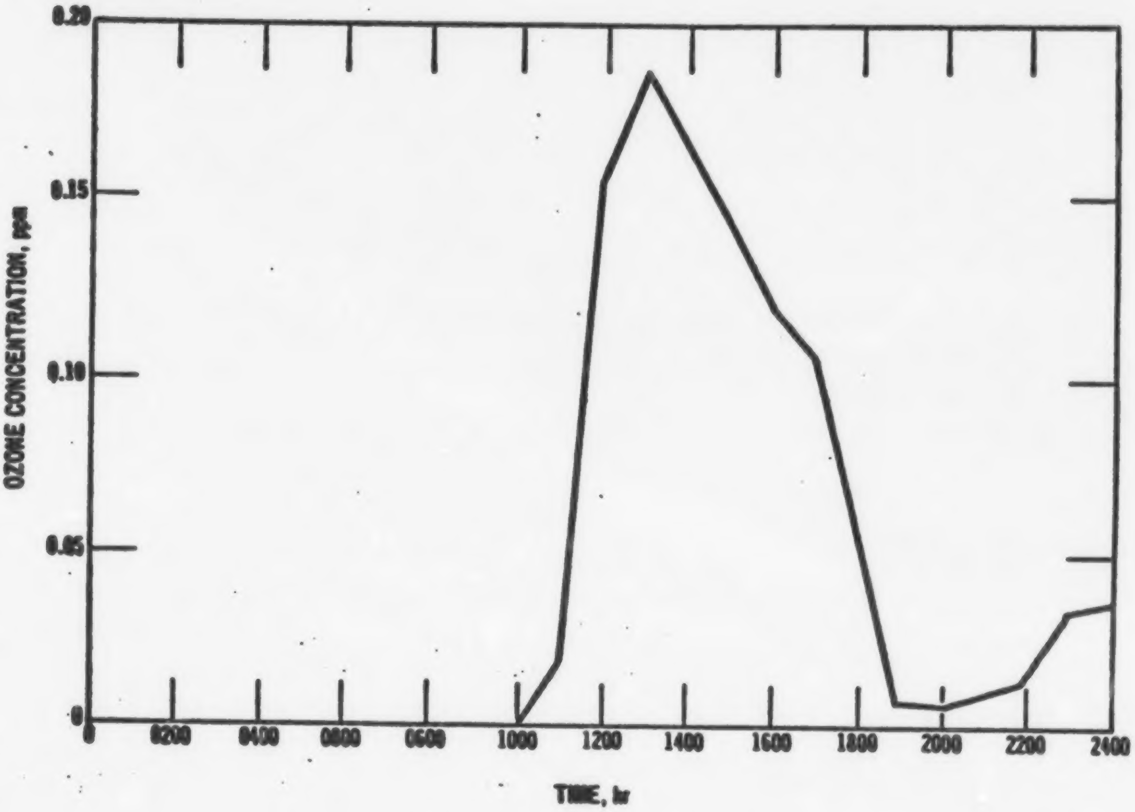

Figure 4-3. Ozone concentrations in Amsterdam, March 10, 1971. (Reprinted with permission from NATO.[7])

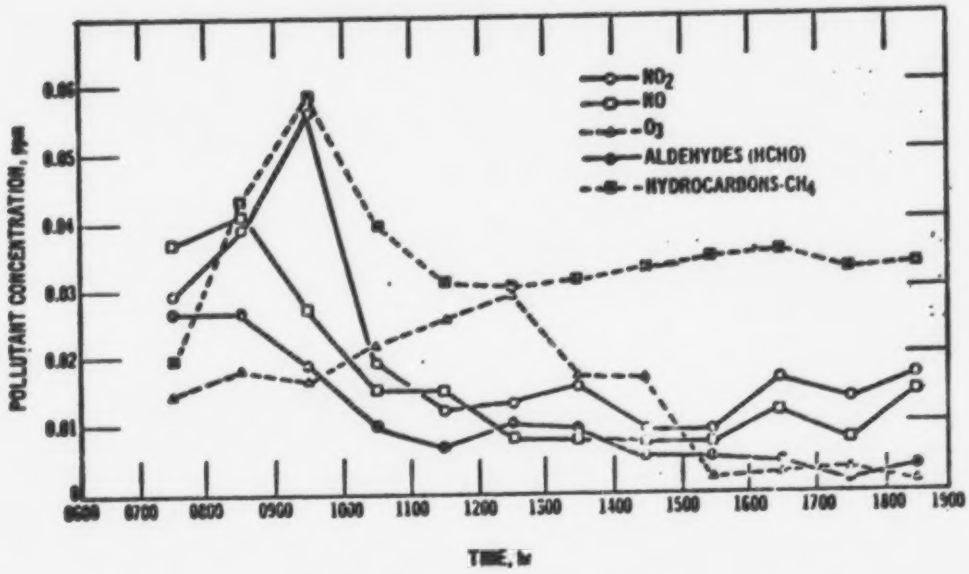

Figure 4-4. Nitrogen dioxide, nitric oxide, ozone, aldehyde, and hydrocarbon concentrations in University City in Rome. (Reprinted with permission from NATO.[7])

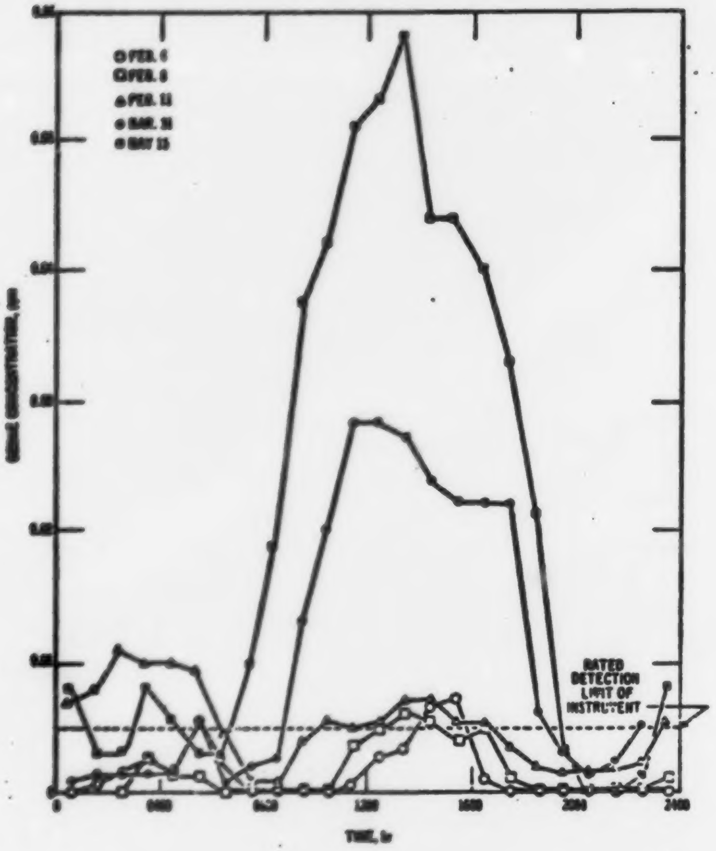

Figure 4-5. Diurnal variation in ozone concentration in Ankara, Turkey, on selected days of 1972. (Reprinted with permission from NATO.[7])

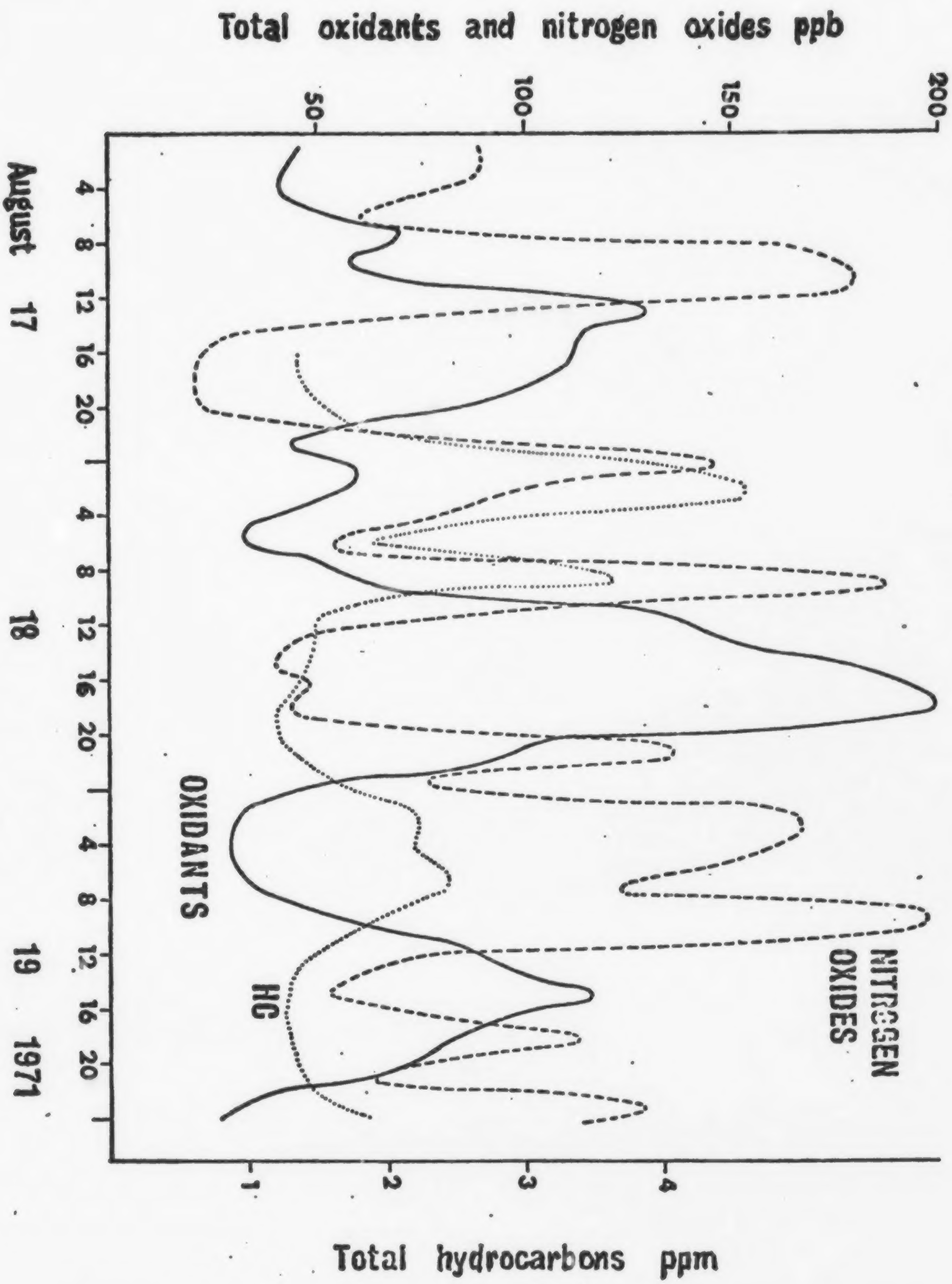

Figure 4-6. Oxidant, nitrogen oxide, and hydrocarbon concentrations in pollution episode in Windsor. (Reprinted from Ref. 15.)

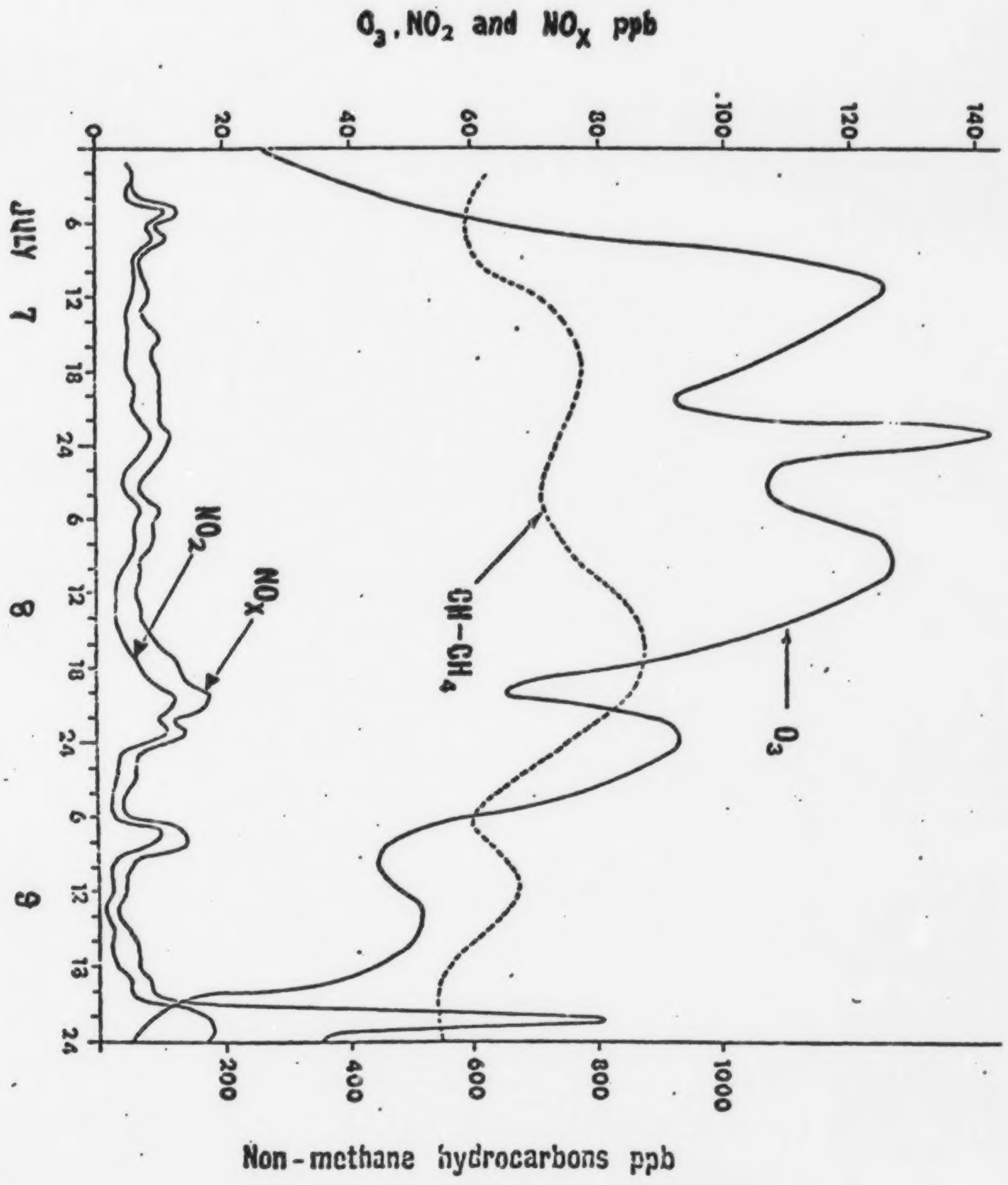

Figure 4-7. Ozone, nitrogen dioxide, NO$_X$, and nonmethane hydrocarbon concentrations in pollution episode at Tunney's Pasture 1973. (Reprinted from Ref. 15.)

Table 4-6

Oxidant Concentrations in Sydney[a]

Year	Portion of Hours with Concentration, %			Annual Maximal 1-hr Average, ppm
	>0.05 ppm	>0.10 ppm	>0.15 ppm	
1971	4.1	0.2	0.01	0.17
1972	5.6	0.9	0.2	0.24
1973	6.1	0.9	0.3	0.28

---

[a] Derived from Bilger.[16]

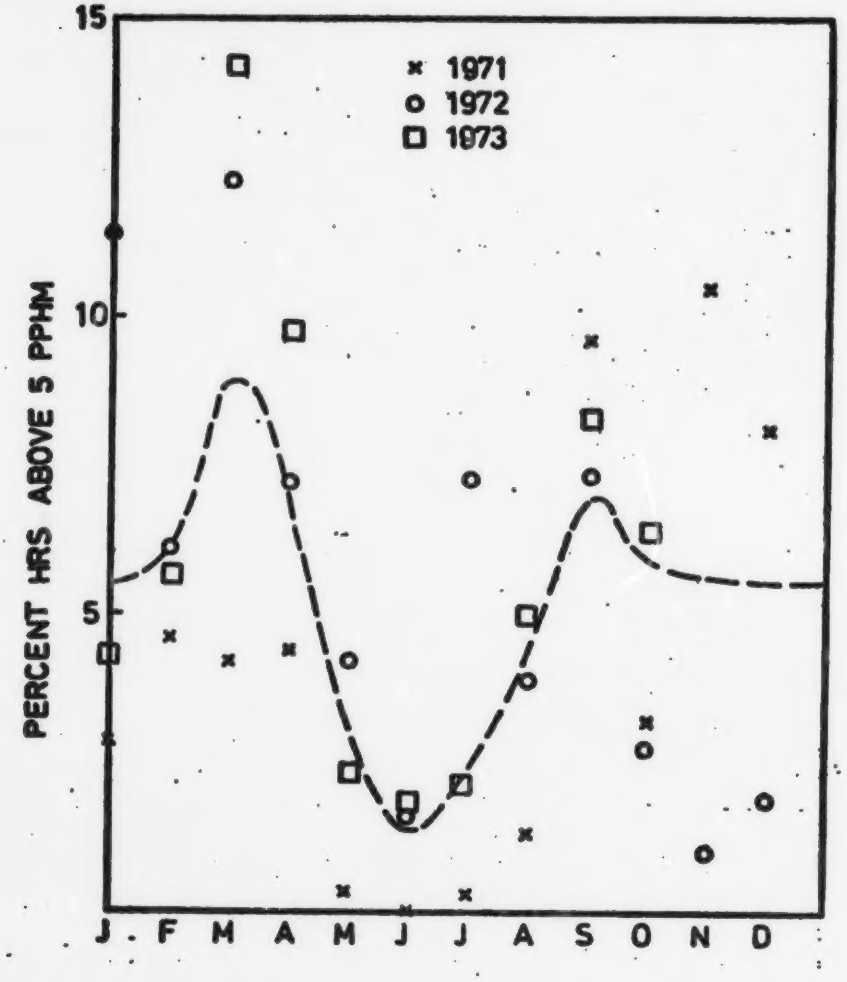

Figure 4-8. Seasonal variations in oxidant concentration in Sydney, (Reprinted with permission from Bilger.[16])

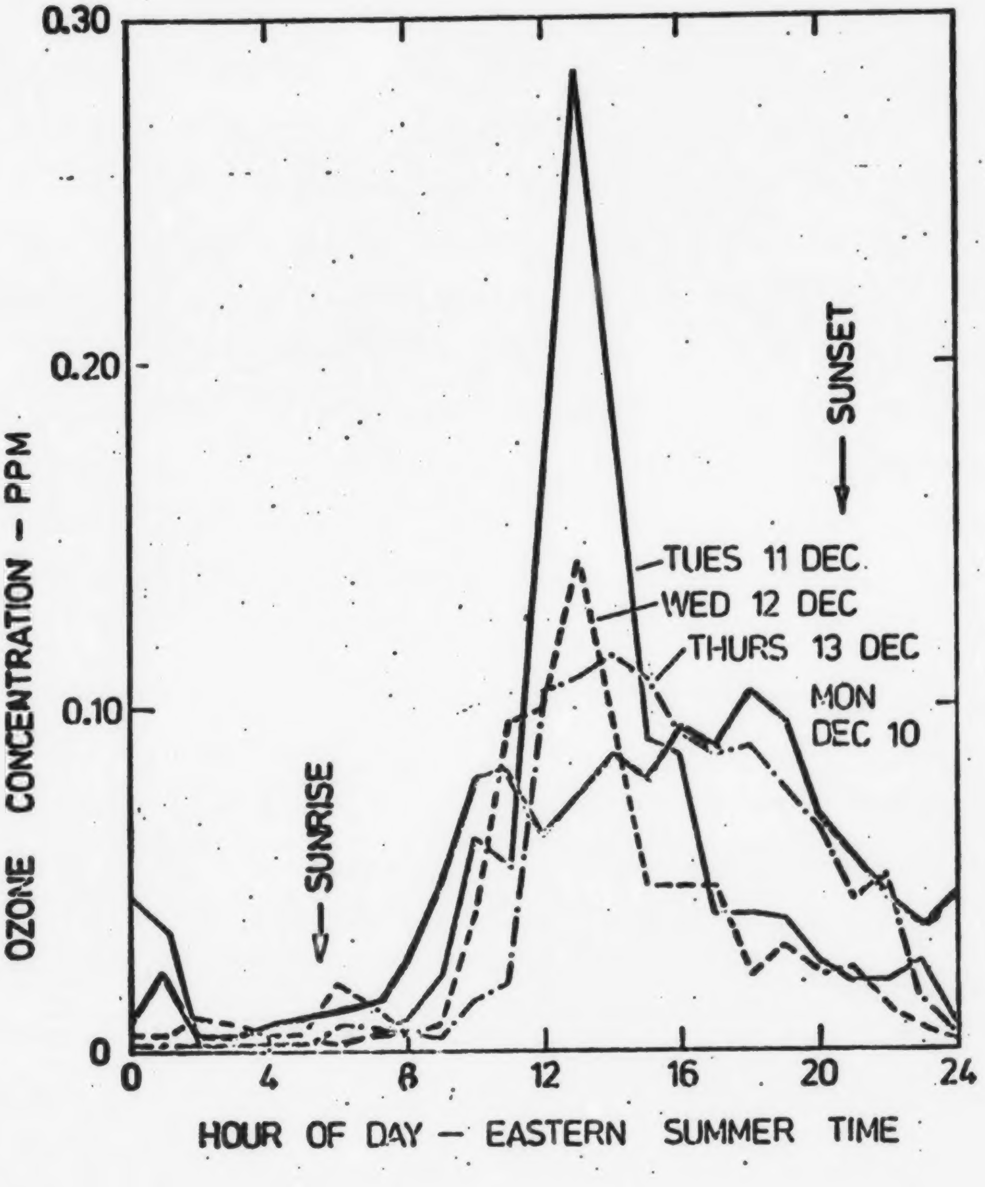

Figure 4-9. Diurnal variation in ozone concentration during December 1973 at Parliament Place, Melbourne--a 3-min average on the hour. (Reprinted with permission from Bilger.[16])

In addition to the analysis of oxidant problems in the United States and Australia, the Organization for Economic Cooperation and Development's Air Management Sector Group[17] has compiled oxidant concentrations measured in Japan during 1970 - 1972. Table 4-7 summarizes maximal hourly oxidant concentrations and the frequencies of concentrations of 0.15 ppm or more. The figures show that, despite the high latitude, rather large maximal hourly concentrations are observed in several of the cities, with the highest being 0.38 ppm in Tokyo in 1972, during which year the oxidant concentration reached or exceeded 0.15 ppm on 25 days.

Another high-latitude area where substantial ozone concentrations have been observed is London. Derwent and Stewart[17a] reported ozone concentrations in excess of 0.1 ppm. These were recorded at Harwell, Brookshire, on July 3, and July 7, 1971, by Atkins _et al_.[17b] The main subject of Derwent and Stewart's paper, however, deals with measurements in central London. Figure 4-9a (from Derwent and Stewart[17a]) shows the time variation of photochemically active pollutants for 3 days in central London. On the second day, the late afternoon peak exceeded 0.1 ppm. It is apparent that some conversion of nitric oxide to nitrogen dioxide was responsible for the ozone buildups, but it is not as clear a chemical pattern in these results as it is for cities in the western United States. The paper did not mention the method of ozone measurement; however, qualitative descriptions of the weather patterns suggest that the days of high ozone were characterized by light winds and considerable sunlight.

Coupled closely with the effect causing horizontal distributions are the vertical distributions of ozone concentrations. These distributions have an intimate influence on the urban-rural interchange of ozone. Miller and Ahrens[18]

Table 4-7

Oxidant Concentrations in Japan, 1970-1972[17][a]

City	Maximal Hourly Oxidant Concentration, ppm			
	1969	1970	1971	1972
Tokyo	0.27	0.34	0.29	0.38
Osaka	0.26	0.24	0.24	0.29
Kanagawa	----	0.21	0.36	0.33
Chiba	----	----	0.25	0.32
Saitama	----	----	0.32	0.28
Aichi	----	----	0.165	0.20
Hyogo	----	----	0.21	0.24

No. Days in 1972 with Oxidant Concentration ≥ 0.15 ppm	
Tokyo district:	an average of 25
Osaka district:	an average of 11
Ise district:	an average of 5
Ibaragi:	16
Okayama:	3
Ehime:	3

---

[a] Derived from OECD.[17]

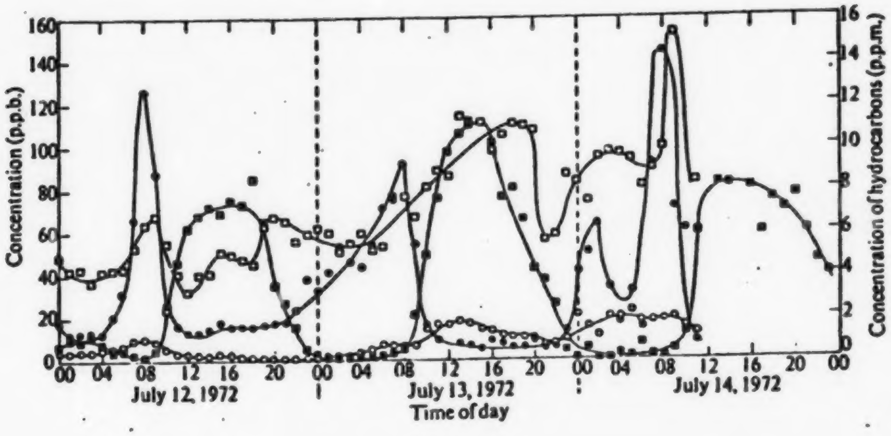

Figure 4-9a. Diurnal variations of air pollutants measured in London from July 12 to July 14, 1972. ■ , Ozone, p.p.b.; ●, nitric oxide, p.p.b.; ▢, nitrogen dioxide, p.p.b.; ○, hydrocarbons, p.p.m. (Reprinted with permission from Derwent and Stewart.[17a])

presented detailed vertical time and space cross sections of ozone concentrations at altitudes up to 2,500 m. A low-altitude temperature inversion may actually lead to lower concentrations of oxidant, because the destruction rate can be increased by the injection of nitric oxide into a shallow mixing layer. Very high oxidant concentrations were observed at the edge of the marine inversion, where the mixing layer is rather deep. Possible high-altitude transport of ozone within the inversion layer and absence of destruction mechanisms could lead to a buildup aloft. Later fumigation caused by surface heating could cause increased ozone concentrations at downwind locations. Horizontal spatial patterns were mapped out with aircraft measurements to indicate the connection between transport from areas where precursor emission occurs and the downwind buildup of ozone after the photochemical reaction.

The compensating factors leading to increased daily maximal oxidant concentration over the years include both decreased destruction rates and increased precursor concentration. The decreased destruction rates theoretically result from urbanization, which tends to destabilize the air and increase vertical mixing. Thus, the very mechanism that leads to greater dispersion also leads to higher ozone concentration. The ozone aloft that comes from polluted air that is transported upward into the inversion has a relatively long lifetime, compared with that at low altitudes.

To determine the relationship of ozone concentrations in the Sierra Nevada mountains with those in the central valley of California, airborne and ground-station measurements were taken of total oxidant, temperatures, and wind from August 17 to August 27, 1970. Miller et al.[19] report the results in a paper that coordinates the measurements on the basis of ozone transport. Figure 4-10 shows concentrations equaling or approaching the national ambient air quality standard for oxidants at stations at 351 and 2,287 m. Comparison with concentrations in an urban center in the central valley, with an altitude of 99 m, shows that the peak concentrations at these very different elevations roughly approximate one another during the afternoon and early evening. At the urban location, however, nighttime values decrease dramatically, probably because of reaction with nitric oxide emitted locally. These results suggest that the ozone-laden layer moves along the terrain, rather than touching the surface at some altitude near the mixing depth. A highly plausible transport mechanism is found in the afternoon up-slope flows induced by surface heating. Aircraft profile measurements at Mineral King (2,287 m) indicated that both temperature and oxidant increased slightly near the surface. The evidence suggests that photochemical oxidant is transported from population centers in the central valley into the higher-altitude mountain valleys. The primary pollutants (oxides of nitrogen and hydrocarbons) may have been the specific pollutants advected (i.e., moved horizontally), and the abundant light in the ultraviolet range at the higher altitudes could have been significant in increasing ozone production during the early morning.

Blumenthal et al.[20] obtained aircraft data by taking vertical soundings over various airports in the Los Angeles basin area. Figure 4-11 shows the results for a vertical sounding over Hawthorne Airport at 9:15 a.m., on September 20, 1972. The vertical distributions of condensation nuclei and temperature suggest a mixing layer approximately 800 ft deep. At the same altitude, there is a decided increase in ozone concentration that persists

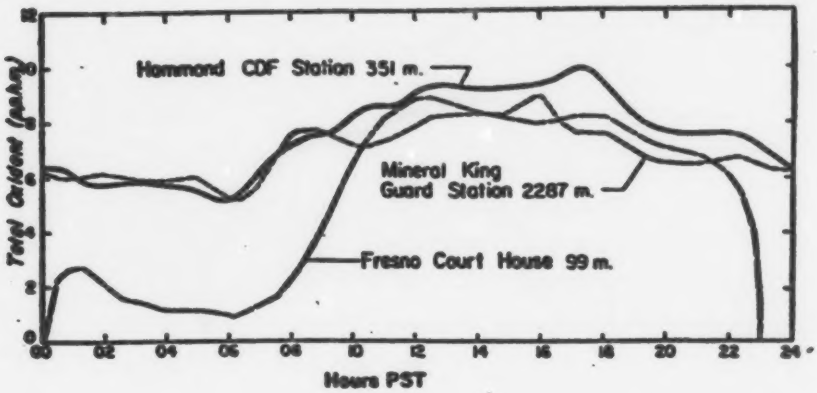

Figure 4-10. Comparison of 10-day means of hourly total oxidant concentrations at Fresno, Hammond, and Mineral King, California. (Reprinted with permission from Miller _et al._[19])

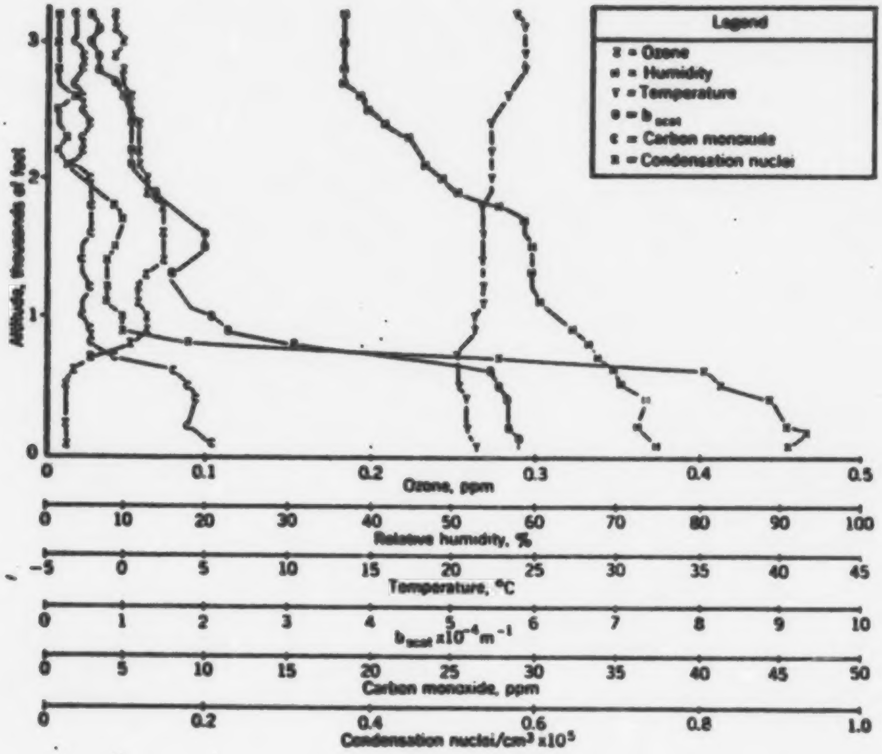

Figure 4-11. Data from vertical sounding over Hawthorne Airport at 9:15 a.m., September 20, 1972. (Reprinted with permission from Blumenthal _et_ _al._[20])

up to a few thousand feet in altitude. This morning profile of ozone up into the inversion layer corroborates other findings of high ozone concentrations in regions that are not well mixed with nitric oxide from the ground. The profiles of carbon monoxide concentration and b_{scat} (a measurement of light scattering in air) also indicate the location of the mixing layer.

Blumenthal and co-workers[21] used the earlier data and a case study of Denver to develop arguments as to the source of high concentrations of ozone or ozone precursors that are found in some nonurban areas. They believe that downwind areas as long as 260 km can exceed the standard because of precursor emission from an urban source. Although they do not present any ozone production estimates related to photochemistry, their data analyses confirm hypotheses of transport from urban to nonurban areas. They point out that rural areas have had concentrations as high as 0.3 ppm with no local source of reactant.

The Los Angeles Reactive Pollutant Program (LARPP) obtained three-dimensional distributions of ozone by using helicopters and ground-based instruments. The instrument platforms were directed to follow an air parcel through the Los Angeles basin by means of radio commands based on the radar tracking of tetroon* arrays that were released below the inversion base and allowed to float along with the air. Preliminary plots of these data[22] show that each vertical distribution of ozone is very nonuniform during the morning, but becomes very uniform toward midday as the values increase. This behavior is shown in Figure 4-12. Vertical profiles of temperature, dew point, and ozone, shown in Figure 4-13, illustrate a case in which the ozone concentration

---

* A neutral buoyancy balloon that follows winds along constant density contours.

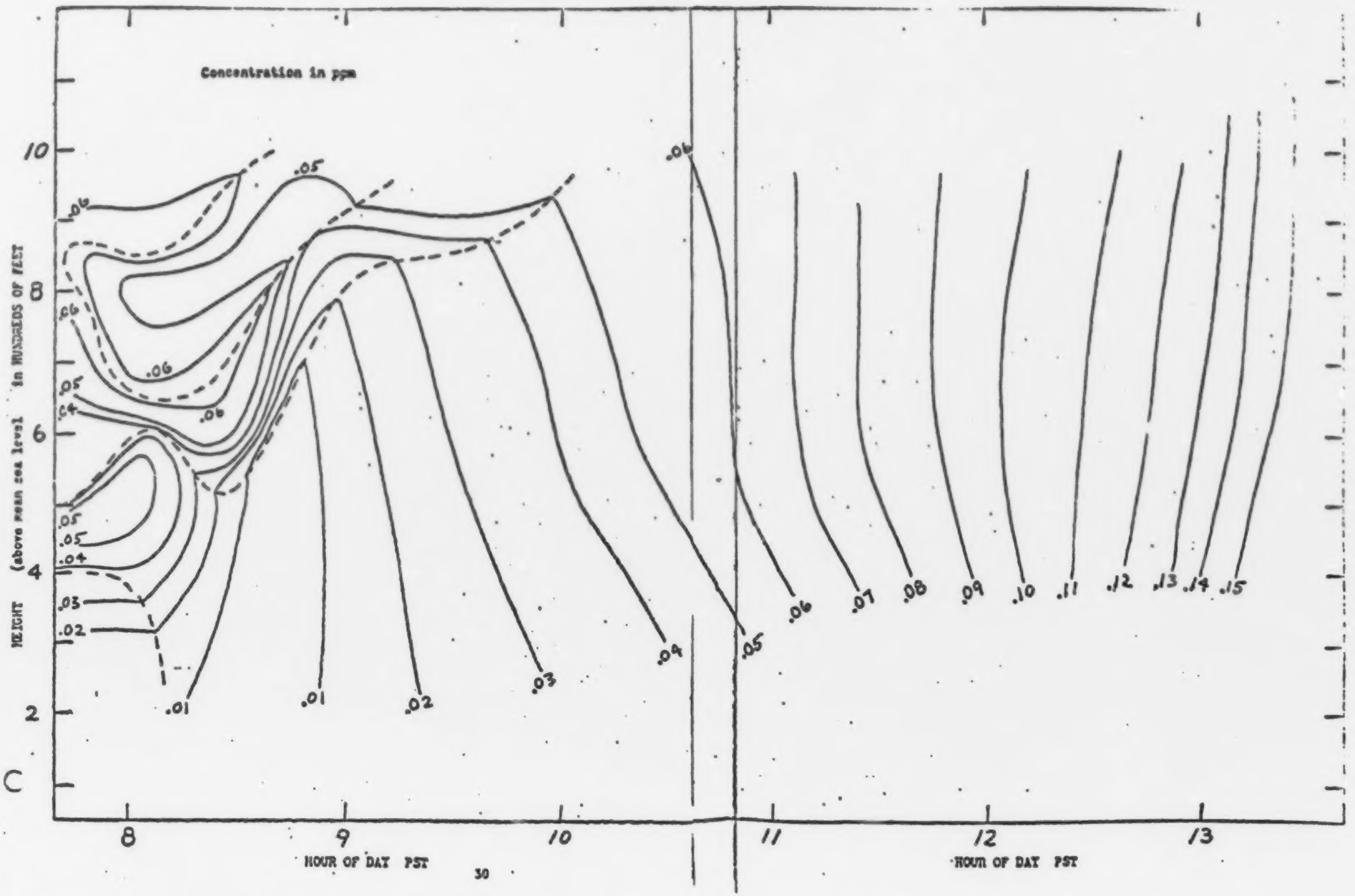

Figure 4-12. Vertical time section for ozone, operation 33, November 5, 1973. (Reprinted with permission from Edinger.[22])

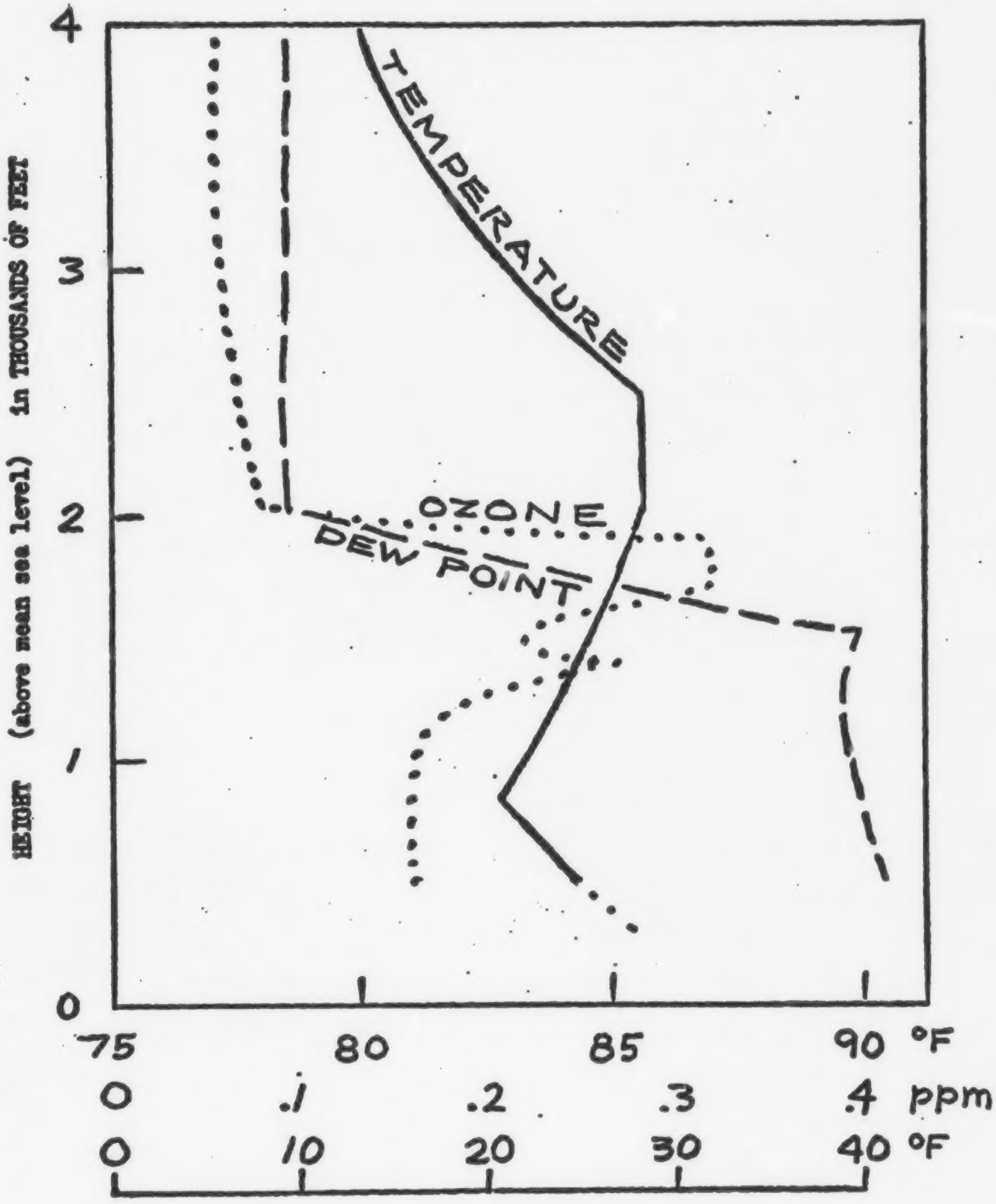

Figure 4-13. Vertical temperature, due point, and ozone sounding for operation 14, Glendale, October 4, 1973, 1:01-1:25 p.m. (Reprinted with permission from Edinger.[22])

in the inversion layer 1,000-2,000 ft above mean sea level was approximately 3 times the concentration near the ground. This finding lends further support to the hypotheses advanced by others regarding the horizontal transport of ozone at high altitudes.

In rural areas of western Maryland and West Virginia, hourly ozone concentrations as high as 0.12 ppm were recorded[23] in August and September 1972. The concentration exceeded the national ambient air quality standard of 0.08 ppm 11% of the time. During one episode, this standard was exceeded for 26 consecutive hours. Precursors were always near background concentrations, and the horizontal spread of ozone was extensive. After mentioning stratospheric sources and ground sinks, the report hypothesizes that clouds of precursors emitted from distant urban areas undergo transformation to ozone during their long journey. Mechanical turbulence is suggested as a transport mechanism that brings the resulting ozone to the surface.

Airborne measurements made for transects across the Los Angeles basin by Edinger[24] confirm the earlier hypotheses that ozone concentrations go through a spatial maximum above the base of the inversion in many situations. Figures 4-14 and 4-15 show space sections of the potential temperature and the oxidant concentrations in a vertical cross section running approximately west to east from the Pacific cost to Rialto, California. These results are for June 20, 1970, at 4:30 p.m. The temperature field exhibits a distinct inversion base that roughly follows the terrain, but increases slightly moving inland—which is typical of the heating effect that occurs during onshore flows. The oxidant field corresponding to it shows peaks in excess of 0.35 ppm at altitudes approaching 1,000 m. At the same time, ground concentrations gradually increase to a maximum of 0.25 ppm 60 miles onshore.

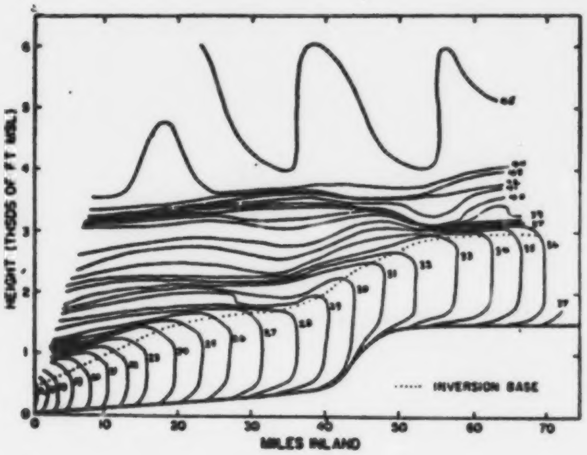

Figure 4-14. Field of potential temperature (°C) in the vertical cross section from Santa Monica to Rialto-Miro, 4:30 p.m., June 20, 1970. (Reprinted with permission from Edinger.[24])

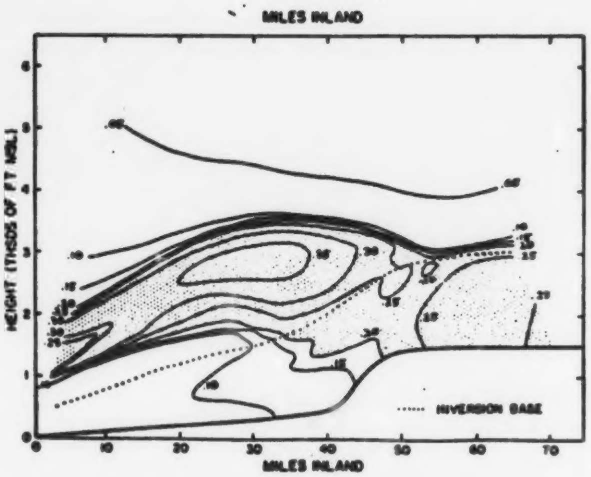

Figure 4-15. Field of oxidant concentrations (ppm) in the vertical cross section from Santa Monica to Rialto-Miro, 4:30 p.m., June 20, 1970. (Reprinted with permission from Edinger.[24])

These data suggest that the oxidant within the inversion layer has been advected into that layer from horizontal injections in the vicinity of heated mountain slopes. This explanation is preferred to vertical mixing, because of the extreme stability within the inversion layer. In fact, that stability insulates the high-ozone air parcel from nitric oxide, which could react rapidly with the ozone and thereby decrease it. Entrapment in the inversion layer also suggests an explanation for long-range horizontal transport that can ultimately lead to the large nonurban ozone concentrations that have been reported.

Ozone and ozone precursor concentrations at nonurban locations in the eastern United States were studied extensively.[25] The three parts of the study were field measurements, a quality assurance program, and an airborne monitoring program. The main objective of the study was to establish a data base for nonurban ozone and precursor concentrations. Simultaneous statistical summaries of the concentrations of nitrogen dioxide and nonmethane hydrocarbons were also provided. Another objective was to search for relationships between ozone concentrations and nitrogen dioxide and nonmethane hydrocarbon concentrations.

Monitoring sites were selected in northwestern Pennsylvania, central Ohio, western Maryland, and southern West Virginia. The field program was conducted between June and September of 1973. Ozone was measured at each of the four sites, and precursor concentrations were measured at three of them. The diurnal patterns of ozone concentration were not similar to the rural site measurements reported for New York State.[9,10] Instead of a gentle ozone peak just after midnight, there was a late afternoon peak that was several times the minimal concentration of ozone, which generally occurred early in the morning. On selected dates, however, nighttime ozone concentration maximums were observed at the Maryland and Ohio sites. It was noted that the National Ambient Air Quality Standard for photochemical oxidants was exceeded during 37, 30, 20, and 15% of the hours at the sites in Maryland, Pennsylvania, Ohio, and West Virginia, respectively, during the sampling interval. Correlation coefficients among hourly ozone concentrations measured at the four stations at the same time were in the range of 0.468-0.678. Evidently, high ozone concentrations at the nonurban locations were spread over extensive areas of the four-state region.

The quality assurance phase of the program was conducted to maximize the comparability of the data generated at the four monitoring sites, as well as data from the mobile laboratory. Real-time data processing permitted quick analysis of the performance of the analyzers. Because the nitrogen dioxide values were very low and the hydrocarbon data from the fixed sites were declared invalid, only ozone was subjected to statistical analysis. The bias of measurements between fixed- and mobile-site analyzers was estimated. The greatest bias observed during the program, 23%, was attributed to span drift of one of the analyzers.

The airborne monitoring program concentrated on the measurement of ozone to provide supplementary air quality data for various altitudes over the fixed sites. The airborne measurements were conducted in a C-45 aircraft that carried a solid-face chemiluminescent ozone monitor. The ozone meter was cycled every 2 min to provide calibration, purge, measurement, and purge at equal intervals. The sparseness of the airborne data precluded detailed analysis, but the comparisons between ozone aloft and ozone at the ground stations showed a high degree of regularity. The airborne values were comparable with those read on the ground 100 - 600 ft below. A general conclusion on the vertical data is that the ozone generated from ground-source precursors is predominant over ozone that might be transported from the stratosphere.

Gloria et al.[26] studied photochemical air pollution with an instrumented aircraft in various air bases in California. They estimated background ozone concentrations for the southern coast air basin to be about 0.03 ppm. Ozone was measured by ultraviolet absorption with a Dasibi ozone photometer. Total oxidant, carbon monoxide, oxides of nitrogen, hydrocarbons, dew point, and temperature were measured simultaneously. East-west ozone sections were made from series of flights following survey patterns mapped on Figure 4-16. Figure 4-17 shows the vertical cross section of ozone isopleths for August 11, 1971, indicating higher ozone concentrations next to the surface than up near the inversion base. Layering of ozone at higher altitudes is shown in the profiles measured at Riverside, California, on August 10-12, 1971. These profiles, illustrated in Figure 4-18, show the entrapment of high ozone concentrations far above the surface in strata. Similar ozone layering was observed in the San Francisco Bay area during the same study.

Atmospheric ozone concentration was measured simultaneously at two rural and four urban sites in New York State.[9] It was noted that during the period August 1-17, 1973, the average hourly ozone concentrations at the rural sites stayed well above the urban concentrations throughout each day and that the urban values peaked at approximately the rural values in the early afternoon (see Figure 4-19). The average rural ozone concentration for the period of observations was around 0.05-0.07 ppm. The authors concluded that violations

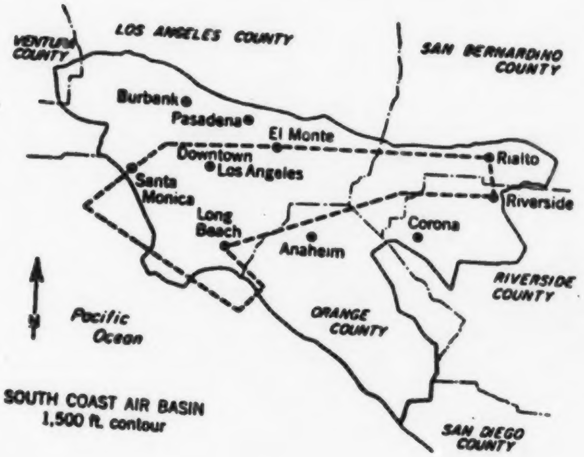
VENTURA COUNTY
LOS ANGELES COUNTY
SAN BERNARDINO COUNTY
Burbank
Pasadena
El Monte
Downtown
Los Angeles
Rialto
Santa Monica
Riverside
Long Beach
Corona
Anaheim
RIVERSIDE COUNTY
N
Pacific Ocean
ORANGE COUNTY
SOUTH COAST AIR BASIN
1,500 ft. contour
SAN DIEGO COUNTY

Figure 4-16. Outline map of the Los Angeles basin area traversed during survey flights, showing general flight paths. (Reprinted with permission from Gloria et al.[26])

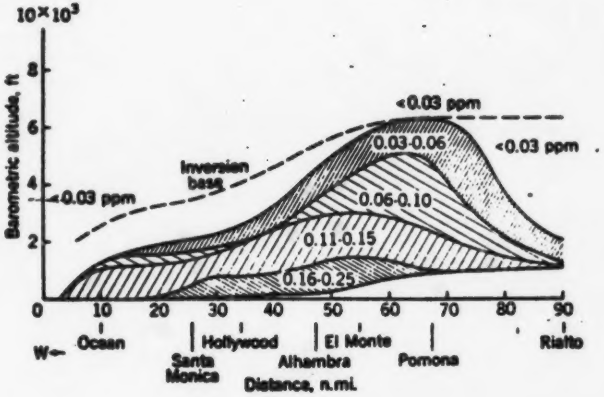

Figure 4-17. Ozone isopleths (vertical cross section) from southern coast air basin survey, August 11, 1971. (Reprinted with permission from Gloria _et_ _al._[26])

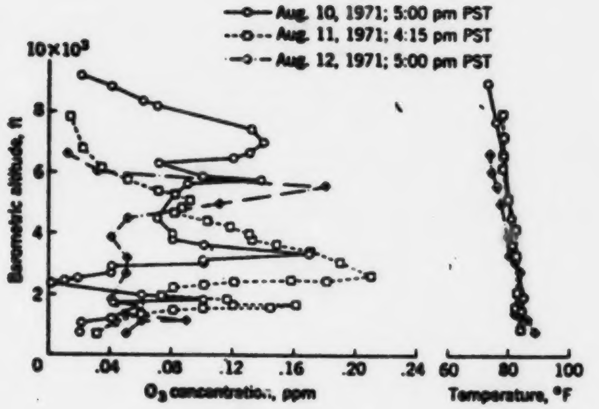

Figure 4-18. Ozone profiles, Riverside, Calif., August 10-12, 1971. (Reprinted with permission from Gloria et al.[26])

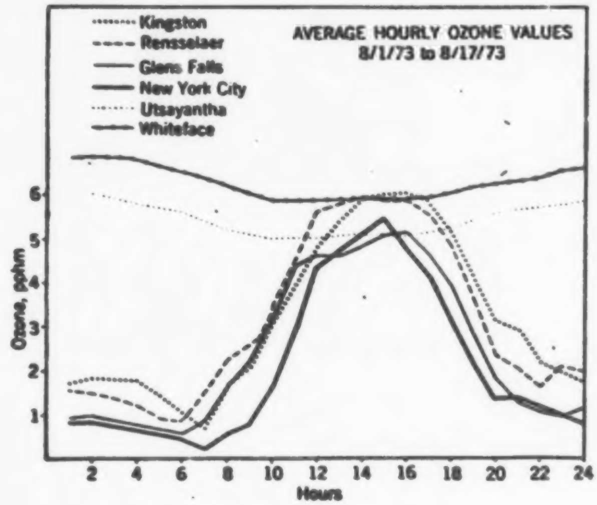

Figure 4-19. Average hourly ozone concentrations during August 1-17, 1973, at selected sites in New York State. (Reprinted with permission from Stasiuk and Coffey.[9])

of the present ambient air quality standard for photochemical oxidants may not be prevented completely by reducing anthropogenic hydrocarbon emission in the state. They compared the weight equivalent of 0.24-ppm hydrocarbon and 0.08-ppm ozone. These numbers were derived from the air quality standards and suggested that one weight of nonmethane hydrocarbon is capable of generating an equivalent weight of ozone photochemically. The questionable nature of these assumptions is brought out by a comparison of the ozone potential for all anthropogenic emission of hydrocarbon in the nation with the influx of ozone by advection into New York State. The two ozone values are approximately equivalent. Clearly, the photochemistry of nitrogen oxides must be included in such estimates. Explanations of the relatively high rural ozone concentrations center on speculation based on the subsidence of stratospheric ozone or on ozone generation by the photooxidation of natural precursors. It is argued that transport of ozone from other urban areas and later reactions with further precursors do not appear to constitute the dominant mechanism. These arguments apparently were based on the assumed weight equivalency between hydrocarbon precursors and ozone in the atmosphere.

The authors later continued the disucssion with the same New York State data.[10] There were close correlations between rural ozone concentrations and some of the urban peak values for the August 1-17, 1973, period, as shown in Figure 4-20. Time correspondences between maximal wind and maximal ozone concentration are cited as evidence to support the hypothesis that high urban ozone concentrations in New York State result from the transport of background ozone into these areas. Correlation coefficients of 0.83 for wind and temperature, 0.81 for wind and ozone, and 0.87 for ozone and temperature were obtained for readings in Kingston, New York. The correlations for the Welfare

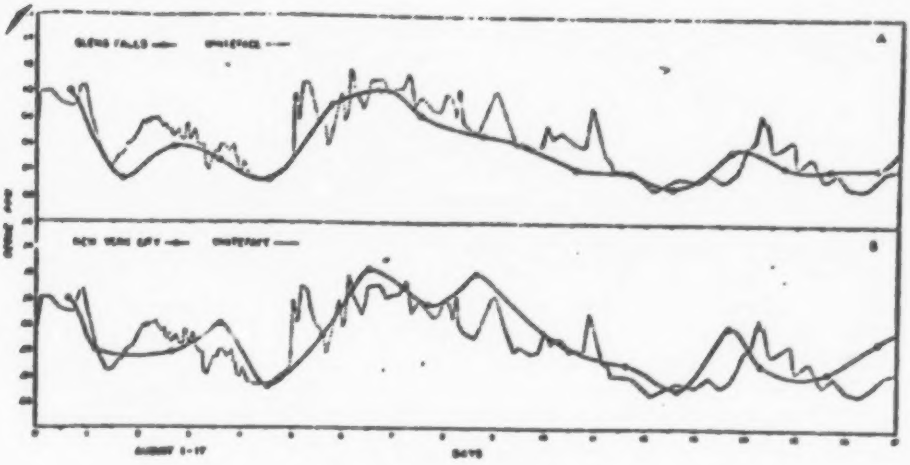

Figure 4-20. Close correlations between the whiteface ozone concentrations from August 1-17, 1973, and the smooth curve drawn between the Glens Falls and New York City daily ozone maximums. (Reprinted with permission from Coffey and Stasiuk.[10])

Island monitoring site in New York City were not nearly as clear as the ones for Kingston. It was concluded that the correlation of photochemical ozone in one area with that in another does not necessarily indicate transport. An alternative mechanism was based on a belief that the observed correlations imply a common ozone source. It was suggested that ozone concentrations exceeding the federal ambient air quality standard exist in rural areas and are transported into urban areas, but no direct evidence is offered beyond the concentration graphs.

Air breakdown due to coronal discharges around high-voltage transmission lines has been considered as a possible rural source of ozone. Several investigations[25,27-30] suggest that this cannot be a significant source.

In a paper presented at the EPA scientific seminar on automotive pollutants,[31] Pitts pointed out that, until the controversy on calibration methods was resolved, most people believed that the urban plume moving eastward from Los Angeles was accompanied by increasing ozone concentrations. This is illustrated in Figure 4-21 for downtown Los Angeles, Pasadena, Pomona, Azusa, Riverside, and San Bernardino. Figures 4-21 through 4-23 all show the numbers of days on which the maximal hourly average oxidant concentration equaled or exceeded 0.20 ppm in 1973. Pitts assumed that all data were adjusted to the Los Angeles Air Pollution Control District (APCD) calibration method by multiplying the non-Los Angeles (i.e., Riverside and San Bernardino) data by 5/7. Figure 4-22 shows that this procedure lowers the numbers for the two easternmost stations relative to those for the eastern portion of Los Angeles County (stations 2, 3, and 4—Pasadena, Pomona, and Azusa). Proceeding to another alternative, Pitts multiplied the numbers for stations 1-4 by 7/5 as a way of converting Los Angeles APCD data to the ARB calibration

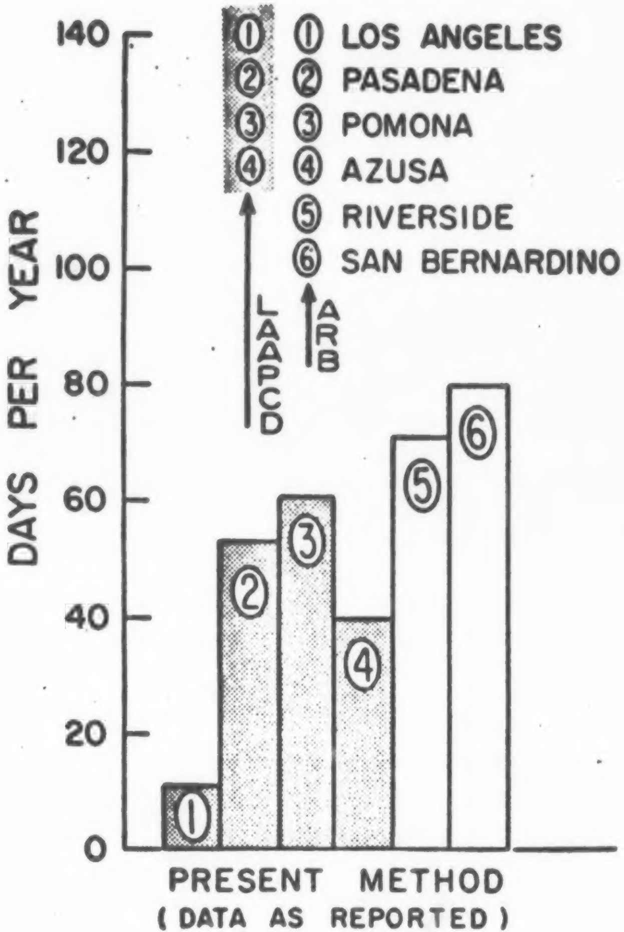

Figure 4-21. Number of days in 1973 on which the maximal hourly average oxidant concentration equaled or exceeded 0.20 ppm at six air monitoring stations in the southern coast air basin. Data as reported: Los Angeles, Pasadena, Pomona, and Azusa reported by Los Angeles County APCD; Riverside reported by Riverside County APCD; and San Bernardino reported by San Bernardino County APCD. (Reprinted with permission from Pitts.[31])

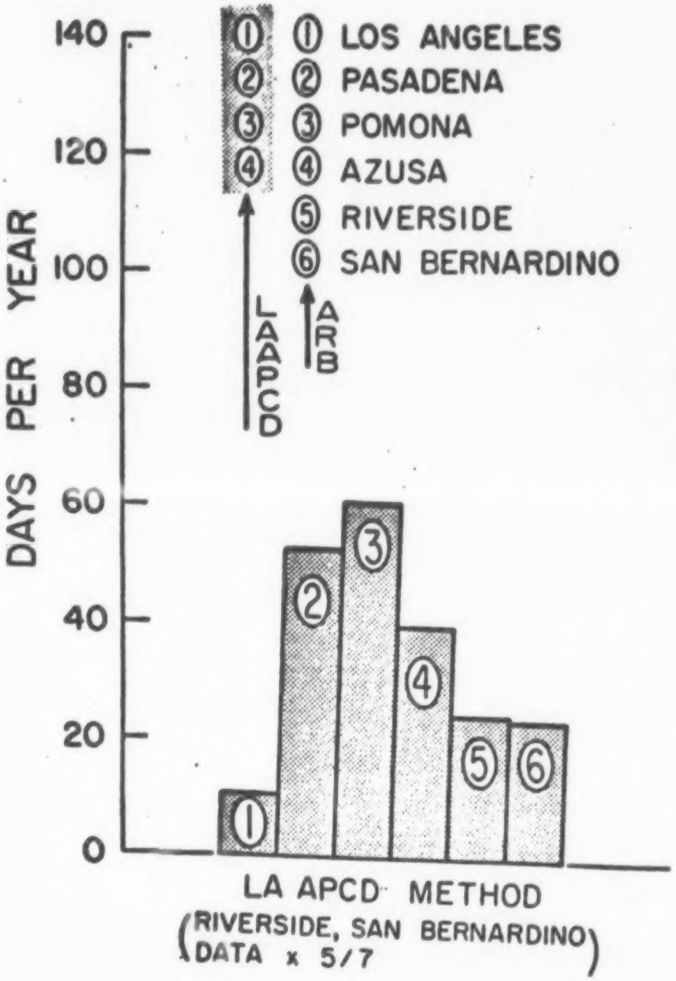

Figure 4-22. Number of days in 1973 on which the maximal hourly average oxidant concentration equaled or exceeded 0.20 ppm at six air monitoring stations in the southern coast air basin. Non-Los Angeles APCD data multiplied by 5/7 to convert to Los Angeles APCD scale. (Reprinted with permission from Pitts.[31])

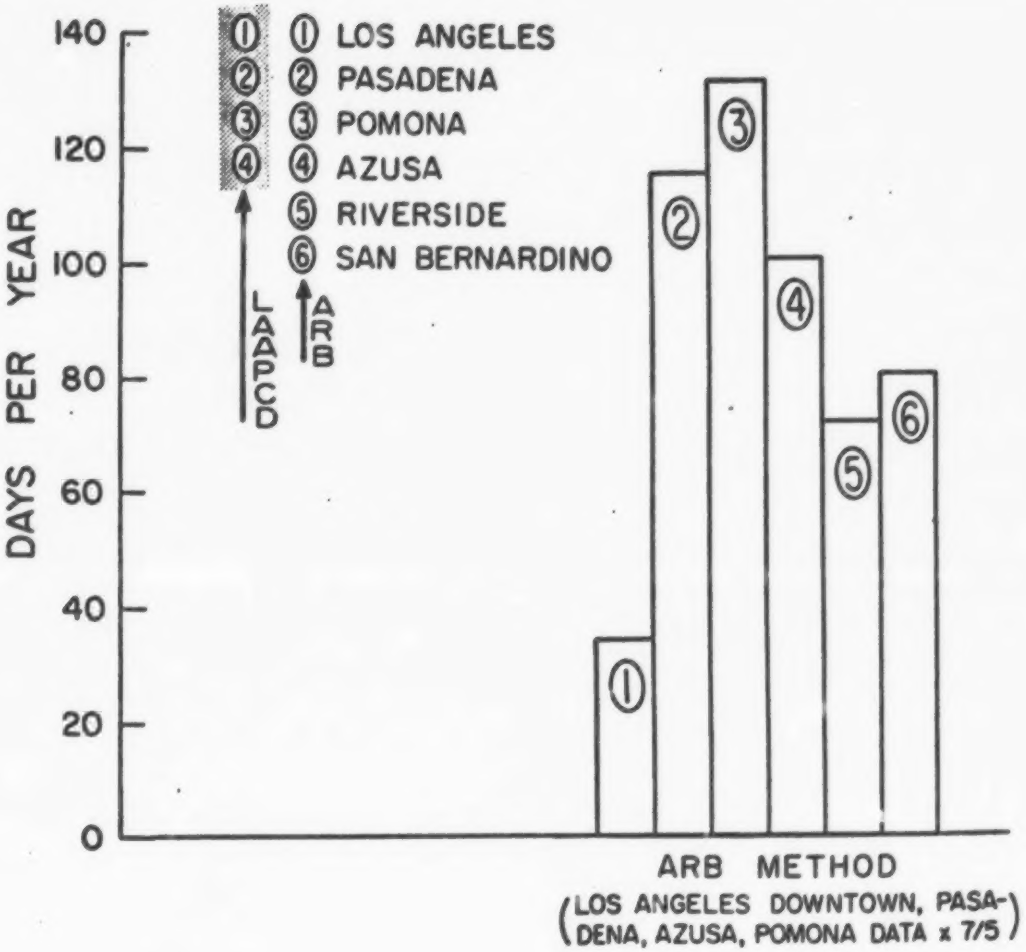

Figure 4-23. Number of days in 1973 on which the maximal hourly average oxidant concentration equaled or exceeded 0.20 ppm at six air monitoring stations in the southern coast air basin. Los Angeles APCD data multiplied by 7/5 to convert to the ARB-EPA scale. (Reprinted with permission from Pitts.[31])

method. The results, illustrated in Figure 4-23, show the numbers for the two easternmost stations to be lower than those for the stations in Los Angeles County. Without saying which agency is correct in the controversy, Pitts points out that a consistent approach with either method produces a conclusion different from the previous one. Previously, it was believed that the eastern counties experienced higher ozone concentrations. Now it appears that the ozone concentration goes through a peak in the eastern portions of Los Angeles County and decreases as the air parcel moves into the counties east of Los Angeles. These results point out that extreme care must be taken in comparing ozone or oxidant measurements taken at different places with instruments that are calibrated by different methods.

The production of ozone in power plant plumes has been suggested to explain ozone spatial distributions in nonurban areas.[32,33] Comparison of oxidation mechanisms competing for sulfur dioxide suggests that three reactions--

$$SO_2 + HO_2 \rightarrow SO_3 + OH \qquad (3)$$

$$SO_2 + OH + M \rightarrow HSO_3 + M \qquad (4)$$

$$SO_2 + CH_3O_2 \rightarrow SO_3 + CH_3O \qquad (5)$$

--are principally responsible for sulfur dioxide removal. Equation 4 is thought to be the first step in a chain that converts nitric oxide to nitrogen dioxide, causing an ozone buildup via the photostationary state mechanism involving the nitrogen dioxide-nitric oxide-ozone cycle. Oxidized species up to HSO_6 are postulated as being responsible for the conversion.

Descriptions of field studies of power plant stack plumes were given by Davis *et al.*[32] The ozone concentration appears to be lower in regions of high sulfur dioxide content. At 32 km downwind from the stacks, it was claimed that the ozone concentration in the plume (now 11 km wide) is higher than the ambient concentration (~0.08 ppm) by approximately 0.02 ppm. Simultaneous measurements of nitric oxide and nitrogen dioxide were integrated across the plume. Values of the ratio of nitric oxide to NO_x concentration decreased monotonically from 0.9 at 2 km to 0.2 at 15 km and beyond. Other, similar observations were cited.

It has been suggested by the analysis of organic components in rainwater that naturally emitted terpene compounds may be the source of some photochemical oxidant.[34] Gas chromatography was used to separate individual components of rainwater that had been purged by helium gas as a carrier. The individual components thus separated were identified by their mass spectra. Rainwater samples were taken at the end of a mid-August 1973 smog episode in the Washington, D.C., area. The episode was characterized by stagnant weather over a large area east of the Appalachian Mountains between New Jersey and North Carolina. It ended on August 13, when a gentle rain occurred and samples were taken. The dominant compound in the rainwater samples was 3-methylfuran. Plausibiluty arguments based on chemical reaction mechanisms were advanced for the existence of 3-methylfuran as a product of the photooxidation of isoprenoid compounds. Some aromatics in the sample were attributed to vehicular hydrocarbon emission, but the relative concentrations suggested that terpenes could have been the most important compound in the smog. No definite conclusions were drawn, but it was inferred that naturally occurring hydrocarbons could cause summer photooxidant smog. This is highly unlikely, in view of measurements made on rain that originated from an air mass different from that in which the smog episode occurred.

In addition to observations in Los Angeles, Blumenthal and White[35] have reported measurements of a power-plant plume and an urban plume 35 and 46 km downwind from St. Louis, Missouri. Figure 4-24 shows the evidence of extensive ozone buildup in the urban plume. Simultaneous measurements of scattering coefficient, b_{scat}, trace the spread and dilution of suspended particulate material. It is interesting that in the urban plume, which spreads to 20 km in width, the ozone increases while the particulate matter decreases; this suggests considerable photochemical production at an altitude of 750 m. Contrary to the statements of Davis and co-workers reported above,[32,33] the power-plant plume causes a decrease, rather than an increase, in ozone. Nitric oxide in the plume reacts with the ozone as it mixes. This is clearly indicated by the distribution of particulate matter, which acts as a tracer.

Rough plots of ozone isopleths from measurements over rural areas of Connecticut have been constructed by Rubino _et al_.[36] Increased concentrations (~0.31 ppm) are traced across the state during the June 10, 1974, episode. The concentrations that built up throughout the day are associated with the trajectory of an air mass that was over the metropolitan New York area during morning peak traffic. The conclusion was that the city is an origin of precursors that cause high ozone concentrations downwind. This is an interesting contrast with (but perhaps not a contradiction of) the suggestions of Coffey and Stasiuk,[10] who believed that ozone of stratospheric origin is transported into the metropolitan New York area. One difference between the two studies

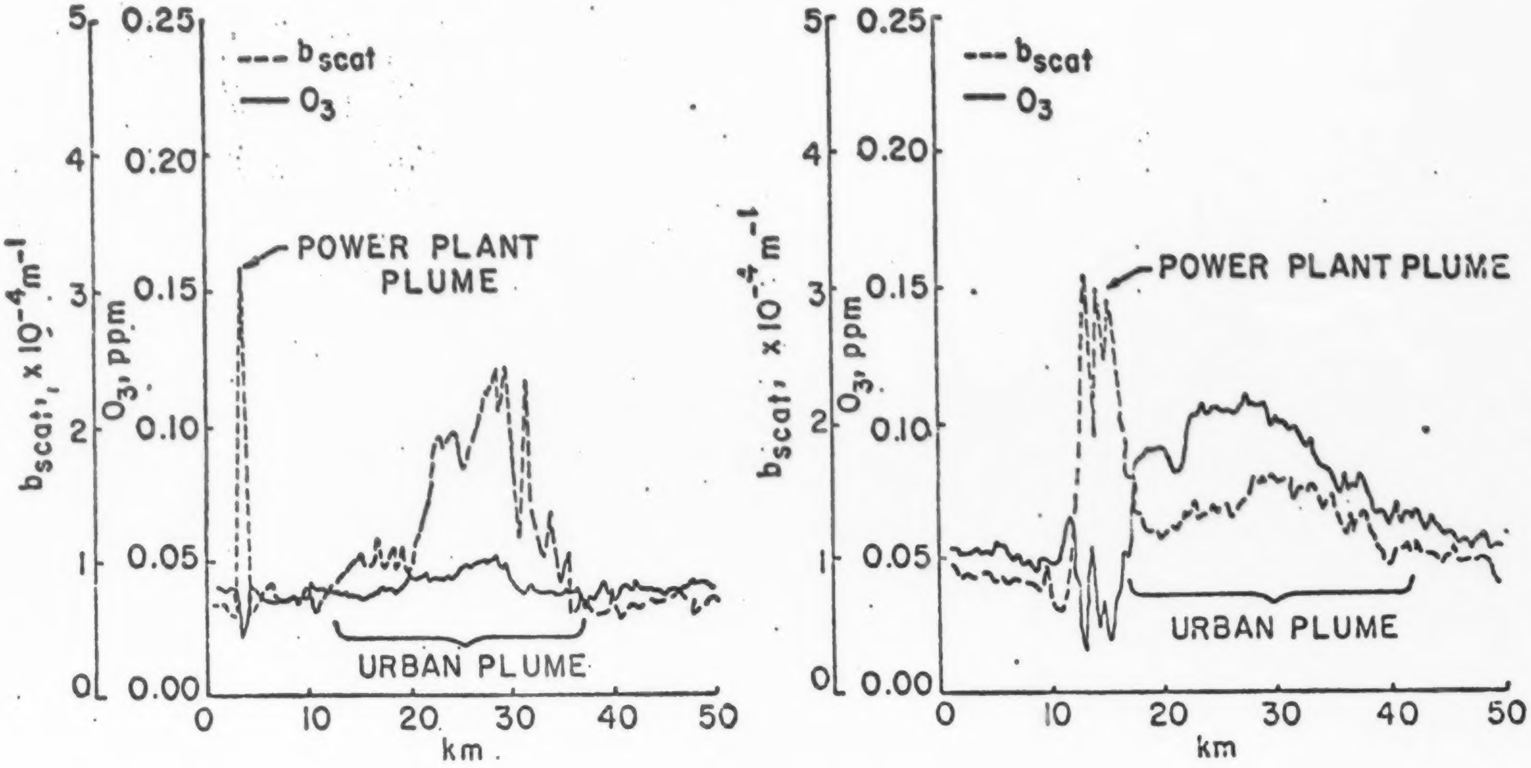

Figure 4-24. Plume measurements on September 6, 1973. Left, traverse at 750 m above mean sea level (msl) 35 km downwind (SW) of Arch-St. Louis, Mo., 11:17-11:37 a.m. Right, traverse at 750 m msl 46 km downwind (SW) of Arch-St. Louis, Mo., 3:30-3:49 p.m. (Reprinted with permission from Blumenthal and White.[35])

is that the Connecticut work traced geographic movement of increased ozone, whereas the New York paper showed temporal variations in urban and rural areas.

Sticksel[37] discussed vertical profile measurements of ozone in the stratosphere and the troposphere over the last several years. Transient ozone maximums in the troposphere are illustrated and explained by three possible mechanisms: a channel-like region conducted ozone from the stratosphere into the troposphere; ozone-laden air descended from the stratosphere and was compressed as it subsided; and ozone-rich layers leaked through the break between the polar and middle tropopauses by differential advection. Surface variations of ozone soundings were mostly attributed to anthropogenic pollution; however, relatively thick high-altitude layers are held out as a potential natural source of high surface ozone concentrations. Sticksel concluded that further investigation was needed to ascertain whether the stratosphere can play a significant role in raising nonurban ozone concentrations.

Johnston[38] has pointed out possibilities of significant transport and transformation of oxidant precursors from the Los Angeles or San Francisco metropolitan air quality control regions to the central valley of California. Emission rates per unit area from sources in Los Angeles County and the Los Angeles metropolitan AQCR are approximately 10-20 times the national average for photochemically active pollutants. The emission rates per unit area in the California central valley are about the national average values for hydrocarbon and carbon monoxide, but only half the national average for NO_x. Despite the much lower emission rates in the central valley, compared with Los Angeles, the valley's ambient concentrations of carbon monoxide, NO_x, and oxidant are half those in Los Angeles. Johnston suggested that a combination of urban-rural transport and confinement without substantial ventilation is responsible for the ambient pollutant concentrations, which are relatively high, compared with emission rates per unit area.

In considering the more general case of ozone in nonurban locations, Johnston considered the problem of downward transport of ozone from the stratosphere, which contains ozone at a peak value of about 10 ppm. He cited Fabian and Pruchniewicz's[39] measurements of ozone at 19 nonurban sites in Europe and Africa--from Tromso, Norway, to Hermanus, South Africa--in 1970-1972. The 19-station network in Europe and Africa averaged approximately 0.022 ppm in the summer. However, some of the central European areas occasionally had higher values.[41] In another survey, a 12-site network was operated from 1963 to 1964 between Thule, Greenland, and Balboa, Canal Zone.[40] Profiles were measured at intervals from ground level to about 30 km. Table 4-8 shows the number of ozone profiles that were made at 0-1 km and the number of ground-level ozone readings that equaled or exceeded 0.08 ppm. Note that the average of the 835 values corresponds closely to the summer values reported from the European-African network. Table 4-9 details the seven readings that equaled or exceeded 0.08 ppm. Five of them occurred at the Bedford, Massachusetts, station.

Johnston argued that, if ozone were formed in the stratosphere and downward transport occurred, there would be a positive concentration gradient extending from 0.5 km to 5 km in altitude. Most of the cases in Table 4-9 obey this situation; however, for the seven high-ozone cases in Table 4-9, the reverse is true. This seems to indicate that the occurrence of ground ozone concentration exceeding 0.08 ppm is characterized by formation reactions near the ground, which suggests that stratospheric sources are not responsible for these cases.

Table 4-8

Ozone Concentrations at Ground Level at 12 Widely Spaced Stations in the Northern Hemisphere, 1963-1964[a]

Station Location	Latitude, degrees	No. cases	Ozone mole fraction, ppm Min.	Ozone mole fraction, ppm Max.	Ozone mole fraction, ppm Ave.	No. Cases at or Above 0.080 ppm
Thule, Greenland	76.5	50	0.010	0.050	0.022	0
Fairbanks, Alaska	64.8	58	0.010	0.050	0.024	0
Churchill, Canada	58.8	67	0.010	0.060	0.026	0
Goose Bay, Labrador	53.3	71	0.010	0.060	0.021	0
Seattle, Washington	47.4	83	0.010	0.100	0.029	1
Madison, Wisconsin	43.1	29	0.010	0.060	0.031	0
Bedford, Mass.	42.5	124	0.010	0.110	0.031	5
Fort Collins, Colo.	40.6	93	0.010	0.050	0.023	0
Alberquerque, N.M.	35.0	102	0.005	0.060	0.026	0
Tallahassee, Fla.	30.4	73	0.005	0.080	0.035	1
Grand Turk, West Ind.	21.5	31	0.010	0.040	0.019	0
Panama, Canal Zone	9.0	54	0.010	0.050	0.017	0
Total		835	5	110	26	7

---

[a] Derived from Hering and Borden.[40]

Table 4-9

Ozone Concentrations (1963-1964) Equal to or Greater than 0.080 ppm at Ground Level (0 - 1 km)[a]

Station Location	Date	Ozone Mole Fraction, ppm	
		0 km	5 km
Bedford, Mass.	June 26, 1963	0.100	0.075
	July 3, 1963	0.080	0.075
	Jan. 20, 1964	0.100	0.065
	July 15, 1964	0.090	0.060
	Aug. 26, 1964	0.110	0.040
Tallahassee, Fla.	Sept. 11, 1963	0.080	0.045
Seattle, Wash.	April 17, 1964	0.100	0.090

---

[a] Derived from Hering and Borden.[40]

Evidently, the high nonurban ozone concentrations observed in 1971-1973 in the continental United States were not of natural origin. This conclusion is supported by comparisons of the data from the 1963-1964 North American study and those from the 1970-1972 European-African study. Because increased concentrations were not traceable to natural processes, anthropogenic sources may be necessary to explain the concentrations of ozone currently observed in the United States. Inhibition of the photochemical smog reaction in the atmosphere by increased NO_x emission could delay the oxidant formation until air parcels move out of urban regions. (The early portion of the vehicle emission control plan had increased NO_x emission, but decreased hydrocarbon and carbon monoxide emission.) Similarly, hydrocarbon substances in the lower paraffin series that are relatively abundant may be reactive over long periods and behave synergistically with other hydrocarbons. The high ozone values in nonurban locations may well result from these processes.

Nonurban oxidant measurements in Ohio were reported by Neligan and Angus.[42] Concentrations of 0.18 and 0.12 ppm were reported for rural sites in Wilmington and McConnelsville, respectively. At the same time, urban sites had similar concentrations. However, the nonurban sites violated the ambient air quality standard more frequently than the urban sites. Trajectory analysis showed that ozone concentrations of 0.04 - 0.06 ppm were found in air masses that had not passed over anthropogenic hydrocarbon sources. These may have been examples of naturally occurring oxidant. Airborne hydrocarbon bag samples were obtained over 6-min periods, and ozone was also measured. At 4,000 ft (1,200 m) above mean sea level (msl), ozone concentrations exceeding 0.20 ppm were observed over northern Ohio and Pennsylvania. Wind was predominantly out of the Southeast. Forty-eight-hour reverse trajectories (apparently based on surface winds) showed that a developing high-pressure system carried air from central New York State and seaboard metropolitan areas into the test region. The correspondence of locations with high ozone concentration and locations with high acetylene, carbon monoxide, and chlorofluoromethanes ("freons") concentrations suggests anthropogenic emission that leads to increased ozone concentrations. Early in the morning, the rural ozone concentration is at a maximum. Profiles at 7:00-9:00 a.m. show increased ozone in nonurban areas at altitudes of several thousand feet and relatively low concentrations at the surface. Daytime profiles show increases in ozone at the surface, with the late afternoon concentrations exceeding the midday concentrations.

Deep mixing of stratospheric ozone can occur during episodes of frontal passage and jet stream interaction. The mechanism for this transfer is the downward advection of air parcels rich in ozone and unaffected by removal processes until they reach the ground. The meteorologic conditions during these events are totally different from those attending high-oxidant episodes over extensive nonurban areas. Therefore, the invocation of stratospheric transport for high nonurban ozone concentrations cannot explain the long-term increases in ozone observed in the studies described above.

INDOOR VERSUS OUTDOOR OXIDANT CONCENTRATIONS

An important aspect of the relationship of indoor to outdoor oxidant concentration is the scavenging of the oxidant by surfaces, e.g., in ventilating systems and in indoor areas.

Ozone decay was measured in an office, a home, and several metal test facilities.[43] Measurements were carried out with a Mast ozone meter and an MEC chemiluminescence ozone detector. The latter was calibrated with a stable ozone source and the EPA neutral buffered potassium iodide procedure. (It was noted over a wide range of concentrations that the MEC meter measurements were consistently higher than those of the Mast meter by a factor of 1.3. That this is essentially identical with the findings of the DeMore committee[2] is interesting.) Ozone generated by a positive corona ionizer was introduced into the test facilities. Ozone decay in a metal-walled room was found to be first-order, with the rate constant highly dependent on the preconditioning of the metal walls with respect to ozone exposure. An activated-carbon filter in the air cleaner for the room markedly increased the rate of decay of ozone. Increases in ambient humidity or temperature also markedly increased the rate of ozone decay. Decay rates in the bedroom and office environment were much greater than those in rooms with aluminum or stainless-steel walls.

During a series of smoggy days in Los Angeles, indoor concentrations of ozone were measured to study the phase relationship of indoor to outdoor ozone buildup.[44] The general mechanism of ozone decay within buildings was investigated with a Dasibi ozone instrument. Various air filters were evaluated with respect to capacity for removing ozone. A computational model was suggested for correlating indoor and outdoor concentrations of ozone as a function of time. Buildups of ozone within buildings lagged behind ambient outdoor buildups by 3 or 4 h, and the maximums indoors were not as high as those outdoors. For example, a small number of measurements suggest that concentrations in private residences reach only about 70% of the peaks attained outside. Sabersky et al.[44] constructed a table of ozone decomposition rates on several common materials. Activated-charcoal and Purafill filters performed better in their tests than fiberglass filters. Approximately 95% of the ozone was removed by the activated charcoal under a wide range of flow conditions. A differential equation model was proposed to calculate concentrations-time relationships for indoor ozone concentration. First-order reactions with empirical constants were assumed, and the predicted ozone concentration patterns were similar to those based on measurement.

A ventilation model for relating indoor to outdoor pollutant concentration was proposed on the basis of an extension of earlier work by these authors.[45] When the outdoor pollutant concentrations change slowly, compared with the indoor changes, a rather simple equation can be used to relate indoor to outdoor concentrations. Further findings of the model study suggest that reductions in indoor concentrations down to 20% of the outdoor concentrations is feasible. Such a program would limit the number of days on which a threshold value of 0.1 ppm is exceeded to 4 or 5 per year, instead of the typical 200 or more days/year for outdoor concentrations. The model was tested with the assumption that the air flow in a building can be approximated by a well-stirred chemical reactor, which is influenced by constant sources and first-order reactions.[46] Monitoring measurements were taken for a laboratory building at the California Institute of Technology to test the model. For a series of locations within the building, the model predicted a good upper-bound curve for the observed indoor pollutant concentrations.

It appeared that ozone concentrations were lower in rooms with excess furniture, books, and papers than in rooms that had concrete floors and contained few books or papers.

The use of ozonizers for deodorizing indoor air has been discussed and evaluated with respect to potential health hazards.[47] In a normal 40-m^3 room, an ozone concentration of 0.1 ppm is established after 3½ h of operation of one of these devices. Evidence on health effects was cited to support the conclusion that inhalation of the quantities of ozone produced by these air conditioners should be avoided and that certainly no beneficial effects should be attributed to ozone inhalation.

PERIODIC TEMPORAL PATTERNS OF OXIDANT CONCENTRATION

Although the previous discussion on spatial differences in ozone contained some references to time dependence, this discussion will explore periodic time dependence further. Specifically, diurnal and seasonal variations will be explored here, with data on various cities in the United States.

The diurnal variations in mean hourly average oxidant concentration are illustrated in Figures 4-25 and 4-26. Several factors influence the shapes of these curves. The primary influence is that of sunlight intensity, inasmuch as photons in the ultraviolet are responsible for the primary photochemical process that leads to ozone formation. Note that the St. Louis curve for June 1966 is broader than that for Los Angeles in August. This is explained by differences in sunlight intensity distribution throughout the day.

Another factor in the curve shapes is the relative proximity of sources of nitric oxide, which reacts with ozone locally and suppresses it. Figure 4-19 shows how the diurnal variations are larger in a city where nitric oxide

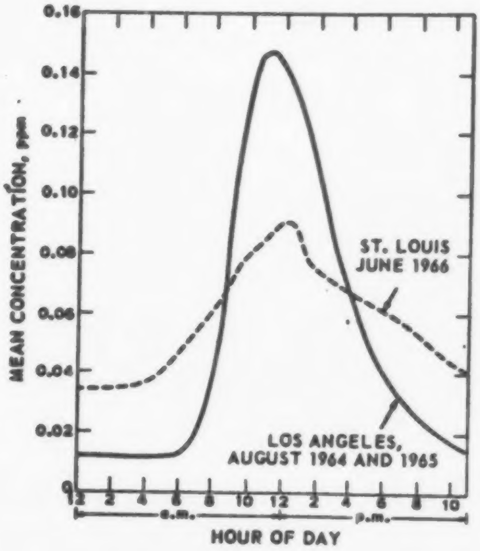

Figure 4-25. Diurnal variation in mean hourly average oxidant concentration in Los Angeles and St. Louis. (Reprinted from U.S. DHEW.[1])

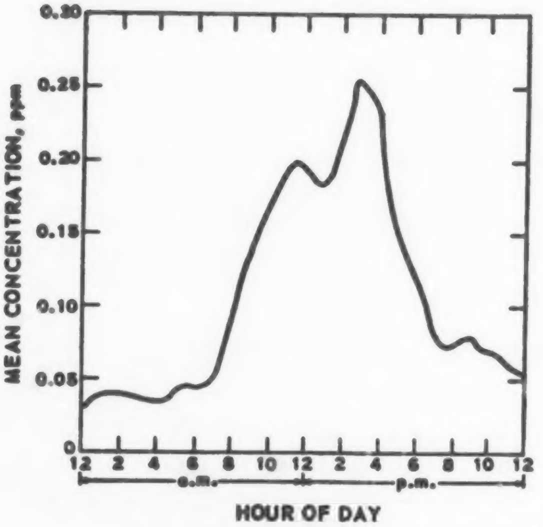

Figure 4-26. Diurnal variation in mean hourly average oxidant concentration in Philadelphia, August 6-8, 1966. (Reprinted from U.S. DHEW.[1])

emission dominates than in a rural area, where the ozone is relatively unaffected. This brings us to a third factor influencing the shape of these curves: advective transport. If movement of ozone from another area is dominant in the local photochemical oxidant concentration, then the wind direction and speed have a great influence on the curve shape. Figure 4-27 shows that, in a central urban area like downtown Los Angeles, the ozone pulse shape is relatively symmetrical about the middle of the day, because of the dominance of local production. In outlying areas, however, such as Azusa and Riverside, the pulse is skewed to the later hours of the afternoon, because of the greater role of transport to the area. Riverside shows this most decidedly, with its own locally produced ozone rising around 8 a.m. and a large secondary peak at 4 p.m., presumably the result of advection from areas to the west. Palm Springs peaks after 8 p.m.

Monthly patterns that show the seasonal variation in oxidant concentration for three cities are presented in Figures 4-28 and 4-29. Again, the combination of availability of sunlight and degree of ventilation governs the shape of these curves. Los Angeles is subject to high late-season oxidant production, because the late spring and early summer months are heavily affected by stratus, which obscures the sunlight. Denver, however, has a more symmetrical seasonal distribution that follows the sunlight pattern. Phoenix has relatively lower oxidant peaks in July, August, and September, because of the dominance of convectively driven mixing, which counteracts the affect of the higher solar intensity.

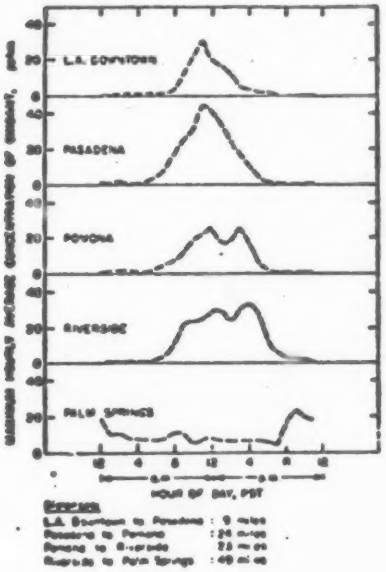

Figure 4-27. Diurnal variation in mean 1-h average oxidant concentration at selected California sites, July 25, 1973. (Reprinted with permission from Pitts et al.[48])

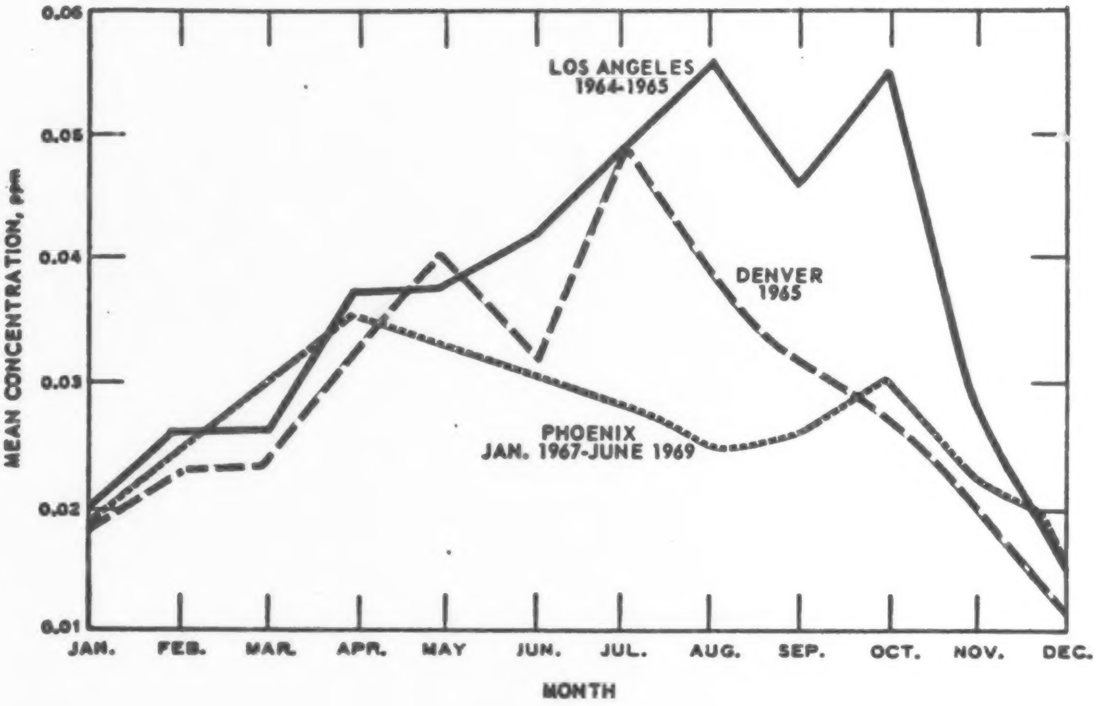

Figure 4-28. Monthly variation in mean hourly oxidant concentration in three selected cities. (Reprinted from U.S. DHEW.[1])

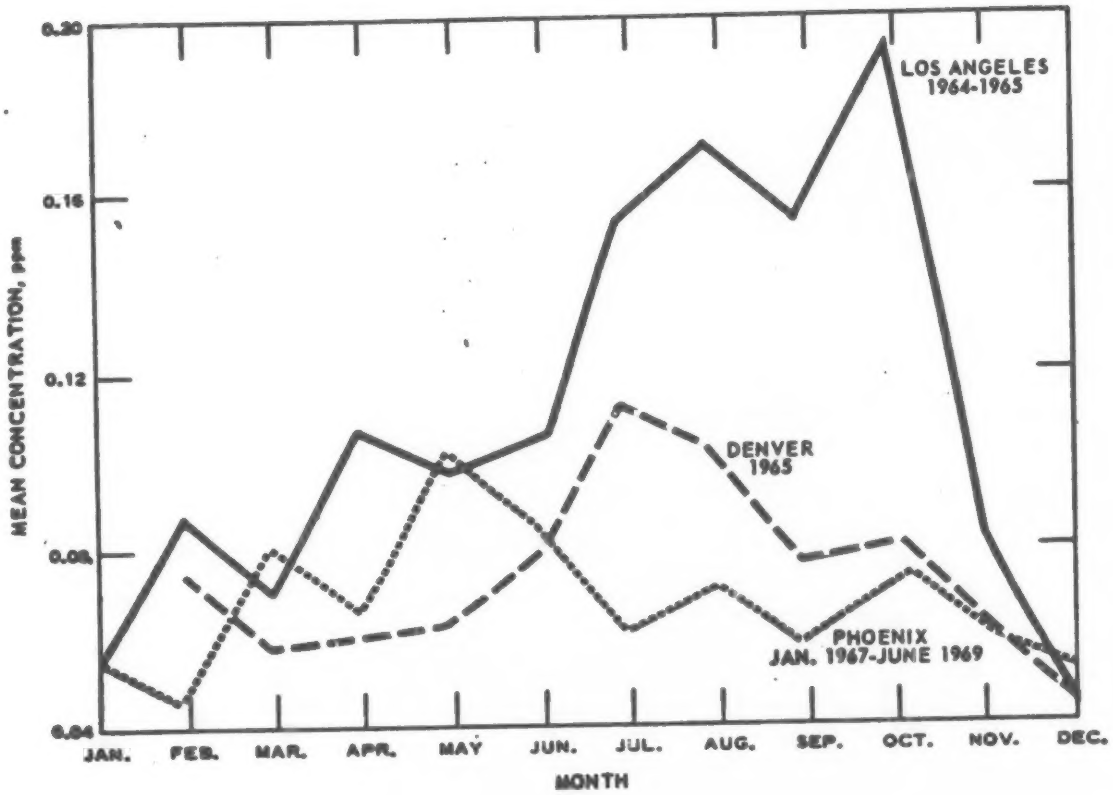

Figure 4-29. Monthly variation in mean daily maximal 1-h average oxidant concentration in three selected cities. (Reprinted from U.S. DhEW.[1])

LONG-TERM TRENDS OF AMBIENT CONCENTRATIONS

The limited sample of photochemical oxidant and ozone data precludes extensive trend analysis for all but a few regions in the United States. Some such analysis has been done by the California Air Resources Board.[49] Its analysis can be applied on a temporal basis to any given location; however, spatial intercomparisons are subject to the problems pointed out by Pitts.[31]

Both annual average and 3-year moving average values of oxidant concentration were plotted in a CARB report by Kinosian and Duckworth[49] for several stations in the southern coastal air basin during 1963-1972. These are shown in Figures 4-30, 4-31, and 4-32. The 3-year moving average is used to smooth the data. Comparing the three cities--Los Angeles, Azusa, and Riverside--they found a distinct downtrend in the 3-year moving average for Los Angeles, a nearly level trend for Azusa, and a slight uptrend for Riverside. It should be pointed out that the variability due to weather is not completely removed by the 3-year averaging process. Thus, the report applies an adjustment factor for temperature aloft and concludes that low oxidant concentrations in 1968 were due to the weather, whereas the lower ones observed in 1970 and 1971 were not.

A report by the National Academy of Sciences Coordinating Committee on Air Quality Studies to the U.S. Senate[50] concluded that "available air monitoring data do not allow conclusions to be drawn about photochemical oxidant trends on a nation-wide basis." This report relied heavily on California data to illustrate trends, because so much information was available for that region. Maximal 1-h concentrations in the New Jersey cities of Bayonne and Newark were compared for 4-year periods between 1966

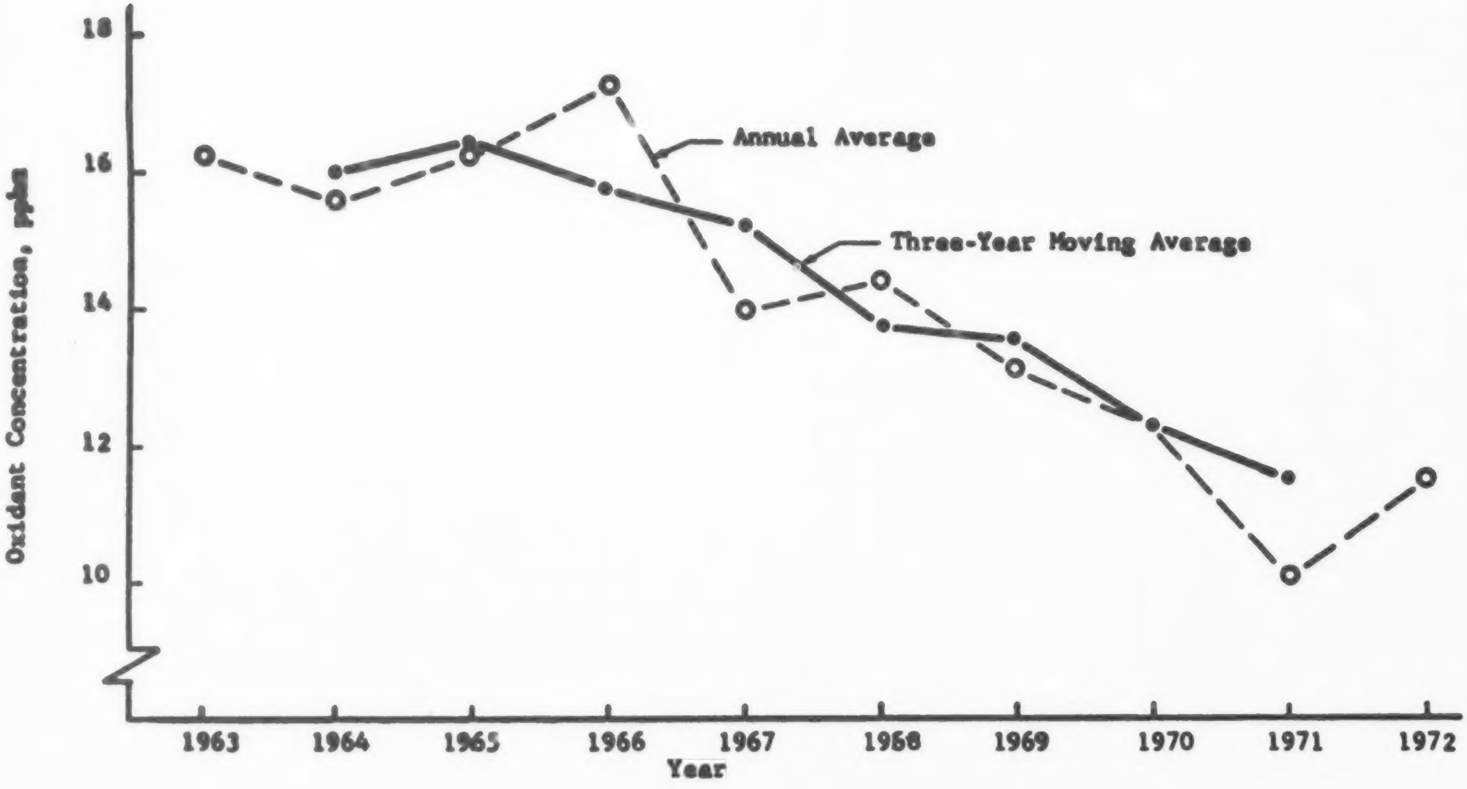

Figure 4-30. Oxidant trends in Los Angeles, 1963-1972. Annual and 3-year moving averages of daily maximal 1-h concentrations for July, August, and September. (Reprinted with permission from Kinosian and Duckworth.[49])

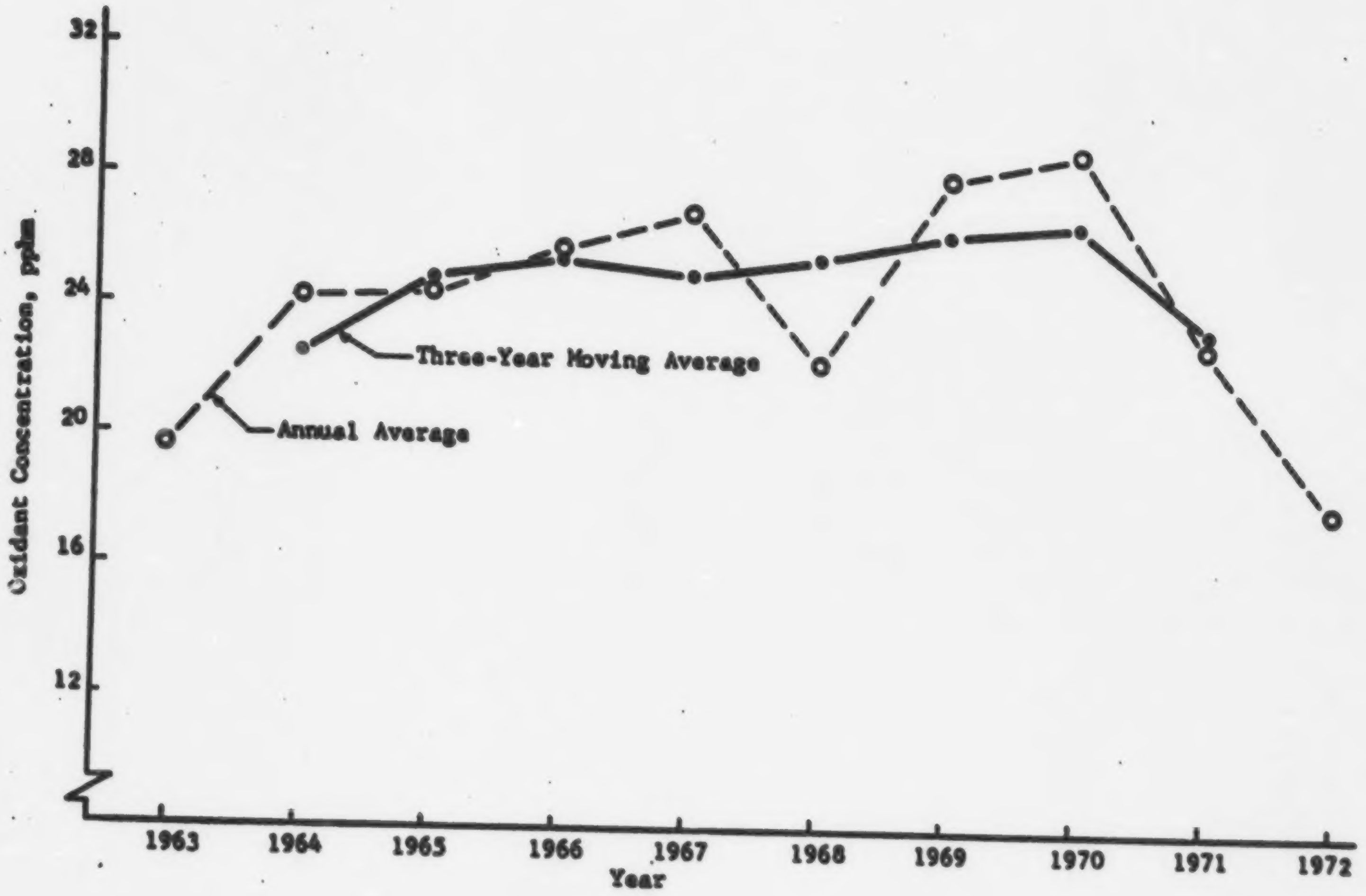

Figure 4-31. Oxidant trends in Azusa, California, 1963-1972. Annual and 3-year moving averages of daily maximal 1-h concentrations for July, August, and September. (Reprinted with permission from Kinosian and Duckworth.[49])

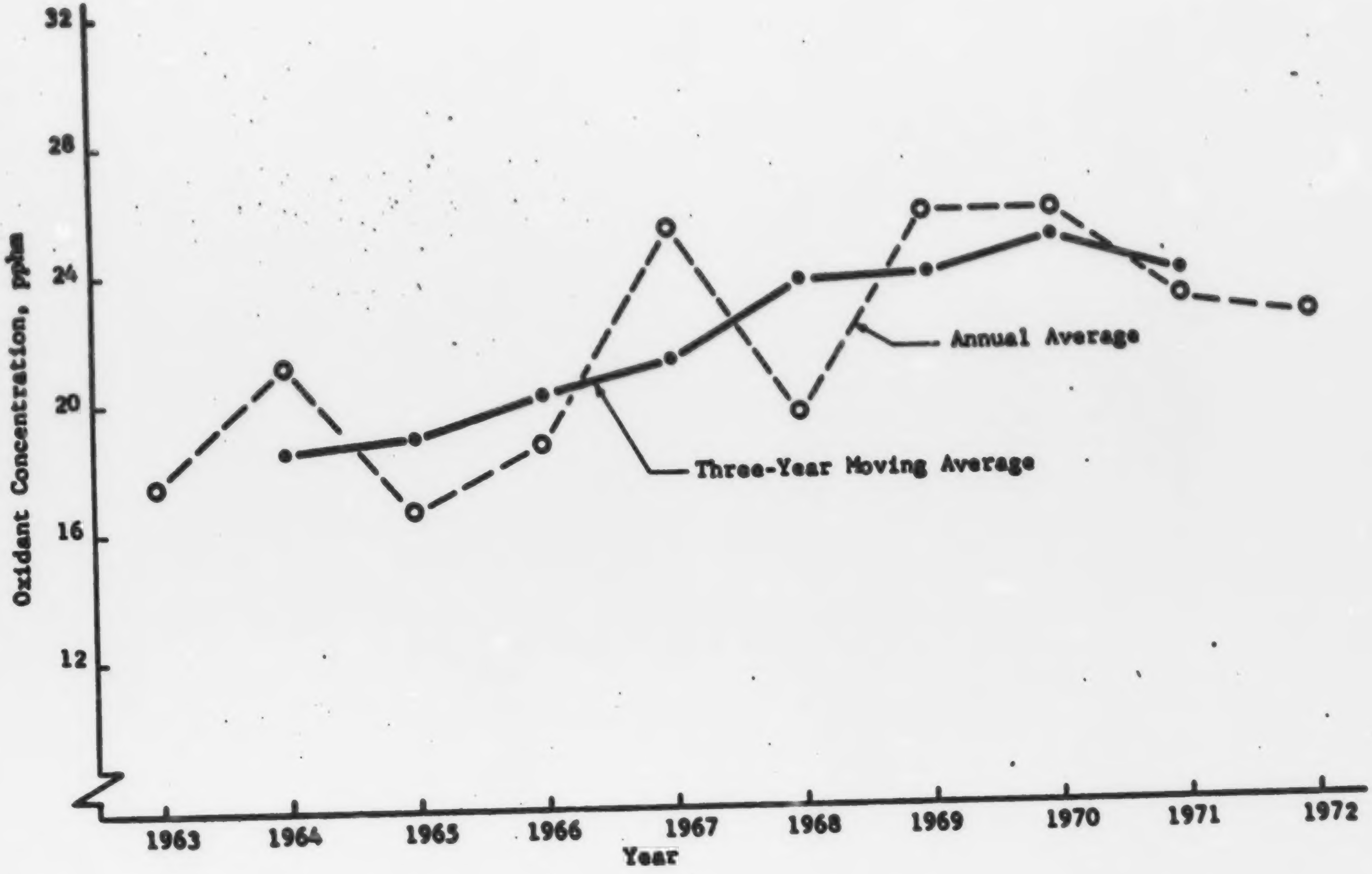

Figure 4-32. Oxidant trends in Riverside, California, 1963-1972. Annual and 3-year moving averages of daily maximal 1-h concentrations for July, August, and September. (Reprinted with permission from Kinosian and Duckworth.[49])

and 1973. These two cities exhibit 24% and 46% decreases, respectively. Emphasis was placed on differences in calibration procedure in various jurisdictions of air pollution control agencies. It is indicated that trend analysis for each station is still valid, despite the differences in calibration procedure. But values from different places must be compared cautiously.

CAMP data presented in Table 4-10 show a generally decreasing trend in total oxidant concentration as measured by neutral buffered potassium iodide. The southern coastal air basin in California is also known as the metropolitan Los Angeles AQCR. The map in Figure 4-33 shows the location of air pollution monitoring stations. However, the boundaries shown in that figure include more than the AQCR referred to. Of Santa Barbara County, only the southern strip bounded on the North by the coastal mountain range is included in that basin; and of San Bernardino and Riverside Counties, only the partially urbanized areas in the western portions are included. Figure 4-34 shows the oxidant trends in the southern coastal air basin. Two selection techniques were used for stratifying the air monitoring data.[51] One is based on the "rule 57" day, which is defined as a day having an inversion base at 4:00 a.m. lower than 1,500 ft, a maximal mixing height below 3,500 ft, and an average wind speed between 6:00 a.m. and noon below 5 mph. Another selection technique stratifies the data for an inversion base less than 3,500 ft. The number of days in each year that exceed an oxidant concentration of 0.25 ppm as defined by these two systems shows a distinct downward trend in the graph.

As a result of recent control activities, the downtown Los Angeles station has experienced successively lower oxidant concentrations,[49,52] as shown in Figure 4-30. It should be noted that Riverside and San Bernardino

Table 4-10

Total Oxidant Concentrations Measured at CAMP Stations by Neutral Buffered Potassium Iodide Method[a]

Station Location	Average of 99th Percentile, $\mu g/m^3$		Change, %	Average of Annual 2nd Highest Value, $\mu g/m^3$		Change, %
	1962-1966	1967-1971		1962-1966	1967-1971	
Chicago	128.1	166	+30	263	299	+14
Cincinnati	192	177	- 8	333	287	-14
Denver	—	—	—	—	—	—
Philadelphia	212	270	-20	459	299	-35
St. Louis	—	—	—	—	—	—
CAMP averages	177	171	- 3	352	295	-16

---

[a] Derived from the National Academy of Sciences Coordinating Committee on Air Quality Studies to the U.S. Senate.[50]

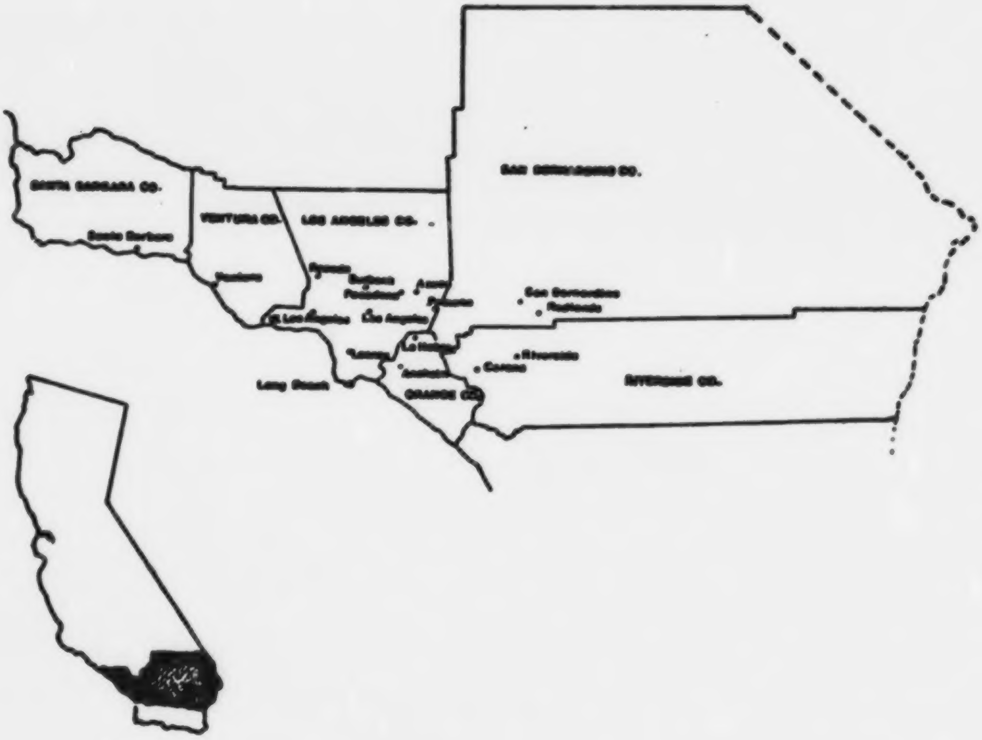
SANTA BARBARA CO.
VENTURA CO.
LOS ANGELES CO.
SAN BERNARDINO CO.
Santa Barbara
Los Angeles
San Bernardino
Redlands
Riverside
Corona
Anaheim
Long Beach
ORANGE CO.
RIVERSIDE CO.

Figure 4-33. Air pollution monitoring network for southern coastal air basin, California. (Reprinted with permission from the National Academy of Sciences Coordinating Committee on Air Quality Studies to the U.S. Senate.[50])

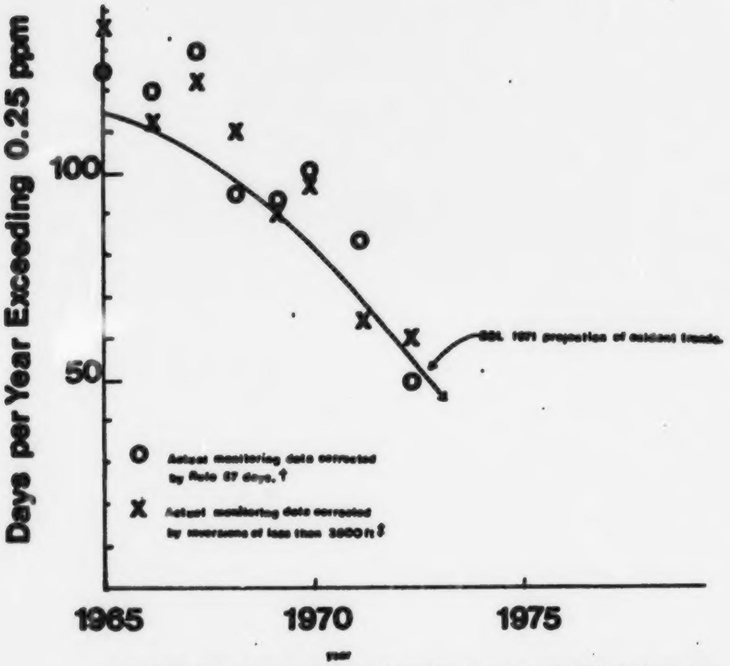

† A rule 57 day is one on which the inversion base at 4 AM (PST) is lower than 1500 feet, the maximum mixing height is not above 3500 feet and the average surface wind speed between 600 AM and 12 noon (PST) does not exceed 5 MPH.

‡ This correction has been adopted by the California Air Resources Board in an attempt to remove this meteorological variability from the analyzing oxidant trends.

Figure 4-34. Southern coastal air basin oxidant trends. (Reprinted with permission from Heitner and Krier.[51])

Counties show great fluctuations in annual average oxidant concentrations, with Riverside actually having an increase. Again, it should be emphasized that differences in calibration methods from place to place will not affect the temporal trend analysis presented here.

It has been argued that the smog reaction has been inhibited by the higher NO_x:hydrocarbon ratios brought about by early emission control systems, thereby increasing concentrations at downwind locations. It has also been argued that increased NO_x concentrations could contribute to the high non-urban values by interacting over long periods with natural methane or terpene to produce ozone.[53,54] It is probable that nitric oxide emission reacts locally to decrease preexisting atmospheric ozone; however, there is little doubt that increased NO_x over a long-time (long-range) trajectory will ultimately make more oxidant, if more hydrocarbon is introduced. In summary, added nitric oxide inhibits ozone locally, but can enhance it regionally.

Altshuller[49] evaluated oxidant results from throughout the United States. CAMP concentration data were analyzed for 8 or more years of measurements available from the period 1964 - 1973. Tables 4-11 and 4-12 summarize the measurements. Data from 2 years were rejected, because the method of eliminating sulfur dioxide interference was not in operation. Interference from nitrogen oxides was removed from the data by subtracting 20% of the combined nitric oxide and nitrogen dioxide concentrations from the total oxidant reading, because all the data used were from the colorimetric potassium iodide method of measurement. Where comparisons were available, colorimetry oxidant data averaged 0.015 ppm higher than the chemiluminescence measurements. It was observed that this difference should be expected, because of possible additional interferences from organic peroxides or peroxyacylnitrates.

Table 4-11

Summary of Total Oxidant Concentrations Recorded at CAMP Sites, 1964-1972[a]

City	Year	No. Days of Valid Data	No. Days with at Least One Hourly Average Equal to or Exceeding 0.05 ppm	0.10 ppm	0.15 ppm	Maximal Hourly Average Oxidant Concentration, ppm
Chicago	1964	254	149	15	0	0.13
	1965	275	120	9	0	0.13
	1966	235	52	6	3	0.19
	1967	255	113	16	1	0.16
	1968	211	113	17	5	0.18
	1969	24	15	0	0	0.07
	1970	200	97	4	3	0.20
	1971	276	90	14	2	1.17
	1972	312	79	4	0	0.14
Cincinnati	1964	303	137	36	5	0.26
	1965	310	182	19	5	0.17
	1966	208	54	1	0	0.10
	1967	228	122	24	1	0.20
	1968	86	65	7	0	0.14
	1969	48	23	5	1	0.16
	1970	7	1	0	0	0.08
	1971	221	96	10	1	0.16
	1972	257	69	3	1	0.15
Denver	1965	285	226	51	14	0.25
	1966	298	187	46	9	0.19
	1967	166	76	12	4	0.21
	1968	151	149	28	5	0.26
	1969	108	70	2	0	0.13
	1970	141	69	9	1	0.18
	1971	184	63	5	1	0.20
	1972	209	94	26	1	0.18

Table 4-11 Cont.

Summary of Total Oxidant Concentrations Recorded at CAMP Sites, 1964-1972[a]

City	Year	No. Days of Valid Data	No. Days with at Least One Hourly Average Equal to or Exceeding			Maximal Hourly Average Oxidant Concentration, ppm
			0.05 ppm	0.10 ppm	0.15 ppm	
Philadelphia	1964	269	124	37	9	0.20
	1965	266	109	23	4	0.33
	1966	315	145	52	19	0.52
	1967	282	124	28	3	0.17
	1968	140	88	18	3	0.21
	1969	92	37	3	0	0.11
	1970	112	29	10	0	0.13
	1971	260	47	5	0	0.14
	1972	47	20	10	1	0.15
St. Louis	1964	253	156	26	6	0.26
	1965	329	206	33	8	0.35
	1966	292	174	33	5	0.22
	1967	289	185	38	4	0.20
	1968	163	100	7	2	0.23
	1969	95	47	5	0	0.12
	1970	96	20	0	0	0.08
	1971	294	77	1	0	0.13
	1972	203	77	9	2	0.16
Washington, D.C.[b]	1964	293	163	40	4	0.20
	1965	284	150	25	3	0.21
	1966	325	134	27	2	0.16
	1967	322	137	27	5	0.26
	1968	217	134	40	9	0.25
	1969	71	30	1	0	0.10
	1970	167	95	10	2	0.16
	1971	299	144	17	0	0.13
	1972	179	45	6	0	0.13

---

[a] Derived from Ref. 7.

[b] Site moved to another section of the city at end of 1968.

Table 4-12

Number of Days and Percentage of Days with Corrected Oxidant Concentration over 0.08 ppm at CAMP Sites in 1964-1973[a]

Corrected Oxidant Concentration, ppm	No. or Percentage of Days[b]						
	Chicago	Cincinnati	Denver	Philadelphia	St. Louis	Washington, D.C.	Total
	No.	No.	No.	No.	No.	No.	No.
0.085-0.095	15(2)	75(8)	64(16)	53(14)	92(18)	87(14)	386(72)
0.10-0.12	22(5)	52(5)	70(10)	77(14)	56(9)	95(12)	372(55)
0.125-0.145	7(3)	32(2)	31(1)	26(2)	19(8)	19(4)	134(20)
0.15-0.195	6(1)	7(2)	20(1)	17(3)	6(1)	11(2)	67(10)
0.20-0.245	0	0	6(0)	3(2)	3(0)	2(0)	14(2)
0.25-0.295	0	1(0)	0	1(0)	0	0	2(0)
0.30-0.345	0	0	0	1(0)	0	0	1(0)
Total	50(11)	167(17)	191(28)	178(35)	176(36)	214(32)	976(159)
	%	%	%	%	%	%	%
At or above 0.10 ppm	70(82)	55(53)	67(44)	70(60)	48(50)	59(56)	60(55)
At or above 0.125 ppm	26(36)	24(24)	30(7)	27(20)	16(25)	15(18)	22(20)
At or above 0.15 ppm	12(10)	5(12)	14(4)	12(14)	5(3)	6(6)	9(8)
At or above 0.20 ppm	0(0)	1(0)	3(0)	3(0)	2(0)	1(0)	2(0)

---

[a] Derived from Altshuller.[55]

[b] Sundays in parentheses.

The fractions of days with valid oxidant data for May - October and for June - August were tabulated for the CAMP sites for 1964 - 1973. The average percentage over all years and all sites was 60%. Seasonal effects were shown by distributing according to month the days with oxidant concentrations exceeding 0.08 ppm. Sunday oxidant concentrations and comparisons of results by location were also discussed. Annual trends in oxidant concentration for the various sites were represented by plotting the number of days with oxidant concentrations over 0.08 ppm (or the California state standard of 0.10 ppm) for each year at each site (see Figure 4-35 and Table 4-13). It was suggested that the relatively infrequent high oxidant concentrations observed in Chicago were due to a site effect involving the lake breeze ventilation and the high concentration of automobile-generated nitric oxide. The higher frequency of high ozone concentrations in Denver was attributed to Denver's high altitude and attendant increases in ultraviolet intensity. No distinct Sunday oxidant effect was noted with respect to exceeding the 0.08-ppm concentration. Neither precursor concentrations nor favorable reactant ratios should lead one to expect more favorable conditions for oxidant formation on Sundays, according to the paper. However, it was noted that in the Los Angeles basin alert concentrations (0.6 ppm) or near-alert concentrations (0.4 - 0.6 ppm) are never observed on Sundays. Extensive discussion was devoted to the apparent downward shifts in oxidant measurements for central urban areas, in contrast with the nearly constant or rising oxidant concentrations in suburban and rural areas.

The latest Los Angeles County APCD profile gives further insights into the measurement of trends and their interpretation. It uses California's ambient air quality standard of 0.10 ppm oxidant (hourly), instead of the

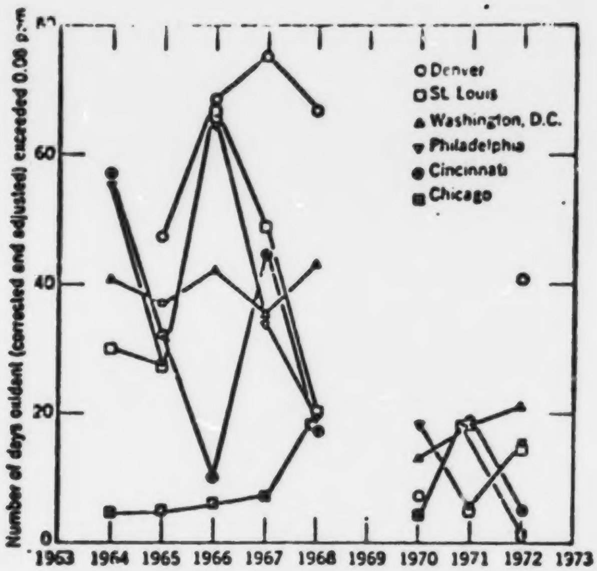

Figure 4-35. Trend in oxidant concentration by year at CAMP sites. (Reprinted with permission from Harrison and Lodge.[57])

Table 4-13

Number of Days on Which State Standard 1-Hour Average of 0.10 ppm for Total Oxidant[a] was Equaled or Exceeded in Los Angeles Basin[b]

	Year																
Month	1957	1958	1959	1960	1961	1962	1963	1964	1965	1966	1967	1968	1969	1970	1971	1972	1973
Jan.	15	26	27	13	23	17	9	9	9	11	10	8	8	5	10	2	0
Feb.	21	21	14	15	22	9	22	16	17	13	22	13	7	11	12	17	1
March	26	15	28	25	18	12	18	12	10	23	18	18	17	19	17	26	3
April	24	25	26	23	22	23	16	15	17	26	14	24	22	19	17	22	12
May	20	30	29	25	24	20	23	22	21	26	22	26	26	26	17	22	26
June	28	30	30	30	29	26	21	27	25	29	24	26	22	27	26	26	25
July	31	31	31	31	31	31	29	31	31	31	31	31	30	31	31	30	31
Aug.	31	31	30	30	30	31	31	30	31	31	31	29	31	31	31	29	29
Sept.	30	29	28	30	25	29	26	30	24	28	28	25	30	29	26	24	27
Oct.	25	29	28	26	22	26	27	27	28	30	31	26	27	24	18	8	24
Nov.	26	27	27	19	22	24	16	10	15	17	20	20	14	17	13	4	7
Dec.	28	28	18	19	15	19	20	3	8	6	8	6	12	2	0	1	0
Total	305	322	316	286	283	267	258	232	236	271	259	252	246	241	218	211	185

---

[a] By potassium iodide method.

[b] Derived from Birakos.[56]

federal standard of 0.08 ppm. Table 4-13 shows the numbers of days on which the state standard for total oxidant (by the potassium iodide method) was equaled or exceeded in the Los Angeles basin (confined here to the county of Los Angeles). From 1957 to 1973, a distinct downtrend in the number of days was observed. On an average over this 17-year period there were 258 days of violation per year. During the last three years tabulated—1971, 1972, and 1973—the numbers were 218, 211, and 185, respectively. This trend is qualified by the observation that climatologic conditions during 1973 were favorable for smog formation, with the lower frequency of inversion and weak winds. It is perhaps more realistic to consider the final 3 years as a group, rather than using 1973 to interpret the trends. Another index that the Los Angeles County APCD uses is the total number of days on which eye irritation was recorded in the Los Angeles basin. This is summarized in Table 4-14. For the same 17-year span, the average number of days characterized by eye irritation is 163. However, during the final 3 years, the numbers were 125, 125, and 124, which seem to correspond to the ozone measurement trend. It is of interest to note the similar statistics (Table 4-15) for violation of the state visibility standard—namely, for one observation, visibility should not be less than 10 miles when the relative humidity is less than 70%. The data in Table 4-15 are reported on the basis of the 1970 state standard through May 1972 and later on the basis of the June 1972 state standard. The average number of days on which the standard was violated over the 12-year period is 328. For the last 3 years of the reporting period, the numbers are 333, 311, and 298. This confirms the improvement trend exhibited in the other two tables.

Table 4-14

Number of Days on Which Eye Irritation was Recorded in Los Angeles Basin[a]

Month	Year 1956	1957	1958	1959	1960	1961	1962	1963	1964	1965	1966	1967	1968	1969	1970	1971	1972	1973
Jan.	12	3	6	11	3	12	10	4	3	2	2	6	2	3	1	8	0	0
Feb.	11	12	6	3	7	12	7	11	7	11	3	6	7	1	4	4	6	0
March	14	11	2	14	19	9	5	8	4	4	18	10	5	9	7	6	15	0
April	8	13	8	18	17	16	19	8	6	15	18	1	7	5	6	7	11	9
May	12	8	20	7	15	8	16	11	13	12	17	11	13	16	12	8	17	18
June	23	17	17	23	24	21	21	13	13	9	22	15	17	12	17	16	17	16
July	23	27	21	28	26	22	28	23	28	24	27	23	27	21	26	23	18	21
Aug.	23	27	31	23	26	28	29	22	22	29	23	26	19	31	26	23	20	23
Sept.	28	25	26	12	21	15	25	19	23	20	20	15	16	24	20	17	15	17
Oct	17	11	21	22	18	19	23	22	21	22	19	23	13	10	11	7	2	17
Nov.	12	10	16	18	14	13	18	7	6	12	6	13	8	4	4	6	4	3
Dec.	16	6	20	9	8	11	13	13	1	4	1	0	0	1	0	0	0	0
Total	199	170	194	188	198	186	214	161	147	164	176	149	134	137	134	125	125	124

---

[a] Derived from Birakos.[56]

Table 4-15

Number of Days on Which State Standard for Visibility was Equaled or Exceeded (Visibility Less than 10 Miles when Relative Humidity is Less than 70%)[a]

Month	Year											
	1962	1963	1964	1965	1966	1967	1968	1969	1970	1971	1972	1973
Jan.	25	29	27	26	26	28	28	24	21	28	26	22
Feb.	18	22	24	24	26	28	26	22	23	24	28	15
March	26	26	24	28	26	29	28	24	27	28	29	16
April	29	21	24	22	30	24	29	28	27	27	27	20
May	25	28	26	31	28	30	30	31	30	28	28	29
June	29	28	29	29	29	28	30	29	30	30	28	28
July	31	31	31	31	31	31	31	31	31	31	28	31
Aug.	31	31	31	31	31	31	30	31	31	31	31	30
Sept.	30	29	30	29	29	30	30	30	29	29	26	30
Oct.	30	30	30	28	31	31	30	28	30	29	24	27
Nov.	29	25	20	19	29	27	27	22	27	29	21	24
Dec.	31	29	21	26	25	26	26	26	26	19	15	26
Total	334	329	317	324	341	343	345	326	332	333	311	298

---

[a] Derived from Birakos.[56]

It is also of interest in interpreting trends to look at the rare event and at the frequency distribution, as well as average values. This can be done by examining the number of ozone alerts called for the series of years under analysis. For a first alert for ozone, the Los Angeles County APCD has set the value at 0.50 ppm. Ninety alerts were declared from the inception of the alert program in 1955 through December 1973. The 1955 - 1972 average is five alerts/year. However, in 1972 and 1973, only one alert was declared each year. The highest number of alerts posted during a single year was 15, in 1955. The highest frequency of alerts occurs during September. January and February have never experienced ozone alerts. Alerts are most frequent on Friday and have never occurred on Sunday.

Frequency distributions of ozone concentrations for Azusa and Goleta, California, are shown in Figures 4-36 and 4-37, respectively. (These curves were prepared by J. R. Martinez of Environmental Research & Technology, Inc.) The Azuse distribution consists of points for 8 years (each taken as an individual sample). The Goleta data are for 1 year only. A year-to-year scatter of approximately ±15% about a mean curve is observed for Azusa; both curvature and slope difference distinguish it from the Goleta distribution. The primary reference standard for the latter followed the CARB procedure; that for Azusa followed the Los Angeles APCD procedure. Although the DeMore et al. report[2] states that zero offsets are suppressed and that direct multiplicative corrections should be applied, one must wonder whether nonlinearities may still emerge from the calibration procedure, in view of the differences in curvature. Another explanation may be that, because of the higher concentrations in Azusa, actual atmospheric nonlinearities occur.

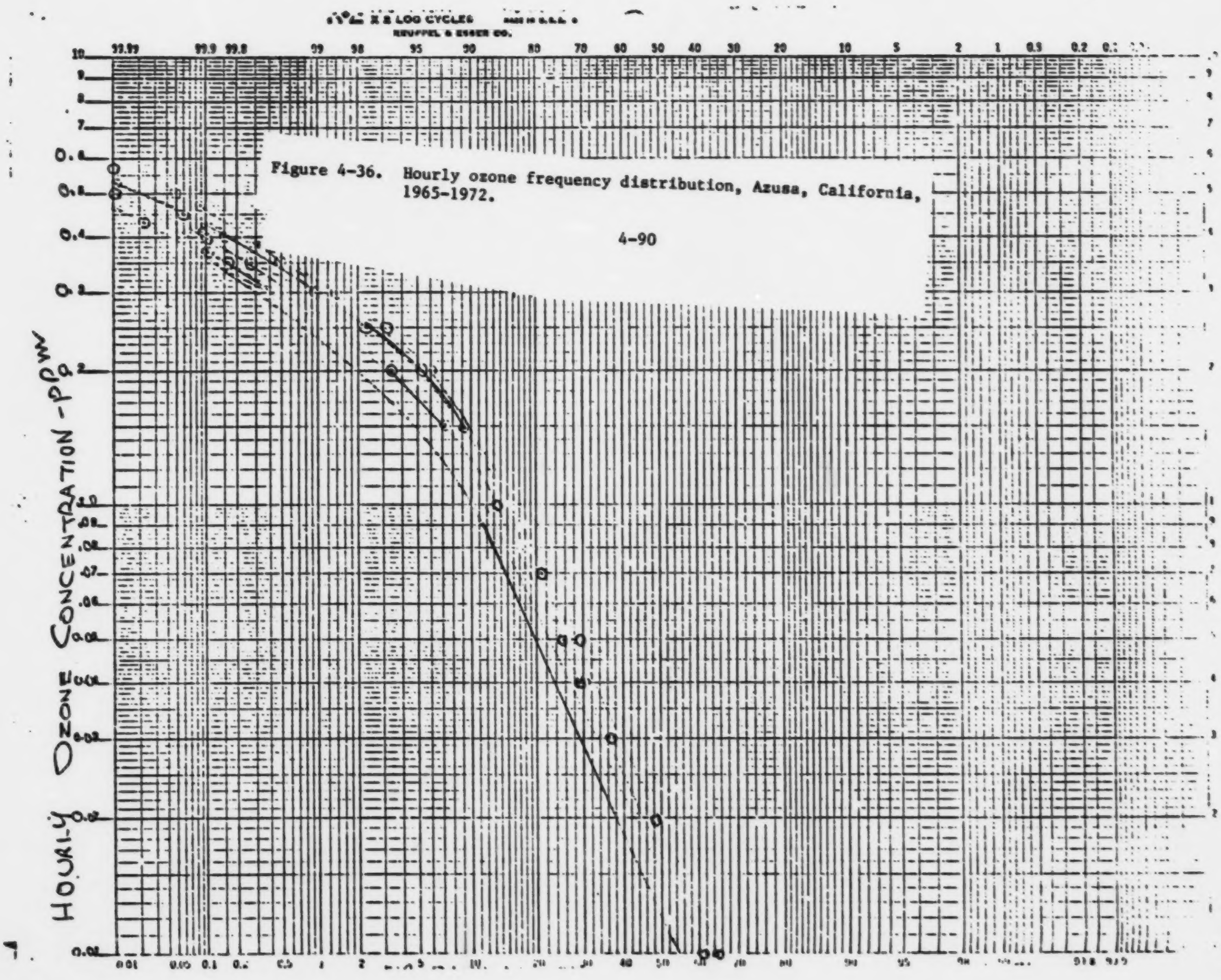

Figure 4-36. Hourly ozone frequency distribution, Azusa, California, 1965-1972.

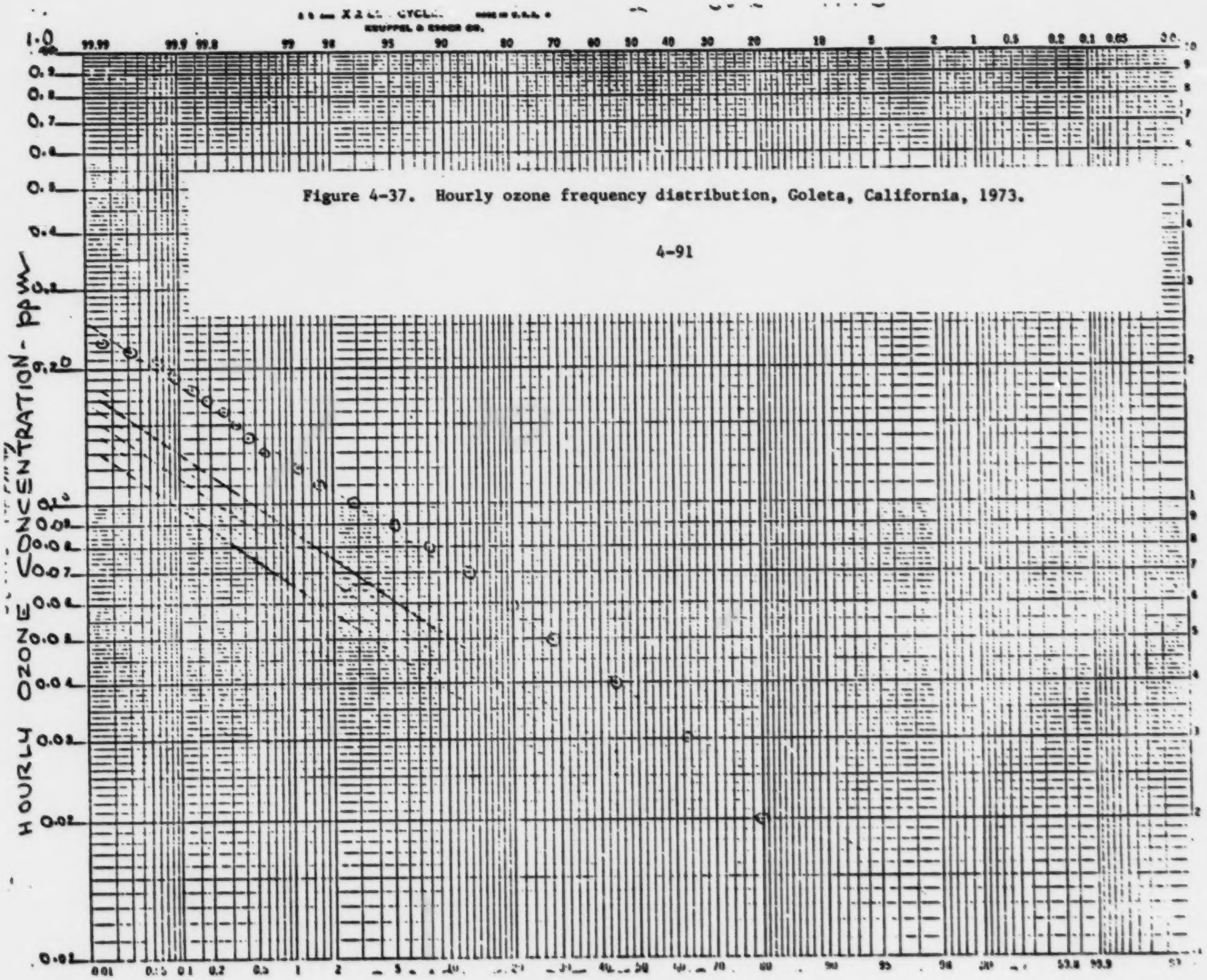

Figure 4-37. Hourly ozone frequency distribution, Goleta, California, 1973.

237

But this will not account for the large slope discrepancy at low concentrations. It should be noted that all Los Angeles APCD distributions qualitatively resemble Azusa's, and that other CARB distributions are like Goleta's.

PHOTOCHEMICAL OXIDANTS OTHER THAN OZONE

As mentioned previously, the scope of photochemical oxidants extends to organic nitrates and other carbonyl compounds. Among the organic nitrates, the one most often cited is peroxyacetylnitrate (PAN). Electron-capture detector techniques applied to the gas chromatograph were used to measure PAN concentrations in Los Angeles late in 1965.[57]

On each of 16 weekdays in September and 19 in October, seven measurements were made. The daily means are plotted in Figure 4-38. Note that the PAN concentrations are considerably below the total oxidant concentrations.

At the University of California at Riverside, the same technique was used beginning in June 1966 to measure PAN. Hourly samples were collected between 7:00 a.m. and 4:00 p.m. Figure 4-39 shows the PAN distribution to exhibit double peaks, which sometimes occur with oxidant concentrations.[1] Note that the relationship between the PAN curve and the oxidant curve in Figure 4-39 is very similar to that in Figure 4-38. Figure 4-40 shows the seasonal variations in PAN concentration and oxidant concentration for portions of 1966 and 1967 at Riverside.

Aldehydes may also be thought of as photochemical oxidants. The definition here becomes a bit hazy, because aldehydes in themselves are photooxidative reactants as well as secondary pollutants that have adverse health effects. Referring to Figure 4-4, we note that aldehyde concentration throughout the day in Rome seems to decay at roughly the same rate as the nitric oxide concentration. It would be expected to track the

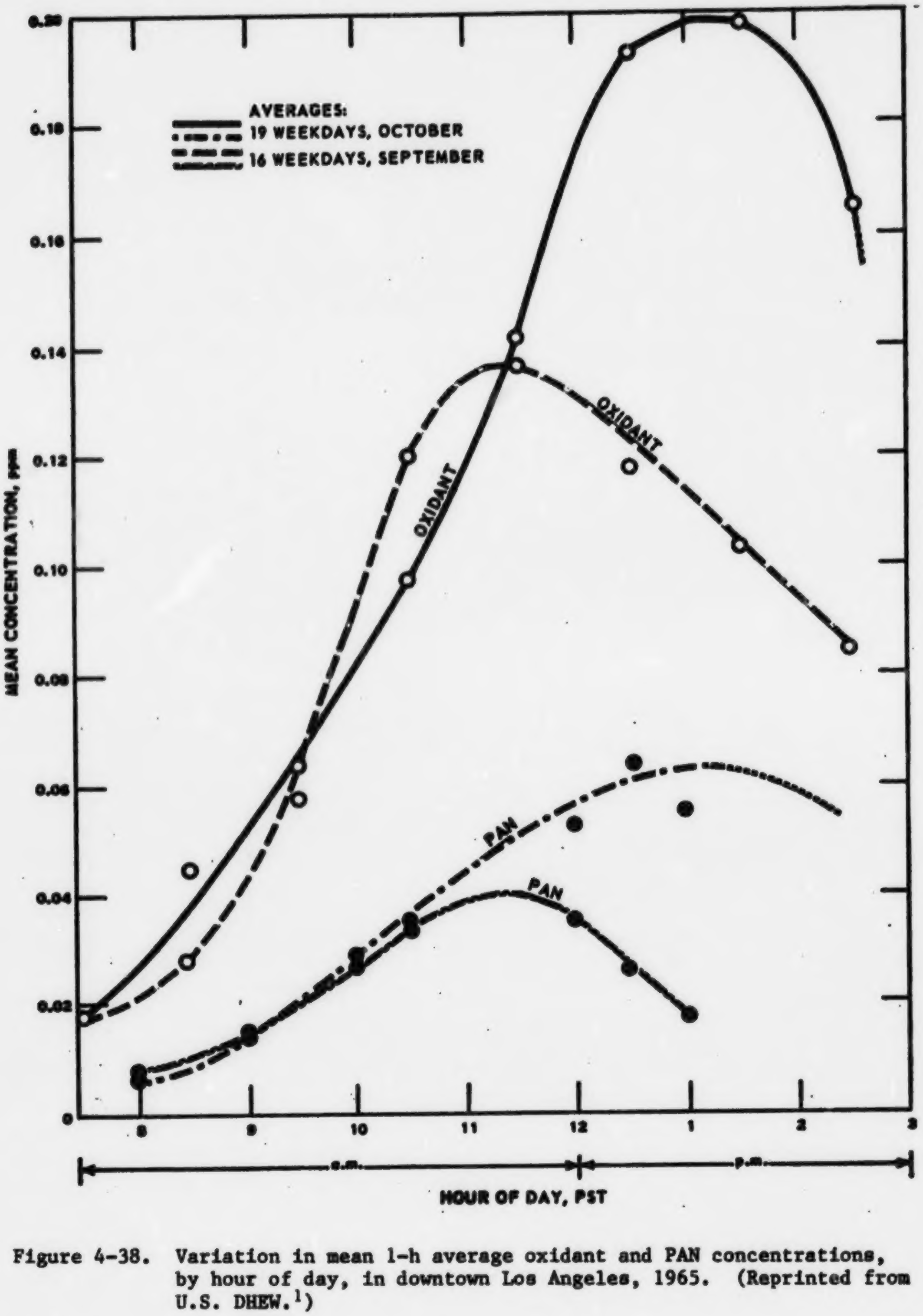

Figure 4-38. Variation in mean 1-h average oxidant and PAN concentrations, by hour of day, in downtown Los Angeles, 1965. (Reprinted from U.S. DHEW.[1])

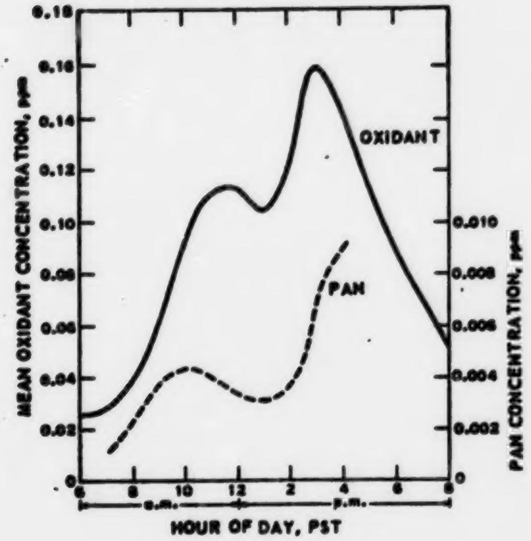

Figure 4-39. Variation in mean 1-h average oxidant and PAN concentrations, by hour of day, at the Air Pollution Research Center, Riverside, California, September 1966. (Reprinted from U.S. DHEW.[1])

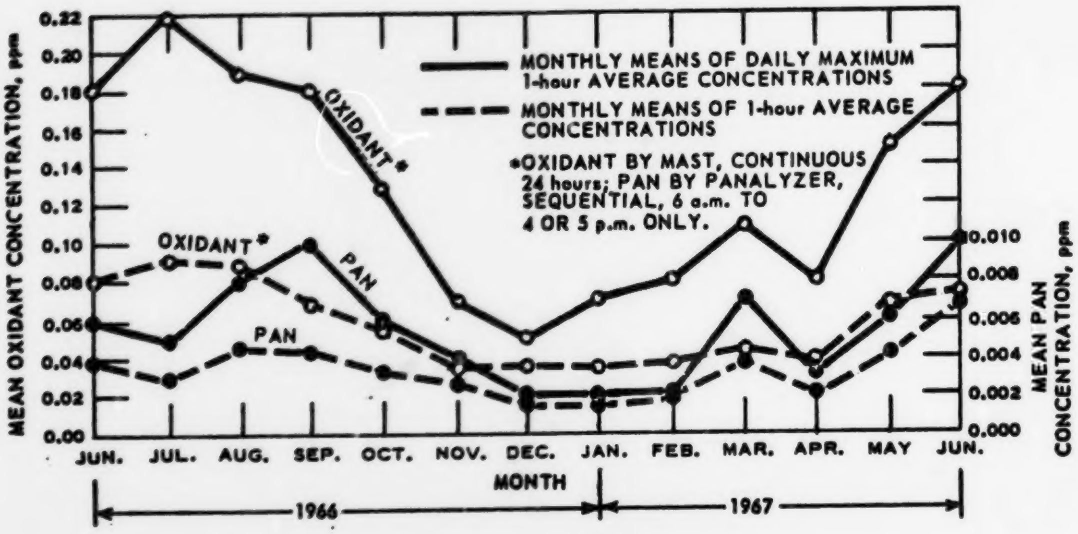

Figure 4-40. Monthly variation in oxidant and PAN concentrations at the Air Pollution Research Center, Riverside, California, June 1966-June 1967. (Reprinted from U.S. DHEW.[1])

reactive fraction of the hydrocarbons, and this is also borne out approximately by the Rome data. A maximum formaldehyde concentration of 39 $\mu g/m^3$ (0.032 ppm) was measured in Berlin, Germany, in 1967 on a street with high traffic density.[58]

Measurements were conducted in Rotterdam during the period January-March 1973, to determine the ambient concentrations of aliphatic aldehydes. The 24-h average concentrations were around 5 $\mu g/m^3$, and the 8:00 a.m. - 4:00 p.m. average concentration was 8.4 $\mu g/m^3$.[59]

Dickinson[60] measured total aldehydes by the bisulfite procedure and formaldehyde by the chromotrophic acid procedure.

Renzetti and Bryan[61] measured total aldehydes, formaldehyde, and acrolein. The maximal acrolein concentration observed was 25.2 $\mu g/m^3$ (0.011 ppm), and the maximal total aldehyde concentration was 0.36 ppm for a 10-min sample. The formaldehyde concentration never exceeded 130 $\mu g/m^3$ (0.10 ppm).

Altshuller and McPherson[62] used spectrophotometry to analyze aldehydes in the Los Angeles atmosphere in the fall of 1961. Table 4-16 shows the diurnal variation in both formaldehyde and acrolein concentrations. Both rise early, remain relatively constant throughout the day, and decrease in the later part of the day. Acrolein apparently accounts for only about 10% of the total olefinic aldehyde in the atmosphere, with most of the latter concentration being accounted for by formaldehyde.

Another nonozone photochemical oxidant observed in urban atmospheres is hydrogen peroxide. Bufalini _et al._[63,64] found this compound to be present at concentrations up to 0.04 ppm in the air in Hoboken, New Jersey, and up to 0.18 ppm on a smoggy day in Riverside, California. Figure 4-41 shows

Table 4-16

Average Aldehyde Concentrations by Hour in Los Angeles, September 25 - November 15, 1961[a]

Sampling Time	Formaldehyde No. Days	Formaldehyde Average Concentration, ppm	Acrolein No. Days	Acrolein Average Concentration, ppm
7 a.m.	7	0.041	2	0.007
8 a.m.	18	0.043	3	0.009
9 a.m.	21	0.045	3	0.009
10 a.m.	28	0.044	5	0.008
11 a.m.	27	0.051	5	0.008
12 noon	23	0.044	3	0.005
1 p.m.	25	0.041	7	0.008
2 p.m.	27	0.034	5	0.007
3 p.m.	25	0.026	4	0.004
4 p.m.	15	0.019	5	0.004

---

[a] Derived from Altshuller and McPherson.[62]

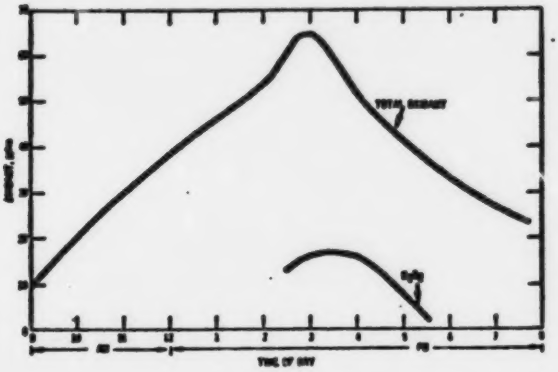

Figure 4-41. Measured oxidant at Riverside, Calif., August 6, 1970.
(Reprinted with permission from Bufalini *et al.*[63])

that the diurnal hydrogen peroxide variation in Riverside on August 6, 1970, nearly parallels that of total oxidant. Figure 4-42 indicates, however, that on at least one occasion (August 11, 1970) it peaked as early as 10:30 a.m.

A dramatic departure of ozone measurements from total oxidant measurements has been reported[65] for the Houston, Texas, area. Side-by-side measurements suggested that either method was a poor predictor of the other. Consideration was given to known interferences due to oxides of nitrogen, sulfur dioxide, or hydrogen sulfide, and the deviations still could not be accounted for. In the worst case, the ozone measurements exceeded the national ambient air quality standard for 3 h, and the potassium iodide instrument read less than 15 ppb for the 24-h period. Sulfur dioxide was measured at 0.01 - 0.04 ppm throughout the day. Even for a 1:1 molar influence of sulfur dioxide this could not explain the low oxidant values. Regression analysis was carried out to support the conclusion that the ozone concentration is often much higher than the nonozone oxidant concentration.

DATA QUALITY

Chapter 6 covers most of the questions influencing data quality. At least three factors enter into the selection of data: the instrumental technique used for measurement, the exposure of the station and the location of the sampling inlet, and the choice of standard calibration method.

Because of interaction with nitric oxide, local decreases in ozone concentrations can occur near large sources, such as power plants or freeways. Consequently, ozone monitoring should not be undertaken near any of these sources if a representative regional ambient concentration is desired. The early portions of the Continuous Air Monitoring Program were evidently focused

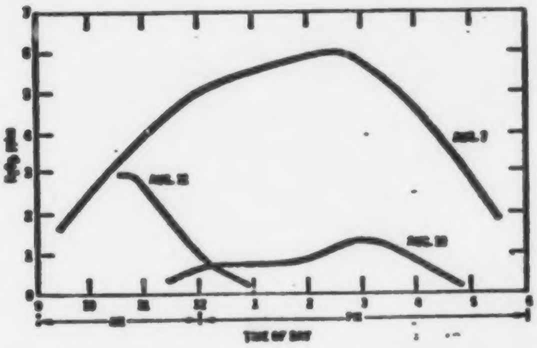

Figure 4-42. Hydrogen peroxide concentrations at Riverside, Calif., in August 1970. (Reprinted with permission from Bufalini *et al.*[63])

on the measurement of community exposure to pollutants, inasmuch as monitoring sites were set up in the centers of urban areas. Because of the source interaction referred to above, this often resulted in an underestimate of the ozone problem. It is now known that stations around the perimeter of a central business district or in surburban areas give higher ozone readings because of the absence of local sources and because of the time required for photochemical reactions to result in ozone buildups in the air. Dark reactions in the inlet manifolding of the sampling train can also distort an instrument's ozone measurements. Large-diameter high-velocity flow systems made of low-reactivity materials should be used to avoid this source of data distortion.

The problems with various primary calibration standards are still being resolved. The earlier discussion of DeMore *et al.*[2] indicates the work undertaken by the CARB in comparing oxidant calibration procedures. It was recommended that all oxidant analyzers in the California network be calibrated by a secondary standard consisting of an ultraviolet ozone analyzer. The primary standard recommended is ultraviolet photometry. These recommendations have been adopted by the CARB. Potassium iodide, indicated as a second choice, requires the application of a correction factor of 0.78.

The fraction of valid data days has been summarized by Altshuller[55] for the six CAMP sites. He noted that, in Cincinnati in the summers of 1969 and 1970 and in Denver in 1971, no results were reported for oxidant. At best, for Washington, D.C., and Chicago, 70 - 75% valid data were obtained; at worst, 40 - 50% valid data were obtained for summer months in Denver and Cincinnati. The findings are summarized in Table 4-17. Altshuller called attention to the large corrections that must be applied to colorimetric

Table 4-17

Percentage of Days for Which Valid Oxidant Data Are Available for May - October and June - August at CAMP Sites[a]

	Percentage of Days[b]										
Site	1964	1965	1966	1967	1968	1969	1970	1971	1972	1973	Average
Chicago	60(75)	85(85)	70(80)	75(75)	75(75)	15(30)	90(95)	90(85)	85(85)	65(85)	70(75)
Cincinnati	80(80)	90(80)	50(45)	70(55)	35(35)	15(0)	5(0)	85(85)	70(65)	80(80)	55(55)
Denver	ND	90(90)	75(65)	30(15)	50(30)	15(20)	60(55)	25(1)	55(55)	65(70)	50(40)
Philadelphia	85(85)	55(45)	80(80)	70(70)	45(55)	25(20)	25(45)	75(75)	15(15)	25(50)	55(50)
St. Louis	90(80)	90(95)	75(60)	80(80)	60(50)	30(30)	30(15)	75(85)	40(60)	85(95)	65(65)
Washington, D.C.	85(80)	80(85)	90(90)	95(100)	75(100)	15(15)	80(90)	95(100)	20(30)	85(80)	70(75)
Average	80(80)	80(80)	75(70)	70(65)	55(55)	20(20)	50(50)	55(70)	50(50)	70(75)	60(60)

---

[a] Derived from Altshuller.[55]

[b] Rounded to nearest 5%. June - August values in parentheses.

oxidant analyzers for peaks that occur at night late in the fall and in winter. He pointed out that the NO_x response correction becomes a major part of the reading, because the instruments are functioning mostly as analyzers of NO_x. What might be considered a valid data base extends much further back in time for the Los Angeles basin. A high fraction of the data for nearly 20 years is available for that area. Before a final judgment on the validity of the data, however, one must carefully assess the problems of calibration consistency and monitoring station siting. It will be found in most local monitoring systems outside California that the bulk of the valid oxidant data has been obtained since 1970. Thus, in 1975, valid data are available for only a few years, because of lags in data processing and editing.

SUMMARY

In comparison with previously available material[1] on atmospheric concentrations of photochemicaloxidants, we now have a far richer data base and a deeper understanding of how to interpret the reported concentrations. The recent information on hydrogen peroxide and the broader geographic coverage of measurements abroad are examples of new data that have come to light.

Subtleties in future standard-setting must consider receptor damage in terms of exposure location and time and receptor distributions and response functions. The formula for damage function points up the need for improved knowledge of spatial and temporal distribution. The use of second-to-worst hourly readings for an ambient air quality standard must give way to a specification stated in terms of a statistically defensible higher-frequency event. This will reduce substantially the uncertainty inherent in confining one's attention to the "worst case."

Long-term trends in oxidant concentration cannot be identified with nearly the degree of certainty that we might like. The data suggest a decrease in oxidant concentrations in central-city areas and an increase in downwind areas. Measurements of nonurban oxidant are exhibiting a higher frequency of violations of the ambient standard than was once believed to occur. Figure 4-43 shows typical ranges of concentrations in various regions in and out of urban complexes.

Probably the most critical question today regarding atmospheric concentrations of ozone and other photochemical oxidants is, "What fraction of the observed values in each locale is susceptible to control by anthropogenic emission reduction?" As brought out in this chapter, there is one school of thought embracing the idea that nature frequently presents us with concentrations that exceed the U.S. national ambient air quality standards. The other point of view is that global background ozone concentrations do not exceed 0.05 - 0.06 ppm at the surface and that higher concentrations than this have anthropogenic sources.

The data presented in the literature reviewed above support the second point of view. The observation of ozone concentrations exceeding the ambient standard in nonurban areas does not demonstrate that this is of natural origin. However, the measurements in remote areas of the northern hemisphere, compared with those in the continental United States, do support the thesis that anthropogenic sources are involved in cases where the standard is exceeded.

This is a very broad conclusion, and additional measurements must be made. Some of this effort (which is goingon) should address the problem of other pollutants and condensation nuclei that accompany the nonurban oxidant.

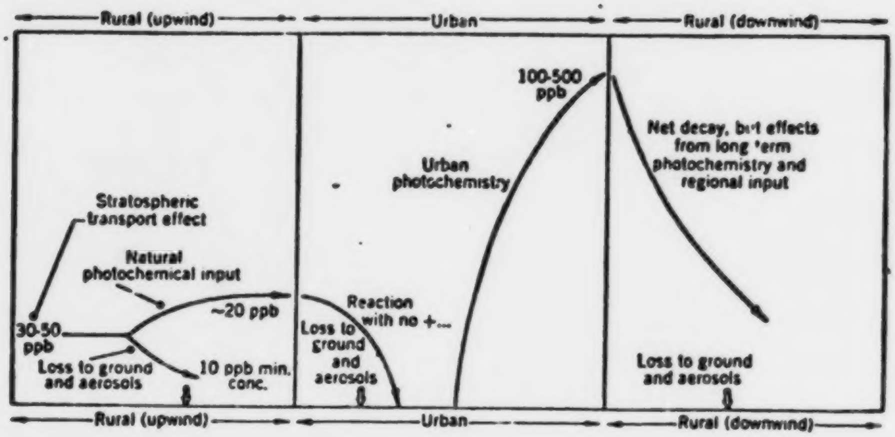
Rural (upwind)
Urban
Rural (downwind)
100-500 ppb
Net decay, but effects from long term photochemistry and regional input
Urban photochemistry
Stratospheric transport effect
Natural photochemical input
~20 ppb
30-50 ppb
Loss to ground and aerosols
10 ppb min. conc.
Reaction with no +...
Loss to ground and aerosols
Loss to ground and aerosols
Rural (upwind)
Urban
Rural (downwind)

Figure 4-43. The tropospheric ozone cycle. (Reprinted with permission from Corn *et al.*[66])

Interpretation of these measurements will increase the specificity of separating anthropogenic sources from natural background sources. Theoretical assessments of the existing observations will shed light on the relative roles played by stratospheric injection, plant emission, background methane, and dry deposition on surfaces in the natural portion of the tropospheric ozone cycle.

Geographically, our best measurements have focused on the Los Angeles, California, region because of the severity of the problem there. The Regional Air Pollution Study and its extensions will, it is hoped, supply an additional rich data base for the St. Louis, Missouri, region. Airborne-pollutant measurements aimed at specific experimental objectives are needed in the central and eastern areas of the United States to broaden the foundations of a national control strategy. Existing ground-based continuous monitoring networks will not provide an adequate basis for the regional control of oxidant. *Ad hoc*, one-shot aircraft measurements have led mainly to speculation that can establish incorrect attitudes on the origin and fate of nonurban ozone. In the vigor of environmental control efforts, incomplete data sets have stimulated hasty targeting on specific sources (for example, rural vehicular emission, power stations, trees, and frontal passages).

Another subject of recent interest has been the question of indoor-outdoor oxidant concentrations. Available measurements and models suggest that indoor exposures may be substantially reduced by appropriate choices of ventilation systems, air filters, and interior surface materials. The cost-benefit relationships may well have a great impact on future decisions based on atmospheric concentrations of oxidant pollutants.

Much care must be exercised in comparing atmospheric concentrations between one place and another because of differences in primary calibration techniques or in instrumentation. Chapter 6 summarizes these problems in detail.

RECOMMENDATIONS

- Nonmethane hydrocarbons and both oxides of nitrogen should be monitored concurrently whenever photochemical oxidant or ozone is monitored.
- Photochemical oxidant monitoring stations should be sited upwind and downwind from urban areas, as well as within those urban areas, wherever possible.
- A common primary calibration standard should be established for all monitoring networks.
- Documentation should be provided in each case to outline the rationale for location and design of monitoring stations and the rationale for data validation for photochemical oxidants.
- A clear indication of what constitutes background concentrations of photochemical oxidants and ozone must be made, in order to form the basis of emission control programs.
- The results of monitoring data must be generalized, in order to relate air quality to emission in a stochastic fashion.

REFERENCES

1. U. S. Department of Health, Education, and Welfare. Public Health Service Environmental Health Service. Atmospheric photochemical oxidant concentrations, pp. 3-1--3-18. In Air Quality Criteria for Photochemical Oxidants. National Air Polution Control Administration Publ. AP-63. Washington, D. C.: U. S. Government Printing Office, 1970.
2. DeMore, W. B., J.C. Romanovsky, M. Feldstein, W. J. Hamming, and P. K. Mueller. Comparison of Oxidant Calibration Procedures. California Air Resources Board Ad Hoc Oxidant Measurement Committee Report, February 3, 1975. (UNVERIFIED)
3. U. S. Environmental Protection Agency. Title 42--Public Health. Part 420. Requirements for preparation, adoption, and submittal of implementation plans. Federal Register 36:15486-15506, 1971.
4. U. S. Environmental Protection Agency. Progress in the Prevention and Control of Air Pollution in 1973. Report to the Congress of the United States, January 1974. pp. 41, 64. (UNVERIFIED)
5. U. S. Environmental Protection Agency. The National Air Monitoring Program: Air Quality and Emissions Trends. Annual Report. Vol. 1. Monitoring and Data Analysis Division, EPA-450/1-73-001-a. Research Triangle Park: U. S. Environmental Protection Agency, 1973.
6. Eschenroeder, A., J. Martinez, and R. Nordsieck. A view of future problems in air pollution modeling, pp. 1013-1027. In Proceedings of the 1972 Summer Computer Simulation Conference. La Jolla, Calif.: Simulation Councils, Inc., 1972. (UNVERIFIED)

7. North Atlantic Treaty Organization. Committee on the Challenges of Modern Society. Atmospheric concentrations, pp. 2-1--2-52. In Air Quality Criteria for Photochemical Oxidants and Related Hydrocarbons. N.29. 1974.

8. Weber, E. Ministry of the Interior, Bonn, Federal Republic of Germany, April, 1973. (UNVERIFIED)

9. Stasiuk, W. N., Jr., and P. E. Coffey. Rural and urban ozone relationships in New York State. J. Air Pollut. Control Assoc. 24:564-568, 1974.

10. Coffey, P. E., and W. M. Stasiuk, Jr. Evidence of atmospheric transport of ozone into urban areas. Environ. Sci. Technol. 9:59-62, 1975.

11. Lahmann, E., J. Westphal, K. Damschke, and M. Lübke. Kontinuierliche Ozon-Messungen in einer verkehrsreichen Strasse. Gesund. Ing. 89:144-147, 1968.

12. Brasser, L. J. of the Research Institute for Public Health Engineering, Delft, The Netherlands, April 1973. (UNVERIFIED)

13. Laboratoria di Inquinamento Atmosferico del CNR, Universita di Roma, Rome, Italy, April 1973. (UNVERIFIED)

14. Muezinoulu, A. Scientific and Technical Research Council of Turkey, Ankara, Turkey, May 1973. (UNVERIFIED)

15. National Research Council. Associate Committee on Scientific Criteria for Environmental Quality. The Effects of Photochemical Smog. July 1974, Draft. (UNVERIFIED)

16. Bilger, R. W. Oxidants and Their Precursors in the Atmosphere. National Summary Report. Department of the Environment and Conservation, Canberra City, Australia, February 19, 1974. (UNVERIFIED)

17. Report on the Problem of Photochemical Oxidants and Their Precursors in the Atmosphere. Issued by the Organization for Econimic Cooperation and Development, Air Management Sector Group, September 9, 1974. (UNVERIFIED)

17a. Derwent, R. G., and H. N. M. Steward. Elevated ozone levels in the air of central London. Nature 241:342-343, 1973.

17b. Atkins, D. H. F., R. A. Cox, and A. E. J. Eggleton. Photochemical ozone and sulphuric acid aerosol formation in the atmosphere over southern England. Nature 235:372-376, 1972.

18. Miller, A., and D. Ahrens. Ozone within and below the west coast temperature inversion. Tellus 22:328-339, 1970. (UNVERIFIED)

19. Miller, P. R., M. H. McCutchan, and H. P. Milligan. Oxidant air pollution in the Central Valley, Sierra Nevada foothills, and Mineral King Valley of California. Atmos. Environ. 6:623-633, 1972.

20. Blumenthal, D. L., T. B. Smith, D. S. Ensor, S. O. Marsh, R. B. Husar, W. White, S. L. Heisler, and P. Owens. Three Dimensional Pollutant Gradient Study--1972 Program. Report to the California Air Resources Board. Altadena, Calif.: Meteorology Research, Inc., 1972. (UNVERIFIED)

21. Blumenthal, D. L., W. H. White, R. L. Peace and T. B. Smith. Determination of the Feasibility of the Long-Range Transport of Ozone or Ozone Precursors. EPA-450/3-74-061. Altadena, Calif.: Meteorology Research, Inc., 1974.

22. Edinger, J. G. Preliminary Analysis of LARPP Data. Informal Report to Coordinating Research Council, Inc., February 1, 1975. (UNVERIFIED)

23. Research Triangle Institute. Investigation of High Ozone Concentration in the Vincinity of Garrett County, Maryland and Preston County, West Virginia. Institute Final Report. EPA-R4-73-019. Research Triangle Park, N. C.: Research Triangle Institute, 1973. 105 pp.

24. Edinger, J. G. Vertical distribution of photochemical smog in Los Angeles basin. Environ. Sci. Technol. 7:247-252, 1973.

25. Research Triangle Institute. Investigation of Ozone and Ozone Precursor Concentrations at Nonurban Locations in the Eastern United States. EPA-450/3-74-034. Research Triangle Park, N. C.: Research Triangle Institute, 1974. [141 pp.]

26. Gloria, H. R., G. Bradburn, R. F. Reinisch, H. N. Pitts, Jr., J. V. Bahar, and L. Zafonte. Airborne survey of major air bases in California. J. Air Pollut. Control Assoc. 24:645-652, 1974.

27. Fern, W. J., and R. I. Brabets. Field Investigation of Ozone Adjacent to High Voltage Transmission Lines. IEEE (Institute of Electrical and Electronics Engineers) Transactions Paper T 74 057-6, Presented at the PES Winter Meeting, New York, New York, Jan. 27-Feb. 1, 1974.

28. Roach, J. F., V. L. Chartier, and F. M. Dietrich. Experimental oxidant production rates for EHV transmission lines and theoretical estimates of ozone concentrations near operating lines, pp. 647-657. In IEEE (Institute of Electrical and Electronics Engineers) Transactions on Power Apparatus and Systems, Mar-April, 1974.

29. Frydman, M., A. Levy, and S. E. Miller. Oxidant measurements in the vicinity of energized 765 KV lines, pp. 1141-1147. In IEEE (Institute of Electrical and Electronics Engineers) Transactions on Power Apparatus and Systems, May-June, 1973.

30. Sherer, H. N., Jr., B. J. Ware, and C. H. Shih. Gaseous effluents due to EHV transmission line corona, pp. 1043-1049. In IEEE (Institute of Electrical and Electronics Engineers) Transactions on Power Apparatus Systems, May-June, 1973.

31. Pitts, J. N., Jr. Air Pollutants and Public Health: Old Problems and New Horizons for NO_x Control. Statewide Air Pollution Research Center Report No. 2. Riverside: University of California, 1975.

32. Davis, D. D., G. Smith, and G. Klauber. Trace gas analysis of power plant plumes via aircraft measurement: O_3, NO_x and SO_2 Chemistry. Science 186:733-736, 1974.

33. Davis, D. D. Atmospheric Gas Phase Oxidation Mechanisms for the Molecule SO_2. Chemistry Department. College Park: University of Maryland, 1974. (in press)

34. Saunders, R. A., J. R. Griffith, and F. E. Saalfeld. Identification of some organic smog components based on rain water analysis. Biomed. Mass Spectrosc. 1:192-194, 1974.

35. Blumenthal, D. L., and W. H. White. The Stability and Long Range Transport of Ozone or Ozone Precursors. Paper 75-07 Presented at 68th Annual Meeting of the Air Pollution Control Association, Boston, Massachusetts, June 15-20, 1975.

36. Rubino, R. A., L. Bruckman, and J. Magyar. Ozone Transport. Paper 75-07 Presented at 68th Annual Meeting of the Air Pollution Control Association, Boston, Massachusetts, June 15-20, 1975.

37. Sticksel, P. R. The Stratosphere as a Source of Surface Ozone. Paper 75-07.6 Presented at 68th Annual Meeting of the Air Pollution Control Association, Boston, Massachusetts, June 15-20, 1975.

38. National Academy of Sciences. National Academy of Engineering. Coordinating Committee on Air Quality Studies. Air Quality and Automobile Emission Control. Vol. 3. The Relationship of Emissions to Ambient Air Quality. U. S. Senate Committee Print Serial No. 93-24. Washington, D. C.: U. S. Government Printing Office, 1974. pp. 76-82.

39. Fabian, P., and P. G. Pruchniewicz. Miriodonal distribution of tropospheric ozone from ground based registrations between Norway and South Africa. Pure Appl. Geophys. 106-108:1025-1035, 1973.

40. Hering, W. S., and T. R. Borden, Jr. Ozonesonde Observations over North America. Volumes I, II, and III. Air Force Cambridge Research Laboratory, Report AFCRL-64-30, January, 1964.

41. Fabian, P., and P. G. Pruchniewicz. Ozonesonde Observations over North America. Air Force Cambridge Research Laboratory, Report AFCRL-64, January 1964. p. 1027.

42. Neligan, R. E., and R. M. Angus. The Validity of the Strategy of Linear Rollback of Hydrocarbons to Achieve Oxidant Air Quality Standards. Presented at the UC-ARB Conference Technical Bases for Control Stratagies of Photochemical Oxidant: Curent Status and Priorities in Research, December 16-17, 1974, Riverside California.

43. Mueller, F. X., L. Loeb, and W. H. Mapes. Decomposition rates of ozone in living areas. Environ. Sci. Technol. 7:342-346, 1973.

44. Sabersky, R. H., D. A. Sinema, and F. H. Shair. Concentrations, decay rates, and removal of ozone and their relation to establishing clean indoor air. Environ. Sci. Technol. 7:347-353, 1973.

45. Shair, F. H., and K. L. Heitner. Theoretical model for relating indoor pollutant concentrations to those outside. Environ. Sci. Technol. 8:444-451, 1974.

46. Hales, C. H., A. M. Rollinson, and F. H. Shair. Experimental verification of linear combination model for relating indoor-outdoor pollutant concentrations. Environ. Sci. Technol. 8:452-453, 1974.

47. King, G. S. Ozone and air conditioning. Royal Soc. Health J. 93:84-86, 1973.

48. Pitts, J. N., Jr., A. C. Lloyd, and J. L. Sprung. Chemical reactions in urban atmospheres and their applications to air pollution control strategies, pp. 27-61. In Proceedings of the International Symposium on Environmental Measurements, Geneva, Oct. 2-4, 1973.

49. Kinosian, J. R., and S. Duckworth. Oxidant Trends in the South Coast Air Basin 1963-1972. California Air Resources Board Report, April 1973.

50. National Academy of Sciences. National Academy of Engineering. Coordinating Committee on Air Quality Studies. Air Quality and Automobile Emission Control. Vol. 3. The Relationship of Emissions to Ambient Air Quality. U. S. Senate Committee Print Serial No. 93-24. Washington, D. C.: U. S. Government Printing Office, 1974. pp. 65-88.

51. Heitner, K., and J. E. Krier. Outline of an Approach to Management Standards. California Institute of Technology, Environmental Quality Laboratory, Memorandum No. 13, January 1974. p. 11.

52. Tiao, G. C., G. E. P. Box, M. Grupe, S. T. Liu, S. Hillmer, W. S. Wei, and W. J. Hamming. Los Angeles Aerometric Ozone Data 1955-1972. University of Wisconsin, Technical Report No. 346, Oct. 1973.

53. Chameides, W., and J. C. G. Walker. A photochemical theory of tropospheric ozone. J. Geophys. Res. 78:8751-8760, 1973.

54. Ripperton, L. A., H. Jeffries, and J. J. B. Worth. Natural synthesis of ozone in the troposphere. Environ. Sci. Technol. 5:246-248, 1971.

55. Altshuller, A. P. Evaluation of oxidant results at CAMP sites in the United States. J. Air Pollut. Control Assoc. 25:19-24, 1975.

56. Birakos, J. N., Ed. 1974 Profile of Air Pollution Control. County of Los Angeles Air Pollution Control District, 1975.

57. Bartel, A. W., and J. W. Temple. Ozone in Los Angeles and surrounding areas. Ind. Eng. Chem. 44:857-861, 1952.

58. Lahmann, E. Luftverunreinigungen durch den Kraftverkehr. Bundesgesundheitsblatt 12:284-286, 1969.

59. Brasser, L. J. Research Institute for Public Health Engineering, TNO Delft, The Netherlands, April, 1973. Private communication to the NATO/CCMS Panel on Air Quality Criteria.

60. Dickinson, J. E. Air Quality of Los Angeles County. Los Angeles County Air Pollution Control District Technical Progress Report, Vol. 2, February, 1961.

61. Renzetti, N. A., and R. J. Bryan. Atmospheric sampling for aldehydes and eye irritation in Los Angeles smog. J. Air Pollut. Control Assoc. 11:

62. Altshuller, A. P., and S. P. McPherson. Spectrophotometric analysis of aldehydes in the Los Angeles atmosphere. J. Air Pollut. Contr. Assoc. 13:109-111, 1963.

63. Bufalini, J. J., B. W. Gay, Jr., and K. L. Brubaker. Hydrogen peroxide formation from formaldehyde photooxidation and its presence in urban atmospheres. Environ. Sci. Technol. 6:816-821, 1972.

64. Gay, B. W., Jr., and J. J. Bufalini. Hydrogen peroxide in the urban atmosphere. Adv. Chem. Ser. 113:255-263, 1972.

65. Severs, R. K. Simultaneous total oxidant and chemiluminescent ozone measurements in ambient air. J. Air Pollut. Control Assoc. 25:394-396, 1975.

66. Corn, M., R. W. Dunlap, L. A. Goldmuntz, L. H. Rogers. Photochemical oxidants: Sources, sinks, and strategies. J. Air Pollut. Control Assoc. 25:16-18, 1975.

CHAPTER 5.

MODELS FOR PREDICTING AIR QUALITY

Trends in air pollutant concentrations can be predicted with simple empirical models based on atmospheric and laboratory data. Concentrations of nonreactive pollutants from point sources can be predicted with accuracy to within a factor of 2; predictions are more likely to be too high than too low, especially predictions of concentration peaks. Concentrations of reactive pollutants, such as ozone and other photochemical oxidants, can be predicted reasonably well with photochemical-diffusion models when detailed emission, air quality, and meteorologic measurements are available; most such predictions of air pollution in Los Angeles have been accurate to within 50%.

Statistical models based on data correlations and on Markov chains are being actively developed and their fidelity evaluated by several research groups. Photochemical-diffusion models based on deterministic equations are also being developed, but because of their complexity will probably be used only as research tools for some time.

As expressed in Eq. 1 of Chapter 4, the spatial and temporal distributions of pollutants must be known to assess their damage to receptors. Traditionally, monitoring station measurements are used to estimate the concentrations for entire regions. Statutory mandates, however, require the prediction of future concentrations under differing emission conditions. More and more refined predictions will be required as the standards become more specific.

An air quality model is a method of relating air quality to emission under specific environmental conditions. There are many types of air quality models, and the purposes of this chapter are to describe models that are available for the analysis of photochemical oxidants and to give some information on how well the models perform.

We must first gain a perspective on present modeling capabilities. The photochemical-diffusion computer programs are aimed at prediction of ozone and nitrogen dioxide concentrations. It must be understood that ozone is used as an indicator or as a surrogate for other oxygenated organic compounds or radicals that may actively cause adverse effects. Most models do not treat aldehydes and oxygenated organic aerosols specifically, although they do address the problems of peroxy-radical and hydrogen peroxide concentrations in some cases.

Because of the dominance of distributed sources over local single sources in the production of photochemical oxidants, point-source models will not be discussed here. Related research regarding the measurement of diffusion or the development of atmospheric chemical submodels will not be emphasized.

Chapter 2 is devoted to the chemical processes that govern atmospheric transformation and removal, and this aspect of the models will not be repeated here.

Numerous reviews of air quality models have appeared in the literature in the last several years. Wanta[1] considered the meteorologic role in air pollution, including the effects of vertical temperature structure, topography, windfields, and dispersion mechanisms. He tabulated in detail numerous characteristics of the mathematical air pollution models that existed in 1967. The relationship of meteorology to air pollution was also reviewed in papers by Pack[2] and Neiburger.[3] Theories of diffusion in the lower atmosphere were outlined by Gifford,[4] who stressed the empirical aspects of both differential equation diffusion theory and Gaussian diffusion formulas, traced the historical connections between the two, clarified their relationship to atmospheric turbulence, and reviewed cases of plume formulas to cover special phenomena, such as plume fluctuation, looping, coning, fumigation, and lofting.

Various meetings on urban diffusion models have been held in recent years. One was a symposium[5] sponsored by the Environmental Protection Agency. Its proceedings include studies of Gaussian plume and puff modeling techniques available in 1969. Each paper on a specific model gave some detail as to the mathematical assumptions and the types of measurements that were used to test it. Several participants noted a need to develop finite-difference numerical techniques to handle the nonlinearities of atmospheric reactions. Another review resulted from a series of meetings and working groups related to Project Clean Air, which was carried out by the University of California in 1969 and 1970. One of the task force reports[6] is especially helpful in its review of mathematical simulation modeling up to 1970. The stated purpose of the review was to identify future research needs for California's Project Clean Air. A tabulation summarized fifteen simulation schemes by commenting on each of nine points of information, including statements of working equations and quantitative aspects of cell size, time resolution, and verification tests. It is gratifying to note that substantial progress has been made on each of the 10 recommendations given for future research.

Another useful collection of papers is the proceedings of the second meeting of the Expert Panel on Air Pollution Modeling, sponsored by NATO.[7] The volume contains 15 papers from both the first and second meetings of the panel. Three of the main topics are: air quality modeling projects that were going on in Ankara, Turkey, and Frankfurt, Germany; applicability of physical models that use hydraulic or aerodynamic replications of flow fields; and problems in atmospheric chemistry of pollutants, with particular emphasis on photochemical transformation. In his review of atmospheric transport processes, Reiter[8] stressed the behavior of the diffusion equations under the combined effects of frictional, buoyant, and Coriolis forces. The distortion of the velocity profile as it approaches the geostrophic wind was discussed. The main approach was theoretical and was based on K theory, but Gaussian plume results were also cited. The fluid dynamic limitations of the Gaussian plume formulas were reviewed critically, and extensive references for various special aspects of the formulas were given.

In another review, Hoffert[9] discussed the social motivations for modeling air quality for predictive purposes and elucidated the components of a model. Meteorologic factors were summarized in terms of windfields and atmospheric stability as they are traditionally represented mathematically. The species-balance equation was discussed, and several solutions of the equation for constant-diffusion coefficient and concentrated sources were suggested. Gaussian plume and puff results were related to the problems of developing multiple-source urban-dispersion models. Numerical solutions and box models were then considered. The review concluded with a brief outline of the atmospheric chemical effects that influence the concentration of pollutants by transformation.

Motivated by statutory mandates for environmental evaluation of transportation systems, Darling[10] solicited information from each originator of an air pollution model by a questionnaire advertised in the Commerce Business Daily, a widely circulated publication in the United States. Of the 78 questionnaires on models sent out, 44 were completed and returned. The questionnaire dealt in some detail with computer programs involved with each model, in addition to the analytic foundations of each approach. Principles, implementation, applications, and validation were discussed in the report. Whenever information was available, there was comparative analysis of the models. An important conclusion of the work was that in 1972 there had been very little performance evaluation of models related to transportation-generated air pollution. Johnson[11] reviewed EPA programs in air quality simulation modeling in 1972, covering the various policy questions that models can help to answer, summarizing modeling approaches, and outlining advantages and disadvantages of the various techniques. The mission of UNAMAP (User Network for Applied Modeling of Air Pollution) was described as a system that would provide easy user access to the models for practical applications.

The third meeting of NATO's Expert Panel on Air Pollution Modeling[12] updated reports of modeling efforts for Cologne, St. Louis, Milan, Ankara, Frankfurt, Stockholm, Oslo, and Manchester. It also included research papers on model-related meteorologic topics and reviews of various national programs and facilities represented by the participants. The fourth meeting of the panel[13] departed from the format of the others, in that it consisted of five workshop sessions, which covered applications of modeling and user's needs, validations of air quality simulation models, regional air pollution studies, empirical-statistical modeling of air quality, and the question of simplicity versus sophistication in air quality modeling. Each workshop discussion was summarized in narrative form, and several prepared papers were included after the workshop sessions.

Lamb and co-workers[14] reviewed techniques of diffusion modeling for air quality with relation to transportation-generated pollution. They discussed the theory and structure of models, presented a series of tabulated comparisons, analyzed the function and design of each model, and offered simple diagrams to illustrate the functions and problems of the various techniques. The report was intended to survey a great deal of unpublished material and therefore was important in bringing the earlier surveys up to date (to about mid-1973).

Air quality simulation models for photochemical pollutants were reviewed by Sklarew[15] for a new edition of Air Pollution. Some of the models developed for simulating photochemical smog were reviewed from the viewpoints of module logic and evaluation results. The Los Angeles-based developments were outlined, including the format and preprocessing of emission inventory data and meteorologic data. Lumped-parameter chemical approaches were described, and smog chamber kinetics validations were outlined.

One of the purposes of this chapter is to add recent material to that collected in the reviews just described. In contrast with previous reviews, however, this chapter will emphasize the critical evaluation of performance. The sections that follow deal with objectives of models (from research to applied control systems), the elements of schemes for predicting air quality, specific methods of modeling, and the evaluation of prediction techniques.

OBJECTIVES OF MODELS

At the heart of the problem of relating improvements in air quality to reductions in pollutant emission is a reliable method of prediction. Only with such a method can there be rational planning for air pollution control through regulation of transportation, indirect sources, and stationary sources. Decision-makers need it as a tool and must specify it in their regulations. Otherwise, their administration of an air quality plan would be based on sheer guesswork tempered by political negotiation.

Pollutant concentrations are related to sources under specified meteorologic conditions by using what is called an air quality model. Models vary from simple arithmetic exercises to complex computer simulations. There are many paths to the needed answers. Which of the available methods is appropriate depends on the specific problem. Most agencies charged with enforcement of air quality rules have used only the most rudimentary models. In some cases, short deadlines have forced the situation. But the recognition of the social costs of air pollution control has led to deeper interest in scrutinizing the results of air quality models, and it is not likely that casual calculation will be accepted by regulatory agencies--especially if the results (in the form of abatement strategies) involve severe socioeconomic dislocation and large financial outlays.

In examining how well a model meets its objectives, one must ask several questions:

- Who will use the model?
- What questions must the model be able to answer?
- How well is the model adapted to the intended application?
- Has the model been thoroughly tested against an adequate data base for validations?
- How readily accessible is the model with respect to practical calculations and computer implementation?

This section examines various purposes of developing and using air quality models.

Scientific Purposes

In any environmental management plan, it is essential to understand the pertinent quality criteria and their relationship to the variables that can be manipulated directly. The construction of mathematical models imposes the requirement of a logical framework that connects causes and effects, identifies all pertinent variables, and defines their interrelationships. Even if a particular technique never becomes practical, the discipline imposed by the logical structure is valuable in highlighting important relationships.

Methods for predicting air quality were first applied in conjunction with field measurement programs and routine monitoring programs. Such applications has emphasized both the strengths and the weaknesses of various modeling schemes and eluciadated the main points of technical understanding that must underlie the establishment of control systems. Considering the responses of models to various inputs, "parametric sensitivity evaluations" carried out in parallel with supporting field programs will continue to be helpful in the development of the understanding on which pollution abatement plans can be based.

Experience has followed an iterative pattern in playing the model exercises against field measurements. Usually, the first indication of the relative importance of variables is seen in bodies of observational data. The next step is to build a model on the basis of either intuition or a deterministic physical equation that reflects the trends seen in the data. The model is then used for the range of conditions in the data base, and uncertainties as to the correctness or completeness of the model become evident. The questions that arise can usually be answered only through further field experimentation. Thus, the models themselves are used in the design of both laboratory and field experiments that will ultimately provide a basis for the improvement of the modeling art.

Regulatory Purposes

Long-term air quality forecasts are implicit in any scheme that is designed to improve the atmospheric environment through specific sanctions on primary pollutant emission. The writing of legislation and regulations is an obvious application of air quality modeling. For example, vehicular emission controls are specified in the U. S. Clean Air Amendments of 1970. Originally, a modeling scheme was used to specify the control that would be required to achieve improvements in air quality. One of the difficulties with such legislation is that the ambient air quality standards are set by an administrative process, whereas the vehicular emission standards are set by the original law. In this case, the extent of control was specified before the establishment of the target reduction of pollution for the future.

A broader regulatory application of air quality modeling is the examination of regional plans for abatement of air pollution. Ideally, each plan should be tested by a reliable model that will tell what the pollutant concentrations will be in the future if emission is reduced as specified by the plan. Therefore, alternative approaches must be evaluated both with respect to their effectiveness in cleaning the air and with respect to their social costs, and cost models and possibly even damage models must be used concurrently with the air quality model. Only in this way can a least-cost abatement strategy be implemented.

The successful application of quantitative predictions to the design of strategies requires full cooperation of the scientific community with the decision-makers. Regulatory and legislative bodies need the most reliable tools available to assess the impact of their decisions. The assessment of environmental impact is an integral part of the process of engineering design, whether the object of the process is a steam generator, a highway, or an airport. As a result of the new requirements, many branches of government--not only the EPA--must be able to predict air quality.

Urban Planning

Human land-use patterns and meteorologic conditions both directly determine the degree of air pollution. Land-use planning includes the design of transportation systems. Air quality models must be able to predict the pollution that will be caused by various patterns of land use. In this application, the predictive scheme is used inversely; i.e., it has to answer the question: Given air quality standards, what patterns of land use are acceptable?

Experience has shown that conventional wisdom can be dangerously misleading in regard to the impact of various land-use and transportation plans on air pollution. In the models to evaluate proposed changes, one gains an understanding of the sensitivity of environmental variables to different types of facilities and to where they are placed.

Emerging from analyses like these is a new concept of population holding capacity. Earlier notions of maximal population density were based on availability of space for transportation systems, subsoil conditions related to the support of buildings, availability of off-street parking space, and many other considerations. With the new set of requirements imposed by environmental quality standards, the earlier criteria will be superseded, in effect, by the output of a model that specifies how great a population can occupy a given region, and where and when. In many urban areas, air quality may already be a controlling factor in the determination of this holding capacity. Hence, accurate forecasts are important.

Episode Control

Systems are now being devised that require a real-time system that uses model logic to control emission sources to maintain acceptable air quality for all meteorologic conditions. In the United States, such control systems may be needed for large combustion sources of air pollution. Such systems use meteorologic and power-demand data to produce load schedules by fuel type. Indeed, the concept of computer-aided controls could be used for the control of sources throughout an urban area, as has been proposed in some prefectures in Japan. For real-time warning systems or control systems, the air quality model provides the logic in the feedback loop that links air quality improvement to emission reduction under specific predicted meteorologic conditions. With the coming need for flexibility in fuel logistics, these systems may become more and more prevalent.

The operational logic for an episode control system must have much finer resolution and higher reliability than that for long-term applications. For forecasts covering a decade or two, progress in a cleanup campaign can be closely monitored, and emission controls can be continually adjusted. Episode management, however, is far more difficult. One the one hand, if too many errors are made by the system, unduly high public exposure to harmful pollutants will result. On the other hand, if the episode control system generates too many false alarms, the social costs in industrial operational modification will become so onerous that public support for the system may fade.

Implicit in the success of any episode control system is the ability to predict weather accurately. Conventional applications of air quality models that use a wide variety of meteorologic information require that such details as wind speed and direction and mixing depth be reliably predicted. Some of the statistical-empirical models that are discussed below obviate such a large mass of prediction by selecting a few sensitive measurements and bypassing the detail of deterministic logic. The episode-control application of models clearly illustrates the need to develop a multiplicity of air quality models. For example, a model that finds a natural application in the regulatory or planning process may be extremely poorly suited to the control of discrete episodes.

ELEMENTS OF AIR QUALITY PREDICTION SCHEMES

Structure of Deterministic Models

All deterministic schemes have some elements in common. The completeness or detail of any of these elements varies greatly from model to model, but a diagrammatic representation of the basic structure will clarify the relationships among the various techniques to be presented. Figure 5-1 shows that three streams of input information enter the preprocessing module, and the background and initial pollutant concentrations may become unimportant if the simulation is run for a long enough period and covers a large enough area. The preprocessing module renders this information useful for the main computational part of the air quality model, transmitting to the main program the various kinds of data shown in Figure 5-1. Depending on the complexity of the logic, one or more of these kinds of data may be unnecessary. Pollutant concentrations constitute the output of any of the models. The form of this output varies in detail, ranging from a single concentration averaged over a long period for an entire region to hourly maps of concentration in three dimensions over the region.

Classification of Types

There are many ways of categorizing air quality models. One differentiation is between statistical and deterministic models. The structure of statistical models is based on the patterns that appear in the extensive measured data. The structure of deterministic models is based on mechanistic principles wherever possible. Most deterministic models contain some degree of empiricism. For example, few models, if any, use turbulent-diffusion formulations that are based on first principles, but rather use measured values of dispersion. The same is

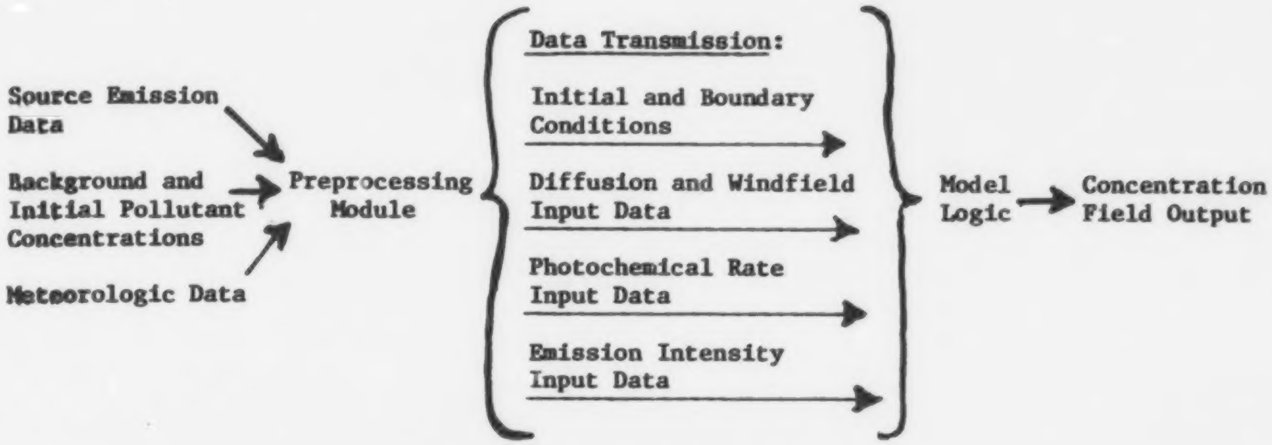
Source Emission Data
Background and Initial Pollutant Concentrations
Meteorologic Data
Preprocessing Module
Data Transmission:
Initial and Boundary Conditions
Diffusion and Windfield Input Data
Photochemical Rate Input Data
Emission Intensity Input Data
Model Logic
Concentration Field Output

Figure 5-1. Diagram of elements of deterministic model.

true in regard to the atmospheric chemistry of photochemical formulations. A common caution is that, if too many disposable quantities exist in a deterministic model, it becomes a statistical model in disguise, because all it accomplishes is a version of curve-fitting.

Another classification of model is related to the time and space scales of interest. Ambient air quality standards are stated for measurement averaging periods varying from an hour to a year. However, for computational purposes, it is often necessary to use periods of less than an hour for a typical resolution-cell size in a model. Spatial scales of interest vary from a few tenths of a meter (e.g., for the area immediately adjacent to a roadway) up to hundreds of kilometers (e.g., in simulations that will elucidate urban-rural interactions). Large spatial scales are also warranted when multiday simulations are necessary for even a moderate-sized urban area. Under some climatologic conditions, recirculations can cause interaction of today's pollution with tomorrow's. Typical resolution specifications couple spatial scales with temporal scales. Therefore, the full matrix of time scales and space scales is not needed, because of the dependence of time scales on space scales. Some typical categories by scale are as follows:

- A roadway impact model in the microscale (~0.1 km; ~10 min-1 h).
- Large-point-source or indirect-source model (~10 km; ~1 h).
- Urban regional scale model (~50 km; ~1 h).
- Urban-rural regional scale model (~300 km; 1 h to 1 week).

The reviews by Johnson[11] and by Seinfeld[16] give helpful guidelines in the classification of models by space and time scale.

Perhaps the most fundamental method of classifying models is by methodology. Examples of specific methods will be discussed later, but a brief summary is appropriate here. Great emphasis on historical data as embodied in empirical formulas is found in the methodology of statistical and rollback models.[17-27] Rollback models embody the principle that reductions in emission are reflected by improvements in air quality, as may be shown by a straight line, a curved line, or a complex surface that expresses some proportionality relationship. These models work best if the geographic and temporal distribution of the emitters is not changed. The straight-line versions can apply only to pollutants that do not undergo chemical transformations in the atmosphere. An example of a proportional linear rollback is a rapidly instituted retrofit control of carbon monoxide emission imposed on an entire vehicle population. Corrections for irregularities in distribution caused by nonuniform growth, however, have been suggested.[22,23] The great advantages of the linear rollback model are its use of aggregated emission statistics and its mathematical simplicity. Suggested improvements of the rollback to account for chemical change have been based on the use of air quality data or smog-chamber data.

Dispersion models may take the form of a simple box model[28-32] or a Gaussian formula. Dispersion models that use superposition of Gaussian plumes improve the rollback approach for nonreacting species by accounting for geographic distribution of emission sources. Emission generally consists of an array of area elements or effective point sources, each characterized by an output intensity. The plumes from the several sources contribute in an additive manner to the pollution at any downwind field point. Summation of the contributions over all sources constitutes the superposition aspect of the approach. Computationally, this is convenient, because it allows sequential consideration of each source element, but the same feature renders the method inapplicable to multireacting systems undergoing chemical transformations. The Gaussian puff approach removes the limitation of steady-state assumptions from the calculation and treats discrete emissions as puffs that spread according to the Gaussian law.

Special balance equation models combine the effects of diffusion, advection and some chemistry and normally may use finite difference techniques for the solution.[33-44] Currently, these are the most elaborate simulations applied to air quality analysis. Both time and space are subdivided into cells in these models, so that the cumulative effects of emission, transport, and (when chemistry is included) reactions are simultaneously accounted for. The potential danger in using this kind of model is that the available data base will be outstripped by mathematical detail. When that happens, the large volumes of data output can delude the user into a high degree of confidence when, in reality, only very sparse data bases are available for verifying the model. The advantage of finite-difference models is the potentially greater fidelity where greater detail exists in the input data base and in the validation testing.

Emission Description

The quantitative expression of the introduction of primary pollutants into the atmosphere is basic to any air quality model. Emission is most generally described as a geographic, temporal, and chemical distribution that requires a rather massive array of numbers. Some simple models need only the aggregated numbers found in ordinary tabulations of emission inventory (e.g., kilograms per day of carbon monoxide, NO_x, etc., for a large air quality control region).

A geographic breakdown of emission is needed, however, if we are to determine key "hot spots" of high pollution to which ambient air quality standards are directed. This spatial distribution of emission is often given on a grid or on a traffic-flow network system. Similarly, the hourly variation in emission must be known if we are to predict the peak hourly averages that are often mentioned in the standards.

For purposes of characterization, emission sources are generally divided broadly into stationary and mobile or transportation sources. Stationary sources are further divided into point and area emitters. Typical point sources must include petroleum refineries and electric power plants. Commercial solvent emission and gasoline marketing emission may generally be represented as area sources. A third category has been defined recently--indirect sources --which takes into account hybrid sources like sports arenas and shopping centers. These have fixed locations, but the traffic that is generated by or attracted to such a facility constitutes the source of emission that is combined with the emission of the facility itself.

Gathering emission data and putting them in condition for use in air quality models are often among the most tedious and time-consuming parts of their handling. For this reason, the preprocessing module is identified as a separate automatic operation in the procedure outlined in Figure 5-1.

Transport Formulation

The movement of pollution from one place to another and its dilution by atmospheric mixing are both based on the meteorologic conditions of the airshed in question. Air flow patterns are in turn based on the interaction of the large-scale flow with the topographic details of the region, with regard to altitude variation, roughness of surface, and heating characteristics. The part of the flow-surface interaction that influences the degree of pollution must be taken into account in a model. Rather than computing the local weather as part of the prediction, most models use meteorologic measurements to construct atmospheric flow fields that represent, on a local scale, the driving factor of the transport mechanisms.

With the velocity field and the atmospheric dispersion mechanisms given, the basic equation is that for mass balance for an individual species, which can be expressed in the following form:

$$\frac{\partial c_j}{\partial t} + \sum_{\ell=1}^{3} \frac{\partial (c_j v_{j\ell})}{\partial x_\ell} = w_j + S_j \qquad (j = 1, 2, 3, \ldots, s), \quad (1)$$

where

c_j = mass concentration of jth species,

t = time,

ℓ = an index referring to each coordinate direction,

$v_{j\ell}$ = velocity of jth species in ℓth direction,

x_ℓ = distance in ℓth direction,

w_j = net molar production rate of jth species per unit volume by chemical reaction,

S_j = source strength for emitters of jth species at some location above the ground, and

s = number of species.

The derivation of the mixture-balance laws has been given for a binary mixture by Chapman and Cowling.[52] Its generalization to multicomponent mixtures, as in Eq. 1 , uses a determination of the invariance of the Boltzmann equation. This development has been detailed by Hirschfelder _et al_.[53] These derivations were summarized in the notes of Theodore von Kármán's Sorbonne lectures given in 1951-1952, and the results of his summaries are stated in Penner's monograph.[54] For turbulent flow, the species-balance equation can be represented in the Boussinesq approximation as:

$$\frac{\partial \bar{c}_j}{\partial t} + \sum_{\ell=1}^{3} \bar{v}_\ell \frac{\partial \bar{c}_j}{\partial x_\ell} = \sum_{\ell=1}^{3} \frac{\partial}{\partial x_\ell} \left(K_{\ell\ell} \frac{\partial \bar{c}_j}{\partial x_\ell} \right) + \bar{w}_j + S_j \qquad (j = 1,2,3,\ldots,s), \quad (2)$$

where overbars denote time-averaged values and $K_{\ell\ell}$ is the eddy diffusivity that relates the flux of a diffusing species to the species concentration gradient, both acting in the same direction. The Boussinesq approximation is best applied to large scale turbulent flow or motions typifying the problems in urban and regional areas.

The development of this form of the equation is given by Bird _et al_.[55] The species-mass-conservation models use numerical integrations of various forms of these equations.

The Gaussian plume formulations, however, use closed-form solutions of the turbulent version of the species-mass-balance equation subject to simplifying assumptions. Although these will not be treated further here, their description is included for comparative purposes. The assumptions are: reflection of species off the ground (that is, zero flux at the ground), constant value of vertical diffusion coefficient, and large distance from the source compared with lateral dimensions. This Gaussian solution to the species-mass-balance equation is obtained under the assumption that chemical transformation source and sink terms are all zero. In some cases, an exponential decay factor is applied for reactions that obey first-order kinetics. A typical solution (with the time-decay factor) is:

$$\bar{c}_j(x_1,x_2,x_3) = \frac{Q_j/\rho}{2\pi\sigma_2\sigma_3\bar{v}_1}\left\{\exp\left[-\frac{x_1}{v_1\tau} - \frac{1}{2}\left(\frac{x_2}{\sigma_2}\right)^2 - \frac{1}{2}\left(\frac{x_3-h}{\sigma_3}\right)^2\right]\right.$$

$$\left. + \exp\left[-\frac{1}{2}\left(\frac{x_3+h}{\sigma_3}\right)^2\right]\right\} , \qquad (3)$$

where

Q_j = emission rate of jth species,

p = air density,

h = source height,

τ = chemical decay time for first-order reaction, and

$\sigma_\ell = (2K_{\ell\ell}\,x_1/\bar{v}_1)^{1/2}$.

The three coordinate directions--1, 2, and 3--are taken to be downwind, crosswind, and vertical. The origin is fixed to the ground at the location of the source.

Physicochemical Transformation Simulation

The atmospheric chemical processes undergone by most pollutants are not readily describable by first-order kinetics. Hence, the simple Gaussian plume solution in Eq. 3 is inapplicable in most cases where physicochemical transformations significantly alter concentrations on a time scale or space scale appropriate to an urban airshed.

The general case must be solved by numerical integration with finite-difference schemes or other approaches to the solution of Eq. 2 for the species of interest. As written, this equation requires that the partial-differential equation be solved for each species in the reactive mixture. In reality, however, the number of partial-differential equations that must be solved can be reduced by imposing stationary-state assumptions. That is, some species are so reactive that their rate of production nearly equals their rate of depletion, and these rates may be effectively equated. This being the case, algebraic expressions are used to relate the stationary-state species concentration to all the reactive compounds and radicals that are responsible for its production and removal. For multicomponent mixtures, these are simultaneous nonlinear algebraic equations that must be solved by numerical techniques, such as Newton's method for finding roots of equations.

A generalized notation for representing chemical reactions is:

$$\sum_{j=1}^{s} \nu_{ij} A_j \xrightarrow{k_i} \sum_{j=1}^{s} \nu'_{ij} A_j \qquad (i = 1,2,3,\ldots.,r), \qquad (4)$$

where, for the jth species participating in the ith reaction,

ν_{ij} = reactant stoichiometric coefficient,

ν'_{ij} = product stoichiometric coefficient,

A_j = chemical formula of jth species,

r = number of reactions, and

k_i = rate coefficient of ith reaction

The generality of the index notation permits any specification of a chemical mechanism that the user desires. With the notation, the source term becomes:

$$w_j = (\mu_j/\mu) \sum_{i=1}^{r} \beta_{ij} k_i \prod_{\lambda=1}^{s} (\mu \bar{c}_\lambda/\mu_\lambda)^{\nu_{i\lambda}} \qquad (j = 1,2,3,\ldots.,s), \qquad (5)$$

where

μ_j = molecular weight of jth species,

μ = molecular weight of mixture (air),

$\beta_{ij} = \nu'_{ij}$, and

λ = dummy species index.

Because of fluctuations in turbulent flows, Eq. 5 is only an approximation. Research is underway to correct this deficiency. The use of Equation 5 instead of specific terms retains a degree of generality in the computer program that greatly simplifies alterations of the mechanism.

For stationary-state species, the partial-differential equation represented by Eq. 2 is replaced by the source term in Eq. 5 set equal to zero. This provides the algebraic means for solving for individual species concentrations. These algebraic formulas are carried along in the calculation as constraints on the remaining partial-differential equations.

Discussions of specific chemical mechanisms are found in Chapter 2, and examples of working mechanisms that have been used in models can be found in Friedlander and Seinfeld,[35] Eschenroeder and Martinez,[36,37] Wayne *et al.*,[40] and Reynolds *et al.*[46,48]

EXAMPLES OF SPECIFIC METHODS

Statistical, Rollback, and Box Models

Both linear rollback and modified rollback models were used by Barth[17] to examine federal motor-vehicle emission goals for standards governing carbon monoxide, hydrocarbon, and oxides of nitrogen. The linear rollback principle was suggested and applied to these primary pollutants.

$$R = \frac{(GF)\ (PAQ) - (DAQ)}{(GF)\ (PAQ) - B}, \qquad (6)$$

where R is the fractional reduction required. GF is the growth factor, PAQ is present air quality, DAQ is desired air quality, and B is background concentration. Linear rollback and related models have been heavily emphasized in the regulatory approaches taken to date.

Linear rollback involved direct application of Eq. 6 to carbon monoxide, hydrocarbon, and oxides of nitrogen emission. Modified rollback implies reading from a graph of peak oxidant versus hydrocarbon concentration the needed hydrocarbon reduction and then using Eq. 6 to relate hydrocarbon emission to atmospheric concentrations. The reduction in nitric oxide emission was chosen to achieve the nitrogen dioxide ambient air quality standard, and the reduction in hydrocarbon was tailored to achieve the oxidant standard via the Schuck _et_ _al_. diagram[18] following the modified rollback scheme. This diagram gives envelope curves of the maximal 1-h oxidant observed versus the 6:00-9:00 a.m. average hydrocarbon concentration in five cities. To avoid the inaccuracies of the linear rollback scheme as applied directly to oxidant, Schuck and Papetti[19] have refined the nonlinear or modified rollback scheme. First, they modified the nonlinear rollback method to include 1968-1971 air quality data from the Los Angeles basin. The new approach to modified rollback used an eight-station concentration average in response to the objection that the hydrocarbon concentrations that caused the oxidant buildup occur somewhere other than the oxidant station location. That is, winds will generally sweep the air with the morning hydrocarbon contamination to a location some distance away. Therefore, averaging eight stations tends to distribute this inaccuracy and, it is hoped, cancel it out. The upper-limit curve is stated to be in agreement with regression analyses done at Chevron Research.[20] Because of NO_x inhibition effects, decreasing hydrocarbon emission faster than nitric oxide emission will reduce ozone even more than is predicted by the curve. Working against this bonus, however, is the effect of growth that must be used to correct the percentage hydrocarbon reductions read directly from the curve. The original rollback formula, of course, included gross growth factors. The nonlinear rollback approach has serious deficiencies and should not be used for planning purposes.

Another approach that uses a linear rollback relating primary pollutants to ambient air quality is described by Hamming _et_ _al_.,[21] who presents a series of graphs to show photochemical smog effects in terms of primary pollutant concentrations. Contours of constant oxidant, eye irritation, peak nitrogen dioxide concentration, and time to nitrogen dioxide peak are plotted on NO_x-versus-hydrocarbon planes. The data for the graphs were based on interpretation of the Los Angeles County Air Pollution Control District's experimental-chamber measurements, as well as those of Korth et al.[56] and of Dimitriades.[57] It is cautioned that the chamber results cannot be transferred to the atmosphere on a one-for-one basis, because of wall effects, dilution effects, and other experimental artifacts. The 6:00-9:00 a.m. concentrations of hydrocarbon and NO_x are traced out on graphs. Projections of hydrocarbon and NO_x concentrations are made for future years, but the method of carrying out these projects is not described. Presumably, linear rollback was used to relate emission to precursor concentrations. Hence, in theory, this procedure is one step more nearly complete than the modified rollback used in the oxidant envelope curves. It reflects the influence of the hydrocarbon:nitric oxide ratio on the four photochemical smog effects contoured on the plots. This would have been a direct extension of the modified rollback method, if atmospheric data had been used; however, the authors cite atmospheric trends that tend to support the conclusions that they draw from chamber-data plots. The lack of any explicit means of considering mixture-ratio effects is a major drawback in the use of modified rollback for the present oxidant control strategies, which impose more rapid reduction in hydrocarbon than in NO_x emission. The technique of Hamming et al. holds out the possibility of eliminating this deficiency.

Chang and Weinstock[22] represent the general rollback formula as integrals over time and space of a population of emitters weighted with influence functions. The influence functions (or source-receptor interaction functions) contain the elements of meteorologic and geometric effects. The analysis is restricted to carbon monoxide or any other pollutant that may be nonreactive. The role of an inhomogeneously distributed growth factor is discussed, and a method of correcting rollback for this effect with a diffusion model to obtain the source-receptor interaction functions is proposed. This follows very closely a methodology introduced earlier by the same authors.[23] The rollback formula was corrected for the nonuniformity of growth with the diffusion model and contrasted with the usual straight tonnage approach. The result is a lessening of the requirement for percentage reductions in emission to achieve a specific air quality goal. For cases with regularity in the forms of the source-receptor interaction function, there appears to be a good chance to make general use of this modified rollback approach.

Statistical relationships between air quality measurements and meteorologic variables are also used for calculating future air quality. It is important to note, however, that the statistical relationships are usually related to a fixed-emission-source distribution pattern or one that changes with time in some regular manner. Peterson[24] analyzed 24-h averaged sulfur dioxide concentrations at 40 sites in St. Louis for the winter of 1964-1965. Assuming some linear relationships, he isolated three basic patterns that accounted for most of the variance in the observations. The method of empirical orthogonal functions was used to get regression equations that related pollutant patterns to meteorologic variables. Because this approach performed better than a diffusion model, it appeared to be useful for forecasting, although it contains no explicit relationship to source emission. It might be possible to add an adaptive algorithm to a model like this one and use continuously updated data to reflect changing emission patterns. With meteorologic forecasts, it could then be useful for short-term pollution forecasts, but it would not be applicable to the long-range study of control strategies.

Forecasting formulas for pollutant concentrations at the downtown Los Angeles monitoring station were developed by Merz et al.,[20] who used a time series analysis of the monitoring data. The logarithm of oxidant was fit to the logarithms of hydrocarbon and nitric oxide concentrations up to second-order terms in the logarithm for each of the dependent variables. The formula obtained was based on 624 data points for eight 3-month periods and yielded a correlation coefficient of 0.55 with a standard error of estimate for the oxidant concentration logarithm (base 10) of 0.5. The diagram was constructed to provide a graphic working basis for the formula derived. This model relates pollutants with one another, but does not relate emission to air quality and, therefore cannot be used for planning emission control strategies.

Trijonis[25] determined statistical empirical relationships for primary and secondary pollutants. The primary-pollutant formula assumed linear rollback for each concentration along the frequency distribution. This was based on the usual supposition that the pollutant is inert and that changes in emission are proportional in space and time. The method was applied to nitrogen dioxide for central Los Angeles on the basis of NO_x emission projections. Another relationship was concerned with photochemical secondary pollutants, specifically oxidant. It followed the assumption that the probability of exceeding a prescribed concentration depends on the extent of emission of primary pollutants that react to form oxidant. The specific oxidant-precursor relationship was implicit in a series of probability curves that depended on morning NO_x concentration in central Los Angeles. Curves were developed for various constant concentrations of morning hydrocarbon (adjusted for methane). The relationships were derived from 5 years of monitoring data. This approach constitutes another method of accounting for the influence of hydrocarbon: NO_x ratios on smog predictions.

Correlations of ozone concentrations with solar radiation, wind speed, and temperature data were prepared by Bruntz et al.[26] for a monitoring station at Welfare Island in New York City. Insights into these correlations were gained by means of a "weathervane plot," which displays ozone versus solar radiation with circular symbols whose diameters are proportional to temperature. Lines on each circle were applied to represent wind speed and direction vectorially. An equation of ozone proportional to $(\text{solar radiation})^{\theta_1} \times (\text{wind speed})^{\theta_2} \times (\text{temperature})^{\theta_3}$ is suggested by an examination of the graph. While interesting correlations emerge from this work, no relationship to emissions is provided.

McCollister and Wilson[27] proposed two time series models based on forecasting some future event by applying a linear formula to a past event. One model uses today's maximal value of peak carbon monoxide or oxidant to predict tomorrow's peak value. The other model uses data averaged over each hour today to predict concentrations for corresponding hours tomorrow. Each model is evaluated by dividing the mean absolute error by the mean value for days in 1972 using coefficients derived from years before 1972. Evaluation results are described later. Again, nothing in this model explicitly shows how emissions affect air quality.

The box model is one of the simplest forms of solutions of Eq. 2 that appears in air quality simulation techniques. It assumes that the air bounded by the ground and the mixing height is uniform. It further considers that the source intensity of pollution emanating from the ground is constant and that the wind speed is constant. The consequence of these assumptions is a simple formula that states that the ambient concentration of some pollutant is directly proportional to the source emission rates and inversely proportional to the wind speed. The constant of proportionality is determined from mixing height or is derived empirically. One form of this type of model was suggested by Hanna.[28] He assumed the constant of proportionality to be taken as the width of the region divided by the average mixing depth appropriate to the scale of the region. This constant is approximately 225 for many cities. Gifford and Hanna[29] conducted tests of the simple model for particulate matter and sulfur dioxide predictions for annual or seasonal averages versus diffusion-model predictions. Hanna[30] went on to apply the simple dispersion model to the analysis of chemically reactive pollutants. This required that each reaction achieve a steady state within the space and time scale of the airshed of interest. It was concluded that chemical concentrations indicate the lack of steady state for nearly calm conditions of low mixing depth, but that the chemistry does not significantly interfere with the use of a simple model for sunny and windy conditions. For calculational purposes in the example taken for Los Angeles, the reactive hydrocarbon emission was assumed equal to the "published propylene emission." Gifford and Hanna state that "detailed urban diffusion models developed so far have the property that they generate more pollution variability than is actually observed to occur. This seems to us to be a strong argument for the use of simpler models." "Variability" is undefined, and the degree of variability that is generated by the simpler models is not stated.

After the application of the simple model to chemically reactive pollutants,[30] Lamb and Seinfeld[31] disagreed sharply with the contention that the simple dispersion model proposed by Hanna could be applied to the photochemical smog problem. They argued that the rate of change depends on more variables than concentration alone, that spatial variations cannot be neglected, that steady-state conditions are highly unlikely, that the height of the pollution layer does indeed extend to the edge of the mixing layer, and that more than local sources influence ground-level pollution concentrations.

In reply to these criticisms, Hanna[32] addressed the objections point by point. He stated that the use of regionally averaged variables is a necessary first step and has no special limitations. He asserted that the simple model formulation does not assume steady-state conditions, but that such conditions often occur. He restated the belief that local sources are the chief influence on ground concentrations. The number of chemical parameters available with the simple model depended on the complexity of the mechanism and was therefore considered to be arbitrarily complex. It was further contended that the reason that there are few restrictive assumptions listed for the simple model is that it has few limitations. Further comparisons with more complex models were drawn on the grounds that the correlation coefficients for observed versus predicted data were comparable or better with the simple model.

On the basis of these discussions it does not appear that the simple model is applicable to chemically reactive pollutants.

Finite-Difference Simulations

Correct modeling of variable diffusivity, time-dependent emission sources, nonlinear chemical reactions, and removal processes necessitates numerical integrations of the species-mass-balance equations. Because of limitations of dispersion data, emission data, or chemical rate data, this approach to the modeling of air pollution may not necessarily ensure higher fidelity, but it does hold out the possibility of the incorporation of more of these details as they become known.

An early analog-computer study of the solution to the species-mass-balance equations was done by Karplus et al.[33] This work consisted on a one-dimensional time-dependent diffusion equation with chemical source terms representing a multicomponent atmospheric kinetic system. An electronic analog computer was used, with one integrator at each node between space cells to handle the combined effects of mass transfer and chemical reaction. Results were obtained for a simple mechanism, but no tests of validity were made. Ulbrich[34] also used a series of boxes that were coupled in a model of the species-mass-balance equations. He integrated a data-management system with a model system for real-time prediction and control. A long-term cost-minimizing strategic command and control system was formulated. Adaptive features were built into this control system. The system model conceived for Los Angeles was a series of seven boxes, each covering 288 square miles. Each box was assumed to be well mixed and was advectively coupled to its neighbors. A smog delay time of 1.5 h was set into the system. The only emission that was considered was that of nitric oxide.

Similarity solutions of the species-mass-balance equations were assumed by Friedlander and Seinfeld[35] for a simple photochemical-smog reaction scheme. (This scheme assumed a steady-state condition for ozone.) Demonstration runs were shown for parametric variations in the system of ordinary differential equations that emerged from the partial-differential equations. Analytic solutions yielded atmospheric reaction criteria that were usable for correlating smog variables.

Pollutants emitted by various sources entered an air parcel moving with the wind in the model proposed by Eschenroeder and Martinez.[36,37] Finite-difference solutions to the species-mass-balance equations described the pollutant chemical kinetics and the upward spread through a series of vertical cells. The initial chemical mechanism consisted of seven species participating in 13 reactions based on smog-chamber observations. Atmospheric dispersion data from the literature were introduced to provide vertical-diffusion coefficients. Initial validity tests were conducted for a static air mass over central Los Angeles on October 23, 1968, and during an episode late in 1968 while a special mobile laboratory was set up by Scott Research Laboratories.[58] Curves were plotted to illustrate sensitivity to rate and emission values, and the feasibility of this prediction technique was demonstrated. Some problems of the future were ultimately identified by this work,[38] and the methodology developed has been applied to several environmental impact studies (see, for example, Wayne _et_ _al_.[40]).

Concern is sometimes expressed regarding the role of surface reactions on aerosol as an interference in the buildup of photochemically produced ozone. An upper-limit analysis was carried out by Eschenroeder, Martinez, and Nordsieck[38] to assess the effect of 200-$\mu g/m^3$ loading of 0.5-μm-diameter particles. Ratios of surface-reaction rates to gas-phase rates for 100% surface reaction efficiencies were computed. Early in the day, nitric oxide and nitrogen dioxide surface reaction rates can be a few hundred times the gas-phase reaction rate, under the assumption that each molecular collision with the particle surface constitutes a successful reactionevent. In the middle of the day, nitrogen dioxide and ozone surface-reaction rates in this limit are 10-50 times the corresponding gas-phase reaction rates, again assuming 100% efficiency. The efficiencies of surface reactions are more nearly in the 10^{-6}-10^{-4} region. Therefore, the high upper-limit values must be reduced considerably to reflect realistic conditions. It is therefore likely that the ozone buildup is affected little by aerosol surface reactions; however, the formation of nitrate in the aerosol, which is observed to take place in the morning, may be marginally important, compared with the gas-phase reaction.

Another Lagrangian photochemical model was developed by Wayne et al.[40] This photochemical model uses a moving "cell" or "air mass" that follows an air trajectory either from a specified source or to a specified receptor. The emission input from the ground-based sources is expressed as a time-dependent influx of primary pollutants. Diffusive spread need not be computed in this model, because the air in the cell is assumed to be homogeneously mixed at all times. This brings about a tremendous advantage in reduced computing time. The chemical mechanism represents reactive hydrocarbons as propylene and lumps others into a generic dummy hydrocarbon. Reactivity is handled by specifying the mix of propylene and generic hydrocarbon. Performance evaluation results are reported for September 30, 1969, on the basis of arbitrarily assigned initial values for hydrocarbon concentrations and neglecting stationary emission of NO_x.

Mahoney and Egan[41,42] developed a two-dimensional time-dependent diffusive and advective model that neglects vertical velocity. Chemical reaction is also neglected. The source term is an effective volume source in the bottom grid mesh cell of the calculation. The authors discussed the pseudodiffusion errors that arise with the large grid spacing that is appropriate to urban-scale calculations. They pointed out that this error is orders of magnitude larger than natural diffusion. A puff example from a volume source was presented in the paper. The scheme proposed avoids pseudodiffusion by using moments of the concentration distribution in the governing equations. The concentration profile was reconstructed by using the computed first and second moments. Egan and Mahoney[43] applied the model to estimate ground concentrations under different meteorologic conditions. Velocity profiles and vertical-diffusivity profiles were introduced on the basis of various stability conditions. Two-dimensional time-dependent solutions with variable advective velocity were obtained. Test cases were presented, including the effects of wind-velocity vector changes with height and the effects of this velocity field distortion on the dispersion of air pollutants. Elevated inversions and time-dependent mixing heights were also investigated. The height variation of the velocity field was shown to be important under stable conditions. Although this model does not treat air chemistry, it can resolve subgrid scale elements because of the moment method used.

A solution to the species-balance equation was generalized by Lamb and Neiburger[44] to allow for the space and time distribution of pollutant

Preceding page blank

emission, diffusion coefficients, and wind field. Pollutant removal at the ground and leakage through the upper boundary were also allowed for in this model. A transformation to a Lagrangian coordinate system was made, and the model was adapted to various source emission configurations. It was tested for carbon monoxide concentrations in the Los Angeles basin for September 23, 1966. It considered vehicular sources based on freeway and surface-street traffic counts. The authors plotted observed versus predicted concentrations for four stations and found that the morning "peak" in concentration was exaggerated by the model, but that the midday "valley" was underestimated.

Seinfield et al.[45] and Reynolds et al.[46] discussed theoretical aspects of urban air pollution modeling in terms of the species-mass-balance equations cast into a problem requiring specification of initial and boundary values of field quantities. Restrictions of K theory in turbulence approximations were reviewed. The vertical coordinate system was mapped between the ground and the inversion base by a linear stretching transformation. The methods were detailed for interpolating discrete data on winds and vertical stability to obtain field values needed for the calculations. The kinetic mechanism that uses lumped parameters for hydrocarbon change was outlined. Eulerian difference equations were integrated numerically, and a method of fractional steps was described. Explicit differencing was used for horizonal coordinates, and implicit differencing for the vertical terms of the equations. In a later paper in the series, Roth et al.[47] gave a detailed description of an emission model and an inventory for the Los Angeles basin. Automotive emission was discussed with a breakdown into surface-street and freeway categories. Average-trip-speed correction factors were allowed for, and cold-start corrections for automotive emission factors were introduced. Spatial distributions of daily vehicle miles traveled were laid out on a 2-mile grid for the Los Angeles basin. An overall temporal distribution was adopted, and deviations from this at various locations were shown to be small. Ground and flight operations of aircraft were discussed, but only ground emission was included in the actual application of the model. Reactivity of hydrocarbon from aircraft was considered to be the same as that from automobiles. Stationary sources were categorized as power plants, refineries, and distributed sources. This paper serves as a prototype for future source-emission inventory processes that are intended to supply modelers with input data.

Reynolds et al.[48] described the process of evaluation of the airshed photochemical model. Kinetic mechanisms were checked against smog-chamber tests, yielding branching factors and rate parameters for the simplified lumped-parameter scheme. A microscale model was established to correct for local effects around monitoring station sites. An evaluation procedure involved preparing data, preparing initial and boundary conditions, checking for agreement with carbon monoxide, and testing computed versus observed values for reactive pollutants. The results agreed rather well with observations, but no statistical performance measure was used at this stage of the work.

Sklarew et al.[49] used a particle-in-cell K theory (PICK) approach to calculate atmospheric diffusion and reaction. The method was applied to carbon monoxide pollution in Los Angeles and predicted daily averaged concentrations reportedly within 20% of measured averages for 12 monitoring stations. Photochemical smog simulation was demonstrated, but the results were hampered by the use of the early prototype of lumped-parameter chemical mechanisms,[36] which did not adequately represent the influence of differing hydrocarbon: NO_x ratios. Also, the carbon monoxide results required inordinately high carbon monoxide emission by the Pacific Ocean.

Knox[50] summarized recent developments at the Lawrence Livermore Laboratory. The computation using the Lagrangian large-cloud dispersion model* was shown to agree moderately well with the measurement of gross beta-particle activity in the cloud of a nuclear test burst. A three-dimensional atmospheric-diffusion particle-in-cell code was described in which marker particles are traced through an Eulerian grid that was distorted to fit topography. A grid followed the cloud center to minimize the number of cells and to minimize pseudodiffusion. Mass-consistent wind-field modeling was also discussed. This form of modeling considers the confining effects of an elevated inversion and the variable topography on the surface wind measurements. A multibox regional air pollution model was run for the San Francisco Bay area for carbon monoxide, and the calculated surface concentrations were approximately 20-50% above the observed concentrations. The frequency distribution predicted for the concentrations, however, paralleled closely the observed frequency distributions.

Gradient diffusion was assumed in the species-mass-conservation model of Shir and Shieh.[51] Integration was carried out in the space between the ground and the mixing height with zero fluxes assumed at each boundary. A first-order decay of sulfur dioxide was the only chemical reaction, and it was suggested that this reaction is important only under low wind speed. Finite-difference numerical solutions for sulfur dioxide in the St. Louis area were obtained with a second-order central finite-difference scheme for horizontal terms and the

---

*A model for calculating the time dependent airborne concentration, surface air concentration, and dry and/or wet deposition of pollutants from large clouds.

Crank-Nicolson technique for the vertical-diffusion terms. The three-dimensional grid had 16,800 points on a 30 x 40 x 14 mesh.

PERFORMANCE OF PREDICTION TECHNIQUES

Before we examine the performance of various models for predicting ambient air quality, it is important to review the criteria for selecting a particular model. In this selection process, it is essential to consider the following factors:

- The precision required for forecasting air quality impact.
- The conditions of high concentrations of air pollutants in the selected region.
- The severity of vehicle-generated pollution relative to that from other sources.
- The availability of meteorologic and air quality data for the selected region.
- The availability of geographic and temporal distributions of emission sources.
- The effect of stack heights associated with large point sources on regional air quality.
- The relative influences of spatial emission distribution, time dependence, and chemical reactions on regional pollution patterns.
- The time and money available for modeling.

Many standard statistical tests are available to evaluate the performance of models against observations. It should be pointed out, however, that graphic checks on the performance of models are also necessary. Anscombe[59] has brought this out strikingly with specific numerical examples. He showed that pure regression analysis can be extremely misleading and demonstrated what can happen in purely numerical analysis of data. In his paper, four artificial data sets of x and y values were given; they are reproduced in Table 5-1. Suppose that x is an observed pollutant concentration, and y is a concentration computed from a model. If standard statistical analytic techniques are performed on these four sets, it can be shown that they posess identical values of the following calculations:

- Number of observations: 11
- Mean of the x's: 9.0
- Mean of the y's: 7.5
- Equation of the regression line: $y = 3 + 0.5x$
- Sum of squares of $x - \bar{x}$: 110.0
- Estimated standard error of slope of regression line: 0.118
- Multiple correlation coefficient: 0.667

Table 5-1

Sample Data Sets Given By F. J. Anscombe[59]

(x = observed pollutant concentration; y = model-computed concentration)

Set 1		Set 2		Set 3		Set 4	
x	y	x	y	x	y	x	y
10.0	8.04	10.0	9.14	10.0	7.46	8.0	6.58
8.0	6.95	8.0	8.14	8.0	6.77	8.0	5.76
13.0	7.58	13.0	8.74	13.0	12.74	8.0	7.71
9.0	8.81	9.0	8.77	9.0	7.11	8.0	8.84
11.0	8.33	11.0	9.26	11.0	7.81	8.0	8.47
14.0	9.96	14.0	8.10	14.0	8.84	8.0	7.04
6.0	7.24	6.0	6.13	6.0	6.08	8.0	5.25
4.0	4.26	4.0	3.10	4.0	5.39	19.0	12.50
12.0	10.84	12.0	9.13	12.0	8.15	8.0	5.56
7.0	4.82	7.0	7.26	7.0	6.42	8.0	7.91
5.0	5.68	5.0	4.74	5.0	5.73	8.0	6.89

Figures 5-2 through 5-5 show the great contrasts in the actual data that are revealed by a graphic presentation, but are totally concealed in the above results of standard analytic procedures. Figure 5-2 shows a typical scatter plot, but the other three reveal regularities that may be missed by linear regression analysis--a smooth curve, a different straight line with an outlier, and x values all the same except for an outlier.

The meaning of this example for model performance evaluation is significant: if measures are confined to the usual statistical tests, a great deal of information can be lost. The loss of information tends to perpetuate biases in the calculations, which might otherwise be eliminated. The message is clear. One should beware of correlation analysis alone. Questions of data regularity that can be resolved by graphic presentations must be pursued, as well as those which pertain to regression analysis alone.

Rollback, Statistical, and Box Model Performance

Eschenroeder[60] compared linear rollback results with photochemical-diffusion model results in assessing the effects of various stages of the original transportation control plan formulated by a federal regulatory agency. Technologic controls without a reduction in the number of vehicle miles traveled (VMT) were considered as a first stage, and successive percentages of VMT reduction were considered as further stages. For the first stage of control, the photochemical-diffusion models suggested more rapid reduction in peak photochemical oxidant concentration than linear rollback, because the latter fails to account for nitric oxide inhibition effects. Reactive hydrocarbon (RHC) is the only precursor considered by the rollback method. In reality, the ratio of RHC to NO_x also has a decided influence on the oxidant production.

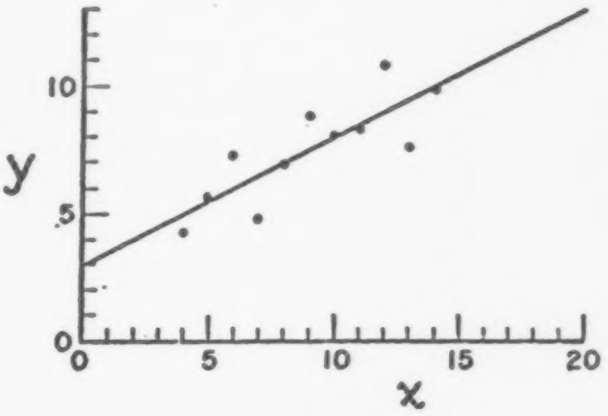

Figure 5-2.
Graph of data in Anscombe's sample set 1[59]
(see Table 5-1)

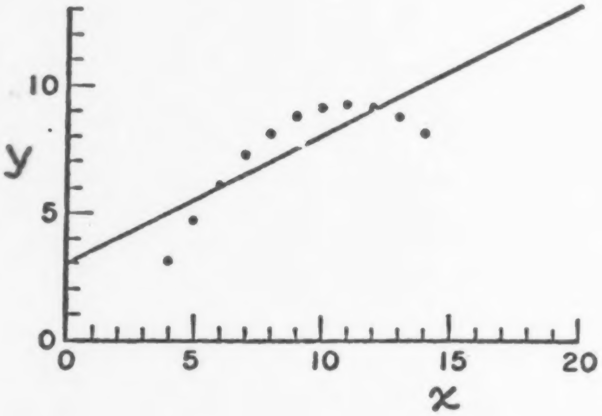

Figure 5-3.
Graph of data in Anscombe's sample set 2[59]
(see Table 5-1)

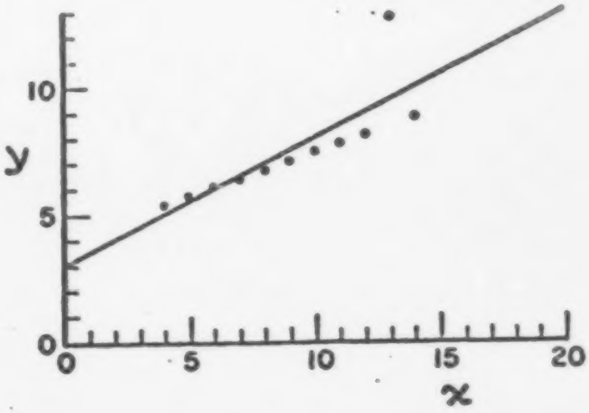

Figure 5-4.
Graph of data in Anscombe's sample set 3[59]
(see Table 5-1)

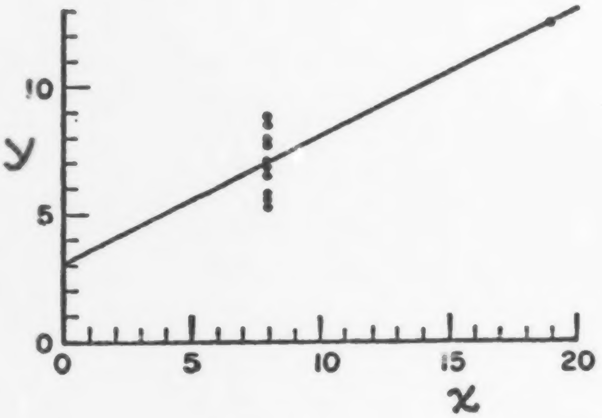

Figure 5-5.
Graph of data in Anscombe's sample set 4[59]
(see Table 5-1)

Excess NO_x slows the production of oxidant. Successive stages of emission control brought about by reductions in VMT show less than proportional reductions in photochemical oxidant according to the photochemical diffusion model. This occurs because RHC and NO_x are being reduced in the same ratio, which has a weaker influence on oxidant than in the case of more rapid reductions in RHC. This comparison illustrates the need to consider nonlinearities in the case of reactive pollutants when using rollback models.

In another study, Martinez and Nordsieck[61] found that comparing linear rollback with a photochemical model gave very nearly the same results for peak oxidant for the year in the distant future when extensive controls would be imposed. The agreement between the two methods, however, was poor in a case in which NO_x controls were frozen at 1974 values, instead of being progressively applied as rapidly as RHC controls. This case is designated 1980d in Table 5-2, which summarizes the results for forecast ozone concentrations on the basis of both linear rollback and the photochemical-diffusion model. The frozen-controls case (1980d) shows the large disparity between the methods because of the failure of rollback to consider the effects of mixture ratios of precursor pollutants on oxidant formation.

Reynolds and Seinfeld[62] compared the statistical model of Trijonis[25] with their dynamic model[45-48] and with linear rollback. Considering 1977 emission with and without one of the EPA abatement plans in effect, they obtained a reduction from 80 to 20 in the number of days on which the oxidant standard is exceeded and from less than 15 days to less than 10 days for exceeding the nitrogen dioxide standard. (The oxidant standard is defined on the basis of hourly average, and the nitrogen dioxide standard is defined as an annual

Table 5-2.

Baseline Values of Maximal Hourly Average Ozone Concentration in Vicinity of Riverside[a]

	Maximal Hourly Average Ozone Concentration, ppm	
Year	Diffusion Kinetics Model	Linear Rollback
1980	0.16	0.16
1990	0.15	0.13
2000	0.15	0.13
1980d	0.12	0.17

---

[a] Derived from Martinez and Nordsieck.[61] See text for explanation.

average.) These findings, which were obtained with the Trijonis model, were limited to one monitoring station because of the method by which that model was calibrated. The dynamic model was run with two ways of specifying future initial conditions and grid boundary conditions for the calculations. It was not stated whether linear or nonlinear rollback was used. Comparisons were then made between 1969 (the reference year) and 1977 both with and without the EPA abatement plan in effect in 1977. The dynamic-model calculation showed a 76% reduction in carbon monoxide from 1969 to 1977 with the EPA abatement plan in effect and only a 65% reduction without it. Rollback agrees with the 65% reduction, because the conditions for its validity with an inert pollutant are fulfilled. Nitrogen dioxide peak concentrations were reduced by 5-8% without the plan and by 60-76% with the plan, according to the dynamic model. Rollback predicted only a 34% reduction with the plan. For ozone, the dynamic-model results suggested that the abatement plan is more effective than the rollback model would predict--namely, that up to a 94% reduction in maximal ozone was predicted by the dynamic model, and a 74% reduction was predicted by rollback. The 1969-1977 ozone reductions without the abatement plan in effect are 39% according to rollback and 65-75% according to the dynamic model. As was the case with the Hamming *et al.*[21] and Eschenroeder[60] calculations, this illustrates for ozone that it is necessary to consider both RHC and NO_x in the rollback calculation, not only RHC. If the RHC emission is reduced faster than the NO_x emission, the ozone concentrations at a given station may decrease in greater proportion than the RHC concentrations.

Peterson[24] used the skill score to evaluate the performance of his empirical statistical model based on orthogonal functions. The skill score equals 1.0

when all calculated and observed concentrations agree, but 0 when the number of correctly predicted results equals that expected by chance occurrences. The statistical technique had a skill score of 0.304. An 89-day, 40-station set of the data was used to check a Gaussian diffusion model, and this technique gave the diffusion model a skill score of only 0.15. It will be recalled that the statistical empirical model was used for 24-h averaged sulfur dioxide concentrations at 40 sites in St. Louis for the winter of 1964-1965.

The time-series analysis results of Merz et al.[20] were expressed in first-order empirical formulas for the most part. Forecasting expressions were developed for total oxidant, carbon monoxide, nitric oxide, and hydrocarbon. Fitting correlation coefficients varied from 0.547 to 0.659. As might be expected, the best results were obtained for the primary pollutants carbon monoxide and nitric oxide, and the lowest correlation was for oxidant. This model relates one pollutant to another, but does not relate emission to air quality. For primary pollutants, the model expresses the concentrations as a function of time.

Bruntz et al.[26] applied multiple regression analysis and found that the method of least squares yielded a set of coefficients that produced an 0.84 correlation of ozone concentration with the data. Adding mixing height to the correlation yielded no statistically significant improvement in agreement with the assertions of Hanna.[30]

The first time-series model of McCollister and Wilson[27] yields results around 0.4 for the mean absolute error divided by the mean value for the days in 1972, on the basis of parameters derived before 1972. By comparison, a persistence model yields about 0.5 for the same parameter, and Los Angeles APCD forecasts lie between the time-series results and the persistence-model results. The hourly oxidant time-series model yields errors from 0.3 to 0.45, whereas persistence yields errors of 0.4-0.5. For carbon monoxide, the hourly-model results lie between 0.15 and 0.5—consistently below the persistence results.

Gifford and Hanna[29] tested their simple model for particulate matter and sulfur dioxide predictions for annual or seasonal averages against diffusion-model predictions. Their conclusions are summarized in Table 5-3. The correlation coefficient of observed concentrations versus calculated concentrations is generally higher for the simple model than for the detailed model. Hanna[30] calculated reactions over a 6-h period on September 30, 1969, with his chemically reactive adaptation of the simple dispersion model. He obtained correlation coefficients of observed and calculated concentrations as follows: nitric oxide, 0.97; nitrogen dioxide, 0.05; and RHC, 0.55. He found a correlation coefficient of 0.48 of observed ozone concentration with an ozone predictor derived from a simple model, but he pointed out that the local inverse wind speed had a correlation of 0.66 with ozone concentration. He derived a "critical wind speed" formula to define a speed below which ozone prediction will be a problem with the simple model. Further performance comparison of the simple box model with more detailed models will be discussed later.

Species-Mass-Balance Model Performance and Comparative Evaluations

Sklarew *et al.*[49] evaluated their particle-in-cell K-theory approach for atmospheric diffusion of carbon monoxide and for photochemical smog. All-day averages of carbon monoxide concentration were predicted to be within 20% of the

Table 5-3.

Test of Simple Model for Particulate Matter and Sulfur Dioxide Predictions[a]

City	No. Sampling Sites	Source Area Size, km^2	Correlation Coefficient, observed vs. calculated concentrations	
			Simple Model	Detailed Model
Memphis	9	25	0.68	0.73
Nashville	16	25	0.91	0.80
Ankara	10	9	0.63	0.59
Bremen	4	16	0.65	0.05
"Test City"	8	25	0.98	0.96

---

[a] Derived from Gifford and Hanna.[29]

measured averages at 12 monitoring stations, and the correlation coefficient of measured with observed concentrations was 0.73.

In his survey,[15] Sklarew covered evaluation studies and summarized the results of correlation coefficients and root-mean-square (rms) errors from a linear regression between observed and calculated values for three photochemical models.[63,64,65] The statistical comparisons are shown in Tables 5-4 and 5-5 for carbon monoxide and ozone, respectively. It is notable that the correlation coefficients are considerably higher than those reported for many Gaussian models. Similarly, the regression lines have slopes closer to unity than those from the Gaussian models. Extreme caution must be exercised in comparing performance measures directly, because of the intrinsic differences between trajectory and grid models and between evaluation test designs. Nappo[66] evaluated eight mathematical models and 24-h persistence with six different measures of performance evaluation for carbon monoxide predictions. The usual measure of correlating the time-averaged concentrations was applied to the computed versus observed values. Table 5-6 summarizes these results, with computer time and computer costs estimated for an IBM 360/65 system. This is one of the few attempts to supply information that could enter a cost-effectiveness analysis. The data base used by Nappo consisted exclusively of computed and observed concentrations that are reported in the literature (see table for references). The averaging time for each data set varied according to the time interval for which each model was run. For example, if a model were designed to predict hourly averages and was run for an 8-h interval, the averaging time for the data set was chosen to be 8 h.

Table 5-4

Statistical Comparison of Model Calculations and Observations of Carbon Monoxide Concentration[a]

Model[b]	Ref.	No. Data Points	Correlation Coefficient	RMS Error, ppm	Regression Line[c] (y = ax + b)	
					a	b
SAI	99	514	0.79	3.4	1.09	0.68
PES	100	71	0.82	3.0	0.91	-0.70
GRC	101	149	0.80	3.7	1.01	-0.37

---

[a] Derived from Sklarew.[15]

[b] SAI = Systems Applications, Inc., PES = Pacific Environmental Services, Inc., GRC = General Research Corporation.

[c] y = observed, x = calculated.

Table 5-5

Statistical Comparison of Model Calculations
and Observations of Ozone Concentration[a]

Model[b]	Ref.	No. Data Points	Correlation Coefficient	RMS Error, ppm	Regression Line[c] (y = ax + b) a	b
SAI	99	574	0.69	0.063	0.76	3.9
PES	100	63	0.49	0.069	0.46	-7.6
GRC	101	151	0.92	0.021	0.84	2.3

---

[a] Derived from Sklarew.[15]

[b] SAI = Systems Applications, Inc., PES = Pacific Environmental Services, Inc., GRC = General Research Corporation.

[c] y = observed, x = calculated.

Table 5-6.

Model Evaluation Based on Temporal Characteristics[a]

Model	Average Temporal Correlation Coefficient	Computer Time for 24-h Prediction, min	Computer Cost for 24-h Prediction, $
MacCracken et al.[67] multibox	0.37	106	350
24-h persistence	0.47	0	0
Roth et al.[68] primitive equation	0.52	60	200
Hanna[69] ATDL simple model	0.60	0	0
Sklarew et al.[70] particle-in-cell	0.65	49	160
Pandolfo and Jacobs[71] primitive equation	0.66	20	70
Reynolds et al.[63] primitive equation	0.73	30	100
Eschenroeder et al.[65] trajectory	0.73	15	50
Lamb and Neiburger[44] trajectory	0.90	35	115

[a] Derived from Nappo.[66]

In addition to the temporal correlation coefficient, the spatial correlation coefficient was calculated approximately for fixed values of time. Except for one of the mathematical models,[69] all techniques showed a better temporal correlation than spatial correlation. The two correlation coefficients are cross plotted in Figure 5-6. Nappo stressed that correlation coefficients express fidelity in predicting trends, rather than accuracy in absolute concentration predictions. Another measure is used for assessing accuracy in predicting concentrations: the ratio of predicted to observed concentration. Nappo averages this ratio over space and over time and extracts the standard deviation of the data sample for each. The standard deviation expresses consistency of accuracy for each model. For example, a model might have a predicted: observed ratio near unity, but with a wide variability of the ratio about its mean value. All the models tested have ratios that average within ±40% of unity (including 24-h persistence), with two exceptions--the Hanna simple model[69] and the Lamb and Neiburger trajectory model.[44] It should be noted that this measure of model performance produced a rank ordering very different from that of the usual temporal correlation test. Figure 5-7 shows the mean ratios of predicted to observed concentration with uncertainty bars characterized by the standard deviation of the ratios about their mean. Figure 5-8 shows the space-averaged temporal standard deviation plotted against the time-averaged spatial standard deviation of these ratios. The models have both standard deviations less than 0.5, except those of Roth et al.,[68] Pandolfo and Jacobs,[71] and Hanna[69] and 24-h persistence.

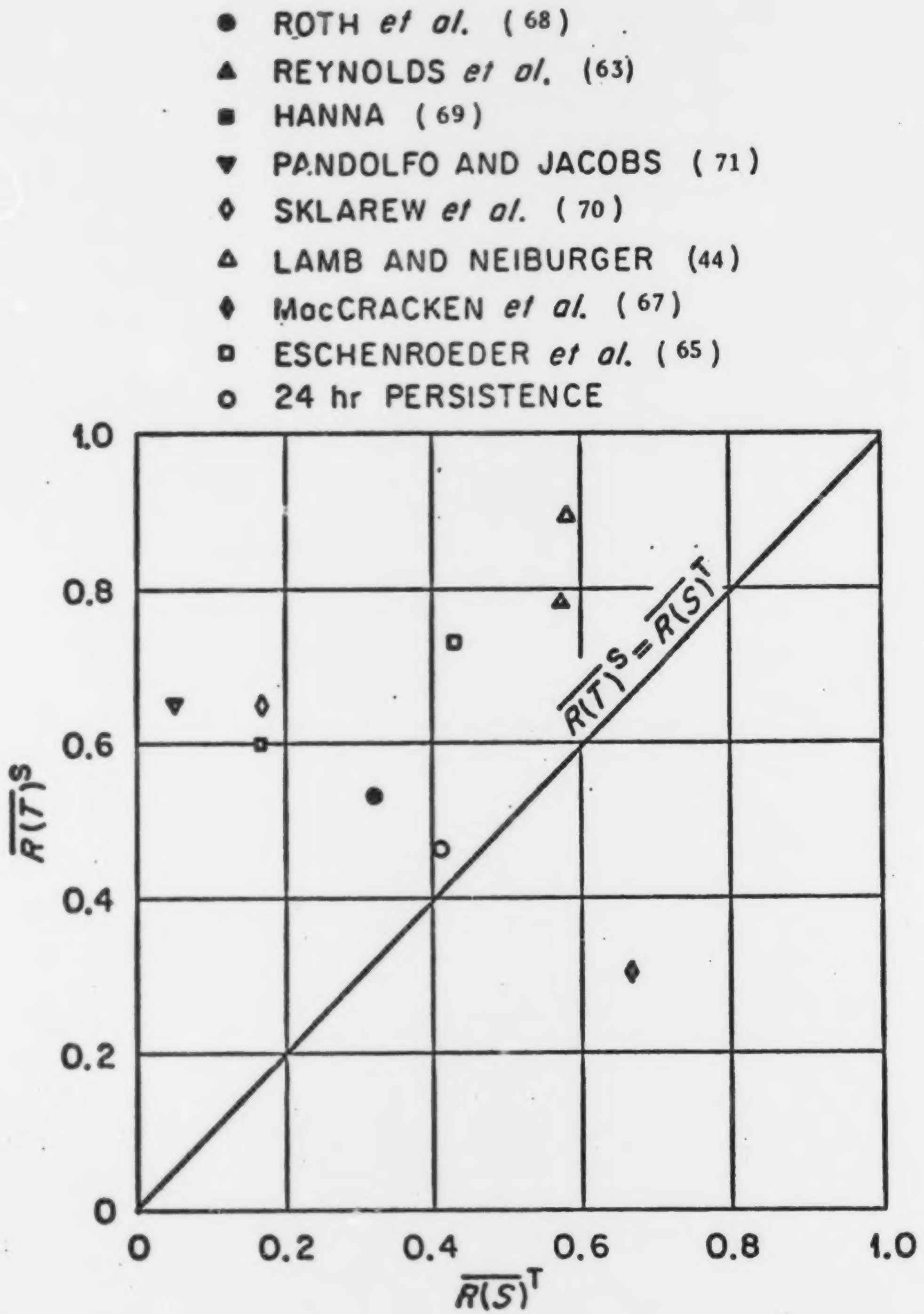

Figure 5-6. $\overline{R(t)}^s$ versus $\overline{R(s)}^t$—space-averaged temporal correlation coefficient versus time-averaged spatial correlation coefficient. Points are averages for each model tested. (Reprinted with permission from Nappo;[66] reference numbers changed to conform with this volume.)

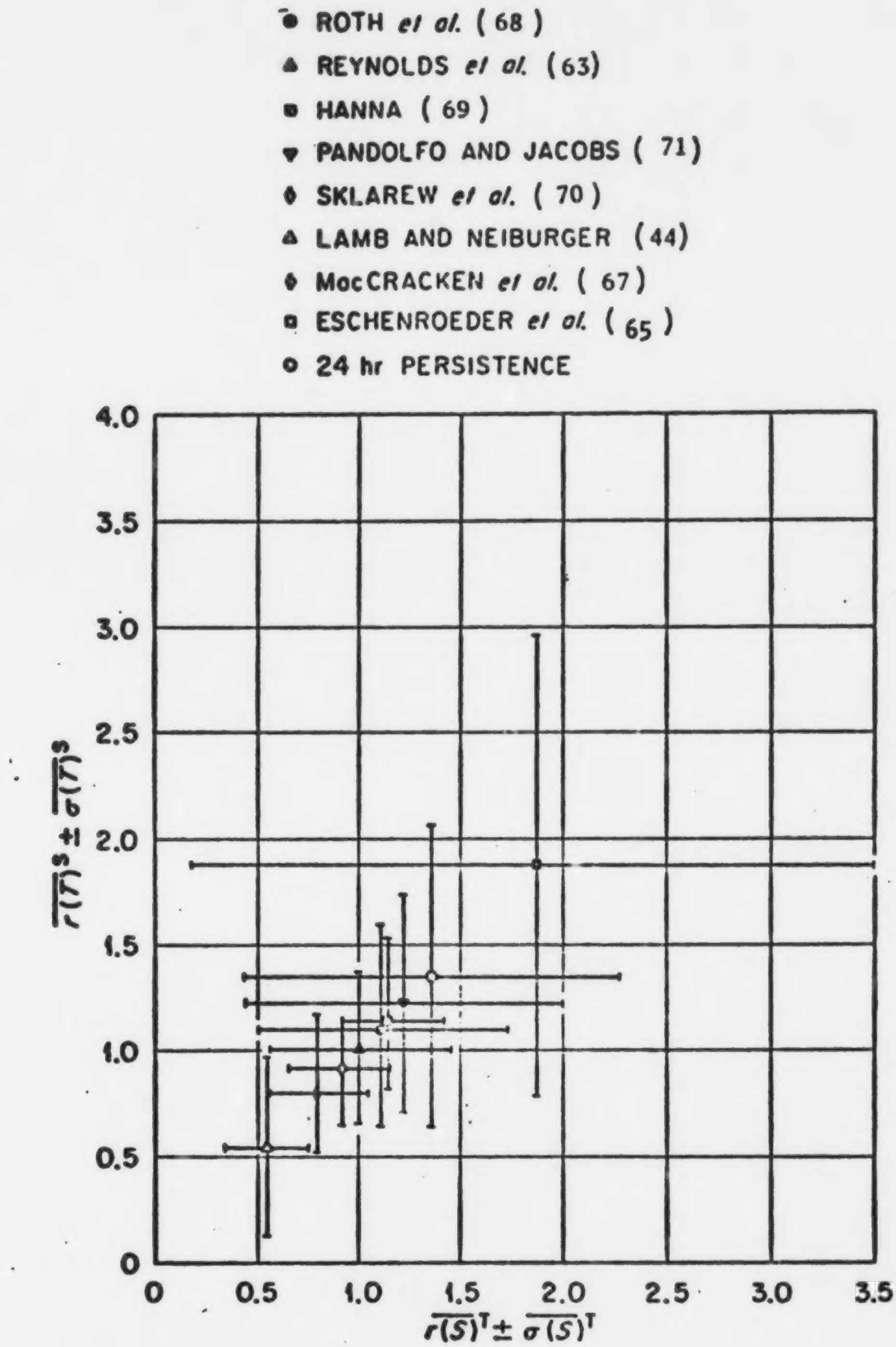

Figure 5-7. $\overline{r(t)}^s \pm \overline{\sigma(t)}^s$ versus $\overline{r(s)}^t \pm \overline{\sigma(s)}^t$ (see text for definitions). Points are averages for each model tested. (Reprinted with permission from Nappo;[66] reference numbers changed to conform with this volume.)

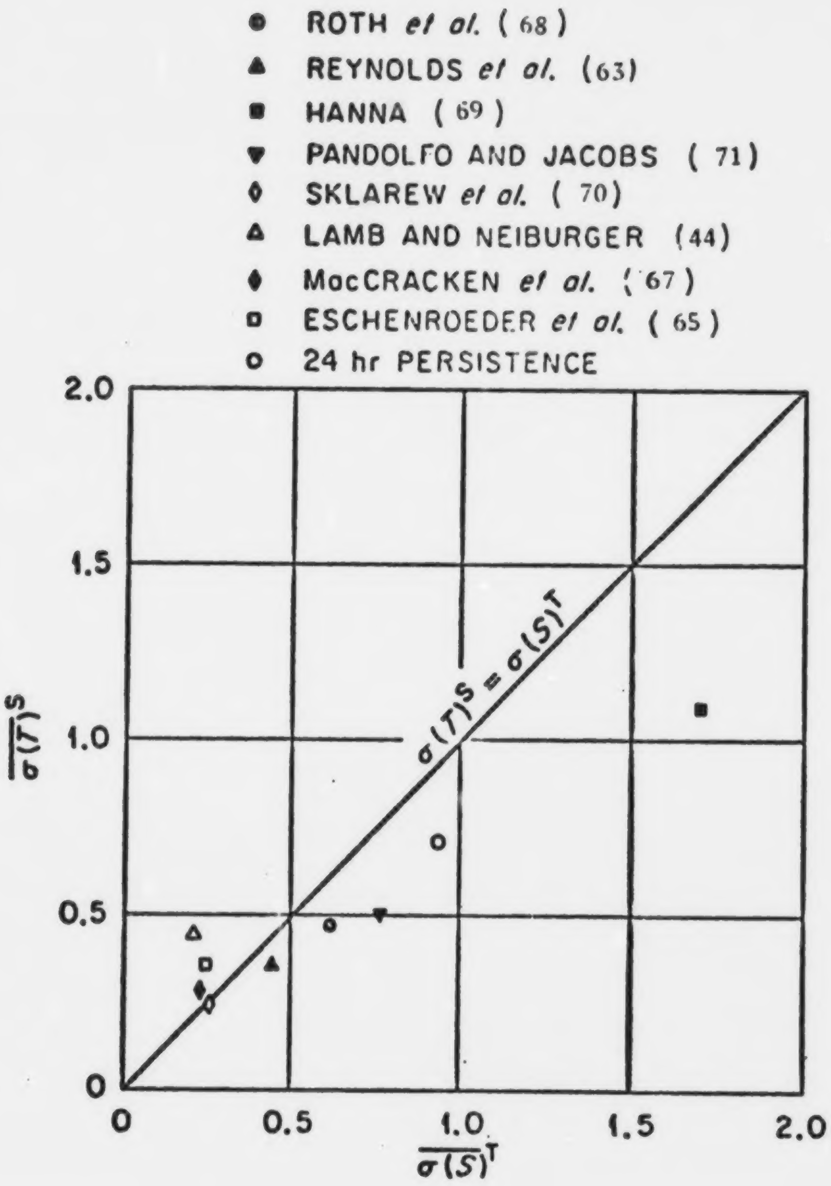

Figure 5-8. $\sigma(t)^s$ versus $\sigma(s)^t$. Points are averages for each model tested. (Reprinted with permission from Nappo;[66] reference numbers changed to conform with this volume.)

Whitney[72] evaluated the evaluation studies of predicted values derived by photochemical models with actual measurements. To assess the validation tests sponsored by the EPA for three different approaches,[63-65] Whitney proposed several statistical evaluation measures of model performance. In addition to the correlation coefficient and the standard deviation, the chi-squared test is imposed. Table 5-7 shows the comparison for four pollutants modeled. The symbol SAIC denotes station values selected from the Systems Applications, Inc., validation runs[63] to be in correspondence as nearly as possible with the station values computed in the Pacific Environmental Services, Inc., validation runs (PESC).[64] This was done in an effort to compare models on a common-denominator basis. Likewise, trajectories are traced through the SAI hourly-grid results, to form the SAIT data set to compare with the General Research Corporation validation runs (GRCT).[65] Clear trends are difficult to identify, but, as the author points out, the SAI model probably excelled in carbon monoxide prediction because it has more detail in advective diffusive coupling, and the GRC model did best with ozone prediction probably because of careful calibration. The PES model had the minimal standard deviation with nitric oxide prediction because the data sample centered on midday concentrations away from the morning traffic peak, which is difficult to predict. The chi-squared test suggested that most of the time none of the models adequately represented the data on the basis of a 10% chance that the results are randomly distributed. Exceptions to this finding are noted with GRCT and SAIT, both passing the chi-squared test to a 90% confidence level for carbon monoxide results.

Table 5-7

Statistical Analyses of Photochemical Air Quality Model Performance for the Los Angeles Basin[a]

Model[b]	Correlation Coefficient[c]	Standard Deviation[d]	Degrees of Freedom	Measured Chi-Squared[e]	Standard Chi-Squared[f]
Carbon monoxide					
PESC	0.68	4.27	143	233.75	171.62
SAIC	0.84	3.52	290	287.35	330.44
GRCT	0.82	3.39	172	75.12	203.32
SAIT	0.79	3.18	175	84.42	206.58
Nitric oxide					
PESC	0.77	3.18	49	227.67	66.05
SAIC	0.87	9.13	277	1,081.01	316.54
GRCT	0.87	8.70	171	1,053.03	202.23
SAIT	0.86	8.13	173	1,042.44	204.41
Nitrogen dioxide					
PESC	0.68	8.36	49	157.15	66.05
SAIC	0.65	6.82	276	310.56	315.47
GRCT	0.43	10.05	172	316.91	203.32
SAIT	0.52	12.62	175	159.81	206.58
Ozone					
PESC	0.50	8.26	53	380.85	70.71
SAIC	0.60	8.56	255	3,480.79	292.97
GRCT	0.91	3.82	127	237.74	154.02
SAIT	0.69	8.75	131	387.30	158.43

---

[a] Data from Whitney.[72]

[b] See text for abbreviations.

[c] Correlation of predicted and actual measurements.

[d] Difference of predicted and actual measurements.

[e] Normalized by σ where σ is assumed to be 0.7 + 0.1 x (observed value).

[f] A 90% confidence level was assigned for the purposes of the chi-squared test.

Other performance measures were carefully chosen to reflect accuracy of prediction. They consisted of scatter plots of predicted versus observed concentrations and four other types of plots involving analyses of residuals. The residual study took the (predicted - observed) values and displayed them in histograms in plots of time against predicted concentrations and against observed (or interpolated) concentrations. The results of the residual analysis are too extensive to review here, but the user who is interested in modeling a particular pollutant or who is considering one of the specific models tested should examine the computer printouts to answer specific performance questions. Whitney has devised a useful set of model performance measures for the task of evaluating the earlier evaluations. The results of similar tests on log statistics would have been interesting. It was not stated whether the residuals were normally distributed.

The sensitivity of diffusion-model output to variations in input has been assessed by workers at Systems Application Inc. and at the California Department of Transportation. In each case, reports are in preparation and are therefore not yet available. It is important to distinguish between sensitivity and model performance. True physical or chemical sensitivity that is reflected by the simulation-model equations is a valid reflection of reality. But spurious error propagation through improper numerical integration techniques may be regarded as an artificial sensitivity. Such a distinction must be drawn carefully, lest great sensitivity come to be considered synonymous with unacceptable performance.

SUMMARY

The literature contains reviews of air quality modeling that stress special purposes. Some concentrate on meteorologic aspects, and others combine this with air chemistry. Proceedings of several conferences are another information resource. Recent surveys have been addressed specifically to photochemical modeling problems. It may be concluded that, although they are relatively complex, the photochemical-diffusion models perform as well as, if not better than, available inert-species models.

A variety of goals and objectives may be met with air quality modeling. They are summarized as:

- Scientific understanding of atmospheric phenomenology.
- Rational application of the regulatory process.
- Land-use planning within environmental constraints.
- Real-time control of episodes.

The fundamental elements of deterministic models involve a combination of chemical and meteorologic input, preprocessing with data transmission, logic that describes atmospheric processes, and concentration-field output tables or displays. In addition to deterministic models, there are statistical schemes that relate precursors (or emission) to photochemical oxidant concentrations. Models may be classified according to time and space scales, depending on the purposes for which they are designed.

Specific model applications to the oxidant problem include both the simple rollback (with modifications) and the photochemical-diffusion techniques. Very little modeling of intermediate complexity seems to have been attempted for the oxidant system.

Preceding page blank

Model performance is now receiving critical attention because of the need for cost-effective control measures. Standard statistical performance descriptors can sometimes mislead a prospective user; therefore, more specialized tests are being devised. Various model types are being compared for a specified set of initial and boundary conditions. It is apparent from these studies that added fidelity is purchased at the expense of added complexity of a logical structure that must represent the controlling phenomenology.

SUGGESTED RESEARCH DIRECTIONS

Internal improvements in deterministic methods will be based on accounting for more physicochemical effects in the logical structure. One challenge to the researcher is to do this without making something that is already complex still more difficult to understand, and another challenge is to avoid needless elaboration of detail. Both pitfalls will be avoided, first, by asking how accurate a modeling job is demanded and, second, by carrying out order-of-magnitude analytic appraisals of the omitted phenomenology.

Perhaps the most important thing that research will contribute is a set of criteria delineating the fidelity of existing models, rather than a single supermodel that will consider all effects. Much remains to be done in statistical modeling. The scientific community is on the threshold of potentially great strides with these methods, because of the veritable explosion of data from measurement programs. It is absolutely essential for all agencies interested in environmental management to begin mounting analysis programs that are carefully designed to capitalize on the data base. Traditionally, support has been more readily obtained for making additional measurements in hope that useful information would emerge directly or that someone would spontaneously dig out the useful information. Seldom has either been the case.

Specific research subjects have emerged with respect to improved descriptions of specific phenomena. Some time ago,[38] it was speculated that gas-solid interactions and turbulence effects on reaction kinetics would be important areas of advance in the modeling art. Gas-solid interactions include both chemical formation of aerosols and reactions on surfaces of preexisting suspended particulate matter. Because of differing effects of a material in the gas phase and in some condensed phase, it will be important to characterize transformation processes. The ACHEX (Aerosol CHaracterization EXperiment) program[89] recently carried out under the direction of Hidy will provide an extensive data base with which to test new ways of treating the gas-solid interaction problem.

The turbulent mixing of emitted reactant gas (such as nitric oxide) with atmospherically formed reactant gas (such as ozone) results in macroscopic heterogeneities, which under some circumstances can significantly change the reaction rate from the value that the mean concentrations used in a rate equation would predict. Airborne measurement from some 40 operational days from the LARPP (Los Angeles Reactive Pollutant Program) study gives 6-s-interval gas-phase data for six gas-phase species simultaneously. This program (under the field management of W. Perkins and under the direction of Coordinating Research Council's CAPA-12 committee, chaired by J. Black) has produced archives of these data that can serve as a test bed for theories of turbulent interactions with kinetics.

In a broader sense, the data obtained from the Regional Air Pollution Study (RAPS) and the California Three-Dimensional Pollutant Gradient Study

Program should also serve as bases of further model development. It is incumbent on the agencies responsible for air quality control to identify resources specifically aimed at using these data for improving techniques for designing pollution abatement strategies.

SUGGESTED APPLICATIONS TO POLLUTION ABATEMENT

Without doubt, the top-priority application of air quality models is the determination of emission controls needed to achieve ambient air quality standards. With the reexamination of transportation control strategies and with the pressures of fuel substitutions, refinements well beyond the traditional proportional models are imperative. Where validated diffusion models are available, they should be used to recalculate the emission requirements that came from initial hasty efforts to implement the Clean Air Act Amendments of 1970. This is the greatest national service that could be performed by the air quality modelers at present. Before this can be achieved, however, the institutional apparatus must provide the impetus and resources called for in a recent National Academy of Sciences report to the U.S. Senate.[90]

Much of the research work will add content to the model structures, but future applications demand simplifications that are oriented toward the nonspecialist user. One of the largest obstacles to the effective use of air quality prediction schemes is the resolution of this apparent conflict. At least two steps can be taken by those who produce models to encourage applications and to aid the user:

- Compile a catalog of air quality models that describes their capabilities in terms of a common set of performance standards.
- Clarify data communication in the input-output interfaces between user and model.

To accomplish the first step, model standards will be evolved on the basis of legislative mandates and regulatory needs. Each of the various types of model has undergone performance evaluation through the application of a set of tests peculiar to its own structure or output. For example, Gaussian models that predict long-term averages are often evaluated by computing only the correlation coefficient between measured and computed concentrations. Early evaluations of species-mass-balance models stressed hour-by-hour comparison of the predicted and observed concentrations. Recently, a broader range of descriptors has evolved, as evidenced by the work of Nappo[66] and Whitney.[72]

The performance indexes must be designed with the model applications in mind. Will the model be used to predict local effects around a highway or a smelter where short-term high doses are as important as long-term averages? Will the model be called on to compare trends in air quality between two different scenarios of urban population growth? Will the model be used to select a control plan that will result in a given hourly air concentration's being exceeded only once a year? A properly designed set of performance standards will allow a potential user to compare models with respect to suitability for any specific application. The particular performance characteristic of interest influences strongly the rank-ordering of models on a scale of goodness.

Fundamental to the definition of an optimal set of performance measures will be the relationship of risk (of health, property, or aesthetic attributes) to exposure (average pollutant concentration, time-integrated pollutant concentration, synergistic combination of pollutant dosages, or dosages integrated with respect to space, time, and population[38]). Derived from the risk factor will be, not a single number, but a distribution of effects for each degree of exposure. For example, a range of pulmonary effects can be expected in a sample population in which each individual has been exposed to ozone at an average concentration of 100 $\mu g/m^3$ for 5 years. The expectation value of the effect will be the risk factor that is the function of exposure described above. The model performance index will utilize these relationships to connect a probability density distribution output from the model (associated with imperfect knowledge) to a probability density distribution of the threat to public health and welfare. Stated in a different way, each model will be assessed on the basis of the uncertainty of damage estimate that arises from it imperfections. This must be done in an unambiguous way for the user, who may not be a specialist.

The second step that will be needed to ensure ready application of air quality models is largely a question of packaging and presentation. User-oriented documentation will be needed for personnel at data processing centers, who may not be specialists in chemistry, mathematics, or meteorology. Experience has shown that the user desires to operate the model in his own data center and wishes to understand enough about the model structure to explain it to others in his field. Models that cannot be adapted to these requirements have not been widely applied. In some cases, an operating manual intended for persons with some knowledge of programing will need to be rewritten to allow the user to supply completed data forms to a computer center and routinely receive output in return. Other adaptations may require a user to punch data in on a teletypewriter and receive output on the same machine in an interactive mode. This involves a network of remote terminals served by the computer center, such as that under development in UNAMAP.[11]

Output displays will be required to bring the abstract aspects of voluminous output data into some form that appeals to the experience of the user. Isopleth maps are useful, as are three-dimensional isometric plots like SYMVU, produced by Harvard University. Printer plots of concentration maps will undoubtedly enjoy an even greater application, because of the common availability of line printers or teletypewriters as output devices. Examples of these techniques are SYMAP and GRID, both produced by Harvard University.

Another aspect of matching output to user needs involves presentation of results in a statistical framework--namely, as frequency distributions of concentrations. The output of deterministic models is not directly suited to this task, because it provides a single sample "point" for each run. Analytic linkages can be made between observed frequency distributions and computed model results. The model output for a particular set of meteorologic conditions can be on the frequency distribution of each station for which observations are available in sufficient sample size. If the model is validated for several different points on the frequency distribution based on today's estimated emission, it can be used to fit a distribution for cases of forecast emission. The fit can be made by relating characteristics of the distribution with a specific set of model predictions. For example, the distribution could be assumed to be log-normal, with a mean and standard deviation each determined by its own function of output concentrations computed for a standardized set of meteorologic conditions. This, in turn, can be linked to some effect on people or property that is defined in terms of the predicted concentration statistics. The diagram below illustrates this process:

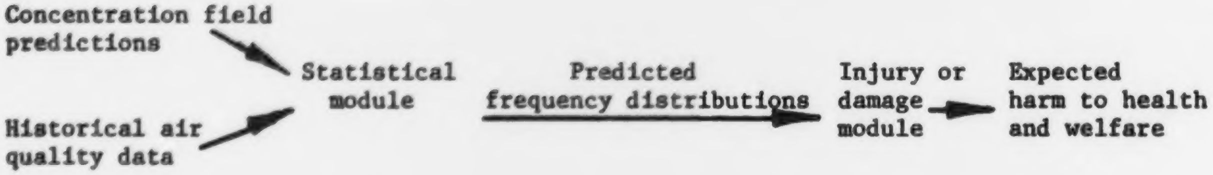
Concentration field predictions
Historical air quality data
Statistical module
Predicted frequency distributions
Injury or damage module
Expected harm to health and welfare

We have seen the wide variety of methods now available to calculate air quality. The priority for adapting these methods to current needs is clearly established. Only through clear expositions of model performance and simple implementation procedures will the present techniques have a favorable impact on air quality management. A growing appreciation by the specialist community of the policy requirements will be essential for the successful fulfillment of these goals.

REFERENCES

1. Wanta, R. C. Meteorology and air pollution, pp. 187-226. In A. C. Stern, Ed. Air Pollution. Vol. 1 (2nd ed.) New York: Academic Press, 1968.

2. Pack, D. H. Meteorology of air pollution. Science 146:1119-1128, 1964.

3. Neiburger, M. The role of meteorology in the study and control of air pollution. Bull. Amer. Meteorol. Soc. 50:957-965, 1969.

4. Gifford, F. A., Jr. An outline of theories of diffusion in the lower layers of the atmosphere, pp. 65-116. In D. H. Slade, Ed. Meteorology and Atomic Energy. Oak Ridge, Tenn.: U. S. Atomic Energy Commission, 1968.

5. Stern, A. C., Ed. Proceedings of Symposium on Multiple-Source Urban Diffusion Models. Air Pollution Control Office Publ. AP-86. Research Triangle Park, N. C.: U. S. Environmental Protection Agency, 1970. [416 pp.]

6. Neiburger, M., J. G. Edinger, and H. C. Chin. Meteorological Aspects of Air Pollution and Simulation Models of Diffusion Transport and Reactions of Air Pollution. Project Clean Air Report of Task Force No. 4. Riverside: University of California, 1970.

7. North Atlantic Treaty Organization. Committee on the Challenges of Modern Society. Proccedings of the Second Meeting of the Expert Panel on Air Pollution Modeling, Paris, France, July 26-27, 1971.

8. Reiter, E. R. Chapter 7, pp. . In Atmospheric Transport Processes. Part 3: Hydrodynamic Traces. AEC Critical Review Series. Oak Ridge, Tenn.: U. S. Atomic Energy Commission, 1972.

9. Hoffert, M. I. Atmospheric transport, dispersion, and chemical reactions in air pollution: A review. Amer. Instit. Aeronaut. Astronaut. J. 10: 377-387, 1972.

10. Darling, E. M., Jr. Computer Modeling of Transportation-Generated Air Pollution, A State of the Art Survey. U. S. Department of Transportation Report DOT-TSC-OST-72-20, June 1972.

11. Johnson, W. B. The status of air quality simulation modeling, pp. 114-127. In Proceedings of the Interagency Conference on the Environment. Washington, D. C.: U. S. Atomic Energy Commission, 1972.

12. North Atlantic Treaty Organization. Committee on the Challenges of Modern Society. Proceedings of the Third Meeting of the Expert Panel on Air Pollution Modeling, Paris, France, October 2-3, 1972.

13. North Atlantic Treaty Organization. Committee on the Challenges of Modern Society. Proceedings of the Fourth Meeting of the Expert Panel on Air Pollution Modeling, Oberursel, Federal Republic of Germany, May 28-30, 1973.

14. Lamb, D. V., F. I. Badgley, and A. T. Rossano, Jr. A Critical Review of Mathematical Diffusion Modeling Techniques for Air Quality with Relation to Motor Vehical Transportation. Washington State Highway Department Research Report 12.1, Research Project &-1540, University of Washington, June 1973.

15. Sklarew, R. C. Air quality simulation models for photochemical pollutants, pp. . In A. C. Stern, Ed. Air Pollution. Vol. . (ed.) New York: John Wiley and Sons, (in press)

16. Seinfeld, J. H. Mathematical models of air quality control regions, pp. 169-196. In A. Atkisson and R. S. Gaines, Eds. Development of Air Quality Standards. Columbus, Ohio: Charles E. Merrill Publishing Co., 1970.

17. Barth, D. S. Federal motor vehicle emission goals for CO, HC. and NO_x based on desired air quality levels. J. Air Pollut. Control Assoc. 20:519-523, 1970.

18. Schuck, E. A., A. P. Altshuller, D. S. Barth, and G. B. Morgan. Relationship of hydrocarbons to oxidants in ambient atmospheres. J. Air Pollut. Control Assoc. 20:297-302, 1970.

19. Schuck, E. A., and R. Papetti. Examination of the photochemical air pollution problem in southern California. Appendix D, pp. . In Technical Support Document for the Metropolitan Los Angeles Intrastate Air Quality Control Region Transportation Control Plan Final Promulgation, Environmental Protection Agency, Oct. 30, 1973. (UNVERIFIED)

20. Merz, Ph. H., L. J. Painter, and P. R. Ryason. Aerometric data analysis--time series analysis and forecast and an atmospheric smog diagram. Atmos. Environ. 6:319-342, 1972.

21. Hamming, W. J., R. L. Chass, J. E. Dickenson, and W. G. MacBeth. Motor Vehicle Control and Air Quality. The Path to Clean Air for Los Angeles. Paper No. 73-73 Presented at 66th Annual Meeting of the Air Pollution Control Association, Chicago, Illinois, June 24-28, 1973. (UNVERIFIED)

22. Chang, T. Y., and B. Weinstock. Rollback modeling for urban air pollution control, pp. 184-189. In Proceedings of the Symposium on Atmospheric Diffusion and Air Pollution, American Meteorological Society, Santa Barbara, California, September 9-13, 1974. (UNVERIFIED)

23. Chang, T. Y., and B. Weinstock. Urban CO concentrations and vehicle emissions. J. Air Pollut. Control Assoc. 23:691-696, 1973.

24. Peterson, J. T. The calculation of sulfur dioxide concentrations over a metropolitan area by using empirical orthogonal functions. American Institute of Aeronautics and Astronautics, Paper 70-113, January 1970. (UNVERIFIED)

25. Trijonis, J. C. Economic air pollution control model for Los Angeles County in 1975. General least cost-air quality model. Environ. Sci. Technol. 8:811-826, 1974.

26. Bruntz, S. M., W. S. Cleveland, B. Kleiner, and J. L. Warner. The dependence of ambient ozone on solar radiation, wind, temperature, and mixing height, pp. 127-128. In Proceedings of the Symposium on Atmospheric Diffusion and Air Pollution, American Meteorological Society, Santa Barbara, California, 1974. (UNVERIFIED)

27. McCollister, G. M., and K. R. Wilson. Linear stochastic models for forecasting daily maxima and hourly concentrations of air pollutants. Atmos. Environ. (in press) (UNVERIFIED)

28. Hanna, S. R. A simple method of calculating dispersion from urban area sources. J. Air Pollut. Control Assoc. 21:774-777, 1971.

29. Gifford, F. A., and S. R. Hanna. Modelling urban air pollution. Atmos. Environ. 7:131-136, 1973.

30. Hanna, S. R. A simple dispersion model for the analysis of chemically reactive pollutants. Atmos. Environ. 7:803-817, 1973.

31. Lamb, R. G., and J. H. Seinfeld. A simple dispersion model for the analysis of chemically reactive pollutants. Atmos. Environ. 8:527-529, 1974. (discussion)

32. Hanna, S. R. Author's reply. [To discussion of "A simple dispersion model for the analysis of chemically reactive pollutants."] Atmos. Environ. 8: 529-530, 1974.

33. Karplus, W. J., G. A. Bekey, and P. J. Pekrul. Atmospheric diffusion of air pollutants: Analog computer study. Ind. Eng. Chem. 50:1657- 1660, 1958.

34. Ulbrich, E. A. Adapredictive air pollution control for the Los Angeles basin. Socio-Econ. Plan. Sci. 1:423-440, 1968.

35. Friedlander, S. K., and J. H. Seinfeld. A dynamic model of photochemical smog. Environ. Sci. Technol. 3:1175-1182, 1969.

36. Eschenroeder, A. Z., and J. R. Martinez. Mathematical Modeling of Photochemical Smog. General Research Corporation IMR-1210. Santa Barbara, Calif.: General Research Corporation, 1969.

37. Eschenroeder, A. Q., and J. R. Martinez. Concept and applications of photochemical smog models. Adv. Chem. Ser. 113:101-168, 1972.

38. Eschenroeder, A. Q., J. R. Martinez, and R. A. Nordsieck. A view of future problems in air pollution modeling, pp. 1013-1027. In Proceedings of the 1972 Summer Computer Simulation Conference. LaJolla, Calif.: Simulation Councils, Inc., 1972.

39. Martinez, J. R., R. A. Nordsieck, and A. Q. Eschenroeder. Morning vehicle-start effects on photochemical smog. Environ. Sci. Technol. 7:917-923, 1973.

40. Wayne, L., R. Danchick, M. Weisburd, A. Kokin, and A. Stein. Modeling photochemical smog on a computer for decision-making. J. Air Pollut. Control Assoc. 21:334-340, 1971.

41. Mahoney, J. R., and B. A. Egan. A mesoscale numerical model of atmospheric transport phenomena in urban areas, pp. 1152-1157. In H. M. Englund and W. T. Beery, Eds. Proceedings of the Second International Clean Air Congress. New York: Academic Press, 1971.

42. Egan, B. A., and J. R. Mahoney. Numerical modeling of advection and diffusion of urban area source pollutants. J. Appl. Meteorol. 11:312-322, 1972.

43. Egan, B. A., and J. R. Mahoney. Applications of a numerical air pollution transport model to dispersion in the atmospheric boundary layer. J. Appl. Meteorol. 11:1023-1039, 1972.

44. Lamb, R. G., and M. Neiburger. An interim version of a generalized urban air pollution model. Atmos. Environ. 5:239-264, 1971.

45. Seinfeld, J. H., S. D. Reynolds, and P. M. Roth. Simulation of urban air pollution. Adv. Chem. Ser. 113:58-100, 1972.

46. Reynolds, S. D., P. M. Roth, and J. H. Seinfeld. Mathematical modeling of photochemical air pollution--I. Formulation of the model. Atmos. Environ. 7:1033-1061, 1973.

47. Roth, P. M., P. J. W. Roberts, M-K. Liu, S. D. Reynolds, and J. H. Seinfeld. Mathematical modeling of photochemical air pollution--II. A model and inventory of pollutant emissions. Atmos. Environ. 8:97-130, 1974.

48. Reynolds, S. D., M-K. Lieu, T. A. Hecht, P. M. Roth, and J. H. Seinfeld. Mathematical modeling of photochemical air pollution. III. Evaluation of the model. Atmos. Environ. 8:563-596, 1974.

49. Sklarew, R. C., A. J. Fabrick, and J. E. Prager. Mathematical modeling of photochemical smog using the PICK method. J. Air Pollut. Control Assoc. 22:865-869, 1972.

50. Knox, J. B. Numerical modeling of the transport diffusion and deposition of pollutants for regions and extended scales. J. Air Pollut. Control Assoc. 24:660-664, 1974.

51. Shir, C. C., and L. J. Shieh. A generalized urban air pollution model and its application to the study of SO_2 distributions in the St. Louis metropolitan area. J. Appl. Meteorol. 13:185-204, 1974.

52. Chapman, S., and T. G. Cowling. Chapter 8, pp. . and Chapter 14, pp. . In The Mathematical Theory of Nonuniform Gases. Cambridge: Cambridge University Press, 1939.

53a. Hirschfelder, J. O., C. F. Curtiss, and R. B. Bird. The equation of state of gases at low and moderate densities, pp. 131-233. In Molecular Theory of Gases and Liquids. New York: John Wiley and Sons, Inc., 1954.

53b. Hirschfelder, J. O., C. F. Curtiss, R. B. Bird, and E. L. Spotz. The equation of state of dense gases and liquids, pp. 234-335. In Molecular Theory of Gases and Liquids. New York: John Wiley and Sons, Inc., 1954

53c. Hirschfelder, J. O., C. F. Curtiss, and R. B. Bird. The transport properties of dense gases and liquids, pp. 611-667. In Molecular Theory of Gases and Liquids. New York: John Wiley and Sons, Inc., 1954.

53d. Hirschfelder, J. O., C. F. Curtiss, R. B. Bird, and E. L. Spotz. The transport properties of dense gases and liquids, pp. 611-667. In Molecular Theroy of Gases and Liquids. New York: John Wiley and Sons, Inc., 1954.

54. Penner, S. S. Chapter 2, pp. . In Introduction to the Study of Chemical Reactions in Flow Systems. London: Butterworths Scientific Publications, 1955.

55. Bird, R. B., W. E. Stewart, and E. N. Lightfoot. Chapter 20 pp. . In Transport Phenomena. New York: Wiley, 1960.

56. Korth, M. W., A. H. Rose, Jr., and R. C. Stahman. Effects of hydrocarbon to oxides of nitrogen ratios on irradiated auto exhaust. Part I. J. Air Pollut. Control Assoc. 14:168-175, 1964.

57. Dimitriades, B. Effects of hydrocarbon and nitrogen oxides on photochemical smog formation. Environ. Sci. Technol. 6:253-260, 1972.

58a. Scott Research Laboratories, Inc. 1969 Atmospheric Reaction Studies in the Los Angeles Basin. Vol. 1. Program Design and Methodology. Data Summary and Discussion. Final Report. Plumsteadville, Pa.: Scott Research Laboratories, Inc., 1970. [113 pp.]

58b. Scott Research Laboratories, Inc. 1969 Atmospheric Reaction Studies in the Los Angeles Basin. Vol. 2. Commerce Ground Data. Final Report. Plumsteadville, Pa.: Scott Research Laboratories, Inc., 1970. 535 pp.

59. Anscombe, F. J. Graphs in statistical analysis. Amer. Statist. 27:17-21, 1973.

60. Eschenroeder, A. Q. Comments on the California Transportation Control Strategy. Invited Testimony before the Environmental Protection Agency Hearing at Santa Barbara, California, March 19, 1973. (Available as General Research Corporation IM-1741, April 1973.)

61. Martinez, J. R., and R. A. Nordsieck. Air Quality Impacts of Electric Cars in Los Angeles. General Research Corporation RM-1905. Santa Barbara: General Research Corporation, 1974.

62. Reynolds, S. D., and J. H. Seinfeld. Interim evaluation of strategies for meeting ambient air quality standard for photochemical oxidant. Environ. Sci. Technol. 9:433-447, 1975.

63. Reynolds, S. D., M. K. Liu, T. A. Hecht, P. M. Roth, and J. H. Seinfeld. Urban Air Shed Photochemical Simulation Model Study. Vol. 1. Development and Evaluation. EPA-R4-73-30a. Systems Applications Incorporated, July 1975.

64. Wayne, L. G., A. Kokin, and M. I. Weisburd. Controlled Evaluation of the Reactive Environmental Simulation Model (REM) Vol. 1. Final Report Santa Monica, Calif.: Pacific Environmental Services, Inc., 1973. [176 pp.]

65. Eschenroeder, A. Q., J. R. Martinez, and R. A. Nordsieck. Evaluation of a Diffusion Model for Photochemical Smog Simulation. EPA-R4-73-012a. Santa Barbara, Calif.: General Research Corporation, 1972. 226 pp.

66. Nappo, J., Jr. A method for evaluating the accuracy of air pollution models, pp. 325-329. In Proceedings of the Symposium on Atmospheric Diffusion and Air Pollution. American Meteorological Society, Santa Barbara, California, September 9-13, 1974.

67. MacCracken, M. C., T. V. Crawford, K. R. Peterson, and J. B. Knox. Development of a Multibox Air Pollution Model and Initial Verification for the San Francisco Bay Area. Lawrence Radiation Lab. No. UCRL-73348, 1971.

68. Roth, P. M., S. D. Reynolds, P. J. W. Roberts, and J. H. Seinfeld. Development of a Simulation Model for Estimationg Ground Level Concentrations of Photochemical Pollutants. Systems Applications Inc., Final Report 71-SAI-21, 1971.

69. Hanna, S. R. Urban Air Pollution Models--Why? ATDL Contribution File No. 83. Atmospheric Turbulence and Diffusion Laboratory, Oak Ridge, Tenn. 1973.

70. Sklarew, R. D., A. J. Fabrick, and J. E. Prager. A Particle-in-Cell Method for Numerical Solution of the Atmospheric Diffusion Equation, and Applications to Air Pollution Problems. Systems, Science and Software Final Report 3SR-844, 1971.

71. Pandolfo, J. P., and C. A. Jacobs. Tests of an Urban Meteorological-Pollutant Model Using CO Validation Data in the Los Angeles Metropolitan Area. Vol. 1. EPA R4-730-025A. Hartford, Conn.: The Center for the Environment and Man, Inc., 1973. 176 pp.

72. Whitney, D. C. Analysis of Results of Past Model Verification Studies. Systems Application, Inc. Draft Report, August 1974.

73. Lissaman, P. B. S. A Simple Unsteady Concentration Model Explicitly Incorporating Ground Roughness and Heat Flux. Aerovironment Report No. 73-129, 1973.

74. Wang, I. T., and D. M. Rote. A Finite Line Source Dispersion Model for Mobile Source Air Pollution. Argonne National Laboratory Paper 75-135, 1973.

75. Beaton, J. L., A. J. Ranzieri, and J. B. Skog. Air Quality Manual: Vol. 1. Meteorology and Its Influence on the Dispersion of Pollutants from Highway Line Sources. Department of Transportation Report FHWA-RD-72-33, 1972.

76. Beaton, J. L., A. J. Ranzieri, and J. B. Skog. Air Quality Manual: Vol. 2. Motor Vehicle Emission Factors for Estimates of Highway Impact on Air Quality. Department of Transportation Report FHWA-RD-72-34, 1972.

77. Beaton, J. L., E. C. Shirley, and J. B. Skog. Air Quality Manual. Vol. 3. Traffic Information Requirements for Estimates of Highway Impact on Air Quality. Department of Transporation Report FHWA-RD-72-35, 1972.

78. Beaton, J. L., A. J. Ranzieri, E. C. Shirley, and J. B. Skog. Air Quality Manual. Vol. 4. Mathematical Approach to Estimating Highway Impact on Air Quality. Department of Transportation Report FHWA-RD-72-36, 1972.

79. Beaton, J. L., A. J. Ranzieri, E. C. Shirley, and J. B. Skog. Air Quality Manual. Vol. 5 (Appendix to Vol. 4) Department of Transportation Report FHWA-RD-72-37, 1972.

80. Beaton, J. L., A. J. Ranzieri, E. C. Shirley, and J. B. Skog. Air Quality Manual. Vol. 6. Analysis of Ambient Air Quality for Highway Projects. Department of Transportation Report FHWA-RD-72-38, 1972.

81. Beaton, J. L., E. C. Shirley, and J. B. Skog. Air Quality Manual. Vol. 7. A Method of Analyzing and Reporting Highway Impact on Air Quality. Department of Transportation Report FHWA-RD-72-39, 1972.

82. Beaton, J. L., and J. B. Skog. Air Quality Manual. Vol. 8. Synthesis of Information on Highway Transportation and Air Quality. Department of Transportation Report FHWA-RD-72-40, 1972.

83. Chen, T. C., and F. March. Effect of highway configurations on environmental problems--dynamics of highway associated air pollution, pp. 35-40. In H. M. Englund and W. T. Beery, Eds. Proceedings of the Second International Clean Air Congress. New York: Academic Press, 1971.

84. Danard, M. B., R. S. Koneru, and P. R. Slawson. A numerical model for carbon monoxide concentrations near a highway, pp. 152-157. In Proceedings of the Symposium on Air Pollution, Turbulence and Diffusion, December 7-10, 1971.

85. Calder, K. L. Air Pollution Concentrations from a Highway in an Oblique Wind. Environmental Protection Agency, Division of Meteorology, Research Triangle Park, N. C., August 1972.

86. Sakuraba, S. Sensitivities of air quality prediction to input erros and uncertainties, pp. 8-11. In A. C. Stern, Ed. Proceedings of Symposium on Multiple-Source Urban Diffusion Models. Air Pollution Control Office Publ. AP-86. Research Triangle Park, N. C.: U. S. Environmental Protection Agency, 1970.

87. Knox, J. B. Numerical Modeling of the Transport, Diffusion and Deposition of Pollutants for Regions and Extended Scales. Lawrence Livermore Laboratory Report UCRL-74666, 1973.

88. Shieh, L. J., P. K. Halpern, B. A. Clemens, H. H. Wange, and F. F. Abraham. A multiple-source diffusion model for New York City, pp. 108-115. In Proceedings of the Symposium on Air Pollution, Turbulence and Diffusion. December 7-10, 1971.

89. Hidy, G. Final Report on the Aerosol Characterization Experiments. State of California Air Resources Board. (in press)

90. National Academy of Sciences. National Academy of Engineering. Coordinating Committee on Air Quality Studies. Conclusion and recommendations [for measuring oxidants], pp. 6-8. In Air Quality and Automobile Emission Control. Vol. 3. The Relationship of Emissions to Ambient Air Quality. Committee Print Serial No. 93-24. (Committee on Public Works, U. S. Senate) Washington, D. C.: U. S. Government Printing Office, 1974.

Chapter 6

MEASUREMENT METHODS

Photochemical oxidants are atmospheric pollutants produced by a series of reactions between hydrocarbons and oxides of nitrogen in the presence of sunlight. The recognized photochemical oxidants that have been measured in ambient air are ozone, the peroxyacyl nitrates (mostly as peroxyacetyl nitrate, abbreviated as PAN), and hydrogen peroxide.[1,2]

Chemical radicals such as hydroxyl, peroxyhydroxyl and various alkyl and aryl species have either been observed in laboratory studies or have been postulated as photochemical reaction intermediates. Atmospheric photochemical reactions also result in the formation of finely divided suspended particles, (secondary aerosols), which create atmospheric haze. Their chemical content is enriched with sulfates (from sulfur dioxide), nitrates (from nitrogen dioxide, nitric oxide and peroxyacyl nitrates), ammonium (from ammonia), chloride (from sea salt), water and oxygenated, sulfurated and nitrated organic compounds (from chemical combination of ozone and oxygen with hydrocarbon, sulfur oxide and nitrogen oxide fragments).[3]

The chemistry of the photochemical reaction milieu including the formation of secondary aerosols is covered in Chapter 3. Table 6-1 lists the substances which have been identified and associated with the impact of photochemical oxidants on breathing, eye irritation, plant damage and visibility reduction. It is important to recognize this chemical complexity when formulating strategies for controlling the emissions of the primary pollutants. It is also important that a review of the issues relates air pollutants to their sources. This requires not only the measurement of end products but also of their precursors. Table 6-1 shows in general terms the present state of monitoring practice for each of these substances.

The effects of photochemical smog initially observed in Los Angeles were severe haze formation, eye irritation, plant damage and rubber tire cracking. Haagen-Smit[4] was the first researcher to recognize that the severity of photochemical smog could be quantified by measuring oxidants. This oxidizing property of smog was subsequently more efficiently monitored by measuring the increase in color intensity produced by the iodine released from potassium iodide solutions in contact with air.[5, 6] As a consequence, photochemical oxidants have been defined by air pollution agencies as atmospheric substances that oxidize certain reagents.

The reagent most frequently used is a neutral phosphate-buffered potassium iodide solution, calibrated with a known source of ozone. This reagent, which is particularly sensitive to ozone, is also somewhat responsive to other atmospheric oxidants such as nitrogen dioxide, the peroxyacyl nitrates, and to a lesser extent, to hydrogen peroxide.[1, 2] Reducing agents present in smog (e.g., sulfur dioxide, SO_2) have an effect on the reagent solution opposite to that of oxidants.

Various terms are used to describe photochemical oxidant concentrations. Two of these, "oxidant" and "total oxidant," are used because the measurement method (usually the potassium iodide method) cannot distinguish between oxidizing and reducing agents, which in

Table 6-1

Substances and Monitoring Practices for Species Present in Photochemical Smog as Precursors or Products

Substance	Formula or Symbol	Monitoring Practice
Gaseous		
ozone	O_3	Routine
peroxyacetyl nitrate (PAN)	$CH_3\overset{\overset{O}{\|}}{C}OONO_2$	Occasional
hydrogen peroxide	H_2O_2	Research
nitrogen dioxide,	NO_2	
nitric oxide	NO	Routine
hydroxyl	$HO^{\bullet}$	Research
peroxy hydroxyl	$HOO^{\bullet}$	None
alkyls	$CH_3(CH_2)_n^{\bullet}, CH_3CO^{\bullet}$, etc.	None
aryls	$C_6H_5CH_2^{\bullet}$ etc.	None
aldehydes, formaldehyde	CH_2O	Occasional
acetaldehyde	CH_3CHO	Occasional
acrolein	$CH_2{=}CHCHO$	Occasional
benzaldehyde	C_6H_5CHO	Occasional
hydrocarbons, total	THC	Routine
methane	CH_4	Routine
total non-methane	NMHC	Routine
alkanes	C_2H_6 to C_nH_{2n+2}	Occasional and research
olefins	C_2H_4 to C_nH_{2n+1}	Occasional and research
diolefins	C_4H_6 to C_nH_{2n-2}	Occasional and research
acetylene	C_2H_2	Occasional and research
aromatics	C_6H_6 to C_nH_{2n-6}	Occasional and research

Table 6-1 (Cont.)

Substances and Monitoring Practice for Species Present in Photochemical Smog as Precursors or Products

Substance	Formula or Symbol	Monitoring Practice
Particulate		
sulfate	$SO_4^{=}$	Routine
nitrate	$NO_3^{=}$	Routine
ammonium	NH_4^{+}	Occasional
chloride	Cl^{-}	Occasional
water	H_2O	Research
oxygenated organics	$HOOC(CH_2)_nCH_2OH$	Research
	$HOOC(CH_2)_nCOOH$	Research
	$HOOC(CH_2)_nCHO$	Research
	$HOOC(CH_2)_nCONO_2$	Research
	Many others	

combination, produce the "net" oxidizing ability of the air. The terms "corrected oxidant" or "adjusted oxidant" are used to indicate that a measurement has been corrected for responses to certain components known to be present (usually sulfur dioxide and nitrogen dioxide), other than ozone, peroxyacetyl nitrate or hydrogen peroxide.[3a] None of these terms: "photochemical oxidant," "total oxidant," "oxidant," "corrected oxidant," and "adjusted oxidant" has an exact meaning since the reaction measured in the potassium iodide method is produced by the presence of a number of substances, each responding differently. Ideally, each of the major oxidants: ozone, nitrogen dioxide, PAN, and hydrogen peroxide, and each of the major reductants: sulfur dioxide and hydrogen sulfide, should be measured separately.

The potassium iodide method has been used extensively in California to measure the net oxidizing properties of atmospheric pollutants without identifying the particular species of oxidizing or reducing agents present. Studies have shown, however, that in California, ozone is the major oxidant.[2,7] At most sampling locations in California the negative interference from sulfur dioxide, and the positive interferences from other oxidants have not substantially altered the perception of the photochemical smog problem.[1,2] This is both because the levels of sulfur dioxide are in general small compared to the relatively high observed ozone levels and because the positive interference from nitrogen dioxide tends to offset the negative interference from sulfur dioxide. In other parts of the United States where the peak ozone concentrations have generally been much lower, the potassium iodide measurement method has produced data which has been useful in establishing that an oxidant pollution problem exists. But because it lacks sufficient specificity,[8,9] it is unreliable for measuring the ozone occurrence in these areas. In contrast, there are specific measurement methods that provide reliable relationships between ozone concentrations and other aerometric variables.[10]

In addition to the specificity of the monitoring method, another important requirement for the measurement of atmospheric pollutants is the accuracy of the calibration technique. The calibration procedure for the measurement of oxidants or ozone utilizes a stable and reproducible sample of dilute ozone in air. The ozone concentration of this sample is established, using a reference method that is not necessarily suitable for monitoring ambient air. This reference method must agree with the scientifically accurate measurement of ozone in the calibration sample.

Whether ozone or oxidant measurements can be correlated with other variables is highly dependent on the choice of sampling site and the manner of sample transfer. The importance of these criteria is discussed in Chapter 5 and the desirable specifications are described in this chapter.

The emphasis here is on the various routinely used measurement processes. These create huge banks of data which become influential in deciding public policy. Measurements made only occasionally or during research (Table 6-1) are more easily scrutinized at the time of data application and therefore are not discussed here. Specifications

Preceding page blank

for most types of available instrumentation have been compiled and discussed by the Environmental Instrumentation Group, Lawrence Berkeley Laboratory.[11]

UNITS OF EXPRESSION

Ozone or oxidant concentrations are commonly reported in the units; volumes of ozone per million volumes of air (ppm), or weight of ozone per cubic meter of air ($\mu g/m^3$). The scale for the units in volume per volume or weight per volume may be varied to avoid small decimals or large whole numbers.

The commonly used units of expression are explained in Table 6-2. Expressing concentration data in $\mu g/m^3$ facilitates relating ambient concentrations to emissions. This practice is generally accepted as standard by the Environmental Protection Agency (EPA) in the United States, and similar agencies in other countries.

Expressions of volume per volume units (ppm, pphm or ppb) simplify measurements because their value is independent of atmospheric temperature and barometric pressure. The volume units are equivalent to the ratio of the number of molecules of ozone to the number of molecules of air. This facilitates quantification of the atmospheric chemical reactions which lead to the formation of ozone. These units are also preferable when the molecular weight of a substance is uncertain, as is the case when reporting total nitrogen oxides or total aldehydes.

Particulate matter components cannot be expressed on a volume to volume basis, but they can be expressed on a mole per unit volume basis, μ moles/m^3, if the molecular weight is known. This would be a convenient unit to use when investigating the relationship between particulates and gaseous species.

Table 6-2

Units of Ozone Concentration and their Interconversion Factors

Units	Explanation	Units
ppm	Volume of ozone per million volumes of air (or molecules of ozone per million molecules of air)	= μl O_3/ℓ air = 100 pphm = 1000 ppb = 1.96 mg O_3/m^3 air* = 1960 μg O_3/m^3 air*
μℓ/ℓ	Microliters of ozone per liter of air	= ppm
pphm	Volume of ozone per hundred million volumes	= 0.01 ppm
ppb	Volume of ozone per billion volumes of air	= 0.001 ppm
mg/m^3	Milligrams of ozone per cubic meter of air at 25 C and 1 atmosphere pressure	= 0.51 ppm
μg/m^3	Microgram of ozone per cubic meter of air at 25 C and 1 atmosphere pressure	= 0.00051 ppm = 0.051 pphm = 0.51 ppb
160 μg/m^3	Ozone air quality standard	= 0.08 ppm

---

* When the temperature is 25 C and the barometric pressure is 1 atmosphere.

Temperature and pressure do not influence the value of the volume of volume units.

The conversion of ppm to $\mu g/m^3$ is calculated with equations (1) and (2):

$$\mu g/m^3 = \frac{(ppm)\ 1.219 \times 10^4\ PM}{T} \qquad (1)$$

and

$$ppm = \frac{(\mu g/m^3)\ T}{(1.219 \times 10^4)\ P\ M}\ , \qquad (2)$$

where M is the molecular weight of the gaseous substance being measured (for ozone, 0_3, M = 48 g/mole),

P is the total gas pressure in atmospheres (atm)

T is the temperature in degrees Kelvin, (degrees Celsius + 273), and the number, 1.219×10^4 is the reciprocal of the gas law constant, R, in units moles T/atm m^3, consistent with the units used in the equations.

As these conversion equations show, in addition to knowing the molecular weight of a measured gaseous pollutant, the temperature and pressure at the time of the measurement must also be known. Since this information is frequently not given in the literature, no attempt has been made in this report to convert to a common unit.

SAMPLE GATHERING

Several sample gathering techniques are available for oxidant and ozone measurements. Typically, outdoor air, taken with a sampling probe is ducted to a sampling manifold located in a temperature regulated space. Air is withdrawn from the manifold either continuously into automated ozone monitoring instruments or intermittently using cumulative ozone absorbers. Because ozone reacts quickly with some substances, reliable measurement requires careful attention to the details of sampling site selection, sampling frequency, and sampling train materials. Ozone measurements are made indoors, outdoors near ground level, and from aircraft, for different though related purposes. Nationwide uniformity in sampling techniques is being achieved through cooperation among the various control agencies in specifying sampling conditions.

The location of the probe necessitates careful design and documentation to ensure that surrounding environmental conditions do not interfere with the subsequent interpretations of the measurement data. Examples of such minimum site descriptions are given in Table 6-3. Some of this information is now included with all the data logged into the Environmental Protection Agency's National Aerometric Data Bank and some was provided by the control agencies. An example of a site description in Southern California based on the requirements of the California Air Resources Board is shown in Table 6-4 (2 pages). In addition to the site description, there is a statement of all the conditions being monitored, the methods used, and the numerical specifications for the sampling probe both for the sampling manifold and for the connections from the manifold to the instruments. A third page

Table 6-3

Monitoring Site Description

Location and Agency	Site Number	Land Use and Site Description	UTM*	Elevation Above SL (meters)
1. New York (AQCR 043) State Dept. of Environmental Conservation, Div. of Air Resources				
Welfare Island (NYC East River)	7093-03	Residential; fairly open area free from obstructions; northern tip of Welfare Island in East River.	589.4E 4513.2N	
Merrick Ave. Eisenhower Pk., L.I.	2950-10	Residential, near Roosevelt Raceway; open area, no obstructions; level topography all around.	619.3E 4511.2N	46 to 61
Mammareseck 5th Ave. at N.Y.S. Twy. Exit 9	5956-01	Residential and commercial; low spot but fairly level. Surrounded by houses. Located in small basin in which the land rises 50' within an 800' radius.	603.9E 4531.8N	
2. New Jersey (AQCR 043) State Dept. of Environmental Protection, Bureau of Air Pollution Control				
Bayonne (Hudson County Park)		Mostly residential between bay and open park 0.5 m long. Over mile from Newark.	574.4E 4503.5N	46
Newark (Brandford Place)		Center city, commercial, surrounded by obstruction, on one corner of a parking lot 1 block square; moved mid May 1975.	569.6E 4509.5N	122
Linden (Tremley Point Sewage Plant)		Suburban, industrial adjacent to refinery	566.0E 4495.4N	61
3. Houston (AQCR 216) Texas Air Control Board				
Deer Park (Mae St.)	4515-60 (Connie 1)	Industrial, open area free from obstruction, near Federal Rd. and IH 10, level topography.	285.1E 3295.4N	64
Aldine (N. Houston)	(Connie 8)	Residential, open area free from obstruction; 1.6 km west of Hwy. 29; 3.2 kms of airport. Prevailing SE wind.	275.4E 3310.2N	579
4. Los Angeles (AQCR 024) Los Angeles County Air Pollution Control District (see Table 6-4).				

---

*Universal Transverse Mercator, 1/10 kilometer units

Table 6-4

State Air Resources Board Sampling Site Report

Date July 1, 1974 Prepared by WDH
Air Monitoring Station No. 60 City Azusa
Street Address 803 North Loren Avenue, Azusa, California
Longitude: W 117 Deg. 55 Min. 22 Sec., Latitude: N 34 Deg 8 Min 9 Sec
Nearest Street Intersection Loren Avenue and Foothill Boulevard
Date Operation Initiated at this Location January 30, 1957
Name of Operating Agency Los Angeles County Air Pollution Control District
Address of Operating Agency 434 South San Pedro Street, Los Angeles, California 90013
District Los Angeles Basin South Coast

SITE DESCRIPTION

CATEGORY
☐ CENTER CITY ☒ SUBURBAN
☐ RURAL
☐ REMOTE

SUBCATEGORY (Dominating Influence)
☒ Industrial ☐ Residential ☐ Commercial ☐ Mobile
☐ Near Urban ☐ Agri ☐ Comm ☐ Ind ☐ None of these

Type of Street Traffic Arterial
(Residential, Expressway, Commercial, Downtown, Arterial)

Outstanding Landmarks and Relation to Site:
Station location at foothills of San Gabriel Mountains. Aerojet plant S.E. 2 miles; Foothill Freeway a mile south.

Surrounding terrain and community characteristics (hills, valleys, flat, bodies of water, residential, industrial, commercial, rural, open, forested, row crops, grassland, orchard, etc.).
San Gabriel Mountains four miles to the north; small manufacturing plants around station site. Some residence near site - single family next door to south, trailer park across Loren to the east. Commercial area of Azusa 2 miles to the east. Flat, gently sloping terrain.

Possible nearby sources (refineries, stacks, chimneys, gasoline stations, power plants, parking lots, traffic, agricultural operations, etc.)

Source	Direction	Distance	Pollutants
Small Iron Foundry (usual equipment)	southeast	1000 feet	Normal
Large Gravel Plant	northwest	1½ miles	Particulate
Large Gravel Plant	southwest	3 miles	Particulate
Freeway	south	1 mile	Auto Exhaust
Limited Parking	east and north	Adjacent	Auto Exhaust
Metal Melting Furnace (no permits on file so apparently a minor source)	southwest	100 feet	Normal - Operated intermittently, regular schedule

Attach 8-½" X 11" portion of local street map indicating station location.

Table 6-4 (Cont.)

Air Monitoring Station No. 60

Gaseous Measurements

Gases		Method	Air Flow L/Min.
O_3			
O_x	X	Potassium Iodide - Colorimetric	3.7
NO	X	Modified Saltzman - Colorimetric	0.225
NO_2	x	Modified Saltzman - Colorimetric	0.225
NO_x	X	Addition of NO and NO_2 from above	--
THC	X	Flame Ionization	0.05
THC-CH_4	X	Flame Ionization	0.05
CO	X	Non-dispersive Infrared	0.5
SO_2	X	Conductivity - Hydrogen Peroxide	20 CFH
OTHER			

Instruments located on 1st floor of 1 story building.

PROBE DESCRIPTION

PROBE

Size 1 inch I.D.

Material Pyrex pipe

Flow rate 30 L/Min.

Length 23 Ft.

Sample Residence Time in Probe 7.1 Sec.

Number of Changes in direction 1

Number of Instruments connected 5

AIR INTAKE

Vertical ______ (up, down)

Angled 45° down ; Direction ______ (degrees, up, down) (N,S,E,W)

Horizontal X Direction S (N,S,E,W)

Height above: Ground level 7 1/3 ft.

sea level 607 ft.; roof - ft.

Horizontal distance to nearest street curb 43 ft.

If the probe does not extend above the roof, indicate the intake distance down from the roof 4 ft.; out from the building wall 1¼ ft.

Note: If more than one probe utilized, provide the above information for each. Attach a single line schematic diagram of probe arrangement(s) indicating inside diameters and cumulative air flows of all segments.

Three to four feet of ¼-inch Teflon tubing connects each instrument to sampling man.

Are wind instruments on same mast as station probe(s) inlet(s)? XXX No. If yes how much higher? - ft. If no, distance and direction from probe(s) 25 ft.; direction W .

Height above: Ground level 24 1/3ft., roof 13 ft., sea level 624 ft.

Nearby obstruction(s) to wind flow: None
Type(s), distance(s), direction(s), size(s)

(not included here) shows a schematic drawing with the dimensions and locations of the bends in the ducting. The sampling probe specifications currently in effect at four major air pollution control agencies are summarized in Table 6-5.

When selecting a monitoring site, it is important to take account of environmental features. For example, ozone measured in or near automotive traffic can drop to 50% of the area-wide value owing to reaction with the nitric oxide from exhaust emissions. While ozone measured 7.5m from a large tree in green leaf can drop to 70% of the area-wide value, it may also be reduced within 1m of shrubs and grass. Paint, asphalt, concrete, dry soil, and dead vegetation are not as reactive and so have a lesser effect. Peak ozone values observed in sunlit-windscreened-concrete and-asphalt courtyards tend to be higher than those recorded on an adjacent rooftop.

A preferred sampling location is open to the free movement of the ambient air, at least 3m above grass, 8m from shrubs, 40m from large trees, and 120m from any heavy automotive traffic. The flat roof of a one-or two-story building is ideal.[1] A probe which projects through a wall and extends about 2m beyond, is an acceptable alternate approximating the roof.

To minimize undesirable gas phase reactions in the probe, the gas flow must be regulated to keep the transit time in the sampling ducts as short as possible. When a probe is longer than 30cm, passage of the ozone-air sample should take less than 20 or 30s. Losses can also occur from reaction with the probe itself or with the accumulated dust which coats the inside.

Table 6-5

Sampling Probe Design

Item	Los Angeles	New York	New Jersey	Houston
Agency	Los Angeles County Air Pollution Control District (LAAPCD)	State Division of Air Resources	State Bureau of Air Resources	Texas Air Control Bd.
Height above ground (m)	2.2 to 22 mostly 3 to 6	4 to 6	3 to 4	6
Material	glass	glass	glass	glass
Shape	inverted U down	inverted U down	inverted U down	inverted U down
Inside diameter, (cm)	2.5	7.6	5 to 7.6	5
Total length, (m)	7 to 16	7 to 11	7 to 9	13
Flow rate (l/min)	15 to 30	560 to 850	283 to 400	283
Sum of sampler flows (l/min)	14	5 to 10	<10	ca 10
Water removal	see no condensation	see no condensation	see no condensation	Manifold lays in trailer light-well. Heat obviates condensation.
Rel. humidity controls	none	none	none	
Temperature controls	±3 C	±2 C (20-22C)	±3 C	±2 C
Inlet filters	none	screen, no filter	no filter, no screen	none

The materials of which probes are constructed must be sufficently inert to trace amounts of ozone to prevent adsorption, absorption, and reaction between the ozone-air sample and the sample line during the transit period. Teflon and glass are both relatively inert, but Teflon has the advantage of being unbreakable and thus more durable. Nalgon vinyl tubing is satisfactory for connectors and even for a short probe, if nothing else is available. Ozone reacts with Tygon vinyl, stainless steel, and aluminum, all of which should not be used.

To prevent the formation of reaction products from the interaction of the ozone-air sample with filters, they are intentionally not used at probe inlets (see Table 6-5). Some of the newer instruments however, require filters at the inlet of their sampling ports to prevent the particulate matter in the ambient air from fouling reaction chamber cells or from clogging the gas-flow controllers. When the same type of filter also precedes the calibration and zero gas sampling ports (which has not always been the practice), the problem is minimized to the extent that similar events occur during the calibration and sampling.

CALIBRATION

Most currently used oxidant and ozone monitors need to be calibrated with a predetermined concentration of ozone in air. Regardless of the principle used to measure ambient ozone or oxidant concentrations, the primary reference standard for calibrating each monitoring device or system should be identical everywhere. This requirement remains to be achieved in practice. Up to June 1975, at least seven calibration procedures were practiced in the U.S. These are listed in Table 6-6 along with the agency, primary use and current status of each method. Comparisons of these methods were recently completed.[12-16]

Ozone Generation

For reliable calibrations, it was necessary to develop a stable and reproducible ozone source which could produce ozone in air at concentrations smaller than ppm. After this was accomplished[19] several different versions were engineered which are now available commercially from most ozone-monitoringvendors of instruments.[20-24] The factors affecting the production and survival of oxygen species other than ozone are discussed in Chapter 12. Care must be taken to prevent these species from creating interference when generating ozone for instrument calibration.

A typical source (see Figure 6-1) consists of an ultraviolet mercury lamp which irradiates a quartz tube through which clean air flows at 5-10 l/min. A small amount of the oxygen in air is converted to ozone by photolysis. It is important that the incoming air is free of moisture nitrogen oxides, sulfur oxides, hydrocarbons and particles to avoid producing inadvertent interferences with subsequent sensors. Ozone concentrations from 0 to 1 ppm can be generated by varying the ultraviolet radiation intensity by means of an adjustable shield around the lamp envelope. The air stream flow rate is controlled by a needle valve and measured by a rotameter or a mass-flow meter. The ozonized air passes to a manifold from which the testing monitor draws its sample. The ozone concentration produced in this way is solely an empirical function of the settings of the lamp

Table 6-6

Primary Reference Standards for Calibration of Ozone or Oxidant Analysis

Principle	Abbreviation	Agency/Application	Status	Ref.
1. Colorimetric; 1% neutral buffered potassium iodide	1% NBKI	USEPA/air monitoring	Official, USEPA	25
2. Colorimetric; 2% neutral buffered potassium iodide	2% NBKI	Calif. ARB/air monitoring	Official, Calif. until June 1975	26
3. Titrimetric; 2% unbuffered potassium iodide	2% UBKI	Los Angeles County/air monitoring	Official	27
4. Gas phase titration of nitric oxide with ozone	GPT	USEPA/verification	Tentative EPA Method.	18 18a
5. National Bureau of Standards ozone generator	$SRM\text{-}O_3^*$	Several/with (1) in air monitoring	Developmental	19
6. Extinction coefficient of ozone in the ultraviolet range at 254 nm	UV-254	Calif. ARB/air monitoring; Research labs.	Official in Calif. since June 1, 1975	13
7. Extinction coefficient of ozone in the infrared range at a frequency of 1053 cm^{-1} (9480 nm)	IR-1053	Research labs.	Research application	17, 14

*SRM - Standard Reference Material

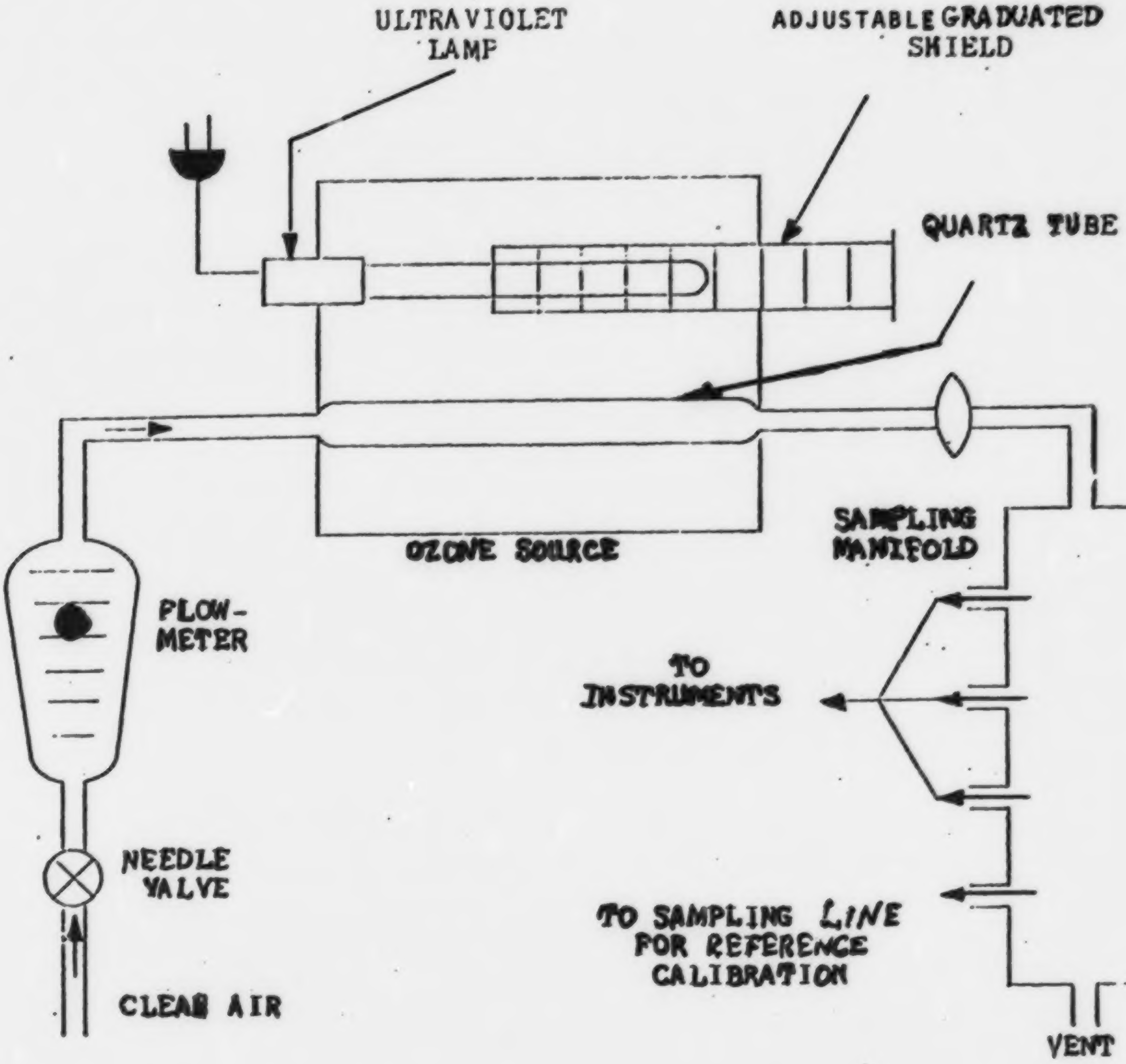
ULTRAVIOLET LAMP
ADJUSTABLE GRADUATED SHIELD
QUARTZ TUBE
OZONE SOURCE
SAMPLING MANIFOLD
FLOW-METER
TO INSTRUMENTS
NEEDLE VALVE
TO SAMPLING LINE FOR REFERENCE CALIBRATION
CLEAR AIR
VENT

Figure 6-1. Ozone source and manifold system.[19]

shield and air flow rate, the air temperature, and the humidity. Therefore, the output concentration must be measured using a scientifically acceptable reference standard.

Ozone Analysis

All of the iodometric reference methods (items 1, 2 and 3, Table 6-6) are similar in principle. They assume that ozone (O_3) when in contact with iodide ions (I^-) in aqueous (H_2O) solution releases a stoichiometric amount of iodine (I_2) according to the following chemical equation:

$$O_3 + 2I^- + H_2O = I_2 + O_2 + 2OH^- \qquad (3)$$

where O_2 stands for oxygen and OH^- for hydroxyl ions.

In California, the Los Angeles County Air Pollution Control District (LAAPCD) and the California Air Resources Board (ARB) both began continuous air monitoring for oxidants more than 20 years ago. Oxidant monitoring at urban sites was begun over 5 years ago by the National Air Pollution Control Administration and continued by the Environmental Protection Agency (EPA). All these groups initially used instruments containing the same absorbing solutions but their iodometric calibration methods differed in detail.

California Air Resources Board (ARB) Procedure (prior to June 26 1975. The ARB reference procedure for ozone uses a 2% neutral buffered potassium iodide reagent. Ozone is generated in air previously humidified to about 50% relative humidity. The air sample to be analyzed is drawn through the reagent in a midget impinger, and the ozone present in the sample air liberates iodine from the iodide reagent. The quantity of iodine liberated is determined using a spectrophotometer which has been calibrated with an iodine solution standardized with sodium thiosulfate solution which, in turn, has been standardized against primary grade potassium biiodate.

U.S. Environmental Protection Agency (EPA) Procedure.[25] The EPA reference procedure for ozone is similar to the ARB procedure except that the ozone is produced from dry air, the reagent is 1% neutral buffered potassium iodide, and the iodine solution is standardized with primary standard grade arsenious oxide. Oxidant minitors outside California have generally been calibrated with this procedure.

Los Angeles County Air Pollution Control District (LAAPCD) Procedure.[27] The LAAPCD reference procedure for ozone uses a 2% unbuffered potassium iodide reagent. Ozone is generated in air previously humidified to about 50%. The air sample to be analyzed is drawn through the reagent in an impinger of LAAPCD design and the ozone present in the sample air liberates iodine from the iodide reagent. The quantity of iodine liberated is determined by titrating the reagent with sodium thiosulfate solution. The sodium thiosulfate used in the titration is standardized with potassium dichromate solution. The procedure utilized by the LAAPCD was modified in January 1974 to include the use of dry ice in the standardization of the dilute sodium thiosulfate in order to improve the precision of the titrations. This does not affect the mean values obtained with their procedure.[28]

These iodometric calibration methods are based on the assumption that there is a stoichiometric reaction between ozone and the iodine in the various potassium iodide procedures. Three essentially independent methods have been used to test the accuracy of this assumption. These are: measuring the absorption of ultraviolet radiation at 254 nm by ozone in air; measuring the absorption of infrared radiation at 9480 nm by ozone in air; and determining the ozone in air concentration by titration with nitric oxide.

The first two determinations by radiation absorption require accurate measurements of the extinction coefficients of ozone (a measurement of the absorption efficiency of the incoming radiation at a maximum absorption wavelength) in the ultraviolet and the infrared. Three different principles have been used over the past 20 years to measure the extinction coefficient of ozone in the ultraviolet at 254 nm: manometric, decomposition stoichiometry and gas-phase titration. The manometric method which is based on pressure measurements of gaseous ozone requires, in at least one case,[34] a substantial and somewhat uncertain correction for decomposition; and the method of decomposition stoichiometry depends on the pressure change that accompanies the decomposition of ozone to oxygen, $2\,O_3 \rightarrow 3\,O_2$. Clyne and Coxon[31] determined ozone concentrations in a flow tube by titration with nitric oxide, a method essentially equivalent to gas phase titration. These methods with their results are summarized in Table 6-7. The best value for the ultraviolet extinction coefficient at 254 nm is considered to be 134 cm^{-1} atm^{-1} at O C and 1 atm (STP).[31a]

Table 6-7

Ozone Extinction Coefficient Measurements

Authors	Reference	Extinction Coefficient cm^{-1} atm^{-1} STP, base 10	Method*
Inn and Tanaka	34	133	Manometric
Hearn	33	134	Decomposition stoichiometry
DeMore and Raper	30	135	Decomposition stoichiometry
Griggs	32	132	Manometric
Clyne and Coxon	31	136 (250 nm)	Gas-phase titration
Becker, Schurath, and Seitz	29	135	Manometric

*Method used to establish the ozone concentration.

Measuring the absorption by ozone in air of ultraviolet radiation at a wave length of 254 nm. With this value for the extinction coefficient, a laboratory photometer is used to measure the primary reference concentration of the ozone in the gas stream used for calibration.[13] A schematic for this arrangement is in Figure 6-2. Highly accurate measurements are attainable with this type of photometer because the pressure, temperature and path length of the light beam in the cell can all be controlled and measured precisely.

The ozone concentration in parts per million is given by:

$$O_3\ (\text{ppm}) = \frac{10^6\ T}{273\ Pk\ell} \log \frac{I_o}{I_t} \qquad (4)$$

where T = temperature, K (kelvin)

P = total pressure, atm.

k = extinction coefficient of ozone is 134 cm^{-1} atm^{-1} at STP

ℓ = path length, cm

I_o = intensity with carrier gas only

I_t = intensity with O_3 present.

Because at concentrations smaller than parts per million, the radiation intensities, I_o and I_t, have to be measured with very great precision, the determination using absolute photometry requires a physical chemistry laboratory with an experienced staff.

Calibrations at monitoring sites, therefore, require a trans-

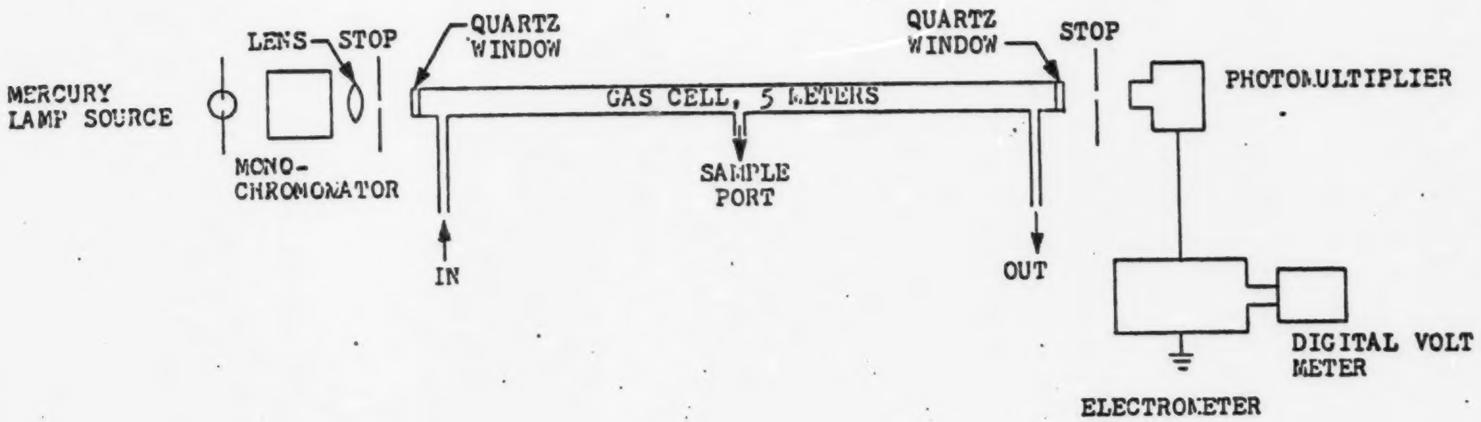
MERCURY LAMP SOURCE
LENS
STOP
MONO-CHROMONATOR
QUARTZ WINDOW
GAS CELL, 5 METERS
SAMPLE PORT
IN
OUT
QUARTZ WINDOW
STOP
PHOTOMULTIPLIER
ELECTROMETER
DIGITAL VOLT METER

-Figure 6-2. Absolute Ultraviolet Ozone Photometer[13] ferable standard. The use of a commercially available photometer, which displays the difference in signals between the ultraviolet light absorbed at 254 nm with and without ozone in the sample cell, is one approach. It has proven to be stable in performance even after transport between different laboratories.[12,15] A schematic diagram of the Dasibi Model 1003-AH ozone monitor is shown in Figure 6-3. The operating principle of the Dasibi instrument has been described by Behl,[36] Bowman and Horak,[37] and by Hodgeson _et al_.[15] An evaluation of this instrument has been carried out by deVera, Jeung and Imada.[35]

As it enters the instrument, the sample is diverted by the valve into a chemical scrubber which changes any ozone present to oxygen. This ozone-free sample then passes through an absorption chamber 71 cm in length, where a detector measures the amount of ultraviolet light at 254 nm transmitted through it. The integrated intensity of the transmitted light is digitized and stored electronically as the reference signal. On completion of this measurement the valve is opened and the absorption chamber is flushed with the ozone-containing sample. The digital counter now records the reduction of ultraviolet light due to the ozone in the sample. This value is subtracted from the stored reference measurement and the difference is displayed in concentration units equivalent to parts per million ozone.

The ozone concentration (c) as measured by the Dasibi ozone meter is in principle given by equation (4), which can be expressed in terms of the instrument itself as:

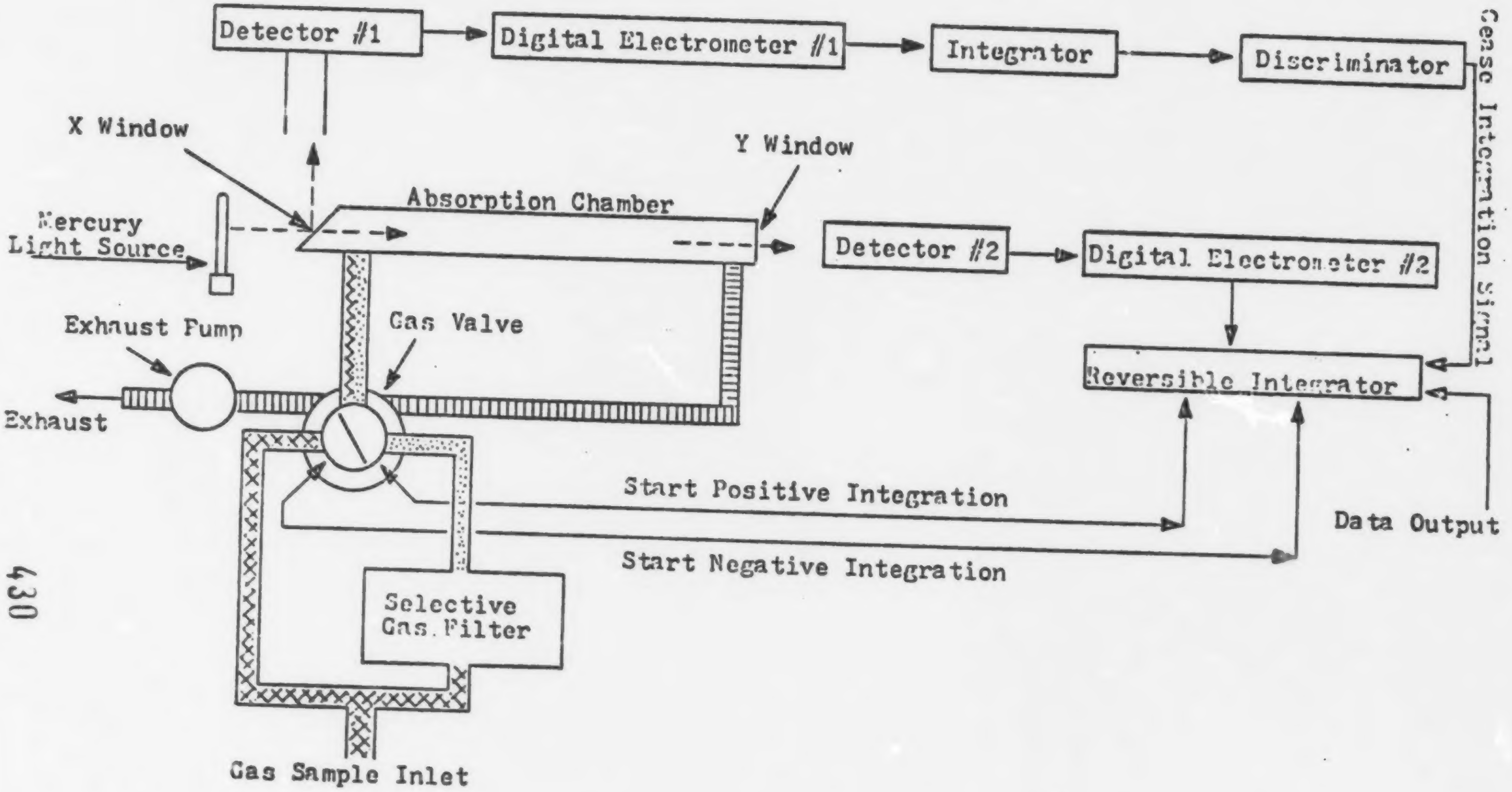
Detector #1
Digital Electrometer #1
Integrator
Discriminator
Cease Integration Signal
X Window
Y Window
Absorption Chamber
Mercury Light Source
Detector #2
Digital Electrometer #2
Exhaust Pump
Gas Valve
Exhaust
Reversible Integrator
Start Positive Integration
Start Negative Integration
Data Output
Selective Gas Filter
Gas Sample Inlet

Figure 6-3. Dasibi ozone monitor, block diagram.[54]

$$O_3\text{(ppm)} = \frac{22.4\ T}{kP}\ \ell n\ \frac{S}{S-R} \qquad (5)$$

where T = temperature, K, degrees kelvin.

S = span setting of instrument, $\propto I_o$

R = instrument reading $\propto (I_o - I_t)$

k = extinction coefficient of ozone is 134 cm^{-1} atm^{-1} at STP

P = pressure, atm.

At low ozone concentrations (R small compared to S), the above expression can be simplified as follows:

$$O_3\text{(ppm)} = \frac{22.4\ T}{k\ P}\left(\frac{R}{S}\right). \qquad (6)$$

The quantity 22.4 T/k P is the theoretical absolute span setting of the instrument. In practice, calibration against the ozone standard is required for maximum accuracy, both because the length of the light path is altered by possible multiple reflections off the inner wall, and because the pressure, temperature and absorption inside the instrument cannot be precisely determined. Hodgeson et al.[15] compared a Dasibi instrument spanned according to equation (4) with the absolute photometer. They obtained the following relationship when repeated (61) measurements were made on different days at ozone concentrations of 0.05 to 2.5 ppm:

$$O_3\text{(phot)} = (1.05 \pm 0.01)\ O_3\text{(Dasibi)} + (0.025 \pm 0.013). \qquad (7)$$

When the span setting of a Dasibi instrument was adjusted to agree with an absolute laboratory photometer and repeated measurements were made on different days, the following relationship with the absolute photometer was obtained:

$$O_3\,(\text{phot}) = (0.999 \pm 0.003)O_3\,(\text{Dasibi}) - (0.007 \pm 0.002). \qquad (8)$$

The uncertainties refer to 95% confidence limits. These small error limits are indicative of the high precision of the readings obtainable from both instruments.

Measuring the absorption by ozone in air of infrared radiation at a wavelength of 9480 nm. This method which is identical in principle to measurement of the absorption in the ultraviolet requires an accurate measurement of the extinction coefficient of ozone at a wavelength of 9480 nm. Making this measurement in the infrared energy region is more complicated because the determination of the extinction coefficient is more strongly influenced by temperature, pressure and instrumental characteristics such as spectral slit width. Also, the extinction coefficient is much smaller than in the ultraviolet. This means that for measurements of concentrations smaller than parts per million, the absorption path length in the infrared infrared has to be about 100 times longer than the 1 meter ultraviolet cell (see Figure 6-2). All these factors create problems which detract from the practicality of this method as a primary reference. Nevertheless, at laboratories experienced in this technique, accurate measurements have recently been made that are in close agreement with the values obtained by absolute ultraviolet photometry.[14] Using the Dasibi ozone meter as a transfer standard, the following agreement has been obtained:

$$O_3\,(\text{Dasibi}) = (0.99 \pm 0.02)\, O_3\,(\text{IR}) + (0.016 \pm 0.011). \qquad (9)$$

The uncertainties are within one standard deviation. Because ultraviolet photometry carried out with the Dasibi instrument is a relatively simple procedure, it may be advisable to calibrate even infrared analyzers, by means of the ultraviolet transfer standard.

Determination of ozone in air by titration with nitric oxide. This calibration technique[18,18a] is based on the application of the rapid gas-phase reaction between nitric oxide (NO) and ozone to produce a stoichiometric quantity of nitrogen dioxide (NO_2) according to the following equation:

$$NO + O_3 \rightarrow NO_2 + O_2 . \qquad (10)$$

The reaction rate is extremely fast so that even at concentrations smaller than parts per million, the reaction is virtually complete after a few seconds when there is an excess of nitric oxide present. Under these conditions the amount of ozone added during the titration is equivalent to the amount of nitric oxide consumed, and to the amount of nitrogen dioxide formed. The accuracy of this calibration method is critically dependent on the accurate measurements of the nitric oxide concentration, and on the nitric oxide and ozone flow rates.

Nitric oxide at about 50 ppm compressed with very pure nitrogen in gas cylinders is provided for this purpose, and the true concentration is established by comparison with that of a compressed gas tank which can be obtained from the National Bureau of Standards, as a standard reference material. The nitric oxide meter is calibrated repeatedly at several concentrations of nitric oxide and the mass flow meters are recalibrated frequently with absolute bubble meters.

The titration is shown schematically in Figure 6-4. Nitric oxide, compressed with nitrogen in a gas cylinder, is then metered into the apparatus along with the clean air stream but without the ozone. In this way, the initial nitric oxide concentration is measured with the nitric oxide meter. When the initial nitric oxide concentration is established, the lamp shield in the ozone generator is withdrawn to various settings and the final nitric oxide concentrations are measured. The initial nitric oxide concentration, the reaction residence times, and the maximum ozone concentration added are established such that the unreacted ozone is negligible (i. e., <1%). Under these conditions, the measured decreases in nitric oxide concentrations then determines the ozone concentrations for various generator settings and serves to calibrate the ozone source. The ozone source may then be used to calibrate ozone meters.

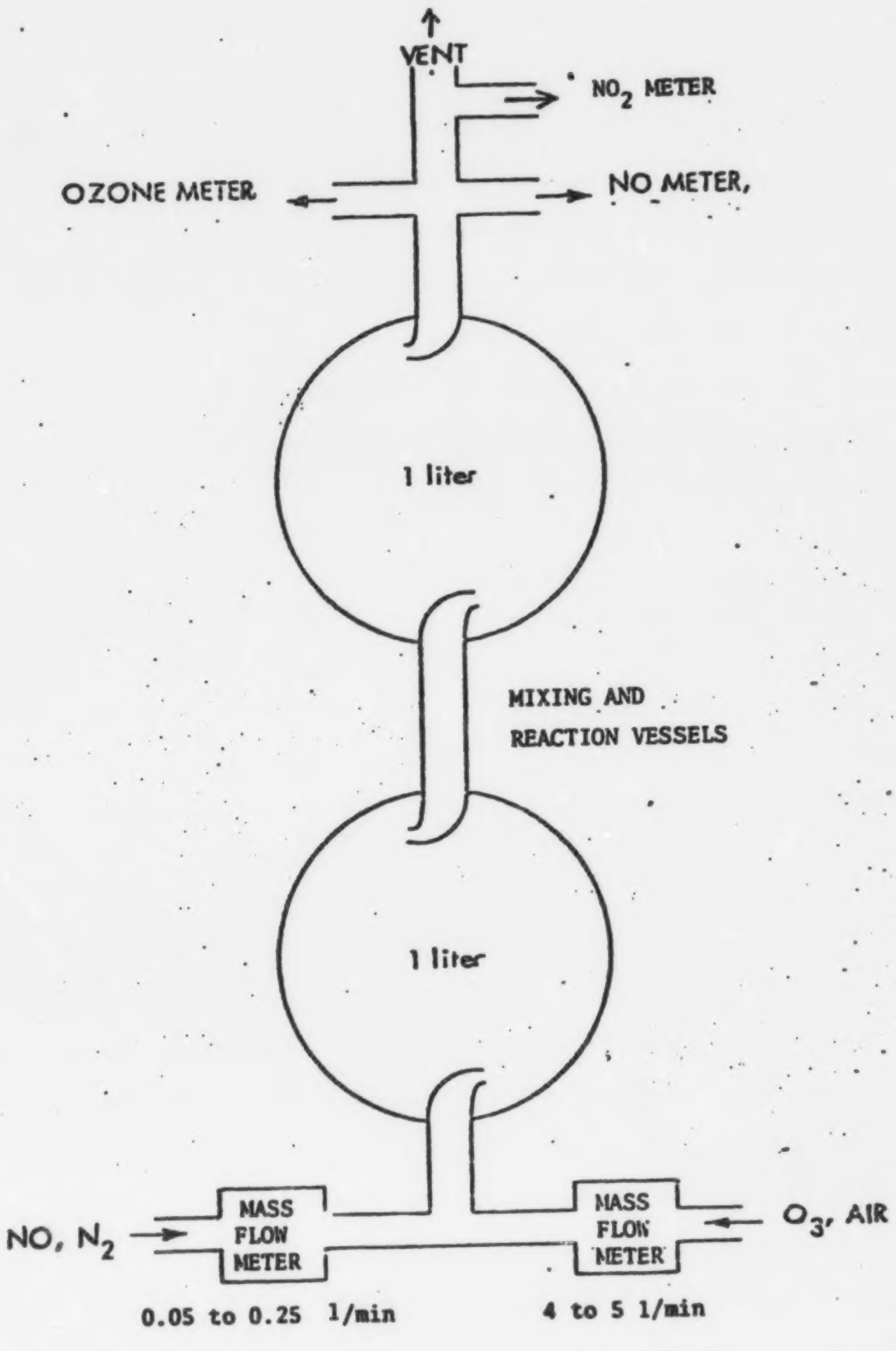
VENT
NO$_2$ METER
OZONE METER
NO METER,
1 liter
MIXING AND
REACTION VESSELS
1 liter
NO, N$_2$
MASS
FLOW
METER
MASS
FLOW
METER
O$_3$, AIR
0.05 to 0.25 l/min
4 to 5 l/min

Figure 6-4. Gas phase titration for determining ozone.[13]

As an option, the nitrogen dioxide concentration produced can also be monitored at the same time. In fact, this is one way to conveniently calibrate nitrogen dioxide meters.

Using the Dasibi ultraviolet ozone analyzer as a secondary reference standard DeMore and Patapoff[13] tested the prediction that the observed change in nitric oxide concentration (ΔNO) would equal the ozone concentration introduced and measured by UV absorption. They found good agreement in which

$$[O_3]_{UV} = (1.00 \pm 0.05)\ \Delta NO - (0.00 \pm 0.01). \qquad (11)$$

Similar conclusions were recently reported both by Hodgeson[15] and by Paur.[16] These findings provide further validation of the ultraviolet method for calibrating air-monitoring instruments and establish gas phase titration as an alternative primary reference method.

PRINCIPLES OF MONITORING

Most of the atmospheric oxidant and ozone data, as well as the experimentally determined exposure data for vegetation, animals, and humans, have been obtained using analyzers which sample, and record the ambient concentrations almost continuously during the period of observation. The response times are usually acceptable for fixed station monitoring because data describing hourly averages are sufficient. Faster responses are needed, however, for studying chemical reaction rates, retention upon inhalation, sampling while in motion, (as from aircraft) and for expediting calibrations. The response times required are therefore a function of the resolution needed.

Definitions of Resolution and Response Times

Resolution: the ability to separate two closely occurring events in space or time at a signal-to-noise ratio of two, expressed as percent of full scale.

Signal-to-noise ratio: the ratio of the magnitude of the response due to the pollutant concentration and of the magnitude of unwanted, spontaneous, short-term responses not caused by variations in pollutant concentration.

Response times: (see Figures 6-5 and 6-6).

Lag time (initial response time), t_l: the interval between the time t_o, when a step change (increase or decrease) in pollutant concentration is made, to the time t_i when the instrument indicates a response equal to twice the noise.

$$t_l = t_i - t_o . \tag{12}$$

Time to 95%, t_{95}: the interval between the time t_o, when a step increase in pollutant concentration is made, to the time t_{95} when the instrument indicates a response equal to 95% of the step increase.

$$t_{95} = t_{95} - t_o \tag{13}$$

Similarly, t_{90} corresponds to the time to indicate 90%, and t_{100} the time to indicate 100% of the step increase in pollutant concentration.

Time to -95%, t_{-95}: the interval between the time t_o when a step decrease in pollutant concentration is made to the time t_{-95} when the instrument indicates -95% of the step decrease.

$$t_{-95} = t_{-95\%} - t_o . \qquad (14)$$

Similarly, t_{-90} corresponds to the time to indicate -90%, and t_{-100} to the time to indicate -100% of the step decrease in pollutant concentration.

Rise time, t_r: the interval between the time of a response equal to 100% of the step increase in pollutant concentration (t_{100}) and the lag time (t_1).

$$t_r = t_{100} - t_1 . \qquad (15)$$

Fall time, t_f: the interval between the time the instrument indicates -100% of the step decrease in pollutant concentration (t_{100}) and the lag time (t_1).

$$t_f = t_{-100} - t_1 . \qquad (16)$$

The fall time does not necessarily equal the rise time.

Pulse time: the minimum time a pollutant concentration must persist for the analyzer to register a peak response equal to the pollutant concentration (see Figure 6-5).

For any event to be accurately recorded, it must persist for the pulse time of the instrument. This time is equal either to the rise time or to the time to 100% response, depending on the design of the instrument. For accurate data from aircraft sampling plumes, for example, it is necessary to obtain rise times of a few seconds or less. This is a

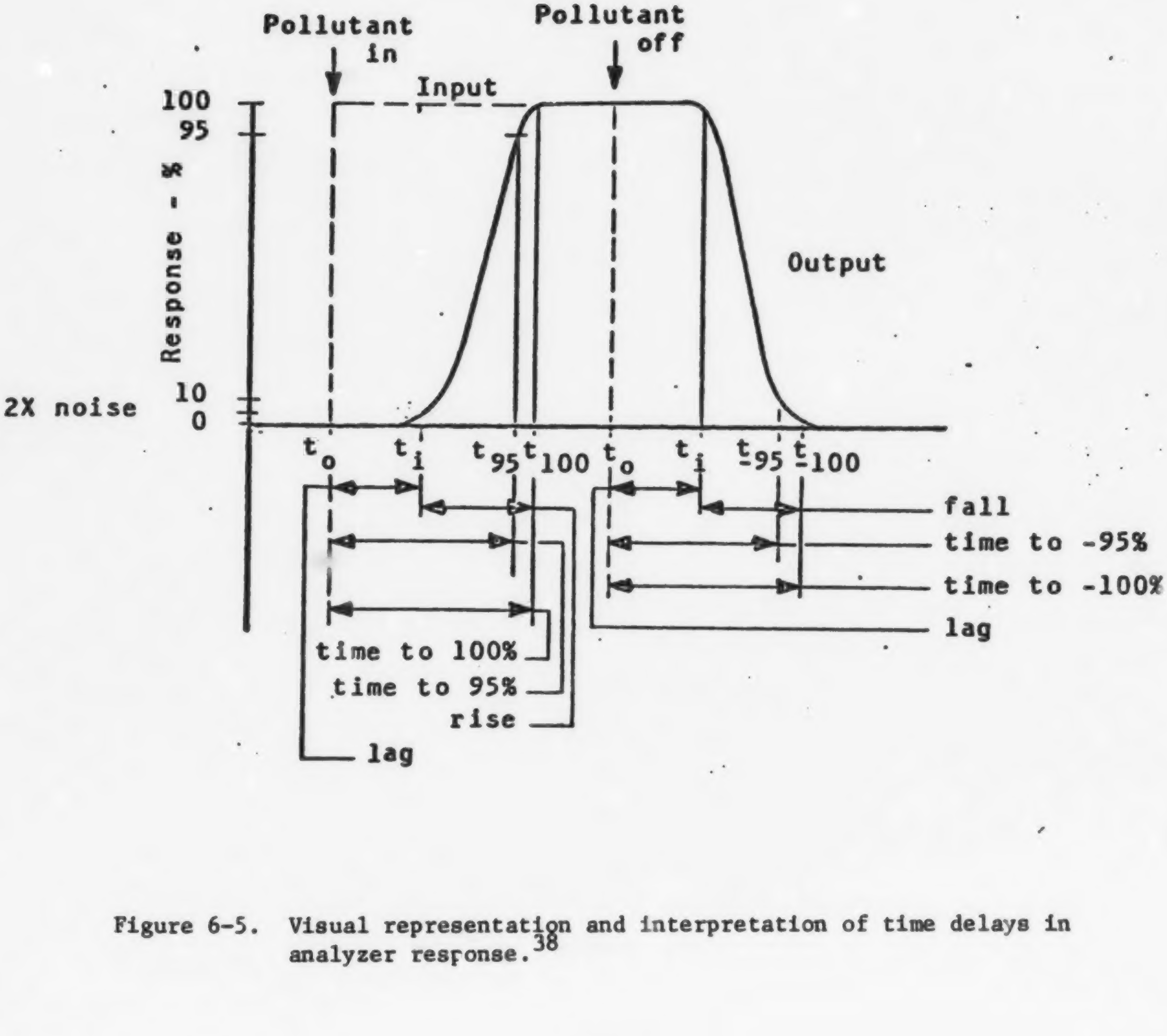
Pollutant in
Pollutant off
Input
Output
100
95
10
0
2X noise
Response - %
t_o
t_i
t_{95}
t_{100}
t_o
t_i
t_{-95}
t_{-100}
fall
time to -95%
time to -100%
lag
time to 100%
time to 95%
rise
lag

Figure 6-5. Visual representation and interpretation of time delays in analyzer response.[38]

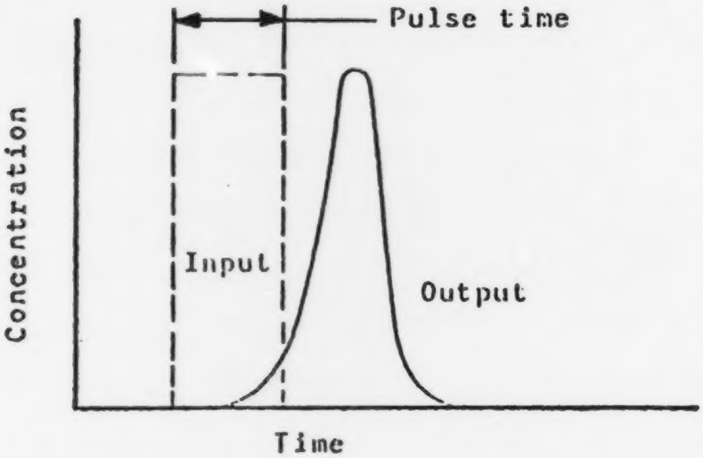
Pulse time
Concentration
Input
Output
Time

Figure 6-6. Diagram of pulse time.[28]

very fast response for an analyzer and has only quite recently become possible for ozone measurements.

The analytical principles which have been applied to accumulate air quality data are: colorimetry, amperometry, chemiluminescence and ultraviolet absorption. Colorimetric and amperometric continuous analyzers employing wet chemical techniques (reagent solutions), have been in use as ambient air monitors for many years. Chemiluminescent analyzers, which measure the amount of chemiluminescence produced when ozone reacts with a gas or solid, were developed to provide a specific and sensitive analysis for ozone, and have also been field-tested. Ultraviolet absorption analyzers are based on a physical detection principle, the absorption of ultraviolet radiation by a substance. They do not use chemical reagents, gases or solids in their operation and have only recently been field-tested. Ultraviolet absorption analyzers are ideal as transfer standards but as discussed earlier they have limitations as air monitors because aerosols, mercury vapor, and some hydrocarbons could interfere with the accuracy of ozone measurements made in polluted air.

Advanced electro-optical methods (e.g., laser resonance absorption), capable of measuring average concentrations over long distances still require extensive research and field testing to demonstrate their practical application to ozone monitoring. Since electro-optical methods have not to date been widely used, they will not be discussed further here.

Colorimetric Analyzers

Colorimetric analyzers spectrophotometrically measure the increase in color (absorbance) of a solution resulting from contact with a measured volume of air. The absorbance is linearly proportional to the concentration of the colored species, within known limits. Continuous colorimetric analysis of total oxidants is carried out using a solution of neutral-buffered potassium iodide (KI). In 1953, Littman and Benoliel[6] developed the first colorimetric oxidant recorder to come into general use. Instruments of this design, using a 20% neutral-buffered potassium iodide solution, later changed to 10%, were incorporated into the Los Angeles County Air Pollution Control District (LAAPCD) air monitoring network in the early 1950's.[1]

The continuous colorimetric instrumental method is described in detail by the Intersociety Committee[39] and the American Society for Testing and Materials,[40] and colorimetric and amperometric analyzers are discussed extensively in the papers both of Tokiwa *et al.*[41] and of Hodgeson.[2]

A typical colorimetric analyzer is illustrated schematically in Figure 6-7.[41] Sample air is drawn at a metered rate into a contact column where the air is scrubbed with a metered flow of potassium iodide buffered at pH 6.8. The reaction of oxidants with the potassium iodide solution produces the yellow colored triiodide ion (I_3^-). The colored solution flows to a colorimeter cell where the absorbance of the triiodide ion is measured at 354 nm. The photometer signal is then electronically recorded as parts per million of oxidant. The reaction of potassium iodide with ozone at pH 6.8 ± 0.2 is given by equation 17.

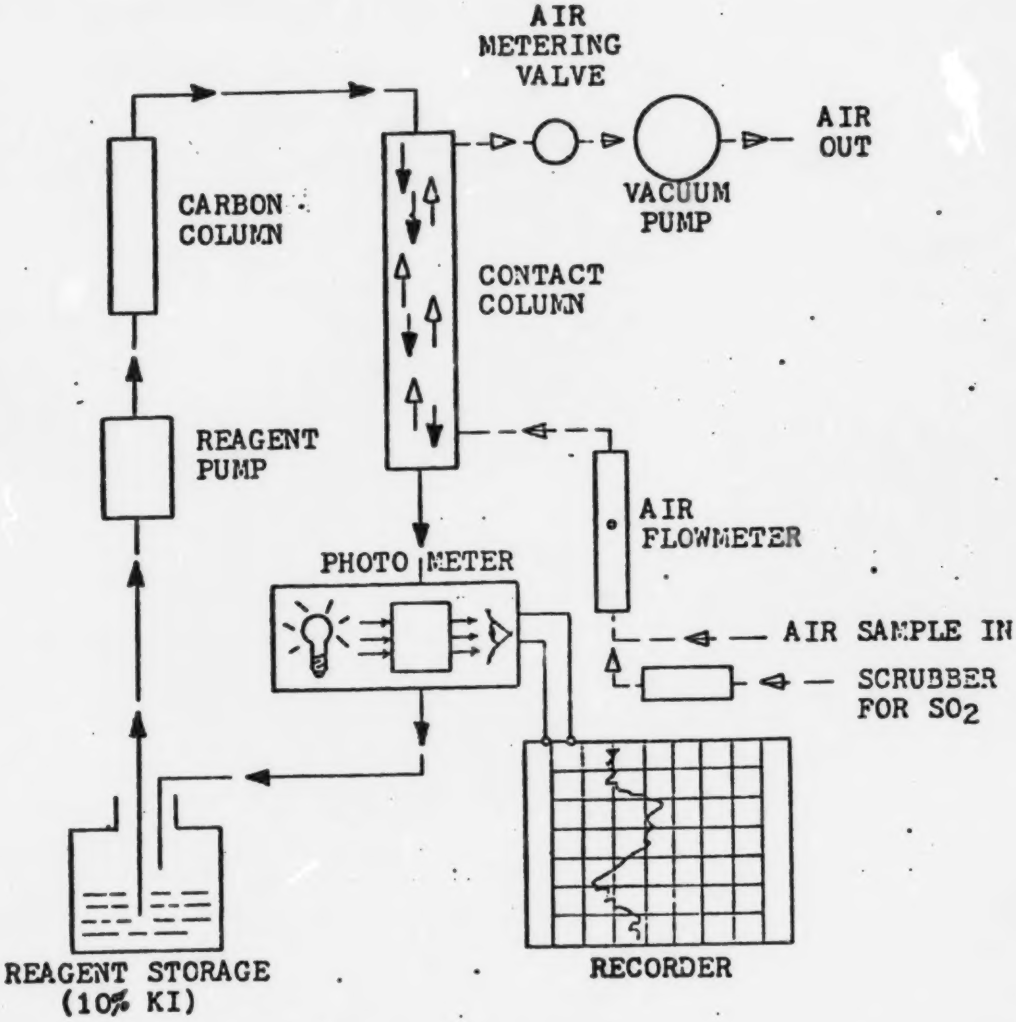
AIR METERING VALVE
AIR OUT
VACUUM PUMP
CARBON COLUMN
CONTACT COLUMN
REAGENT PUMP
AIR FLOWMETER
PHOTO METER
AIR SAMPLE IN
SCRUBBER FOR SO_2
REAGENT STORAGE (10% KI)
RECORDER

Figure 6-7. Colorimetric oxidant analyzer.[41]

$$O_3 + 3KI + H_2O \rightarrow K^+I_3^- + 2KOH + O_2 . \qquad (17)$$

Colorimetric oxidant analyzers operate most reliably at atmospheric oxidant levels ranging from 20-2000 $\mu g/m^3$ (0.01 - 1.0 ppm) of ozone or other equivalent oxidant. A usable response can be obtained from oxidant levels equivalent to as much as 100 ppm ozone, but at such high levels the stability and speed of response are inferior to those attainable at lower concentrations.[39]

When sulfur dioxide (SO_2) is present in the polluted air, it causes a negative interference equal to 100% of an equimolar concentration of oxidant.[40] The response to the pollutant, nitrogen dioxide (NO_2), varies with the reagent formulation and scrubber design. For 10% potassium iodide, nitrogen dioxide produces a positive interference of approximately 21%; for 20% potassium iodide, the interference produced is approximately 30%.[41]

Filters and scrubbers have been used for removing sulfur dioxide, but detailed information about their performance is not available. A brief review of performance characteristics of sulfur dioxide scrubbers is given by Hodgeson.[2] One device consists of glass fiber strips impregnated with chromium trioxide and sulfuric acid.[42] An even better scrubber consists of a bed of small pellets of porous chromatography grade firebrick or alumina impregnated with chromium trioxide.[38] These scrubbers, that convert only a portion of the ambient nitric oxide to nitrogen dioxide, require an additional correction factor. Despite these drawbacks, this is the most generally used technique for removing sulfur dioxide interference, particularly during periods of high sulfur dioxide concentrations. When sulfur dioxide levels are less than 20% of the nitric oxide concentration, this filtering system is not recommended.[39] In this case, the correction for nitrogen dioxide interference in the oxidant reading can be determined by measuring the instrument response to a known stream of nitrogen dioxide while concurrently analyzing for nitrogen dioxide in the atmosphere; then the appropriate subtraction can be made.[40]

Amperometric Analyzers

Amperometric analyzers are often referred to as "coulometric" analyzers. Coulometry is a mode of analysis in which the quantity of electrons (charge) necessary to oxidize or reduce a desired substance is measured. Because it is the current and not the charge which is measured by these instruments, "coulometric" analyzers are more properly called amperometric analyzers. This principle has been implemented for oxidant monitoring using either a galvanic (Hersch) cell[47] or an electrolytic (Brewer or Schulze) cell.[44-46] A schematic illustration of this instrument using a Brewer cell is shown in Figure 6-8. (Instruments using Hersch or Schulze cells are not widely used.)

The operational principles of the amperometric analyzer are described in the Intersociety Committee's manual of methods for ambient air sampling and analysis.[43] The contactor-sensor consists of a rod wound with many turns of a fine platinum wire (cathode) and two turns of a heavier wire (anode) axially mounted in a plastic block with a hole about 0.6 cm inside diameter and 5 cm long. The reagent is usually a mixture of 2% potassium iodide and 5% potassium bromide buffered at pH 6.8 0.01 M with 0.026 M disodium hydrogen phosphate and 0.018 M sodium dihydrogen phosphate.[41] Sample air and reagent pass concurrently through the annular

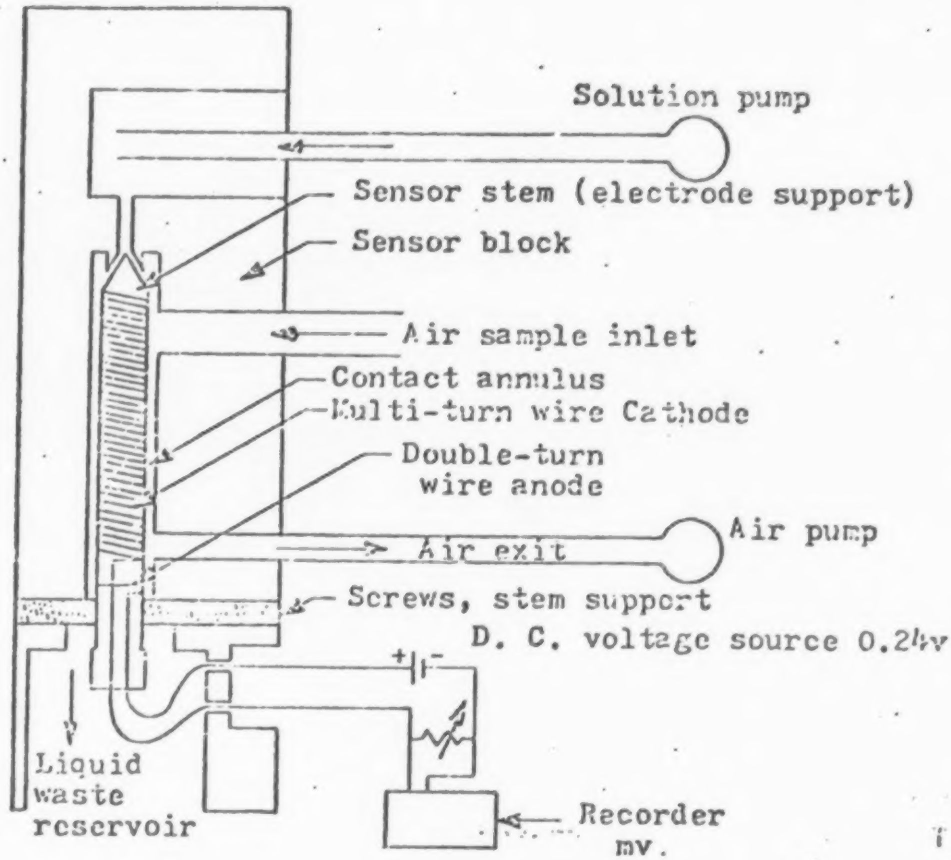
Solution pump
Sensor stem (electrode support)
Sensor block
Air sample inlet
Contact annulus
Multi-turn wire Cathode
Double-turn wire anode
Air pump
Air exit
Screws, stem support
D. C. voltage source 0.24v
+ -
Liquid waste reservoir
Recorder mv.

Figure 6-8. Amperometric analyzer using Brewer type electrolytic cell.[43]

space (about 0.2 cm) between the support rod and the cylinder wall. Ozone in the air transferred to the reagent reacts with the iodide to produce triiodide ions which in turn react with the hydrogen, polarizing the cathode. As a result of these reactions, current flows to repolarize the cathode in proportion to the amount of hydrogen removed. This current, which is directly proportional to the ozone concentration, is recorded.[44,45]

The presence of nitrogen dioxide in the sample causes a positive interference. When the concentration of the potassium iodide reagent is 2%, then the interference is about 6% of the nitrogen dioxide concentration. This is typical for amperometric analyzers which have been marketed specifically for ozone or oxidant measurements.[41] The exact level of the detector's specific response to nitrogen dioxide depends on the instrument design, the composition of the sensing solution, the operating conditions, and other unknown factors.[43] Therefore, the specific response for each detector should be determined experimentally. The oxidant measurements can be corrected for nitrogen dioxide interference by subtracting the response due to the nitrogen dioxide from the total detector response.

Sulfur dioxide in the sample causes a negative interference of approximately 1 mole of ozone per mole of sulfur dioxide because it reduces the iodine formed by ozone back to potassium iodide. When sulfur dioxide levels do not exceed those of the oxidants, a method commonly used to correct for its interference is to add the amount of sulfur dioxide determined by an independent method to the total detector response. A second method is to remove the sulfur dioxide from the sample stream by using solid[38,46,48] or liquid[47] chromium trioxide scrubbers. Because the data on the performance of these sulfur dioxide scrubbers is inadequate, the performance for each oxidant system must be established experimentally.

Because of the interference problems with both colorimetric and amperometric analyzers, they are being replaced by instruments based on other principles. (Colorimetric analyzers are no longer commercially available.) One such recently improved technique developed for the specific detection and measurement of ozone is by detecting the absorption of ultraviolet radiation by the ozone molecule. (This method is described in the Calibration section.) Another, is by measuring the chemiluminescence produced when ozone reacts with a specific gas or solid.

Chemiluminescence

In 1965, a gas-phase chemiluminescent reaction between ozone and ethylene was reported by Nederbragt et al.,[49] and subsequently the sensitivity of this technique was improved by Warren and Babcock.[50] The reaction between ozone and ethylene yields chemiluminescent emission in the 300 to 600 nm region with maximum intensity at 435 nm.[51] The intensity of this emission is directly proportional to the ozone concentration.

A diagram of a typical gas-phase (ozone-ethylene) chemiluminescent ozone analyzer[54] is shown in Figure 6-9. The detector responds linearly to ozone concentrations between 0.003 and 30 ppm; no interferences were initally observed.[51] More recently, however, it has been established that when going from 0 to 60% relative humidity in the temperature range of 20 to 25 C, water vapor produces a small positive signal which results in about an 8% increase in the ozone concentration measurement. This potential

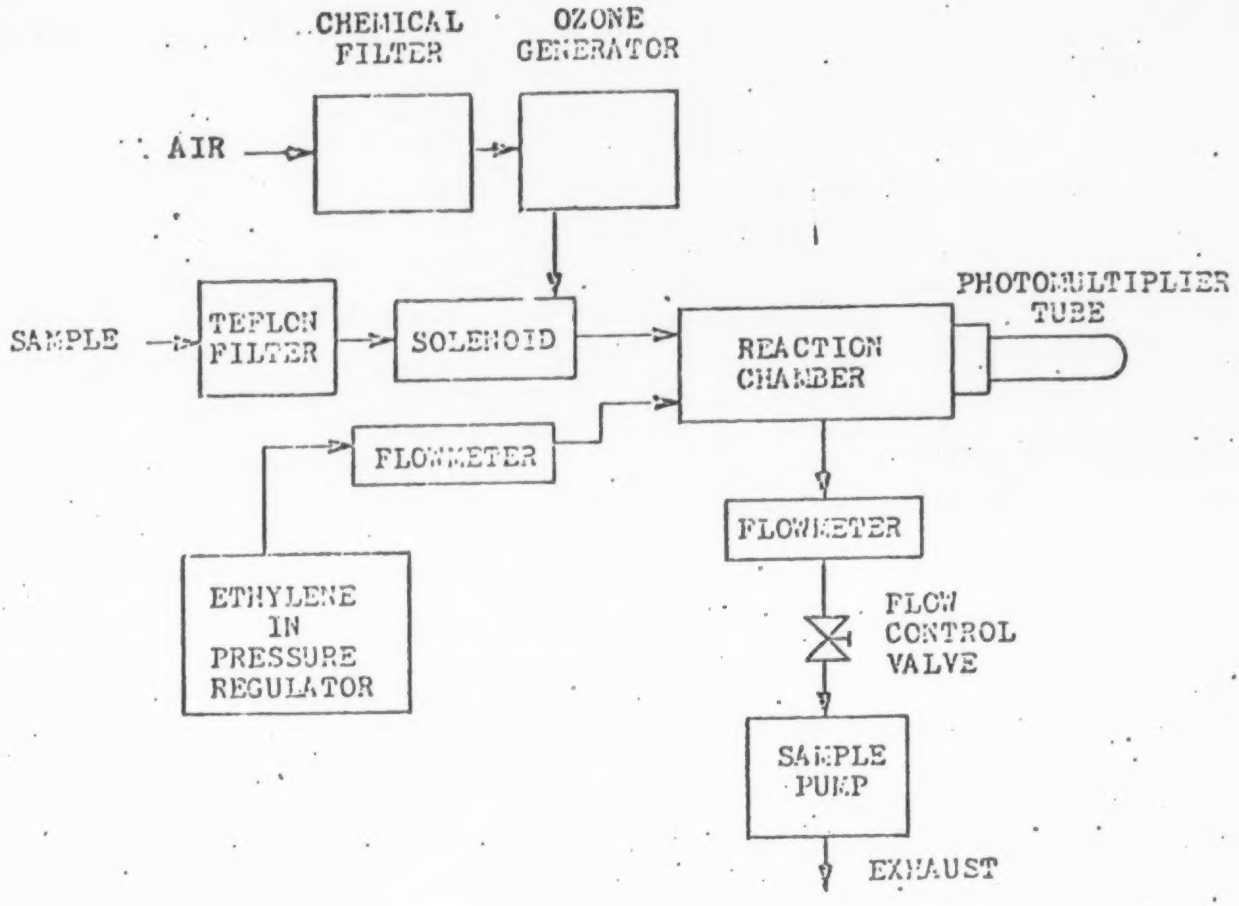
CHEMICAL FILTER
OZONE GENERATOR
AIR
SAMPLE
TEFLON FILTER
SOLENOID
REACTION CHAMBER
PHOTOMULTIPLIER TUBE
FLOWMETER
FLOWMETER
ETHYLENE IN PRESSURE REGULATOR
FLOW CONTROL VALVE
SAMPLE PUMP
EXHAUST

Figure 6-9. Gas-phase (ozone-ethylene) chemiluminescent ozone monitor, block diagram.[54]

source of error can be minimized by using humidified rather than dry ozone in air streams when calibrating.

Slight improvements in sensitivity can be achieved by cooling the phototubes used to detect the emitted light or by increasing the ethylene flow rate. Chemiluminescence produced by the reaction of ozone with ethylene has been designated by the EPA as the reference method for the monitoring ozone.[25, 57] Several different commercially produced instruments are available.

OTHER OXIDANTS AND PRECURSORS

Besides ozone, the main indicator of photochemical pollution, other important concomitant products are: peroxyacetyl nitrate (PAN), hydrogen peroxide, nitrogen dioxide, hydroxyl radicals and various aldehydes which are both products and primary pollutants; and the particulates; sulfates, nitrates, ammonium, chloride, water, and various types of oxygenated organic compounds. The most important precursors of photochemical pollution are nitric oxide and hydrocarbons. The measurement procedures for the hydrocarbons are not as highly developed as those for ozone and the nitrogen oxides.

Many deleterious effects have been associated with photochemically polluted air: ozone is definitely associated with respiratory problems, plant damage and material damage; PAN has definitely been associated with plant damage and some other members of this class of chemical compounds have been associated with eye irritation; the hydroxyl radical is considered to be an important factor in the conversion of gas phase intermediates to end products, such as sulfur dioxide to particulate sulfate; the particulate complex is responsible for haze formation and has also been associated with eye irritation and respiratory effects. The aldehydes have been associated with eye irritation. Ozone and PAN itself do not cause eye irritation. For purposes of control, much more research is needed in order to relate the laboratory data about the levels of these various materials which have significant effects to their formation in the atmosphere from emissions and their atmospheric distribution. The lack of convenient measurement methods has hindered progress in gaining this understanding.

The chief precursors for both oxidant and suspended particulate matter formation in the atmosphere, which are directly emitted into the atmosphere, are nitrogen oxides, hydrocarbons and their derivatives, ammonia, and sulfur dioxide. The measurement of particulate components is discussed in Chapter 2. This section describes briefly the measurement of nitrogen oxides, hydrocarbons, free radicals and other precursors.

Nitrogen Oxides

The technology for the routine measurement of the nitrogen oxides (nitrogen dioxide, NO_2, and nitric oxide, NO) is fairly well advanced. The Environmental Protection Agency is on the verge of officially proposing that chemiluminescence produced by the reaction of nitric oxide with ozone should be the reference method for nitrogen dioxide.[57] This method is even more suitable for nitric oxide. Since no national air quality standard has been promulgated for nitric oxide, no reference method will be specified. However, its measurement in the atmosphere is crucial for establishing the relationship of its emission to the formation of atmospheric ozone and other photochemical oxidants.

Most of the data for nitrogen oxides prior to 1970 have been obtained by continuous measurements with a colorimetric analyzer which was similar in principle to the colorimetric oxidant analyzer shown in Figure 6-7.[41] The scrubbing agent is a mixture of N-(1-Naphthyl) ethylenediamine, sulfanilic acid and acetic acid in aqueous solution. The color is produced when both nitrogen dioxide and nitrites react with this reagent to form an azo dye. The color is not affected by any nitric oxide present in the air sample.

The quantification of the nitrogen dioxide depends on the acceptance of an empirical factor which relates the response of this reagent such that one mole of NO_2 scrubbed from the gas phase produces the same amount of color as 0.72 mole of nitrite added in solution. Upon alterations of reagent composition and scrubber design this factor may change. For most of the air monitoring activities in the United States using this reagent this factor appears to have been verified.[57a] Evaluations remain to be conducted using gas phase titration with a known ozone source.

To determine nitric oxide with this method, it is oxidized to nitrogen dioxide by passing the air sample through a reaction vessel containing either potassium permanganate or chromium trioxide.[38] For an accurate measurement, however, any nitrogen dioxide originally present must first be selectively removed by passing the air sample through a triethanolamine scrubber.[58] This precaution has, unfortunately, not been the practice. Rather, the air sample containing both nitric oxide and nitrogen dioxide has been passed first through the oxidizer and then to the reagent scrubber, which gives a measurement of total nitrogen oxides (NO_x). The assumption is made that no nitrogen dioxide is lost.

In another technique, the air stream exiting from the nitrogen dioxide reagent scrubber is taken to the oxidizer and then to a second reagent scrubber. This gives separate measurements for nitrogen dioxide and nitric oxide. Here the assumption is that all the nitrogen dioxide is retained in the first reagent scrubber and no nitric oxide is lost. Neither of the assumptions made for these methods of measuring nitric oxide is completely correct. For this reason, there is a great deal of uncertainty about the amount of error in existing data banks. The nitrogen dioxide data, on the other hand, is believed to be reasonably accurate particularly where there has been proper instrument calibration and maintenance.[38]

The diurnal patterns of ozone, nitric oxide and nitrogen dioxide concentrations observed during photochemical oxidant episodes in California, have been confirmed by smog chamber studies. There may be, however, a decrease in reliability with decreasing concentration of values less than 0.1 ppm that were measured by the colorimetric method. The magnitude of these uncertainties among the various monitoring networks in the United States has still to be assessed.

In the chemiluminescent detection of nitrogen oxides, a constant source of ozone is reacted with a metered air sample containing nitric oxide. Fontijn _et_ _al_.[52] suggested that this method could also be used for ozone detection by using a constant nitric oxide source for reaction with ozone in the air sample. The ozone-nitric oxide reaction is carried out at reduced pressure to avoid quenching the chemiluminescent reaction. Detection of the emissions in the spectral region involved (600-3000 nm) requires using a near-infrared sensitive photomultiplier tube. The noise of such a photomultiplier tube is reduced by cooling it to about -20 C.[56]

To measure nitrogen dioxide with this technique it is thermochemically converted to nitric oxide by reaction with molybdenum at about 200 C. The extent of possible interferences at various monitoring sites from nitrogen compounds other than ammonia, which does not interfere unless the temperature is considerably higher than 200 C, remains to be assessed. The instrumentation of this procedure is inherently more reliable than the original colorimetric analyzers. Unfortunately, the mutual equivalency under monitoring situations of data obtained from these two techniques has not yet been evaluated. This is particularly important for the data from California, where nitrogen oxide measurements have been made over the past 20 years using the colorimetric method.

At present, two primary calibration standards are available for nitrogen oxides. One is a nitrogen dioxide generator in which the source is a permeation tube, certified by the National Bureau of Standards, in a temperature- and flow-controlled gas diluter. The amount of nitrogen dioxide generated is determined by the loss in weight of the permeation tube.

The other standard is a cylinder of compressed nitric oxide in oxygen-free nitrogen certified in the range of 50 ppm by the National Bureau of Standards. To obtain concentrations smaller than one part per million, this cylinder has to be connected to a dilution apparatus carefully regulated for flow and temperature.

The calibration of a chemiluminescent analyzer using these standards is verified when both the nitrogen dioxide and nitric oxide channels respond similarly to charges from the cylinder of diluted nitric oxide. Agreement with the response of the nitric oxide channel should also be obtained when titrating the standard nitric oxide mixture with a previously established source of ozone. While chemiluminescent instruments have simplified monitoring of nitrogen oxides, achieving accurate calibration requires well-trained personnel.

Hydrocarbons

For the measurement of the hydrocarbon precursors of photochemical oxidants, the naturally occurring methane must be separated from the other so-called non-methane hydrocarbons. Only one procedure, gas chromatography coupled with flame ionization detection, is available for this separation and measurement. Although instrumentation for routinely accomplishing this process is commercially available, its maintenance (continued operation) requires a degree of operational know-how which may be too costly for most public agencies in the United States to support. Consequently, there is at present insufficient data to relate the occurrence of photochemical oxidants and ozone accurately to some of their most important precursors, the non-methane hydrocarbons.

In addition, it is widely recognized, based on chamber studies, that some of the non-methane hydrocarbon compounds are far more important than others in causing the formation of photochemical oxidants and aerosols. These are referred to as the reactive hydrocarbons. To date it has only been possible to measure them by means of a more sophisticated gas-chromatographic process than described above. Therefore, their measurement in the atmosphere has been limited to research or to short-term episodic types of studies. While these are useful for understanding the phenomena of photochemical pollution formation, they have been too costly for determining the effectiveness of hydrocarbon control programs with respect to the changes in the occurrence and concentration of reactive hydrocarbons in air. Consequently, there is very little data about those hydrocarbon compounds in the atmosphere which may be precursors for the formation of atmospheric haze.

Particulate Sulfates and Nitrates

The sulfate and nitrate content of atmospheric particles comes primarily from the conversion of sulfur dioxide and nitrogen dioxide. Photochemically initiated atmospheric reactions and transient free radicals are often associated with this process (Chapter 2). At over 3500 locations in the United States, the total suspended particulate matter is regularly sampled at least once per week for a 24 h period.[57] The particles are usually collected on glass-fiber filter mats which are then sent to a central laboratory. There the sulfate and nitrate contents are extracted with hot water and determined by standardized chemical analytical procedures. Recently, there has been a detailed review of these procedures covering their reliability, their limitations, and the alternatives available for their improvement (emphasizing sulfates).[59]

There are several potential sources of error in these methods. The filters routinely used have a relatively high and somewhat variable sulfate content, so that at concentrations lower than 10 $\mu g/m^3$ and sampling periods less than 24 h, the reliability of the sulfate measurement is reduced. Several different types of filtering media adsorb sulfur dioxide during the first few hours of sampling, which alters the amount of sulfate observed. This interference can become critical when sampling periods are less than 24 h and the ratio of the concentrations of sulfur dioxide to sulfate is greater than 5 to 1. Interference can also be introduced by the hot water extraction, when reduced sulfur compounds such as sulfite are present, because they are oxidized to sulfates in this process. Another possible error source is that some of the various analytical procedures used for sulfate determination may be influenced by other substances also present in the particulate matter.

Current developments for minimizing these limitations in the analytical procedures are: selecting filtering media for sampling which have low blanks and do not adsorb significant amounts of sulfur dioxide and nitrogen oxides; and designing analytical methods which are specific for sulfates and nitrates in the presence of other particulate substances. In addition, more sensitive procedures for studying short-term (hourly) variations are being developed. These procedures will permit the investigation of how the formation and occurrence of these particulate components relate to atmospheric reactions and to the acute effects both when inhaled and when deposited on surfaces.

Other Substances

As shown in Table 6-1 (and reviewed in Chapter 2), there are other substances monitored occasionally, which are important in the photochemical oxidant milieu. These are the peroxy alkyl and aryl nitrates (PAN's) and the aldehydes.

The PAN's have been monitored by directly injecting the air at the sampling site into a specifically designed gas chromatograph. Aldehydes (formaldehyde is the major one in the atmosphere) are generally sampled in liquid absorbers using reagents which develop a color. These are sensed continuously with an instrument comparable in design to the colorimetric oxidant analyzer (Figure 6-7). To obtain information about specific aldehydes, the material collected in the absorber is sent to a central laboratory where individual aldehydes are analyzed by gas chromatography and mass spectroscopy.

There are a number of significant oxygenated organic particulate compounds and gas-phase free radicals formed by the reactions of gas-phase hydrocarbons (see Table 6-1 and Chapter 2). The measurement methods for these substances are complicated and in the research stage. Their description is beyond the scope of this chapter. It is of major importance to develop methods for measuring hydroxyl and peroxyhydroxyl radicals as well as the various oxygen species formed together with ozone (see Chapter 12).

EVALUATION

In the final analysis, the purpose of measurement is to provide numerical values as the basis both for making policy decisions and for enforcing regulations. It is critical therefore to know whether measurement data is reliable. It is also essential that all the data be intercomparable. This includes data obtained from laboratory studies of chemical reactions, plant and material damage, and animal and human toxicology; from field studies of air quality, vegetation and ecosystem effects, and population exposures. In all such studies (see Chapters 2, 4, 8, 9, 11, 12, and 13), irrespective of the measurement method used, the measurement of oxidants is based on a "standardized" source of ozone.

Unfortunately, and probably unavoidably, from the earliest research until the present, investigators have not used the same standardization process. Furthermore, standardization practices within different research groups have only rarely followed the meticulous series of in-house calibrations, verifications and inter-laboratory comparisons long prescribed by the community of measurement specialists. There are several quantitatively crucial studies, however, which have followed sound measurement procedures (e.g., Hackney, Chapter 9).

The chief objective of this section is to provide a perspective concerning the reliability of atmospheric oxidant data. The expected performance of atmospheric oxidant monitors is given in Table 6-7. To judge the reliability of measurements, information about the following five factors is required:

(1) Accuracy; agreement with respect to a primary reference standard.

(2) Reproducibility; the precision with which measurements can be repeated both within a single measurement group and among different groups in different laboratories.

(3) Interferences; substances that exist simultaneously with ozone and alter the response of the measurement method.

(4) Comparisons among different measurement methods.

(5) Practices and maintenance of measurement operations.

The fundamental factors which govern the accuracy of primary reference standards were discussed in the section of this chapter on calibration. Even though an improved reference standard has been advocated, most of the existing air monitoring and laboratory exposure data have as their reference the potassium iodide procedure used by either the California Air Resources Board (ARB), or the Los Angeles County Air Pollution Control District (LAAPCD), or the EPA. The relationship of these three variations of the potassium iodide procedure to the ultraviolet method are as follows:

$$O_3(\text{ARB}) = 1.29\, O_3(\text{UV}) - 0.005 \qquad (18)$$

$$O_3(\text{LAAPCD}) = 0.96\, O_3(\text{UV}) - 0.032 \qquad (19)$$

$$O_3(\text{EPA}) = 1.11\, O_3(\text{UV}) - 0.035. \qquad (20)$$

Table 6-7

Expected Performance Specifications for Oxidant Monitors[60]

Performance Characteristic	Specification
Range	0 to 0.5 ppm
Noise	0.005 ppm
Lower detectable limit	0.01 ppm
Interference equivalent	
Each interferent	±0.02 ppm
Total interferent	0.06 ppm
Zero drift, 12 and 24 h	±0.02 ppm
Span drift, 24 h	±0.025 ppm
Lag time	20 min
Rise time	15 min
Fall time	15 min
Precision, standard deviation range	0.01 ppm
as % of 0.08 air quality standard ppm	12.5%
Accuracy with respect to primary reference standard	not specified

While the differences between these several primary reference procedures are of some concern, the practice and performance of these procedures since 1952 has been remarkably consistent. For instance, several studies by different investigators and laboratories have shown an average ratio of 1.37, between the LAAPCD and ARB methods (with extremes in this value not exceeding 5%).[12] The EPA primary reference procedure using potassium iodide has also been evaluated recently by several laboratories. When the concentration range of ozone was 0.005 to 0.5 ppm, the standard deviation among the laboratories during a 4-day continuous measurement of the same atmosphere was ± 6 to 10%.

With respect to stablized ozone generators supplied and calibrated by the National Bureau of Standards, the participating laboratories obtained values that were about 15% lower on the average, at an ozone concentration of about 0.2 ppm.[61] Therefore, while acceptable repeatability within and among laboratories can be achieved even with the potassium iodide bubbler method as a reference procedure, there are unpredictable variables inherent in this procedure which contraindicate its continued acceptance.

Differences in measurement methods include analyzer systems based both on the same and on different measurement principles. The average standard deviation in the performance of different chemiluminescent ozone instruments which are sampling the same ambient air both with and without an added ozone concentration of 0.002 to 0.5 ppm is 6 to 10%. Field studies comparing an ultraviolet monitor with several chemiluminescent monitors showed correlation coefficients for hourly averages of from 0.80 to 0.95

between various pairs of instruments. Hourly averages for about 500 pairs of values at ambient ozone concentrations of from 0.005 to 0.100 ppm showed deviations of from 3 to 23% between the average values for paired instruments.

Typical colorimetric and amperometric analyzers have been compared both in the laboratory, using ozone concentrations of 0 to 0.6 ppm (with and without added NO_2 at a similar concentration range), and at field locations where the oxidant concentration was 0 to 0.2 ppm.[41] When both instruments were corrected for NO_2 interference, the field results showed highly correlated ($r = 0.96$) hourly averages. Nevertheless, the colorimetric readings were consistently 6% higher than the amperometric readings. The responses showed the following relationship:

$$O_3\,(\text{amp}) = 0.942\, O_3\,(\text{col}) - 0.0038\ \text{ppm}. \qquad (21)$$

To summarize, the results of comparing and evaluating air oxidant analyzers indicate that when the use of similar primary reference procedures is coupled with meticulous operational practices, agreement within about 20 to 30% can be expected. A monitoring network operated by a single tightly managed group, however, can achieve even better agreement.

SUMMARY, CONCLUSIONS AND RECOMMENDATIONS

With the exception of calibration, the measurement problems which were apparent in 1970, at the time of publication of the first air quality criteria document on photochemical oxidants, have essentially been solved for ozone. This remarkable achievement is the result of unstinting efforts by individuals working at EPA's National Environmental Research Center, North Carolina; the National Bureau of Standards; private research contractors sponsored primarily by EPA; private instrument manufacturers; the Jet Propulsion Laboratory of the California Institute of Technology; the Air and Industrial Hygiene Laboratory, California Department of Health; the Air Pollution Research Center of the University of California at Riverside, and the California Air Resources Board (CARB).

Due to the focus on the problem brought about by the CARB , a significant advance in the accurate calibration of instruments for monitoring ozone in ambient air was achieved during 1975. As a result, this agency adopted the measurement of ozone in the ultraviolet region at 254 nm as a primary calibration reference standard. They have also adopted statewide, as a transfer standard for calibrating ozone and oxidant monitoring instruments at air monitoring stations, a commercially available instrument (coupled with the precise controlled generation of ozone in air), which measures the differential absorption of ultraviolet radiation.

It is important to separate conceptually, and in practice, the calibration process from the monitoring process. Photochemical oxidants consisting primarily of ozone were first continuously measured in Southern California by measuring the color change of potassium iodide solutions brought into contact with the ambient air. This measurement continues to yield valid photochemical oxidant data in California. However, it has yielded questionable data at ambient air monitoring sites elsewhere in the United States. For this reason at the end of 1971, EPA officially adopted a continuous monitoring process that measures the chemiluminescence produced when ozone in air is brought into contact with the gas ethylene. This reference procedure when calibrated with the primary reference procedure using ultraviolet absorption is widely accepted.

Instruments based on differential ultraviolet absorption still need to be evaluated, and possibly modified, prior to their acceptance for monitoring ozone in polluted atmospheres on a nationwide scale. The California Air Resources Board and other air pollution control agencies are currently conducting multi-year programs for evaluating ultraviolet absorption side-by-side with chemiluminescent and potassium iodide based instruments, to determine their applicability and needed modification, as well as to assure continuity in the data base while the older monitoring instruments are being replaced.

Thus despite the remarkable progress in the monitoring for ozone, nitrogen oxides and non-methane hydrocarbons, which has strengthened the implementation and evaluation of control programs, substantial research and development is still required to help resolve the uncertainties in our knowledge which are inhibiting the actual achievement of desired air quality standards.

The areas in which further research and development are needed, in sequence of priority are:

- Evaluation of primary calibration procedures applicable nationwide for ozone measurement.
- Development of principles and instruments which can easily track the sources of those hydrocarbons reactive in the production of ozone and those which are reactive in the production of particles.
- Chemical identification of both gas and particle phase compounds occurring in the atmosphere, which cause eye irritation and respiratory difficulties.

- Methods for the direct and continual measurement of those chemicals in the particles of the atmospheric haze, that are known to be formed during photochemical pollution episodes and are already suspect as respiratory irritants. By implementing such measurements it will be possible to find out to what extent the occurrence of such substances can be reduced by various emission controls. To assess actual population exposures, it is also necessary that these measurement methods be easily carried out indoors and in vehicles.

- Improved measurement methods suitable for observations from airborne platforms so that the regional scale impacts of urban emissions can be accurately assessed. This is needed because some control options for solving the urban-scale problem have the potential of transferring pollution from one geographic area to other areas.

REFERENCES

1. U. S. Department of Health, Education, and Welfare. Public Health Service. Environmental Health Service. National Air Pollution Control Administration. Air Quality Criteria for Photochemical Oxidants. NAPCA Publ. AP-63. Washington, D. C.: U. S. Government Printing Office, 1970.

2. Hodgeson, J. A. Review of analytical methods for atmospheric oxidants measurements. Int. J. Environ. Anal. Chem. 2:113-132, 1972.

3. Schuetzle, D., D. Cronn, and A. L. Crittenden. Molecular composition of secondary aerosol and its possible origin. Environ. Sci. Technol. 9: 838-845, 1975.

3a. Altshuller, A. P. Evaluation of oxidant results at CAMP sites in the United States. J. Air Pollut. Control Assoc. 25:19-24, 1975.

4. Bradley, C. E., and A. J. Haagen-Smit. The application of rubber in the quantitative determination of ozone. Rubber Chem. Technol. 24:750-755, 1951.

5. Smith, R. G., and P. Diamond. The microdetermination of ozone. Preliminary studies. Amer. Ind. Hyg. Assoc. Quart. 13:235-238, 1952.

6. Littman, F. E., and R. W. Benoliel. Continuous oxidant recorder. Anal. Chem. 25:1480-1483, 1953.

7. Cherniack, I., and R. J. Bryan. A comparison study of various types of ozone and oxidant detectors which are used for atmospheric air sampling. J. Air Pollut. Control Assoc. 15:351-354, 1965.

8. Graedel, T. D. Private communication, Bell Telephone Labs, Murray Hills, N. J., 1975.

9. Lewis, N. Private communication, N. J. State Bureau of Environmental Control, Trenton, N. J., 1975.

10. Bruntz, S. M., W. S. Cleveland, T. E. Graedel, B. Kleiner, and J. L. Warner. Ozone concentrations in New Jersey and New York: Statistical association with related variables. Science 186:257-259, 1974.

11. Environmental Instrumentation Group. Photochemical oxidant monitoring instrumentation, pp. . In Instrumentation on Environmental Monitoring--Air. Berkeley: Lawrence Berkeley Laboratory, University of California, 1973.

12. DeMore, W. B., J. C. Romanovsky, M. Feldstein, W. J. Hamming, and P. K. Mueller. Interagency comparison of iodometric methods for ozone determination, pp. . In Proceedings of American Society for Testing and Materials Symposium on Calibration Problems and Techniques, Boulder, University of Colorado, Aug. 5-7, 1975. (in press) (UNVERIFIED)

13. DeMore, W. B., and M. Patapoff. Comparison of ozone determinations by ultraviolet photometry and gas phase titration. Environ. Sci. Technol. (in press)

14. Pitts, J. N., J. M. McAfee, W. D. Long, and A. M. Winer. Longpath infrared spectroscopic investigation at ambient concentrations of the 2% neutral buffered potassium iodine method for determination of ozone. Environ. Sci. Technol. (in press)

15. Hodgeson, J. A., C. L. Bennett, H. C. Kelly, and B. A. Mitchell. Ozone measurements by iodometry, ultraviolet photometry and gas-phase titration, pp. . In Proceedings of American Society for Testing and Materials Symposium on Calibration Problems and Techniques, Boulder, University of Colorado, Aug. 5-7, 1975. (in press)

16. Paur, R. Comparison of uv photometry and gas phase titration as candidate methods for absolute calibration of ozone generator output in the sub-part-per million range, pp. . In Proceedings of American Society for Testing and Materials Symposium on Calibration Problems and Techniques, Boulder, University of Colorado, Aug. 5-7. 975. (in press)

17. Hanst, P. L., E. R. Stephens, W. E. Scott, and R. C. Doerr. Absorptivities for the infrared determination of trace amounts of ozone. Anal. Chem. 33: 1113-1115, 1961.

18. Hodgeson, J. A., R. E. Baumgardner, B. E. Martin, and K. A. Rehme. Stoichiometry in the neutral iodometric procedure for ozone by gas-phase titration with nitric oxide. Anal. Chem. 43:1123-1126, 1971.

18a. Rehme, K. A., B. E. Martin, and J. A. Hodgeson. Tentative Method for the Calibration of Nitric Oxide, Nitrogen Dioxide and Ozone Analyzers by Gas Phase Titration. EPA-R2-73-246. Research Triangle Park: U. S. Environmental Protection Agency, Office of Research and Monitoring, 1974. 16 pp.

19. Hodgeson, J. A., R. K. Stevens, and B. E. Martin. A stable ozone source applicable as a secondary standard for calibration of atmospheric monitors, pp. 149-158. In J. Scales, Ed. Air Quality Instrumentation. Vol. 1. Selected Papers from International Symposia Presented by the Instrument Society of America. Pittsburgh: Instrument Society of America, 1972.

20. Bendix Corp., Process Instruments Div., P. O. Drawer 477, Ronceverte, W. Va. 24970

21. Dasibi Corporation, 161 East Colorado St., Glendale, CA, 91205.

22. McMillan Electronics Corporation, 7327 Ashcroft, Houston, TX 77036.

23. Monitor Labs, Inc., 4202 Sorrento Valley Blvd., San Diego, CA, 92121.

24. Ultra-Violet Products, Inc., 5114 Walnut Grove Ave., San Gabriel, CA, 91778.

25. U. S. Environmental Protection Agency. Title 40. Protection of environment. Part 50. National primary and secondary ambient air quality standards. Federal Register 36:22384-22397, 1971.

26. California Department of Health. Air and Industrial Hygiene Laboratory. Calibration and Standardization of Continuous Photometric Analyzers of Atmospheric Oxidants. Recommended Method No. 5B. Berkeley: California Department of Health, 1970. 17 pp.

27. Los Angeles County Air Pollution Control District. Ozone Calibration Procedure for Monitoring Instruments (Titrimetric Method). Los Angeles: Air Pollution Control District, 1975. 15 pp.

28. Imada, M. Comparison of LAAPCD's Original and Modified Methods for Standardizing 0.002 N Sodium Thiosulfate Solutions. Letter to W. B. Demore, Feb. 7, 1975. (see Ref. 11.)

29. Becker, K. H., U. Schurath, and H. Seitz. Ozone-olefin reactions in the gas phase. 1. Rate constants and activation energies. Int. J. Chem. Kinet. 6:725-739, 1974.

30. DeMore, W. B., and O. Raper. Hartley band extinction coefficients of ozone in the gas phase and in liquid nitrogen, carbon monoxide, and argon. J. Phys. Chem. 68:412-414, 1964.

31. Clyne, M. A. A., and J. A. Coxon. Kinetic studies of oxy-halogen radical systems. Proc. Roy. Soc. A303:207-231, 1968.

31a. Hampson, R. F., W. Braun, R. L. Brown, D. Garvin, J. T. Herron, R. E. Huie, M. J. Kurylo, A. H. Laufer, J. D. McKinley, H. Okabe, M. D. Scheer, W. Tsang, and D. H. Stedman. Survey of photochemical and rate data for twenty-eight reactions of interest in atmospheric chemistry. J. Phys. Chem. Ref. Data 2:267-311, 1973.

32. Griggs, M. Absorption coefficients of ozone in the ultraviolet and visible regions. J. Chem. Phys. 49:857-859, 1968.

33. Hearn, A. G. The absorption of ozone in the ultra-violet and visible regions of the spectrum. Proc. Phys. Soc. (London) 78:932-940, 1961.

34. Inn, E. C. Y., and Y. Tanaka. Absorption coefficient of ozone in the ultraviolet and visible regions. J. Optic. Soc. Amer. 43:870-873, 1953.

35. deVera, E. R., E. Jeung, and M. Imada. Equivalency Determination and Calibration Procedure for a UV Absorption Ozone Monitor. AIHL Report No. 160. Berkeley: California State Department of Health, 1974. (UNVERIFIED)

36. Behl, B. A. Absolute Continuous Atmospheric Determination by Differential U.V. Absorption. Presented at the 65th Annual Meeting of the Air Pollution Control Association, June 1972. (UNVERIFIED)

37. Bowman, L., D. Horak, and F. Richard. A Continuous Ultraviolet absorption ozone photometer. ISA AID 72430 (103-108), 1972 (UNVERIFIED)

38. Mueller, P. K., Y. Tokiwa, E. R. deVera, W. J. Wehrmeister, T. Belsky, S. Twiss, and M. Imada. A Guide for the Evaluation of Atmospheric Analyzers. Air and Industrial Hygiene Laboratory Report No. 168. Berkeley: California State Department of Public Health, 1973. (UNVERIFIED)

39. Intersociety Committee. Tentative method for the continuous analysis of atmospheric oxidants (colorimetric), pp. 356-364. In Methods of Air Sampling and Analysis. Washington, D. C.: American Public Health Association, 1972.

40. Standard method of test for continuous analysis and automatic recording of the oxidant content of the atmosphere. Designation: D 2011-65 (Reapproved 1972), pp. 924-928. In 1973 Annual Book of ASTM Standards. Part 23. Water; Atmospheric Analysis. Philadelphia: American Society for Testing and Materials, 1973.

41. Tokiwa, Y., S. Twiss, E. R. de Vera, and P. K. Mueller. Atmospheric ozone determination by amperometry and colorimetry, pp. 109-130. In G. Mamantov, and W. D. Shults, Eds. Determination of Air Quality. Proceedings of the ACS Symposium, Los Angeles, 1971. New York: Plenum Press, 1972.

42. Saltzman, B. E., and A. F. Wartburg, Jr. Absorption tube for removal of interfering sulfur dioxide in analysis of atmospheric oxidant. Anal. Chem. 37: 779-782, 1965.

43. Intersociety Committee. Tentative method for continuous monitoring of atmospheric oxidant with amperometric instruments, pp. 341-350. In Methods of Air Sampling and Analysis. Washington, D. C.: American Public Health Association, 1972.

44. Brewer, A. W., and J. R. Milford. The Oxford-Kew ozone sonde. Proc. Roy. Soc. A256:470-495, 1960.

45. Mast, G. M., and H. E. Saunders. Research and development of the instrumentation of ozone sensing. Instrum. Soc. Amer. Trans. 1:325-328, 1962.

46. Schulze, F. Versatile combination ozone and sulfur dioxide analyzer. Anal. Chem. 38:748-752, 1966.

47. Hersch, P., and R. Deuringer. Galvanic monitoring of ozone in air. Anal. Chem. 35:897-899, 1963.

48. Wartburg, A. F., A. W. Brewer, and J. P. Lodge, Jr. Evaluation of a coulometric oxidant sensor. Air Water Pollut. 8:21-28, 1964.

49. Nederbragt, G. W., A. Van Der Horst, and J. Van Duijn. Rapid ozone determination near an accelerator. Nature 206:87, 1965.

50. Warren, G. J., and G. Babcock. Portable ethylene chemiluminescence ozone monitor. Rev. Sci. Instrum. 41:280-282, 1970.

51. Stevens, R. K., and J. A. Hodgeson. Applications of chemiluminescent reactions to the measurement of air pollutants. Anal. Chem. 45:443A-446A, 449A, 1973.

52. Fontijn, A., A. J. Sabadell, and R. J. Ronco. Homogenous chemiluminescent measurement of nitric oxide with ozone. Anal. Chem. 42:575-579, 1970.

53. Altshuller, A. P. Analytical problems in air pollution control, pp. 245-286. in W. W. Meinke and J. K. Taylor, Eds. Analytical Chemistry: Key to Progress on National Problems. Proceedings of 24th Annual Summer Symposium on Analytical Chemistry, National Bureau of Standards, Gaithersburg, Maryland, 1971. National Bureau of Standards Special Publication 351. Washington, D. C.: U. S. Government Printing Office, 1972.

54. Coloff, S. G., M. Cooke, R. J. Drago, and S. F. Sleva. Ambient air monitoring of gaseous pollutants. Amer. Lab. 5(7):10-22, 1973.

55. California Air Resource Board. A Study of the Effect of Atmospheric Humidity on Analytical Oxidant Measurement Methods. Sacramento: State of California, Air Resources Board, Report of a Interagency Study, July 9, 1975. 14 pp.

56. Altshuller, A. P. Analytical problems in air pollution control, pp. 245-286. In W. W. Meinke and J. K. Taylor, Eds. Analytical Chemistry: Key to Progress on National Problems. Proceedings of 24th Annual Summer Symposium on Analytical Chemistry, National Bureau of Standards, Gaithersburg, Maryland, 1971. National Bureau of Standards Special Publication 351. Washington, D. C.: U. S. Government Printing Office, 1972.

57. Hoffman, A. J., T. C. Curran, T. B. McMullen, W. M. Cox, and W. F. Hunt. EPA's role in ambient air monitoring. Science 190:243-248, 1975.

57a. Intersociety Committee. Tentative method of analysis for nitrogen dioxide content of the atmosphere (Griess-Saltzman Reaction), pp. 329-336. In Methods of Air Sampling and Analysis. Washington, D. C.: American Public Health Association, 1972.

58. Levaggi, D. A., W. Siu, M. Feldstein, and E. L. Kothny. Quantitative separation of nitric oxide from nitrogen dioxide at atmospheric concentration ranges. Environ. Sci. Technol. 6:250-252, 1972.

59. Mueller, P. K., and G. H. Hidy. Measurement Technology of Sulfates, Appendix D. In Electric Power Research Institute Report 485. Menlo Park, Calif.: Electric Power Research Institute, (in press)

60. U. S. Environmental Protection Agency. Part 53--Ambient air monitoring reference and equivalent methods. Federal Register 40:7044-4063, 1975.

61. McKee, H. C., R. E. Childers, and V. B. Parr. Collaborative Study of Reference Method for Measurement of Photochemical Oxidants in the Atmosphere (Ozone-Ethylene Chemiluminescent Method) EPA 650/4-75-016. San Antonio, Texas: Southwest Research Institute, 1975. 49 pp.

Chapter 7

RESPIRATORY TRANSPORT AND ABSORPTION

This chapter discusses the transport and absorption of ozone and other photochemical oxidants within the respiratory tract. It includes lung morphology and flow aspects of respiratory physiology and emphasizes methodologic approaches to modeling.

Although the theory of the uptake of inert gases is well developed, there is no adequate theory for gases like ozone, which are reactive and metabolized by body tissues and fluids. Thus, it is not possible to predict local tissue dosage at critical airway sites that can be reliably related to toxic effects. In this chapter, the background information necessary for the development of a realistic model of lung uptake of reactive gases is presented, and subjects needing further study are identified. A successful model would help in correlating observations in animal and man and estimating the effective dose at reactive sites in man. Combined with a knowledge of biologic mechanisms of toxicity, it allows the prediction of health effects in man outside the range of conditions in which observations are made.

The radical or reactive intermediates discussed in Chapter 2 are included in the term "photochemical oxidants" for the purpose of this chapter. Of the reactive intermediates discussed, only the hydroperoxy, HO_2, and singlet oxygen, O_2 (a $^1\Delta$), radicals have a lifetime long enough to allow transport of significant quantities into the lungs before deactivation. Modeling of oxygenated organic aerosols will not be considered in detail in this chapter. According to the discussion in Chapter 3, most of the oxygenated organic aerosols have a diameter less than 0.5 μm, the range in which diffusion is the controlling mechanism of deposition. Regional particle deposition models[90,119g,123] can account for their deposition and clearance in the tracheobronchial tree and pulmonary regions. Work by Hounam[67a] suggests that Landahl's model[84] can be used to predict the deposition of oxygenated organic aerosols that are highly diffusive, as condensation nuclei in the nasopharynx.

This chapter first reviews and discusses selected research on local dose aspects of ozone toxicity, the morphology of the respiratory tract and mucous layer, air and mucus flow, and the gas, liquid, and tissue components of mathematical models. Next, it discusses the approaches and results of the few models that exist. A similar review[60] was recently done to define an analytic framework for collating experiments on the effects of sulfur oxides on the lung. Pollutant gas concentrations are generally stated in parts per million in this chapter, because experimental uptake studies are generally quoted only to illustrate behavior predicted by theoretical models. Chapter 5 gives a detailed discussion of the conversion from one set of units to another.

EFFECTIVE TISSUE DOSE

In this section, sites of action in the respiratory tract will be discussed, along with experimental studies of gas uptake in animals. Cumulative dose and dosage at critical sites of action will be defined, as well as the general characteristics required for modeling the transport and absorption in the respiratory tract.

Sites of Action

The sites of action and effects of ozone and other photochemical oxidants are described in Chapters 8 and 9. Recent work with primates[38] has suggested that ozone is absorbed along the entire respiratory tract, penetrates more into the peripheral nonciliated airways, and causes more lesions in the respiratory bronchioles and alveolar ducts as the inhaled ozone concentration increases from 0.2 to 0.8 ppm. The most common and most severe tissue damage was observed in the respiratory bronchioles. The ciliated cells in the terminal bronchioles and the type 1 cells in the epithelial layer of the proximal alveoli of rats were the primary sites of action of ozone at 0.5 and 0.9 ppm.[117a] Recent work in rabbits[22] and rats[113] suggests that the mucous layer in the large airways does not completely protect the underlying cells from ozone damage. Specifically, Boatman and Frank noted patches of desquamated ciliated cells along the conducting airways after acute exposures to ozone at 0.25, 0.5, and 1 ppm; these desquamated patches were most often found at bifurcations.

Table 7-1 gives an overview of various irritant and nonirritant gases commonly found in the atmosphere, their solubility in water, and their main sites of action. The Henry's law constant indicates the relative solubility in waterlike lung fluid. Although most of the information goes back to 1924, it is supported and extended by numerous studies of the effects of war gases and industrial irritants.[25,27,28,39,50,51,62,78,128,134]

Studies that have measured the uptake of pollutant and irritant gases in different regions of the respiratory tract of animals and man and in experimental airway models provide the most useful data for development and verification of gas transport models.[1,9a,10,24,29a,33,40,41,45,46,47,68,79,94,100,116,127,138,139,140] They generally show that the very

Table 7-1

Physical Properties of Pollutant Gases and Their Site of Action or Absorption in the Respiratory Tract[a]

Gas	Ambient Concentration, ppm	Henry's Law Const.[b] at 37 C, 1 atm, mole fraction in air / mole fraction in water	Major Site of Action or Absorption[c]
Ammonia[d]	0.02-0.2	3.5	URT
Sulfur dioxide[d]	0.01-0.5	59.7	URT and large bronchi
Hydrogen sulfide[d]	0.03	704	URT and large bronchi
Formaldehyde[d]	0.3	791	URT
Carbon dioxide	330	2,190	PULM
Ozone	0.05-0.5	9,700	TBT and PULM
Nitrogen dioxide	0.05-0.5	Converts to nitric and nitrous acids in water	TBT and PULM
Nitric oxide	0.05-2	33,900	TBT and PULM
Oxygen	209,460	51,800	
Carbon monoxide	1-100	67,400	PULM
Nitrogen	780,840	100,700	PULM

---

[a] Derived from Haggard.[55]

[b] Data from International Critical Tables[68a] and Perry *et al*.[102]

[c] URT = upper respiratory tract (nose, mouth, pharynx, larynx);
TBT = tracheobronchial tree (ciliated airways);
PULM = pulmonary region (alveolated airways and alveoli).

[d] For these highly water-soluble gases, Henry's law may be assumed to apply over the ambient concentration range.

soluble nonreactive gases--like ammonia, sulfur dioxide, and formaldehyde--are nearly totally removed by absorption in the nasal passages during normal breathing. Less water-soluble gases--like ozone and nitrogen dioxide--penetrate more peripherally into the lung and are partially exhaled. Total uptake depends on tidal volume, respiration rate, and in some cases initial inhaled concentration. For example, data from dogs[139] show that nearly 100% of sulfur dioxide inhaled through the nose is removed before reaching the first bifurcation, whereas only 27-70% of the ozone is removed in this same region.

Inhalation of gas or aerosol-gas mixtures may shift the site of action of the separate gases. Generally, the absolute quantity of irritant gases absorbed by suspended particles is negligible at ambient gas and aerosol concentrations; however, the irritation may be significantly increased by the transport of soluble gases by particles deeper into the lung. Insoluble particles, like carbon, and partially water soluble particles, may absorb ozone, sulfur dioxide, and other gases, in the water phase. Likewise, partially soluble particles with catalytic properties may oxidize absorbed gases and convert them to more toxic chemical forms (e.g., sulfur dioxide oxidized to sulfur trioxide in the liquid phase of particles with the aid of metallic catalysts). Gaseous mixtures that are chemically unreactive in the environment may react rapidly with each other in the special conditions of the respiratory tract to form other toxic compounds. The synergism observed by Bates and Hazucha[16] and by Bell _et al_.,[20] when human subjects were exposed to mixtures of sulfur dioxide and ozone may be caused by one of these physicochemical interactions. Another example of synergism related to physicochemical interaction of gases and particles was described by Mezentseva, _et al_.,[93] who observed edema in the lungs of animals exposed to hydrochloric acid derived from the hydrolysis of titanium chloride, $TiCl_4$, but not in those exposed to similar concentrations of pure gaseous hydrogen chloride.

Indexes of Critical Dose

To model the uptake of ozone and other gases for establishing dose-response relationships at specific sites, local dose must be accurately defined. In the past, this has not been done for specific sites. Fairchild and Graham,[42] Stokinger *et al.*,[118] and Stokinger[119a] have developed expressions for the effective dose of ozone, which depend only on the inhaled concentration and exposure time. "Dose" may be the mass or moles of the toxic gas delivered to the site of interest, and the average dose may be measured in micrograms per square centimeter of surface.

For acute exposure in a specific airway, the average rate or flux to the epithelial tissue or mucous layer may be the critical quantity and is measured in micrograms per square centimeter per second (in the unit is micrograms per square centimeter per breath). Chronic effects are probably related to the time integral over the period of exposure. When sensory receptors are involved in the acute response, the local flux to the small surface areas containing the receptor sites may be crucial.

Controlling Factors in Ozone Uptake

The major respiratory factors in the control of ozone uptake are the morphology (including the mucous layer), the respiratory flow, the physical and chemical properties of mucus, and the physical and chemical properties of ozone. The next two sections discuss models of the morphology and the air and mucus flow. The physical and chemical properties of bronchial secretions have been reviewed by Barton and Lourenco[13a] and Charman _et_ _al_.[26] The relevant physical and chemical properties of ozone are its solubility and diffusivity in mucus and water and its reaction-rate constants in water, mucus, and tissue.

Solubility data for mucus are not available, but Table 7-1 indicates that the Henry's law constant for ozone in water in lung conditions is 9,700. Solubility data for pure ozone and other physical properties are available from various sources.[74,122] _Air Quality Criteria for Photochemical Oxidants_[124] reports an ozone solubility of 0.494 ml/100 ml of water at 0 C for ozone at 760 mm Hg; extrapolation of data from Thorp[122] indicates 1.09 g/liter of water at 0 C and approximately 0.31 g/liter of water at 37 C for 100% ozone. The value for 37 C agrees closely with the solubility calculated from the Henry's law constant for pure ozone at 760 mm Hg.

The diffusivities of ozone in mucus, tissue, and water are unknown. As an approximation, the diffusivity of oxygen in water (2.5×10^{-5} cm^2/s) may be used for the diffusivity of ozone in water and in the mucous layer. Although reactivities of ozone in mucus and tissue are unknown, the results of Alder and Hill[3] and Hoigne and Bader,[65a] which describe the decomposition of ozone in aqueous solutions, may be used as a first approximation.

MORPHOLOGY OF THE RESPIRATORY TRACT AND MUCOUS LAYER

Human and Animal Airway Models and the Real Lung

The airways and the tissue lining of the human respiratory tract have a very complex structure and dynamic behavior, which vary with age, sex, and state of health.[56,61] Horsfield[66] reviewed the structure and function of the respiratory tract and described how it can be simplified into airway models for calculating gas and particle transport. Phalen[103] has summarized the limited available data concerning the similarities and differences between the airways of humans and several animal species. Hausknecht and Ziskind[60] have also reviewed airway models for gas uptake. Most mathematical models for particle deposition are based on circular cylindrical, rigid models of the conducting airways with dimensions representative of the normal adult. Diameter, length, and branching angle of the airways at the same generation of the treelike branching structures are usually assumed equal.

Although the airway model of Findeisen,[43] which was later modified by Landahl,[85] has a very unrealistic branching structure, it has been used widely for particle-deposition.[119g] Weibel's model "A"[130] has a more realistic symmetric dichotomous branching pattern and is currently popular. His complete model has 16 generations of conducting airways in the tracheobronchial region and seven partially or completely alveolated generations in the pulmonary zone. Table 7-2 shows the numbers and diameters of the conducting airways that are representative of an adult with a lung volume of 4,800 cm^3 at 75% inflation.

Other human airway models have been developed by Davies,[34] Horsfield *et al.*,[67] Phalen *et al.*,[104] and Yeh *et al.*[137] The asymmetric model of Horsfield *et al.* is more realistic than Weibel's, but is more difficult to use for calculations. Yeh *et al.* described a Monte Carlo technique for constructing a realistic lung model from extensive morphometric data. Such a lung model should have statistical distributions of the geometric characteristics similar to those of an actual lung and will permit separate deposition calculations for each lobe of the lung. Data on the airflow distribution between lobes of the lung[5] can be used to verify the model structure. Phalen *et al*. compared the airway morphology of the human, dog, rat, and hamster. The human tracheobronchial tree was found to be more symmetric with respect to diameter ratios and branching angles than those of the other species (but closest to that of the dog). Phalen[103] found that the bronchial tree structure is variable from species to species, from lobe to lobe within a given lung, and from one depth to another in the lung. Other animal airway models have been developed for the rat,[49,76] the guinea pig,[75] and the rabbit.[77] If bifurcations continue to be viewed as critical sites for gas and particle deposition and dose-response relationships, more refined airway models will be needed that define in more detail the structure of bifurcation regions.

Because of the complexity of the actual structures, the emphasis in modeling has been on obtaining an average representation, and the variability among individuals tends to be neglected. There are two experimental studies of variability of airway dimensions in living humans as revealed by aerosol deposition studies. Lapp *et al*.[86a] assessed the size of alveolar spaces in terms of half-life of aerosol persistence during breathholding and obtained a coefficient of variation of 20-25%. Palmes and Lippmann[98a] report the variability of a measure reflecting the influence of anatomic factors in tracheaobronchial deposition as revealed by *in vivo* retention of γ-tagged microspheres in the human thorax; they found a coefficient of 60-70%. Variability of direct anatomic measurements of numbers and sizes of airways in man is given by Matsuba and Thurlbeck,[91a] Angus and Thurlbeck,[11a] and Thurlbeck and Haines.[122a] In addition to expressing one cause of differences in the susceptibilities of individuals, the variability in model measures indicates a bias in the results of calculations that are based only on average values of the measures. Proctor and Swift[107] described the complex anatomy of the human nose and constructed a morphologic model of the nasal airways from actual casts, which may require simplification. Similar models need to be developed for animal upper airways.

Mucus and Alveolar Tissue Models

Because the mucous layer or the underlying cells may serve as either final accumulation sites of toxic gases or layers through which the gases diffuse en route to the blood, we need simplified models of these layers. Altshuler *et al.*[8] have developed the only available model for these layers that can be used in a comprehensive system for calculating tissue doses of inhaled irritants. It assumes that the basement membrane of the tracheobronchial region is covered with three discrete layers: an inner layer of variable thickness that contains the basal, goblet, and ciliated cells; a 7- μm middle layer composed of waterlike or serous fluid; and a 7-μm outer layer of viscous mucus. Recent work by Boatman and Luchtel[23] in rabbits supports the concept of a continuous fluid layer; however, airways smaller than 1 mm in diameter do not show separate mucous and serous fluid layers.

FLOW ASPECTS OF RESPIRATORY PHYSIOLOGY

Respiratory Airflow Patterns in Lung Models versus the Real Lung

Flow Analysis in Weibel's Model "A". Tidal volume and respiratory frequency are used with the anatomic dimensions to model airflow patterns in the respiratory tract.

During the respiratory cycle, the volumetric flow rate of air varies from zero up to a maximum and back. Usually, the expiratory phase is longer than the inspiratory phase, and there may be intervening pauses between the two, especially after expiration. Silverman et al.[115] studied the respiratory airflow patterns of healthy young men at rest and under a wide range of workloads. The maximal inspiratory flow rate increased from a mean value of 40 liters/min in sedentary subjects to 100 liters/min at an exercise workload of 622 kg/min and to 286 liters/min at 1,660 kg/min. The corresponding values for maximal expiratory flow rates were 32, 107, and 322 liters/min.

When a quiet breathing rate of 15 cycles/min and a tidal volume of 450 cm^3 are assumed in Weibel's model "A," the time-averaged velocities are as shown in Table 7-2. Reynolds number and entrance length are calculated by treating each branch as a straight smooth tube. Analysis of these data suggests that there is plug (uniform) flow in the trachea through the third generation, partially developed laminar flow in the fifth through seventh generations, and developed Poiseuille flow for an increasing fraction of each branch in the eighth through sixteenth generations. With maximal inspiratory and expiratory effort, however, velocities and Reynolds numbers (Re) may be 22-45 times larger than during quiet breathing. This suggests turbulent flow in the upper generations. Furthermore, because of variations in compliance and resistance, ventilation is not equally distributed throughout the lung; consequently, branches of the same generation may have different flow rates.

Skewed Profiles and Secondary Flows. The preceding flow analysis neglects the complicated flow behavior initiated at the bifurcations and transferred to the daughter branches. Schroter and Sudlow[112] and Schreck and Mockros[111] measured the velocity profiles for steady flow in the daughter branches of airway models that were geometrically similar to Weibel's model. For

Table 7-2

Airflow Analysis of Weibel's Model "A" for a Normal Resting Breathing Rate of 15 Cycles/Min and a Tidal Volume of 450 cm^3 [a]

Generation (z)	No. (N_z)	Diameter (D_z), cm	Length (L_z), cm	Time-Averaged Velocity (U_z), cm/s	Reynolds Number[b] (Re $\frac{D_z\bar{U}_z}{\nu}$)	Entrances Length[c] / Length of Generation $\left(\frac{0.057 \mathrm{Re} D_z}{L_z}\right)$
0[d]	1	1.8	12.0	88.6	960.7	8.21
1[e]	2	1.22	4.76	96.6	710.0	10.37
2[f]	4	0.83	1.90	105.6	528.0	13.15
3[g]	8	0.56	0.76	112.5	379.5	15.94
4	16	0.45	1.27	90.7	245.9	4.97
5	32	0.35	1.07	72.3	152.4	2.84
6	64	0.28	0.90	56.8	95.8	1.70
7	128	0.23	0.76	44.1	61.1	1.05
8	256	0.186	0.64	32.4	36.3	0.60
9	512	0.154	0.54	23.5	21.8	0.35
10	1,024	0.130	0.46	16.8	13.2	0.21
11	2,048	0.109	0.39	11.5	7.55	0.12
12	4,096	0.095	0.33	7.81	4.47	0.073
13	8,192	0.082	0.27	5.06	2.50	0.043
14	16,384	0.074	0.23	3.24	1.44	0.026
15	32,768	0.066	0.20	1.99	0.79	0.015
16	65,536	0.060	0.165	1.25	0.45	0.009

[a] Derived from Bell.[18]

[b] ν = kinematic viscosity of air in lung.

[c] Equation from Langhaar.[86]

[d] Trachea.

[e] Primary bronchi.

[f] Lobar bronchi.

[g] Segmental bronchi.

Poiseuille or plug flow in the parent tube, the flow is symmetrically split by the carina, and the higher axial velocities are directed off the daughter-tube axis along the inside wall. The shear rates along the inside wall are about 4 times larger than those along the outside wall, and the peak axial velocity is twice the average bulk flow velocity. The flow is also skewed as a result of the lateral convection or secondary flows generated at the bifurcation (Figure 7-1).

Although secondary flows increase the uniformity of the flow distribution distally along the branch, this is significant only in the slower regions. The flow profiles in the daughter branches become more complicated when this asymmetric flow reaches a second bifurcation; however, they follow the same general trends.

Sudlow and Schroter observed secondary flows at all flow rates (Reynolds number, 50-4,500), regardless of the shape of the entry profile. On inspiration, a pair of symmetric vortices is formed in each daughter branch (Figure 7-1). They are strong enough to complete one helical cycle within three branch diameters. On expiration, a set of four vortices is generated in the parent tube.

These results suggest that simple parabolic flow is ensured only in the conductive airways where the Reynolds number is less than 1.0. There, the fluid inertia is negligible, and the convective fluid transport is less than the molecular transport.

Turbulence. The simplified flow analysis of Weibel's model "A" indicates undeveloped flow with a flat profile in the trachea for Reynolds numbers (Re) up to approximately 2,000.[110] However, this does not consider disturbances produced by the rough walls, the eccentricity of the cross section, and the larynx.

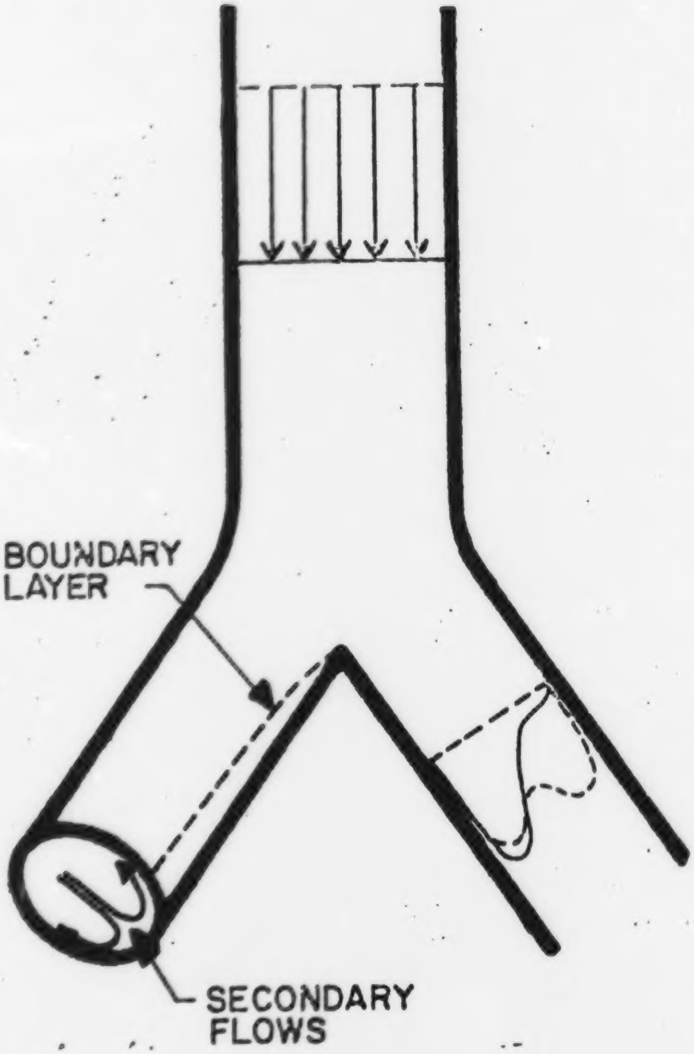

Figure 7-1. Schematic representation of flow in daughter branches of bifurcation model for steady inspiratory flow with flat profile in parent branch. Velocity profiles in plane of bifurcation (——) and in normal plane (----) are indicated in right branch. Orientation of secondary flows and position of laminar boundary layer are shown in left branch. (Reprinted with permission from Bell.[18])

For steady inspiratory flow in hollow casts of the trachea and the first bifurcation, Dekker[36] observed that a Reynolds number of 1,800 was required for initiation of turbulence. Similarly, for stead inspiratory flow in casts containing a larynx with the glottis in a natural open position, the required Reynolds number was 450. West[131] observed turbulence in the trachea of lung casts during exhalation at a Reynolds number of 800, although his hollow casts did not include a larynx. As the position of the vocal cords changes in the real lung,[141] the glottis of the larynx functions as a variable orifice. During inspiration, a jet of turbulent air enters the trachea and is directed against its ventral wall. Although the length of the trachea would be insufficient for the complete development of turbulent flow, the additional turbulence created by the jet and the corrugated walls may cause the turbulence to approach a fully developed state by the end of the trachea for a Reynolds number greater than 3,000.

A model developed by Owen[98] indicates that turbulence will gradually decay in any branch in which the Re is less than 3,000. Assuming a peak Re of 1,865 in the trachea--corresponding to a 1.9-s, 450 -cm^3 inhalation--Owen's model predicts a 10% decay in the trachea and in each of the first two generations of bronchi. According to Batchelor's theory[14] for the change in turbulent energy at regions of rapid flow contraction, decays of 15, 16, and 10% occur in the first three generations of bifurcation, respectively. Therefore, turbulence generated in the trachea at an Re of 1,865 will have approximately 50% of its initial intensity when it enters the third generation of bronchi. At inspiratory flow rates with an Re greater than 3,000, decay would be even slower.

These decay calculations neglect the possible effects of the strong secondary flows generated at the bifurcation. The regions of very high and very low shear rate caused by the secondary flows could also be regions of high and low turbulence and dissipation. However, Pedley, Schroter, and Sudlow[101] argued that the boundary layer remains laminar in the daughter tube for an Re less than 15,000 and had experimental evidence to verify this assumption for a parent-tube Re up to 10,000. Thus, the turbulent eddies are localized in the core, and the arguments given above are sufficient for predicting their rate of decay.

Detailed descriptions of the convective airflow patterns in cast replicas of the human respiratory tract during steady inspiration were given by Olson *et al*.[97] Their results show that the effect of the larynx is such that flow patterns typical of smooth bifurcating tubes (secondary motions and high shear rates along the inside wall) do not occur until the lobar bronchi. Turbulent eddies produced by flow separation below the larynx do not decay as rapidly as predicted by theory.[98] Indeed, small eddies were observed as far down as the sublobar bronchi with 200-ml/s flows in the trachea.

Wall and Flow Oscillations. Another flow complication is the effect of heartbeat. West[131] measured flow oscillations attributed to beating of the heart in the segmental bronchi and found that they were detectable only during breathholding or during pauses between inspiration and expiration. The peak oscillatory flow rate observed was 0.5 liter/min, which is approximately 20% of the peak flow rate in the segmental bronchi during quiet breathing. These oscillations will improve gas mixing.

The minor variation in airway dimensions during expansion and contraction of the lungs in breathing can generate radial velocities that would be significant only in the peripheral airways with the smallest axial velocities.

Schroter and Sudlow[112] estimated that the macroscopic corrugations in the airways are below the critical protuberance height at which laminar flow can be disturbed.

Quasisteady Flow. Most mathematical models for particle and pollutant transport assume steady flow conditions. However, flow actually varies approximately sinusoidally over time, and breathing frequency ranges from eight breaths per minute for sedentary conditions to 50 breaths per minute during sustained work and exercise.

Quasisteady flow may be a more accurate description. This means that the pulsatile flow in the lungs can be analyzed as a continuous sequence of steady-flow profiles. However, there are different and sometimes conflicting criteria for quasisteady flow in the airways.[72,112,135]

Bell[18] suggested that the quasisteady flow is probably a valid approximation at quiet-breathing frequencies and that velocity and pressure profiles in the lung during quiet breathing can be obtained from experimental steady-flow data. The same conclusions cannot be generally applied to experimental particle deposition or gas-transfer measurements.

For regions in which the flow is not quasisteady, a transient-flow solution may be possible. For example, Lakin[82] and Lakin and Fox[83] developed a two-dimensional transient-flow solution for an idealized symmetric bifurcation during the period at the end of inspiration and before expiration. Their finding that vorticity decreases at the carina or bifurcation apex suggests that particle- and gas-deposition rates may be increased at these sites in the respiratory tract. It also suggests that reactive gas deposition rates during normal oscillatory breathing differ significantly from those predicted for steady flow--a view suggested by Bell[18] for particles.

Convective and Diffusive Transport and Mixing. Another complication with unsteady, periodic flows is the mixing of residual air in the respiratory tract with the tidal air. The secondary flows and turbulence both increase the mixing of inhaled gases and particles with dead-space air. There have been numerous theoretical and experimental studies of convective and diffusive gas or aerosol mixing in the respiratory tract, but there is no general agreement on their relative significance in specific regions of the tract.

Work by Altshuler et al.[7] with 0.4- μm particles and a tidal volume of 500 ml showed that only about 11-27% of new air in each successive breath actually mixes with residual air. Theoretical particle-deposition models developed by Altshuler,[6] Beeckmans,[17] and Davies[35] have accounted for the mixing of inhaled aerosol with residual air.

Whipple, Chen, and Wang[132] showed that the distribution of an inhaled aerosol bolus depends on the orientation of the successive airway bifurcations and the volume of the bolus. On the basis of skewed velocity profiles, they made theoretical calculations of the distribution of aerosol boli in branching airways that were in fair agreement with the experimental data. Their results suggested that slow and shallow breaths should show greater differences in dispersion of irritant gases in the airways.

Baker et al.[13] theoretically analyzed simultaneous gas flow and diffusion in Weibel's symmetric model. They applied a time-varying flow with simultaneous longitudinal diffusion and concluded that convective mixing is much less important than mixing induced by molecular diffusion.

By analogy with heat-transfer data in curved tubes[114] and branching systems, the local transfer rates of easily absorbed gases are expected to be significantly affected by convective mixing in the large conducting airways. In the terminal bronchi and pulmonary regions, where convection is very slight, molecular diffusion is clearly dominant.

In a recent paper by Taulbee and Yu,[120] convective mixing of particles or gases in lung airways was defined in terms of an apparent diffusion coefficient. This was derived by assuming the inhaled particles or gases to follow the average air velocity in each airway and assuming the average velocity to be normally distributed among airways of the same generation. Their calculations indicated that this apparent diffusion coefficient is dominant and accounts for the pulmonary air mixing process.

As pointed out by Altshuler,[9] the flexibility and curvature of the airway walls and the gross inhomogeneities in the expansion and contraction of the lung structure cause flow separation and vortex motion that are directly related to convective mixing and flow irreversibility. To estimate the transport and uptake of inert and irritant gases within the pulmonary region better, one could use the alveolar-duct model and the calculation methods proposed by Altshuler for convective and diffusive mixing. He pointed out the significance of the fact that almost the entire wall of the alveolar ducts is open to the alveoli.

Wilson and Lin[133] described precisely the three transport mechanisms that act during the flow of a nonuniform gas in a tube: pure convection, Taylor diffusion (where radial diffusion and axial convection are coupled to produce an effective block or plug flow), and axial diffusion. They defined regions in the respiratory tract where each of these mechanisms dominates. By using Weibel's airway model[130] and these three mechanisms, they developed and analyzed a model to describe the transport of inert gases within the conducting airways. For quiet breathing, pure convection dominated the transport in the zero- through seventh-order generations, Taylor diffusion dominated in the eighth through eleventh, and axial diffusion dominated in the twelfth through seventeenth.

Later research by La Force and Lewis[81] showed that gaseous concentration gradients are negligible during quiet breathing (contradicting the work of Cumming _et al_.[30]). Their anatomic models of the alveolated airways and their calculation methods should be compared with those used or proposed by Altshuler[9] and Taulbee and Yu[120] in the establishment of a model for pollutant-gas uptake in the alveolated airways.

Airflow in the Nose and Nasal Airway Models. The complex anatomic structure of the nose is ideal for humidification, temperature regulation, and pollutant scrubbing of inspired air. Proctor and Swift[107] studied nasal airflow by observing and measuring the flow of water through a clear plastic model of the walls of the nasal passages. They used steady flow with a Reynolds number equivalent to that for air in the human nose. For an inspiratory flow of 0.4 liter/s (quiet breathing), the linear inspiratory velocity at the nasal entrance reached at least about 4.5-5 m/s and at most 10-12 m/s. These values are significantly larger than the peak linear velocity of 2 m/s in the bronchial tree during quiet breathing.

As the cross-sectional area expands beyond the entrance, flow separation occurs and results in turbulence and eddies, which continue as the air goes through the passages around the turbinates. The linear velocity also decreases sharply in this region, and the air stream then bends downward into the nasopharyngeal region. Because of these complex flow patterns and the large surface area of the nasal mucosa, the nose effectively scrubs particles and some gases from the inspired air.

Proctor and Swift's nasal passage model[107] and their charts of the direction and linear velocity of airflow in the model could be used for estimating the local uptake of gaseous pollutants and the total scrubbing efficiency of the nose. The degree of swelling of the nasal mucosa significantly affects the scrubbing efficiency, so more refined airway models should simulate the morphology and flow behavior during different states of swelling.

Mucus Flow Patterns in the Respiratory Tract

The dynamic properties of the mucous, serous fluid, and epithelial layers of the respiratory tract are important for the transport, absorption, and desorption of reactive gases. The cilia beat at a fairly constant frequency within the stationary serous layer and cause the outer mucous layer to move up the respiratory tract. Clearance of deposited particles and absorbed gases in the ciliated tracheobronchial tree depends partly on the movement of this mucous layer.

There have been a number of studies of the thickness and velocity of the mucous layer, with different results. Dalham[31] reported a thickness of 5 μm in the trachea of rats. Similarly, Alder _et al._[4] reported 10 μm and less in cats, and Comroe[29] reported 10-15 μm. Velocity has been measured at 13.5 mm/min in rats,[31] 0-35 mm/min in cows and 5-14 mm/min in dogs,[64] 10.5 ± 3.7 mm/min in cats,[4] and 15 mm/min in human trachea and 3.75 mm/min in human main bronchus.[64]

Clearance in the upper, or ciliated, region is governed by the rate of mucus transport along the airways. These rates have been measured in the human nose[48] and in dogs, rats, and other species. Asmundsson and Kilburn,[12] Hilding,[65] and Iravani[69] established that mucociliary clearance rates increase from the distal bronchi toward the trachea. Because bronchial openings retard mucus flow, bifurcations receive an accumulation of mucus and associated particles. The rate of mucus production and mucus thickness and velocity vary from one person to another. Thickness increases and velocity decreases greatly when some toxic elements are present in the airway.[119b,119c,119d,119e,119f]

New techniques have been developed for the direct measurement of mucociliary transport rates in the trachea. Yeates _et al._[135a] used an external gamma camera to follow a bolus of labeled microspheres deposited in the large airways by aerosol inhalation; they fitted a log-normal distribution to their measurements and obtained a geometric mean of 3.6 mm/min and a coefficient of variation of 75% among 42 healthy nonsmokers. (The short-term coefficient of variation was considerably less, with a value of 25%.) Santa Cruz _et al._[109a] used a cinebronchofibroscopic method on subjects whose larger airways were anesthetized and observed the movement of small Teflon disks (0.68 mm in diameter and 0.13 mm thick) that were blown into the trachea through the fibroscope; they reported an arithmetic mean of 21.5 mm/min (standard deviation, 5.5 mm/min) in 16 normal nonsmokers and a much smaller value of 1.7 mm/min in older patients with chronic obstructive lung disease. The large discrepancy in the values reported for normal nonsmokers has several sources: different statistical distributions, different methods, and a complicated heterogeneity in local mucus velocities. It appears that the invasive aspect of the bronchofibroscopic technique caused some of the increase in the measured transport rate.

Mucus flows in the bronchial airways have not been directly measured. The measurements of particle clearance for radioactively tagged particles depend on a mixture of deposition sites and mucus flow rates. However, such measurements have shown reproducibility in the individual and a large variation among individuals.[2a]

Altshuler *et al.*[8] developed a method for estimating the thickness and velocity of mucus throughout the tracheobronchial region. They matched a particle clearance time with Landahl's lung model and assumed a constant rate of mucus production per unit surface area and a uniform mucus thickness throughout the tract, except for terminal bronchioles. The calculated values are given in Table 7-3. From these values, mucus velocity in each region can be obtained by dividing the length of the region by the corresponding transit time. Jacobi,[71] Thomas,[121] and Haque and Collinson[57] also devised mucus clearance models for estimating the lung-tissue dosage of short-lived alpha emitters.

The calculated velocities are based on the assumption that mucus flows axially in each region. Actually, the bronchial openings represent obstructions to this parallel flow. Some have observed that the mucus stream has a spiral path sweeping over the carina.[58] According to Hilding,[63] mucus streams move axially and parallel in each section of airway. The streams that intersect the carina bend 90°, pass parallel to the carina, and then move upward. Others continue their flow undisturbed. Hilding stated that the reasons for this flow behavior may be the change in direction of cilia beat and the presence of small whirlpools in the middle of the margin of bronchial openings.

Some studies indicate that the mucous layer is not a continuous blanket. Direct observations of the airways of normal and bronchitic rats *in vitro* by Iravani and Van As[70] and Van As and Webster[125] failed to find a mucous blanket at any level of the tracheobronchial tree.

Table 7-3

Anatomic Model of the Bronchial Tree and Mucous Layer[a]

Region	Diameter, cm	Length, cm	Total Circumference, cm	Total Surface Area, cm^2	Mucus Transit Time, min	Mucus Thickness, μm
Trachea	1.6	12	5.0	60	8	7
Main bronchi	1.0	6.0	6.3	38	6	7
Lobar	0.4	3.0	15	45	11	7
Segmental	0.2	1.5	63	94	37	7
Subsegmental	0.15	0.5	360	180	82	7
Terminal	0.06	0.3	11,000	3,400	1,980	4.2

[a] Derived from Altshuler et al.[8]

Further work by Van As and Webster[126] supports the discontinuity of mucus and shows that it is transported in well-defined streams in the larger airways of the rat. In addition to small regions of stagnation, local retrograde movement was observed. One must also consider the possibility that some of the serous fluid and mucus may be reabsorbed as it moves up the respiratory tract. This could influence the local tissue and mucous layer concentration of absorbed gas with time. Morphologic examination confirmed that mucus is present as flakes, droplets, and plaques. Droplets 0.5-1 μm in diameter are believed to be the primary unit of mucus, and they aggregate to form flakes, which in turn forms plaques. The smaller flakes may be transported individually over individual metachronal fields of cilia, but the plaques are transported en masse by the combined action of numerous metachronal fields. The assumption of a continuous, stationary, and uniform layer of serous fluid also needs critical examination, especially in nonciliated areas.

Recent unpublished studies by Boatman and Luchtel[23] in rabbits show that the mucous field is indeed continuous in the medium and smaller airways. Their morphologic techniques are currently being extended to the large airways. Differences in techniques may account for the discrepancy between this work and that of Van As and Webster.[126] Further studies of the structure of the mucous layer in animals are therefore needed to resolve the continuity-discontinuity question.

Mucociliary clearance from the nose or upper airways of man has been measured and described by Proctor and co-workers,[105,106,107,107b] Anderson _et al_.,[10,11] and Quinlin _et al_.[108] Through the use of radioactive particles as tracers, mucus has been observed to move everywhere toward the nasopharynx, although indirectly. The mucociliary stream from the paranasal sinuses joins the nasal stream all along the middle meatus and above the posterior end of the middle turbinate. This flow field ensures that the region of the nose receiving the greatest desposition of toxic gases and aerosols is better protected. Mucus that reaches the nasopharynx, where the cilia disappear, is moved downward during swallowing, because the soft palate wipes the posterior nasopharyngeal wall.

Anderson *et al.*[9a] found a weak positive association between tracheobronchial clearance and nasal clearance with a saccharine-particle method. A strong positive correlation would have indicated that information about the tracheobronchial clearance rate can be derived by studying clearance rates in the nose, which is more accessible. The saccharine method was shown to be a useful clinical tool for evaluating the status of the nasal mucociliary function in human subjects exposed to ambient pollutants or to controlled concentrations of specific pollutant gases or aerosols.

Effects of Inhaled Irritants and Airway Abnormalities on Air and Mucus Flow

A particular pulmonary irritant may alter air or mucus flow, and this in turn is one of the factors determining the local tissue dosage of the irritant. Such positive or negative feedback effects should also be incorporated into a dynamic model.

Acute exposure to irritant gases or particles present in urban air and in cigarette smoke at high concentrations can change the physical and chemical properties of mucus and cause retardation or cessation of mucociliary clearance.[10,31,32,73,117] Chronic exposure to some of the same irritants appears to cause hypertrophy of the mucus-secreting elements and glands of the upper airways, with a parallel increase in the production and secretion of airway mucus, and the bronchioles may show a marked increase in the goblet cells, resulting in excessive mucus production and airway obstruction, owing to ineffective clearance.[91]

Bronchoconstriction caused by acute exposures to ozone or sulfur dioxide may be expected to change the ventilation distribution, local aerodynamics, and tissue dosage. Edema resulting from exposures to toxic gases may alter the gas-absorptive capacity of the airways, in addition to the aerodynamics. Reaction of irritant gases with surfactant material in the alveoli may alter the absorptive capacity and physical properties of the surfactant, influence edema formation, and alter the clearance of inhaled particles.

GAS PHASE OF MODELS FOR POLLUTANT-GAS TRANSPORT IN THE RESPIRATORY TRACT

This section is concerned mainly with the approach to modeling the gas-phase behavior of single reactive gases. The basic approach can also apply to sulfur dioxide, ammonia, and other pollutant gases in which water solubility alone controls the rate of uptake. The simpler case of inert gases has been reviewed in a conference report edited by Papper and Kitz.[99]

Boundary Conditions

The simplest boundary condition between the gas and liquid phases is the assumption that the gas concentration at the surface of the mucus is zero. This same boundary condition is used for particles, so the deposition theory for highly diffusive particles may also be applicable. It may be adequate for predicting the net uptake of highly soluble gases like sulfur dioxide during single-breath inhalations at low gas-phase concentrations and could also apply to cases in which a pollutant gas undergoes rapid chemical reaction at the surface of the mucus (i.e., if the rate of chemical reaction exceeds the rate of transfer from the gas phase). Experimental data[15,139] have suggested that the rate of transfer of ozone from the air to the mucosal lining may be partially influenced by its capacity for undergoing chemical transformation in the liquid phase. If this zero-conconcentration boundary condition is to be used, data are needed on the rate of chemical transformation of ozone in mucus.

A realistic boundary condition must account for the solubility of the gas in the mucous layer. Because ambient and most experimental concentrations of pollutant gases are very low, Henry's law ($y = Hx$) can be used to relate the gas- and liquid-phase concentrations of the pollutant gas at equilibrium; y is the partial pressure of the pollutant in the gas phase expressed in mole fraction at a total pressure of 1 atm, x is the mole fraction of absorbed gas in the liquid, and H is the Henry's law constant. Gases with high solubilities have a low value of H. When experimental data for solubility in lung fluid are unavailable, the Henry's law constant for the gas in water at 37 C can be used (see Table 7-1). Gas-absorption experiments in airway models lined with water-saturated filter paper[68] gave results for the general sites of uptake of sulfur dioxide and nitrogen dioxide that agree with uptake and histopathologic data on animals.

The Henry's law constant in water is used in the McJilton et al. uptake model[92] to determine the equilibrium concentration of ozone and sulfur dioxide at the surface of a simulated mucous film along the airways in Weibel's symmetric model.[130] It is also used to determine the concentration of absorbed gas at the surface of the mucus when the pollutant gas undergoes a homogeneous or heterogeneous chemical reaction within the mucous layer.

An additional complexity that has not been modeled is the simultaneous inhalation, absorption, and chemical reaction in the gas or liquid phase of two or more gases (e.g., sulfur dioxide and ozone). For sufficiently dilute mixtures, Henry's law can be used for each gas. If droplet aerosols and one or more reactive gases are simultaneously present, absorption with or without chemical conversion in the droplets must be considered.

Transport Equations

As noted earlier, air-velocity profiles during inhalation and exhalation are approximately uniform and partially developed or fully developed, depending on the airway generation, tidal volume, and respiration rate. Similarly, the concentration profiles of the pollutant in the airway lumen may be approximated by uniform partially developed or fully developed concentration profiles in rigid cylindrical tubes. In each airway, the simultaneous action of convection, axial diffusion, and radial diffusion determines a differential mass-balance equation. The gas-concentration profiles are obtained from this equation with appropriate boundary conditions. The flux or transfer rate of the gas to the mucous boundary and axially down the airway can be calculated from these concentration gradients. In a simpler approach, fixed velocity and concentration profiles are assumed, and separate mass balances can be written directly for convection, axial diffusion, and radial diffusion. The latter technique was applied by McJilton *et al.*[92]

To calculate more precisely the average uptake or the local variation in uptake in each airway, the local variations in velocity and concentration profiles must be taken into account. For example, thin momentum and concentration boundary layers occur at bifurcations and gradually increase in thickness with distance downstream. Bell and Friedlander[19] showed that particle and gas transfer to the airway wall is greatest where the boundary layers are thinnest, e.g., at the carina or apex of bifurcations.

Experimental data (e.g., from Yokoyama and Frank[139]) demonstrate that the concentrations of ozone and other gases reaching the trachea depend heavily on whether nose or mouth breathing is used. Detailed gas-transport equations for the nose and mouth are difficult to formulate. A simple approach used by La Belle _et al._[80] assumed that the nose behaved like a scrubbing tower used in chemical processing. By varying the number of transfer units (defined as a portion of the dose sufficient to permit equilibration between gas and liquid phases) and the molar ratio of inhaled air to liquid, one may control the uptake of a soluble gas to match experimental data. Another simple approach was used by Aharonson _et al._[1] A quasisteady state was considered for unidirectional flow in a one-dimensional model of the nose. A local mass balance was made for the transfer of the soluble vapor from the air to the mucus-tissue layer. The local transfer rate was strictly proportional to the local partial pressure of the vapor in the gas phase, and the average transfer rate--i.e., the overall uptake--could be determined by integrating the local transfer rates over the entire length of the nose.

Local and Average Mass-Transfer Coefficients

The rate of mass transfer of a pollutant gas from the gas phase to the wall of an airway can be written as:

$$\frac{dm}{dt} = -K_G A(C - C^*), \qquad (1)$$

where K_G is the average mass-transfer coefficient, in centimeters per second, over the entire exposed surface area, A, of the airway; C is the average pollutant mass concentration in the gas phase in the airway; and C* is the concentration of pollutant gas at equilibrium with the absorbed gas in the wall.[102] Local mass-transfer coefficients can be similarly defined for subsegments of an airway wall.

K_G can be defined as a gas-phase transfer coefficient, independent of the liquid layer, when the boundary concentration of the gas is fixed and independent of the average gas-phase concentration. In this case, the average and local gas-phase mass-transfer coefficients for such gases as sulfur dioxide, nitrogen dioxide, and ozone can be estimated from theoretical and experimental data for deposition of diffusion-range particles.[18] This is done by extending the theory of particle diffusion in a boundary layer to the case in which the dimensionless Schmidt number, ν/D, approaches 1 (ν is the kinematic viscosity of the gas, and D is the molecular diffusivity of the pollutant). Bell's results in a tubular bifurcation model predict that the transfer coefficient depends directly on the square root of the average airway velocity, the diffusion coefficient raised to the 2/3 power, and the bifurcation angle.

The prediction of such "hot spots" of gas transfer at bifurcations are supported by experimental data on ozone-exposed rabbits.[22] Longitudinal slices of airways from these rabbits showed at low magnification that desquamation of the ciliated epithelium cells was focal and sometimes more intense at a bifurcation.

The dependence of the local and average transfer coefficients on the square root of the average airflow rate is supported by the experimental data and analysis of Aharonson et al.[1] for ozone, acetone, ether, and sulfur dioxide.

Values for the average vapor-transfer coefficient from the gas phase to the airway epithelium can also be estimated from heat-transfer data in straight, curved, or bifurcating cylindrical tubes by using the analogy between heat transfer and mass transfer. Such an approach has been used by Yeh[136] to predict the diffusional deposition of small particles in the conducting airways.

LIQUID-TISSUE PHASE OF MODELS FOR POLLUTANT-GAS TRANSPORT IN THE RESPIRATORY TRACT

The important properties of the mucous and serous layers for gas-transfer models are thickness, viscosity, velocity gradients, the diffusion coefficients of pollutant gases in the mucous and serous fluid, and the chemical properties of these layers in the case of gases. Nonreactive gases like sulfur dioxide must diffuse through this liquid layer and the underlying cellular tissue layers before being absorbed by the blood. Figure 7-2 is an idealized cross-sectional model of part of a conducting airway showing separate tissue- and blood-layer components of the liquid-tissue phase. In preliminary studies designed to predict the average uptake in each generation, complexities like detailed velocity gradients in the liquid phase are unwarranted. Velocity gradients could be important in predicting local dosage to tissue; however, there are no experimental data. The mucous and serous layers may or may not be continuous and may constitute a homogeneous layer in some airways; thus, a single homogeneous liquid layer of constant thickness in each airway should be assumed until a more detailed description seems justified. Similarly, in the future it may be advantageous to subdivide the tissue layer into cell layers to reflect the pathologic evidence of ozone damage on some cell types and layers.

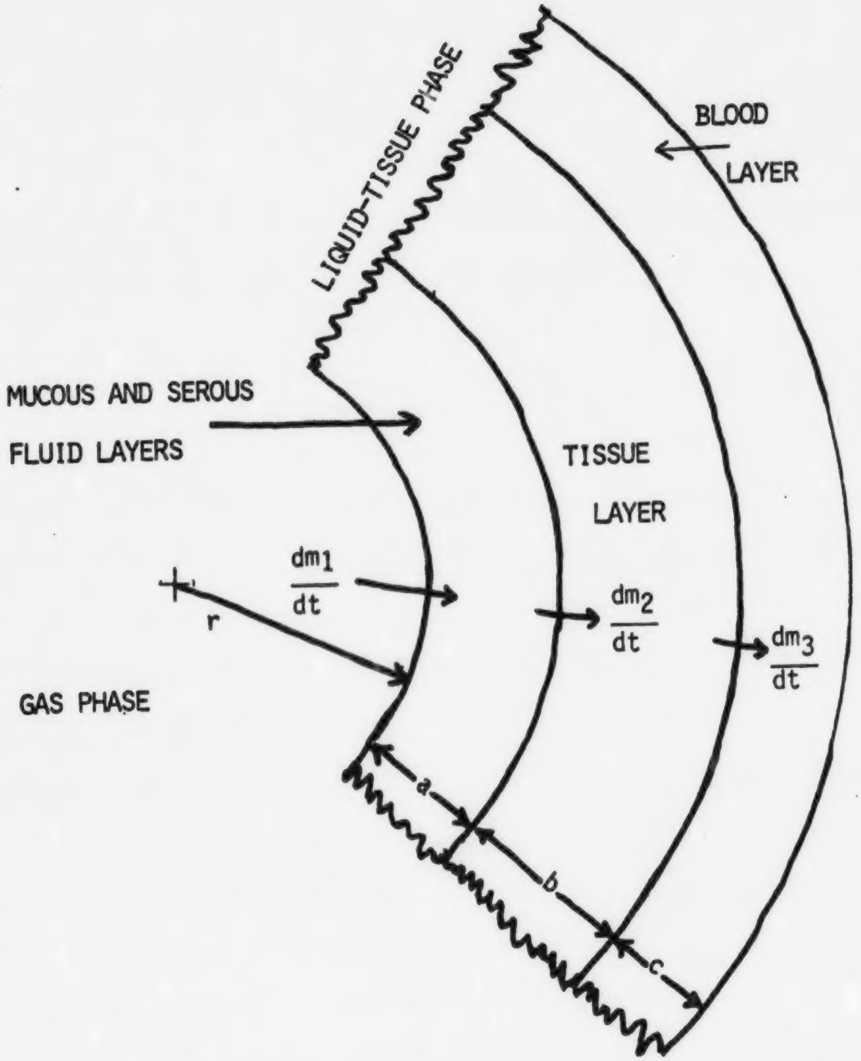
LIQUID-TISSUE PHASE
BLOOD
LAYER
MUCOUS AND SEROUS
FLUID LAYERS
TISSUE
LAYER
$\frac{dm_1}{dt}$
$\frac{dm_2}{dt}$
$\frac{dm_3}{dt}$
r
GAS PHASE
a
b
c

Figure 7-2. Cross-sectional model of part of a conducting airway in the respiratory tract, showing a gas phase and a liquid-tissue phase subdivided into mucous- and serous-fluid, tissue, and blood layers. (Derived in part from McJilton *et al.*[92])

Aharonson et al.[1] combined the mucous and tissue phases in their conceptual model of the nose into one layer that separates the air and blood. The different resistances of each interface and layer are lumped into their local transfer coefficient.

Figure 7-2 illustrates a three-compartment structure assumed by McJilton et al.[92] for describing radial diffusion. It consisted of a gas phase in the lumen of the airway, a liquid layer that lined the airway, and a tissue compartment. The rate of movement of the gas into the liquid layer, dm_1/dt, is a function of the solubility of the gas in the liquid, as defined by the Henry's law constant. The rate of movement of the gas molecules across the liquid layer to the tissue compartment, dm_2/dt, is a function of the diffusion coefficient of the gas in the mucous and serous layer. The concentration of ozone was assumed to be zero at the liquid-tissue boundary. This means that ozone is instantaneously converted by chemical reaction when it reaches the tissue layer, but undergoes no chemical reaction within the mucous layer. Such a model may be useful for ozone, if the rate of chemical reaction is very low. Ozone is known to react with hydroxyl ions at a very low rate,[3] but it probably reacts more rapidly with organic molecules in the mucus.

The mass-transfer coefficient in Eq. 1, K_G, which averages over the interface between the gas phase and the mucous-fluid layer, is given by $K_G = 1/[(1/kg)+(H/k_\ell)]$, where k_g is the gas-phase mass-transfer coefficient and k_ℓ is the liquid-phase coefficient. This is the two-film model for interfacial mass transfer in which a gas molecule encounters resistance from both phases as it diffuses from the bulk vapor to the bulk liquid.[88,102] McJilton et al. assumed that $k_g >> k_\ell/H$ and used empirical data to evaluate k_ℓ for several gases. An alternative procedure is to evaluate k_ℓ from penetration theory:[102]

$$k_\ell = \sqrt{\frac{4D}{\pi t}} \quad , \qquad (2)$$

where D is the diffusivity of the absorbed gas in the mucous layer and t is the gas-liquid contact time during inhalation or exhalation. Using the diffusivity of the absorbed gas in water may overestimate the actual transfer rate, because diffusivity may be much smaller in a viscous mucous fluid. Values of k_g can be determined as described in the previous section.

If the gas is converted by chemical reaction in the liquid layer, k_ℓ is modified according to the order of the reaction and whether it is reversible or irreversible. For example, if ozone reacts rapidly and irreversibly with organic molecules in the mucous layer, k_ℓ could be 10-100 times higher than the estimate based on penetration theory.

To model sulfur dioxide absorption by the blood through the walls of the upper airways, as demonstrated by Frank _et al._,[46] one must include the transport rates of sulfur dioxide across a mucus-tissue interface, a tissue layer, and a tissue-blood interface (Figure 7-2). For the case of release of dissolved gas back into the exhaled air, which is depleted of gas in the lower lung, the mucous layer would still represent the greatest resistance to transfer. Consequently, the overall transfer coefficient, K_G, would still be given by k_ℓ /H.

The processes of convection, axial diffusion, radial diffusion, and chemical reaction in the liquid and tissue layers all occur simultaneously. A rigorous approach requires solution of several simultaneous differential equations. To avoid this complexity in preliminary models, the transfer processes can be calculated in successive steps, as was done by McJilton et al.

The average dose rate or mass flux to tissue in each airway generation, defined as the mass transferred per unit time to the surface area of the generation, is given by dm_2/dt, the rate of mass transfer across the liquid-tissue interface in Figure 7-2. The dosage to tissue is found by integrating the mass flux over time or a number of breaths. The local dose rate and dosage are defined in analogous ways.

DISCUSSION OF RESULTS WITH VARIOUS MODELS

Most models of gas uptake in the respiratory tract have been concerned with carbon dioxide, carbon monoxide, oxygen, and anesthetic gases like chloroform, ether, nitrous oxide, benzene, and carbon disulfide (e.g., Lin and Cumming[89a] and Papper and Kitz.[99]) Unfortunately, there are only a few preliminary models of pollutant-gas transport and uptake in the respiratory tract.

Models of Nasal Uptake

La Belle et al.[80] modeled the absorption of various gases in the nasal passages of rats by applying principles of scrubbing-tower design. Their important characteristics were the Henry's law constant, the molar ratio of inhaled gas to absorbing liquid in the nose, and the number of transfer units. One transfer unit was defined as a portion of the nose sufficient to permit equilibration. The blood flowing through the nasal epithelial linings, rather than the moving mucous layer, was assumed to be the principal absorbing liquid. and the Henry's law constants for water were used. The number of transfer units, N, was guessed to be between 1 and 10. Results of the calculations for various gases are summarized in Table 7-4. For oxygen through acrolein (relatively insoluble through moderately soluble gases), the penetration was controlled largely by the Henry's law constant. For ozone, with a Henry's law constant of 9,700 at 37 C, the La Belle _et al_. model predicts 99% penetration. For more soluble gases like sulfur dioxide and ammonia, the penetration also depends on the number of transfer units and the molar ratio of gas to blood.

This model appears inadequate, for a number of reasons. Although experimental data show that less sulfur dioxide than ozone penetrates the nasal passages in animals, as predicted by the model, much more ozone is predicted to penetrate than was demonstrated by Yokoyama and Frank[139] in dogs. The most likely explanation is that the model does not account for chemical reactions of ozone in the mucus and epithelial tissue. Another problem is that the nose is believed to behave more like a scrubbing tower with fresh liquid at each level, inasmuch as the blood supply is not continuous for the entire length of the nose,[24] as assumed in the model. Neglecting the surface area, volume, flow, and thickness of the mucous layer in the nose will probably also give erroneous results for soluble gases with a small diffusion coefficient in mucus and for single-breath inhalations of a low concentration of any gas.

However, recent work by Loring and Tenney[89b] partially supported the La Belle _et al_. model by suggesting that the properties of the mucous layer in the nose may be irrelevant for modeling the absorption of relatively water-insoluble gases, such as nitrogen, oxygen, carbon

Table 7-4

Calculated Penetration of Gases through the Nasal Passages in Rats[a]

Gas	Henry's Law Constant, mole fraction gas / mole fraction in solution	Fraction of Gas that Penetrates to Lung,[b] %		
		N = 1	N = 5	N = 10
Oxygen	50,000	100	100	100
Nitric oxide	31,000	100	100	100
Nitrogen	10,000	99	99	99
Ozone	9,700	99[c]	99[c]	99[c]
Nitrous oxide	2,560	98	98	98
Carbon dioxide	1,900	95	95	95
Hydrogen sulfide	610	90	90	90
Chloroform	475	90	90	90
Bromine	160	80	80	80
Ethyl ether	68	70	70	70
Acetaldehyde	25	60	60	60
Acrolein	20	52	50	50
Chlorine	12	28	25	20
Sulfur dioxide	10	26	18	9
Acetic acid	7	25	7	2
Formaldehyde	3.8	10	4	0.2
Hydrogen cyanide	2.5	8	2	0.05
Ammonia	1.5	6	1.1	0.02
Phenol	0.4	5	0.8	0.01
Hydrogen bromide	0.003	5	0.7	0.01
Hydrogen chloride	0.001	5	0.6	0.01
Hydrogen iodide	0.0008	5	0.6	0.01

---

[a] Dervied from La Belle *et al*.[80]

[b] N = number of transfer units.

[c] Extrapolated values.

dioxide, and nitrous oxide. They observed that the flux of these gases from the frontal sinuses of cats was explained best by a perfusion-limited blood absorption mechanism.

An accurate nasal model must also account for the airflow rate and the concentration of the inspired gas. Aharonson _et_ _al_.[1] conclusively demonstrated that the "uptake coefficient," or average mass-transfer coefficient, over the entire nose for acetone, ozone, sulfur dioxide, and ether increased with increasing airflow rate.

Yokoyama and Frank,[139] Frank _et_ _al_.,[47] Brain,[24] and Egle[40,41] largely overlooked this flow-dependent relationship, because they did not normalize their retention data into the average-transfer-coefficient form. In fact, failure to do this led Yokoyama and Frank to the erroneous conclusion that "the uptake of O_3 was inversely rated to flow."

Aharonson _et_ _al_.[1] discussed four explanations for the increased uptake with increased flow: misinterpretation of data owing to a dependence of the average transfer coefficient on vapor concentration, decrease in the gas-film resistance, increased perfusion of nasal tissue, and increase in the effective surface area for uptake. For a gas like ozone, which is fairly insoluble but probably highly reactive in the mucous layer, the gas film or concentration boundary layer represents the major resistance to uptake. As discussed earlier, the gas-phase average or local transfer coefficient in airways of the tracheobronchial tree is predicted to depend on the square root of the average airflow rate in the airway and is independent of gas-phase concentration. Because the data analyzed by Aharonson _et_ _al_. agree roughly with this square-root dependence, the properties of the boundary layers in the nose may be similar to those in the tracheobronchial tree. The vapor concentration enters only in calculation of the average flux to the tissue from the product of the transfer coefficient and the concentration gradient between the gas phase and the liquid-tissue phase. The overall transfer coefficient, K_G, in Eq. 1 may be concentration-dependent, if the vapor is reacting reversibly in the liquid layer or reacting reversibly with a second dissolved vapor in an inert liquid layer.

Models of Tracheobronchial Uptake

There are no published models that adequately describe ozone uptake in the tracheobronchial tree. To present the methodology, a few published and unpublished models of the uptake of various gases will be reviewed.

The McJilton et al. model of ozone uptake has been widely cited, although not formally published. It is described here because it was the first attempt to model the absorption of pollutant gases in each generation of the tracheobronchial tree.

They used mass-balance expressions in finite-difference form to approximate the convection and diffusion of the pollutant gas in a 25-segment airway model that started at the trachea and was a modified version of Weibel's model. A sinusoidal breathing cycle and uniform plug flow were assumed in each of the first 20 segments. Beyond the twentieth segment, where the segmental volume was greater than 5 ml, uniform convective mixing was assumed. The cylindrical airways were assumed to be lined with a stationary mucous-fluid layer and a tissue layer as shown in Figure 7-2. The mucus was assumed to have the properties of water and thicknesses of 10 μm in the upper generations, 3-5 μm in the alveolar ducts, and 0.3 μm in the alveoli. There were no chemical reactions in the mucus.

Finite-difference techniques were also used to calculate the rate of diffusion of the pollutant gas from the airway to the mucous layer and through the mucous layer to a perfectly absorbing sink at the mucus-tissue interface. The mass of pollutant lost from the airway or transferred across the air-mucus interface during each breathing cycle was divided by the segmental surface area to obtain the dosage, in micrograms per square centimeter per breath.

Although convection, axial diffusion, and radial diffusion actually occur simultaneously, a multistep procedure was adopted in the finite-difference calculation. For each 5-cm^3 increment in tidal volume and for each time increment, Δt, the differential mass-balance equations were solved for convection, axial diffusion, and radial diffusion in that order. This method may slightly underestimate the dosage for weakly soluble gases, because the concentration gradient in the airway may be decreased.

Although the authors view their results with this model as only preliminary, a few of the results are presented here to contrast the expected behavior of water-soluble gases (e.g., sulfur dioxide) with that of fairly insoluble gases (e.g., ozone).

Figure 7-3 shows the percentage of total gas uptake for the steady state (after five or six breaths of 500-cm^3 tidal volume with 2-s inspirations). Uptake increases from about 75% for a relatively insoluble gas with a Henry's law constant of about 10^4 to a peak of 95% for soluble gases with a Henry's law constant of 20 or less. Figure 7-4 shows why there is only a 20% variation in uptake over a wide range of the Henry's law constant (10-10^4). The model predicts that the dosage of gases of

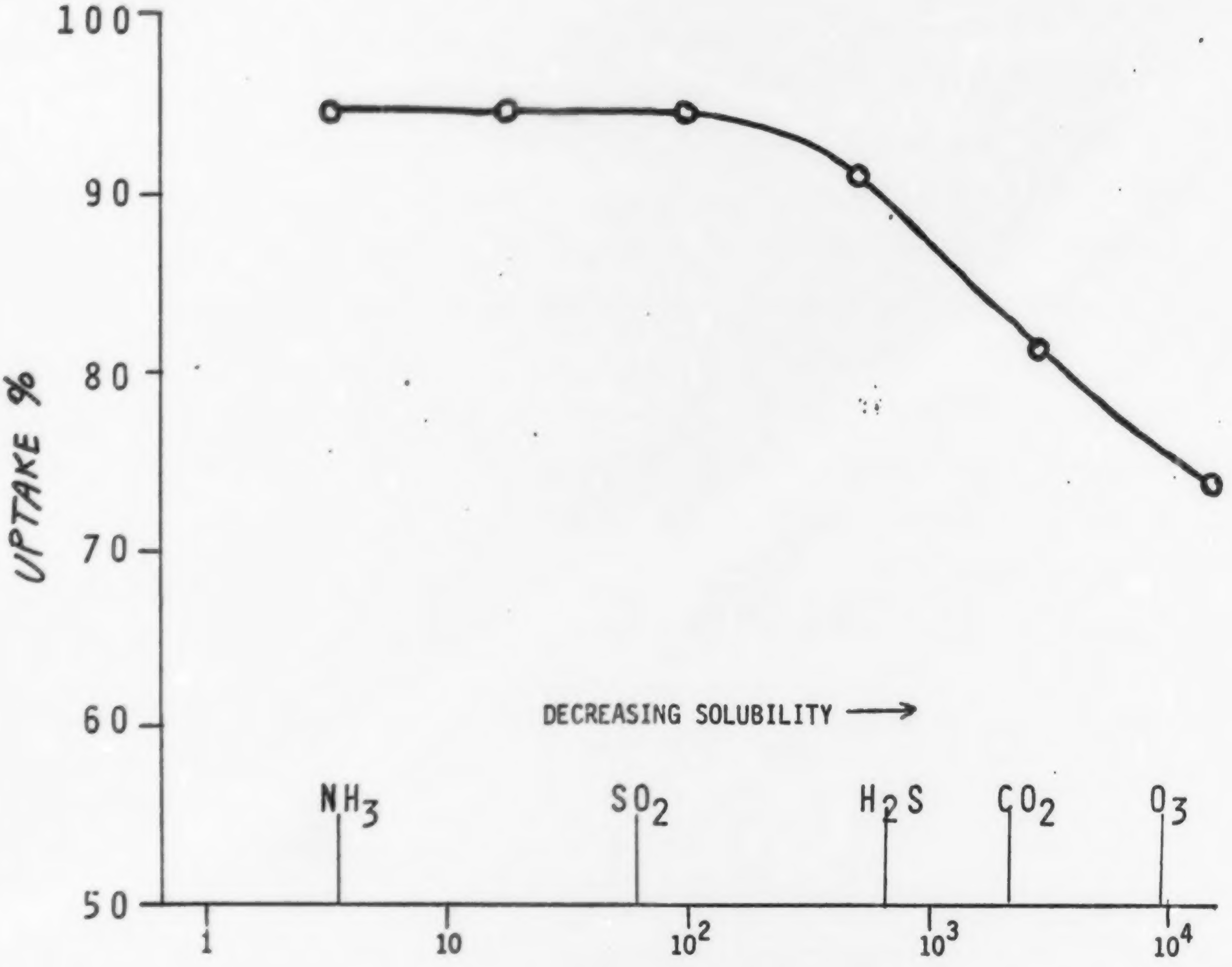

H, Henry's Law Constant at 37 C

Figure 7-3. Uptake of pollutant gases in the entire tracheobronchial tree and pulmonary region at steady state as a function of Henry's law constant. (Modified from the model results of McJilton *et al*.[92])

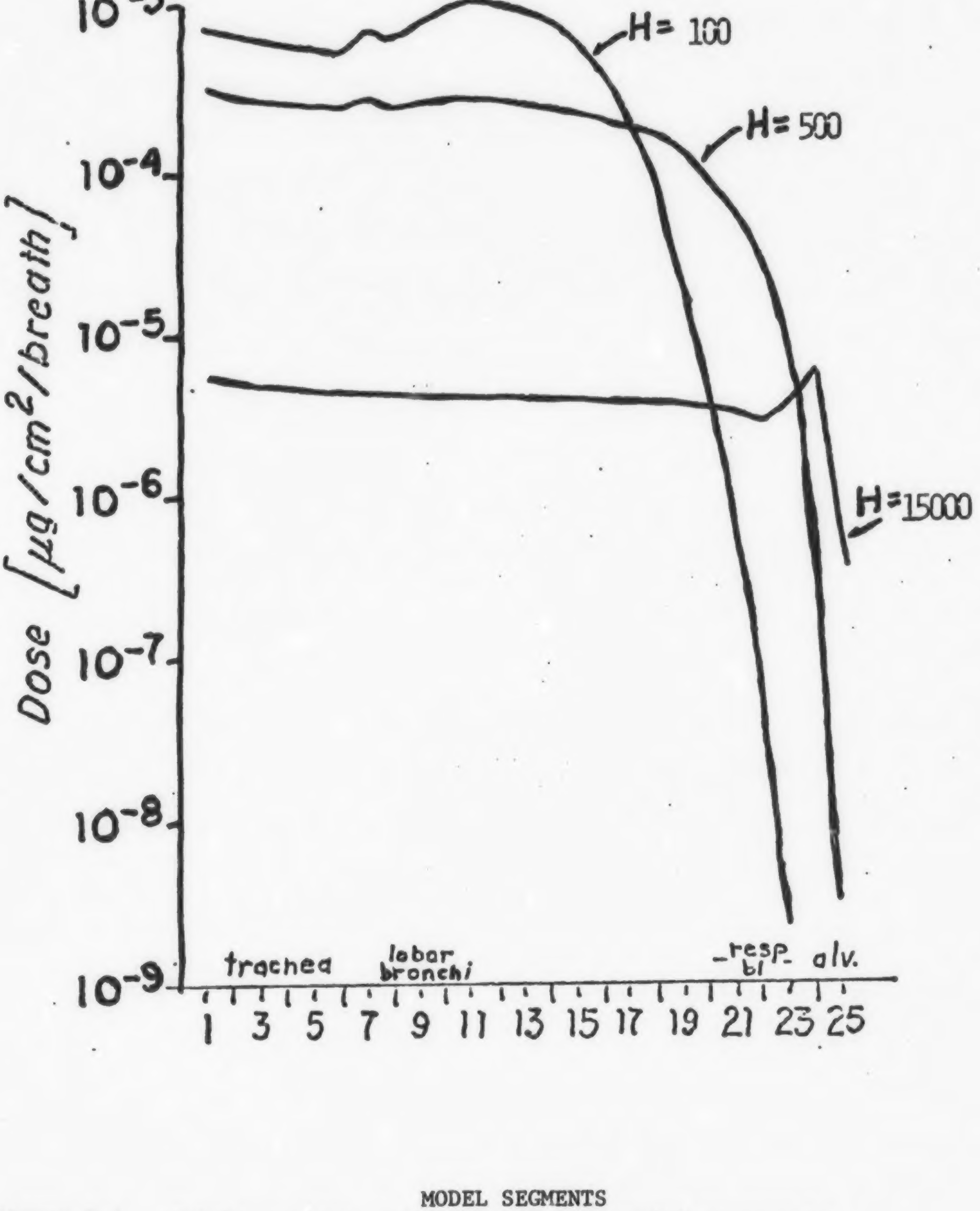

Figure 7-4. Uptake or dose predicted for each model segment by McJilton et al. for gases of different solubilities at 37 C. Tidal volume = 500 cm^3. Inspiration time = 2 s. (Modified from McJilton et al.[92])

low solubility is fairly uniform throughout most of the airways until the alveoli are reached, whereas gases of high solubility are predominantly removed in the upper airways of the tracheobronchial tree.

The model also predicts an increase in uptake as tidal volume increases over a constant breathing period. As the breathing period increases at a constant tidal volume, the uptake also increases. In the former case, increased ventilation of peripheral airways with a high surface:volume ratio increases uptake. In the latter, the period for radial diffusion is increased in every segment.

Figure 7-5 contrasts the steady-state uptake of sulfur dioxide and ozone per breath in each segment of the McJilton _et al_. model when the inhaled gas concentration at the entrance to the trachea is 1,000 $\mu g/m^3$. The patterns for the uptake of the highly soluble sulfur dioxide and the relatively insoluble ozone are strikingly different. The segmental dosage of sulfur dioxide peaks at 1.2×10^{-3} $\mu g/cm^2$-breath in segments 11 and 12 (immediately beyond the lobar bronchi). Ozone dosage is fairly uniform around 8.5×10^{-6} $\mu g/cm^2$-breath in segments 1-18. It then dips sharply to 5×10^{-6} $\mu g/cm^2$-breath in segment 22 and peaks again at 8.3×10^{-6} $\mu g/cm^2$-breath in respiratory bronchioles. A much smaller dosage of 2×10^{-7} $\mu g/m^3$-breath is calculated in the alveoli, mainly because of the large surface area.

There are no experimental data to verify the detailed dosage distribution among airway segments; however, experimental data on mouth-breathing animals and man support the general concept of rapid absorption of sulfur dioxide and greater peripheral absorption of ozone.[24,46,140]

Recently, Corn et al.[29a] measured an overall mass-transfer coefficient for sulfur dioxide and nitrogen dioxide in the upper airways of the tracheobronchial tree in cats during controlled respiratory cycles. Their measured transfer coefficient for sulfur dioxide was nearly 100 times larger than the average transfer coefficient predicted between the trachea and segmental bronchi from Figure 7-5. Their coefficients for sulfur dioxide were also slightly dependent on concentration, but they were independent of concentration for nitrogen dioxide. At a fixed tidal volume, the measured transfer coefficients were consistent with the square root of the breathing frequency or average flow rate, as predicted by the previously discussed theory based on the boundary layer model, and as shown by the uptake data for sulfur dioxide in the nasopharyngeal region.

In general, the McJilton et al. model appears to be useful for estimating the uptake in the tracheobronchial tree and pulmonary region of water-soluble and relatively water-insoluble gases that are nonreactive with the mucous layer. Nonreactive gases that are only partially soluble in tissue or blood (sulfur dioxide, oxygen, carbon dioxide, and anesthetic gases) may exert a backpressure that inhibits the gas uptake from the airways. Modifications, including the local blood flow rate and the tissue thickness (Figure 7-2) are required to handle these gases properly. The major weakness is the requirement of nonreactivity of gases in the mucous layer. Very weakly reactive gases may be treated as nonreactive. However, the uptake of ozone, which is known to decompose in water and is expected to react rapidly with biopolymers and other organic molecules in the mucous layer, is probably underestimated in the upper airways and

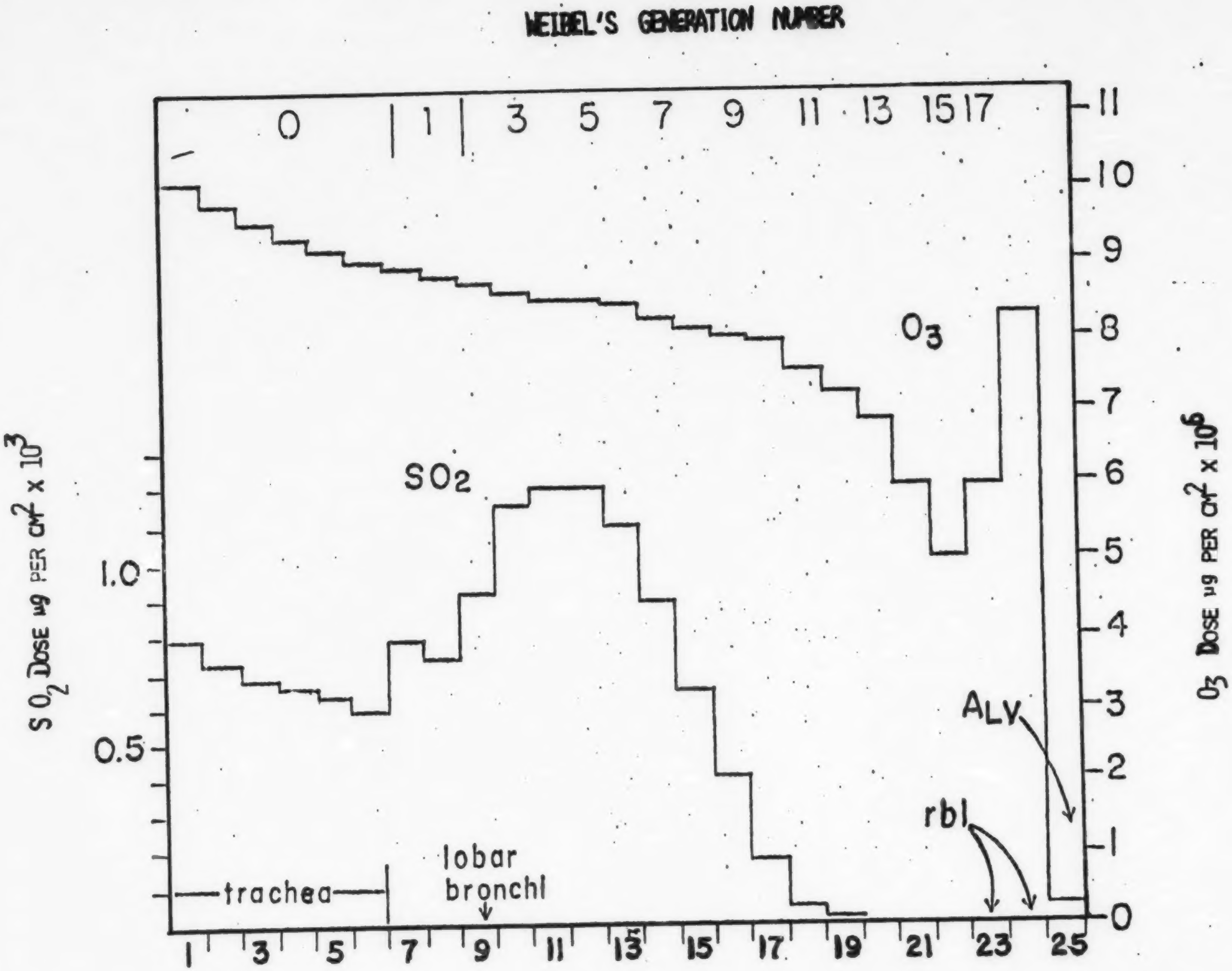

Figure 7-5. Comparison of dosage of sulfur dioxide and ozone predicted per breath for each model segment by McJilton *et al.* Inhaled concentration = 1,000 µg/m^3. Tidal volume = 500 cm^3. Inspiration time = expiration time = 2 s. (Modified from McJilton *et al.*[92])

overestimated in the terminal airways of their model. Thus, their model represents a worst-case estimate of dosage of ozone to the terminal airways, which are unprotected by mucus. Too little is known of the chemical and physical properties of the mucous layer, and there is great uncertainty in the values of the diffusivity of ozone or other gases to be used in the liquid-tissue phase of gas uptake models.

Gases that do not react irreversibly with epithelial tissue, such as anesthetic gases, may diffuse into the bloodstream and will ultimately be eliminated from the body. A different and earlier model developed by DuBois and Rogers[37] estimates the rate of uptake of inhaled gas from the tracheobronchial tree in terms of diffusion through the epithelial tissue, rate of blood flow, and solubility of the gas in blood. The rate of uptake from the airway lumen is determined by the equation:

$$\frac{\dot{V}_c}{P_o} = \frac{\alpha DA\dot{Q}}{(x\dot{Q}+DA)760} , \qquad (3)$$

where $\dot{V}_c$ is the rate of uptake of gas from the lumen, P_o is the partial pressure of the gas in the lumen, α is the solubility of the gas in blood, D is the coefficient of gas diffusion in tissue, A is the surface area of the bronchial segment, $\dot{Q}$ is the bronchial blood flow, and x is the thickness of the bronchial epithelium between lumen and blood flow. DuBois and Rogers used this equation to calculate the uptake of several gases of different solubilities from the first 16 generations of Weibel's model during acute exposures.

The absorption distribution between generations of Weibel's model had the same trend for acetone, nitrous oxide, and sulfur hexafluoride, which are soluble, moderately soluble, and insoluble, respectively, in blood or water. Absorption decreased by one-third from the trachea through the third generation and then increased rapidly and continuously with depth in the tracheobronchial tree; absorption in the sixteenth generation was 15-25 times that in the trachea. The relative magnitude of absorption at each generation was directly related to solubility. The distribution for nitrous oxide, whose solubility is slightly greater than that of ozone in water, differs radically beyond the third generation from the distribution predicted by McJilton _et al_. for ozone (Figure 7-5). Similarly, the uptake distribution for acetone, whose solubility is close to that of sulfur dioxide, differs significantly from the prediction for sulfur dioxide (Figure 7-5). This is plausible, because the tissue thickness decreases and the blood flow per generation increases with depth beyond the third generation in the DuBois and Rogers model, whereas, in the McJilton _et al_. model, blood absorption is neglected, the mucous-layer thickness decreases only slightly with depth, and the coefficient of transfer across the air-mucus interface decreases rapidly.

An improved gas-uptake model should incorporate the features of the DuBois and Rogers model and the McJilton _et al_. model. As shown in Figure 7-2, the model for gas uptake in the airways should include separate layers for mucous-serous fluid, epithelial tissue, and blood. Development of such a model awaits reliable data and methods for predicting the coefficient of diffusion of pollutant gases in tissue and information on the rates of local perfusion of blood and lymph in the bronchial epithelium.

Experimental data from humans and animals[52,53,54,138] on the rate of sulfur dioxide absorption in blood could be used to make improved estimates of the tissue diffusion coefficients in vivo.

New or improved methods are needed to measure local uptake experimentally. Such data can be used to verify the detailed dosage distribution predicted by the models. For example, the retrograde catheter and tracheal cannula system used by Corn et al.[29a] appears promising for transfer-coefficient measurements within segments of the tracheobronchial tree. A similar method was used by Battista and Goyer[16a] to measure the absorption of acetaldehyde vapor in the dog lung.

Radioactive lung-scanning techniques that use tagged irritant gases could give regional uptake data similar to scans obtained from radioactive-particle deposition and clearance studies. With methods of chemical separation and quantitation of the radioactivity in compounds isolated from the mucous layer, the reactions of ozone with biopolymers may be determined. Autoradiographic methods may also be useful for measuring the local uptake of tagged soluble gases within specific airways.

Bell[18] described how deposition of particles by convective diffusion in the respiratory tract can be used to estimate the average and local rates of gas transfer. For example, local inhomogeneities in pollutant-gas transfer can be included in uptake models. This is done by multiplying the local-transfer coefficients for 0.088-μm-diameter particles (Figure 7-6) by $(D_{gas}/D_{particle})^{2/3}$; D is the coefficient of diffusion of the gas or particle in the gas phase. When the boundary is perfectly absorbing, the local gas-phase transfer coefficients are to be multiplied by the gas concentration, the surface area between appropriate contours in Figure 7-6, and the inhalation time to determine the local gas dosage. Figure 7-7

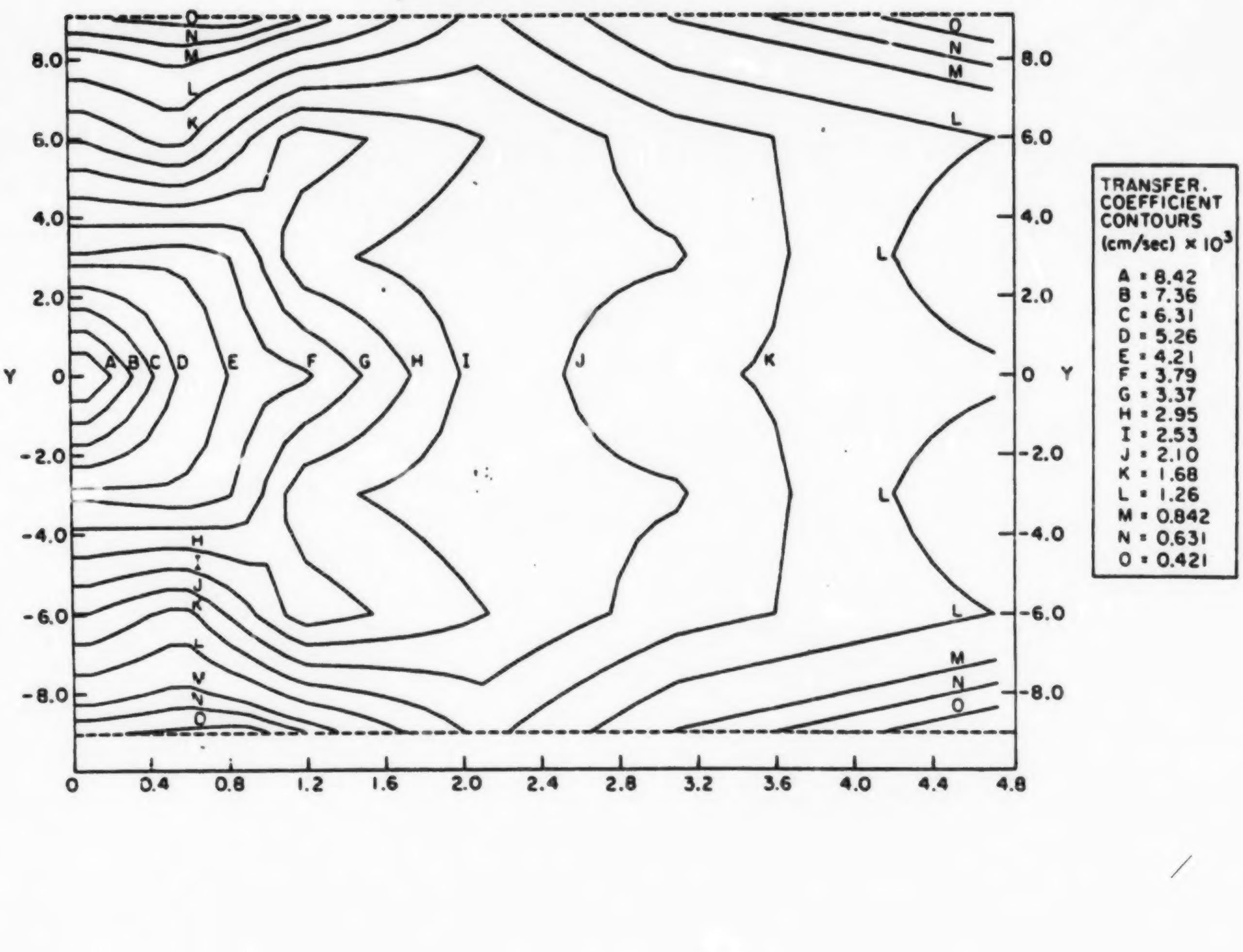

Figure 7-6. Transfer-coefficient contours for 0.088-μm-diameter particle deposition in the daughter branch of the three-dimensional bifurcation model shown in Figure 7-1 during inhalation. The time-averaged velocity in the parent branch, $\overline{U}$, is 100 cm/sec. Total surface area = 18.6 cm.^{2} X = distance (in centimeters) downstream from the carina; Y = deposition locations around the branch circumference with Y = 0 at the carina. Each unit of the ordinate corresponds to a distance of 0.215 cm. (Adapted from Bell.[18])

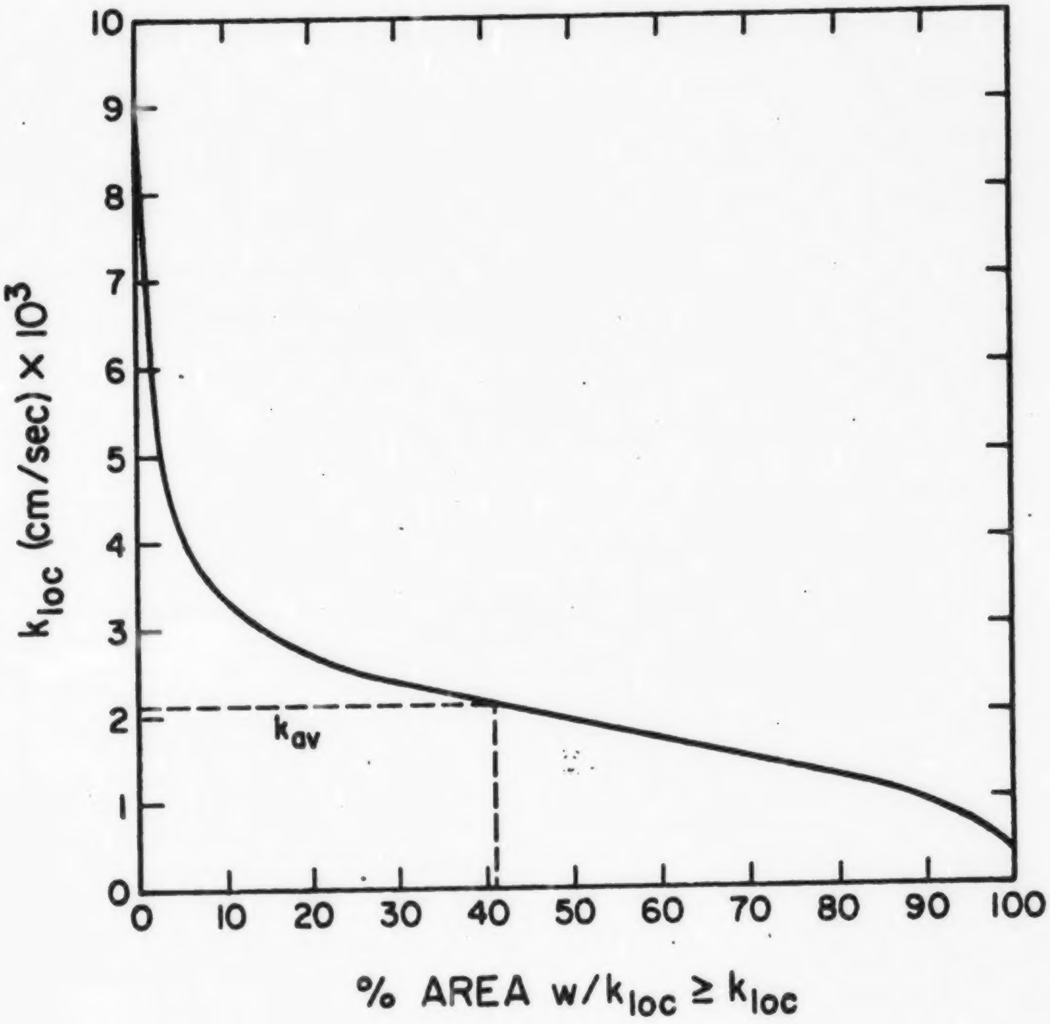

Figure 7-7. Cumulative surface-area distribution for Figure 7-6, showing the fraction of surface area of daughter branch with local transfer coefficient equal to or greater than stated value (d_p = 0.088 μm, $\bar{U}$ = 100 cm/sec). (Reprinted with permission from Bell.[18])

allows a rapid determination of the area between contours. When the boundary is not perfectly absorbing, the local gas-phase transfer coefficient must be substituted for k_g in the expression $1/K_G = 1/k_g + H/k_\ell$. Here, K_G is redefined as the coefficient of local transfer across the air-liquid interface. Local nonuniformities of gas transfer would be most prevalent in single-breath experiments, during the transient periods before equilibrium is attained, and in exposures with pollutant gases that react rapidly with the mucous layer.

Dose-Response Correlations

Modeling of gas transport is also useful for correlating dose-response data obtained under different conditions. Brain[24] suggested that the total dose of an inhaled gas is related to ventilation rate, duration of exposure, and gas concentration before inhalation. Folinsbee *et al.*[44] exposed human subjects to ozone at 0.37, 0.5, or 0.75 ppm for 2 h while they were at rest or exercising intermittently. The primary response of the subjects was an alteration in the exercise ventilatory pattern. They showed an increase in respiratory rate and a decrease in tidal volume that were correlated with the total dose of ozone (expressed as the volume of ozone inspired during exposure). Other pulmonary function data, like the flow at 50% of vital capacity, also appeared to be related to the volume of ozone inspired.

Fairchild and Graham,[42] Stokinger *et al.*,[118] and Stokinger[119a] showed that the toxic effect of ozone in experimental animals is cumulative. They found that the effective dose depends on the product of ozone concentration and exposure duration for short-term single exposures.

When the pulmonary response is activated by irritant receptors in the nose, response for different flows and concentrations would not be expected to correlate with the volume of inspired gas but rather with regional dosage (e.g., nasal) or the local dosage of gas to irritant receptors lining the airway.[2]

SUMMARY

This chapter has discussed the general approach required to model the transport and absorption of ozone and other pollutant gases in the respiratory tract. For unreactive or very weakly reactive gases, there are a few models that are qualitative descriptions for assessing total dosage and dosage in major regions. However, there is no adequate model for gases like ozone, which are strongly reactive within the mucous and tissue layers.

RECOMMENDATIONS

The development of models requires more knowledge about the chemical, physical, morphologic, and flow properties of the mucous layer; the kinetics of the reactions of ozone in the mucous and tissue layers; and the molecular diffusivity of ozone in these layers. Similar information is needed for the hydroperoxy, HO_2, and singlet oxygen, O_2 (a $^1\Delta$), free radicals, which are reactive intermediates in photochemical smog.

Furthermore, a realistic model based on such knowledge needs to be verified by measurements of uptake and tissue dosage in the various regions of the respiratory tract. These are currently difficult to make, but are required to establish accuracy and reliability. New methods of sampling and techniques using tagged gases should be developed, so that local uptake can be measured.

An extensive effort is needed in studies of pollutant-gas transfer, absorption, and reaction in the respiratory tract. After some of the experimental questions about behavior of ozone in the mucous layer and adjacent tissue are answered, available methods for calculating the local dosage to critical airway sites can be used in new uptake models. Gas-absorption and particle-deposition models for the upper respiratory tract (nose, mouth, pharynx, larynx) also need to be improved. Experimental data now available can be used to develop semiempirical relations for gas uptake in the nose in a procedure analogous to that used to model particle deposition. Development of a more refined model for nonreactive gases requires data on gas diffusivities in the mucus and tissue, local blood perfusion rates in the nasal epithelium, and physiologic and pharmacologic factors affecting the mucosa and local blood flow rates. Models need to be developed for mixtures of gases that may interact chemically in the gas phase, in the mucus, or in aerosol droplets to form other species. This requires theoretical and experimental studies of dissolution, absorption, adsorption, and desorption of gases in or on aerosols in the respiratory tract.

Improved modeling is needed for the design and interpretation of animal experiments and controlled human studies, and for the collation of diverse data from animal and human exposures to ozone. Calculations of local dose at reactive tissue sites can help to explain the mechanisms of toxicity and are needed to extrapolate animal and human data for assessing population risks under different environmental conditions.

REFERENCES

1. Aharonson, E. F., H. Menkes, G. Gurtner, D. L. Swift, and D. F. Proctor. Effect of respiratory air flow rate on removal of soluble vapors by the nose. J. Appl. Physiol. 37:654-657, 1974.

2. Alarie, Y. Sensory irritation by airborne chemicals. CRC Crit. Rev. Toxicol. 2:299-363, 1973.

2a. Albert, R. E., M. Lippmann, H. T. Peterson, Jr., J. Berger, K. Sanborn, and D. Bohning. Bronchial deposition and clearance of aerosols. Arch. Intern. Med. 131:115-127, 1973.

3. Alder, M. G., and G. R. Hill. The kinetics and mechanism of hydroxide ion catalyzed ozone decomposition in aqueous solution. J. Amer. Chem. Soc. 72:1884-1886, 1950.

4. Alder, K. B., O. Wooten, and J. M. Dulfano. Mammalian respiratory mucociliary clearance. Arch. Environ. Health 27:364-369, 1973.

5. Altman, E. I., and P. G. Men. Aerodynamical characteristics of the bronchial tree of the right human lung. Biofizika 20:303-307, 1975. (in Russian, summary in English)

6. Altshuler, B. Calculation of regional deposition of aerosol in the respiratory tract. Bull. Math. Biophys. 21:257-270, 1959.

7. Altshuler, B., E. D. Palmes, L. Yarmus, and N. Nelson. Intrapulmonary mixing of gases studied with aerosols. J. Appl. Physiol. 14:321-327, 1959.

8. Altshuler, B., N. Nelson, and M. Kuschner. Estimation of lung tissue dose from the inhalation of radon and daughters. Health Phys. 10:1137-1161, 1964.

9. Altshuler, B. Behaviour of airborne particles in the respiratory tract, pp. 215-231. In G. E. W. Wolstenholme and J. Knight, Eds. Circulatory and Respiratory Mass Transport. A CIBA Foundation Symposium. Boston: Little, Brown and Co., 1969.

9a. Andersen, I., P. Camner, P. L. Jensen, K. Philipson, and D. F. Proctor. A comparison of nasal and tracheobronchial clearance. Arch. Environ. Health 29:290-293, 1974.

10. Andersen, I., G. R. Lundquist, P. L. Jensen, and D. F. Proctor. Human response to controlled levels of sulfur dioxide. Arch. Environ. Health 28:31-39, 1974.

11. Andersen, I., G. R. Lundquist, and D. F. Proctor. Human nasal mucosal function in a controlled climate. Arch. Environ. Health 23:408-420, 1971.

11a. Angus, G. E., and W. M. Thrulbeck. Number of alveoli in the human lung. J. Appl. Physiol. 32:483-485, 1972.

12. Asmundsson, T., and K. H. Kilburn. Mucociliary clearance rates at various levels in dog lungs. Amer. Rev. Resp. Dis. 102:388-399, 1970.

13. Baker, L. G., J. S. Ultman, and R. A. Rhoades. Simultaneous gas flow and diffusion in a symmetric airway system: A mathematical model. Respir. Physiol. 21:119-138, 1974.

13a. Barton, A. D., and R. V. Lourenço. Bronchial secretions and mucociliary clearance. Biochemical characteristics. Arch. Intern. Med. 131:140-144, 1973.

14. Batchelor, G. K. The Theory of Homogeneous Turbulence. London: Cambridge University Press, 1953. p. 74. (UNVERIFIED)

15. Bates, D. V. Air pollutants and the human lung. The James Waring Memorial Lecture. Amer. Rev. Resp. Dis. 105:1-13, 1972.

16. Bates, D., and M. Hazucha. The short-term effects of ozone on the human lung, pp. 507-540. In National Research Council.. Assembly of Life Sciences. Proceedings of the Conference on Health Effects of Air Pollutants, October 3-5, 1973. Senate Committee on Public Works Print Serial No. 93-15. Washington, D. C.: U. S. Government Printing Office, 1973.

16a. Battista, S. P., and M. M. Goyer. Studies of the pulmonary absorption of acetaldehyde vapor in the dog. Fed. Proc. 33:569, 1974. (abstract)

17. Beeckmans, J. M. The deposition of aerosols in the respiratory tract. I. Mathematical analysis and comparison with experimental data. Can. J. Physiol. Pharmacol. 43:157-172, 1965.

18. Bell, K. A. Aerosol Deposition in Models of a Human Lung Bifurcation. Ph.D. Thesis. Pasadena: California Institute of Technology, 1974. 426 pp.

19. Bell, K. A., and S. K. Friedlander. Aerosol deposition in models of a human lung bifurcation. Staub-Reinhalt Luft. 33:178-182, 1973.

20. Bell, K. A., W. S. Linn, and J. D. Hackney. Effects on pulmonary function of humans exposed to mixtures of ozone, sulfur dioxide, and their reaction products. Fed. Proc. 34:428, 1975. (abstract)

Delete 21--omitted

22. Boatman, E. S., and R. Frank. Morphologic and ultrastructural changes in the lungs of animals during acute exposure to ozone. Chest 65(Suppl.) 9S-18S, 1974.

23. Boatman, E. S., and D. Luchte. University of Washington, Seattle, Washington. Personal communication, August 1975.

24. Brain, J. D. The uptake of inhaled gases by the nose. Ann. Otol. 79:529-539, 1970.

25. Cameron, G. R., J. H. Gaddum, and R. H. D. Short. The absorption of war gases by the nose. J. Path. 58:449-455, 1946.

26. Charman, J., M. T. Lopez-Vidriero, E. Keal, and L. Reid. The physical and chemical properties of bronchial secretion. Brit. J. Dis. Chest 68: 215-227, 1974.

27. Clay, J. R., and R. G. Rossing. Histopathology of exposure to phosgene. An attempt to produce pulmonary emphysema experimentally. Arch. Path. 78: 544-551, 1964.

28. Coman, D. R., H. D. Bruner, R. C. Horn, Jr., M. Friedman, R. D. Boche, M. D. McCarthy, M. Gibbon, and J. Schultz. Studies on experimental phosgene poisoning: I. The pathologic anatomy of phosgene poisoning with special reference to the early and late phases. Amer. J. Pathol. 23:1037-1073, 1947.

29. Comroe, J. H., Jr. Physiology of Respiration. An Introductory Text. Chicago: Yearbook Medical Publisher, Inc., 1965. p. 27

29a. Corn, M., N. Kotsko, and D. Stanton. Mass transfer coefficient for sulfur dioxide and nitrogen dioxide removal in cat upper respiratory tract, pp. . In Proceedings of the 4th International Symposium on Inhaled Particles and Vapors, British Occupational Hygiene Society, Edinburgh, September, 1975.

30. Cumming, G., J. Crank, J. Horsfield, and I. Parker. Gaseous diffusion in the airways of the human lung. Respir. Physiol. 1:58-74, 1966.

31. Dalhamn, T. Mucous flow and ciliary activity in the trachea of healthy rats exposed to respiratory irritant gases (SO_2, H_3N, and HCHO). A functional and morphologic (light microscopic and electron microscopic) study with special reference to technique. Acta Physiol. Scand. 36(Suppl. 123):1-161, 1956.

32. Dalhamn, T. A method for studying the effect of gases and dusts on ciliary activity in living animals, pp. 315-319. In C. N. Davies, Ed. Inhaled Particles and Vapours. Proceedings of an International Symposium organized by the British Occupational Hygiene Society, 1960. New York: Pergamon Press, 1961.

33. Davies, C. N. Filtrations of droplets in the nose of the rabbit. Proc. R. Soc. Lond. Ser. B 133:282-299, 1946.

34. Davies, C. N. A formalized anatomy of the human respiratory tract, pp. 82-91. In C. N. Davies, Eds. Inhaled Particles and Vapours. Proceedings of an International Symposium Organized by the British Occupation Hygiene Society, 1960. New York: Pergamon Press, 1961.

35. Davies, C. N. An algebraical model for the deposition of aerosols in the human respiratory tract during steady breathing. J. Aerosol Sci. 3: 297-306, 1972.

36. Dekker, E. Transition between laminar and turbulent flow in human trachea. J. Appl. Physiol. 16:1060-1064, 1961.

37. DuBois, A. B., and R. M. Rogers. Respiratory factors determining the tissue concentrations of inhaled toxic substances. Respir. Physiol. 5:34-52, 1968.

38. Dungworth, D. L., W. L. Castleman, C. K. Chow, P. W. Mellick, M. G. Mustafa, B. Tarkington, and W. S. Tyler. Effect of ambient levels of ozone on monkeys. Fed. Proc. 34:1670-1674, 1975.

39. Durlacher, S. H., and H. Bunting. Pulmonary changes following exposure to phosgene. Amer. J. Path. 23:679-693, 1947.

40. Egle, J. L., Jr. Single-breath retention of acetaldehyde in man. Arch. Environ. Health 23:427-433, 1971.

41. Egle, J. L., Jr. Retention of inhaled acetone and ammonia in the dog. Amer. Ind. Hyg. Assoc. J. 34:533-539, 1973.

42. Fairchild, E. J., and S. L. Graham. Thyroid influence on the toxicity of respiratory irritant gases, ozone and nitrogen dioxide. J. Pharmacol. Exp. Ther. 139:177-184, 1963.

43. Findeisen, W. Über das Absetzen kleiner, in der Luft suspendierter Teilchen in der menschlichen Lunge bei der Atmung. Pfluegers Arch. 236:367-379, 1935.

44. Folinsbee, L. J., F. Silverman, and R. J. Shephard. Exercise responses following ozone exposure. J. Appl. Physiol. 38:996-1001, 1975.

45. Frank, N. R. Studies on the effects of acute exposure to sulphur dioxide in human subjects. Proc. R. Soc. Med. 57:1029-1033, 1964.

46. Frank, N. R., R. E. Yoder, E. Yokoyama, and F. E. Speizer. The diffusion of $^{35}SO_2$ from tissue fluids into the lungs following exposure of dogs to $^{35}SO_2$. Health Phys. 13:31-38, 1967.

47. Frank, N. R., R. E. Yoder, J. D. Brain, and E. Yokoyama. SO_2 (^{35}S labeled) absorption by the nose and mouth under conditions of varying concentration and flow. Arch. Environ. Health 18:315-322, 1969.

48. Fry, F. A., and A. Black. Regional deposition and clearance of particles in the human nose. J. Aerosol Sci. 4:113-124, 1973.

49. Granito, S. M. Calculated Retention of Aerosol Particles in the Rat Lung. M. S. Thesis. Chicago: University of Chicago, 1971. (UNVERIFIED)

50. Gross, P., W. E. Rinehart, and T. Hatch. Chronic pneumonitis caused by phosgene. An experimental study. Arch. Environ. Health 10:768-775, 1965.

51. Gross, P., W. E. Rinehart, and R. T. P. deTreville. The pulmonary reactions to toxic gases. Amer. Ind. Hyg. Assoc. J. 28:315-321, 1967.

52. Gunnison, A. F., and A. W. Benton. Sulfur dioxide: Sulfite. Interaction with mammalian serum and plasma. Arch. Environ. Health 22:381-388, 1971.

53. Gunnison, A. F., and E. D. Palmes. Persistence of plasma S-sulfonates following exposure of rabbits to sulfite and sulfur dioxide. Toxicol. Appl. Pharmacol. 24:266-278, 1973.

54. Gunnison, A. F., and E. D. Palmes. S-sulfonates in human plasma following inhalation of sulfur dioxide. Amer. Ind. Hyg. Assoc. J. 35:288-291, 1974.

55. Haggard, H. W. Action of irritant gases upon the respiratory tract. J. Ind. Hyg. 5:390-398, 1924.

56. Ham, A. W. The respiratory system, pp. 744-771. In Histology. (5th ed.) Philadelphia: J. B. Lippincott Co., 1965.

57. Haque, A. K. M. M., and A. J. L. Collinson. Radiation dose to the respiratory system due to radon and its daughter products. Health Phys. 13:431-443, 1967.

58. Hatch, T. F., and P. Gross. Pulmonary Deposition and Retention of Inhaled Aerosols. New York: Academic Press, 1964. pp. 12, 74, 82, 88.

59. Hatch, T. F. Significant dimensions of the dose-response relationship. Arch. Environ. Health 16:571-578, 1968.

60. Hausknecht, D. F., and R. A. Ziskind. Definition of an Analytic Framework for Collating Experiments on the Effects of Sulfur Oxides on the Lung. Final Report by Science Applications, Inc. (Contract RP-205-2) Prepared for the Electric Power Research Institute, Palo Alto, California, February 28, 1975. (UNVERIFIED)

61. Hayek, H. von. The Human Lung. (Translated by V. E. Krahl) New York: Hafner Publishing Company, Inc., 1960. 372 pp.

62. Henderson, Y., and H. H. Haggard. Noxious Gases and the Principles of Respiration Influencing Their Action. New York: Reinhold Publishing Corporation, 1943. 294 pp.

63. Hilding, A. C. Ciliary streaming in the lower respiratory tract. Amer. J. Physiol. 191:404-410, 1957.

64. Hilding, A. C. Ciliary streaming through the larynx and trachea. Relation to direction of ciliary beat and significance in sites of respiratory disease. J. Thorac. Surg. 37:108-117, 1959.

65. Hilding, A. C. Phagocytosis, mucous flow, and ciliary action. Arch. Environ. Health 6:61-73, 1963.

65a. Hoigné, J., and H. Bader. Ozonation of water: Role of hydroxyl radicals as oxidizing intermediates. Science 190:782-784, 1975.

66. Horsfield, K. The relation between structure and function in the airways of the lung. Brit. J. Dis. Chest 68:145-160, 1974.

67. Horsfield, K., G. Dart, D. E. Olson, G. F. Filley, and G. Cumming. Models of the human bronchial tree. J. Appl. Physiol. 31:207-217, 1971.

67a. Hounam, R. F. The deposition of atmospheric condensation nuclei in the nasopharyngeal region of the human respiratory tract. Health Phys. 20:219-220, 1971. (letter)

68. Ichioka, M. Model experiments on absorbability of the airway mucous membrane of SO_2 and NO_2 gases. Bull. Tokyo Med. Dent. Univ. 19:361-375, 1972. (UNVERIFIED)

68a. Washburn, E. W., Ed. National Research Council of the U. S. A. International Critical Tables of Numerical Data, Physics, Chemistry and Technology. Vol. 3. New York: McGraw Hill, 1928. 444 pp.

69. Iravani, J. Clearance function of the respiratory ciliated epithelium in normal and brochitic rats, pp. 143-148. In W. H. Walton, Ed. Inhaled Particles III. Vol. 1. Proceedings of an International Symposium organized by the British Occupational Hygiene Society, 1970. Surrey: Unwin Brothers Limited, 1970.

70. Iravani, J., and A. van As. Mucus transport in the tracheobronchial tree of normal and bronchitic rats. J. Path. 106:81-93, 1972.

71. Jacobi, W. The dose to the human respiratory tract by inhalation of short-lived ^{222}Rn- and ^{220}Rn-decay products. Health Phys. 10:1163-1174, 1964.

72. Jaffrin, M. Y., and T. V. Hennessey, Jr. Pressure distribution in a model of the central airways for sinusoidal flow. Bull. Physiopath. Respir. 8: 375-390, 1972.

73. Kilburn, K. H., and R. Rylander. An interpretive summary of the Bermuda worshop. Arch. Intern. Med. 126:508-511, 1970.

74. Kirk, R. E., and D. F. Othmer, Eds. Encyclopedia of Chemical Technology. Vol. 9. Metal Surface Treatment to Penicillin. New York: The Interscience Encyclopedia, Inc., 1952. 943 pp.

75. Kliment, V., J. Libich, and V. Kaudersová. Geometry of guinea pig respiratory tract and application of Landahl's model of deposition of aerosol particles. J. Hyg. Epidemiol. Microbiol. Immunol. 16:107-114, 1972.

76. Kliment, V. Similarity and dimensional analysis, evaluation of aerosol deposition in the lungs of laboratory animals and man. Folia Morphol. 21: 59-64, 1973.

77. Kliment, V. Dichotomical model of respiratory airways of the rabbit and its significance for the construction of deposition models. Folia Morphol. 22:286-290, 1974.

78. Kowitz, T. A., R. C. Reba, R. T. Parker, and W. S. Spicer, Jr. Effects of chlorine gas upon respiratory function. Arch. Environ. Health 14:545-558, 1967.

79. Kulle, T. J., and G. P. Cooper. Effects of formaldehyde and ozone on the trigeminal nasal sensory system. Arch. Environ. Health 30:237-243, 1975.

80. La Belle, C. W., J. E. Long, and E. E. Christofano. Synergistic effects of aerosols. Particulates as carriers of toxic vapors. A.M.A. Arch. Ind. Health 11:297-304, 1955.

81. La Force, R. C., and B. M. Lewis. Diffusional transport in the human lung. J. Appl. Physiol. 28:291-298, 1970.

82. Lakin, M. B. Oscillatory Flow Simulation in an Idealized Bifurcation. Ph.D. Thesis. Denver: University of Denver, 1973. 223 pp.

83. Lakin, M. B., and V. G. Fox. Transient flow characteristics in an idealized bronchial bifurcation. Respir. Physiol. 21:101-117, 1974.

84. Landahl, H. D. On the removal of air-borne droplets by the human respiratory tract. II. The nasal passages. Bull. Math. Biophys. 12:161-169, 1950.

85. Landahl, H. D. On the removal of air-borne droplets by the human respiratory tract: I. The lung. Bull. Math. Biophys. 12:43-56, 1950.

86. Langhaar, H. L. Steady flow in the transition length of a straight tube. J. Appl. Mech. 9:A55-A58, 1942.

86a. Lapp, N. L., J. L. Hankinson, H. Amandus, and E. D. Palmes. Variablitity in the size of airspaces in normal human lungs as estimated by aerosols. Thorax 30:293-299, 1975.

87. Levich, V. G. Physicochemical Hydrodynamics. Englewood Cliffs, N. J.: Prentice Hall, 1962. 700 pp. (Translated by Scripta Technica, Inc.,)

88. Lewis, W. K., and W. G. Whitman. Principles of gas adsorption. Ind. Eng. Chem. 16:1215-1220, 1924.

89a. Lin, K. H., and G. Cumming. A model of time-varying gas exchange in the human lung during a respiratory cycle at rest. Respir. Physiol. 17: 93-112, 1973.

89b. Loring, S. H., and S. M. Tenney. Gas absorption form frontal sinuses. Arch. Otolaryngol. 97:470-474, 1973.

90. National Research Council. Committee on Medical and Biologic Effects of Environmental Pollutants. Airborne Particles. Washington, D. C.: National Academy of Sciences, (in press)

91. Macklem, P., and K. H. Kilburn. Tracheobronchial response to insult, pp. 31-35. In D. H. K. Lee, Ed. Environmental Factors in Respiratory Disease. New York: Academic Press, 1972.

91a. Matsuba, K., and W. M. Thurlbeck. The number and dimensions of small airways in nonemphysematous lungs. Amer. Rev. Resp. Dis. 104:516-524, 1971.

92. McJilton, C., J. Thielke, and R. Frank. Ozone uptake model for the respiratory system. Paper No. 45. In Abstracts of Technical Papers. American Industrial Hygiene Conference, May 14-19, 1972.

93. Mezentseva, N. V., E. A. Melnikova, and O. Ya. Mogilevskaya. Titanium, pp. 35-44. In Z. I. Izrael'son, Ed. Toxicology of the Rare Metals. Jerusalem: Israel Program for Scientific Translations, Ltd., 1967. (Translated by Y. Halperin, edited by E. Lieber)

94. Moorman, W. J., J. J. Chmiel, and J. F. Stara. Comparative decomposition of ozone in the nasopharynx of beagles. Arch. Environ. Health 26:153-155, 1973.

95. Morrow, P. E. Airborne contaminants, pp. 71-90. In D. H. K. Lee, Ed. Environmental Factors in Respiratory Disease. New York: Academic Press, 1972.

96. Washburn, E. W., Ed. National Research Council of the U. S. A. International Critical Tables of Numerical Data, Physics, Chemistry and Technology. Vol. 3. New York: McGraw Hill, 1928. 444 pp.

97. Olson, D. E., M. F. Sudlow, K. Horsfield, and G. F. Filley. Convective patterns of flow during inspiration. Arch. Intern. Med. 131:51-57, 1973.

98. Owen, P. R. Turbulent flow and particle deposition in the trachea, pp. 236-252. In G. E. W. Wolstenholme and J. Knight, Eds. Cirulatory and Respiratory Mass Transport. A CIBA Foundation Symposium. Boston: Little, Brown and Co., 1969.

98a. Palmes, E. D., and M. Lippmann. Influence of respiratory air space dimensions on aerosol deposition, pp. . In Proceedings of the 4th International Symposium on Inhaled Particles and Vapors, British Occupational Hygiene Society, Edinburgh, Sept. 1975.

99. Papper, E. M., and R. J. Kitz, Eds. Uptake and Distribution of Anesthetic Agents. New York: McGraw-Hill Book Co., 1963. 321 pp.

100. Pattle, R. E. The retention of gases and particles in the human nose, pp. 302-311. In C. N. Davies, Ed. Inhaled Particles and Vapours. Proceedings of an International Symposium organized by the British Occupational Hygiene Society, Oxford, 1960. Oxford: Pergamon Press, 1961.

101. Pedley, T. J., R. C. Schroter, and M. F. Sudlow. Flow and pressure drop in systems of repeatedly branching tubes. J. Fluid Mech. 46:365-383, 1971.

102. Emmert, R. E., and R. L. Pigford. Mass-transfer fundamentals, pp. 14-13--14-19. In R. H. Perry, C. H. Chilton and S. D. Kirkpatrick, Eds. Chemical Engineers' Handbook. (4th ed.) New York: McGraw-Hill Book Company, 1963.

103. Phalen, R. F. Summary of a Respiratory Tract Morphology Conference. Lovelace Foundation for Medical Education and Research, Albuquerque, New Mexico. Report LF-47, June 1974.

104. Phalen, R. F., H. C. Yeh, and D. J. Velasquez. Bronchial tree structure in the human, beagle, rat, and hamster, LF-49, pp. 289-292. In 1973-1974 Annual Report of Inhalation Toxicology Research Institute. Lovelace Foundation for Medical Education and Research, 1974.

105. Proctor, D. F. Physiology of the upper airway, pp. 309-345. In W. O. Fenn and H. Rahn, Eds. Handbook of Physiology. Section 3: Respiration. Vol. 1. Washington, D. C.: American Physiological Society, 1964.

106. Proctor, D. F., and H. N. Wagner. Clearance of particles from the human nose. Preliminary report. Arch. Environ. Health 11:366-371, 1965.

107. Proctor, D. F., and D. L. Swift. The nose--a defense against the atmospheric environment, pp. 59-70. In W. H. Walton, Ed. Inhaled Particles III. Proceedings of an International Symposium organized by the British Occupational Hygiene Society in London, 1970. Surrey: Unwin Brothers Limited, 1971.

107a. --deleted

107b. Proctor, D. F., I. Andersen, and G. Lundqvist. Clearance of inhaled particles from the human nose. Arch. Intern. Med. 131:132-139, 1973.

108. Quinlan, M. F., S. D. Salman, D. L. Swift, H. N. Wagner, Jr., and D. F. Proctor. Measurement of mucociliary function in man. Amer. Rev. Respir. Dis. 99:13-23, 1969.

109 deleted--omitted

109a. Santa Cruz, R., J. F. Landa, J. Hirsch, and M. A. Sackner. Tracheal mucous velocity in normal man and patients with obstructive lung disease; effects of terbutaline. Amer. Rev. Respir. Dis. 109:458-463, 1974.

110. Schlichting, H. Boundary-Layer Theory. (6th ed.) New York: McGraw-Hill, 1968. 747 pp. (translated by J. Keatin)

111. Schreck, R. M., and L. F. Mockros. Fluid Dynamics in the Upper Pulmonary Airways. American Institute of Aeronautics and Astronautics Paper No. 70, 1970. p. 788.

112. Schroter, R. C., and M. R. Sudlow. Flow patterns in models of the human bronchial airways. Respir. Physiol. 7:341-355, 1969.

113. Schwartz, L. W., W. S. Tyler, and D. L. Dungworth. Pulmonary changes induced by ambient levels of ozone: A morphological study, pp. 367-383. In Proceedings of the 5th Annual Conference on Environmental Toxicology. Wright-Patterson Air Force Base, Ohio, Sept. 24-26, 1974. AMRL-TR-74-125. Wright-Patterson AFB, Ohio: Aerospace Medical Research Laboratory, 1974.

114. Seban, R. A., and E. F. McLaughlin. Heat transfer in tube coils with laminar and turbulent flow. Int. J. Heat Mass Transfer 6:387-395, 1963.

115. Silverman, L. G. Lee, T. Plotkin, L. A. Sawyers, and A. R. Yancey. Air flow measurements on human subjects with and without respiratory resistance at several work rates. A.M.A. Arch. Ind. Hyg. Occup. Med. 3:461-478, 1951.

116. Speizer, F. E., and N. R. Frank. The uptake and release of SO_2 by the human nose. Arch. Environ. Health 12:725-728, 1966.

117. Spiegelman, J. R., G. D. Hanson, A. Lazarus, R. J. Bennett, M. Lippmann, and R. A. Albert. Effect of acute sulfur dioxide exposure on bronchial clearance in the donkey. Arch. Environ. Health 17:321-326, 1968.

117a. Stephens, R. J., M. F. Sloan, M. J. Evans, and G. Freeman. Early response of lung to low levels of ozone. Amer. J. Path. 74:31-44, 1974.

117b. Stevens, R. J., M. F. Sloan, M. J. Evans, and G. Freeman. Alveolor type 1 cell response to exposure to 0.5 ppm O_3 for short periods. Exp. Molec. Path. 20:11-23, 1974. (UNVERIFIED)

118. Stokinger, H. E., W. D. Wagner, and P. G. Wright. Studies of ozone toxicity. I. Potentiating effects of exercise and tolerance development. A.M.A. Arch. Ind. Health 14:158-162, 1956.

119a. Stokinger, H. E. Evaluation of the hazards of ozone and oxides of nitrogen. Factors modifying toxicity. A.M.A. Arch. Ind. Health 15:181-190, 1957.

119b. Sullivan R. J. Preliminary Air Pollution Survey of Arsenic and Its Compounds. A Literature Review. National Air Pollution Control Administration Publication No. APTC 69-26. Bethesda, Md.: Litton Systems, Inc., 1969. 60 pp.

119c. Sullivan, R. J. Preliminary Air Pollution Survey of Chromium and Its Compounds. A Literature Review. National Air Pollution Control Administration Publication No. APTD 69-34. Bethesda, Md.: Litton Systems, Inc., 1969. 75 pp.

119d. Sullivan, R. J. Preliminary Air Pollution Survey of Iron and Its Compounds. A Literature Review. National Air Pollution Control Administration Publication No. 69-38. Bethesda, Md.: Litton Systems, Inc., 1969. 94 pp.

119e. Sullivan, R. J. Preliminary Air Pollution Survey of Nickel and Its Compounds. A Literature Review. National Air Pollution Control Administration Publication No. 69-41. Bethesda, Md.: Litton Systems, Inc., 1969. 69 pp.

119f. Sullivan, R. J. Preliminary Air Pollution Survey of Manganese and Its Compounds. A Literature Review. National Air Pollution Control Administration Publication No. 69-39. Bethesda, Md.: Litton Systems, Inc., 1969. 54 pp.

119g. Task Group on Lung Dynamics. Deposition and retention models for internal dosimetry of the human respiratory tract. Health Phys. 12:173-207, 1966.

120. Taulbee, D. B., and C. P. Yu. A theory of aerosol deposition in the human respiratory tract. J. Appl. Physiol. 38:77-85, 1975.

121. Thomas, J. A method for calculation of the absorbed dose to the epithelium of the respiratory tract after inhalation of daughter products of radon. Ann. Occup. Hyg. 7:271-284, 1964.

122. Thorp, C. E. Bibliography of Ozone Technology. Vol. 2. Physical and Pharmacological Properties. Chicago: Armour Research Foundation, Illinois Institute of Technology, 1955. (UNVERIFIED)

122a. Thurlbeck, W. M., and J. R. Haines. Bronchial dimension and stature. Amer. Rev. Respir. Dis. 112:142-145, 1975. (UNVERIFIED)

123. U. S. Department of Health, Education, and Welfare. Public Health Service. Air Quality Criteria for Particulate Matter. National Air Pollution Control Administration Publ. No. AP-49. Washington, D. C.: U. S. Government Printing Office, 1969. 211 pp.

124. U. S. Department of Health, Education, and Welfare. Public Health Service. Air Quality Criteria for Photochemical Oxidants. National Air Pollution Control Administration Publ. No. AP-63. Washington, D. C.: U. S. Government Printing Office, 1970.

125. Van As, A., and I. Webster. The organization of ciliary activity and mucus transport in pulmonary airways. S. Afr. Med. J. 46:347-350, 1972.

126. Van As, A., and Webster, I. The morphology of mucus in mammalian pulmonary airways. Environ. Res. 7:1-12, 1974.

127. von Nieding, G., and H. M. Wagner. Absorption of NO_2 in low concentrations in the respiratory tract and its acute effects on lung function and circulation. Paper Presented at the 2nd International Clean Air Congress, Washington, D. C., 1970.

128. Wada, S., et al. Neoplasms of the respiratory tract among poison gas workers. Hiroshima Med. J. 16:728-745, 1963.

Delete 129--omitted

130. Weibel, E. R. Morphometry of the Human Lung. New York: Academic Press, Inc., 1963. 151 pp.

131. West, J. B. Observations on gas flow in the human brochial tree, pp. 3-7. In C. N. Davies, Ed. Inhaled Particles and Vapours. Proceedings of an International Symposium organized by British Occupational Hygiene Society, 1960. New York: Pergamon Press, 1961.

132. Whipple, R. T., W. R. Chen, and C. S. Wang. The Dispersion of Aerosol Boli in a System of Repeatedly Branching Tubes. Paper Presented at the 75th Meeting of the AIChE, Detroit, Michigan, June 3-6, 1973.

133. Wilson, T. A., and K.-H. Lin. Convection and diffusion in the airways and the design of the bronchial tree, pp. 5-19. In A. Bouhuys, Ed. Airway Dynamics. Physiology and Pharmacology. Springfield: Charles C Thomas, 1970.

134. Winternitz, M. C. Collected Studies on the Pathology of War Gas Poisoning. New Haven: Yale University Press, 1920. 165 pp.

135. Womersley, J. R. Oscillatory motion of a viscous liquid in a thin-walled elastic tube. I. The linear approximation for long waves. Phil. Mag. Ser. 7 46:199-221, 1955.

135a. Yeates, D. B., N. Aspin, M. T. Jones, and A. C. Bryan. Mucociliary tracheal transport rates in man. J. Appl. Physiol. 39:487-495, 1975.

136. Yeh, H.-C. Use of a heat transfer analogy for a mathematical model of respiratory tract deposition. Bull. Math. Biophys. 36:105-116, 1974.

137. Yeh, H. C., A. J. Hulbert, R. F. Phalen, and O. G. Roabe. Mathematical considerations for particle deposition in the tracheobronchial tree: Equations and lung model, LF-49, pp. 298-302. In 1973-74 Annual Report of Inhalation Toxicology Research Institute, Lovelace Foundation for Medical Education and Research, 1974.

138. Yokoyama, E., R. E. Yoder, and N. R. Frank. Distribution of ^{35}S in the blood and its excretion in urine of dogs exposed to $^{35}SO_2$. Arch. Environ. Health 22:389-395, 1971.

139. Yokoyamo, E., and R. Frank. Respiratory uptake of ozone in dogs. Arch. Environ. Health 25:132-138, 1972.

140. Yokoyama, E. Comparisons of the penetration rate of inhaled O_3, NO_2, and SO_2 into the respiration passages. Taiki Osen Kenkyo (J. Jap. Soc. Air Pollut.) 7:192, 1972. (in Japanese)

141. Zamel, N., J. H. M. Austin, P. D. Graf, H. H. Dedo, M. D. Jones, and J. A. Nadel. Posdered tantalum as a medium for human laryngography. Radiology 94:547-553, 1970.